BIOLOGICAL EVALUATION OF A NOVEL PTEROSTILBENE-DERIVATIVE AS POTENT ANTICANCER AGENT

Ph.D THESIS

by

KUMAR NIKHIL

DEPARTMENT OF BIOTECHNOLOGY
INDIAN INSTITUTE OF TECHNOLOGY ROORKEE
ROORKEE - 247 667 (INDIA)
FEBRUARY, 2015

BIOLOGICAL EVALUATION OF A NOVEL PTEROSTILBENE-DERIVATIVE AS POTENT ANTICANCER AGENT

A THESIS

Submitted in partial fulfilment of the requirements for the award of the degree of

DOCTOR OF PHILOSOPHY

in

BIOTECHNOLOGY

by

KUMAR NIKHIL

DEPARTMENT OF BIOTECHNOLOGY
INDIAN INSTITUTE OF TECHNOLOGY ROORKEE
ROORKEE - 247 667 (INDIA)
FEBRUARY, 2015

INDIAN INSTITUTE OF TECHNOLOGY ROORKEE
ROORKEE

<u>CANDIDATE'S DECLARATION</u>

I hereby certify that the work which is being presented in the thesis entitled **"Biological evaluation of a novel pterostilbene-derivative as potent anticancer agent"** in partial fulfilment of the requirements for the award of the degree of Doctor of Philosophy and submitted in the Department of Biotechnology of the Indian Institute of Technology Roorkee, Roorkee is an authentic record of my own work carried out during the period from July, 2009 to February, 2015 under the supervision of Dr. Partha Roy, Professor, Department of Biotechnology, Indian Institute of Technology Roorkee, Roorkee, India.

The matter presented in this thesis has not been submitted by me for the award of any other degree of this or any other institute.

(KUMAR NIKHIL)

This is to certify that the above statement made by the candidate is correct to the best of my knowledge.

(Partha Roy)

Dated: Supervisor

Abstract

Cancer is defined as uncontrolled growth and spread of cells which can affect almost any part of the body. The growths often invade surrounding tissue and can also metastasize to distant sites. Many cancers can be prevented by avoiding exposure to common risk factors, such as tobacco smoke. In addition, a significant proportion of cancers can be cured, by surgery, radiotherapy or chemotherapy, especially if they are detected early. Over the years, the design of cancer chemotherapy has become increasingly sophisticated. Yet there is no cancer treatment that is 100% effective against disseminated cancer. At present cancer therapy interfering with a single biological molecule or pathway has been successfully utilized. Still the problem of drug resistance and a general belief that agents modulating more than one target could have superior efficacy compared to single target drugs has led to the search for molecules modulating multiple targets. The present thesis entitled **"Biological evaluation of a novel pterostilbene-derivative as potent anticancer agent"** deals with synthesis followed by evaluating the anticancer properties of a novel pterostilbene-isothiocyanate conjugate and further understanding it's mode of action in preventing breast and prostate cancer progression

At the beginning, **Chapter 1** introduces briefly the present scenario of the chemotherapeutic drugs available to prevent steroid related cancer (breast and prostate cancer). It also deals with the key factors and the major signaling pathway present in these cancer cells that need to be targeted for its prevention. These cancer cell characteristics can serve as major points to guide the screening of novel molecule for their respective efficacy. Finally detailed objective to be attained in this study is specified here.

Followed by this, **Chapter 2** presents (i) a detailed review of set of characteristics that defines cancer - Hallmarks of cancer; (ii) a vivid description on endocrine related cancer with special emphasis on breast and prostate cancer; (iii) Understanding the role of inflammation and angiogenesis with major focus on molecular pathways and their therapeutic targets; (iv) recent research detailing benefits of phytochemical and their characteristics to target multiple pathways in cancer therapy; (v) detailed account of the design strategies employed for the synthesis of anticancer agents via molecular hybridization techniques and finally (v) the hypothetic idea behind the present thesis to manipulate the cancer cells towards death. Each of these hypotheses was further explored in subsequent chapters of the thesis.

The main objective of the present work is synthesis and biological evaluation of novel pterostilbene conjugate as anticancer agent and understanding its mode of action. There are

several *in vitro* assays which are already established to confirm a molecule to be anti-cancerous. All these parameters are elaborated in **Chapter 3** of this thesis. In this concern, this chapter contains the overall principles and methodology of all the experimental assays that were performed to identify a molecule to be anticancer compound. The stage I includes biochemical parameters like MTT assay, FACS analysis, cell cycle analysis, DNA fragmentation patterns, activation of caspase which were used initially to check for anticancer effect; and in stage II, the principles of the biological mechanisms are studied at transcriptional and translational levels of various genes to understand how a molecule acts intracellularly, mainly the assays which show the basic determination of the underlying pathways. Further several cell lines used for the study have been discussed in detail.

Cancer is a multifactorial disease, thus agents that concomitantly address more than one biological target for cancer treatment is preferred choice. Over the last few years, molecular hybridization strategy has emerged as a novel approach that involves conglomeration of two or more pharmacophores in one molecular scaffold to develop hybrid multifunctional molecules. The latter have multiple biological activities, modified selectivity profile, different or dual modes of action and/or reduced undesired side effects due to mixing of pharmacophores in one molecule. Using this approach we have synthesized and further characterized a novel compound (Pterostilbene-isothiocyanate conjugate) by appending an isothiocyanate moiety on pterostilbene (PTER) backbone which is described in **Chapter 4.** Moreover, we have tested the anticancer properties of the above said compound on different cancer cell lines in comparison to its parent compound i.e. PTER. Our results showed that all the cancer cell lines as tested by us were more sensitive to conjugate treatment as compared to PTER.

Next, in **Chapter 5**, after the initial screening finally the pathways leading to apoptosis were checked biochemically and then at the transcriptional and translational level in hormone-dependent breast cancer cell line (MCF-7) *in vitro*. Our result confirmed that the pro-apoptotic effect of conjugate is mediated through the activation of caspases, and is correlated with the blockade of the AKT and ERK signaling pathways in MCF-7 cells. Finally the compound was tested on Ehrlich ascitic cell induced mouse tumor models and the characteristic pathways which lead to the reduction in tumor volume was investigated.

PPARγ is a nuclear receptor which is widely expressed in many tumors and cell lines, and has become a promising target for anticancer therapy. This molecule is considered as the most promising target for metabolic syndrome, anti-inflammation and cancer in the 21st

Century. Furthermore this receptor has a critical role in breast cancer proliferation, survival, invasion, and metastasis. Hence in **Chapter 6** we tested whether PTER-ITC mediates its anti-proliferative and pro-apoptotic effects in breast cancer cells through activation of the PPARγ signaling cascade. Our results showed that PTER-ITC activated PPARγ expression in a dose-dependent manner, followed by downregulation of anti-apoptotic genes (Bcl-2 and survivin) to induce noteworthy levels of apoptosis in hormone-dependent (MCF-7) and independent (MDA-MB-231) breast cancer cells.

Androgen and AR functions play a pivotal role in carcinogenesis and progression of prostate cancer (PCa), as well as in normal prostate development. Hence in the next section (**Chapter 7**), the effect of PTER-ITC on regulation of AR signaling in PCa was studied on both androgen dependent (LNCaP) and androgen independent (PC-3) cell lines. Our study showed that PTER-ITC effectively inhibited proliferation of both these PCa cells by inducing apoptosis and causing cell cycle arrest. Both PI3K/AKT and MAPK/ERK pathways played an important and differential role in PTER-ITC-induced apoptosis of these PCa cells. Further PTER-ITC inhibited the AR transcription and translation and also inhibited the localization of AR to the nucleus as seen in the AR-GFP transfection studies suggesting its AR antagonist nature.

Breast cancer as a heterogeneous disease is characterized by activation of multiple signal pathways which stimulate tumor growth, proliferation, inhibit apoptosis, and promote the formation of new blood vessels (angiogenesis), as well as invasion and metastasis. Angiogenesis is essential for tumor progression by supplying sufficient oxygen and nutrients required for tumor growth and metastasis . Targeting angiogenesis is an exciting and attractive area in the treatment of cancer. Human umbilical vein endothelial cells (HUVECs) are cells derived from the endothelium of veins from the umbilical cord and are used as a laboratory model system for the study of the function and pathology of endothelial cells including angiogenesis. **Chapter 8** of this thesis described the isolation and characterization of HUVEC cells from human umbilical cord. In the later part we examined the anti-angiogenic activity of PTER-ITC using a combination of *in vitro* and *in vivo* angiogenesis assays. This was followed by understanding the pathway targeted for preventing angiogenesis.

Chronic inflammation has been linked to various steps involved in tumorigenesis, including cellular transformation, promotion, survival, proliferation, invasion, angiogenesis, and metastasis. Numerous evidence clearly shows that inflammatory pathways are critical targets in both prevention and therapy of cancer. Therefore, identification of agents/drugs that

can suppress these pathways has enormous potential in cancer prevention. In **Chapter 9** of this thesis we further attempted to investigate the anti-inflammatory potential of PTER-ITC followed by understanding its probable mode of action in lipopolysaccharide (LPS) stimulated RAW264.7 macrophages. In addition, the *in vitro* study was followed by *in vivo* studies on λ-carrageenan-induced rat paw edema model. Our data showed that non-toxic doses of PTER-ITC could inhibit inflammatory responses against LPS-stimulated RAW264.7 cells through down regulation of both IKK/NFκB and MAPK/AP-1 signaling

Inflammation and tumors contribute to osteolysis causing bone pain and debilitating skeletal instability. Skeletal integrity depends on bone homeostasis which is achieved by balanced function of bone cells. Bone formation by osteoblasts and bone resorption by osteoclasts are lifelong events delicately balanced in healthy individuals. This homeostasis is compromised under pathologic conditions such as metabolic and inflammatory diseases including osteoporosis, inflammatory osteolysis, and skeletal tumor metastases, wherein heightened osteoclast activity leads in most cases to increased bone loss. Gene targeting studies have shown that the transcription factor nuclear factor-κB (NFκB) has a crucial role in osteoclast differentiation, and blocking NFκB is a potential strategy for preventing inflammatory bone resorption. The **Chapter 10** deals with understanding the role PTER-ITC on preventing RANKL induced osteoclast differentiation in RAW264.7 and understanding the underlying mechanism.

Finally, the **Chapter 11** summarizes the primary contributions of this research and provides suggestions for future work in this area. The scientific findings dealt with in this thesis may be of use to the future researchers working in this area. Last but not the least, the **Chapter 12**, listed the bibliography which was consulted in course of the present work.

Acknowledgements

"Life is not a journey to the grave with the intention of arriving safely in one pretty and well-preserved piece, but rather to skid in broadside, totally worn out and proclaiming, Wow, What a Ride!!!!" - <u>Mavis Leyrer</u>

And again, WOW, WHAT A RIDE!, this is the best expression I can apply to the adventure of becoming a doctor in India. The pursuit of the doctoral degree has been a rigorous, but rewarding journey. Of course, none of all this amazing experience could be possible without the unconditional help and advice of incredible people who not only contributed in my professional journey but also in the personal one. Before beginning a new chapter of my life, I would like to extend a heartfelt thanks to the following people who supported, guided and inspired me throughout the journey of my PhD tenure.

First and foremost I would like to express my profound gratitude to my PhD supervisor **Prof. Partha Roy** *for providing me with an opportunity to work in his lab. I also thank him for all his unwavering support, encouragement and guidance throughout my doctoral discourse. I am grateful for his constructive criticism and invaluable advice whenever needed while his unbounded optimism has always kept my spirits high.*

At the outset I would like to express my gratitude to members of my advisory committee, Prof. R.P. Singh, Dr. A.K. Sharma, both from Department of Biotechnology and Prof. R.Jayaganthan from Department of Metallurgical and Materials Engineering for their encouragement and insightful comments.

I am highly grateful to Professor Partha Roy, the present Head of the Department and all the faculty members of the Department of Biotechnology, IIT Roorkee for providing the necessary infrastructure and facilities and also their support at various time points to complete my thesis.

I take this opportunity to sincerely acknowledge the **Council for Scientific and Industrial Research** *(CSIR), Government of India, New Delhi, for providing financial assistance which buttressed me to perform my work comfortably.*

Most importantly I am thankful to Professor Ilpo Huhtaniemi Imperial College of London, London, UK; Dr. Richard G. Pestell's of Kimmel Cancer Centre, Thomas Jefferson

University, Philadelphia, USA; Dr. Ronald M. Evans (The Salk Institute for Biological Studies, California, USA) and Dr. Michael R. Stallcup (University of Southern California, Los Angeles, USA) for providing me with important research materials which were very essential to complete the study. Without their help this thesis would have been impossible.

*The members of the **Molecular Endocrinology lab** have contributed immensely to my personal and professional time. My thanks are due to the former members of my lab Dr. Shambha, Dr. Ajanta, Dr. Rajani and Dr. Swati for being a source of inspiration for me in my early years as a research scholar which kept me going at the beginning. I also wish to thank my colleagues Shruti and Narender for their invaluable suggestions, motivation and encouragement in the process of this research work. A special thanks to my labmates Snehashish, Ritu and Rutusmita for all the scientific as well as non-scientific discussions and all the off-work enjoyment in lab and trips time we were together. I extend my thanks to the current and past members of my lab, Dr Vishwa Deepak, Dr. Tapas Mandal and Dr. Asvene Sharma for providing me with a peaceful and friendly academic environment. Above all the group has been a source of friendships as well as good advice and collaboration.*

I am highly grateful to Dr.R.K. Peddinti, Department of Chemistry, Indian Institute of Technology Roorkee and his students Mr. Nagaanjaneyulu and Mr Sreenivas who synthesized pterostilbene and its conjugate for the study. I am also thankful to Dr. V. Grover, Abhilasha Nursing Home, Roorkee, India and all midwives and assistant nurses at the labour and delivery ward for their enthusiasm and support for providing the umbilical cord sample.

I further acknowledge all the bachelor and masters students who did their thesis under my supervision. I would like to particularly thank Rahul, Preeti, Sachin, Rohan, Disha, Abhishek, Shifa and Arka, for helping me with experiments and providing me with an opportunity to improve my research skills.

I would like to extend a huge, warm thanks to all other research scholars and MSc students of Department of Biotechnology, IIT Roorkee. Special thanks to the non teaching staff especially the administrative staff and the staff from the BTech and MSc labs who were always so helpful and provided me with their assistance throughout my dissertation.

*I am especially thankful to my wife and labmate **Shruti Sharan** for her constant encouragement and support and also helping me technically at different stages of my thesis work. She had supported me in the most stressful periods and always cheered me to make me*

strong. Many a times when I have yielded to stress of the circumstances, she has taken every pain to patiently transform all my shattered hopes carefully into a perfect mould. She has always contributed her best to the success of all my present endeavors.

My work would not have been so easy without the specific help of all my friends and colleagues from HCU, PGIMER, JNU, AIIMS, NII, NIPER and ICGEB who has contributed directly or indirectly towards the successful completion of my work. Although they were physically far from me, but electronically were really close to me and all their encouraging messages kept me going even in the hard times. I am also thankful to all other friends and colleagues whose names have been unknowingly left. Thank you very much for all your support.

I wish to extend my hearty thanks to Mrs. Roopa Roy, for all her support and her culinary dishes that helped me to find a "home away from home".

Lastly I would like to express my heartfelt thanks to my parents Mr Anil Singh and Mrs Anita Singh and my sisters Neha and Riya for their constant support and abundant patience shown throughout the years. I wouldn't have achieved all this without their unconditional love and encouragement. I dedicate my doctoral thesis to them.

Besides this, I would like to thank everyone who has knowingly or unknowingly helped me in the successful completion of this thesis.

Kumar Nikhil ....

List of Publications

1. **Nikhil K**, Sharan S, Singh AK, Chakraborty A, Roy P. (2014). Anticancer Activities of Pterostilbene-Isothiocyanate Conjugate in Breast Cancer Cells: Involvement of PPARγ. *PloS on*e 9(8), e104592.

2. **Nikhil K**, Sharan S, Chakraborty A, Roy P. (2014). Pterostilbene-Isothiocyanate Conjugate Suppresses Growth of Prostate Cancer Cells Irrespective of Androgen Receptor Status. *PloS one* 9(4), e93335.

3. **Nikhil K**, Sharan S, Chakraborty A, Bodipati N, Peddinti RK, Roy P. (2014). Role of isothiocyanate conjugate of pterostilbene on the inhibition of MCF-7 cell proliferation and tumor growth in Ehrlich ascitic cell induced tumor bearing mice. *Exp cell Res* 320(2), 311-328.

4. **Nikhil K**, Sharan S, Roy P. (2013). A brief overview of androgen receptor: Its structure, functions and role in health and disease. *J Endocrinol Reprod* 17(1):19-30.

5. **Nikhil K**, Sharan S, Palla SR, Sondhi SM, Roy P. (2015) Assessment of the role of a pterostilbene derivative as anti-inflammatory agent and understanding its mode of action *(Under revision, International Immunopharmacology)*.

6. **Nikhil K**, Sharan S, Roy P. (2015) PTER-ITC inhibits osteoclastogenesis by suppressing the activation of NFκB and MAPK in RANKL-induced RAW 264.7 cells *(Under revision, Pharmacological Reports)*.

7. **Nikhil K**, Sharan S, Aggarwal R, Roy P. (2015) Pterostilbene-isothiocyanate, a resveratrol derivative inhibits 17β-Estradiol induced cell migration and proliferation in HUVECs *(In Communication)*.

x

List of Abbreviations

%	Percentage
°C	Degree Centigrade
μg	Microgram
μl	Microliter
μM	Micromolar
5FU	5 Fluorouracil
AMPK	AMP-activated protein kinase
ANOVA	Analysis of Variance
AO	Acridine orange
AP1	Activator Protein 1
AR	Androgen Receptor
ARE	Androgen Response Element
BCA	Bicinchonic acid
bp	Basepair
BSA	Bovine Serum Albumin
CAM	Chick embryo chorioallantoic membrane
CDKs	Cyclin dependent kinases
cDNA	Complementary DNA
COX	Cyclooxygenase
CTR	Calcitonin receptor
DAPI	4',6-diamidino-2-phenylindole
DCIS	Ductal carcinoma in situ
dH_2O	deionised water
DHT	Dihydrotestosterone
DISC	Death-Inducing Signalling Complex
DMSO	Dimethyl Sulphoxide
DNA	Deoxy Nucleic Acid
dNTPs	deoxy Nucleotide Triphosphates
DRs	Death receptors
DTT	Dithiothreitol
E2	Estradiol
EAC	Ehrlich ascitic cell

EB	Ethidium bromide
ECL	Enhanced chemiluminescence
EDTA	Ethylene diamine tetra acetic acid
EGFR	Epidermal growth factor receptor
EMSA	Electrophoretic mobility shift assay
EMT	Epithelial mesenchymal transition
ER	Estrogen Receptor
ERE	Estrogen Response Element
ERK	Extracellular-signal regulated kinases
FACS	Fluorescence activated cell sorter
FADD	Fas Associated Death Domain
FAK	Focal Adhesion Kinase
FBS	Fetal bovine serum
FGF	Fibroblast Growth Factor
g	gram
GSK-3	Glycogen synthase kinase 3
h	Hour
H2O2	Hydrogen peroxide
HIF	Hypoxia inducing factor
HPLC	High performance liquid chromatography
HRMS	High Resolution– Mass spectroscopy
HRP	Horseradish peroxidase
HRPC	Hormone-refractory prostate cancer
HSP	Heat shock proteins
HUVECs	Human umbilical vein endothelial cells
IC50	Half inhibition concentration
IKK	IκB kinase
IL	Interleukin
iNOS	Inducible nitric oxide synthase
ITC	Isothiocyanate
IU	International Unit
IκB	Inhibitor of kappa B
JNK	c-Jun N-terminal protein kinases
kD	KiloDalton

kg	Kilogram
L	Liter
LCIS	Lobular carcinoma in situ
LPS	Lipopolysaccharide
m	Meter
M	Molar
MAPK	Mitogen associated protein kinases
mg	Milligram
min	Minute
mL	Milliliter
mM	MilliMolar
MMPs	Matrix metalloproteinase
mRNA	Messenger Ribonucleic acid
mTOR	Mammalian Target of Rapamycin
MTT	3-(4,5-dimethylthiazol-2-yl)-2,5-diphenyltetrazolium bromide
MYD88	Myeloid differentiation factor-88
NCBI	National Centre for Biotechnology Information
NCCS	National Centre for Cell Sciences
NFAT	Nuclear factor of activated T cells
NFκB	Nuclear Factor of κB
ng	Nanogram
nM	NanoMolar
NO	Nitric oxide
OD	Optical density
OPGL	Osteoprotegerin ligand
OPLS	Optimized potential for liquid simulations
PBS	Phosphate buffered saline
PCa	Prostate cancer
PCR	Polymerase Chain Reaction
PI3K	Phosphatidylinositide 3-kinases
PKB	Protein kinase B
PMSF	Phenyl methyl sulphonyl fluoride
PPAR	Peroxisome proliferator-activated receptors
ppm	Parts Per Million

PPRE	Peroxisome proliferating response element
PR	Progesterone Receptor
PTEN	Phosphatase and TENsin homologue
PTER	Pterostilbene
PVDF	Polyvinylidene fluoride
RANK	Receptor activator of nuclear factor kappa-B
RANKL	Receptor activator of nuclear factor kappa-B ligand
RB	Retinoblastoma
RESV	Resveratrol
RMSD	Root mean square deviation
RNA	Ribo Nucleic Acid
ROS	Reactive oxygen species
rpm	Revolution per Minute
RTK	Receptor Tyrosine Kinases
RT-PCR	Reverse Transcriptase- Polymerase Chain Reaction
SAR	Structure activity relationship
SDS-PAGE	Sodium dodecyl sulphate-Poly acrylamide gel electrophoresis
sec	Second
SEM	Standard error mean
SERM	Selective ER modulator
SRC1	Steroid receptor co-activator 1
TAE	Tris Acetate EDTA
TE	Tris Acetate
TERT	Telomerase Reverse Transcriptase
TLR	Toll-like receptor
T_m	Melting Temperature
TNF-α	Tumor necrosis factor-α
TRADD	TNF receptor associated death domain
TRAF-6	TNF receptor associated factor-6
TRAP	Tartrate resistant acid phoaphatase
TSP-1	Thrombospondin-1
U	Units
UV	Ultra Violet
VEGF	Vascular Endothelial Growth Factor

List of Contents

List of Figures

receptor as determined by green fluorescent protein (GFP)-androgen receptor construct in presence/absence of 10 nM DHT for 2 h.

List of Tables

Chapter 1. Introduction

1.1 Basic Introduction

Cancer is a group of diseases characterized by uncontrolled growth of abnormal cells and is a major worldwide problem. It is a fatal disease that's stand next to the cardiovascular disease in terms of both morbidity and mortality. Although recent cancer research has led to a number of new and effective solutions, the medicines used as treatments have clear limitations and unfortunately cancer is expected as the primary cause of death in the future [Gibbs, 2000; Varmus, 2006]. Chemotherapy is one of the important approaches among cancer therapies and currently there is a huge scientific and commercial interest in the discovery of potent, safe and selective anticancer drugs. Physicians and scientists all over the world are vigorously investigating different ways to improve the efficacy of chemotherapy by developing new chemotherapeutic agents, refining therapeutic approaches, and optimizing combination treatment strategies. As cancer cells are highly heterogeneous in nature and exhibit deregulation in multiple cellular signaling pathways therefore, treatments using specific agents or inhibitors that target only one biological event or a single pathway usually fail in cancer therapy. In order to achieve higher efficacy and overcome this failure, combination treatments using multiple agents having distinct targets have been considered more promising, resulting in better cancer cell killing. Therefore the principle is that by attacking or blocking multiple important pathways which are responsible for promoting cancer cell survival and growth multi-targeted cancer therapy can be considered to be more effective in inhibiting cancer cell growth and inducing apoptotic cell death.

The endocrine system is vital for growth, maturation, and coordination of the human body. However, malignancies can also arise from the organs which are influenced by endocrine-system-secreted hormones. Among these malignancies, the most widely studied are breast cancer and prostate cancer in women and men respectively. Although these tumors seem to be considerably different due to diverse anatomical and physiological features of the organs where they arise, they share a common feature of hormonal-dependence [Risbridger et al., 2010]. The key driver for breast and prostate cancer includes specific steroid hormone receptors, such as estrogen receptor (ER), progesterone receptor (PR), and androgen receptor (AR). Being hormone-dependent tumors, antihormone therapies usually are effective in prevention and treatment. However, the emergence of resistance is common, especially for locally advanced tumors and metastatic tumors, in which case resistance is predictable. The underlying mechanisms of these phenotypes are complicated, involving not only sex hormones

and sex hormone receptors, but also several growth factors and growth factor receptors, with different signaling pathways existing alone or together, and with each pathway possibly linking to one another. The phosphatidylinositol 3-kinase (PI3K)/AKT/mammalian target of rapamycin (mTOR) and the Raf/mitogen-activated and extracellular signal-regulated kinase kinase (MEK)/extracellular signal-regulated kinase (ERK) signaling pathways are critical for normal human physiology, and also commonly deregulated in several human cancers, including breast and prostate cancer. Researches have shown that inhibition of one or both of these pathways plays a more profound effect on tumor cell development and death, making them attractive as a combinational target in cancer therapy. Therefore estrogen receptor (ER), androgen receptor (AR), AKT and ERK could be potential targets for the treatment of both breast and prostate cancer.

In recent years, dietary and compounds harvested from nature (natural compounds) have received increased attention primarily because epidemiological studies have shown their consumption is associated with reduced risk of several types of cancers [Gordaliza, 2007]. Natural products, with their ability to interact with more than one target, in medicinal chemistry, represents, a significant source of inspiration for the design of structural analogues with improved pharmacological profile. 3,5,4-trans-trihydroxystilbene (Resveratrol; RESV), a well-known natural polyphenol present in large amount in grapes and has been reported to exert multiple biological activities including anti-inflammatory [Udenigwe et al., 2008], anti-oxidant [Burns et al., 2000], inhibition of platelet aggregation (Pace-Asciak et al., 1995), antitumor, and induction of apoptosis [Athar et al., 2007; Brisdelli et al., 2009; Carter et al., 2014]. Structure-activity relationship (SAR) studies, performed on a number of RESV analogues established the chemical features responsible for the antitumor and the proapoptotic activities; for example the 3,5-dimethoxyphenyl moiety was identified to play a pivotal role in conferring both the antitumor and the proapoptotic activities [Simony et al., 2006, Roberti et al., 2003; Pettit et al., 2002]. In general, the presence of number of methoxy groups seems to be a fundamental requirement to obtain potent cytotoxic agents. Trans-3,5-dimethoxy-4'-hydroxystilbene (Pterostilbene; PTER) is a naturally occurring dimethyl ether analogue of RESV. The structure of PTER is very similar to resveratrol, although the 3,5-dihydroxy part of RESV (the two hydroxyl groups on the benzene ring to the left) are replaced with methoxy groups. This makes PTER more potent and selective than the parent RESV in the inhibition of the cancer cell growth [Li et al., 2013; Nutakul et al., 2011; Chiou et al., 2011]. In addition PTER has higher oral bioavailability and enhanced potency as compared to RESV [Kapetanovic et al., 2011] and proposed to have similar properties as RESV including anticancer, anti-inflammation,

antioxidant, apoptosis, antiproliferation, and analgesic potential [McFadden, 2013; Denise and MC Fadden., 2012].

On the other hand isothiocyanate (ITC) are naturally occurring small molecules characterized by the presence of reactive $-N=C=S$ group [Fahey et al., 2001]. These chemo protective agents are formed by hydrolysis of their precursor parent compounds known as glucosinolates found in a wide variety of cruciferous vegetables like broccoli, cauliflower, cabbage, Brussel sprouts and kale [Clarke et al., 2008]. Many ITC, both natural and synthetic, display anticarcinogenic activity because they reduce activation of carcinogens and increase their detoxification. Diets high in ITC containing cruciferous vegetables have been shown to protect against a number of malignancies including non-Hodgkin's lymphoma and the cancers of liver, prostate, ovary, lung, colon and gastro intestinal tract [Murillo et al., 2001]. Recent studies show that they exhibit anti-tumor activity by affecting multiple pathways including apoptosis, MAPK signaling, oxidative stress, and cell cycle progression [Wu et al., 2009].

Over the last few years, with the progress in medicinal chemistry, the hybrid approach has received significant attention since it allows obtaining molecules with improved biological activities with respect to the corresponding lead compounds [Nepali et al., 2014]. Thus, the design and synthesis of hybrid molecules encompassing two pharmacophores in one molecular scaffold is a well established approach to the synthesis of more potent drugs. In addition, the hybrids may also minimize the unwanted side effects and allow for synergic action [Nepali et al., 2014]. Using this approach, several research groups have recently designed and synthesized hybrid molecules by coupling a number of bioactive molecules such as: RESV, maleimide, alpha-lipoic acid, coumarine, chalcone, chlorambucil etc. which resulted in new molecules endowed with increased antioxidant, anticancer and anti-inflammatory properties [Vilar et al., 2006; Melagraki et al., 2009; Song et al., 2009; Sashidhara et al., 2010; Wittman et al., 2001; Gupta et al., 2010] Inspired by this the present study was undertaken to synthesize a novel class of hybrid compound by introducing an ITC moiety on PTER backbone and understanding its mode of action in prevention of breast and prostate cancer and its associated complications.

1.2 Aims and Objectives

Cancer is a leading cause of death worldwide, accounting for 8.7 million deaths (around 14% of all deaths) in 2012. The pharmacological fight against cancer has made significant progress in the last twenty years. Although many chemotherapeutic agents have been developed to treat different kinds of cancer effectively, some side effects could occur simultaneously [Bird and Swain, 2008; Beadle et al., 2009; Praga et al., 2005; Vardy, 2009; Falleti et al., 2005, de Ruiter et al., 2012]. Multifunctional compounds (MFCs) are designed broadly as hybrid or conjugated drugs or as chimeric drugs from two or more pharmacophores/drugs having specific pharmacological activities. These are capable of eliciting multiple pharmacological actions and have emerged as magic bullets in treatment of multifactorial diseases like cancer. The major focus of this work is to study the potential of PTER-ITC conjugate, a novel class of hybrid compound synthesized by appending an ITC moiety to the PTER backbone, in prevention of breast and prostate cancer and further understanding its mechanism of action. This is one among the hundreds of new findings to figure an ideal drug for the treatment of cancer. Overall, the study attempted to achieve the following objectives.

1. Synthesis, characterization and comparative analysis of PTER and PTER-ITC in prevention of breast and prostate cancer.

2. Understanding the mode of action of PTER-ITC in prevention of breast cancer in relation to activation of cell death machinery and involvement of PPARγ.

3. Understanding the mode of action of PTER-ITC in prevention of prostate cancer leading to growth arrest in prostate cancer and its cross talk with androgen receptors.

4. Understanding the anti-angiogenic effect PTER-ITC in HUVEC cells after its isolation and characterization.

5. Assessing the role of PTER-ITC as anti-inflammatory agent and understanding its mode of action.

6. Understanding the role of PTER-ITC in preventing RANKL induced osteoclastogenesis.

Chapter 2 Literature Review

2.1. Introduction

The present chapter provides comprehensive reviews regarding different traits/hallmarks that govern the transformation of normal cells to cancer (malignant or tumor) cells. This will be followed by a discussion on different aspect of breast and prostate cancer (PCa) as well as new approaches for evaluating and treating breast and prostate tumors based on improvements in technologies and molecular knowledge. As we were interested in studying the various signaling cascades which control transformation of normal cell into cancer cell, few selected signaling cascades such as apoptosis pathway, ER signaling pathway, AR signaling, PI3K/AKT signaling, MAPK, NFκB, LPS and RANKL signaling pathways and their involvement in cancer and associated diseases have been discussed further. The next part of the chapter deals with a brief review on the role of phytochemicals on cancer chemoprevention with special emphasis on polyphenolic compounds like RESV and PTER. The last part of the review deals with promise and challenges in drug discovery and development of hybrid anticancer drugs.

2.2 Cancer in general

Cancer is a class of diseases in which a group of cells display uncontrolled growth, invasion and sometimes metastasis (spread to other locations in the body via lymph or blood). It mainly occurs when the information in cellular DNA is corrupted leading to abnormal patterns of gene expressions. This leads to increase in expression of normal gene that control cell growth, survival and spread while those genes that suppress these effects are repressed. The main mechanism by which this corruption of the genetic code occurs is through (i) impairment of a DNA repair pathway; (ii) the transformation of a normal gene into an oncogene and (iii) the malfunction of a tumor suppressor gene. Aberrant gene expression leads to a number of key changes in fundamental biological processes within cancer cells – the so-called 'hallmarks' of cancer.

2.3 Hallmarks' of cancer

All cancer cells possess a set of characteristics that define them. These are certain disorders, or biological capabilities in a way, that make these cells different form normal cells. Any cell can be termed as cancerous if it possesses all these features. These are: sustaining proliferative signaling, evading growth suppressors, resisting cell death, enabling replicative immorality, inducing angiogenesis, activating invasion and metastasis, tumor promoting

inflammation, genomic instability and mutation, evading immune destruction and deregulating cellular energetics. These capabilities are together termed as the "hallmarks of cancer". The first six of these hallmarks were published by cancer biologists Weinberg and Hanahan in the journal Cell in the year 2000 [Hanahan and Weinberg, 2000]. The last four were added to the original six, as the hallmark capabilities of cancer cells after another decade of research in the field of oncology and cancer biology and were reviewed by the same two scientists in the year 2011 [Hanahan and Weinberg, 2011][Fig. 2.1].
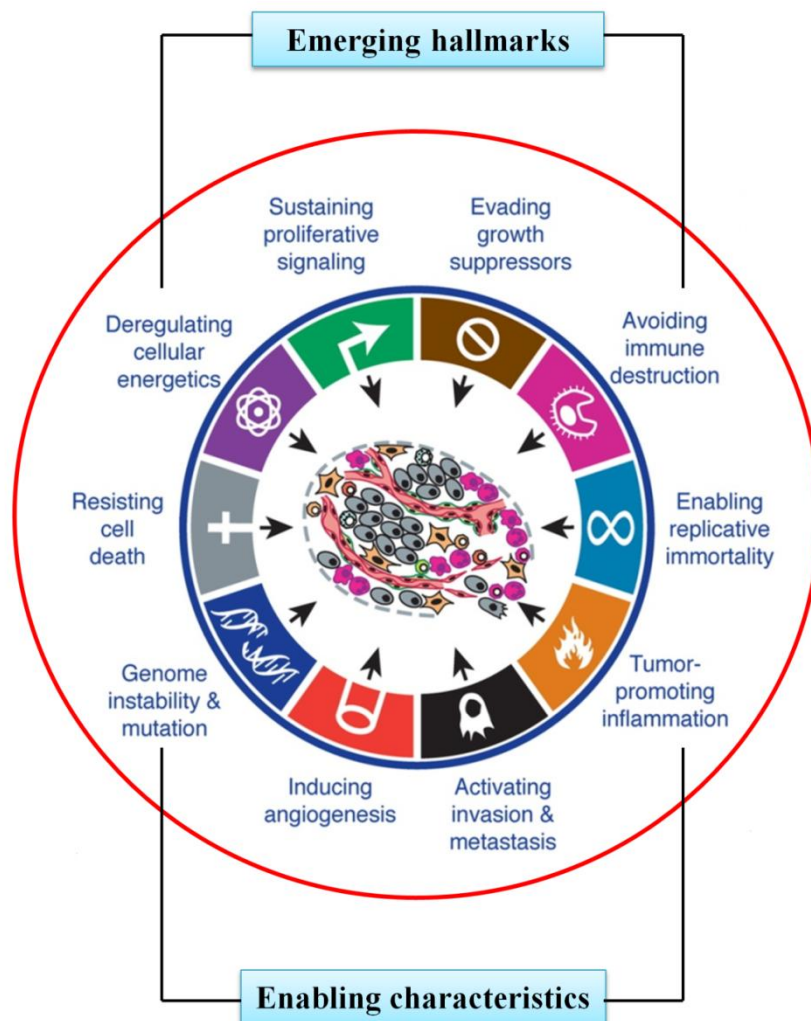
Figure 2.1: The Ten Hallmarks of Cancer [Hanahan D, Weinberg RA. Hallmarks of cancer: the next generation. *Cell*. 2011, 144(5):646-74]

2.3.1 Sustained proliferative signaling

One of the most important terminal characteristics of cancer cells is that they divide continuously in an uncontrolled, uninhibited manner. During the process of transformation, somewhere something goes wrong due to which the regulatory control over the cell cycle

progression and cell division is lost. This off-course is the result of the deregulation of the signaling mechanisms underlying cell division, leading to a continuous flux of proliferation related signals. Mitogen mediated signaling is very well understood in cancer cells [Lemmon and Schlessinger, 2010; Witsch et al., 2010]. Cancer cells can acquire the ability to proliferate continuously in a number of ways. Firstly, through autocrine signaling, they produce ligands for the growth factor receptors present on their surface. Secondly, by paracrine signaling, in which they stimulate the normal cells constituting their microenvironment to produce ligands, which could attach with the growth receptors on their surfaces, thus activating the corresponding signaling pathways. Thirdly, by over expressing the receptors for mitogens on their surfaces.

Constitutive proliferation can also be the result of certain mutations in the genome of cancer cells. It has been reported that almost 40% of human melanomas contain mutations which affect the activity of the B-Raf protein, leading to constitutive signaling of this protein to the MAP-Kinase pathway [Davies and Samuels, 2010]. Several mutations have been reported in the isoforms of the PI3-kinase enzyme, in several tumor types [Jiang and Lu, 2009]. These serve to hyperactivate the PI3-kinase signaling circuit. Finally, the hyper-proliferative signaling of cancer cells can also be a result of defects in negative feedback loop mechanisms that control cell proliferation and the associated signaling pathways as a part of normal homeostasis [Wertz and Dixit, 2010; Amit et al., 2007].

2.3.2 Evading growth suppressors

In order to be able to undergo uncontrolled and uninhibited cell division, cancer cells must be able to escape the several mechanisms that exist within normal cells that suppress cell proliferation. This would mean that tumor cells must be able to circumvent the functions of two well known tumor suppressors: TP53 and Retinoblastoma (Rb) genes. TP53 halts the cell cycle whenever a defect in DNA is encountered. TP53 monitors the overall stress levels in the cell. It checks the abnormality sensors to decide if or not are the intracellular circumstances good enough for the cell to go ahead with its normal cell and divide. If the level of damage to the genome is found to be beyond the level of sustenance or if the levels of nucleotide pools, growth-promoting signals, glucose or reactive oxygen species in the cells is found to be above the level of sustenance, then it may halt the cell cycle till the conditions are normalized. In cases in which the damage level is found to be irreparable, it may decide to push the cell into apoptosis, thereby preventing it from dividing under circumstances which may lead to the development of mutations in the replicating genome that contribute to the genome-instability

which is implicated in the process of transformation. For all these reasons TP53 is referred to as the "guardian of genome" [Lim et al., 2007; Gomez-Lazaro et al., 2004; Lam and Crawford, 1986; Meulmeester et al., 2008; Saha et al., 2013]. The Rb protein is also involved in the cell's decision making on whether or not to proceed with the cell cycle. It interacts with and suppresses the activity of cyclins and cyclin dependent kinases (CDKs), which are essential for cell division. It thus arrests the cells in between G_1 to S phase [Vurusaner et al., 2012; Burkhart and Sage et al., 2008].

2.3.3 Resisting cell death

Programmed cell death is perhaps the greatest natural barrier to transformation or cancer progression. As any other signaling pathway, apoptosis also has upstream regulators and downstream components (effectors). The regulators, in turn, are divided into two major circuits, one receiving and processing extracellular death-inducing signals (the extrinsic apoptotic program, involving for example the Fas ligand/Fas receptor), and the other sensing and integrating a variety of signals of intracellular origin (the intrinsic program). Both these pathways involve a number of proteases called caspases. The extrinsic pathway culminates in the activation of caspase 8 and the intrinsic pathway leads to the activation of caspase 9, while caspase 3 is a downstream component common to both these pathways [Adam and Cory, 2007].

Apoptosis is controlled by a fine balance between the anti-apoptotic and pro-apoptotic regulatory proteins. The Bcl-2 family of proteins is anti-apoptotic, acting chiefly by suppressing the function of two pro-apoptotic proteins: Bax and Bak, which are normally cytosolic proteins but relocate to the outer mitochondrial membrane, in response to intracellular apoptotic signals. There they mediate the creation of pores in the mitochondrial membrane thus causing the release of proapototic factors from the mitochondrion, the most important of which is cytochrome c [Jia et al., 2012]. Research in the recent past has revealed that a carefully regulated balance between apoptosis, necrosis and autophagy-related pathways is one aspect of normal cell physiology which controls the life of a cell [Nikoletopoulou et al., 2013; Maiuri et al., 2007; Dikshit et al., 2006]. Hence this is one aspect of cancer research as of now.

2.3.4 Enabling replicative immorality

Just as important as it is to have a continuous flux of replication related signaling, is also the ability to undergo repeated cell cycles, for cancer cells. There exist two barriers to this capability, which a cell must pass in order that it can get 'transformed' from a normal to a cancerous state. The first is 'senescence' and the second is a 'crisis phase'. The second follows

the first, when the cells are subjected to repeated sub-culturing *in vitro*. The small fraction of the initial population emerging successful out of the second phase is said to have been immortalized. The most important factor imparting replicative immortality to the cell is telomerase activity. Telomerase expression is very faint in normal cells, but significant in the majority of spontaneously immortalized cells. Telomere length, which is a function of telomerase activity, is a sought of 'biological clock' regulating the lifetime or number of the progeny resulting from a given cell. Apart from this well understood role of the telomerase in cancer progression, new arrays of functions have been attributed to it. Recent studies report that the telomerase is a regulator of all the classical hallmarks of cancer [Low and Tergaonkar, 2013]. The telomerase subunit: Telomerase Reverse Transcriptase (TERT) is involved in metabolic reprogramming and transcriptional regulation [Park et al., 2009]. Thus, the complete role of the telomerase in tumorigenesis is still far from being completely understood.

2.3.5 Inducing angiogenesis

Angiogenesis, the process of formation of new blood vessels from pre-existing blood vessels, occurs continuously only during embryogenesis. In the embryo, endothelial cells are produced and assembled into tube like structures to form blood vessels (vasculogenesis). Also new blood vessels sprout from the existing ones (sprouting angiogenesis). However, in adult the process of angiogenesis acts as a switch, being activated only in case of a tissue injury, or as a part of the female reproductive cycle in order to facilitate healing. In contrast to this, a tumor mass is characterized by sustained angiogenesis, which facilitates its growth and later, metastasis to other sites in the body [Hanahan and Folkman, 1996]. Angiogenesis regulators are most commonly signaling proteins that bind to stimulatory or inhibitory cell-surface receptors displayed on the surface of vascular endothelial cells. The most well known inducer and inhibitor respectively, of angiogenesis are: Vascular Endothelial Growth Factor (VEGF)-A and Thrombospondin-1 (TSP-1) [Baeriswyl and Christofori, 2009]. The VEGF-A protein induces angiogenesis during embryonic development, during the homeostatic survival of endothelial cells and also under certain pathological and physiological conditions in the adult. The expression of VEGF-A gene can be up-regulated by both hypoxia and oncogenic signaling [Ferrara, 2009; Gabhann and Popel, 2008]. Some other signaling proteins such as members of the Fibroblast Growth Factor (FGF) have been implicated in sustaining tumor angiogenesis if their expression is chronically up regulated [Baeriswyl and Christofori, 2009].

The main angiogenesis mechanism in tumor masses revolves around VEGF-A production by tumor cells and the subsequent proliferation of vascular endothelial cells brought

about by VEGF binding to its receptor(s) [Gomes et al., 2013]. VEGF mediates its effects by binding to 3 types of receptors: VEGFR-1, VEGFR-2 and VEGFR-3. VEGF binds with high affinity to VEGFR-1 and VEGFR-2, but with differing affinity to VEGFR-3 [Hoff and Machado, 2012]. VEGFR-1 binds VEGF with the strongest affinity, 10 times as compared to that of VEGFR-2 binding to VEGF. However, the receptor tyrosine activity of VEGFR-2 is much higher than that of VEGFR-1. VEGF binding to VEGFR-1 is seemingly required for most of the physiological effects of VEGF [Shibuya, 2010; Shalaby et al., 1995; Ferrara, 2005]. VEGFR-1 is also up regulated in some of the tumor types, suggesting a possible role in tumorigenesis [Hoff and Machado, 2012]. VEGFR-2 on the other hand mediates responses related to endothelial cell survival, proliferation, migration, vascular permeability and focal adhesion turnover. VEGFR-2 receptor is highly expressed in breast cancers (all types) [Guo et al., 2010; Gonzalez et al., 2009]. Owing to such evidences from research, VEGF, VEGFR-1, VEGFR-2 are all good targets for anti-angiogenic therapy against breast cancer. VEGFR-2 expression levels have also been found to be elevated in colon cancer cell lines, ovarian cancer clinical samples and also in small cell lung cancer cells [Giatromanolaki et al., 2007; Higgins et al., 2006; Tanno et al., 2004].

2.3.6 Activating invasion and metastasis

Any cancer becomes more of a problem when it becomes metastatic and begins to spread to other parts of the body through the blood vascular system or the lymphatic system. Till now, three distinct modes of metastasis have been identified. Transformed epithelial cells can acquire the ability to invade or metastasize primarily by a developmental switch known as epithelial mesenchymal transition (EMT) [Gos et al., 2008; Thiery et al., 2009]. EMT induced metastasis is known as "mesenchymal" metastasis. This program can be activated transiently or stably and to different extents during the course of invasion and metastasis by epithelial cells. Developmental genetics has identified a number of transcription factors such as Snail, Slug, Twist and Zeb1/2 that are involved in coordinating the program of EMT and related migratory processes during embryonic development [Lander et al. 2011; Martin et al., 2005; Micalizzi et al., 2010]. A current area of concern in metastasis research is to understand the function the role of these factors in orchestrating the process of EMT. The second type of metastasis known is the amoeboid type metastasis in which cancer cells show an amoeboid type movement, moving through the existing interstitial sites in between the tissues, in an extracellular matrix [Madsen and Sahai, 2010].

Yet another type of metastasis although known but not very well studied is currently an emerging concept. In this type of metastasis it is believed that cancer cells secrete certain chemo-attractants to cause a buildup of inflammation associated cells around them. These cells then produce the necessary matrix degrading enzymes that enable migration of cancer cells to off-origin sites [Qian and Pollard, 2010].

2.3.7 Tumor promoting inflammation

The seventh hallmark, newly added to the list of the six original one explained beautifully by Weinerg and Hanahan [Hanahan and Weinberg, 2000; Hanahan and Weinberg, 2011] is "inflammation" or more appropriately- 'cancer related inflammation'. Inflammation occurring in the tumor microenvironment facilitates the proliferation and survival of malignant cells, angiogenesis, metastasis, reduction in response to hormones and chemopreventive agents etc [Colotta et al., 2009]. It has been shown that cancer and inflammation are closely related to each other [Ben-Neriah and Karim, 2011]. Cancer and inflammation can have two types of associations with each other. In the intrinsic association or pathway, the genetic changes that occur in neoplasia initiate inflammation related pathways. These then direct the creation of an inflammatory microenvironment which in-turn promotes tumor progression. In the extrinsic pathway, an inflammatory condition directly facilitates the development of tumor. NFκB is a key player in innate immunity/inflammation and NFκB de-regulation has been observed in many cancers [Dolcet et al., 2005]. In addition to the usual modes of activation, NFκB activation can also result from cell-autonomous genetic alterations (amplification, mutations or deletions) in cancer cell genome. Additionally, NFκB can also be activated in response to hypoxia [Eltzschig and Carmeliet, 2011]. Numerous evidences suggest the existence of compensatory pathways between the NFκB and hypoxia inducing factor (HIF)-1α, linking innate immunity to the hypoxic response. NFκB induces the expression of inflammatory cytokines, adhesion molecules, key enzymes in the prostaglandin synthase pathway (COX-2), nitric oxide (NO) synthase and angiogenic factors.

2.3.8 Genome instability

All the above explained hallmark capabilities of cancer cells ultimately results from the accumulation of several oncogenic mutations in the genome. This feature of a cancer cells is referred to as genome instability [Negrini et al., 2010]. Genome instability arises due to two reasons. The first is increased sensitivity to mutagens due to a breakdown in one or several components of the genomic maintenance machinery [Carr and Lambert, 2013]. The second and the probably significant reason is the failure of DNA repair machinery or of the various genes

which keep a check on the status of the genome, such as the TP53 gene, and prevent or delay the onset of division till the errors in the genome have been rectified to sustainable levels, or initiate apoptosis if the level of damage is found to be beyond sustenance [Otozai et al., 2014; Jackson and Bartek, 2009]. Kinzler and Vogelstein in 1997 identified certain genes involved in the DNA-maintenance machinery-as "caretakers of the genome". This group of genes includes those whose products i) detect DNA damage and activate DNA repair machinery, ii) directly repair damaged DNA, iii) inactivating or intercepting mutagenic molecules before they have damaged the DNA [Venkitaraman, 2002]. Mutant copies of these genes have been inserted in mice (knock in), with the results of increased cancer incidence, thus strongly suggesting their involvement in cancer development and progression [Bames and Lindahl, 2004].

2.3.9 Deregulating cellular energetic

Uncontrolled cell proliferation referred as fundamental characteristic of neoplastic cell involves not only deregulated cell proliferation but also corresponding adjustment of energy metabolism. During aerobic condition normal cell utilizes glucose first to pyruvate through glycolysis in cytosol followed by carbon dioxide under anaerobic conditions in mitochondria. However, it was Otto Warburg who first noticed an anomalous behaviour of cancer cells energy metabolism where cancer cells favoured glycolysis as a metabolic program over mitochondrial oxidative phosphorylation even in the presence of oxygen (termed aerobic glycolysis) [Warburg, 1930, 1956a, 1956b]. This "metabolic switch" seems counter-intuitive, as the efficiency of glycolysis is 18-fold lower than oxidative phosphorylation. Cancer cells compensate for this, at least in part, by up-regulating glucose receptors (GLUT1) to import more glucose into the cytoplasm [Jones and Thompson, 2009; De Berardinis et al., 2008; Hsu and Sabatini et al., 2008]. Indeed, increased uptake and utilization of glucose has been reported for many human tumors. The functional rationale for this metabolic switch has not yet been elucidated. Preferential glycolysis has been associated with activated oncogenes and loss of tumor suppressors, both of which confer other hallmark capabilities on cancer cells. One possible explanation for the switch is that it enables diversion of glycolytic intermediates into other pathways, such as those responsible for synthesizing amino acids, nucleosides, and macromolecules.

Intriguingly, some tumors have two subpopulations of cells with different energy metabolism programs. One subpopulation exhibits the Warburg effect, favoring glycolysis and generating lactate along with those useful intermediates. The other subpopulation preferentially imports lactate, using it as the main energy source by harnessing part of the citric acid cycle

[Kennedy and Dewhirst, 2010; Feron, 2009; Semenza, 2008]. This apparently symbiotic relationship within tumors has provocative implications for the study and treatment of human cancers. It is particularly because components of the citric acid cycle, specifically isocitrate dehydrogenases 1 and 2 (IDH1 and IDH2) have recently emerged as oncogenes that are recurrently mutated in gliomas and leukemias.

2.3.10 Evading immune destruction

Recent evidences from clinical epidemiology and genetic engineered mice have revealed that immune system posses' a significant barrier to tumor formation and progression. For instance, carcinogens induced tumor develops more oftenly and progresses more rapidly in immunodeficient mice as compared to wild type mice. Further, NK cells or T-cells depletion in mice have shown increased tumor incidence, suggesting the involvement of both innate and adaptive immunity to immune surveillance. Another important concept which link immunity to cancer is "immunoediting". When carcinogen induced tumors which arise in immunodeficient mice are transplanted into wild type mice these tumors are eliminated by the intact immune system of the new host. However, in contrast, tumors induced in wild-type mice often grow when transplanted to other wild-type mice. Most probably, tumors induced in immunodeficient mice are highly immunogenic, and therefore gets easily identified and removed by a healthy immune system. However, tumors induced in wild-type mice have arisen in spite of an intact immune system. The selective pressure of the competent immune system "edits" the tumor by selecting for cells that can avoid immune destruction. Thus, by the time they are macroscopic, these tumors are poorly immunogenic, and more resistant to immune-mediated destruction.

2.4 Endocrine related cancer

The endocrine system is important for growth, maturation, and coordination of the human body. Yet, malignancies can also result from the organs which are directly influenced by these endocrine-system-secreted hormones. Breast cancer and prostate cancer (PCa) the two most common invasive cancers in women and men, respectively are the most widely accepted malignancies which fall under this category (Fig 2.2). Both these cancers begin in organs that differ in terms of their anatomical and physiological function and both of them require gonadal steroids for their development. The tumors developing from such cancer are typically hormone-dependent and have remarkable underlying biological similarities. These two types of cancer are similar in their epidemiological patterns and possess similar pathological entities. Both of them are hormone related cancers which have their growth and development controlled by endocrine system. To mediate hormone effects on the initiation and progression of diseases

they utilize specific steroid hormone receptors, such as estrogen receptor (ER), progesterone receptor (PR), and androgen receptor (AR). With the recent improvement in diagnostic methodologies, the incidence of both these type of cancer have increased, which is presumably accredited to early diagnosis. However recent advances in understanding the pathophysiology of breast and prostate cancers have paved the way for new treatment strategies. Nonetheless, to date curative treatments for both advanced cancers have not yet been established. Therefore, understanding the underlying pathogenesis of disease progression is the critical prerequisite for developing effective therapeutic and preventive strategies of these two cancers.

Estimated New Cases*

Males				Females		
Prostate	233,000	27%		Breast	232,670	29%
Lung & bronchus	116,000	14%		Lung & bronchus	108,210	13%
Colorectum	71,830	8%		Colorectum	65,000	8%
Urinary bladder	56,390	7%		Uterine corpus	52,630	6%
Melanoma of the skin	43,890	5%		Thyroid	47,790	6%
Kidney & renal pelvis	39,140	5%		Non-Hodgkin lymphoma	32,530	4%
Non-Hodgkin lymphoma	38,270	4%		Melanoma of the skin	32,210	4%
Oral cavity & pharynx	30,220	4%		Kidney & renal pelvis	24,780	3%
Leukemia	30,100	4%		Pancreas	22,890	3%
Liver & intrahepatic bile duct	24,600	3%		Leukemia	22,280	3%
All Sites	**855,220**	**100%**		**All Sites**	**810,320**	**100%**

Estimated Deaths

Males				Females		
Lung & bronchus	86,930	28%		Lung & bronchus	72,330	26%
Prostate	29,480	10%		Breast	40,000	15%
Colorectum	26,270	8%		Colorectum	24,040	9%
Pancreas	20,170	7%		Pancreas	19,420	7%
Liver & intrahepatic bile duct	15,870	5%		Ovary	14,270	5%
Leukemia	14,040	5%		Leukemia	10,050	4%
Esophagus	12,450	4%		Uterine corpus	8,590	3%
Urinary bladder	11,170	4%		Non-Hodgkin lymphoma	8,520	3%
Non-Hodgkin lymphoma	10,470	3%		Liver & intrahepatic bile duct	7,130	3%
Kidney & renal pelvis	8,900	3%		Brain & other nervous system	6,230	2%
All Sites	**310,010**	**100%**		**All Sites**	**275,710**	**100%**

Figure 2.2: Ten leading cancer types along with estimated new cancer cases and death by sex, United States, 2014. * Estimates are rounded to the nearest 10 and excluded basal cell and squamous cell skin cancers and in situ carcinoma except urinary bladder. [Siegel et al. Cancer statistics, 2014. CA: *A Cancer Journal for Clinicians*. 2014, 64: 9-29].

2.5 Breast Cancer – An overview

Breast cancer is the most common malignancy in the women worldwide, and the second leading cause of cancer death [Jemal et al., 2014]. Breast cancer arises in the breast tissue that is made up of glands for milk production, called lobules, and the ducts that connect the lobules to the nipple. The remainder of the breast is made up of fatty, connective, and lymphatic tissues. One in nine women in the UK and USA will develop the disease in their lifetimes. It is more common in Western countries, and many factors have been implicated in its etiopathogenesis [Weinberg et al., 2005]. These include age, genetics, family history, diet, alcohol, obesity and physical inactivity. Others are endocrine factors (both endogenous and exogenous) mammographic density and previous benign disease [Dumitrescu and Cotarla, 2005]. Latest statistics estimated almost 232,670 new cases of the invasive breast cancer occurring among women during 2011 and about 2,360 new cases in men. For the year 2014, almost 40,000 deaths due to breast cancer are expected along with 232,670 new cases.

2.5.1 Breast cancer development and types

Around 95% of the breast cancers are epithelial in origin and hence are termed as carcinomas. They can be categorized into following two major types:

2.5.1.1 Non-invasive

These types of breast cancer are predominantly localized to the ducts or the lobules. They are further characterized based on the location.

Ductal carcinoma in situ (DCIS) is a spectrum of abnormal breast changes that initiates in the cells lining the breast ducts. It is considered a noninvasive form of breast cancer since the abnormal cells are confined to the duct where they originated with no evidence of invasion through the basement membrane [Richie and Swanson, 2003]. It is the most common type of in situ breast cancer that accounts for about 83% of in situ cases diagnosed during 2006-2010. DCIS may or may not progress to invasive cancer; in fact, some of these tumors grow so slowly that even without treatment they would not affect a woman's health. Studies suggest that more than one-third of DCIS cases will progress to invasive cancer if left untreated [Allred DC, 2010]. Thus identifying subtypes of DCIS that are most likely to recur or progress to invasive cancer is an active area of research.

Lobular carcinoma in situ (LCIS, also known as lobular neoplasia) is not a true cancer but an indicator of increased risk for developing invasive cancer. This type of cancer arises and is confined to the milk producing glands or lobules. The proportion of LCIS in benign breast disease is low, ranging between 0.5% and 4%, but the majority of these lesions are multicentric,

suggesting a more widespread process [Visvanathan K, 2011]. LCIS is much less common than DCIS, accounting for about 12% of female in situ breast cancers diagnosed during 2006-2010. Other in situ breast cancers encompass characteristics of both ductal and lobular carcinomas or have unknown origins.

2.5.1.2 Invasive

Majority of breast cancers are invasive, or infiltrating. These types of cancer spread outside the ductal or glandular walls where they originated and grow into surrounding breast tissue. As a result, the cancer cells either remains confined to the breast or metastasize to other parts of the body, such as lymph nodes in the armpit or beyond, to the brain, bones, liver, or lungs hence giving rise to metastatic breast cancer (MBC). The prognosis of invasive breast cancer is strongly influenced by the stage of the disease – that is, the extent or spread of the cancer when it is first diagnosed. Around 80 % of all breast cancer is invasive ductal carcinoma that spreads through the cells of the ducts while 10-14 % is invasive lobular carcinoma that starts spreads through the lobules [Evans et al., 2002].

2.5.2 Molecular classifications of breast cancer

Breast cancer is a heterogeneous group of disease which includes several cell types with distinct biological features and clinical behavior. Hence, classification of breast cancer cannot be limited to those which are based on localization and the extent of the tumor. In addition various research groups have further classified breast cancer in to five major subtypes which includes: - luminal A, luminal B, HER2+/ER–, basal-like and normal breast–like. These classifications are based on molecular basis by making use of different molecular techniques and comprehensive gene profiling analysis [Perou CM, 2000; Hu et al, 2006; Sorlie et al., 2001; Schnitt SJ, 2010].

Luminal A This is the most common type of breast cancer subtypes and accounts for about 40% [Perou and Borresen, 2011]. These types of tumors are ER+ and/or PR+ and HER2-, slow-growing, and are comparatively less aggressive than other subtypes. Luminal A tumors are associated with the most favorable short-term prognosis, in part because expression of hormone receptors is predictive of a favorable response to hormonal therapy; however, long-term survival is similar to or even lower than some other subtypes.

Luminal B About 10% to 20% of breast cancers are luminal B [Perou and Borresen, 2011; Voduc et al., 2010]. Like luminal A tumors, most luminal B tumors are ER+ and/or PR+, but

they are distinguished by either expression of HER2 or high proliferation rates (high numbers of cancer cells actively dividing).

Basal-like Around 10% to 20% of breast cancers are basal-like, and are referred to as "triple negative" since they lack ER, PR, and HER2. These types of tumor are common among African American women, premenopausal women, and those harboring BRCA1gene mutation [Perou and Borresen, 2011]. Women diagnosed with such cancer have a poorer short-term prognosis as compared to other subtypes because there are no targeted therapies for such types of tumors.

HER2 enriched. About 10% of breast cancer subtypes are referred as HER2 since they produce excess HER2 (a growth-promoting protein) and lack expression of hormone receptors (ER- and PR-) [Perou and Borresen, 2011]. As compared to the basal-like these cancers subtypes grow and spread more aggressively than other breast cancers and are related with poorer short-term prognosis compared to ER+ breast cancers [Blow et al., 2010] However, the use of targeted therapies for HER2+ cancers has reversed much of the adverse prognostic impact of HER2 over expression.

2.5.3 Treatment Options

Treatment decision for breast cancer are made by the patient and the physician after consideration of the optimal treatment available for the stage and biological characteristics of the cancer, the patient's age, preferences, and the risks or benefits associated with each treatment protocol. Instead of just one or two, various treatment options are available for breast cancer which could be characterized as follows

2.5.3.1 Local treatment options:

This category of treatment exclusively targets the tumor cells while the remaining parts of the body remain unaffected. It mainly constitutes the following procedures.

Surgery - Surgical treatment of breast cancer involves mastectomy or breast conserving surgery (BCS). In such type of surgery also refereed as partial mastectomy, quadrantectomy and lumpectomy removal of complete breast is avoided and only cancerous tissue plus a border of normal tissue are removed. However in patients with advanced stage of breast cancer, a total mastectomy is done. This involves complete removal of breast with a lymph node biopsy. For a more advanced tumor radical mastectomy is advised that includes removal of breasts along with removal of lymph nodes in the armpits and chest. Surgeries accompanied with

radiotherapy or chemotherapy is the preferred mode of treating breast cancer. Fifty-seven percent of women diagnosed with early stage (I or II) breast cancer have BCS, 36% have mastectomy, 6% have no surgery, and about 1% do not receive any treatment [Siegel et al., 2012] In contrast, among women with late-stage (III or IV) breast cancer, 13% undergo BCS, 60% have mastectomy, 18% have no surgical treatment, and 7% do not receive any treatment [Siegel et al., 2012].

Radiation therapy - Radiation therapy involved use of high-energy beams or particles to kill cancer cells. Radiation therapy is mainly accompanied after surgical removal of tumor to remove residual microscopic cells [Apantaku LM, 2002]. Mastectomy is almost always followed after radiation therapy because it not only reduces the risk of cancer recurrence by about 50% but also reduce the risk of breast cancer death by about 20% [Fisher et al., 2011]. Radiation therapy can be given either internally or externally or in combination depending on cancer type, stage, and location of the tumor, as well as doctor and patient preference.

2.5.3.2 Systemic treatment options

Systemic therapy involves treatment given through bloodstream which affects all the organ of the body and not just the cancer. Systemic therapy includes chemotherapy, hormone therapy, and targeted therapy, all of which work through different mechanisms. Systemic therapy is the preferred choice of treatment for women with metastatic breast cancer since they may not benefit from surgery as the disease have been widespread.

Chemotherapy - Chemotherapy is a type of systemic treatment option mainly recommended for women with an invasive breast cancer. The treatment is usually given through blood steam or administered orally. Alternatively, regional chemotherapy involves administration of drugs directly into the cerebrospinal fluid, an organ, or a body cavity such as the abdomen, which mainly affects cancer cells in those areas. Several therapeutic drug options are available for the treatment through chemotherapy.

Hormone therapy - Hormone therapy involves removal of hormones or blocks their action and thus prevents cancer cells from growing. Estrogen is a key hormone produced by the ovaries that promotes the growth of many breast cancers. Women with hormone receptor (estrogen or progesterone receptors) positive breast cancer can be given hormone therapy to lower estrogen levels or to block the effects of estrogen on the growth of breast cancer cells. For instance, hormone therapy with tamoxifen is often given to patients with early stages or with metastatic breast cancer [Boughey et al., 2008]. Additionally aromatase inhibitor as hormone therapy is

also given to some postmenopausal women who have hormone-dependent breast cancer. Fulvestrant (Faslodex) is another drug (given by injection monthly) that blocks estrogen binding and also reduces the number of estrogen receptors on breast tumors. It is often effective in postmenopausal women who are no longer responsive to tamoxifen. Removal or suppression of the ovaries (primary source of estrogen prior to menopause) may also benefit premenopausal women with hormone-sensitive tumors. In addition the ovarian ablation therapy may also allow some other hormone therapies to work better.

Targeted therapies – Targeted therapies mainly involves targeting a specific downstream protein or a metabolite. HER2 and VEGF protein which play a critical role in tumor progression and chemoresistance are some of the preferred therapeutic targets. Everolimus (an inhibitor of mTOR), bevacizumab (an anti-VEGF-A antibody), sorafenib and sunitinib (multitarget drugs) are some of the drugs which are commonly used for targeted therapies [Mukhai H, 2010]. Furthermore, lapatinib (HER1 and HER2 dual inhibitor), pertuzumab, trastuzumab-DM1 and neratinib constitute promising drugs/ antibodies used for targeting HER2. Besides to these drugs, there are numerous other drugs that are already developed or are in the process of developing which can targets various cancer hallmarks e.g. sustaining proliferative signaling, avoiding immune destruction, activating invasion and metastasis, resisting cell death and so on [Hanahan and Weinberg, 2011]. Figure 2.3 summarizes all targeted drug possibilities established or under study.
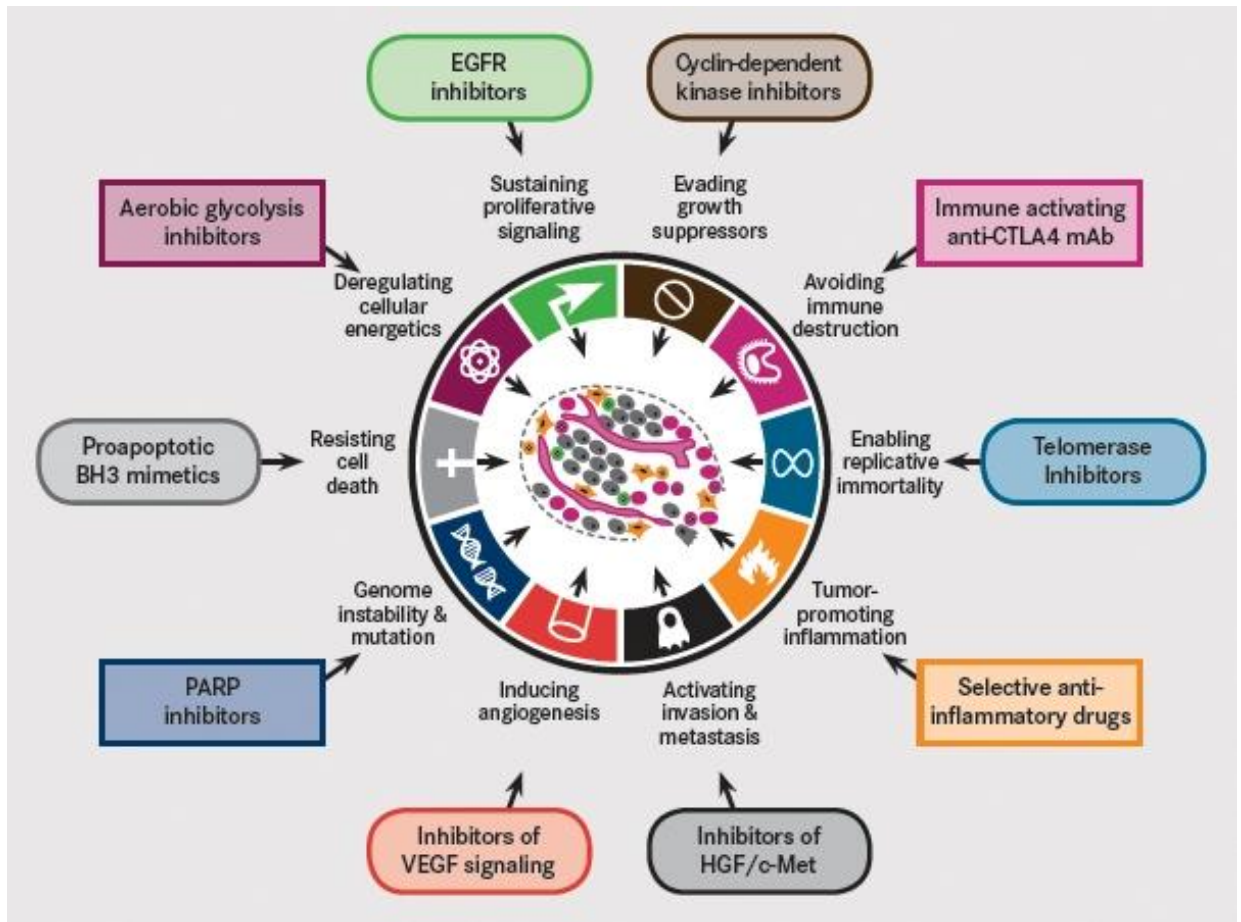
Figure 2.3: Targeting hallmarks of cancer for therapy. Summary of all possible therapeutic target ptoteins/metabolites opening up new therapeutic field for cancer. Some of these targeted therapies are already being used and others are understudy or clinical trials. [Hanahan D, Weinberg RA. Hallmarks of cancer: the next generation. *Cell*. 2011, 144(5):646-74]

2.6 Prostate cancer- An Overview

PCa is the most commonly diagnosed non-cutaneous cancer in males and the second leading cause of cancer-related death for men in United States, [Siegel et al., 2014]. The American Cancer Society estimates that there will be approximately 233,000 men diagnosed with PCa and that 29,480 will die from PCa related causes in 2014 [Siegel et al., 2014]. The disease typically appears in men 65 and older. According to the American Cancer Society, PCa is most common in black men, followed by Caucasians, and least common in Asians.

2.6.1 Aetiology and risk factors

A direct cause of PCa is not well understood and appears to involve a complex interaction between ageing, genetic predisposition, hormonal changes, growth, and environmental features.

Familial - a number of studies have shown the occurrence PCa within certain families suggesting its familial or hereditary nature. Characteristic feature of such type of cancer are (a) when three or more generation of people are being affected by the same disease (b) existence of two men with early onset prostate (age below 55 years) cancer in the same family (c) grouping of three or more man with the disease in nuclear family

Age - Age is the most important predetermining conditions for PCa development. The cancer rarely develops in men aged <50 years, but the chance of its occurrence increases drastically with advancing age. The probability of its occurrence is 1 in 10,000 in man aged <40 years is while it is 1 in 8 for men aged between 60–79 years.

Diet - Diets appears to have a major influence on both the prevention and risk of PCa. Studies have shown that diet rich in vitamins E and D as well as trace elements serves as protecting agent for PCa. On the other hand dietary fat are risk factor for development of PCa. For instance dairy products and red meats consumption are higher in region mostly affected with this disease (e.g. USA).

Testosterone - The growth and function of prostate gland is majorly controlled by testosterone and its main metabolite, dihydrotestosterone. This was confirmed by presence of high testosterone concentration in African-American men with increased cancer incidences as compared to Caucasian man.

Other risk factors - in addition there are numerous other factors like vasectomy, environmental (e.g. exposure to cadmium) and viral factors that are considered risk factors for PCa.

2.6.2 Symptoms and Diagnosis

Prostate tumors' are usually slow growing and symptoms may not occur for many years. In the early stages of PCa, there are often no symptoms. However, due to its location surrounding the urethra, symptoms for the disease most commonly affect urination. PCa symptoms include frequent urination, increased urination during the night, (nocturia), difficulty in maintaining a steady stream of urine, blood in the urine (hematuria) and painful urination (dysuria). It can also affect sexual function, for example difficulty in achieving erection or painful ejaculation. If the cancer is advanced, it can spread to other organs, causing bone pain in the pelvis or ribs. Many of the urinary symptoms also occur in other prostate diseases, such as benign prostate hyperplasia, along with an enlargement of the prostate.

2.6.3 Tumor staging and tumor grading

Once a patient has been diagnosed with a prostate tumor, the cancer must be staged to determine if it has spread beyond the prostate. Staging also provides a better insight into the risk of the disease spreading further so the correct treatment option is selected. The TNM stage was developed by the American Joint Committee on Cancer/International Union Against Cancer (AJCC/UICC) [Wallace et al., 1975]. It is used to evaluate the extent of the primary tumor (T), the affected regional lymph nodes (N) and if it has spread or metastasized (M). There are four stages; in stage I only a small part of the prostate is cancerous, most of the cells are normal and the gland feels normal. In stage II, a lump can be felt in the prostate to the examining finger and a larger part of the prostate is affected. In stage III, the tumor has spread beyond the prostate and in stage IV; it has spread to lymph nodes or nearby organs.

Tumors are graded to allow better predictions for prognosis. The Gleason Grading System is the most commonly used system, where cancers are scored according to their appearance under a microscope. During biopsy, a sample of the prostate tissue is obtained and prepared on microscope slides. Two grade scores are assigned for the two most common tumor patterns, and these scores added together for a final Gleason sum. Gleason scores range from 1 to 5, where 5 has the poorest prognosis and Gleason sums range from 2 to 10. For the primary grade, pathologists identify which pattern corresponds with at least 50% of the tumor and the secondary grade represents the minority of the tumor. The prognosis for PCa can be variable. More aggressive tumors, with Gleason sum 8, 9 or 10, can lead to death in a short space of time, however lower grades, with Gleason sum of 6 or lower, may not see any clinical consequences [Gjertson and Albertsen, 1995].

2.6.4 Treatment options

2.6.4.1 Localized prostate cancer

Watchful waiting/active surveillance - This involves the wait and watch situation and are most appropriate for men aged >70 years and/or those with significant comorbidity. This type of treatment is mostly preferred when the cancer is of low volume with low gleason score. During such cases careful follow up of patients and monitoring of prostate specific antigen with regular digital rectal examination is important. However if the cancer progresses proper counseling and active treatment should be given.

Radical prostatectomy - in radical prostatectomy the entire prostate gland is removed which reduces the disease recurrence. The procedure involves making a horizontal or vertical incision

on the lower abdomen while taking care not to damage the delicate nerves on either side of the prostate; thus reducing the risk of impotency. The seminal vesicles are removed along with the prostate gland. The urethra is then anastomosed to the base of the bladder. A catheter is left for two weeks while the urethra and bladder heal. Side effects include erectile dysfunction as seen in about 50% of patients, but this can be greatly improved with phosphodiesterase-5 inhibitors. Additionally 2–3% of patients are affected with stress incontinence which can also be improved with pelvic floor exercises, physiotherapy and/or anticholinergics.

External-beam radiotherapy - This therapy is perfect approach for localized and locally advanced disease. Pelvic lymph nodes are included in the treatment field. In this therapy radiation beam are directly focused on the prostate gland. This type of treatments has fewer side effects, but proctitis, rectal bleeding and haematuria can occur. In addition there is also a 1–3% risk of incontinence. External-beam radiotherapy provides a 15-year overall survival just like radical prostatectomy however in this case the cancer cannot be treated by surgery if recurrence occurs.

Brachytherapy - This treatment involves direct deployment of radioactive seeds into the prostate gland. It can be done either as a one-stage or two-stage (two visits to hospital; to be measured and then implanted with the seeds) procedure. Brachytherapy can also be given in combination with external-beam radiotherapy in patients with high risk of recurrence. This treatment is most perfect for patients with lower-risk cancers and with small or medium-sized prostate glands. In one-stage brachytherapy 15–20 needles are inserted into the prostate gland through the perineum under transrectal ultrasound guidance procedure and under general anaesthesia. Recent data from the USA suggest that the outcome of brachytherapy is comparable to that of radical prostatectomy and external-beam radiotherapy.

Cryotherapy - This therapy is similar to brachytherapy, but is less commonly used. In this therapy liquid nitrogen is passed through needles which are inserted into the prostate gland thus, creating an 'ice-ball' which destroys cancer cells. The urethra is protected by a warming urethral catheter. Pain, urinary retention and erectile dysfunction are the associated side effects of this therapy.

2.6.4.2 Locally advanced prostate cancer

Hormonal therapy- This therapy works by preventing the production of testosterone at different levels since testosterone and its metabolite dihydrotestosterone are the important

players governing PCa growth. Hormonal therapy can be used alone or before external-beam radiotherapy

Analogues of luteinizing hormone-releasing hormone- are usually given as a depot injection every three months. They act by over-stimulating luteinizing hormone-releasing hormone receptors in the pituitary gland and, via negative feedback, stop the release of luteinizing hormone from the pituitary gland. The concentration of circulating testosterone is reduced to castration levels. The main side effects are a reduction in sex drive and impotence, which are reversible upon ceasing medication; they can also cause hot flushes. These agents reduce the size of the cancer and slow progression, but do not eradicate the disease.

Anti-androgens- Anti-androgens are chemicals which functions by inhibiting the action of testosterone on the prostate gland. They retard the progression of PCa but do not cure it. Their side effects include breast enlargement, soreness, mild stomach upset and damage to the liver. However they do not have such a profound effect on potency and libido compared to luteinizing hormone-releasing hormone analogues.

2.6.4.3 Metastatic prostate cancer

About 70% of men with metastatic PCa die from their cancer within five years. Progression can be delayed for several years by the treatments discussed below.

Bilateral orchidectomy- this involves surgical removal of both testicles to stop complete testosterone production. However in some case only the cells of the testes are removed while capsule is left intact called subcapsular orchidectomy. The main side effects include hot flushes, loss of libido and impotence. Around 80% of men respond to this treatment, where disease progression is slowed for about 18 months.

Analogues of luteinizing hormone-releasing hormone- the response to this treatment in metastatic cancer is about 80%, and benefits last for 18–36 months. A large rise in circulating testosterone may be seen when the injection is first given, causing bone pain and even spinal cord stenosis; anti-androgens are given to protect against this 'tumor flare'.

Luteinizing hormone-releasing hormone analogues and anti-androgens in combination- confer complete testosterone blockade. It is not clear whether this combination therapy significantly increases the time to progression or overall survival. Combination therapy is probably best suited to younger, relatively fit men with advanced PCa because it may result in a longer period before disease progression.

2.7 Angiogenesis-central hallmark of cancer

There are more than 100 different types of cancer with considerable tumor heterogeneity within each tumor type. However a considerable similarity exists in the pathological traits which collectively drive the tumor growth. Sustained angiogenesis is considered to be one of the hallmarks in most if not all malignancies. Angiogenesis, defined as formation of new blood vessels from pre-existing blood vessel is one of the most critical steps in hematogenous metastasis since it provides the escape route for the tumor cells to a distant organ from a confined primary tumor. This complex multistep process involves a series of events that leads to neovascularisation (a) Angiogenic stimuli cause increased endothelial cell permeability and cellular proliferation, which continues as the new capillary sprout elongates [Pepper, 2001]. (b) Proteolysis of basement membrane matricellular components promote the invasion of endothelial cells into the stroma of the neighboring tissue [Mignatti and Rifkin, 1996]. This requires cooperative action of both plasminogen activator system and MMPs (c) Migrated endothelial cells trigger lumen formation as the sprout forms a multicellular structure. Then, a new capillary channel is formed. (d) Finally the capillary is stabilized through the construction of basement membrane, adherent junctions, and endothelial cells (Fig. 2.4). In normal physiology, angiogenesis is necessary for repair and healing of tissues.

1. Angiogenic factor (VEGF, FGF) bind to EC receptors

2. Degradation of basement membrane by MMP and uPAR

3. Proliferation and migration of endothelial cell

4. Tube formation, elongation and remodeling

5. Vessel stabilization
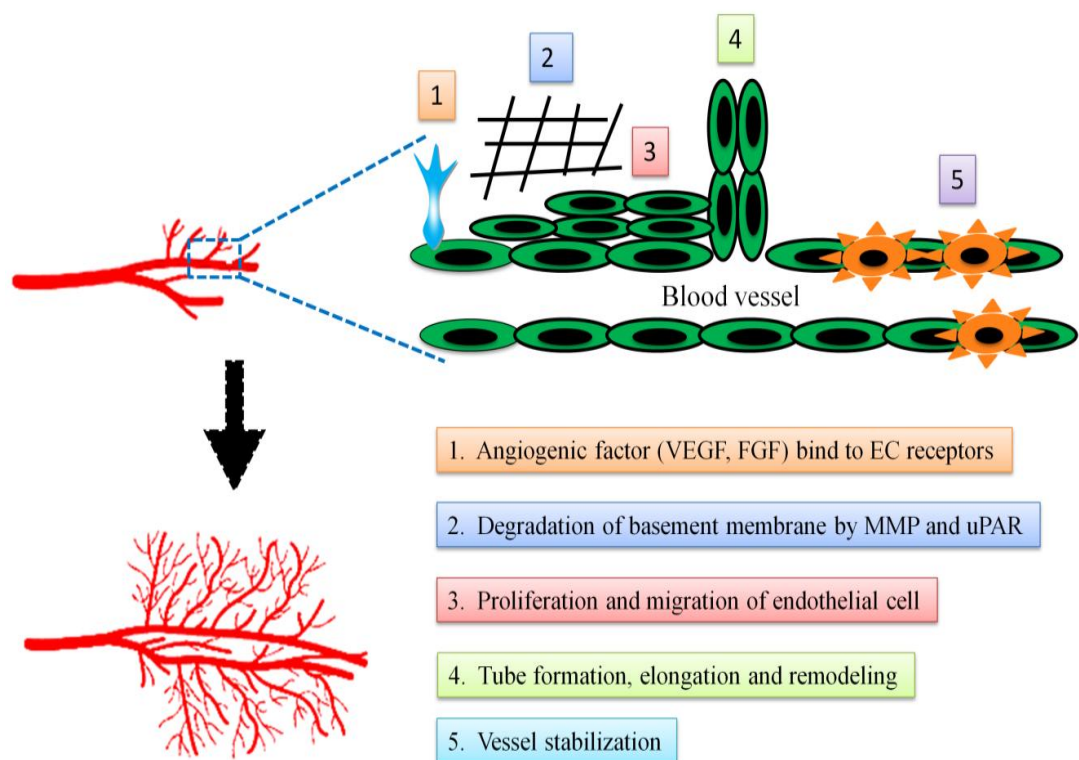
Figure 2.4: Key steps in the process of angiogenesis

25

2.7.1 Types of angiogenesis

Classically, there are three sub-types of angiogenesis

Sprouting angiogenesis - This involves stimulation of endothelial cells to proliferate into the surrounding matrix and form solid sprouts extending towards the angiogenic stimulus leading to the formation of an entirely new vessel [Risau, 1998].

Intussusception – This is also known as splitting angiogenesis. In this type of angiogenesis the capillary wall that extends into lumen splits into two resulting in formation of two vessels [Burri et al., 2004]. Basically it is just the reorganization of existing cells which allows increase in number of capillaries without increasing the number of endothelial cells. This type of angiogenesis is found during embryonic development.

Vasculogenesis - This is the formation of vasculature from endothelial stem cells or angioblasts, which proliferate into de-novo endothelial cells [Patan, 2004].

2.7.2 Angiogenic Factors and Regulation of Angiogenesis

Like most homeostatic process in cellular system angiogenesis is also a complex and highly regulated process which is under tight control of two sets of balancing factors– angiogenic activators and inhibitors [Goh et al., 2007]. These factors are commonly used as a target in strategies to manipulate angiogenesis.

Angiogenic activators: There are more than dozen different proteins which belong to this category. This includes vascular endothelial growth factor (VEGF), TGF-α, TGF-β, bFGF, angiogenin, platelet derived endothelial growth factor, granulocyte colony-stimulating factor, TNF-α, hepatocyte growth factor, epidermal growth factor, placental growth factor, IL-8. VEGF is a strong angiogenic agent in both normal, as well as in neoplastic tissues. Under the influence of certain cytokines and other growth factors, the VEGF family appears in cancerous tissue and the adjacent stroma, and plays an important role in neovascularization [Folkman 1990, 1995a, 1995b]. During last few decades VEGF family and their receptors (VEGFR) have received considerable interest in the field of neoplastic vascularization. Tumor cells feed on the new blood vessels by producing VEGF and then secreting it into the surrounding tissue. When the tumor cells encounter endothelial cells, they bind to receptors on the outer surface of the endothelial cell. The binding of VEGF to its receptor activates relay proteins that transmit a signal into the nucleus of the endothelial cell. The nuclear signal prompts a group of genes to make products needed for new endothelial cell growth. Endothelial cells activated by VEGF

produce MMPs. The MMPs break down the extracellular matrix which fills the spaces between cells and is made of protein and polysaccharides. This matrix permits the migration of endothelial cells. The Endothelial cells begin to divide as they migrate into the surrounding tissues. Soon they organize into hollow tubes that evolve gradually into a mature network of blood vessels with the help of an adhesion factor, such as integrin α or β [Mizejewski 1999; Nelson et al 2000]. Newly formed blood vessels need to stabilize or mature. Angiotensin-1, -2, and their receptor Tie-2 can stabilize and govern vascular growth.

Among the VEGF family members, VEGF-A, VEGF-B, VEGF-C and VEGF-E cause proliferation of blood vessels by binding to their respective receptor, while VEGF-C and VEGF-D are involved in lymphangiogenesis [Neufeld et al 1999; Mandriota et al 2001; Rafii and Skobe 2003].

Inhibitors of angiogenesis: Up-regulation of the activity of angiogenic factors is in itself not enough to initiate blood vessel growth, and the functions of negative regulators or inhibitors of vessel growth may need to be down-regulated. There are many naturally occurring proteins that can inhibit angiogenesis, including angiostatin, endostatin, interferon, platelet factor 4, thorombospondin, prolactin 16 kd fragment, and tissue inhibitor of metalloproteinase-1, -2, and -3. Angiostatin is composed of one or more fragments of plasminogen [Stack et al 1999]. It induces apoptosis in endothelial cells and tumor cells, and inhibits migration and the formation of tubules in endothelial cells [Claesson-Welch et al 1998; Lucas et al 1998]. Endostatin is a 20 kDa C-terminal fragment of type XVIII collagen [O'Reilly et al 1997], a component of the basement membrane. It binds to the $\alpha5\beta1/\alpha v\beta3$ integrin, the major fibronectin receptor in endothelial cells [Rehn et al 2001; Wickstrom et al 2002] and may block endothelial cell focal adhesions [Wickstrom et al 2002]. Endostatin also inhibits the growth factor (eg, bFGF and VEGF-A), and induces proliferation and migration of endothelial cells *in vitro* and *in vivo* [O'Reilly et al 1997; Dhanabal et al 1999; Olsson et al 2004].

2.7.3 Angiogenesis and cancer

Angiogenesis plays a critical role in both development and spread of cancer. Most tumors (less than 2-3 mm3) can persist in situ for months to years without neovascularization. However to spread from the primary site of their origin, they need to be supplied by blood vessels which can bring nutrient and oxygen supply as well as help in removing metabolic waste. In tumors with more than 2 mm3 volume, oxygen and nutrients have difficulty diffusing to the cells in the center of the tumor thus creating a state of cellular hypoxia which marks the onset of tumoral angiogenesis. If there is no vascular support, tumors may become necrotic or

even apoptotic [Holmgren et al 1995; Parangi et al 1996]. Therefore, new blood vessel development (angiogenesis) is an important factor in the tumor progression. Angiogenesis is regulated by a group of protein termed as angiogenic factor/regulators which includes both activator and inhibitor molecules. A change in the local equilibrium between positive and negative angiogenic regulators of the growth of microvessels is involved in the switch to the angiogenic state [Nishida et al., 2006, Yoo and Kwon, 2013] (Fig. 2.5). In the past decades a large number of angiogenic factors have been identified that directly or indirectly induce proliferation and differentiation of endothelial cells. Of the angiogenic inducers, those that are most commonly found in tumors appear to be VEGF and bFGF. Their angiogenic activities are synergistic [22]. VEGF plays a critical role in vasculogenesis and angiogenesis during fetal development. In a knockout mouse model, VEGF or VEGFR inactivation resulted in defects in vasculogenesis in the early stages of development and was embryonic lethal [Ferrara et al., 1996].
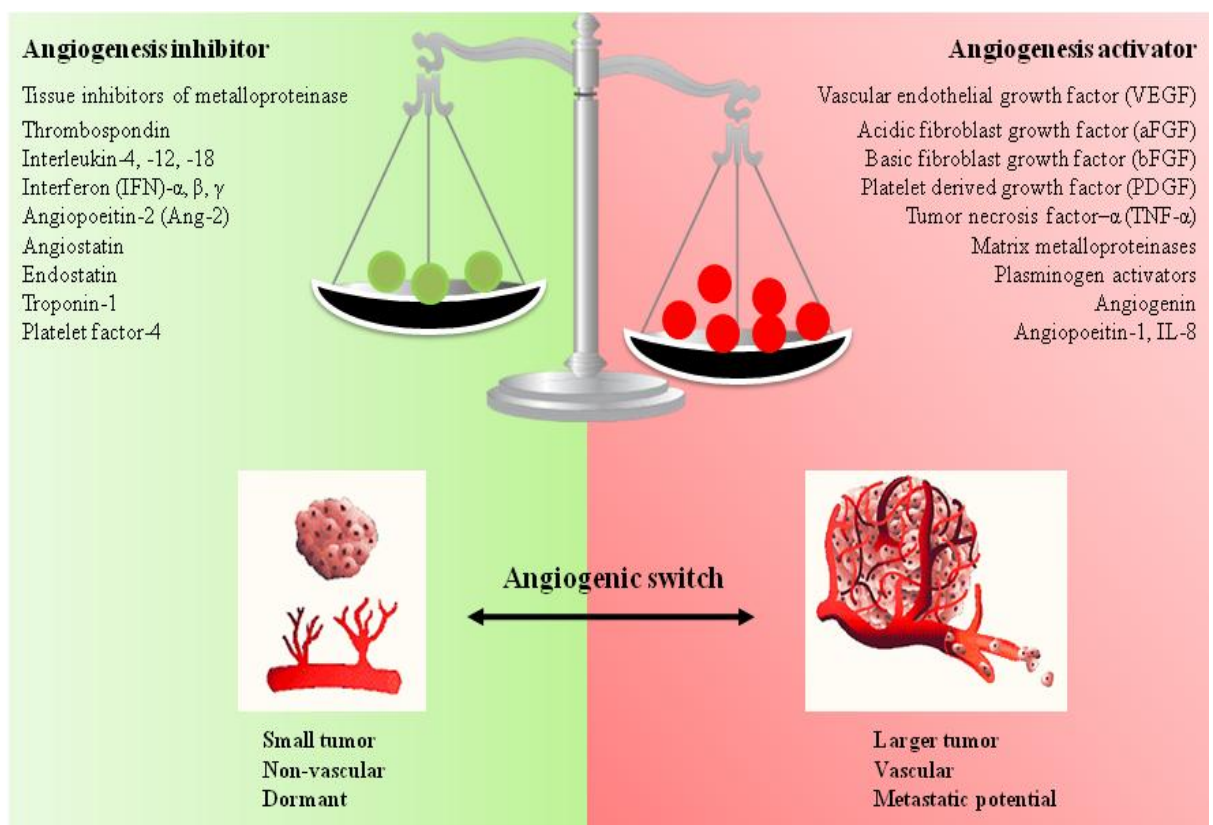
Figure 2.5: Schematic representation of an angiogenic switch- a key process in tumor growth

2.7.4 Antiangiogenic treatment of cancer

Since angiogenesis plays a critical role in the growth and spread of tumor therefore agents that inhibit this process would be of great therapeutic value. With the discovery of endostatin, the concept of anti-angiogenic therapy was launched and popularized by Dr. Folkman [2006]. Since then a plethora of anti-angiogenic drug have been discovered from both natural and synthetic source. These inhibitors can interfere with angiogenesis in various ways. Based on functionality, the anti-angiogenic drugs can be sub-divided into three main groups:

(i) Drugs that inhibit growth of endothelial cells. e.g. Endostatin and combretastatin A4, cause apoptosis of the endothelial cells [Kerbel and Folkman, 2002]. Thalidomide is also a potent inhibitor of endothelial cell growth [D' Amato et al., 1994].

(ii) Drugs that block angiogenesis signaling. e.g. anti-VEGF antibodies (Avastin, FDA approved for colorectal cancer), Interferon-alpha (inhibits the production of bFGF and VEGF) [Kerbel and Folkman, 2002].

(iii) Drugs that block extracellular matrix breakdown. e.g. inhibitors of MMPs [Chan et al., 2008].

2.8 Inflammation - a key event in cancer development

Inflammation (derived from Latin word ''inflammatio,'' to set on fire) is defined as the body's immediate response to either internal or external environmental stimuli and was characterized by the first century Roman physician Cornelius Celsus as that which consists of heat (calor), redness (rubor), pain (dolor), and swelling (tumor). The inflammatory response serves to neutralize the insult acquired by these stimuli to the host. Hallmarks of inflammation are vasodilatation, oedema and leukocyte infiltration. Vasodilation i.e. widening of the blood vessels is the main feature of inflammatory response and is characterized by redness and warmth at the site of injury. Vasodilation increases the blood flow to the infected area thus facilitating the local delivery of soluble mediators and inflammatory cells. The degree to which these occur is normally proportional to the severity of the injury and the extent of infection. The white blood cells or leucocytes have a critical role in inflammation; they extravasate from the capillaries into tissue, and carry on as phagocytes picking up bacteria and cellular debris. They may also aid by walling off an infection and preventing its spread (Fig. 2.6).
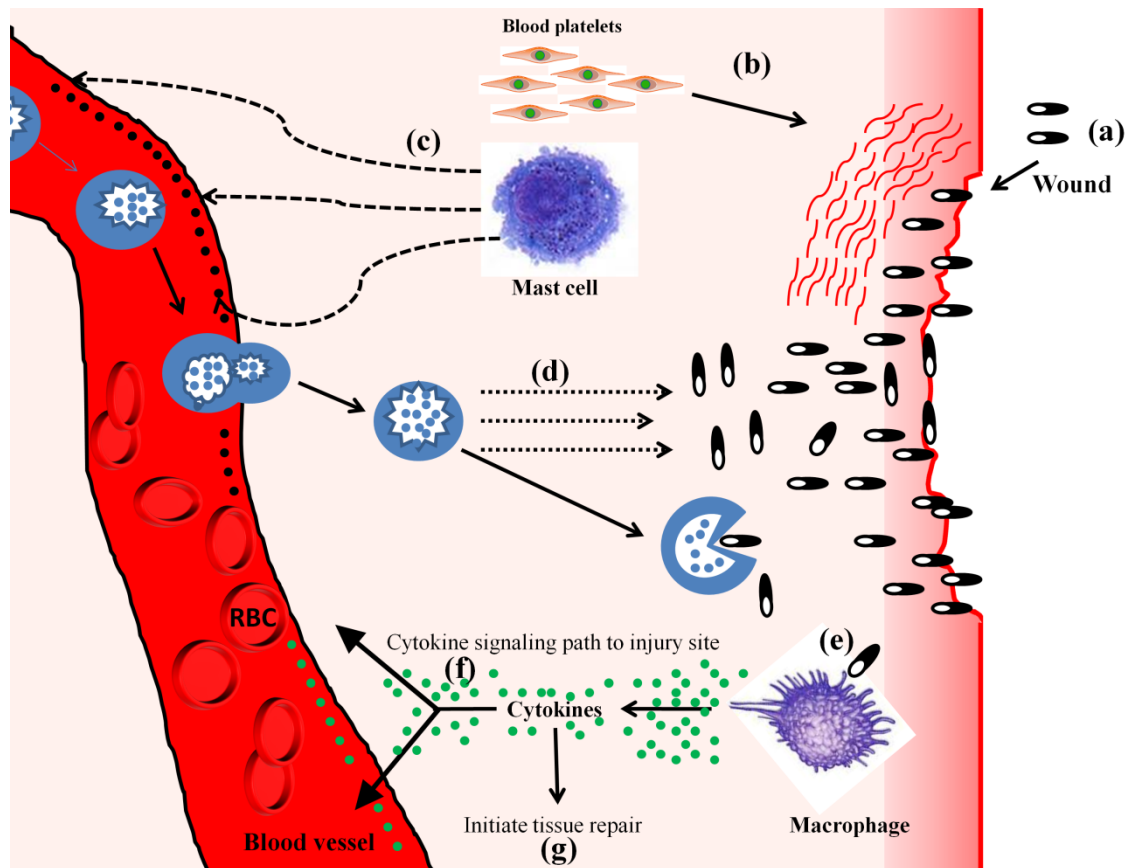
Figure 2.6: Process of inflammation. **(a)** bacteria and other pathogen enters the wound **(b**) platelets from blood release blood-clotting proteins at the wound site **(c)** Mast cell secrete factors that mediates vasodilation and vascular constriction. Delivery of blood, plasma and cells to injured areas increases. **(d)** neutrophils secrete factors that kill and degrade pathogens. **(e)** Macrophage secretes hormones called cytokines that attracts immune system cells to the site and activate cells involved in the tissue repair. **(f)** Inflammatory response continues until the foreign material is eliminated and the wound is repaired.

There are mainly two types of inflammation, acute and chronic. Acute inflammation is an initial stage of inflammation which is mediated through activation of the immune system (innate immunity) and helps the body defend against infections. This type of inflammation lasts for very short period of time and is generally regarded as therapeutic inflammation. However, if the inflammation continues for a long period of time, the second stage of inflammation, i.e., chronic inflammation occurs [Lin and Karin, 2007]. A wide variety of disease such as cancer, diabetes, arthritis, cardiovascular disease, pulmonary diseases, and autoimmune diseases are found to be linked with chronic inflammation. How inflammation is diagnosed and what are its associated biomarkers have not been completely understood. However, the role of different proinflammatory cytokines, chemokines, adhesion molecules and inflammatory enzymes and their association with chronic inflammation are well established (Fig 2.7).

```
STRESS                    Environmental pollutants        Viruses
(chemical, physical, psychological)   (cigarette and diesel)   (HTLV1, HPV, HBV, HCV1, EBV)

Food Factors                                              Bacteria
(Grill, Fried, red meat)                          (eg. Helicobacter pylori)
```

Reactive oxygen species
Tumor necrosis factor-α
Interleukins-1
Interleukins-6
Interleukins-8
Interleukins-18
Nuclear factor-kB
Hypoxia-inducible factor
Cycloxygenase-2
5-Lipoxygenase
Inducible nitric oxide synthase
Matrix metalloproteinase-9
Chemokines

Acute Inflammation
•Innate Immunity
•Humoral Immunity
•Immune surveillance

Therapeutic Inflammation

Chronic Inflammation
•Tumor cell survival
•Tumor cell proliferation
•Tumor cell invasion
•Tumor angiogenesis
•Tumor metastasis
•Tumor chemoresistance
•Tumor radioresistance

Pathologic Inflammation

Figure 2.7: Various faces of inflammation and its role in tumorigenesis

2.8.1 Chronic inflammation and cancer

The association between inflammation and cancers, rather than a recent concern, was noticed ~ 150 years ago by german physicist Rudolf Virchow. In the year 1863 Virchow noticed leucocytes in neoplastic tissues and made a connection that cancers tend to occur at sites of chronic inflammation [Balkwill and Mantovani, 2001]. Lately, it was reported that acute inflammation contributed to the regression of cancer [Philip et al., 2004]. However, accumulated epidemiologic studies support that chronic inflammation conditions, caused by genetic mutations, autoimmune diseases, and exposure to environmental factors can increase the risk of cancer. Epidemiological studies have attributed up to 25% of cancer deaths worldwide to chronic inflammation [Balkwill and Mantovani, 2001]. Chronic inflammation associated with microbial infections (Helicobacter pylori), autoimmune diseases (inflammatory bowel disease), inflammatory conditions of unknown origin (prostatitis) and smoking are well documented to increase the risk of certain cancers [Slattery et al., 2009]. Inflammatory diseases are also frequently associated with increased risk of cancers [Hussain et al., 2003; Mantovani et al., 2008; Wu and Zhou, 2010]. The inflammatory states provides a suitable condition to promote cancer progression and accomplish the full malignant phenotype like tumor tissue

remodeling, angiogenesis, metastasis and the suppression of the innate anticancer immune response. Tumor-infiltrating leucocytes as well as cytokine related signaling pathways are critical components in the development of the inflammatory tumor microenvironment. Understanding the roles of each type of cell and signaling pathway involved in cancer initiation and progression is critical to the discovery of biomarkers specifically targeting cancer inflammation [Chechlinska et al., 2010; Demaria et al., 2010; Rao et al., 2010]. Increased cancer risk is attributed to the observation that chronic inflammation can cause genetic damage via production of oxidizing compounds, such as reactive oxygen and nitrogen species. These products can induce the formation and accumulation of mutagenic, toxic, and/or genome-destabilizing DNA lesions [Hussain et al., 2003; Colotta et al., 2009; Federico et al., 2007; Nishikawa M, 2008; Maynard et al., 2009].

2.8.2 Key molecular players linking inflammation to cancer

During chronic inflammation leukocytes and inflammatory cells are activated and recruited to inflammatory sites by signaling network that involves large number of growth factor, cytokines and chemokines. The key molecular players that drive transitions from inflammation to cancer and further development of inflammation associated cancer are described below.

Cytokines - Cytokines are diverse group of secreted or membrane-bound molecules that play an important role in the growth, differentiation, and activation of immune cells [Dranoff, 2004]. Cytokine signaling can assist in tumor progression either by stimulating of cell growth and differentiation or by inhibiting apoptosis of altered cells at the inflammatory site [Hudson et al., 1999; Pollard, 2004]. Cytokines produced through both tumor cells as well as host stromal cells contributes to immune response against tumor. Tumor-derived cytokines, like Fas ligand, VEGF, and transforming growth factor-β, may assist the suppression of immune response to tumors [Smyth et al., 2004]. Additionally, inflammatory cytokines have also been reported to facilitate the spectrum of tumor development [Smyth et al., 2004; Dranoff, 2004; Philip et al., 2004]. For example, there are numerous evidence which suggest that increase in IL-6 level contributes to colon cancers [Becker et al., 2004; Chung and Chang, 2003; Schneider et al., 2000] while the inhibition of its production and signaling suppress colon cancer [Becker et al., 2004]. Numerous studies reports that TNF and chemokines are candidate linking molecules between inflammation and cancer [Balkwill, 2002; Huang et al., 1999; Micheau and Tschopp, 2003]. TNF are mainly produced by activated macrophages and in addition by tumor cells, and thus initiates its signal by binding to membrane-bound homotrimeric receptors TNFRI and

TNFRII [Locksley et al., 2001]. During inflammation, TNF plays an important role in both tissue destruction as well as damage recovery by maintaining the reversibility of microenvironments, stimulating cellular change, and tissue remodeling [Balkwill, 2002]. In addition TNF can also initiate an inflammatory cascade by involving various other inflammatory cytokines, chemokines, growth factors, and recruitment of variety of activated cells at the site of tissue damage [Balkwill, 2002]. TNF can perform both anticancer and procancer actions due to diverse modification of TNF receptor complexes triggering opposite pathways [Balkwill, 2002; Micheau and Tschopp, 2003]. High dose of TNF can destruct tumor vasculature through necrosis while TNF is also required for chemical carcinogen induced skin carcinogenesis. TNF can induce DNA damage [Jaiswal et al., 2000], inhibit DNA repair [Jaiswal et al., 2000], and act as a growth factor for tumor cells [Wu et al., 1993] and is also a major inducer of NFκB activation.

Chemokines - Chemokines are family of small cytokines that have pleiotropic biological effects. They play an important role in regulating the recruitment and trafficking of leukocytes to sites of inflammation. In addition they also play several important roles in cancer progression, including angiogenesis, inflammation, cell recruitment, and migration. Member of chemokine family are classified into four types based on the positions of key cysteine residues: C, CC, CXC, and CX3C. Numerous reports suggest the involvement of some chemokines in facilitating tumor invasion and metastasis in various cancer types [Daniel et al., 2003; Wilson and Balkwill, 2002; Ardestani et al., 1999]. Mechanistically, chemokines controls tumor invasion and metastasis by allowing a directional migration of tumor cells to specific distal organ via circulation just as it controls leukocyte migration [Hanahan, 2000]. Moreover they assist tumor cells metastasis of by inducing the expression of matrix metalloproteinases (MMPs) and collagenase, which further degrade the basement membrane [Luca et al., 1997; Inou et al., 2000; Muller et al., 2001; Scotton et al., 2001]. Human breast cancer cells, malignant breast tumors, and metastasis have high expression of chemokine receptors such as CXCR4 and CCR7 [Lespagnard et al., 1999].

Nuclear FactorκB - NFκB is a collective term for inducible dimeric transcription factors composed of members of the Rel family [Karin and Neriah, 2000]. It is predominantly located in the cytoplasm, as inactive NFκB-IκB complex in which IκB inhibits NFκB [Viatour et al., 2005] (Fig. 2.8). Upon receiving external stimuli, such as cytokines, IκB gets phosphorylated followed by ubiquitination, and proteolytic degradation either through canonical IκB kinase (IKK) complex-dependent pathway or through a noncanonical NFκB-inducing kinase pathway

[Karin and Neriah, 2000; Viatour et al., 2005]. Degradation of IκB releases NFκB from the complex which then translocates to the nucleus [Baldwin et al., 1996], and binds in the promoter regions of its target genes [Sweeney et al., 2004]. The optimal NFκB activation requires phosphorylation of NFκB itself. Targets of NFκB transcription factor include genes involved in immunity, inflammation, apoptosis, cell proliferation and genes encoding negative regulators of NFκB [Karin et al., 2002]. Additionally NFκB participates in dendritic cell maturation [Caamano et al, 2002] and lymphocyte development [Li and Verma, 2002; Mora et al., 2001; Hettmann et al., 1999]. NFκB regulates the expression of a wide range of inflammatory molecules like cytokines, adhesion factors and thus acts as a critical mediator of inflammation progress, [Tak and Firestein, 2001; Perkins, 2000; Dasgupta et al., 2010]. Furthermore, NFκB activates the expression of growth factor genes, proto-oncogene c-Myc, and cell cycle regulator cyclinD1 and thus contributes to tumor development [Karin et al., 2002; Guttridge et al., 1999; Hinz et al., 1999]. An inflammatory stimulus activates NFκB and its constitutive activation is found in cancer [Karin et al., 2002]; As a result, NFκB is considered as a critical promoter facilitating the development from inflammation in to cancer [Karin et al., 2002]. NFκB is considered as a promising link between inflammation and cancer because NFκB is association with induction of proinflammatory cytokines (IL-6 and TNF-α), chemokines (IL-8), adhesion molecules, COX-2, iNOS and MMPs [Li and Verma, 2002]. Adhesion molecules, such as E-selectin, vascular cell adhesion molecule-1, and intercellular adhesion molecule-1, are responsible for the requirement of NFκB in leukocyte adhesion and migration, which are required for both inflammation and the inflammatory microenvironment of cancer [Chen et al., 1995]. In addition NFκB contributes to genomic instability either by promoting the production of reactive oxygen species which cause mutations [Karin et al., 2002]; or by using its antiapoptotic activity to prevents mutated precancerous cells from being eliminated [Karin et al., 2002].
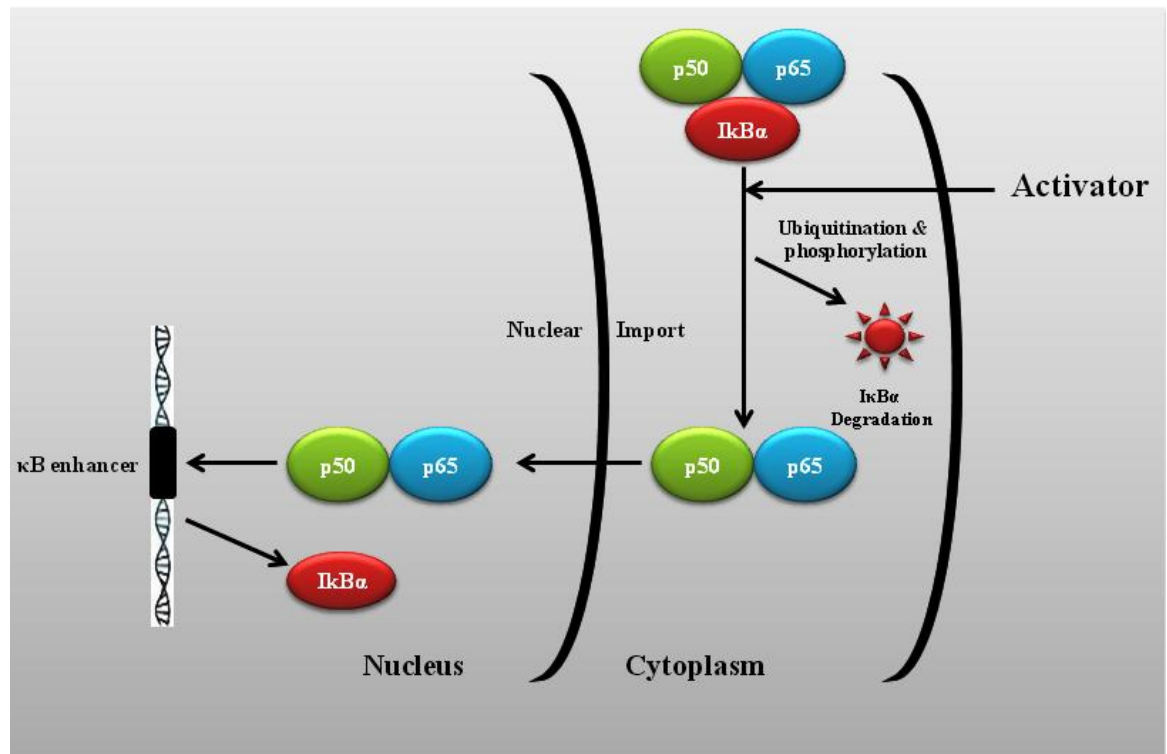
Figure 2.8: NFκB activation pathway**.**

Cyclooxygenase-2 - COX is a rate-limiting enzyme which converts arachiodonic acids to prostaglandins such as PGE2. Two isoforms of COX, which are namely COX-1 and COX-2, have been characterized. A third COX isoform produced as an alternate splice variant of COX-1 has recently been identified as COX-3 (or COX-1b) [Aid and Bosetti, 2011]. COX-1 is expressed constitutively in many types of cells and maintains normal physiological functions (Fig. 2.9). In contrast, COX-2 is an inducible enzyme, which is up-regulated by pro-inflammatory stimuli, including mitogens, cytokines, and bacterial lipopolysaccharide (LPS) in response to infection or inflammatory diseases [Dinarello, 2010]. Evidences from numerous studies indicated that COX-2 is primarily associated with inflammatory disease and is induced in various premalignant and malignant tissues, suggesting that COX-2 plays an important role in inflammation and tumorigenesis [Dinarello, 2010; de Soza Pereira, 2009]. Thus, developing drugs which inhibit the COX-2 expression is considered to be a promising approach to protect against inflammation and tumorigenesis. COX-2 is also over expressed in various types of cancer and involved in cellular proliferation, antiapoptotic activity, angiogenesis, and an increase of metastasis [Tsuji et al., 1997; Prescott and Fitzpatrick, 2000; Eberhart et al., 1994; Ristimaki et al., 1997; Hwang et al., 1998; Okami et al., 1999; Hida et al., 1998]. COX-2 is expressed at an intermediate or high level in epithelial cells of invasive breast cancers [Half et al., 2002]. Expression of COX-2 in breast cancer correlates with poor prognosis, and COX-2

enzyme inhibitors reduce breast cancer incidence in humans. COX-2 over expression has been also found in the mammary gland of transgenic mice induced mammary cancer [Kundu et al., 2002].
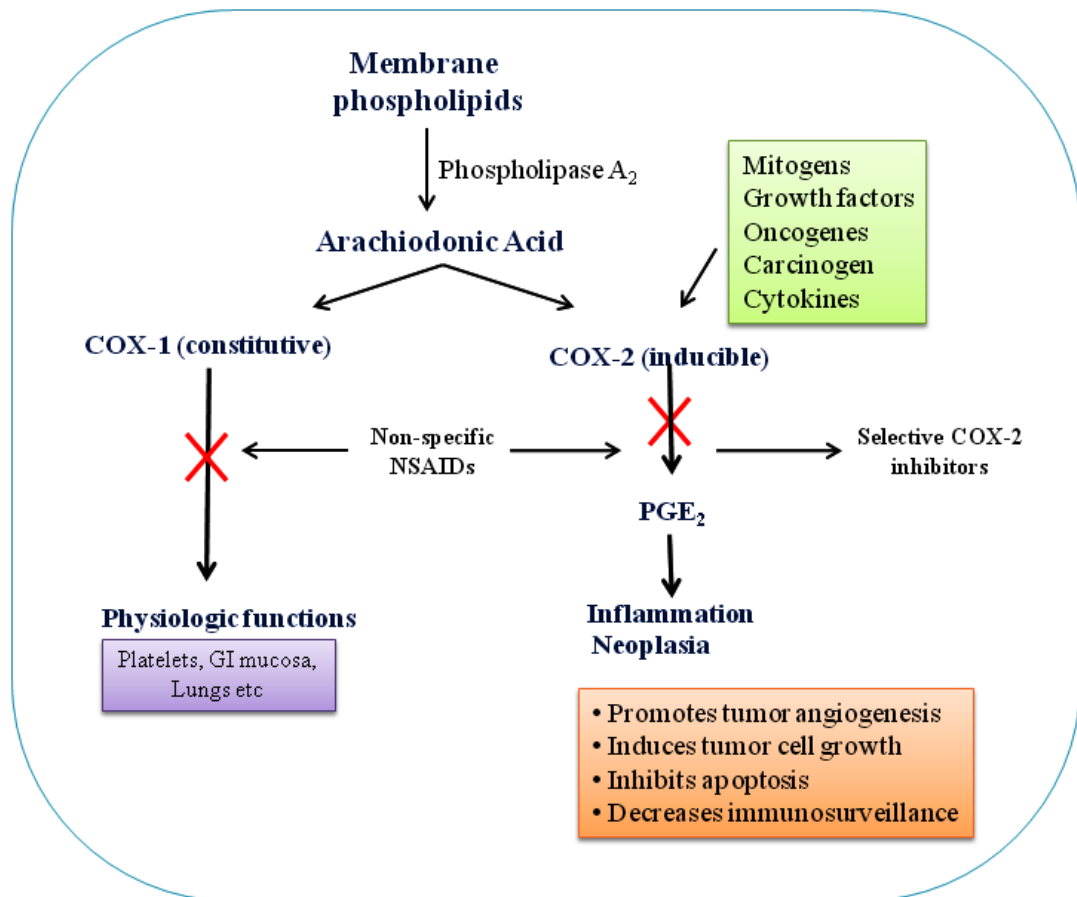
Figure 2.9: The COX-2 signaling pathways.

Inducible nitric oxide (NO) synthase (iNOS) - iNOS is one of three key enzymes generating nitric oxide (NO) from the amino acid l-arginine [Bogdan, 2001a]. Its expression is controlled by various pro-inflammatory mediators such as TNF-α, IL-1β, and IFN-γ [Bogdan, 2001b]. The expression of iNOS is also regulated by various transcription factors including NFκB, signal transducer and activator of transcription, activator protein 1, nuclear factor interleukin-6, 1α interferon-regulatory protein 1 and high-motility group I (Y) protein [Nathan, 1992]. Role of iNOS has been implicated in different stages of cellular changes that lead to malignancy: transformation of normal cells; growth of transformed cells; angiogenesis and metastasis of malignant cells [Geller and Billiar, 1998]. Expression of iNOS has been detected in variety of human malignant tumors, e.g. breast, lung, prostate, bladder, colorectal cancer, and malignant melanoma [Lirk et al., 2002]. Additional studies are required to determine the exact role of

NO/iNOS pathway in tumorigenesis and to establish the use of iNOS inhibitors as chemoprevention agents.

Hypoxia-inducible factor-1 - HIF-1 is a heterodimeric transcriptional complex consisting of an alpha and a beta subunit. The HIF-1α subunit is generally unstable and is proteasomaly degraded during normoxia, while the β subunit is permanently present in nuclei irrespective of the state of oxygenation [Hellwig-Burgel et al., 2005]. Recent literature suggests that even under normoxic conditions a number of peptidic and nonpeptidic mediators of inflammation can activate HIF-1 [Metzen et al., 2004]. This includes cytokines, hormones (insulin, IGF-1, IGF-2) and vasoactive peptides (angiotensin II) [Bilton and Booker, 2004]. Expressions of genes that promote inflammatory reaction (erythropoietin, VEGF, VEGF-R, iNOS, COX-2, glucose transporters, and a number of glycolytic enzymes) are also stimulated by HIF-1α [Hellwig-Burgel et al., 2005]. In contrast to benign tumors and normal tissue accumulation of HIF-1α in the absence of apparent hypoxic stimulation has been demonstrated in a number of different cancers, [Castle et al., 2001]. Thus, HIF-1α is important for conferring a growth and survival advantage to tumor cells, particularly under conditions of metabolic stress.

Oxidative stress - Oxidants also referred as reactive oxygen intermediates, are derivatives of molecular oxygen which includes superoxide, hydroxyl radical, hypochlorous acid, hydrogen peroxide and singlet oxygen. Normally, phagocyte-derived oxidants serve a protective function by killing invading bacteria and parasites. However, they can also have detrimental effects, causing tissue damage and contributing to the development or progression of numerous diseases including cancer [Babior, 2000]. Chronic inflammation is accompanied by increased production of tissue reactive oxygen and nitrogen intermediates. Reactive oxygen species (ROS) can alter signal transduction cascades as well as induce changes in transcription factors such as NFκB and AP-1 that mediate immediate cellular stress responses [Closa and Folch-Puy, 2004]. The proneoplastic activity of reactive oxygen species is mainly due to their ability to cause DNA damage [Marnett, 2000]. Proteins and lipids are also significant targets for oxidative attack, and modification of these molecules can increase the risk of mutagenesis [Schraufstatter et al., 1998]. Agents that either scavenge reactive oxygen intermediates or prevent their formation inhibit induction of DNA damage, mutagenesis, and transformation by inflammatory phagocytes. This forms the basis for the theory that dietary antioxidants can inhibit the development or progression of cancer [Aggarwal et al., 2006].

Overall the above information provides evidence for a strong link between chronic inflammation and cancer. Thus inflammatory biomarkers described here can be used to monitor

the progression of the disease or can be exploited further for development new anti-inflammatory drugs to prevent and treat cancer (Fig. 2.10). These newly discovered drugs can be used in combination with currently available chemotherapy and radiotherapy, which by themselves activate NFκB and mediate resistance. A large number of anti-inflammatory agents including synthetic and those isolated from natural sources have been shown to exhibit chemopreventive activities [Aggarwal et al., 2006a, 2006b], and thus can be used for treatment of cancer. However the lack of toxicity associated with the natural agents combined with their cost provides additional advantages over synthetic chemicals

.
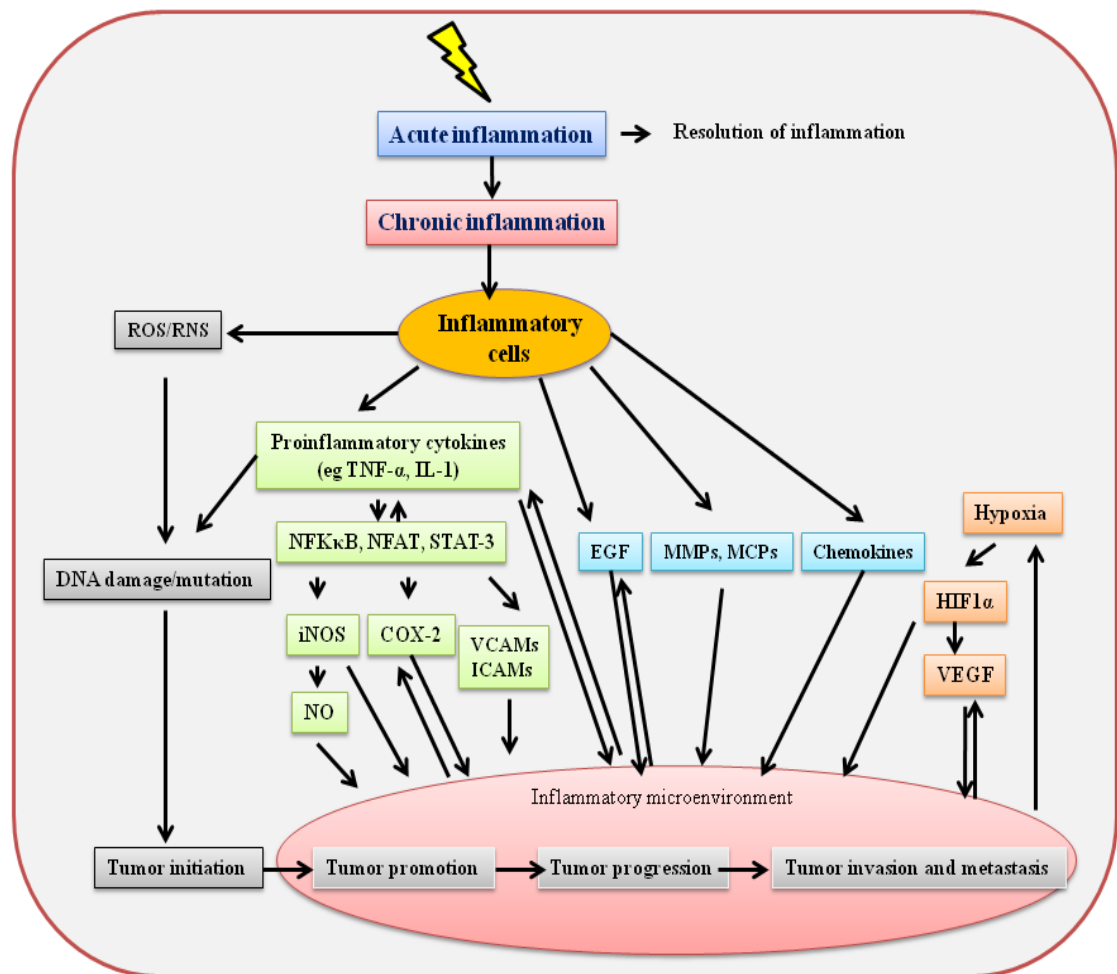
Figure 2.10: Summary of mechanism for the involvement of inflammation in cancer development.

2.9 Dissecting major signaling pathways in development of cancer

The aberrant behavior of cancer reflects upregulation of certain oncogenic signaling pathways that promote proliferation, inhibit apoptosis, and enable the cancer to spread and evoke angiogenesis. Theoretically, it should be feasible to decrease the activity of these pathways or increase the activity of pathways that oppose them with noncytotoxic agents. Since

multiple pathways are dysfunctional in most cancers, and cancers accumulate new oncogenic mutations as they progress, the greatest and most durable therapeutic benefit will likely be achieved with combination regimens that address several targets. Thus, a multifocal signal modulation therapy of cancer is proposed.

2.9.1 Apoptosis pathway

Homeostasis within a living organism is maintained by an intricate balance between cell death and cell survival while its deregulation in any form may leads to cancer. This balance within an individual is maintained by a highly ordered and orchestrated cellular process termed as apoptosis or programmed cell death. Apoptosis is defined as a process by which cell undergoes self destruction (or commit suicide) to control a myriad of physiological and pathological processes like prevention or development of oncogenic transformation. It is a tightly regulated and efficient cell death program which involves multiple factors and understanding its mechanism would provides the basis for developing novel targeted therapies for development of anticancer drugs.

There are two major well studied apoptotic pathways- extrinsic (or death receptor) pathway and intrinsic (or mitochondrial) pathway (Fig. 2.11). Death receptor pathway is triggered through the Fas death receptor, a member of the TNF receptor superfamily while intrinsic pathway as the name implies begins within the cell and leads to the release of cytochrome-c from the mitochondria and activation of the death signal. Both these pathways converge to a final common pathway involving the activation of a cascade of proteases called caspase that cleave regulatory and structural molecules, culminating in the death of the cell. A third less well-known initiation pathway is the intrinsic endoplasmic reticulum pathway [O' Brien and Kirby, 2008]. Apoptosis is characterized by a series of morphological and biochemical markers like shrinkage of cell, chromatin condensation, ultrastrutural modification of cytoplasmic organelles, nuclear fragmentation, membrane blebbing and rapid phagocytosis by neighbouring cells [Saraste and Pulkki, 2000]. Although the features of apoptosis are not a synonym to programmed cell death but it is obviously a sequestration of events definitely leading to cell death. Biochemically apoptosis can be distinguished by the activation of proapoptotic family of proteins (Bax, Bak, Bid etc.), activation of the apoptotic enzyme cascade of caspases, mitochondrial membrane potential dissipation resulting in the mitochondrial membrane permeabilization, oligonucleosomal DNA fragmentation and phosphatidyl serine exposure [Saraste and Pulkki, 2000].

Extrinsic pathway

The extrinsic pathway as the name implies initiates through binding of death receptor ligands to the death receptor. Although there are number of death receptor the best known death receptors includes TNFR1 (Tumor Necrosis Factor Receptor 1) related protein called Fas and their ligands, TNF and Fas ligand (FasL) respectively. The death receptor comprises an intracellular death domain which recruits adaptor protein such as TNF receptor associated death domain (TRADD), Fas Associated Death Domain (FADD) and cysteine proteases like caspase 8. The resulting complex formed between ligand-receptor-adaptor proteins is termed as the Death-Inducing Signalling Complex (DISC), which initiates the assembly and activates pro caspase-8. Active caspase-8 then processes downstream effector caspases which subsequently cleave specific substrates resulting in cell death [Rebecca, 2011; Leena et al., 2012].
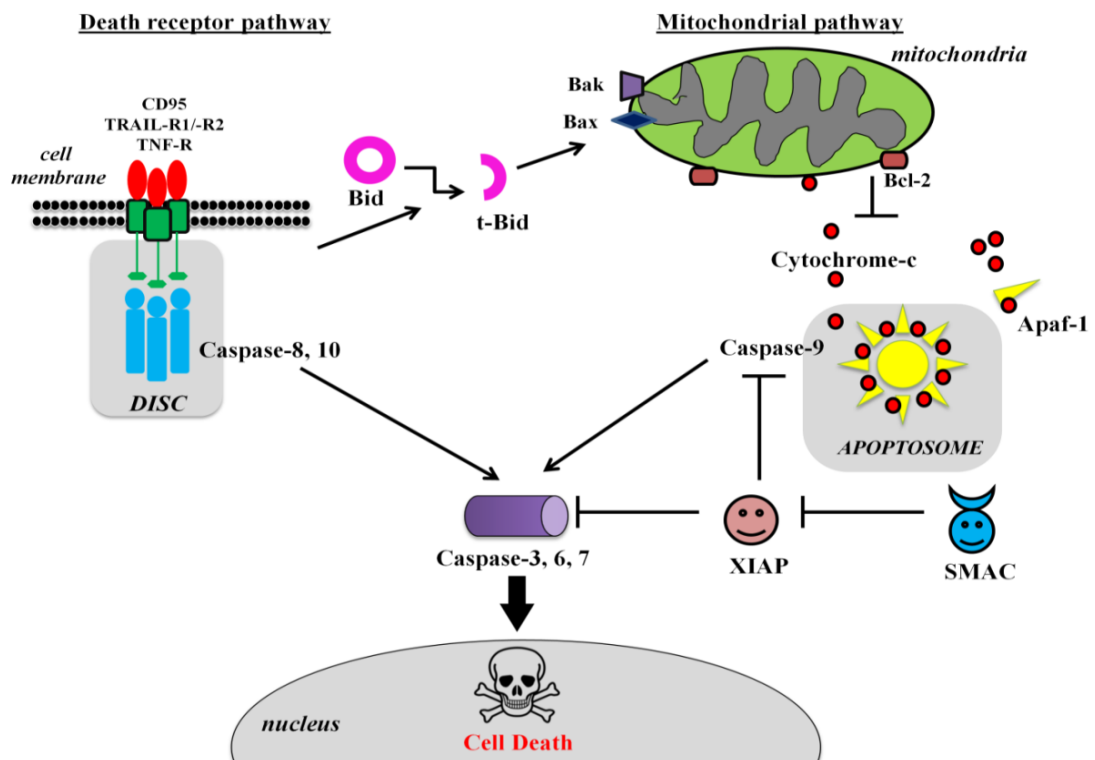
Figure 2.11: Schematic representation of the general apoptotic pathways

Intrinsic pathway

As the name implies this pathways is initiated by stimulus arising within the cell. Internal factors like genetic damage, hypoxia, oxidative stress and high concentration of cytosolic calcium ions trigger the initiation of the mitochondrial pathway resulting in increased mitochondrial permeability and subsequent release of proapoptotic molecules such as

cytochrome-c in the cytoplasm. One of the most important regulators of this pathway is the Bcl-2 family of proteins which includes both proapoptic (Bax, Bak, Bad, Bcl-Xs, Bid, Bik, Bim, and Hrk) and antiapoptotic (Bcl-2, Bcl-XL, Bcl-W, Bfl-1, and Mcl-1) members [Reed, 1994; Leena et al., 2012; Jana et al., 2004]. While the proapoptotic Bcl-2 members acts as activators the antiapoptotic members functions as inhibitor by preventing the release of cytochrome-c. In response to apoptotic stimuli, the outer mitochondrial membrane becomes permeable, leading to the release of cytochrome c. Cytochrome c, once released in the cytosol, interacts with Apaf-1, leading to the activation of caspase-9 proenzymes. Active caspase-9 then activates caspase-3, which subsequently activates the rest of the caspase cascade and leads to apoptosis. [Reed, 1997; Sridaran et al., 1998; Hengartner, 2000; Maity et al., 2010; Leena et al., 2012].

Common pathway

The final pathway which leads to execution of death signal involves the activation of a series of caspases. Caspase-8 and Caspase-9 acts as initiator/upstream caspase for extrinsic pathway, the intrinsic pathway respectively. Both the intrinsic and extrinsic pathways converge to caspase 3 which then cleaves the inhibitor of the caspase-activated deoxyribonuclease, which is responsible for nuclear apoptosis [Reed, 1997; Leena et al., 2012; Hengartner, 2000; Jana et al., 2001]. Additionally, the downstream caspases induce cleavage of protein kinases, cytoskeletal proteins, DNA repair proteins and inhibitory subunits of endonucleases family. They also have an effect on the cytoskeleton, cell cycle and signalling pathways, which together contribute to the typical morphological changes in apoptosis [Reed, 1997; Leena et al., 2012; Hengartner, 2000].

Regulator of apoptosis

The extrinsic and intrinsic apoptotic pathways are regulated by different proteins (p53, NFκB) and pathways (PI3K and ubiquitin proteosome pathway) (Fig. 2.12). P53 protein functions as transcription factor and controls various downstream genes involved in DNA repair, cell cycle arrest and apoptosis. This protein is mutated in a large number of cancers including breast and prostate. Upon DNA damage, p53 arrest the cell at a checkpoint until the damage is repaired. However if the damage is irreversible, apoptosis is triggered. The mechanism by which p53 promotes apoptosis is still not fully understood [Benchimol, 2001; Yu et al., 200]. Similarly NFκB is a nuclear transcription factor which regulates the expression of a different genes involved in the regulation of apoptosis, tumorigenesis and inflammation [Maldonado et al., 1997]. Various stimuli like growth factors, cytokines, lymphokines,

radiation, pharmacologic agents, and stress activates NFκB. Upon activation NFκB provides resistance to apoptotic stimuli by activating many complex proteins including TNF receptor-associated factor, IAP, and X-linked IAP [Lareu et al., 2003]. However NFκB activation may also leads to apoptosis in response to different stimuli which causes activation of few proapoptotic proteins such as interferon-regulated factor-1, c-myc, p53, and caspases such as caspase 1 [Kuhnel et al., 2000].
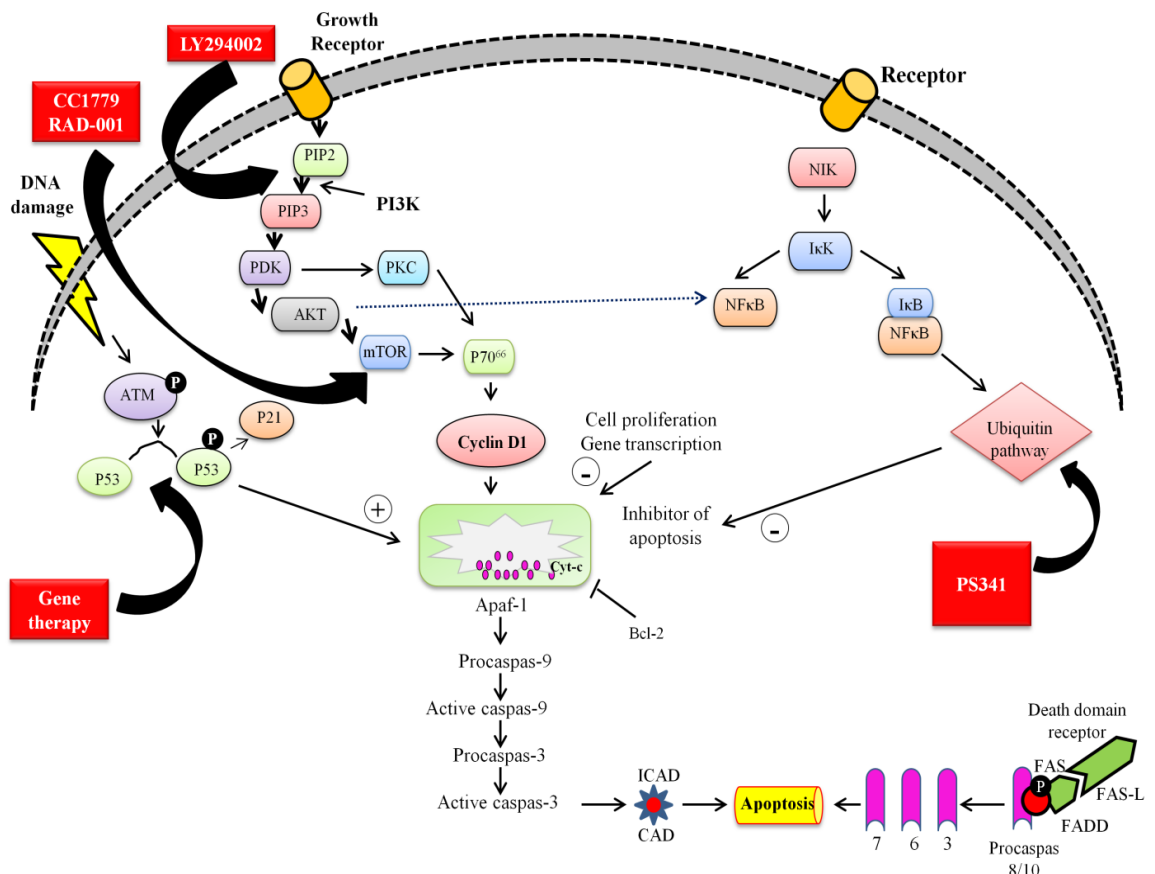
Figure 2.12: Schematic diagram representing apoptosis regulation by p53, NFκB, PI3K, ubiquitin/proteosome system and the anticancer agents (CCI-779, RAD001, PS341, LY294002 and anti-p53 gene therapy) targeting these pathways.

Cellular growth and apoptosis is also regulated by the ubiquitin/proteosome system which contains large proteinase complex required for turnover of most intracellular proteins [Myung et al., 2001] (Fig. 2.12). Many cell cycle regulators (cyclins and cyclin-dependent kinase inhibitors) and transcription factors (p53, NFkB) are regulated by the ubiquitin/proteosome system [Adams et al., 2000; Myung et al., 2001]. Many of the Bcl-2 family members are substrates of the ubiquitin/proteosome [Adams et al., 2000]. Identification of genes that regulates apoptosis or understanding their mode of action has opened up new

avenues for discovery of novel drugs targeting apoptosis. Different pro and anti-apoptotic protein members regulate apoptosis and various strategies have been employed to target these proteins. Among all the apoptosis-based drug targets, strategies that target caspase are the most preferred one. Despite various caspase inhibitors have yielded encouraging results both *in vitro* and *in vivo* yet there are several key issues which remain unanswered that are critical for the success of apoptosis-based therapies. However with the advancement of modern technology involving structural biology and combinatorial chemistry many new drugs have emerged which brings hope that apoptosis-based therapies

2.9.2 Estrogen receptor signaling pathway

Estrogens are a group of structurally related, hormonally active molecules that plays a crucial role in regulating cellular signaling pathways and thus control cell proliferation, differentiation and homeostasis [Poutanen M, 2012]. Additionally they play an important role in development and maintenance of sexual and reproductive function and their effects has also been linked with initiation, development and progression of breast cancer. The most potent estrogen produced in the body is 17β-estradiol (17β-E2). The biological effect of estrogen is mediated through two ERs, ERα and ERβ, which are member of large superfamily of nuclear receptor. The two ERs share a high degree of sequence homology except in their NH_2-terminal domains, and they have similar affinities for E2 and bind the same DNA response elements. The classical mechanism of ER action involves binding of estrogen to its receptors in response to estradiol. Thereafter ER undergoes a conformational change which allows receptor dimerization and recruitment of co activators [Daverey et al., 2009]. Thereafter the whole complex gets translocated inside nucleus and bind to specific response elements known as estrogen response elements (EREs) located in the promoters of target genes (Fig. 2.13). However, there are numerous evidence which suggests the existence of signaling pathways deviating from this classical model. It is now well accepted that ERs can regulate gene expression by a number of distinct mechanisms. In one of the mechanism ERs can regulate its gene expression without directly binding to DNA but modulating the function of other classes of transcription factors through protein-protein interactions within nucleus. Several genes are activated by 17β-estradiol through the interaction of ERs with Fos and Jun proteins at AP-1 binding sites. Such genes include those for ovalbumin, IGF-I, collagenase, and cyclin D1.
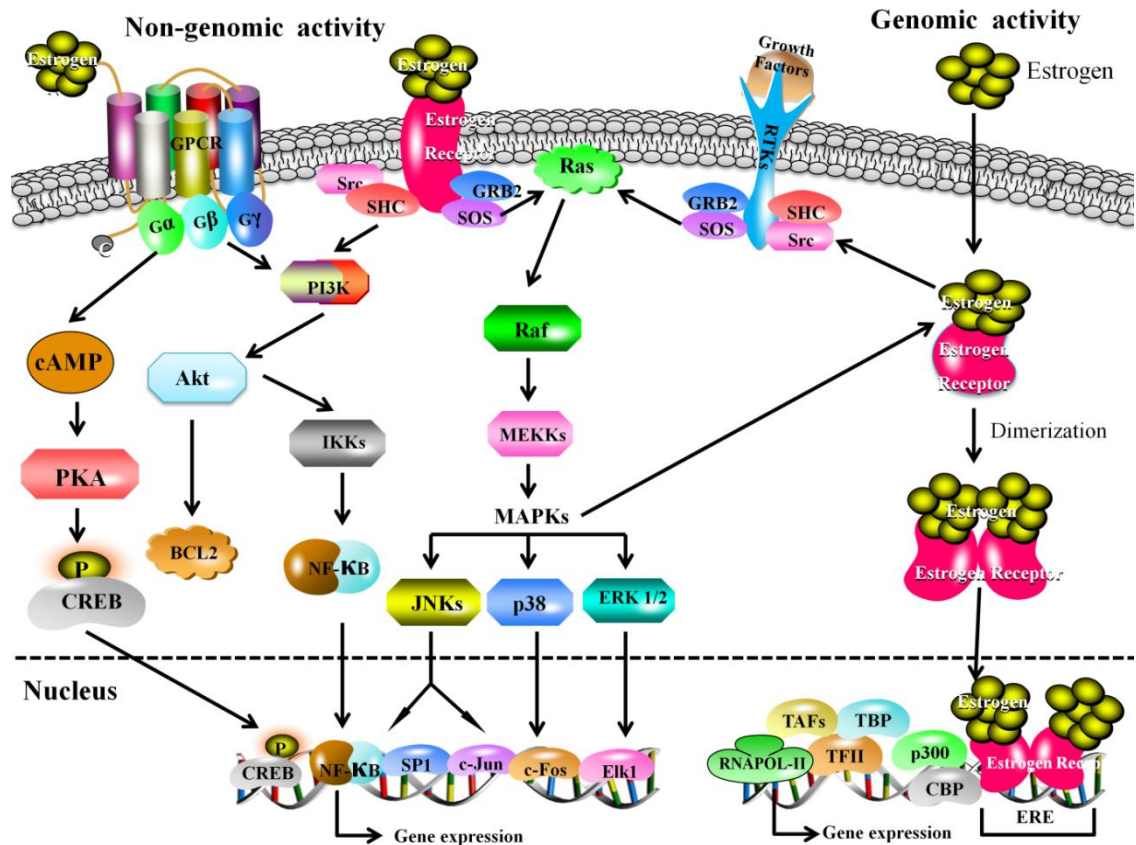
Figure 2.13: Schematic illustration of genomic and non-genomic actions of estrogen receptor (ER)

In addition to the classical genomic action estrogens exert some of their effects independent of ER transcriptional activity. These effects of estrogens are very rapid (i.e. in seconds to minutes) and cannot depend on the activation of RNA and protein synthesis. These actions are known as nongenomic actions and are believed to be mediated through membrane-associated ERs (Fig. 2.13). Various signaling pathways are activated upon E2 binding to ERs. These rapid events may be classified into four main signaling cascade: phospholipase C (PLC)/protein kinase C (PKCs) [Morley et al., 1992; Marino et al., 1998; Marino et al., 2001; Manna et al., 2009], Ras/Raf/MAPK [Watters et al., 1997; Russell et al., 2000; Dos Santos et al., 2002], PI3K/AKT [Bjornstorm and Sjoberg, 2005, Levin, 2005; Park et al., 2012; Marino et al., 2003] and cAMP/ protein kinase A (PKA) [Farhat et al., 1996; Picotto et al., 1996]. These pathways present numerous interactions with several other pathways. The ERα-E2 complex interacts with the IGF-1 receptor, leading to IGF-1 receptor activation and hence to MAPK signaling pathway activation. In addition, the ERα-E2 complex activates the EGF receptor by a mechanism that involves activation of guanine nucleotide exchange proteins (G-proteins), Src, MMPs, leading to an increase in ERK and PI3K/AKT activities [Drigger and Segar, 2002; Zhang et al., 204; Kupzig et al., 2005]. In endothelial cells the Src/PI3K/AKT pathway

mediates rapid E2-dependent activation of eNOS and the release of NO. AKT and PKC could also modulate the MAPK pathway through Raf phosphorylation. It is important to note that activation of signaling pathways by E2 is cell type-specific. Indeed, the effect of E2 on PKC activity has been observed in the preoptic area of female rat brain slices, but not in the hypothalamus or cortex [Ansonoff and Etgen, 1998]. The activation of G-protein/Src/PI3K/MAPK pathway by E2 was evident in late, but not early, differentiated rat preadipocytes [Dos Santos et al., 2002]. The differential requirement of Src/ PI3K or intracellular calcium for MAPK activation is also observed in diverse cell types [Bjornstorm and Sjoberg, 2005; Kupzig and Walker, 2005; Dos Santos et al., 2002]. Different PKC isoforms are rapidly activated by E2 in HepG2 and MCF7 cells. As a whole, these studies indicate that the rapid actions of E2 depend on a number of conditions such as the set of signal transduction molecules and downstream targets present in the target cell, thus the responses are likely to be diverse. All these results point to the concept that ERα is the primary endogenous mediator of rapid E2 actions. Less information is available on the role played by the ERβ-E2 complex to activate rapid non-genomic mechanisms.

2.9.3 Androgen receptor signaling pathway

AR is a member of steroid and nuclear receptor superfamily that plays an important role in the normal growth and development of the prostate gland, and also in prostate carcinogenesis [Kumar et al., 2006; Song et al., 2012]. The AR is expressed to some degree in nearly all primary PCa. AR-mediated signaling is necessary for PCa cell proliferation and an important target for therapeutic drug development [Lee et al., 2003]. In the absence of ligands AR is located predominantly in the cytoplasm where it remains associated with heat shock proteins (HSPs) and other chaperones via cytoskeleton proteins. Binding of the cognate ligands i.e., testosterone or DHT to AR, induces a conformational change in AR thereby resulting in dissociation of AR from HSP and allowing AR to interact with co-regulators such as ARA70 (binds to AR-DBD and AR-LBD), Filamin-A and importin, which bind to the AR nuclear localization signal (NLS). These interactions facilitate nuclear dimerization and import of AR to nucleus. Once inside the nucleus, AR binds to specific recognition sequences known as androgen response elements (AREs) in the promoter and enhancer regions of target genes, recruits coregulators, and forms the transcriptional machinery for AR-regulated gene expression. This AR-signaling pathway, known as the genomic pathway, relies on AR nuclear translocation and AR-DNA binding for cell proliferation. The genomic pathway is thought to

occur over several hours and is characterized by increased expression of specific AR-regulated genes (Fig. 2.14).

In addition to the well characterized genomic pathway numerous studies have reported the existence of a rapid and reversible AR signaling that occurs within minutes and results in regulation of PCa cell proliferation. This AR signaling pathway, known as the non-genomic pathway, requires neither AR nuclear translocation nor AR-DNA binding. Instead, cytoplasmic AR-signaling may function through release of intracellular calcium and activation of protein kinases such as MAPK (ERK), protein kinase A (PKA), AKT and protein kinase C (PKC) (Fig. 2.14). AR can interact directly with, numerous growth factor signaling molecules at the plasma membrane and stimulate the signaling cascades. AR-NTD interacts directly with the p85 regulatory subunit of PI3K, activating the key downstream effector molecule i.e., AKT. This non-genomic action of AR is initiated following androgen treatment. It does this by interacting with the Src homology 3 (SH3) domain of Src by rapidly stimulating Src kinase activity leading to ERK2 activation. Src and the MAPK signaling proteins, Shc and ERK1/2, can be found located in caveolae membrane structures [Okamoto et al., 1998]. Caveolae are known to house many signaling proteins and membrane receptors. This interaction may be necessary prior to non-genomic AR activity originating from caveolae structures. The regions of AR that are responsible for genomic activities are distinct from the ones responsible for these non-genomic cascades [Kousteni et al., 2001]. Differences arise in AR non-genomic signaling when comparing androgen-dependent and androgen-independent cell lines. In androgen-dependent LNCaP cells, activation of the Src/MEK/ERK/CREB pathway relies upon androgen stimulation. In contrast, constitutive activation of the same pathway in androgen-independent LNCaP cells has highlighted an AR-associated redundancy [Unni et al., 2004]. Additionally, re-expression of AR in androgen-independent PC3 PCa cell line interferes with epidermal growth factor (EGF) receptor signaling and internalization and PI3K activation, inducing a less invasive phenotype [Bonaccorsi et al., 2004]. However, in androgen-independent LNCaP cells, AR can localise to caveolin-negative rafts and interact and activate AKT independently of PI3K, which is normally required for downstream activation of AKT [Cinar et al., 2007]. In comparison, androgen-dependent LNCaP cells mediate EGF-induced signaling via AKT, but independently of AR [Zhuang et al., 2002]. Irrespective of the pathway and cell model investigated, AR non-genomic signaling appears to either contribute to or inhibit PCa progression, which needs further validation. Individual cell-signaling fingerprints most likely exist for each cell line or cancer, giving the impression of contrasting AR non-genomic activity when actually individual cancers and cell lines cannot be compared directly with confidence. It

is possible that AR non-genomic activity ultimately serves to influence AR genomic activity and that of other nuclear receptors. AR-activated kinases can phosphorylate AR, regardless of AR-ligand binding status, thus creating an autocrine positive feedback loop. Kinases such as ERK1/2, PI3K and AKT can phosphorylate and activate AR with and without androgen, illustrating the adaptive nature of AR genomic activity in environments with varying levels of androgen.
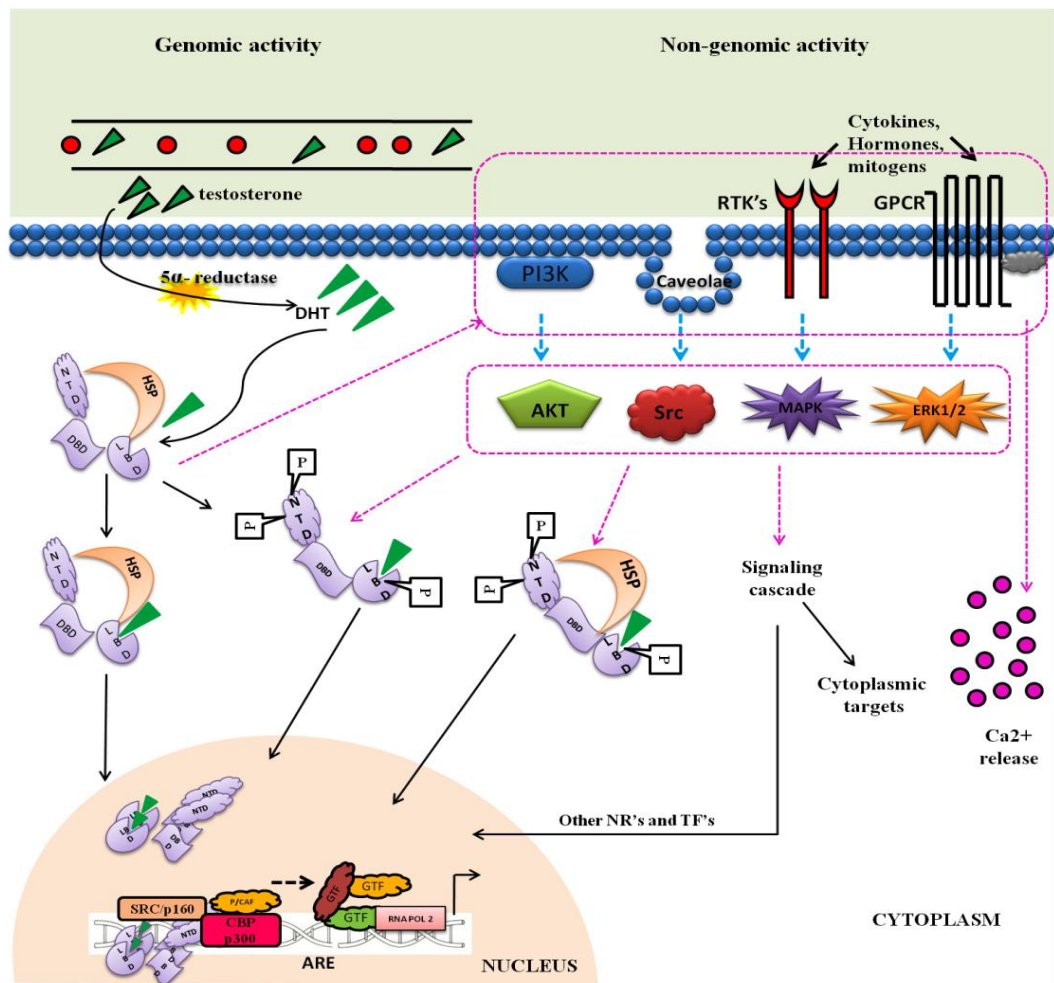
Figure 2.14: Schematic illustration of genomic and non-genomic actions of androgen receptor (AR). AR (purple) is illustrated as a modular protein with each of its domains represented; NTD (N-terminal transactivation domain), DBD (DNA-binding domain), the hinge and the LBD (ligand binding domain). Non-genomic pathway of AR is highlighted in broken lines.

2.9.4 The Map Kinase/ERK Pathway

Growth-promoting signals are relayed to the interior of the cell through a series of different pathways. The RAS-Mitogen Activated Protein Kinase (MAPK) pathway plays an integral part in transducing signals from cytokines and growth factors through Receptor

tyrosine kinases (RTK) to promote cell adhesion, proliferation, migration and survival [Katz et al., 2007] (Fig. 2.15). Central to this signaling cascade is RAS, a small membrane-bound GTPase that shuttles between two conformational states: active GTP-bound and inactive GDP-bound. RAS is activated by Son Of Sevenless (SOS), a guanine exchange factor usually found in the cytoplasm of the cell. Upon receptor signaling SOS shuttles to the cell membrane to catalyze the nucleotide exchange reaction of RAS. Activated GTP-bound RAS activates the serine/threonine kinase RAF that, in turn activates MAPK also known as ERK. ERK1/2 translocate to the nucleus where they activate the Jun/Fos transcription factors. Numerous factors inhibit the activity of this pathway: RKIP, RAF Kinase Inhibitor Protein obstructs phosphorylation of MAPK; RAS and RAB Interactor 1 (RIN1) competes with RAF for binding of GTP-bound RAS; MKP1-3, MAPK phosphatases abolish signal transmission by dephosphorylation of MAPK/ERK. Lastly, the MAPK pathway can also be activated by extracellular matrix molecules and changes in focal adhesion, however, most of these signals are relayed through Focal Adhesion Kinase (FAK) and PI3K.
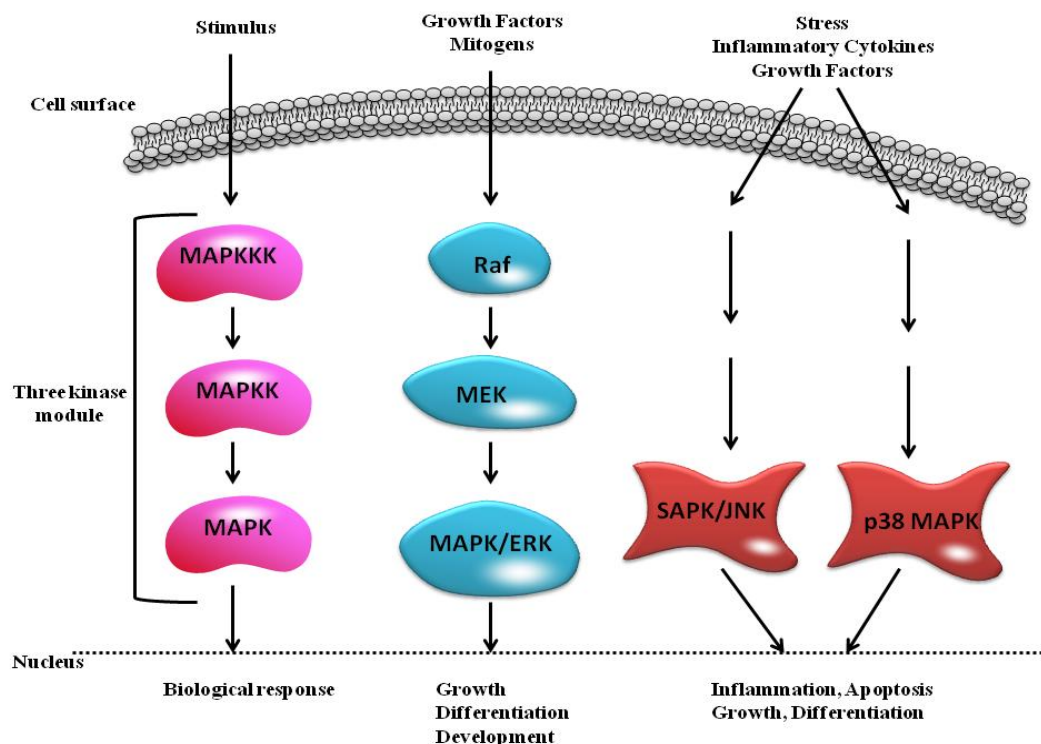
Figure 2.15: The mitogen activated protein kinase (MAPK) signaling cascade

Because of its central role in cell proliferation, it is not surprising that the SOS-Ras-Raf-MAPK signaling cascade is deregulated in a broad spectrum of human tumors. Most of these mutations occur in RAS and RAF and result in constitutive pathway activation and the adoption

of a hyperproliferative state. RAS mutations are found in ~45% of colon cancers and ~90% of pancreatic cancers [Katz et al., 2007]. RAF mutations, in turn, are found in roughly two thirds of all melanoma [Sebolt-Lepold et al., 2004]. Consequently this pathway is a formidable target for therapeutic intervention and has received tremendous attention.

2.9.5 PI3K/AKT Pathway

Similar to the MAPK/ERK pathway, the PI3K/AKT pathway responds to a variety of extra- and intracellular signals, relayed through hormonal receptors, transmembrane tyrosine kinase-linked receptors and intracellular factors and regulates cellular proliferation, cell death and cytoskeletal rearrangements [Hennessy et al., 2005]. Class-I PI3K are heterodimers, consisting of an adaptor / regulatory p85 subunit and a p110 catalytic kinase subunit. Activation of class-I PI3K occurs through interaction of the p85 subunit with various activating proteins such as protein kinase C, RHO, RAC, mutated RAS, SRC and leads to activation of the p110 catalytic subunit. Upon activation PI3K phosphorylates phosphatidylinositol-4,5-biphosphate (PIP2) at a 3-position, converting it to phosphatidylinositol-3,4,5-biphosphate (PIP3). PI3K/AKT signaling is counteracted by the Phosphatase and TENsin homologue (PTEN) (and SHIP1, SHIP2), which dephosphorylates PIP3–PIP2. One major downstream mediator of PIP3 is AKT. The AKT protein kinase binds PIP3 with high affinity through its Pleckstrin Homology (PH) domain. Activated AKT is localized at the cell membrane where it interacts with and is phosphorylated by Phophoinositide Kinase 1 (PDK1). As discussed below, activated AKT regulates a number of downstream targets, implicated in a variety of human diseases (Fig. 2.16).

Activated PI3K/AKT signaling has a variety of downstream effectors that mediate cellular energy metabolism, cell proliferation and survival. There is significant cross-talk between the PI3K/AKT and other pathways, such as the apoptosis pathways and the NFκB and possibly the Wnt pathway. With respect to apoptosis, activated AKT directly and indirectly (through PAK1 and c-RAF) inhibits apoptosis mediators BAD and pro-caspase 9 [Vivanco et al., 2002]. On a transcriptional level, AKT upregulates transcription of the NFκB inhibitor IκB. Furthermore, PDK1 phosphorylates a negative regulator of NFκB signaling, IKKβ and targets it for degradation. AKT directly activates MDM2, a negative regulator of p53. p53 is responsible for DNA damage surveillance and in response, initiates cell cycle arrest and DNA repair. Interestingly, AKT also inhibits Glycogen Synthase Kinase-3 (GSK-3), a negative regulator of Wnt signaling. Deregulated PI3K/AKT signaling has been observed in various cancers. Mutations in the PI3K/AKT pathway inhibitor and tumor suppressor PTEN has been

found in glioblastomas, lung carcinomas and melanomas whereas AKT overexpression or overactivation has been found in breast, ovarian, thyroid and a variety of other cancers [Vivanco et al., 2002]. In conclusion, the PI3K/AKT pathway is constitutively active in numerous human cancers. Activation of this pathway can promote cell survival and proliferation. However, PI3K/AKT signaling further stimulates proliferation by activation of the NFκB and Wnt signaling pathways.
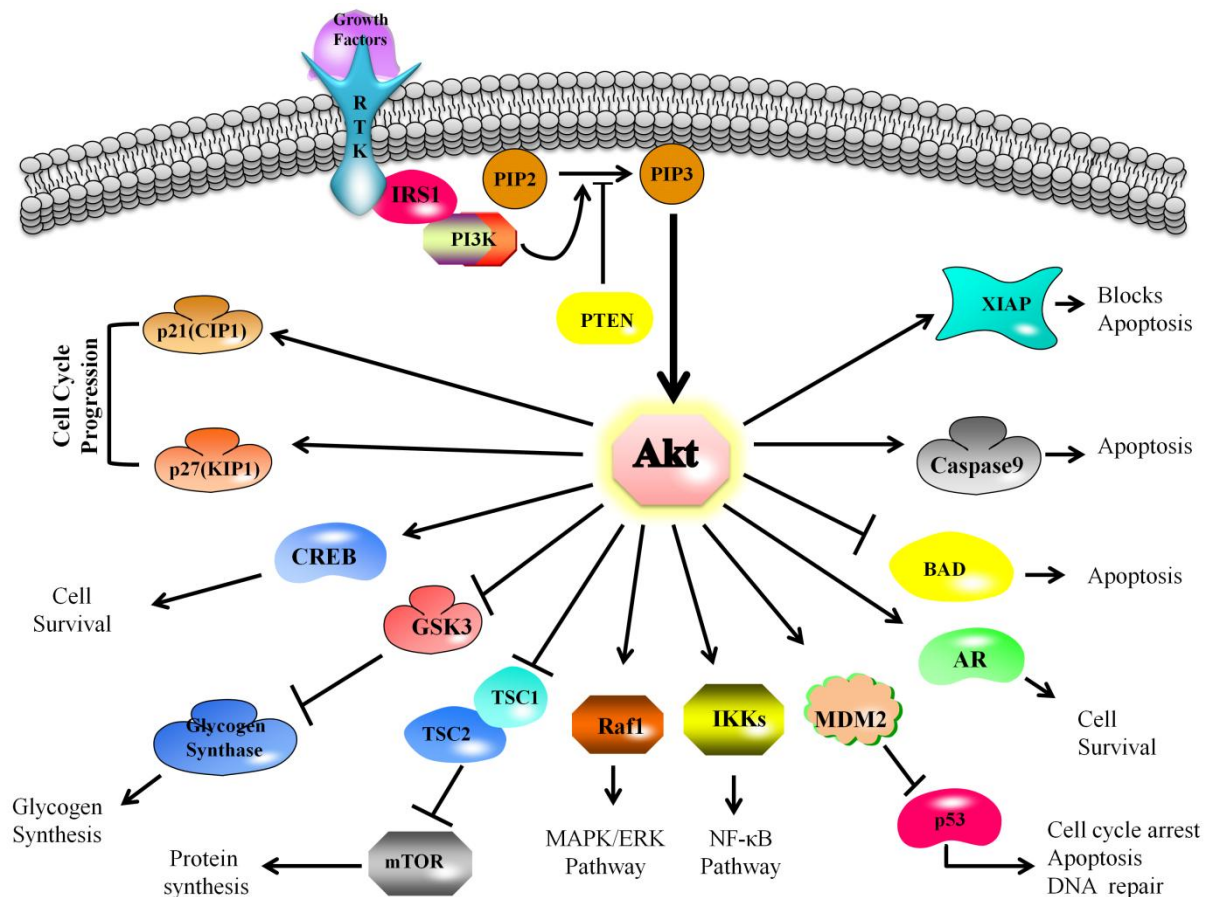
Figure 2.16: Schematic overview of the PI3K/AKT signaling pathway and some of its target molecule

2.9.6 The NFκB Pathway

The NFκB pathway regulates genes involved in key cellular processes such as proliferation, stress response, innate immunity and inflammation [Brivanlou and Darnell, 2002; Courtois and Gilmore, 2006]. In vertebrates, the NFκB transcription factor family consists of p50/p105, p52/p100, c-Rel, RelA and RelB that regulate transcriptional expression of hundreds of target genes. P105 and p100 are proteolytically processed to give rise to p50 and p52, respectively. In contrast c-Rel, RelA and RelB contain a C-terminal transactivation domain and are not processed. c-Rel, RelA, RelB, p50 and p52 can form homo- and heterodimers, shuttle to

the nucleus where they bind DNA regulatory κB sites. In the absence of signaling, NFκB dimers are located in the cytoplasm and inactivated by their interaction with IκB inhibitory proteins. NFκB signaling is activated by a variety of extracellular factors such as the TNF-α, interleukin-1, growth factors, bacterial or viral infections, oxidative stress and pharmaceutical compounds. In response to such stimuli, IκB is rapidly phosphorylated on serine 32 and 36 by the IκB kinase (IKK). Phosphorylated IκB is ubiquitinated by the E3 ubiquitin ligase complex and targeted for degradation by the 26S proteasome. The liberated NFκB dimers can then translocate to the nucleus and activate transcription of target genes (Fig. 2.17).
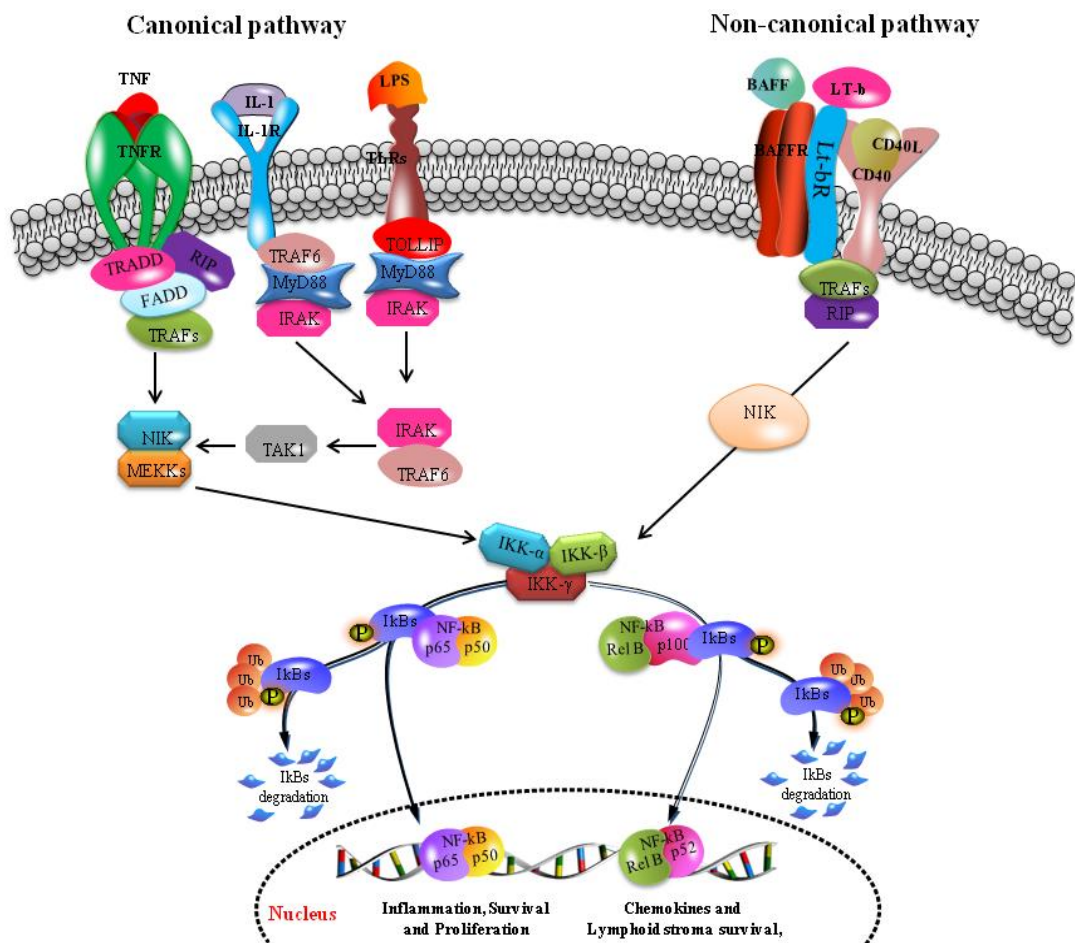
Figure 2.17: Canonical and non-canonical pathway leading to the activation of NFκB

Mutations and miss-regulation of NFκB signaling has been involved in a variety of cancers, for example human B-cell malignancies. The human REL gene, encoding one of the five NFκB transcription factors is amplified in ~50% of Hodgkin's lymphoma, ~10–20% of non-Hodgkin's B-cell lymphomas and ~40% natural killer T-cells lymphomas. It has been

suggested that amplification of the REL gene and overexpression of the protein outcompetes the inhibitory effects of IκB in the cytoplasm, leading to constitutive transcription of NFκB target genes and increased mature B-cell proliferation and survival. Consistent with this model, overexpression of human REL is sufficient to transform and immortalize primary chicken lymphoid cells in culture, whereas diminished levels of REL inhibit B-cell proliferation [Gilmore et al., 2001]. Immunohistochemical analysis of patient-derived lymphoma samples with REL amplifications has confirmed nuclear REL expression in several cases [Barth et al., 2003].

2.9.7 VEGF signaling pathway

De novo formation of blood vessels is an essential factor that governs the growth of human tumors and development of metastases. New blood vessels formation is tightly regulated by specific growth factors which target RTKs. VEGF and its receptor VEGFR-2/KDR/Flk-1 are the key player that governs the endothelial cell-specific factor signaling pathway required for pathological angiogenesis, and tumor neovascularization. Binding of VEGF to VEGFR-2 results in autophosphorylation of the tyrosine residues within the kinase-insert domain and thus creates a binding site for the VEGFR-associated protein either directly through PLC-gamma, VRAP (VEGF Receptor-Associated Protein), and Sck, or by indirect mechanisms, such as Src and PI3K. Binding of PLCγ1 activates protein kinase C, which in turn activates mitogenic signaling via the Ras-Raf1-MEK-ERK pathway (Fig. 2.18). PLC-Gamma catalyzes the hydrolysis of PIP2 (Phosphatidylinositol-4,5-Bisphosphate), creating IP3 (Inositol Trisphosphate) and DAG (Diacylglycerol), which stimulate the release of Ca2+ from internal stores and activate PKC. VEGF-A-induced Ca2+ mobilization is involved in short-term production of NO and prostaglandin resulting in increased vascular permeability and cellular migration. VEGFR-2 also regulates the cell survival signaling by activating PI3K/AKT pathway and its downstream targets such as proapototic proteins BAD, FKHR1 (Forkhead Transcription Factor-1), and Caspase-9, whose phosphorylation inhibits apoptosis. In addition expression of antiapoptotic protein family members such as BCL_2, XIAP (Xenopus Inhibitor of Apoptosis), and Survivin are also induced in response to VEGF. Interaction of VEGF and VEGFR-2 also induces induces cytoskeletal reorganization and cell migration by activation of FAK and Paxillin and recruitment of downstream protein such as Talin and Vinculin (Fig. 2.18).
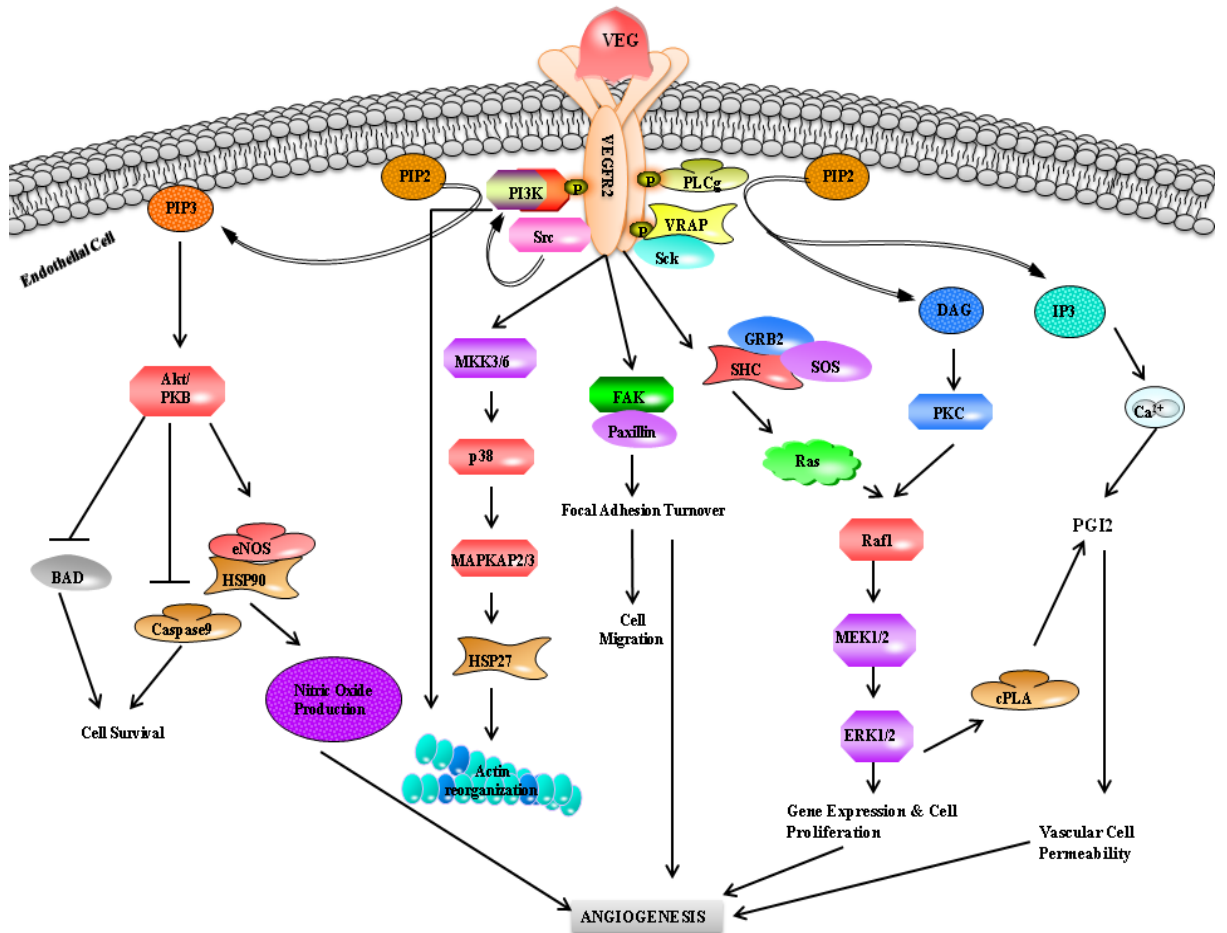
Figure 2.18: Vascular endothelial growth factor signaling pathway

2.9.8 RANKL signaling pathway

Inflammation and tumor are the primary cause of osteolysis leading to bone pain and debilitating skeletal instability. This skeletal integrity mainly relies on proper homeostasis between bone cells ie bone formation by osteoblasts and bone resorption by osteoclasts [Wada et al., 2006]. Osteoclasts are principal bone regulating cells of the body while receptor activator of NF-kB ligand (RANKL) is the cytokines required for osteoclast differentiation. The RANKL/RANK signaling pathway plays an important role in osteoclast differentiation due to its critical role in majority of osteolytic response. RANKL/RANK signaling cascade is initiated by the assembly of signal transduction complex at the cytoplasmic tail of RANK. The binding of RANKL to its receptor RANK leads to recruitment of TNF receptor associated factor 6 (TRAF6) to the cytoplasmic domain of RANK [Takayanagi et al., 2002; Wada et al., 2006]. Subsequently, several downstream targets of TRAF-6 include transcription factors such as NFkB, AP-1, and nuclear factor of activated T cells (NFAT), as well as the MAPK such as p38

MAP kinases, c-Jun N-terminal kinases (JNK), and ERK are recruited to the complex and undergo activation (Fig. 2.19). The downstream target of TRAF6, the PI3K/AKT pathway is also activated by RANKL. Moreover, TRAF6 is also involved in the activation of transcription factor, NFATc1, which plays an important role in osteoclastogenesis. RANKL-induced recruitment of TRAF6 mobilizes intracellular calcium, which results in the activation of calcineurin. Activated calcineurin in turn dephosphorylates and activates NFAT1, resulting in its translocation into nuclei to form a ternary complex with cFos and c-Jun at the promoter for NFATc1 gene to stimulate the expression of NFATc1. NFATc1 can directly regulate a number of osteoclast-related marker genes, including tartrate resistant acid phosphatase (TRAP), calcitonin receptor (CTR), MMP-9, cathepsin K, and NFATc1 itself (Fig. 2.19).
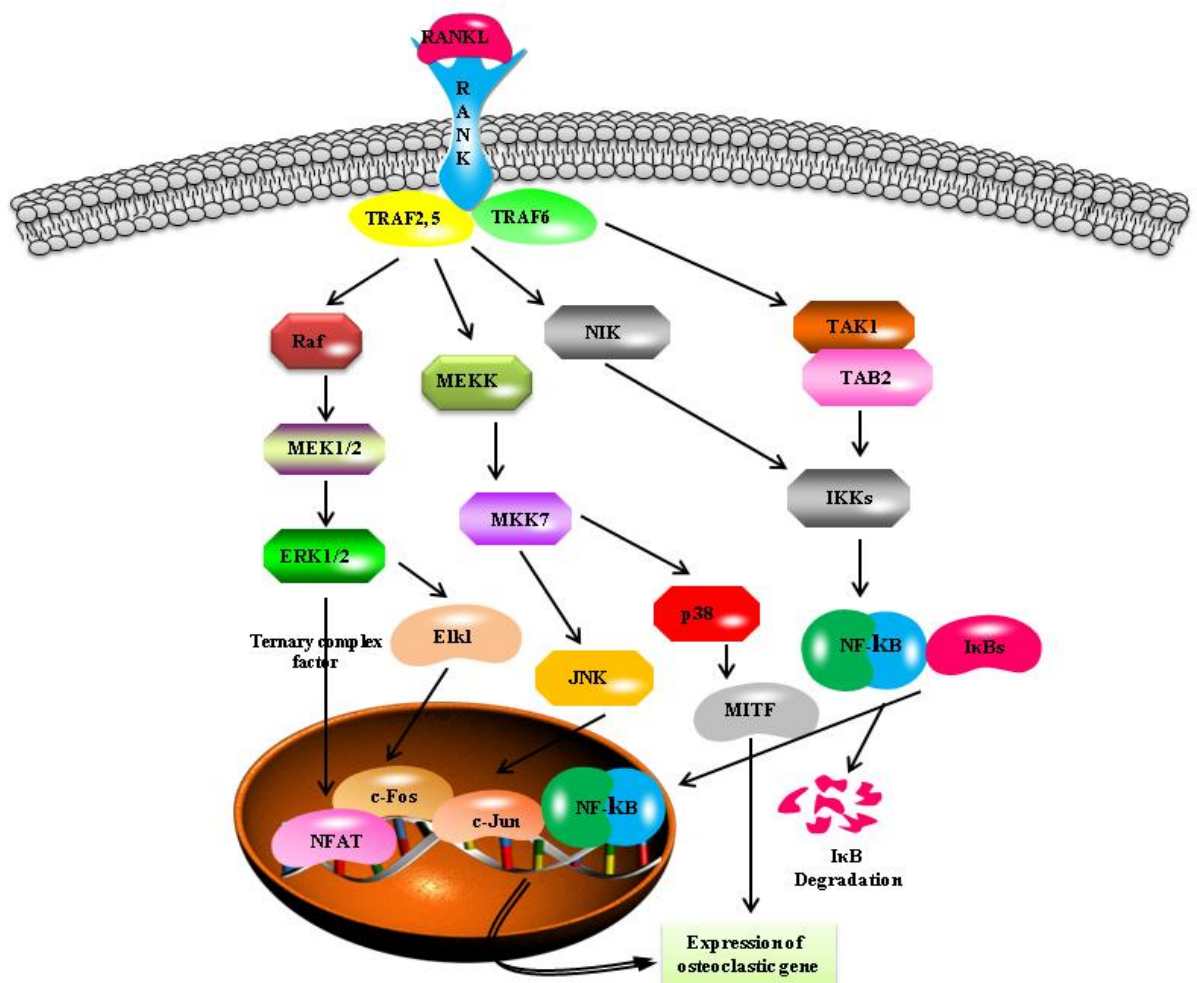
Figure 2.19: Schematic diagram showing the RANKL signaling cascade during osteoclastogenesis

2.10 Cancer chemoprevention

Despite tremendous progress in development of anticancer therapies, the incidence of different types of cancers and the number of cancer-related deaths are still on the rise. Increased cases of chemotherapy failure, recurrence of certain tumors after primary cure, deterioration of patient's quality of life and spiraling healthcare costs of treatment limit the real success of chemotherapy in fighting cancer [Baer-Dubowska, 2006]. One approach with enormous potential is chemoprevention which is defined as the use of natural or synthetic compounds to prevent, suppress, or reverse the development of invasive carcinoma. Chemoprevention aims to reduce the occurrence of cancer by inhibiting or inducing key critical pathways that play a role in the carcinogenesis process. The progression toward invasive cancer is characterized by the accumulation of mutations and increased proliferation. Carcinogenesis is a multistage process with distinct molecular and cellular alteration and latency of many years or decades, thus providing considerable opportunity for intervention. Various studies have shown that chemopreventive agents possess strong cancer-protective properties that might interrupt the carcinogenesis process by interfering at the initiation, promotion, and progression stages of cancer. They might also lead to the modulation of proteins in diverse pathways and require the integration of different signals for the final chemopreventive and/or therapeutic effect. According to a conventional classification chemopreventive agents are subdivided into 2 main categories - blocking agents and suppressing agents [Wattenberg, 1985]. Compounds classified as blocking agents prevent carcinogens from reaching or interacting with critical target sites while suppressing agents prevent the evolution of the neoplastic process. Blocking mechanisms include alteration of drug metabolizing activities and scavenging of reactive oxygen species. Mechanisms that suppress tumorigenesis often involve modulation of signal transduction pathways, like altered gene expression leading to cell cycle arrest, and apoptosis.

A wide variety of plant constituents (phytochemicals) with structurally diverse classes of compounds such as flavonoids, terpenoids, alkaloids and saponins are known to possess antioxidant and anti-inflammatory properties. That some of these chemopreventive phytochemicals possess the ability to sensitize multidrug-resistant cancer cells to undergo apoptosis and block the tumor angiogenesis and metastasis has continued to fuel the search for novel anticancer therapies from edible or non-edible plant sources.

2.10.1 Synthetic or natural agents for cancer chemoprevention

Over the years cancer chemoprevention has involved the use of both natural as well as synthetic compounds. Some of the natural compounds have been in the form of crude and

others in the form of a chemically defined extract. While natural compounds from dietary sources are preferred some of the chemopreventive agents have been identified from non-dietary sources. In addition, efforts have been made to modify bioactive food components for better activity. This, to my thinking falls in developing a synthetic compound. Synthetic compounds are generally target specific, have few off target effects and need to pass thorough a labyrinth of regulatory stages before their recommendation could be made for public use. In addition, their long term use as is expected for effective cancer chemoprevention in humans poses a great risk for unexpected toxic effects down the road. The use of natural agents from dietary sources is generally preferred as they are often termed as nature's gift molecules endowed with cancer preventive properties. Many of them have anti-oxidant activity and some also exhibit anti-inflammatory and anti-proliferative properties. An important fact in favor of natural agents is that they are perceived as non-toxic and humans have naturally acquired the ability to consume them without documented side effects. Another important fact is that natural agents are cost effective and have wide human acceptance. Any agent which is synthetic in nature will only be marketed as a "drug" and there are steps and costs associated with developing drugs which a pharma has to recover. This makes "drugs" expensive. Further, to date there is no single "drug" developed for any disease that is devoid of toxicity. Phytochemicals have great potential in cancer prevention because of their presumed safety, low cost and high oral bioavailability.

2.10.2 Polyphenols in cancer chemoprevention

Polyphenols are a group of plant derived chemical characterized by the presence of more than one phenol unit or building block per molecule. They can be divided into different classes on the basis of number of phenol rings present and the structural elements that bind these rings to one another [Stevenson & Hurst, 2007]. The main groups of polyphenols are shown in Fig 2.20. Among these, the largest and most studied polyphenols are the flavonoids, which comprise several thousands of compounds, including flavonols, flavones, catechins, flavanones, anthocyanidins, and isoflavones [Lotito & Frei, 2006]. Polyphenols are an integral part of the human diet, and are mainly found in berries, grapes/wine, tea, chocolate/cocoa, coffee, soybeans, and other fruits and vegetables [Manach et al., 2004]. Polyphenols are currently, regarded as primary chemopreventive agents due to their tremendous health beneficial effects which includes anti-oxidative, anti-inflammatory, and anti-carcinogenic activities. Polyphenols are synthesized by plants for defense against infection and provide protective effects against stress such as ultraviolet light, pathogens and physical damage

[Robbins, 2003]. Among the interesting biological properties exhibited by plant polyphenols, in recent years, there has been increasing interest regarding cancer prevention. Indeed, a number of *in vitro* and *in vivo* studies have shown that plant polyphenols could be used as chemopreventive agents against different types of cancer [Ramos, 2008; Korkina et al., 2009].
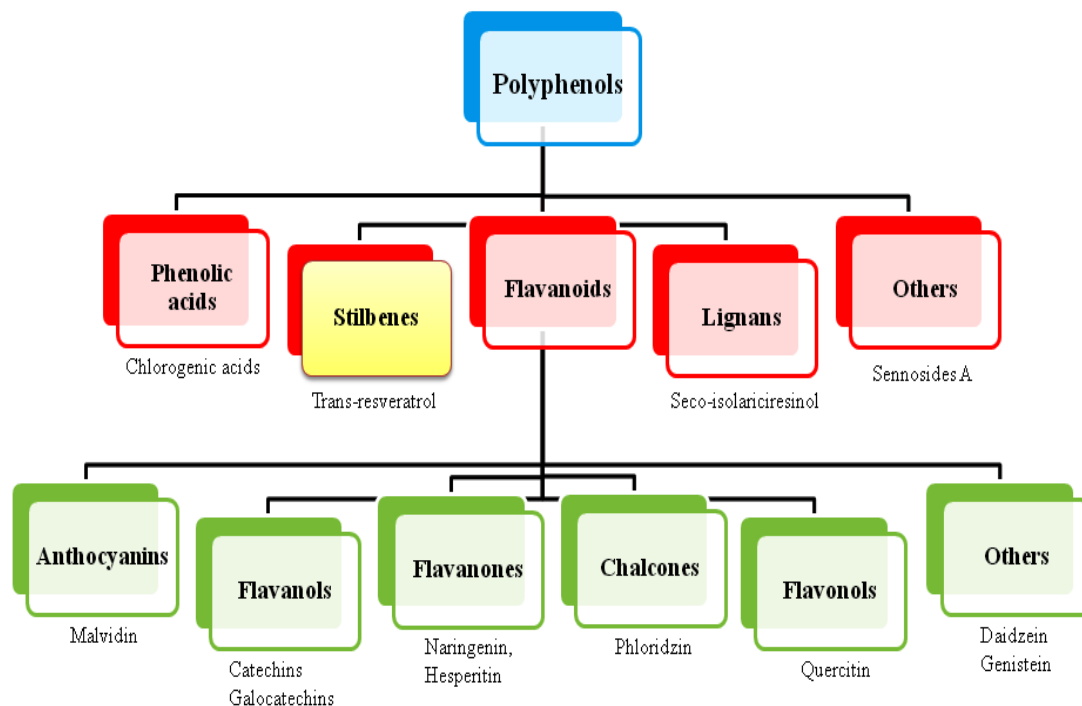
Figure 2.20: Classification of polyphenols

Stilbene

Stilbene or stilbenoids are small molecular weight (approximately 200-300 g/mol) and naturally occurring non-flavonoids polyphenol having 1, 2-diphenylethylene as the core structure. These compounds are mainly stress metabolites, produced in the leaves as well as in sapwood in response to viral and microbial attack, ultra violet exposure and disease [Langcake and Pryce, 1977; Hart and Shrimpton, 1979]. These molecules are synthesized via the phenylpropanoid pathway and share some structural similarities to estrogen. Although known as plant defense compounds, these phytochemicals have diverse pharmacological activities on human health. The effects include its role as an inducer of cell differentiation, a mediator of anti-inflammatory action, its effects as an antioxidant and anti-aging agent, as antimicrobial agent, inhibition of human platelet aggregation and as cancer-chemopreventive natural

products. Over the years, stilbene-based compounds have attracted the attention of many researchers due to their wide range of biological activities.

Resveratrol (trans-3,5,4'-trihydroxystilbene; RESV)

RESV is a prominent and extremely well studied member of stilbene family. It is generally a byproduct of the anthocyanin biosynthetic pathway in the plants [Chong et al., 2009]. The starting molecule being phenylalanine is converted to 4-coumaroyl-CoA by various enzymatic pathways. This molecule is then converted to RESV by resveratrol synthase [Melchior and Kindl, 1991; Schoppner and Kindl, 1984]. These compounds exist in foods and beverages (e.g. in grapes and red wine) and are widely consumed. The medicinal value of RESV was of very little interest until 1990. However in 1997 when Jang and colleagues [Jang et al., 1997] published a seminal article demonstrating its anti carcinogenic effects there has been a rapid progress in uncovering the molecular mechanisms of anti-carcinogenic properties of RESV [Aggarwal et al., 2004]. Due to its broad-spectrum health beneficial effects, such as anti-infective, anti-oxidant, and cardioprotective functions, RESV is considered as the state-of-the-art nature's medicine [Baur and Sinclair, 2006]. The chemopreventive property of RESV has been reflected by its ability to block the activation of various carcinogens and/or to stimulate their detoxification, to prevent oxidative damage of target cell DNA, to reduce inflammatory responses and to diminish proliferation of cancer cells. Several *in vitro* and *in vivo* studies showed that RESV has powerful growth-inhibitory and apoptosis-inducing effects on various solid tumor cells, including colon, breast, prostate, cervical, and pancreatic cancers [Schneider et al., 2000; Mgbonyebi et al., 1998; Sheth et al., 2012; Liu et al., 2013; Garcia-Zepeda et al., 2013; Liu et al., 2013]. Despite its promising properties, RESV's rapid metabolism and low bioavailability have precluded its advancement to clinical use [Aggarwal et al., 2004]. Various pharmacokinetics study of RESV conducted in human volunteers confirmed that even high dose of RESV are insufficient to achieve the required concentration *in vivo* required for the systemic prevention of cancer [Boocock et al., 2007]. This was further confirmed by additional studies in animal cancer models, which showed the ineffectiveness of RESV *in vivo* due to its poor systemic bioavailability [Athar et al., 2007; Niles et al., 2006;

Wenzel et al., 2005]. Analysis of structure–activity relationships revealed that the substitution of hydroxyl groups of RESV to methoxy groups substantially potentiated RESV's cytotoxic activity [Lee et al., 2003]. Therefore, a series of methoxylated analogs of RESV have been prepared with the aim of increasing the antitumor activity of RESV [Fulda S, 2010]. Furthermore, a 3,5-dimethoxy motif was found to be important for conferring the proapoptotic activity to stilbene derivatives. Since then a number of attempts have been made to synthesize and search for natural and synthetic analogues of RESV with improved pharmacokinetics and superior pharmacological potencies that hold greater potential as natural anticancer drugs.

Pterostilbene (*trans*-3,5-dimethoxy-4-hydroxystilbene; PTER)
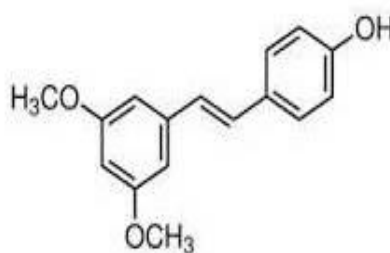
PTER is a naturally occurring dimethylated analog of RESV. PTER shows pleiotropic health benefits, including anti-oxidant, anti-inflammatory, anti-aging, cardioprotective, and neuroprotective activities [Brisdelli et al., 2009]. Both RESV and PTER share similar pharmacologic properties, however PTER has several advantages over RESV. The major chemical difference between PTER and RESV lies in its structure; while RESV has three hydroxyl groups, PTER contains one hydroxyl and two methoxy groups. The two methoxy groups provide lipophilic character to PTER thus increasing its oral absorption and rendering a higher potential for cellular uptake. For stilbenoids, the essence of bioactivity is bioavailability. When administered orally, PTER shows 95% bioavailability while RESV only has 20% bioavailability [Lin et al., 2009]. PTER's half-life is also seven times longer than RESV, 105 min *versus* 14 min [Remsberg et al., 2008]. The greater bioavailability of PTER indicates that PTER could potentially be developed for clinical applications. PTER has been shown to be an effective antioxidant in multiple cancer cell lines, which may facilitate its function as an anti-carcinogenic agent. Recently, PTER induces apoptosis in pancreatic cancer cells [Elango et al., 2014], breast cancer MCF-7 cells [Chakraborty et al., 2010; Chakraborty et al., 2012], docetaxel-induced multiple drug resistance (MDR) lung cancer cells [Hsieh et al., 2014], osteosarcoma cells [Liu et al., 2013], PCa (PC-3 and LNCaP) cells [Lin et al., 2012], leukemia K562 cells, MDR and BCR-ABL-expressing leukemia cells [Tolomeo et al., 2005], colon cancer cells [Nutakul et al., 2011], hepatocellular carcinoma cells and, and gastric carcinoma

cells [Pan et al., 2007]. The mechanisms of the anticancer action have been investigated and include pro-apoptosis, pro-autophagy, alteration of the cell cycle, telomerase inhibition, DNA damage, anti-angiogenesis, anti-metastasis, and immuno-stimulatory effects [McCormack and Mc Fadden, 2012; Hong et al., 2013; Mena et al., 2012; Mak et al., 2013; Chen et al., 2012; Huang et al., 2013; Perecko et al., 2013; Tippani et al., 2014; Pan et al., 2009; Elango et al., 2014; Chakraborty et al., 2012; Hseih et al., 2014; Liu et al., 2013; Lin et al., 2012; Tolomeo et al., 2005; Nutakul et al., 2011; Pan et al., 2007]. In *in vivo* tests, PTER inhibits tumorigenesis and metastasis with minor toxicity [McCormack and Mc Fadden, 2012; Mena et al., 2012]. The human clinical trial demonstrated that PTER is safe in doses up to 250 mg/day. PTER deserves more investigation in preclinical studies or clinical trial as a potential anticancer agent [McCormack and McFadden, 2012]. To improve the anticancer efficacy and safety of PTER, our laboratory designed and synthesized a novel PTER derivative PTER-ITC.

2.11 Hybrid anticancer drug

Over the years the design of cancer chemotherapy has become increasingly sophisticated yet there is no cancer treatment that which is 100% effective against disseminated cancer. Presently cancer therapy interfering with a single biological molecule or pathway has been successfully utilized [Sawyers C, 2004; Petrelli and Giordano, 2008] still the problem of drug resistance exists. A general belief that agents modulating more than one target could have superior efficacy compared to single target drugs [Bode and Dong, 2009; Xhan and Liu, 2009] has led to the search for molecules modulating multiple targets. Cocktail of drugs (Combination therapy), is one of the strategies which now a days are employed by clinicians to treat unresponsive patients [Viegas-Junior et al., 2007; Gediya and Njar, 2009]. This strategy has further encouraged the researchers and scientist globally towards the design of ligands comprising two pharmacophores in a single biological entity. It is a new concept in drug design and development that produce a new hybrid compound endowed with improved affinity and efficacy, when compared to the parent drugs. Pharmacophore hybridization is believed to be analogous to conventional combination therapy, with the exception that the two drugs are covalently linked and available as a single entity [Tietze et al., 2003].

PTER (trans-3,5-dimethoxy-4-hydroxystilbene) is an antioxidant that is predominantly present in blueberries. Numerous studies confirm that PTER exhibits the characteristics hallmark of an effective anticancer agent based on its antineoplastic properties in number of common malignancies. Similarly isothiocyanates (ITC) constitute one of the important families of natural chemoprotective agents which are formed by hydrolysis of their precursor parent

compounds known as glycosinolates present in variety of cruciferous vegetables like broccoli, cauliflower, cabbage, brussel sprouts, and kale [Keum et al., 2004]. Diets high in ITC containing cruciferous vegetables have been shown to protect against a number of malignancies including non-Hodgkin's lymphoma and cancers of the liver, prostate, ovary, lung, colon, and gastrointestinal tract [Murillo and Mehta, 2001]. Previous study showed that the hybrid drug comprising of COX-2 inhibitor nimesulide and ITC side chain was found to be a very potent anticancer agent for inhibiting COX-positive as well COX-negative pancreatic cancers at much lower doses (3-5 μM) than the parent nimesulide ligand (35 μM) [Sarkar et al., 2007]. Similarly the copper complex of henna-ITC hybrid was found to inhibit human myeloma KBM-5 cells ($IC_{50} = 0.3$ μM) through blockade of transcription factor NFκB [Shirisha et al., 2007]. Due to such versatile effects of PTER and ITC on tumor signaling and proliferation, we postulated that a compound containing both these pharmacaphore could be an effective combination for anti-cancer activity.

2.12 The problem addressed in present thesis

The present thesis deals with development of a novel compound for prevention and treatment of cancer. The initial part of this thesis dealt with synthesis and characterization of a novel PTER-ITC conjugate. In the next part the major focus was to understand the mode of action of this hybrid compound in prevention of breast and prostate cancers. Finally the successive chapters reported the anti-inflammatory, anti-angiogenic and anti-osteoclastogenic effect of this novel conjugate. PTER, although established as an anti-cancer and anti-inflammatory agent, but synthesizing its new hybrid with more potent action is a new finding that is dealt with in the present thesis. It was also quite interesting to find that not only this stilbene conjugate has different modes of action when compared to PTER, but it also differentially activates some pathways in tumor cells.

Chapter 3. Materials and Methods

3.1 Introduction

This chapter provided in detail the experimental procedure carried throughout the thesis to establish a novel molecule as anti-cancerous agent. It also deals with various techniques that are used to unveil the underlying molecular pathways of action of this molecule/compound.

3.2 Chemicals, enzymes and hormones used

All cell culture reagents including media, trypsin, fetal bovine serum (FBS) and other supplements were purchased from GIBCO (Life Technologies, Grand Island, NY). Antibiotics (penicillin and streptomycin), dimethyl sulphoxide (DMSO), MTT [3-(4,5-dimethylthiazol-2-yl)-2,5-diphenyltetrazolium bromide], 5-Fluorouracil and all analytical grade chemicals were purchased from HiMedia (Mumbai, India). Polyfect transfection reagent was purchased from QIAGEN (Valencia, CA). Resveratrol, Dihydrotestosterone (DHT), Lipopolysaccharide (LPS), Receptor activator of nuclear factor-κB (NFκB) ligand (RANKL), mitomycin-c, 4',6-diamidino-2-phenylindole (DAPI), rosiglitazone, A6730 (inhibitor of AKT kinase, PD98059 (MAPK/ERK inhibitor), SB203580 (p38 MAPK kinase inhibitor), SP600125 (JNK inhibitor), Z-VAD-FMK (pan-caspase inhibitor), Z-LEHD-FMK (caspase-9-specific inhibitor), Z IETD-FMK (caspase-8-specific inhibitor), GSK0660 (PPARβ/δ inhibitor), GW9662 (PPARγ inhibitor), Parthenolide (NFκ-B inhibitor) and BCA protein estimation kits were from Sigma-Aldrich (St. Louis MO). Pifithrin-α (p53 inhibitor), all primary antibodies and small interfering RNA (siRNA) against AKT (sc-43609), ERK (sc-35335), PPARγ (sc-29455) and control (sc-37007; negative control for targeted siRNA transfection experiments; each consists of a scrambled sequence that will not specifically degrade any known cell mRNA) were purchased from Santa Cruz Biotechnology (Santa Cruz, CA). All secondary antibodies and chemicals for RT-PCR were purchased from Genei (Bangalore, India). ECL detection kit was obtained from Amersham (GE healthcare life science, UK). AP1-luciferase and NFκB-luciferase plasmids were from Promega. The pSG5-hAR-puro and pMMTV-neomycin-luciferase plasmids were a kind gift from Professor Ilpo T Hutaniemi, Imperial College London, UK. The pEGFP-hAR constructs were kindly donated by Dr. Richard G. Pestell's of Kimmel Cancer Centre, Thomas Jefferson University, Philadelphia, USA. The PPAR plasmid and co-regulator plasmid were kind gift from Dr. Ronald M. Evans (The Salk Institute for Biological Studies, California, USA) and Dr. Michael R. Stallcup (University of Southern California, Los Angeles, USA) respectively.

3.3 In vitro experimental models

3.3.1 Cell lines and cell culture

Breast cancer cells MCF-7, T47D, MDA-MB-231 and MDA-MB-468; Prostate cancer cells PC3, LNCaP; Lung cancer cells NCIH-522; Ovarian cancer cells PA-1; Liver cancer cells HepG2; mouse macrophage cell line RAW 264.7 and non-cancer cells, CHO and COS-1 cells were used in this study. All these cell lines were purchased from National Centre for Cell Sciences, Pune, India

MCF-7 cells **(from passage number 14-20)** and **MDA-MB-231 (from passage number 5-10)** were grown in DMEM with 10% fetal bovine serum (heat inactivated) and 1% antibiotic (100 U/mL of penicillin and 100 µg/mL streptomycin) mix at 37 ℃ in humidified atmosphere in a CO_2 incubator. The medium of the cells was changed after every two days to avoid nutrient stress. Drugs were added after washing the cells twice with PBS followed by addition of complete medium.

T47D cells **(from passage number 65-70)** were grown in high glucose RPMI with 10% fetal bovine serum, 2 mM L-glutamine, 0.2 U/mL of insulin (porcine) (Sigma, St. Louis, MO, USA) and 1% antibiotic (100 U/mL of penicillin and 100 µg/mL streptomycin). The culture flasks were maintained in humidified atmosphere in a CO_2 incubator at 37 ℃. The spent medium was replaced by fresh medium on every third day.

MDA-MB-468 (from passage number 16-18) cells was grown in Leibovitz L-15 supplemented with 2 mM L-glutamine, 10% fetal bovine serum and 1% antibiotic (100 U/mL of penicillin and 100 µg/mL streptomycin) mix in a hypoxic environment at 37 ℃ in humidified atmosphere in a CO_2 incubator. The medium was changed by fresh media every alternate day.

The prostate cancer cells **PC3 (from passage numbers 30-32)** were grown in HAM's F12K medium supplemented with 10% fetal bovine serum (heat inactivated), 2 mM L-glutamine and 1% antibiotic (100 U/mL of penicillin and 100 µg/mL streptomycin) mix at 37 ℃ in humidified atmosphere in a CO_2 incubator. The culture medium was changed every third day with fresh HAM's-F12K (complete).

LNCaP cells (from passage numbers 11-15) were maintained in RPMI-1640 medium supplemented with 2 mM L-glutamine, 10 mM HEPES, 1 mM sodium pyruvate, 10% fetal bovine serum (FBS) (heat inactivated) and 1% antibiotic (100 U/mL of penicillin and 100 µg/mL streptomycin) under 5% CO_2 at 37 ℃. The medium of the cells was changed after every two days to avoid nutrient stress.

RAW 264.7 mouse macrophage (from passage number 52-56) cells were cultured in DMEM supplemented with 10% fetal calf serum, 2 mM L-glutamine, 0.1 mM nonessential amino acids and 1 mM sodium pyruvate along with penicillin (10^5 U/L), streptomycin (100 mg/mL). Cell cultures were maintained at 37°C in a humidified atmosphere of 5% CO_2 incubator.

HepG2 (from passage number 45-50) cells were grown in DMEM with 10% fetal bovine serum (heat inactivated) and 1% antibiotic (100 U/mL of penicillin and 100 μg/mL streptomycin) mix at 37 °C in humidified atmosphere in a CO_2 incubator. The medium of the cells was changed after every two days to avoid nutrient stress.

NCIH522 (from passage number 86-90) cells were grown in RPMI 1640 medium supplemented with 10% fetal bovine serum (heat inactivated) and 1% antibiotic (100 U/mL of penicillin and 100 μg/mL streptomycin) mix at 37 °C in humidified atmosphere in a CO_2 incubator. The medium of the cells was changed after every three days to avoid nutrient stress.

PA-1 (from passage number 348-350) cells were grown in MEM supplemented with 10% fetal calf serum, 2 mM L-glutamine, 0.1 mM nonessential amino acids and 1 mM sodium pyruvate and 1% antibiotic (100 U/mL of penicillin and 100 μg/mL streptomycin) mix at 37 °C in humidified atmosphere in a CO_2 incubator. The medium of the cells was changed after every two days.

CHO (**from passage number 20-22**) and **COS-1** (**from passage number 30-35**) cells were grown in DMEM with 10% fetal bovine serum (heat inactivated) and 1% antibiotic (100 U/mL of penicillin and 100 μg/mL streptomycin) mix at 37 °C in humidified atmosphere in a CO_2 incubator. The medium of the cells was changed after every two days to avoid nutrient stress.

3.3.2 Isolation of human umbilical vein endothelial cells (HUVECs)

An umbilical cord usually contains three large blood vessels of which the vein is the largest. Two arteries are also present which are usually closed by contraction of the vessels. Isolation and culture of HUVECs were performed according previous report [Baudin et al., 2007] with minor modifications.

Collection and storage of umbilical cords- After delivery, the umbilical cord cords were cut from the placenta and placed in ice cold PBS till further used.

Isolation and culture of HUVECs- The isolation process was done in a laminar flow hood, using sterile gloves and laboratory coat for protection from infection. The umbilical cord was inspected for clamped and damaged areas, which should be discarded. Then small piece was

cut from one end to obtain a fresh cut. The cord surface was then sterilised by washing with 70% ethanol followed by washing with PBS. A 3-way stopcock was then inserted into the vein of cord and tied with a cable tie. A syringe filled with 20 mL of PBS was injected into umbilical vein and flushed slowly to remove blood clots from the vein. The other side of umbilical cord was clamped by haemostatic clamp and the vein was filled with 25 mL collagenase solution. The filled vessel was incubated for 30 min at $37^{o}C$ in CO_2 incubator. The clamps were removed and the contents of the veins were collected into 50 mL sterile plastic tube and the vein was flushed with additional 20 mL of RPMI. The tube was centrifuged for 7 min at 1000 rpm and the pelleted cells were resuspended in 10 mL RPMI + l0 % FBS. The suspended cells were seeded into 1% gelatine coated 25 cm^2 flask and incubated at $37^{o}C$ in a humidified incubator with 5% CO_2. The adherent endothelial cells (attached cells to dish substratum) were washed one day after isolation, the medium was renewed and the cells were inspected using phase-contrast microscope. The medium was renewed every 3 days.

Subculture of HUVECs- The confluent cells (all the available growth area was utilized and the cells made close contact with one another) were washed twice using PBS, and then 1 mL of trypsin/EDTA was used to detach the cells from the dish substratum for 5 min in CO_2 incubator. As soon as the cells started to detach they were gently tapped from the side of the flask to ensure detachment of all cells. RPMI medium with l0% FBS was added immediately to the cells to inhibit further trypsin activity. The cells were subcultured every, 5 days at a density of 2 x 10^5 cells into gelatine coated culture flask.

3.4 In vivo experimental models

3.4.1 *Animals and tumor development*

Female laboratory mouse: Phylum: Chordata

Subphylum: Vertebrata

Class: Mammalia

Order: Rodentia

Family: Muridae

Genus: *Mus*

Species: *M. musculus*

were purchased from All India Institute of Medical Sciences (AIIMS), New Delhi, India. Animals were in healthy condition at the time of purchase and were housed in a well-ventilated animal house with 12 h light/dark schedules. The animals were fed with a balanced animal feed (Ashirwad Animal Feed Industries, Punjab, India) and had free access to normal drinking

water. The animals were acclimatized for about 10 days prior to initiation of any experiments. This study was carried out in strict accordance with the recommendations in the Guidelines for Laboratory Animal Facility of the Committee for the Purpose of Control and Supervision on Experiments on Animals (CPCSEA), India. The experimental design of the present study was approved by the Institutional Animal Ethics Committee of the Indian Institute of Technology Roorkee, India **(Permit Number: IAEC/10/02 of 30th Nov 2010)**. After the experiments, the mice were sacrificed by cervical dislocation under ether anaesthesia and their blood was obtained by cardiac puncture for further biochemical analyses.

The Ehrlich ascitic cells (EAC) were obtained from National Centre for Cell Sciences (NCCS), Pune, India. EAC is a murine spontaneous breast cancer cell that serves as the original tumor from which an ascitic variant was obtained. EAC resembles human tumor which are more sensitive to chemotherapy due to the fact that they are undifferentiated and has a rapid growth rate. The EAC were maintained in our laboratory by serial intraperitoneal (i.p.) passage in female swiss albino mice at 7-10 days of interval. The tumor cells were withdrawn and then after diluting in phosphate buffer saline (PBS) were counted in a neubauer hemocytometer using trypan blue dye exclusion method. The viability of the cells was found to be 95% or more. The cells were then re-injected (15×10^{6} cells/animal) subcutaneously to the right hind limb (thigh) of the experimental animals for the development of solid tumor. The day of tumor implantation was assigned as day '0'. On day 1, the animals were randomized and divided into six groups (n = 6) as follows

Group-1 Control normal mice

Group-2 Tumor bearing mice (EAC control)

Group-3 Tumor bearing mice treated with PTER (200 mg/kg bw)

Group-4 Tumor bearing mice treated with PTER-ITC (20 mg/kg bw)

Group-5 Tumor bearing mice treated with PTER-ITC (100 mg/kg bw)

Group-6 Tumor bearing mice treated with 5-FU (20 mg/kg bw).

Treatment was initiated from day 6 after tumor implantation and continued for next 30 days. The dosage used in this study were based on earlier existing reports for PTER [Min-Hsuing et al., 2009; McCormack et al., 2011] and 5-FU [Tulika et al., 2011] while for the PTER-ITC it was much below the lethal dose as determined by the pilot study. The treatment was administered orally every alternate days and the tumor mass was measured every 10 days from the day treatment was initiated. The volume of tumor mass was calculated using the formula $V = 4/3\pi r_1^2 r_2$ where r_1 and r_2 are the radii of the tumor from two directions [Kuttan et al., 1990].

Approximately after 24 h of final treatment, the rats were sacrificed as described earlier. The blood was collected by cardiac puncture for determination of the hematological parameters and the tumor was excised out for further analysis. Their body weight and the weight of the major organs namely, liver, kidney and spleen were recorded separately.

3.4.2 Carrageenan-induced paw edema
Male laboratory rats: Phylum: Chordata

Subphylum: Vertebrata

Class: Mammalia

Order: Rodentia

Family: Muridae

Genus: *Rattus*

Species: *R. norvegicus*

were procured from All India Institute of Medical Sciences, New Delhi, India. Animals were in healthy condition at the time of purchase and were housed in a well-ventilated animal house with 12 h light/dark schedules. The animals were fed with a balanced animal feed (Ashirwad Animal Feed Industries, Punjab, India) and had free access to normal drinking water. After a two-week adaptation period, the rats were assigned randomly to six groups (n = 6) for further experiments.

Group-1 Normal saline treated

Group-2 Carrageenan only

Group-3 Indomethacin (10 mg/kg BW) + Carrageenan

Group-4 PTER-ITC (10 mg/kg BW) + Carrageenan

Group-5 PTER-ITC (50 mg/kg BW) + Carrageenan

Group-6 PTER (50 mg/kg BW) + Carrageenan

Carrageenan-induced paw edema model was used for the assessment of anti-inflammatory activity [Winter et al., 1962]. Animals were treated with normal saline, indomethacin (10 mg/kg) and PTER-ITC (10 mg/kg and 50 mg/kg) or PTER (50 mg/kg) 30 min prior to injection of 1% carrageenan suspension in 0.9% NaCl solution. Carrageenan was injected subcutaneously into the planter aponeurosis of the hind paw, and the volume was measured by a water plethysmometer apparatus immediately after carrageenan injection and at 1, 2, 3, 4, and 5 h later. Edema was calculated as follows:

Edema = paw volume at every hour - the paw volume at zero hour

3.5 MTT assay for cell viability

The cytotoxicity as caused by various test compounds was measured according to the protocol reported by Mosmann [1983], which is detailed below. A sub-confluent layer of cells were trypsinized and collected in the respective cell culture media. In brief, 5 X 10^3 cells in 200 μL of medium were seeded in 96-well plates (Griener, Germany*).* Serial dilutions of drugs to be tested were dissolved in ethanol (or DMSO) and were added to the monolayer. The control cells were treated with 0.1% DMSO (vehicle control). The effects of compounds on different cancer cell lines were tested along a range of concentrations under similar conditions. The cultured cells were assayed after 24 h by adding 20 μl of 5 mg/mL MTT followed by incubating at 37°C for 4 h. The MTT containing media was then aspirated and 200 μL DMSO (Himedia, Mumbai, India) was added to dissolve the formazone crystals. The optical density (OD) was measured at 570 nm using ELISA plate reader (Fluostar optima, BMG Labtech, Germany). The percentage inhibition was calculated as:

$$100 - \left[\left(Mean\ OD\ of\ treated\ cell \times 100\right) \div \left(Mean\ OD\ of\ vehicle\ treated\ cells\right)\right]$$

The dose response curve and IC_{50} values were obtained by nonlinear regression analysis [non-linear regression (sigmoidal dose response with variable slope)] using Graph Pad Prism, version 5.02 software (**Graph Pad Software Inc**., CA, USA).

3.6 Apoptosis assay

3.6.1 Assay for apoptotic cells by flow cytometry

Induction of apoptosis in cancer cells caused by test compound was quantitatively determined by flow cytometry using the Annexin V-conjugated Alexafluor 488 Vybrant apoptosis assay kit (V-13241; Molecular Probes, Eugene, Oregon, USA) following the manufacturer's instructions. Briefly, after treatment of cells with test compound for 24 h, the cells were harvested, washed with PBS and incubated with Annexin V Alexafluor 488 (Alexa488) and propidium iodide for cellular staining in binding buffer at room temperature for 15 min in dark. The stained cells were then analyzed by fluorescence activated cell sorter (FACS Calibur, BD Biosciences, San Jose, CA, USA) and the data were analyzed using Cell Quest 3.3 software.

3.6.2 Acridine orange staining

In order to check the plasma-membrane permeability, nuclear morphology and the chromatin condensation, the cells were stained with Acridine orange (AO) / Ethidium bromide (EB) dye mixture (100 μg/mL AO and 100 μg/mL EB) according to the protocol

described earlier [Takahashi et al., 2004]. In brief, 0.5 X 10^6 cells were seeded for the assay in a 6-well plate and incubated with test compound for 24 h and then washed properly with PBS. Then 500 μL AO/EB dye mixture dissolved in PBS was added to the plate and observed under fluorescent microscope (Zeiss, Axiovert 25, Germany).

3.6.3 DAPI Staining

Changes in nuclear morphology of apoptotic cells were examined by fluorescence microscopy of DAPI-stained cells. In brief, 0.5 x 10^6 cells were seeded in a 6-well plate and incubated (24 h) with different concentrations of test compound. The cells were then washed with PBS and incubated with 500 μL DAPI (0.5 μg/mL; 10 min, in the dark) and observed by fluorescence microscopy (Zeiss, Axiovert 25).

3.6.4 DNA fragmentation assay

The pattern of DNA cleavage due to cell cytotoxicity introduced by drugs was analyzed by isolating DNA from drug treated cells and running it on agarose gel according to the protocol described earlier [Sanchez alcazar et al., 1997]. In brief, 3 X 10^6 cells were exposed to the test compound for 24 h. Subsequently the drug treated cells were centrifuged and then washed with PBS, and the pellet was lysed with 400 μL of hypotonic buffer solution [containing 10 mM Tris (pH 7.5), 1 mM EDTA and 0.2% Triton X-100] for 15 min at room temperature and then centrifuged for 15 min at 12,000 rpm. Then 350 μL of the supernatant was again lysed in 106 μL of the second lysis buffer [containing 150 mM NaCl, 10 mM Tris-HCl (pH 8.0), 40 mM EDTA, 1% SDS, 0.2 mg/mL Proteinase K at final concentration] for 4 h at 37 ºC. The DNA was extracted with phenol/chloroform/isoamyl alcohol (25:25:1) and the pellet thus obtained was washed with ethanol and resuspended for RNase digestion in 15 μL of 10 mM Tris, 1 mM EDTA (pH 8.5), and 50 μg/mL RNase for 1 h at 37 ºC. The DNA was then analyzed by electrophoresis at 50 V/cm in a 2% agarose gel.

3.6.5 Single cell gel electrophoresis

DNA damage due to cytotoxicity of drug was assesed after drug treatment by evaluating DNA comet tail area in accordance with previously described protocol [Bentle et al., 2006] with slight modifications. Briefly, MCF-7 cells (5 X 10^5 cells) were treated with test compound in fresh medium and harvested after 24 h. Slides preparation was done according to the method of Tice et al [2000]. Briefly, 0.3 X 10^6 cells were mixed with 1% low melting agarose (50 μL) at 37 ºC in PBS and sandwiched between 1% normal melting agarose in previously prepared slide. Thereafter the prepared slide was stored at 4 ºC for 10 min followed

by incubating it in lysis buffer [containing 2.5 M NaCl, 10 mM Tris-base, 100 mM EDTA (pH 10), 1% Triton X-100 and 1% Sodium lauryl sarcosinate] at 4 ºC for 2 h. The slides was then electrophoresed for 5 min at 25 V in 300 mM NaOH, 1 mM EDTA and precooled to 4 ºC. This was followed by neutralization with Tris–Cl at pH 7.5. The nuclei were then stained with EB and visualized under a fluorescent microscope. Comet tail length was calculated as distance between the nuclei heads and end of each tail. Tail moments were defined as the product of % DNA in each tail, and the distance between mean of head and tail distributions [Bentle et al., 2006] and presented as:

$$\% \text{ DNA (tail)} = TA \times TAI \times 100 / [(TA \times TAI) + (HA \times HAI)]$$

Where TA= tail area, TAI= tail area intensity, HA= head area and HAI= head area intensity.

3.6.6 Caspase assay

Caspase activity was determined by using ApoTarget^{TM} caspase colorimetric protease assay sampler kit (Catalog number: KHZ1001; Invitrogen, USA) according to the manufacturer's instructions. Briefly, cells were treated with different drugs for 24 h. The cells were then collected, washed in PBS, and lysed in 50 μL of lysis buffer on ice for 10 min. After centrifugation, the supernatant containing 150 μg protein were incubated with 200 μM caspase-7 (Ac-DEVD-pNA), caspase-8 (Ac-IETD-pNA) and caspase-9 (Ac-LEHD-pNA) substrates in reaction buffer at 37 ºC for 1 h respectively. The levels of released pNA were measured with a microplate reader (Fluostar optima, BMG Labtech, Germany) at 405 nm wavelength. The fold-increase in caspase-7, -8, and -9 activities were determined by direct comparison to the level of the un-induced control, which was considered as 1. For caspase inhibitor assay, the cells were pretreated with a synthetic universal-caspase inhibitor (20 μM, Z-VAD-FMK) and caspase-8 and -9 inhibitors (20 μM, Z-IETD-FMK and Z-LEHD-FMK, respectively) for 1 h followed by treatment with test compound for another 24 h. On completion of incubation the cell death was finally determined by MTT assay as described earlier.

3.7 Cell cycle analysis

In order to determine the cell cycle distribution patterns, 10^5 cells/well were plated in 6 well plate and treated with different drugs for 24 h. After treatment, the cells were collected by trypsinization, fixed in 70% ethanol and washed with PBS. Subsequently the cells were treated with RNase A (50 μg/mL), stained with propidium iodide (PI) (50 μg/mL) and incubated in the

dark for 30 min at room temperature. The DNA content of the stained cells was analyzed using Cell Quest 3.3 Software with the FACS Calibur flow cytometry (BD Biosciences, CA, USA).

3.8 Scratch assay

The migrations capacity of cells was investigated using *in vitro* scratch assay as described previously [Yi et al., 2008]. Briefly, the cells were seeded in a 6 well microtiter plate until about 90% confluent. The media was then removed and equal size 'scratch' was created using pipette tip and then rinsed with PBS to remove detached cells. The medium with the indicated concentrations of test compound was then added for 24 h incubation in presence of mitomycin-c (5 μg/mL) to control alteration in cell proliferation. The microscopic observations of the cells were recorded at different time interval after treatment. The images were captured using fluorescent microscope (Zeiss, Axiovert 25, Germany) under 100X magnification and analyzed using T-Scratch software v7.8.

3.9 Measurement of intracellular Reactive Oxygen Species (ROS) levels

For determination of the intracellular accumulation of ROS, the $2',7'$-dichlorofluorescein diacetate (H_2-DCF-DA) method was used [Kang et al., 2010]. After treatment of the cultured cells (in 6-well plates) with respective compounds for 24 h, H_2-DCF-DA (at a final concentration of 2 μM) was added to each well and incubated for an additional 20 min at 37 °C. Thereafter the cells were washed with PBS twice and intracellular ROS accumulation was observed and photographed using a fluorescent microscope (Zeiss, Axiovert 25, Germany). The fluorescent intensity was analyzed using ImageJ 1.43 software (NIH, USA).

The generation of ROS was also detected using nitroblue tetrazolium (NBT) reduction assay as previously described [Ishii et al., 2008] with slight modifications. A 100 μL of cell suspension containing 10^6 cells from various treatments were mixed with 100 L of NBT solution (1.4 mM NBT, 1 mM EDTA, 1 mM phenylthiourea) and incubated at 37 °C for 4 h. The samples were centrifuged 1000 ×g for 10 min and then washed with 500 μL of 70% methanol and NBT reduction was measured by dissolving the pellet in extraction solution containing 1 mL of 2 M KOH and 1.5 mL of dimethyl sulphoxide followed by vigorous mixing. The samples were centrifuged at 3500 ×g for 20 min and the O.D was measured at 630 nm. In order to check the exact ROS generated as a result of apoptosis, specific free radical scavengers namely, NaN_3 (singlet oxygen scavenger), KI (hydroxyl ion scavenger) and catalase (hydrogen peroxide scavengers) were added to inhibit their further production [Azmi et al., 2005] in the cell culture medium along with the treatments with the test compounds. After 24 h

of combined incubation of compounds and the ROS scavengers, the intracellular ROS was measured similarly as mentioned above.

3.10 NO production

RAW264.7 (1 X 10^5) cells were seeded in 24-well plates, and then pretreated with different concentrations of PTER and PTER-ITC for 1 h. After 1 h, the cells were stimulated with LPS (1 µg/mL) for the next 18 h. After the incubation period the NO production was determined by estimating the accumulation of nitrite, the primary stable breakdown product of NO, in the culture medium with the Griess reagent [mixture of equal volume of 1% sulfanilamide in 5% H_3PO_4 and 0.1% N-(1-naphthyl) ethylenediamine dihydrochloride in H_2O] [Banerjee et al., 2009]. The amount of nitrite produced was quantified spectrophotometrically at 540 nm using a microplate reader (BMG Labtech, Germany). Concentrations of nitrite was determined using a standard curve of sodium nitrite prepared in the culture medium.

3.11 Oil Red O staining procedure

The production of intracellular neutral lipid was stained and quantified by oil red o (ORO) procedure. Approximately 10^5 cells were grown on glass coverslips in a 6-well plate. The cells were treated with test compounds for various time durations (24 to 72 h), followed by fixing them with 3.7% paraformaldehyde for 1 h at room temperature. They were then washed two times with PBS. Thereafter the cells were stained by ORO dissolved in 60% isopropanol for 30 min. After washing the excess stain, the images were captured with a Zeiss Axiovert40 inverted wide field microscope. The lipids were quantified by dissolving the ORO stain in 100% isopropanol and the absorbance was measured at 510 nm according to published procedure [Vosper et al., 2001].

3.12 Osteoclast differentiation

For differentiation of osteoclasts, RAW264.7 cells (2×10^4, in 24-well plate) were cultured in DMEM, supplemented with 10% FBS in presence of RANKL (50 ng/mL), and other test chemicals. Cells were then maintained in osteoclast formation medium for 6 days with daily change of medium

3.13 Tartrate resistant acid phosphatase (TRAP) staining

The staining is a technique commonly used to visualize osteoclasts. The principle behind staining of TRAP involves the use of napthol AS phosphates in conjunction with fast red violet BB salts for the detection of acid phosphatase. This diazonium fast red violet salt was selected because it couples rapidly at acidic pH, forming insoluble dye deposits. Napthol AS-

MX, released by enzymatic hydrolysis, couples immediately with fast red violet BB salt, resulting in the formation of insoluble pink deposits at sites of activity. Tartaric acid was used in order to demonstrate the presence of tartrate-resistant acid phosphatase. Hence, the cells containing tartrate-sensitive acid phosphatase are devoid of activity, and only the cells containing tartrate acid-resistant phosphatase show pink dye deposits at the sites of activity.

For this staining, the cells were first washed with PBS and fixed with 3.7% paraformaldehyde (pH 7.4) for 15 min at RT. Cells were then permeabilized in 0.1% Triton X-100 for 10 min. After permeabilization the cells were washed and incubated in TRAP stain (0.3 mg of Fast red violet BB salt per mL of TRAP buffer) till the pink color gets developed. Each 100 mL of TRAP buffer contained 50 mL of 0.1M Acetate buffer, 10 mL of 0.3 M Sodium tartarate, 1 mL of 10 mg/mL Napthol AS-MX phosphate and 38.9 mL of milli Q water. Cells with more than three nuclei were counted as osteoclast, and total number of osteoclasts per well were counted under the microscope.

3.14 Karyotyping

For karyotyping of the isolated cells metaphase chromosomes were prepared according the method described earlier [Dev et al, 2012]. Briefly to accumulate mitosis, 0.04% colchicine at final concentration of 2.8 μg/mL was added into actively proliferating cultures for 1–1.5 h. Then 0.56% KCl was applied for hypotonic treatment for 15 min at room temperature (RT) followed by a spin at 2000 rpm for 2 min. The cell pellets were then suspended and fixed with methanol and glacial acetic acid mixture (3:1) on ice for 10 min. Finally, the cell suspension was dropped on wet, cooled slides and air dried at room temperature, followed by Giemsa staining of the slides. Slides were then dried and observed under light microscope at 40X objective.

3.15 Ex-Ovo Chick chorioallantoic membrane (CAM) assay

This is a standardized assay performed to study the effect of a drug on angiogenesis. In this assay the drug is directly tested on a live chick embryo, to see the effect of the drug on the formation of blood vessels (angiogenesis). The procedure followed was according to previously described methods [Dohler et al., 2009]. Briefly, the fertilized chicken eggs were purchased from local markets (Roorkee, India) and incubated at 37.5°C with the relative humidity 60-62% for 72 h. Before starting incubation, dirt, feathers and excrement are carefully removed from the egg shells mechanically by dry wiping with common, gray zigzag hand paper towels, which have a rough rather than a soft surface structure. The eggs are held horizontally and cracked on the edge, keeping close to the bottom of a petri dish and content of the egg transferred to the

petri dish with the embryo and the yolk vessels lying on top of undamaged yolk. As a carrier, a 3x3 mm whatman filter disk pretreated by test compound with or without estradiol was put onto the chorioallantoic membrane (CAM). The ex ovo cultures are returned to an incubator and kept at 38.2 °C and 60% humidity for another 5 days. Then the CAM was observed under microscope, and the neovascularization was quantified. Two independent experiments were performed.

3.16 Transwell migration assay

Cell invasion assay was performed using Transwell chambers (Corning, MA, USA) with 6.5-mm diameter polycarbonate filters (8 μm pore size). HUVECs (2 X 10^4 cells/well) suspended in 100 μl serum free RPMI1640 medium were seeded to each insert (upper chamber), and the bottom chamber contained 600 μl of complete RPMI1640 medium supplemented with 10 nM 17β-E2. RESV and PTER-ITC at different concentrations (5–20 μM) was added into the medium of lower and upper chambers. The plate was then placed at 37°C in 5% CO2/95% air for 12 h. Thereafter the non-migrating cells were removed from the upper surface of the membrane by gentle scrubbing using cotton tipped swabs. Migrated cells on the lower surface of membrane were then fixed with cold 4% paraformaldehyde, permeabilized with 100% methanol and stained with giemsa stain for 15 minutes and finally washed with PBS. Afterward, the filter was mounted onto glass slides and the invasive cells on the lower side of the filter were counted under 100X magnification from three random fields. Migration was normalized to percent migration, with migration in the presence of 17β-E2 representing the scale of 100%.

3.17 Transformation of bacterial cells

All the procedures were strictly performed under sterile conditions. DH5α strain of *Escherichia coli* was grown at 37 °C and 250 rpm in shaker incubator to an OD_{600} of 0.8. The culture was then allowed to chill at 4 °C in a pre-chilled falcon tube. These cells were pelleted at 5000 rpm for 10 min at 4 °C and re-suspended in 35 mL of pre-chilled 80 mM $CaCl_2$ and 20 mM $MgCl_2$ solution. The cells were then re-pelleted and suspended in 2 mL of 0.1 M $CaCl_2$ to obtain the competent cells. An aliquot of these cells were added with 5 ng of plasmid DNA, mixed well and incubated at 4 °C for 30 min. Proper negative and positive controls with no plasmid and known plasmids respectively were included to ascertain the transformation procedure. The cells were subjected to heat shock at 42 °C for 90 sec and immediately transferred to ice. LB broth was added to each tube and incubated at 37 °C for 45 min. The

transformed cells were finally spread plated on antibiotic containing plates corresponding to the antibiotic resistant gene in the plasmid. The plates were incubated overnight at 37 °C.

3.18 Plasmid isolation

The transformed bacteria were inoculated in LB broth containing an antibiotic and incubated overnight at 37 °C and 250 rpm in shaker incubator. A small aliquot of 1.5 mL culture was pelleted by centrifugation at 5000 rpm for 10 min and the bacterial pellet was resuspended in 100 µL of 50 mM glucose, 25 mM TrisCl (pH 8.0), 10 mM EDTA (pH 8.0) solution. To the suspended cells, 200 µL of freshly prepared 0.2 N NaOH, 1% SDS solution was added and mixed by inverting the tube gently and then incubated for 5 min at room temperature. After the incubation, 150 µL of ice-cold 5 M potassium acetate (pH 4.7) solution was added and the tubes were incubated on ice for 10 min. The solution was then centrifuged at 15,000 rpm for 15 min, at 4 °C and the supernatant was precipitated for the plasmid DNA by adding two volumes of ethanol. The DNA was pelleted at 14,000 rpm for 20 min at 4 °C. Finally, the pellet was washed with 70% (v/v) ethanol, re-pelleted, air dried and finally suspended in nuclease free water. The quality of the plasmid DNA was confirmed by running the DNA on the agarose gel.

3.19 Quantification of DNA using spectrophotometer

For this estimation 2 µL of the DNA/RNA sample was diluted in 1 mL of nuclease free water and its OD was determined at 260 nm and 280 nm against nuclease free water as blank. The ratio of the OD260/OD280 was calculated to check the purity of the nucleic acid. The quantity of DNA and RNA was calculated using the standard value-

For DNA: 1 OD_{260} nm = 50 µg/ mL

For RNA: 1 OD_{260} nm = 33 µg/ mL

3.20 Transfection of DNA into mammaliam cell lines

The day before transfection, 8×10^5 cells per 60 mm dish were seeded in complete growth media. The cells were then incubated at 37 °C in a 5% CO_2 incubator until they grew to 40-80% confluency on the day of transfections. Then, 2.5 µg of DNA was dissolved in TE buffer pH 7.0 (minimum DNA concentration of 0.1 µg/µL) and diluted with cell growth medium without serum or antibiotic to a total volume of 150 µL (in case of co-transfection with two plasmids, the receptor containing plasmid DNA and the reporter plasmid DNA were taken in the ratio of 1:4 concentrations respectively). As an internal control for transfection, β-gal plasmid was also transfected with the luciferase reporter plasmids. The solution was mixed and

spun down for a few seconds. Then 15 µL of polyfect reagent (Superfect transfection reagent, Qiagen, CA, USA) was added to the DNA solution and mixed well by pipetting up and down several times. The samples were then incubated for 5 to 10 min at RT to allow the complex formation. During the incubation, the cell medium was aspirated from the petriplate and the cells were washed twice with PBS. To the plate, 3 mL of medium was added and then allowed to stand. After the incubation of the transfection mix, 1 mL of complete growth medium was added to it and gently mixed. The whole transfection mix was then added to the petriplate. The plate was gently swirled to ensure uniform distribution of the complexes. The cells were incubated with the complexes at 37 °C and 5% CO_2 for next 24 h.

3.21 Luciferase assay

On completion of treatment the cells were lysed with the lysis buffer containing 0.6 M NaCl, 0.1 M EDTA, 0.2 M $MgSO_4$, 0.2 M DTT, Triton X-100 and 0.08 M Tricine. The cell lysates were then analyzed for the relative luciferase activity using luciferin as substrate. The values of luciferase activity for each lysates were normalized to the β-gal activity of the respective lysates. Each experimental point was performed in triplicates. The value of luciferase for each lysates was normalized to the luciferase inductions in response to treated cells and was expressed as fold luciferase activity with respect to vehicle treated cells.

3.22 siRNA transfection

The cells were transfected with siRNAs (at a final concentration of 100 nM) using polyfect transfection reagent (Qiagen, CA, USA) according to manufacturer's instructions. After 24 h of transfection, the cells were washed properly and replaced with fresh medium. The cells were then treated with test compound for 24 h, and finally protein lysates were prepared on completion of treatment followed by immunoblot analysis.

3.23 RNA Isolation

Total RNA was extracted from the treated cells according to the method described earlier [Chomczynski and Sacchi, 1987]. Initially, 1×10^4 cells were seeded in a 6-well plate. After the respective drug treatments the cells were washed twice with PBS and harvested. In case of *in vivo* model, 100 mg of the tissue were taken and powdered in liquid nitrogen. The cells therefore obtained from *in vitro* or *in vivo* were lysed with 0.5 mL of Solution D (4 M guanidinium thiocyanate, 25 mM sodium citrate, 0.5% sodium lauryl sarcosinate and 0.1 M β-mercaptoethanol). Then 50 µl of 2 M sodium acetate (pH 4.0), 250 µl of phenol and 250 µl of choloform mix (chloroform: isoamyl alcohol, 49:1) were sequentially added to the lysate

followed by brief vortexing. The separation of the aqueous and organic phases was achieved by a centrifugation at $14,000 \times g$ for 30 min at 4 °C. The upper aqueous phase which contained total RNA from the cell lysate was collected and the RNA was precipitated with isopropanol at -20 °C overnight. Finally, the RNA pellet was washed twice with 75% ethanol and dissolved in DEPC (diethylpyrocarbonate) treated water. In order to finally obtain the DNA-free RNA, the samples were treated with DNase (5 U/20 μg total RNA) for 30 min followed by phenol-chloroform extraction. This was done in order to remove all traces of genomic DNA contamination in the total RNA isolated. Finally 2 μL of the total RNA isolated was dissolved in nuclease free water and its O.D (optical density) was determined at 260 nm against nuclease free water as blank. The protein contamination in the sample was also measured at an absorbance of 280 nm. The isolated RNA was electrophoresed in a formaldehyde agarose (denatured) gel and observed under an UV illuminator. Finally, the RNA was quantified and stored in -80 °C refrigerator. The RNA samples which had a ratio of $OD_{260} : OD_{280} > 1.8$ was further analyzed by RT-PCR. For RT-PCR, total RNA extracted from the control and test samples were quantified and equal amounts from these samples were then reverse transcribed. The reaction was carried out in two steps: cDNA synthesis and PCR amplification.

3.24 Semi quantitative reverse transcriptase PCR (RT-PCR)

3.24.1 First strand cDNA synthesis (reverse transcription)

As the first step, total RNA was reverse transcribed to form cDNA by adding approximately 100 ng of RNA and sterile water was added to 0.2 mL tubes to bring the volume to 9 μL. To this, 1 μL of Oligo(dT)$_{18}$ primer was added and the vial was placed at 65 °C for 10 min and then at room temperature for another 2 min (to remove any secondary structures). The following reagents were added sequentially–

1 μL RNase inhibitor (10 U/μL)

1 μL DTT (0.1 M)

4 μL RT buffer (5X)

2 μL dNTP mix (30 mM)

0.5 μL M-MuLV Reverse transcriptase (50 U/μL)

1 μL sterile water

The solutions were mixed well and incubated at 37 °C for 1 h, followed by incubation at 95 °C to denature RNA-cDNA hybrids. The samples were then spun briefly and quickly placed on ice.

3.24.2 PCR Amplification

All the primers used for PCR were purchased from Ocimum Biosolutions (Hyderabad, India) and are listed in Table 3.1.

PCR amplification for a 25 µL reaction volume with the desired number of cycles was performed by preparing a PCR cocktail consisting of following components:

14.2 µL	sterile water
2.5 µL	10x PCR buffer
1 µL	30 mM dNTP mix
1 µL	Forward primer (100 ng/µL)
1 µL	Reverse primer (100 ng/µL)
0.3 µL	Taq polymerase (3 U/µL)
4 µL	DNA (obtained above)

Once the PCR cocktail was ready, PCR was performed in the thermo cycler machine (PTC-200 thermal cycler, MJ Research, USA) using the following program,

		Temperature	Time
Step1	(Denaturation)	94 °C	2 min
Step2	(Denaturation)	94 °C	45 min
Step3	(Annealing)	** °C	30/45 sec
Step4	(Extension)	72 °C	2 min
Step5	Goto Step2 for 30-35cycles		
Step6	(Final extension)	72 °C	10 min
Step7	End		
Step8	(Product storage)	4 °C	1 h

** annealing temperature depends on the primer length and base composition. The products were stored at -80 °C refrigerator and run in an agarose gel as described below.

3.25 Agarose gel electrophoresis

For a 0.8% gel, 0.4 g of agarose was added to 50 mL 1X TAE Buffer [24.2 g Tris base, 5.71 mL glacial acetic acid, 2 mL of 0.5 M EDTA (pH 8.0) for 100 mL]. The mixture was heated in a microwave oven till the agarose was completely dissolved. Then 2 µL of ethidium bromide (10 mg/mL stock) was added after the solution became lukewarm. This solution was then poured into the gel casting tray fitted with appropriate comb and then allowed to solidify. This gel was used for the submerged electrophoresis for separating the DNA samples using 1X

TAE as the running buffer. DNA samples (isolated plasmids) were mixed with 6X gel loading dye (10 mM TrisCl pH 7.6, 0.03% bromophenol blue, 0.03% xylene cyanol FF, 60% glycerol, 60 mM EDTA pH 8.0) and loaded into the wells. Samples were then electrophoresed at 7-8 V/cm for 1 h till the dye front reached the last one-third of the gel. The agarose gel was observed under UV-visible transilluminator.

3.26 Immunoblotting

For immunoblotting, 5×10^4 cells were plated onto 6-well plates and exposed to test compounds for various time intervals. Cell lysates were prepared by harvesting cells in lysis buffer [20 mM Tris pH 7.2, 5 mM EGTA, 5 mM EDTA, 0.4% (w/v) SDS and 1X protease inhibitor cocktail]. Protein was quantified with a BCA protein estimation kit (Sigma). Total protein samples (~40 μg) were analyzed on 12% polyacrylamide gels, followed by immunoblot analysis using a standard protocol. In brief, the proteins were transferred to nylon membrane, which was blocked with TBS-T buffer (20 mM Tris-HCl, pH 7.5, 150 mM NaCl, 0.05% Tween-20) containing 5% skim milk powder. The blots were washed with TBS-T buffer and incubated (overnight, 4ºC) in the same buffer containing appropriate amount of primary antibodies in a respective dilutions given in Table 3.2. Blots were then washed and incubated with HRP (horseradish peroxidase)-conjugated anti-rabbit or -mouse secondary antibody (1:20,000). Color was developed in the dark using the ECL kit (GE Healthcare, Bucks, UK) and blots were analyzed by densitometry with ImageJ 1.43 using β-actin as internal control.

3.27 Coimmunoprecipitation

The LNCaP cells were plated in 100 mm culture dishes and treated with PTER-ITC or DHT for 24 h. The whole-cell lysates were prepared as described previously [Yuan et al., 2005] in immunoprecipitation (IP) buffer containing 50 mM Tris-HCl (pH 8.0), 150 mM NaCl, 5 mM EDTA, and 1% Triton X-100. Protein aliquots of 500 μg were then incubated overnight at 4°C using 2 μg of antibody directed against AR. The Protein A-Cl Agarose beads were then added and further incubated for 6 h at 4°C. The immunoprecipitates were washed four times with the IP buffer and the immunocomplexes were recovered by boiling in SDS sample buffer. Finally the western blot was carried out using anti-AR, anti-SRC-1 and anti-GRIP-1 antibodies (Santa Cruz, CA, USA).

Table 3.1: List of primers used for semi-quantitative RT-PCR

Primers	Sense (5-3)	Antisense (5-3)	PCR Conditions		Product (bp)
Caspase 8 (Human)	AATGAAAAGCAAA CCTCGGG	ATGTACCAGGTTC CCTCTGCA	94 ^{o}C 1 min, 57 ^{o}C 45 sec, 72 ^{o}C 2 min	30 cycles	600
Caspase 9 (Human)	TGGTGGAAGAGCT GCAGGT	TGGGCAAACTAGA TATGGCGT	94 ^{o}C 45 sec, 60 ^{o}C 45 sec, 72 ^{o}C 2 min	30 cycles	500
Bcl2 (Human)	CGACTTTGCAGAG ATGTCCA	ATGCCGGTTCAGG TACTCAG	94 ^{o}C 45 sec, 58 ^{o}C 45 sec, 72 ^{o}C 2 min	25 cycles	148
Bax (Human)	TGCAGAGGATGAT TGCTGAC	GAGGACTCCAGCC ACAAAGA	94 ^{o}C 45 sec, 60 ^{o}C 45 sec, 72 ^{o}C 2 min	25 cycles	317
DR-5 (Human)	AAGACCCTTGTGCT CGTTGT	GACACATTCGATG TCACTCCA	94 ^{o}C 45 sec, 61 ^{o}C 45 sec, 72 ^{o}C 2 min	30 cycles	350
Bcl-Xl (Human)	AACTCTTCCGGGAT GGGGTAA	AATTCTGAGGCCA AGGGAACT	94 ^{o}C 45 sec, 60 ^{o}C 45 sec, 72 ^{o}C 2 min	25 cycles	200
cJUN (Human)	GGAAACGACCTTC TCTGACG	GAACCCCTCCTGC TCATCTGTCACGT TCTT	94 ^{o}C 45 sec, 63 ^{o}C 30 sec, 72 ^{o}C 2 min	30 cycles	316
AIF (Human)	GGATCCTGGGGCC AGGGTACTGAT	CTCGGGGAAGAGT TGAATCACTTC	94 ^{o}C 45 sec, 61 ^{o}C 45 sec, 72 ^{o}C 2 min	30 cycles	550
AR (Human)	TCCATCTTGTCGTC GTCTTCGGAA	GGGCTGGTTGTTG TCGTGT	94 ^{o}C 45 sec, 57 ^{o}C 45 sec, 72 ^{o}C 2 min	25 cycles	250

PTEN (Human)	ACCAGGACCAGAG GAAACCT	GCTAGCCTCTGGA TTTGACG	94 ^{o}C 45 sec, 58 ^{o}C 45 sec, 72 ^{o}C 2 min	28 cycles	241
PPARγ (Human)	TCTGGCCCACCAAC TTTGGG	CTTCACAAGCATG AACACCA	94 ^{o}C 45 sec, 55 ^{o}C 45 sec, 72 ^{o}C 2 min	28 cycles	360
COX-2 (Mouse)	GGAGAGACTATCA AGATAGT	ATGGTCAGTAGAC TTTTACA	94 ^{o}C 45 sec, 60 ^{o}C 45 sec, 72 ^{o}C 2 min	30 cycles	861
iNOS (Mouse)	AATGGCAACATCA GGTCGGCCATCACT	GCTGTGTGTCACA GAAGTCTCGAACT C	94 ^{o}C 45 sec, 60 ^{o}C 45 sec, 72 ^{o}C 2 min	30 cycles	454
Bax (Mouse)	GTTTCATCCAGGAT CGAGCAG	CATCTTCTTCCAG ATGGTGA	94 ^{o}C 45 sec, 53 ^{o}C 45 sec, 72 ^{o}C 2 min	30 cycles	487
TRAP (Mouse)	GGTAATGGCTGAG GCAGGAT	CACAAGCCGCCCA ATCTTTC	94 ^{o}C 45 sec, 63 ^{o}C 30 sec, 72 ^{o}C 1 min	30 cycles	475
NAFTC1 (Mouse)	CAGGACCCGGAGT TCGACTT	CTTCGGGGAAAAC CCTCCTC	94 ^{o}C 45 sec, 64 ^{o}C 30 sec, 72 ^{o}C 1 min	30 cycles	620
MMP-9 (Mouse)	CTGTCCAGACCAA GGGTACAGCCT	GTGGTATAGTGGG ACACATAGTGG	94 ^{o}C 45 sec, 60 ^{o}C 30 sec, 72 ^{o}C 1 min	30 cycles	263
Cathepsin K (Mouse)	AATGGCAACATCA GGTCGGCCATCACT	GCTGTGTGTCACA GAAGTCTCGAACT C	94 ^{o}C 45 sec, 63.5 ^{o}C 30 sec, 72 ^{o}C 1 min	30 cycles	513
c-Fos (Mouse)	GTCGACCTAGGGA GGACCTT	AGGCCTTGACTCA CATGCTC	94 ^{o}C 45 sec, 60 ^{o}C 30 sec, 72 ^{o}C 1 min	30 cycles	209

VEGF **(Human)**	CTGCTGTCTTGGGT GCATTG	TTCACATTTGTTG TGCTGTAG	94 ^{o}C 45 sec, 57 ^{o}C 45 sec, 72 ^{o}C 2 min	35 cycles	378
VEGFR1 **(Human)**	CTAGGATCCGTGA CTTATTTTTTCTCA ACAAGG	CTCGAATTCAGAT CTTCCATAGTGAT GGGCTC	94 ^{o}C 45 sec, 62 ^{o}C 45 sec, 72 ^{o}C 2 min	35 cycles	241
VEGFR2 **(Human)**	CCTGGGGTAAAGA TTGATGAAG	AGTTGGGGTGTGG ATGCT	94 ^{o}C 45 sec, 65.3 ^{o}C 45 sec, 72 ^{o}C 2 min	35 cycles	776
CD31 **(Human)**	CAACGAGAAAATG TCAGA	GGAGCCTTCCGTT CTAGAGT	94 ^{o}C 45 sec, 57 ^{o}C 45 sec, 72 ^{o}C 2 min	30 cycles	259
vWF **(Human)**	GTTCGTCCTGGAAG GATCGG	CACTGACACCTGA GTTGAGAC	94 ^{o}C 45 sec, 60 ^{o}C 45 sec, 72 ^{o}C 2 min	30 cycles	697
β-Actin **(Human)**	TCACCCACACTGTG CCCCATCTACGA	CAGCGGAACCGCT CATTGCCAATGG	94 ^{o}C 45 sec, 57 ^{o}C 45 sec, 72 ^{o}C 1 min	20 cycles	300

Table 3.2 List of primary antibodies used for western blotting

Primary antibody	Cat # Santacruz	Dilutions	Secondary antibody	Dilutions	Chromogen
Caspase 3	SC-7148	1: 500	Anti-rabbit	1:20000	ECL
Caspase 9	SC-7885	1: 500	Anti-rabbit	1:20000	ECL
Bcl-2	SC-492	1: 500	Anti-rabbit	1:20000	ECL
Bax	SC-526	1: 500	Anti-rabbit	1:20000	ECL
PTEN	SC-7974	1: 500	Anti-mouse	1:20000	ECL
Survivin	SC-17779	1: 500	Anti-mouse	1:20000	ECL
p-53	SC-126	1: 500	Anti-mouse	1:20000	ECL
AIF	SC-9416	1: 500	Anti-goat	1:20000	ECL
Bcl-Xl	SC-8392	1: 500	Anti-mouse	1:20000	ECL
AR	SC-816	1: 500	Anti-rabbit	1:20000	ECL
PPARγ	SC-7273	1: 500	Anti-mouse	1:20000	ECL
COX-2	SC-1745	1: 500	Anti-goat	1:20000	ECL
iNOS	SC-651	1: 500	Anti-rabbit	1:20000	ECL
VEGF	SC-507	1: 500	Anti-rabbit	1:20000	ECL
TSP-1	SC-12312	1:500	Anti-goat	1:20000	ECL
SRC-1	SC-8995	1: 500	Anti-rabbit	1:20000	ECL
ERα	SC-542	1: 500	Anti-rabbit	1:20000	ECL
ERβ	SC-8974	1: 500	Anti-rabbit	1:20000	ECL
GRIP-1	SC-8996	1: 500	Anti-rabbit	1:20000	ECL
AKT	SC-1619	1: 500	Anti-goat	1:20000	ECL
p-AKT	SC-7985	1: 500	Anti-rabbit	1:20000	ECL
ERK	SC-154	1: 500	Anti-rabbit	1:20000	ECL
p-ERK	SC-7383	1: 500	Anti-mouse	1:20000	ECL
p-NFκB p65	SC-101749	1: 500	Anti-rabbit	1:20000	ECL
p-IκB-α	SC-101713	1: 500	Anti-rabbit	1:20000	ECL
p-JNK	SC-6254	1: 500	Anti-mouse	1:20000	ECL
p-p38	SC-17852	1: 500	Anti-rabbit	1:20000	ECL
β-actin	SC-130656	1: 1000	Anti-rabbit	1:20000	ECL

3.28 Immunofluroscence

For immunofluorescence staining, the cells were washed with PBS, fixed in 3% paraformaldehyde, permeabilized with 0.1% Triton X-100 and finally blocked with 1% BSA for 30 min at room temperature. The cells were then incubated with primary antibody of Cytochrome-c, AR, PPAR-γ, COX-2, p-NFκB and p-IκBα diluted 1:200 in blocking buffer for 1 h at RT. Finally, the cells were washed with PBS and incubated with FITC-labelled anti-rabbit secondary antibody diluted 1:1000 in blocking buffer for 30 min at room temperature and then washed with PBS to remove the excess unbound antibodies. The cells were then visualized and imaged under a fluorescence microscope (Zeiss, Axiovert 25, Germany).

3.29 Electrophoretic mobility shift assay (EMSA)

EMSAs were performed to measure the DNA-binding ability of selected protein (transcription factor) and double-stranded oligonucleotides taken from the promoters of respective target genes. For this 10 μg nuclear extracts prepared from RAW 264.7 cells were incubated in a total volume of 15 μL at room temperature for 30 min in 5X binding buffer (750 mM KCl, 0.5 mM dithiothreitol, 0.5 mM EDTA, 50 mM Tris, pH 7.4) and 1 μM concentration of double-stranded oligonucleotide. Then, 15 μL of the EMSA reaction was loaded onto a 6% of native polyacrylamide gel, and electrophoresis was carried out in 1X TBE buffer at room temperature. The gel was analyzed by using a fluorescence based EMSA kit (Molecular Probes, USA). The gels were then stained with fluorescent dyes and visualized by a gel documentation system (BioRad, USA). The oligonucleotide sequences used as probes for EMSA are presented in Table 3.3.

Table 3.3 List of oligonucleotides used as probe for EMSA

Name	Function	Sense Sequence	Annealed with complement
NF-kB binding sequence	NF-kB response element	AGTTGAGGGGACTTTCCC AGGC	GCCTGGGAAAGTCCC CTCAACT
AP1 binding sequence	AP1 response element	GCTTGATGACTCAGCCCG GAAC	GTTCCGGCTGAGTCAT CAAGC

3.30 Histopathology

The tissues from different organs were collected from all groups of animals and fixed in 10% neutral buffered formalin solution. The fixed tissues were dehydrated in series of ethanol gradations from 30 to 100%, then cleared in xylene for 1 h with two changes and finally embedded in wax at 60 ℃ (two changes). Paraffin blocks of tissues were sectioned at 5 µm thickness and fixed on glass slides. The sections were de-paraffinated in xylene followed by hydrations in gradations of alcohol (100-70% ethanol). The slides were kept of 2 min in each of alcohol gradation. Thereafter, the sections were stained with Harry's haematoxylin (30 s) and, washed with tap water (1 min). These sections were again dehydrated in ethanol (70-90%) 2 min each and counter stained with eosin (2 min), followed by dehydration again in 90% and absolute ethanol for 2 min each. The sections were finally passed through xylene (1 min) and mounted with DPX (according to the methods described earlier by Mukherjee, 2003).

3.31 Molecular docking study

Docking simulations were performed with Glide using the Maestro module of the Schrödinger suite (Suite 2011: Maestro v. 9.2, Schrödinger, New York NY). The crystal structure of PPARγ bound to ligand Telmisartan was used as the starting model (PDB ID 3VN2) [Berman et al., 2000]. Using the protein preparation wizard, the complex was prepared by addition of hydrogens and sampling at neutral pH. The structure was refined with the optimized potential for liquid simulations (OPLS) 2005 force field [Jorgenson et al., 1996] and minimized to a root mean square deviation (RMSD) of 0.30Å. The Telmisartan binding pocket, which lies within the protein ligand-binding domain (LBD; residues 225-505), was identified on the PPARγ/Telmisartan complex and the receptor grid was generated. During this process, no Van der Waal radius sampling was done; the partial charge cut-off was set at 0.25 and no constraints were enforced [Sherman et al., 2006]. Ligands under study were drawn with ChemDraw [Mills, 2006] and 3-D structure files were generated at Online SMILES Translator and Structure File Generator (http://cactus.nci.nih.gov/services/translate/), followed by preparation with the Maestro LigPrep wizard. Each ligand was subjected to a full energy minimization in the gas phase employing OPLS2005 force field [Jorgenson et al., 1996], with the generation of structures by different combinations of ionized states and considering all possible tautomeric states in a pH range of 5 to 9. Docking calculations were done using the Extra Precision (XP) mode of Glide [Friesner et al., 2006], maintaining the receptor fixed and ligand flexible. This mode incorporates a more refined and advanced scoring function for

protein-ligand docking, which gives an overall approximation of the ligand binding free energy. The function is given by

$$XPGlideScore = E_{coul} + E_{vdw} + E_{bind} + E_{penalty}$$

where Ecoul is coulomb interaction energy; Evdw is Van der Waals interaction energy; Ebind is binding energy and Epenalty is energy due to disolvation and ligand strain. Finally, post-docking energy minimization was used to improve the geometry of the poses.

3.32 Statistical analysis

Data are expressed as mean ± SEM. The level of statistical significance was determined by one-way analysis of variance (ANOVA) followed by Bonferroni post hoc test for multiple comparison using Graph Pad Prism 5.04 (Graph Pad Software, San Diego, CA, USA). A p-value of less than 0.05 was considered to be statistically significant.

Chapter 4.1 Synthesis and Characterization of PTER and PTER-ITC

4.1.1 Introduction

The word 'Cancer' is not a new challenge for the global biological and biomedical research community. Ever since its first description by the Greek physician 'Hippocrates' about 2500 years ago, the disease has been puzzling the human mind [Hajdu, 2011]. However, in the past 4 decades we have come to know a great deal about cancer, chiefly due to the tremendous advancements in our knowledge of molecular biology, cellular physiology and signaling and the improvements made in laboratory techniques such as those of, molecular probing, profiling, analysis, cell and tissue culture, transgenics, microscopy and medical imaging. Although the number of cancer deaths worldwide has declined from their peak value of 215.1 individuals per 100,000 in 1991 to 173.1 individuals per 100,000 in 2009, the disease is certainly on the rise with 14.1 million cases being diagnosed globally in 2012 [Siegal et al., 2013]. So any research addressing the issue of cancer detection or treatment, would address the cause of these 1.7 million patients and of many more, thus being of utmost relevance to the betterment of global healthcare.

Over the years, the design of cancer chemotherapy has become increasingly sophisticated. Yet there is no cancer treatment that is 100% effective. Currently there is increased interest in use of combination therapy employed by clinicians and scientist all over the world for prevention and cure of cancer. Molecular hybridization (combination therapy) is a new concept in drug design and development which involves conglomeration of two or more pharmacophores in one molecular scaffold to generate a new hybrid compound with improved affinity and efficacy as compared to the parent drugs [Nepali et al., 2014]. The resulting molecule is endowed with multiple biological activities, modified selectivity profile, different or dual modes of action and/or reduced undesired side effects due to mixing of pharmacophores in one molecule. Using this approach, several research groups have designed and synthesized many hybrid molecules by coupling different bioactive group [Vilar et al., 2006; Melagraki et al., 2009; Song et al., 2009; Sashidhara et al., 2010; Wittman et al., 2001; Gupta et al., 2010].

3,5,4′-trihydroxy-trans-stilbene (RESV), a naturally occurring phytoalexin, is the most extensively studied stilbene derivative. This compound was shown to exert several beneficial effects, including anti-inflammatory and cancer chemopreventive activities [Udenigwe et al., 2008, Athar et al., 2007; Brisdelli et al., 2009; Carter et al., 2014]. Structure–activity relationship (SAR) studies, performed on a number of RESV analogues, allowed to establish the chemical features responsible for the antitumor and the proapoptotic activities. In general,

the number and position of the hydroxyl groups present on the benzene rings determine their radical-scavenging activity and cyclooxygenase-2 inhibitory activity, while methoxyl groups are mainly related to their antitumor and apoptosis-inducing activity [Wang et al., 1999; Murias et al., 2004; Murias et al., 2005]. For example, the 3,5-dimethoxyphenyl moiety was identified to play a pivotal role in conferring both the antitumor and the proapoptotic activities [Simony et al., 2006, Roberti et al., 2003; Pettit et al., 2002]. Generally, the presence of a number of methoxy groups seems to be a fundamental requirement to obtain potent cytotoxic agents, and trans-3,5-dimethoxy-4'-hydroxystilbene (PTER) proved to be more potent and selective than the parent resveratrol in the inhibition of the cancer cell growth [Li et al., 2013; Nutakul et al., 2011; Chiou et al., 2011]. PTER is a naturally occurring dimethyl ether analogue of resveratrol, which has higher oral bioavailability and enhanced potency as compared to RESV [Kapetanovic et al., 2011] and proposed to have similar properties as RESV including anticancer, anti-inflammation, antioxidant, apoptosis, antiproliferation, and analgesic potential [Denise and MC Fadden., 2012; McFadden, 2013].

Isothiocyanates $(R–N = C = S)$ (ITC) are known to be the major bioactive compounds present in cruciferous vegetables and responsible for anti-cancer activity [Wu et al., 2009; Adsule et al., 2010; Fimognari et al., 2004; Fimognari et al., 20012]. Many isothiocyanates, both natural and synthetic, display anticarcinogenic activity because they reduce activation of carcinogens and increase their detoxification. Recent studies show that they exhibit anti-tumor activity by affecting multiple pathways including apoptosis, MAPK signaling, oxidative stress, and cell cycle progression [Wu et al., 2009; Fimognari et al., 2004; Fimognari et al., 20012]. Due to such versatile effects on tumor signaling and proliferation, they are considered to be one of the most promising chemopreventive and therapeutic anticancer agents. However, the existing literatures are somewhat ambiguous about the chemopreventive activity of ITC which suggests that not all of them are suitable for their use as chemopreventive agents [Fimognari et al., 2004]. Due to their electrophilic reactivity, some ITCs are able to form adducts with DNA and induce mutations and chromosomal aberrations [Fimognari et al., 2012]. PTER, on the other hand, has not yet been reported to have any genotoxic effects. Based on these reports we hypothesized that by combining PTER with ITC, the newly developed conjugate molecule could bypass some of their individual toxic effects and at the same time would complement each other for inhibition of cancer.

Hence, inspired by this we have synthesized and characterized a novel compound that have both PTER and ITC entities in one molecule and have evaluated them for their anticancer and anti-inflammatory potential. The present chapter deals with synthesis and characterization

of this novel PTER-ITC conjugate. In the second part of the present chapter, this novel compound along with the parent molecule PTER was tested for cytotoxic properties against different cancer cells with major focus on breast and prostate cancer.

4.1.2 Brief Methodology

4.1.2.1 General

Unless otherwise mentioned, all reactions were performed in oven-dried glassware. All starting materials and reagents were obtained from commercial suppliers (Acros, Aldrich) and used without further purification. Solvents used in the reactions were purified before use. Tetrahydrofuran was distilled from sodium and benzophenone. Dichloromethane was distilled over P_2O_5 and dimethylformamide was distilled over CaH_2. Reactions were monitored by thin-layer chromatography (TLC) carried out on 0.25 mm E. Merck silica gel plates (60F-254) using UV light as visualizing agent. Silica gel (particle size 100-200 mesh) was used for column chromatography.

4.1.2.2 Synthesis of compounds

5-Bromo-2-hydroxybenzaldehyde
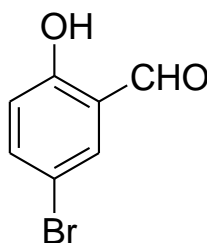
To a mechanically stirred solution of anhydrous magnesium dichloride (4.76 g, 50 mmol), solid paraformaldehyde (2.25 g, 75 mmol) and triethylamine (5.06 g, 50 mmol) in dry tetrahydrofuran (100 mL) was added a solution of 4-bromophenol (4.32 g, 25 mmol) in tetrahydrofuran (50 mL) at room temperature, resulting in an opaque, light pink mixture. When this mixture was immersed in an oil bath at about 70 °C (bath temperature), soon it turned into a bright orange color. The reaction mixture was stirred for 4 h at the same temperature then the reaction mixture was cooled to room temperature and 50 mL of diethyl ether was added. The resulting mixture was washed successively with 1N HCl (3 x 50 mL) and water (3 x 50 mL), dried over anhydrous sodium sulfate, and filtered. The solvent was evaporated in vacuo and the compound was purified by silica gel column by using 10% ethyl acetate/hexanes as eluent; yield: 4.25 g (84%) as pale yellow color solid, m.p. 54-55 °C (lit[1]: m.p. 52-53 °C).

^{1}H NMR (500 MHz, CDCl$_3$): δ = 11.60 (br s, 1H), 9.85 (s, 1H), 6.94 (t, J = 7.8 Hz, 1H), 7.55 (dd, J = 7.5, 1.5 Hz, 1H), 7.75 (dd, 7.5, 1.5 Hz, 1H) ppm. ^{13}C NMR (125 MHz, CDCl$_3$): δ = 196.0, 157.9, 139.9, 133.0, 121.2, 120.7, 111.0 ppm.

1,3-Dimethoxy-5-vinylbenzene
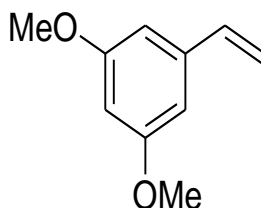
To a suspension of methyl triphenylphosphonium bromide (23.2 g, 65 mmol) in dry THF (100 mL), potassium *tert*-butoxide (8.5 g, 76 mmol) was added in one portion. The mixture was stirred for 2 h at room temperature, then cooled to -70 to -80 °C. Then a solution of 3,5-dimethoxybenzaldehyde (9.0 g, 54.2 mmol) in dry THF (50 mL) was added dropwise at -70 to -65 °C. After the addition, the cooling bath was removed, and the mixture was allowed to warm to room temperature. Now, the reaction was quenched with dry MeOH (10 mL). The volatiles were removed under reduced pressure and the residue was passed through a short pad (6 cm) of silica gel using hexanes/ethyl acetate, 15:1 as eluent to give 8.54 g (96%) of 3,5-dimethoxystyrene as a colorless oil.

^{1}H NMR (500 MHz, CDCl$_3$): δ = 6.66 (dd, J = 17.5, 10.5 Hz, 1H), 6.59 (d, J = 2.5 Hz, 2H), 6.41 (t, J = 2.5 Hz, 1H), 5.75 (dd, 17.5, 10.5 Hz, 1H), 5.26 (dd, J = 17.5, 10.5 Hz, 1H), 3.80 (s, 6H) ppm; ^{13}C NMR (125 MHz, CDCl$_3$): δ = 160.8, 139.5, 136.8, 114.2, 104.2, 99.9, 55.1 ppm.

4-Hydroxy-3',5'-dimethoxystilbene
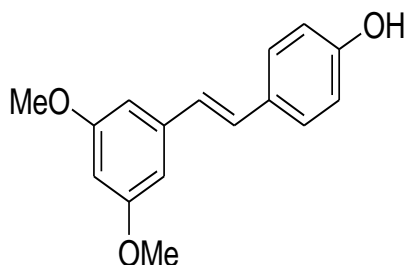
A solution of 1,3-dimethoxy-5-vinylbenzene (1.14 g, 7 mmol), 4-bromophenol (0.86 g, 5 mmol), palladium(II) acetate (0.011 g, 1 mol%), tri-*o*-tolylphosphine (0.060 g, 4 mol%) and triethylamine (0.707 g, 7 mmol) in dimethylformamide (20 mL) was stirred at 100 °C under

nitrogen for 6 h. Then the reaction mixture was cooled to room temperature, water (20 mL) was added and the compound was extracted with ethyl acetate (3 x 10 mL). The organic layer was sequentially washed with 1N HCl (3 x 5 mL) and water (3 x 5 mL), dried over anhydrous sodium sulfate and filtered. The solvent was evaporated in vacuo and the compound was purified by silica gel column by using 5% ethyl acetate/hexanes as eluent; yield 8.25 g (66%) as pale yellow color oil.

^{1}H NMR (500 MHz, CDCl$_3$): δ = 7.39 (d, J = 8.5 Hz, 2H), 7.02 (d, J = 16.0 Hz, 1H), 6.88 (d, J = 16.0 Hz, 1H), 6.82 (d, J = 8.5 Hz, 2H), 6.65-6.64 (m, 2H), 6.38 (t, J = 2.5 Hz, 1H), 5.57 (br s, 1H), 3.82 (s, 6H) ppm; ^{13}C NMR (125 MHz, CDCl$_3$): δ = 160.9, 155.5, 139.7, 130.0, 128.7, 128.0, 126.5, 115.6, 104.4, 99.6, 55.4 ppm.

1-Formyl-2-hydroxy-3',5'-dimethoxystilbene
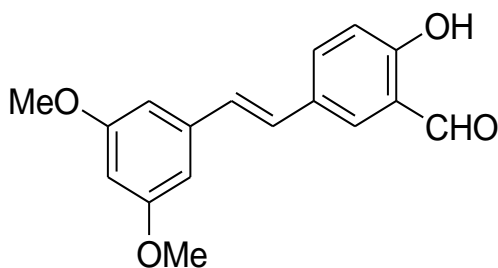
A solution of 1,3-dimethoxy-5-vinylbenzene (1.14 g, 7 mmol), 5-bromo-2-hydroxybenzaldehyde (1.02 g 5 mmol), palladium(II) acetate (0.011 g 1 mol%), tri-*o*-tolylphosphine (0.060 g, 4 mol%) and triethylamine (0.707 g, 7 mmol) in dimethylformamide (20 mL) was stirred at 100 ^{o}C under nitrogen for 6 h. Then the reaction mixture was cooled to room temperature, water (20 mL) was added and the compound was extracted with ethyl acetate (3 x 10 mL). The organic layer was washed with 1N HCl (3 x 5 mL) and followed by water (3 x 5 mL) dried over anhydrous sodium sulfate and filtered. The solvent was evaporated in vacuo and the compound was purified by silica gel column by using 5% ethyl acetate/hexanes as eluent; yield 8.64 g (60%) as pale yellow viscous oil.

^{1}H NMR (500 MHz, CDCl$_3$): δ = 11.01 (br s, 1H), 9.94 (s, 1H), 7.71 (dd, J = 8.5, 2.5 Hz, 1H), 7.66 (d, J = 2.5 Hz, 1H), 7.04 (d, J = 16.0 Hz, 1H), 7.01 (d, J = 8.5 Hz, 1H), 6.95 (d, J = 160. Hz, 1H), 6.66-6.65 (m, 2H), 6.41 (t, 2.5 Hz, 1H), 3.83 (s, 6H) ppm; ^{13}C NMR (125 MHz, CDCl$_3$): δ = 196.6, 161.3, 156.2, 141.6, 128.9, 128.7, 127.6, 126.4, 121.2, 119.7, 109.2, 105.2, 99.5, 55.4 ppm.

Pterostilbene-isothiocyanate conjugate
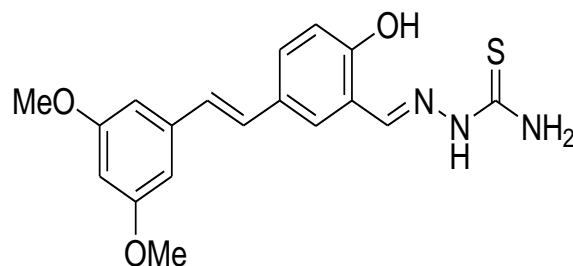
A solution of 1-formyl-2-hydroxy-3',5'-dimethoxystilbene (0.852 g, 3 mmol) and thiosemicarbazide (0.273 g, 3 mmol) in dry methanol (10 mL) was stirred at room temperature for 5 h. The product was precipitated in the reaction medium and filtered. The compound was further purified by recrystallization in methanol.

1H NMR (500 MHz, DMSO-d6): δ = 11.42 (br s, 1H), 9.65 (s, 1H), 7.62 (dd, J = 8.5, 2.5 Hz, 1H), 7.62 (d, J = 2.5 Hz, 1H), 7.01 (d, J = 16.0 Hz, 1H), 6.98 (d, J = 8.5 Hz, 1H), 6.95 (d, J = 16.0 Hz, 1H), 6.67-6.65 (m, 2H), 6.42 (t, J = 2.5 Hz, 1H), 4.24 (br s, 2H), 3.81 (s, 6H) ppm; 13C NMR (125 MHz, DMSO-d6); δ = 191.2, 180.4, 162.2, 157.5, 140.2, 128.7, 127.9, 127.6, 126.4, 122.5, 119.4, 109.3, 105.2, 99.6, 55.3 ppm

4.1.2.3 Instrumentation

4.1.2.3.1 NMR Spectroscopy

NMR spectra were recorded in CDCl3 using TMS as internal standard on Brüker AMX-500 instrument. Chemical shifts of 1H NMR spectra were given in parts per million with respect to TMS and the coupling constant *J* was measured in Hz. The signals from solvent CDCl3, 7.26 and 77.0 ppm, are set as the reference peaks in 1H NMR and 13C NMR spectra, respectively. The signal from solvent DMSO-d6, 2.50 ppm is set as the reference peak in 1H NMR.The following abbreviations were used to explain the multiplicities: s = singlet, d = doublet, t = triplet, q = quartet, m = multiplet, b = broad.

4.1.2.3.2 High-performance liquid chromatography

The LC-2010HT consist of a membrane on-line degasser unit, quaternary low-pressure gradient unit, 2LC-10ADvp pump unit, mixer, ultra fast SIL-10ADvp auto sampler, column oven, a UV-VIS detector (SPD-10A(V) vp with a thermostatted flow cell, and LC solution, DAO (data access objects) 3.5 operating software was from Shimadzu, Kyoto (Japan).

4.1.2.3.3 Mass Spectroscopy

High resolution mass spectra (HRMS) were recorded on microOTOF-Q 11.

4.1.3 Results and Discussion

In the present study we have designed and synthesized PTER and its novel conjugate using the method described above. Both the synthesized compounds were characterized by 1H NMR, 13C NMR, HRMS, HPLC and IR. The detailed scheme for the synthesis of PTER and PTER-ITC is shown in Fig. 4.1.1.

(A)

(B)
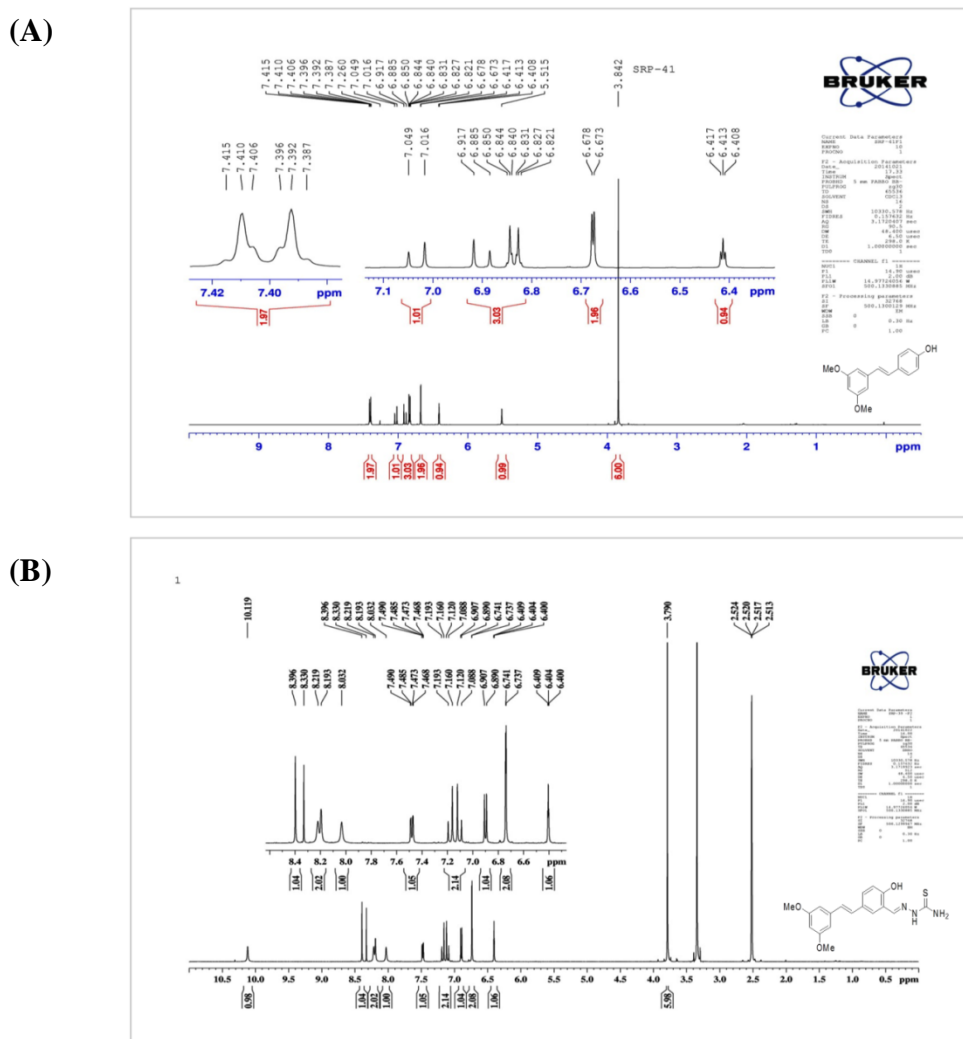
Figure 4.1.2: NMR spectra for (A) PTER and (B) PTER-ITC

4-bromophenol

5- Bromo-2-hydroxybenzaldehyde

3,5-dimethoxybenzaldehyde

1,3-Dimethoxy-5-vinylbenzene

1,3-Dimethoxy-5-vinylbenzene

4-bromophenol

4-Hydroxy-3',5'-dimethoxystilbene (PTER)

5 Bromo-2-hydroxy benzaldehyde

1,3-Dimethoxy-5-vinylbenzene

1 Formyl-2-hydroxy-3',5'dimethoxystilbene

Thiosemicarbazide

1Formyl-2-hydroxy-3',5'-dimethoxystilbene

Pterostilbene-isothiocyanate conjugate (PTER-ITC)

Figure 4.1.1: Scheme for the synthesis of PTER and PTER-ITC

4.1.3.1 HPLC purification

The purity of synthesized PTER and PTER-ITC was checked through HPLC. The elute showed single major peak for both PTER (Fig. 4.1.3A) and PTER-ITC (Fig. 4.1.3B). The purity of both the compound was found to be more than 99%.

(A)

Detector A Ch1 254nm

Peak#	Ret. Time	Area	Height	Area %	Height %
1	7.780	44891927	1052472	99.140	98.940
2	10.149	389257	11273	0.860	1.060
Total		45281183	1063744	100.000	100.000

(B)

Detector A Ch1 254nm

Peak#	Ret. Time	Area	Height	Area %	Height %
1	5.946	123619	2138	0.060	0.054
2	7.610	204934682	3915339	99.142	99.234
3	9.948	1060790	25334	0.513	0.642
4	15.059	589386	2758	0.285	0.070
Total		206708478	3945570	100.000	100.000

Figure 4.1.3: Purity of PTER and PTER-ITC as confirmed through HPLC. The figure represents chromatogram of (A) PTER and (B) PTER-ITC
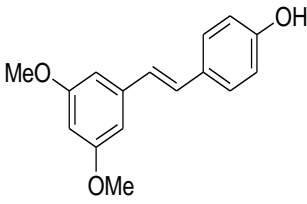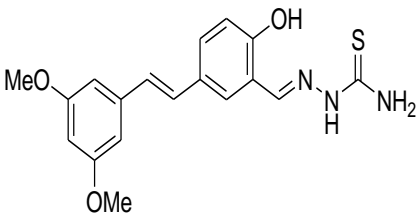
4.1.3.2 Mass spectroscopy

The molecular weight of both PTER and PTER-ITC was further established by HR-MS (Table 4.1.1). The observed molecular weights of PTER (257.11) and PTER-ITC (380.10) are in excellent agreement with the calculated values, which verify the proposed molecular formula for the compound (Fig. 4.1.4A, B).

4.1.3.3 Preparation of the final stock of PTER and PTER-ITC for biological studies

From the mass spectral analysis, the molecular mass of PTER and PTER-ITC was found to be 257.11 and 380.10 respectively. The compounds were further dissolved in DMSO at a concentration of 100 mM. Serial dilutions from the mother stock were made in order to check the biological activities of the compound.

Table 4.1.1 Structure, purity, molecular weight and melting point for PTER and PTER-ITC

Compound	Purity (HPLC)	HRMS	Melting Point
PTER	**> 99%** (99.140%)	Calculated for [C16H16O3+H]: **257.1172** Found: 257.1172	106-108 ^{o}C
PTER-ITC	**> 99%** (99.142%)	Calculated for [C18H19N3O3S+Na]: **380.1039** Found: 380.1039	216-218 ^{o}C

(A)

(B)
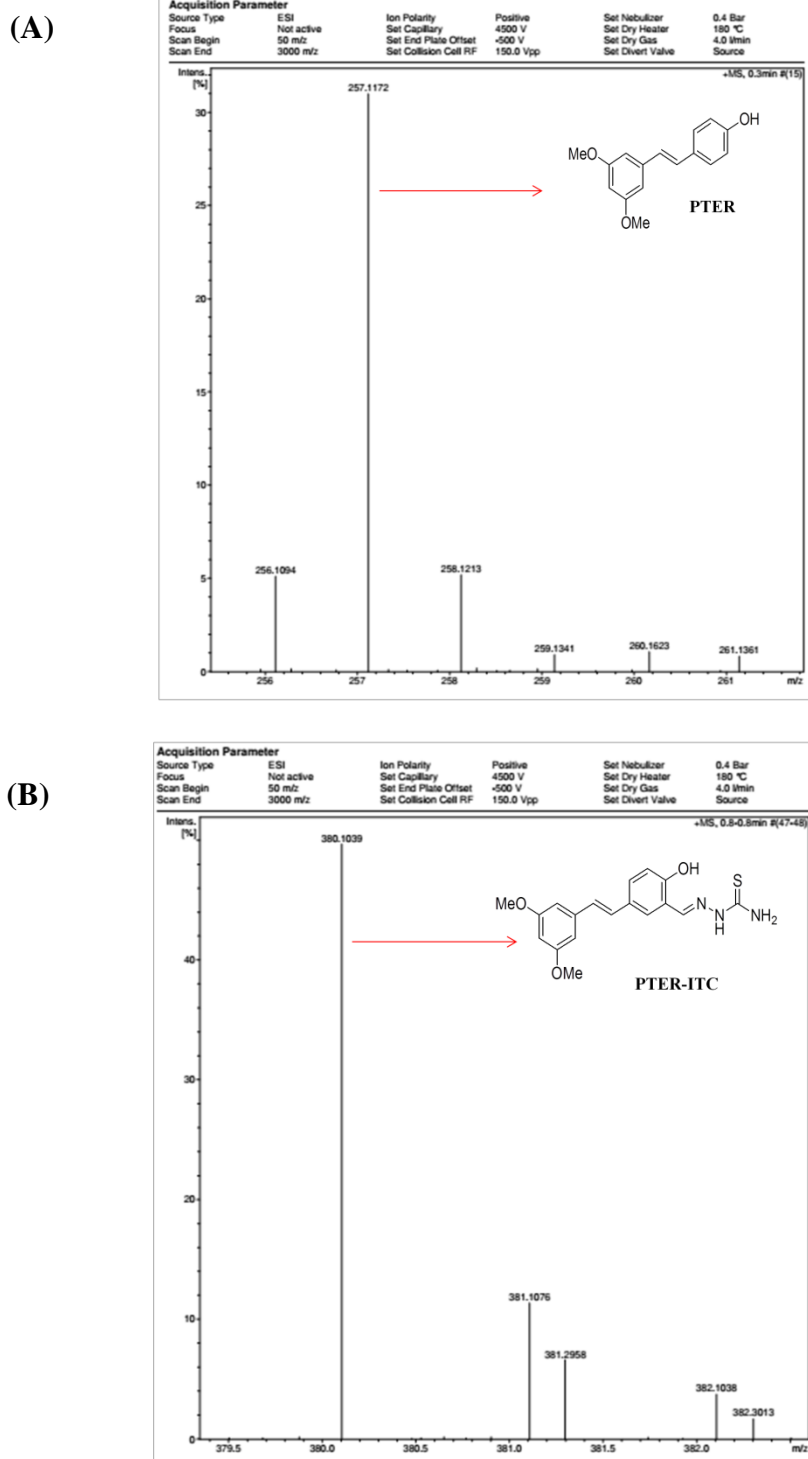
Figure 4.1.4: High resolution mass spectrometry data for (A) PTER and (B) PTER-ITC.

Chapter 4.2 PTER and PTER-ITC as Anti-cancer Agent- A comparative analysis

4.2.1 Introduction

Cancer is a major health problem worldwide and is the leading cause of human mortality exceeded only by cardiovascular disease [Varasmus, 2006]. Most of the currently available anti-cancer drugs fail to differentiate between normal and neoplastic cells or to overcome primary or secondary resistance mechanisms involved in cancer cells. Thus, there is an urgent need of anti-cancer drugs with high potency, less toxicity to non cancerous cells and unique target of actions [Chari, 1998]. Since cancerous cells exhibit deregulation in multiple cell signaling pathways therefore treatments using specific agents that target only one specific pathway usually fails in cancer therapy. Modulating multiple targets simultaneously can be achieved by a combination of multiple drugs with different modes of action or using a single drug that could modulate several targets of multifactorial disease [Sarkar et al., 2009].

Recently the concept of hybrid anti-cancer compound has attracted much attention for tackling the alarming problem of drug resistance, as these molecules often act on multiple therapeutic targets because of the presence of two different covalently fused pharmacophores [Mayur et al., 2009; Solomon et al., 2009]. By adopting this approach, several research groups have recently reported hybrid molecules by coupling different bioactive molecules like isothiocyanate-progesterone conjugate [Adsule et al., 2010], coumarine-chalcone hybrid (Sashidhara et al., 2010), paclitaxel-chlorambucil hybrid [Wittman et al., 2001], estradiol-chlorambucil hybrid [Gupta et al., 2010] and 17β-estradiol-platinum hybrid [Mandeville et al., 2008]. Inspired by this we designed and synthesized a novel compound that has both pterostilbene (PTER) and isothiocyanate (ITC) entities in a single scaffold. The synthesis and characterization of this novel compound has been described in detail in Chapter 4.1. In the present chapter we systematically compared the anticancer effect of PTER and PTER-ITC as an anti-cancer molecule in breast (MCF-7) and prostate cancer (PC-3) cell lines.

PTER, an analogue of resveratrol (RESV), is a phytoalexin polyphenolic compound (trans-3, 5-dimethoxy-4'-hydroxystilbene) isolated from *Pterocarpus marsupium* stem heart wood. This phytochemical has attracted intense interest in recent years because of its diverse pharmacological effects including anti-cancer, anti-proliferative, pro-apoptotic, anti-oxidant, anti-inflammatory, anti-invasive and anti-metastatic functions in a variety of human cancer cell lines *in vitro* and *in vivo* animal models [Paul et al., 2010; Mannal et al., 2010; Schneider et al., 2010; Pan et al., 2009; Pan et al., 2007; Chakraborty et al., 2010; Mena et al., 2012]. The other part of conjugate used in this study was ITC which are naturally occurring small molecules

characterized by the presence of reactive $-N=C=S$ group [Fahey et al., 2001]. These chemo protective agents are formed by hydrolysis of their precursor parent compounds known as glucosinolates found in a wide variety of cruciferous vegetables like broccoli, cauliflower, cabbage, Brussel sprouts and kale [Clarke et al., 2008]. Diets high in ITC containing cruciferous vegetables have been shown to protect against a number of malignancies including non-Hodgkin's lymphoma and the cancers of liver, prostate, ovary, lung, colon and gastro intestinal tract [Murillo and Mehta, 2001].

Based on these prior observations, we postulated that a compound containing both stilbene and ITC pharmacophores could be an effective combination for anti-cancer activity. Herein, we performed an initial comparison on the cytotoxic effect of PTER and its conjugate in different cancer cell lines with a major focus on breast and prostate cancer.

4.2.2 Brief Methodology

4.2.2.1 Test Compounds

PTER and PTER-ITC used in the experiment were synthesized as described previously (Chapter 4.1). 5-Flurouracil (5-FU) was used as positive control for some assay and was purchased from HiMedia (Mumbai, India).

4.2.2.2 Cell lines

In order to test the cytotoxicity of PTER and PTER-ITC a series of cancerous cell lines from different organs were used for initial screening. Human estrogen receptor positive, MCF-7 (adenocarcinoma) and T47D (ductal carcinoma) breast cancer cells; androgen receptor negative, PC-3, and androgen receptor positive, LNCaP, human prostate cancer cells; human lung cancer cells, NCIH-522; human ovarian cancer cells, PA-1 and human liver cancer cells, HepG2 were all obtained from National Center for Cell Science (NCCS),

4.2.2.3 Cytotoxicity assays

Cytotoxicity was determined by the MTT assay as described in Chapter 3 (3.5).

4.2.2.4 Flow cytometry

Induction of apoptosis and cell cycle arrest in MCF-7 and PC-3 cells caused by PTER and PTER-ITC was quantitatively determined by flow cytometry according the procedure described in Chapter 3 (3.6).

4.2.2.5Acridine orange/Ethidium bromide screening assays

The MCF-7 and PC-3 cells were incubated with the test compound for 24 h and thereafter analyzed for chromatin condensation by AO/EB staining and observed under fluorescent microscope. Detailed protocol of the assay is mentioned previously in chapter 3 (3.6.2).

4.2.2.5 DNA fragmentation assay

Single cell gel electrophoresis assay and DNA fragmentation assay were performed according to the methods detailed in Chapter 3 (3.6.4)

4.2.3 Results

4.2.3.1 Estimation of cytotoxicity

The synthesized conjugate molecule (PTER-ITC conjugate) and PTER were initially tested for their cytotoxic activity in selected human cancer cell lines by MTT assay. The results showed that both PTER and PTER-ITC caused a dose dependent inhibition in the viability of the cancer cells. Among these, MCF-7 and HepG2 cells were more sensitive to PTER-ITC and PTER treatment whereas NCIH-522 was least sensitive. As shown in Table 4.2.1, all the cancer cell lines were more sensitive to PTER-ITC treatment as compared to PTER as depicted by the lower IC_{50} values in all of them. Interestingly, in spite of the fact that both T47D and MCF-7 are ER-positive hormone dependent cell lines with additional expression of AR, they showed differential responses to PTER-ITC treatment. This could be attributed to the fact that several classes of proteins are expressed differentially within these two cell lines. For example, while T47D expresses proteins which are specifically involved in cell growth stimulation, anti-apoptosis mechanisms and carcinogenesis (G1/S specific cyclin D3 and prohibitin), in case of MCF-7 cells, proteins implicated in transcriptional repression and apoptotic regulation (NF-X1, nitrilase homolog 2 and interleukin 10) are predominantly expressed (Aka and Lin, 2012). In case of prostate cancer cells, PC-3 cells were more resistant to the PTER-ITC-mediated antiproferative effect than LNCaP cells. Furthermore, when tested in noncancer cell lines like CHO and COS-1, both PTER and PTER-ITC were found to non-toxic at dose below 100 μM. Thus the growth of human cancer cells was apparently more sensitive to PTER-ITC treatment than that of normal cells

Table 4.2.1 Comparison of cytotoxicity caused by PTER and PTER-ITC *in vitro* on different cancer and noncancer cell lines.

Cell lines	IC$_{50}$ Value[a]	
	PTER (μM)[b]	PTER-ITC (μM)[b]
Breast cancer		
(1) MCF-7	65±0.42	25±0.38*
(2) T47d	69±1.58	45±1.15*
(3) MDAMB-231	58±2.21	35±3.18*
Prostate cancer		
(4) LNCaP	70.4±4.39	40±4.12*
(5) PC-3	75±3.55	45±2.0*
Lung cancer		
(6) NCIH-522	85±2.64	80±1.37
Liver cancer		
(7) HepG2	73±1.81	30±3.55*
Ovary cancer		
(8) PA-1	120±2.00	60±3.98*
Non-cancer		
(9) CHO	>100	>100
(10) COS-1	>100	>100

a *50% growth inhibition as determined by MTT assay (24h drug exposure).*
b *Compound tested in triplicate, data expressed as mean value ± SEM of three independent experiments*
* *p<0.001 between PTER and PTER-ITC treated group*

4.2.3.2 Effect of PTER-ITC on the morphological changes of MCF-7 and PC-3 cells

MCF-7 and PC-3 cells were either left untreated (normal media) or exposed to different concentrations (5, 15, 30 and 50 μM) of PTER and PTER-ITC. Thereafter the cells were and examined microscopically for up to 24 h. Marked morphological changes could be observed after 24 h with characteristic shrinkage of cells and loss of original confluent monolayer (Fig. 4.2.1), indicating apoptotic cell death which was more prominent in a dose dependent manner. Those morphological changes, however, were not observed in vehicle treated (control) cells.
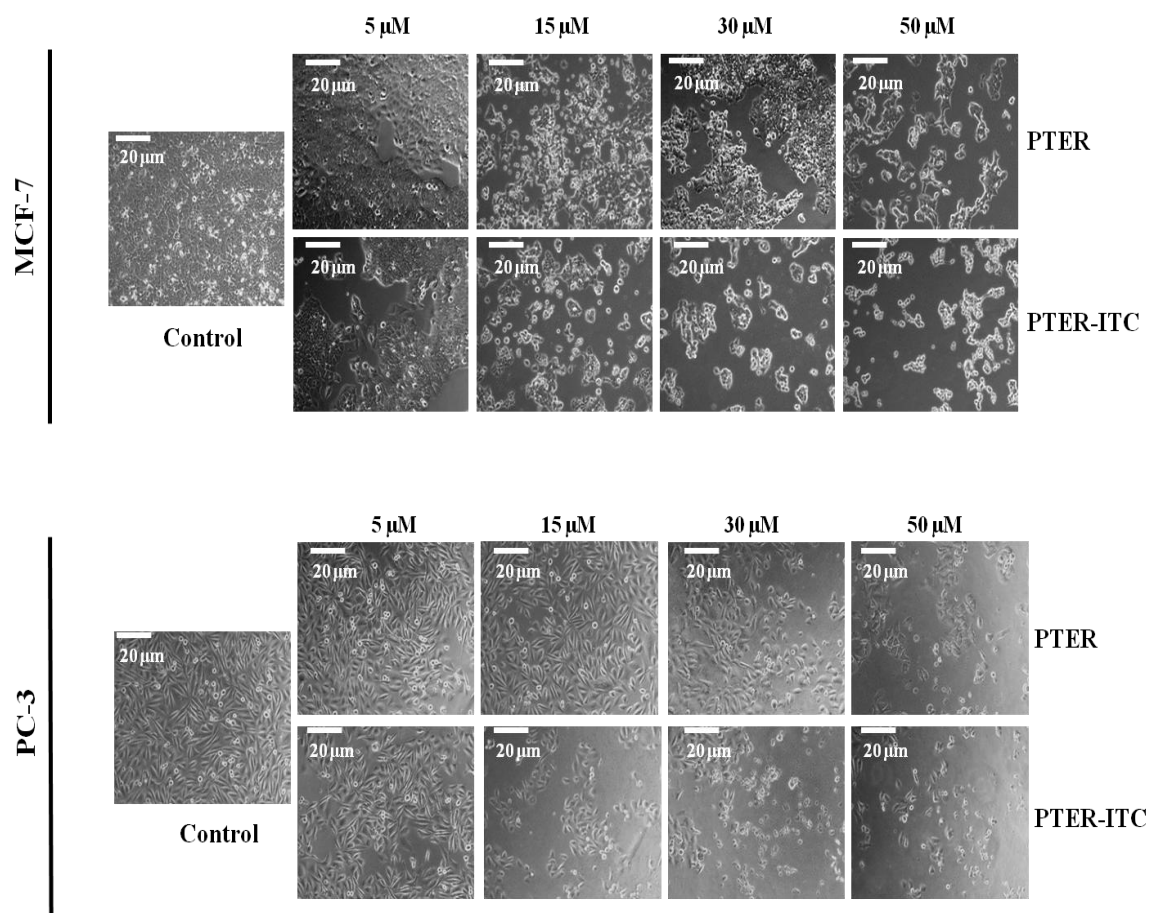
Figure 4.2.1: Effect of PTER and PTER-ITC on the morphology of MCF-7 and PC-3 cells. Cytotoxicity and morphological changes of MCF 7 cells and PC-3 cells treated with PTER and PTER-ITC in a dose dependent (5, 15, 30 and 50 μM) manner as visualized by phase contrast microscope. The data are the representative of four independent experiments.

4.2.3.3 PTER-ITC shows stronger apoptosis inducing effect in breast and prostate cancer cells than PTER

In milieu of the MTT assay results, we extended our study to examine whether breast and prostate cancer cells are undergoing apoptosis after PTER-ITC treatment by using flow cytometry. The number of apoptotic cells was determined as late apoptotic cells shown in upper right quadrant (Q2), and early apoptotic cells as shown in lower right quadrant (Q4) of the fluorescence-activated cell sorting histograms (Fig. 4.4.2A, B). When MCF-7 cells were treated with PTER, PTER-ITC and 5-FU at concentrations of 60, 20 and 55 µM respectively, clear apoptosis was observed after 24 h of incubation. The percentage of total apoptotic cells (sum of early and late apoptotic cells) were found to be 61.5, 47.35 and 56.08% in PTER-ITC, PTER and 5-FU treated cells, respectively, as compared to vehicle treated cells (Fig. 4.2.2A) ($p<0.05$). Similarly in case of PC-3 cells treatment with PTER, PTER-ITC and 5-FU at concentrations of 70, 40 and 65 µM showed 55, 80 and 60% of total apoptotic cells (sum of early and late apoptotic cells) respectively after 24 h of treatment (Fig. 4.2.2B) ($p<0.05$).

Live cells under the stress of early and late apoptosis can also be distinguished by the clear chromatin condensation and percentage uptake of AO: EB dye mixture. AO permeates all cells and makes the nucleus appear green while EB is taken up by the cells only when the cytoplasmic membrane integrity is lost as in late apoptosis or in necrosis staining the nucleus red. As shown in the Fig. 4.2.3, the vehicle treated (control) group had maximum number of viable cells showing acridine orange staining with normal cell morphology. On the contrary, the PTER-ITC, PTER and 5-FU treated cells showed increased number of EB stained cells as compared to vehicle treated cells and out of those, the PTER-ITC showed a marginally higher number of apoptotic cells as compared to other two compounds in both the cancer cells (Fig. 4.2.3).
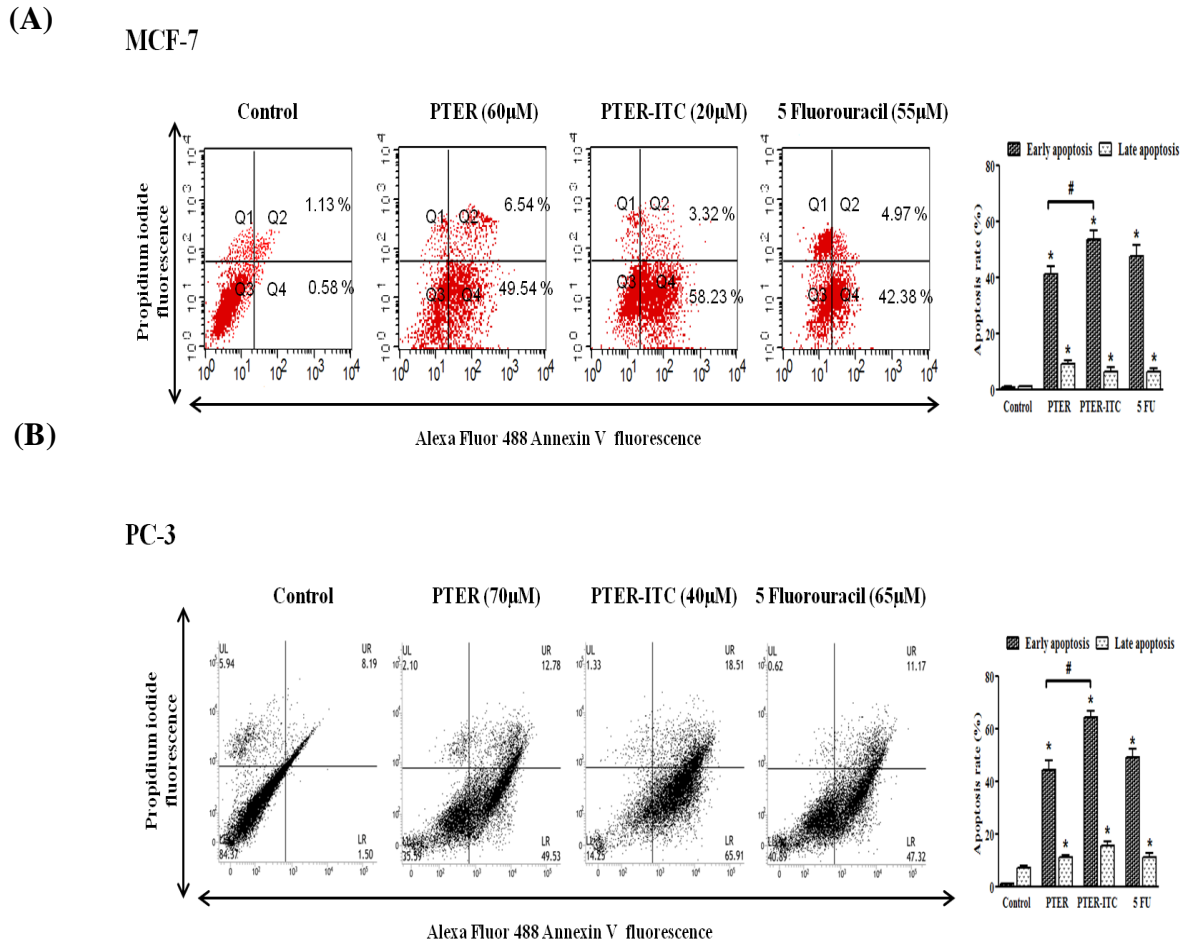
Figure.4.2.2: Effect of PTER and PTER-ITC on apoptosis induction in MCF-7 and PC-3 cells. FACS analysis of (A) MCF-7 and (B) PC-3 cells using Annexin V as marker. Right panel of each figures shows histogram of the analyzed cells in various quadrants. Each bar indicates mean of three experiments; * and # represents statistically significant difference with respect to vehicle and PTER treated cells respectively at $p<0.05$.
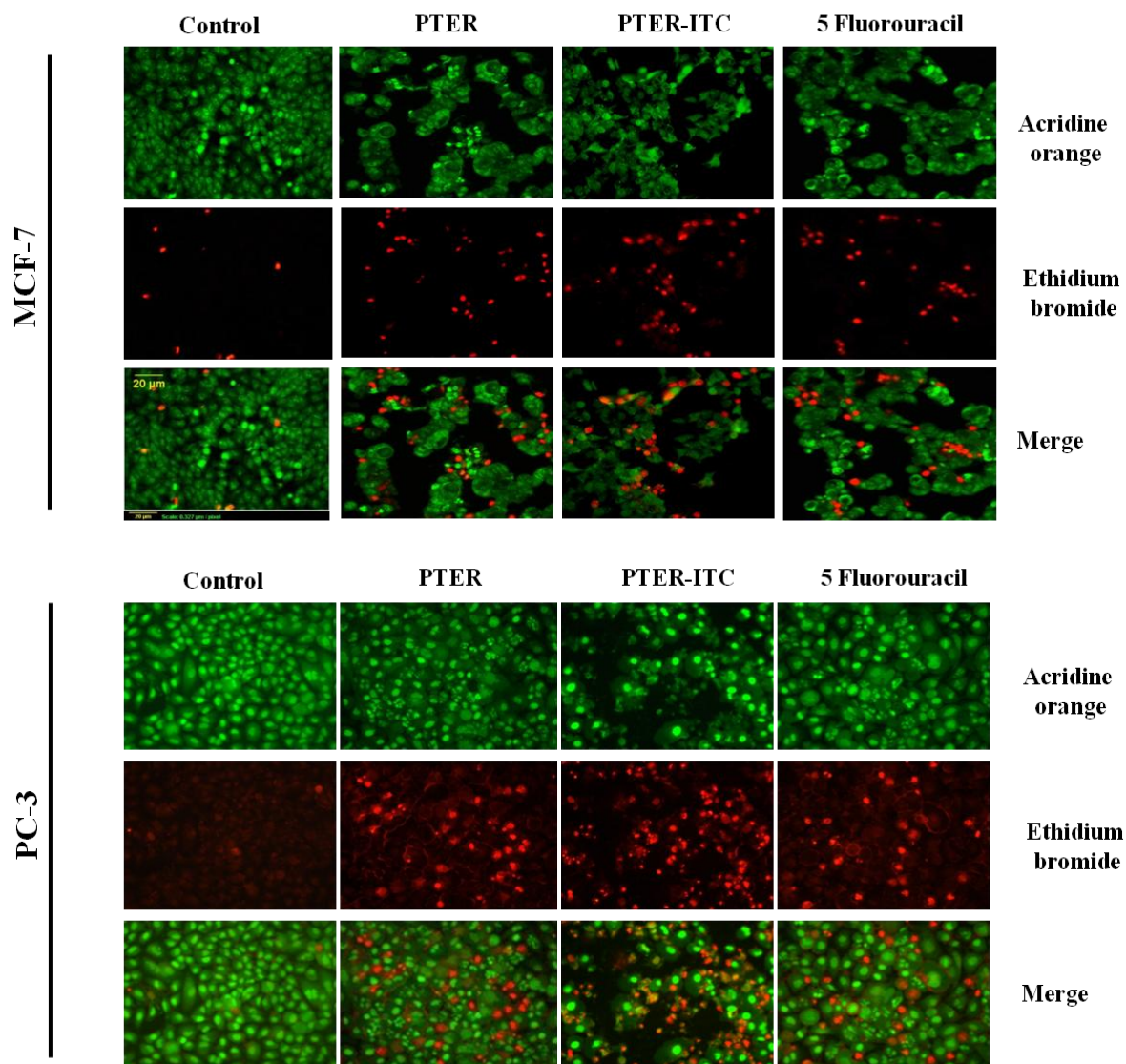
Figure 4.2.3: Evaluation of apoptosis by using Acridine orange/Ethidium bromide staining on MCF-7 and PC-3 cells treated with PTER, PTER-ITC and 5-FU for 24 h. The green staining indicates that the cell membrane integrity does not allow the entrance of ethidium bromide in the cytoplasm. Apoptotic cells are stained in red due to the entrance of the ethidium bromide. The nuclear staining was visualized at 200X magnification of fluorescent microscope. The experiment was performed in triplicate and a representative data are presented. Scale bar represents 20 μm

4.2.3.4 PTER-ITC is more potent than PTER in induction of DNA fragmentation

To further confirm the above results, classical hallmark of apoptosis such as DNA fragmentation assay was carried out. As shown in Fig. 4.2.4A, both PTER-ITC and PTER were almost equally potent and caused an intensified fragmentation of DNA in MCF-7 cells when treated at 20 and 60 μM concentrations respectively. On the other hand, 5-FU showed marginally less DNA fragmentation as compared to other two chemicals. In case of PC-3 cells PTER-ITC at 40 μM showed stronger DNA fragmentation in comparison with PTER and 5-FU (Fig. 4.2.4B).

The above result was further validated by comet assay where a single cell was visualized under fluorescent microscope. Similar to the previous observation, the MCF-7 cells showed a significant DNA damage (Fig. 4.2.4C) as compared to PC3 cells (Fig. 4.2.4D) as shown in single cell gel electorphoresis. The comet tail area of 100 cells showed a significantly high level of DNA tailing in both MCF-7 and PC3 cells ($p<0.05$). The comet tailing was comparatively higher in PTER-ITC treated MCF-7 cells than PC-3 when compared to drug treated groups. Control untreated cells showed no prominent tailing. In case of MCF-7 cells the percentage DNA in each comet tail was found to be 40.06, 33.2 and 32 in PTER-ITC, PTER and 5-FU treated cells, respectively, as compared to 1.22 in vehicle treated cells (Fig. 4.2.3C) ($p<0.001$). On the other hand in case of PC-3 cells, percentage DNA in each comet tail was found to be 27, 19.3 and 15.6 in PTER-ITC, PTER and 5-FU treated cells, respectively, as compared to 1.22 in vehicle treated cells (Fig. 4.2.3D) ($p<0.001$).
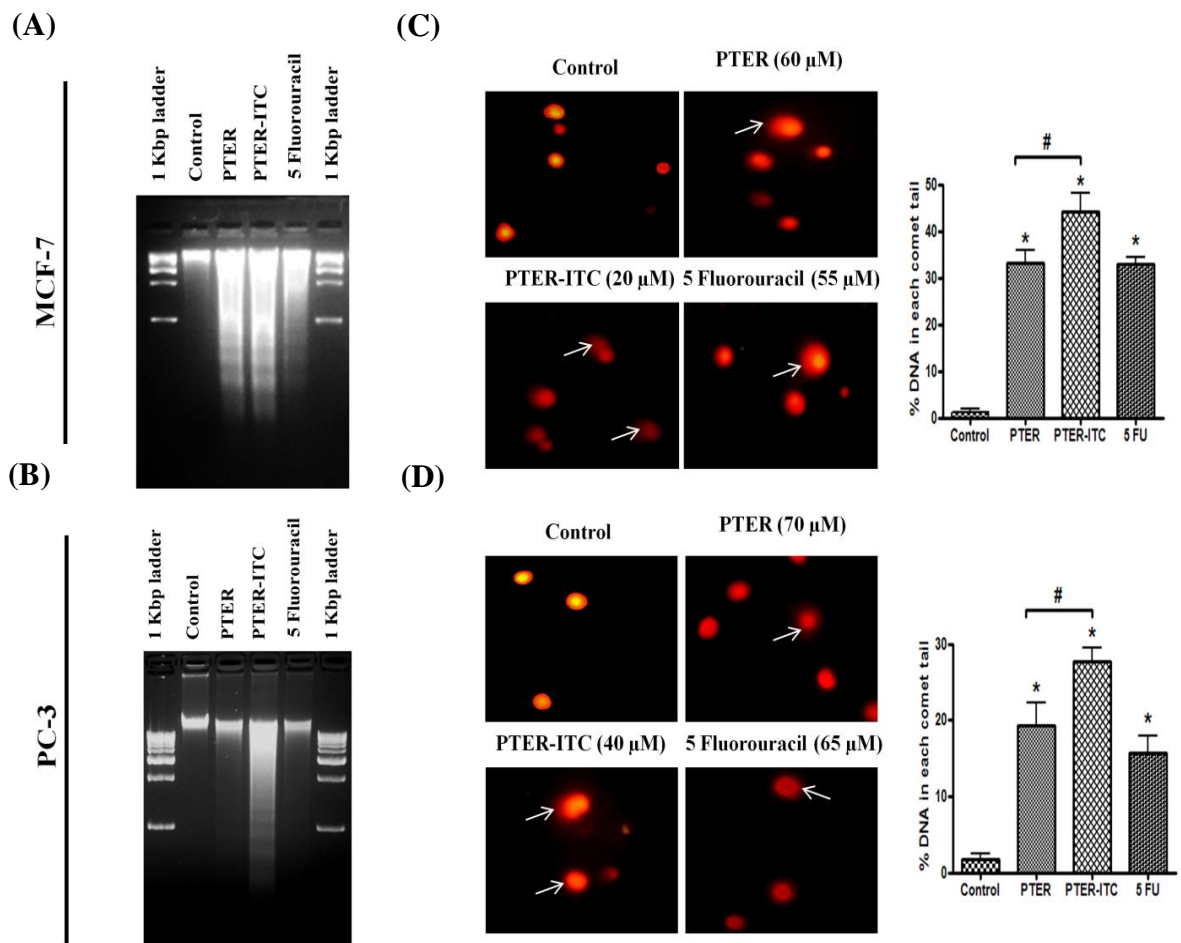
Figure 4.2.4: Induction of DNA fragmentation by PTER and its PTER-ITC in (A) MCF-7 and (B) PC-3 cells. Single cell alkaline gel electrophoresis showing DNA fragmentation in (C) MCF-7 and (D) PC-3 cells. Nuclear staining was visualized under 200X objective of fluorescent microscope. The DNA breaks from individual cells are well visualized as comet tails (marked by arrows). Scale bar represents 20 μm. Histogram on the right shows percentage of DNA in comet tail following PTER and PTER-ITC treatment. * and # indicates statistically significant ($p<0.05$) levels of DNA in comet tail with respect to control and PTER treated cells respectively.

4.2.3.5 PTER-ITC induces G2/M-phases cell cycle arrest in breast and prostate cancer cells

The data presented above clearly suggests that PTER-ITC induced cell death in both breast and prostate cancer cells. In order to test whether the cell death was preceded or accompanied by a growth arrest program, we analyzed the effect of PTER-ITC on cell cycle progression using flow cytometry. Cell cycle distribution analysis showed that PTER-ITC hampered the cell cycle progression by arresting the cells in S and G2/M-phases in both MCF-7 and PC-3 cells (Fig. 4.2.5A, B). On the contrary, PTER caused mainly S-phase arrest of both the breast and prostate cancer cells (Fig. 4.2.4A, B). In MCF-7 cells, after 24 h of treatment the proportion of cells in S-phase increased from 16% (control cells) to 28 and 43% in PTER-ITC and PTER treated cells respectively. Similarly, the cells in G2/M-phase increased from 33% (control cells) to 51 and 37% in PTER-ITC and PTER treated cells respectively. In case of PC-3 cells, after 24 h of treatment the proportion of cells in S-phase increased from 14% (control cells) to 27 and 49% in PTER-ITC and PTER treated cells respectively. Similarly, the cells in G2/M-phase increased from 24% (control cells) to 48 and 20% in PTER-ITC and PTER treated cells respectively. In summary, the data depicts that the PTER-ITC mainly arrests the cells in G2/M-phase while in case of PTER it is predominantly in S-phase.
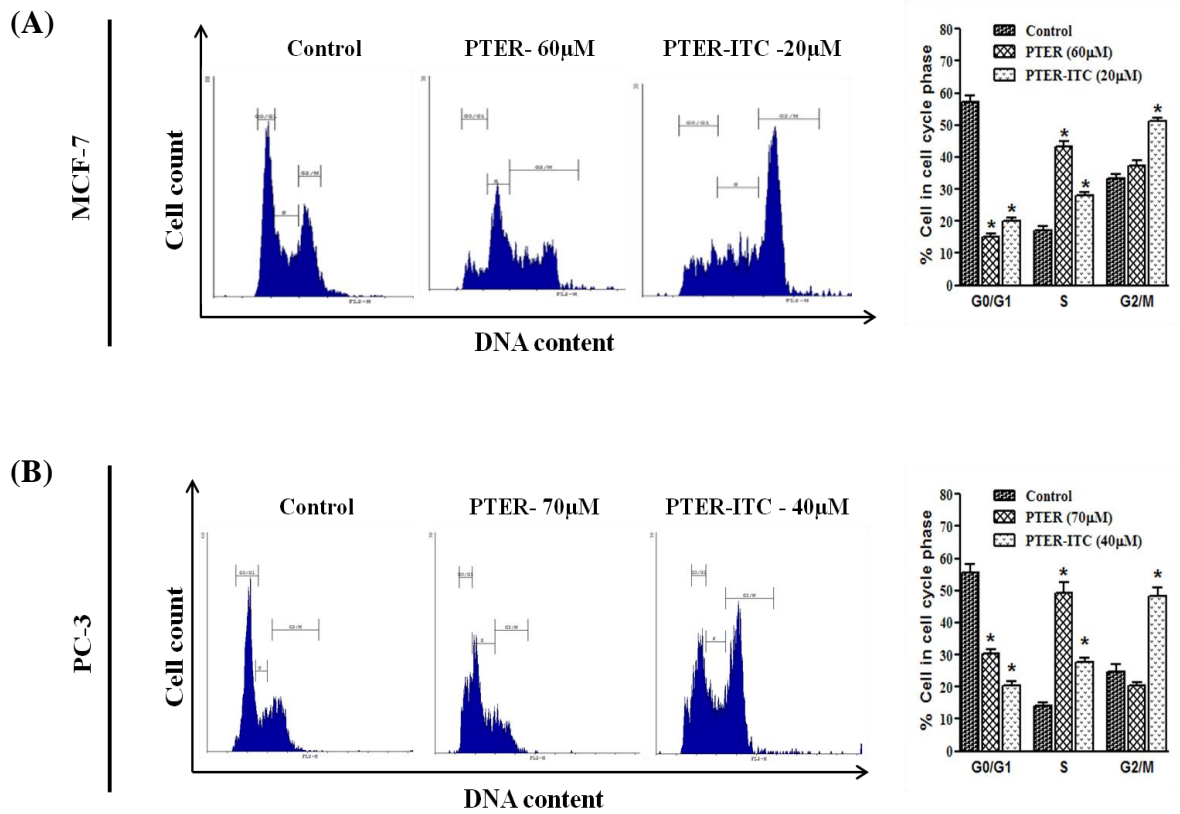
Figure 4.2.5: Cell cycle distribution of (A) MCF-7 and (B) PC-3 cells upon treatment with PTER and PTER-ITC. The right panel represents the histogram of the analyzed data from left panel. Results are presented as means ± SEM of three independent experiments. ∗ indicates $p<0.05$ as compared to respective control.

4.2.3.6 PTER-ITC shows superior anti-metastatic effect than PTER in breast and prostate cancer cells

To ascertain the inhibitory effect of PTER-ITC on cancer metastasis, we investigated the effects of PTER-ITC and normal PTER on the migration potential of MCF-7 and PC-3 cells using the 'wound healing' assay. A 'wound' was created with a pipette tip and the migration of cancer cells to fill up the 'wound' was recorded by microscopic observations. As shown in Fig. 4.2.6A, in case of MCF-7 cells, 24 h after the 'wound' was created the vehicle-treated cells had filled in the cleared area by about 60% while PTER and PTER-ITC showed only 46 and 20% of cell migration respectively in the cleared area. Similarly in case of PC-3 cells the vehicle-treated cells had filled in the cleared area by about 90% while PTER and PTER-ITC showed only 65 and 26% of cell migration respectively in the cleared area (Fig. 4.2.6B). The above data thus suggest that migration of cancer cells were significantly reduced in both PTER-ITC and only PTER treated plates and interestingly it was significantly more prominent in the former as compared to latter (Fig. 4.2.6A, B) (*p<0.05*).

4.2.4 Discussion

Since most of the existing treatment options for breast and prostate cancer resulted in partial fulfillment of their efficacies, there is an urgent need to develop novel preventive approach for this malignancy. One such strategy involved chemoprevention using non-toxic, naturally occurring and/ synthetic agents. PTER, a natural dimethylated analog of RESV, has been recently considered to be one such compound. We have previously established that PTER is a potent anti-cancer molecule having multiple targets of actions [Chakraborty et al., 2010; Chakraborty et al., 2012]. In continuation to that, the present study was aimed to check if modification of this compound by conjugating ITC group to it may further improve the efficacy of this molecule as an anti-cancer agent. The present data clearly showed that PTER-ITC conjugate, a hybrid molecule between PTER and ITC, exhibited more potent anti-proliferative and pro-apoptotic effects *in vitro* at a comparatively lower dose as compared to its parent molecule, PTER.

We determined the inhibitory effects of PTER-ITC and PTER on the growth of human cancer cells of different organ like breast, prostate, liver, lung, ovary etc. These cells have different genetic aberrations and gained different growth aggressiveness. In the present study the cell proliferation assay data showed that the PTER-ITC molecule was more effective at a comparatively lower dose than PTER in various cancer cell lines tested (Table 4.2.1). These data are consistent with various other conjugate molecules already under investigation for their
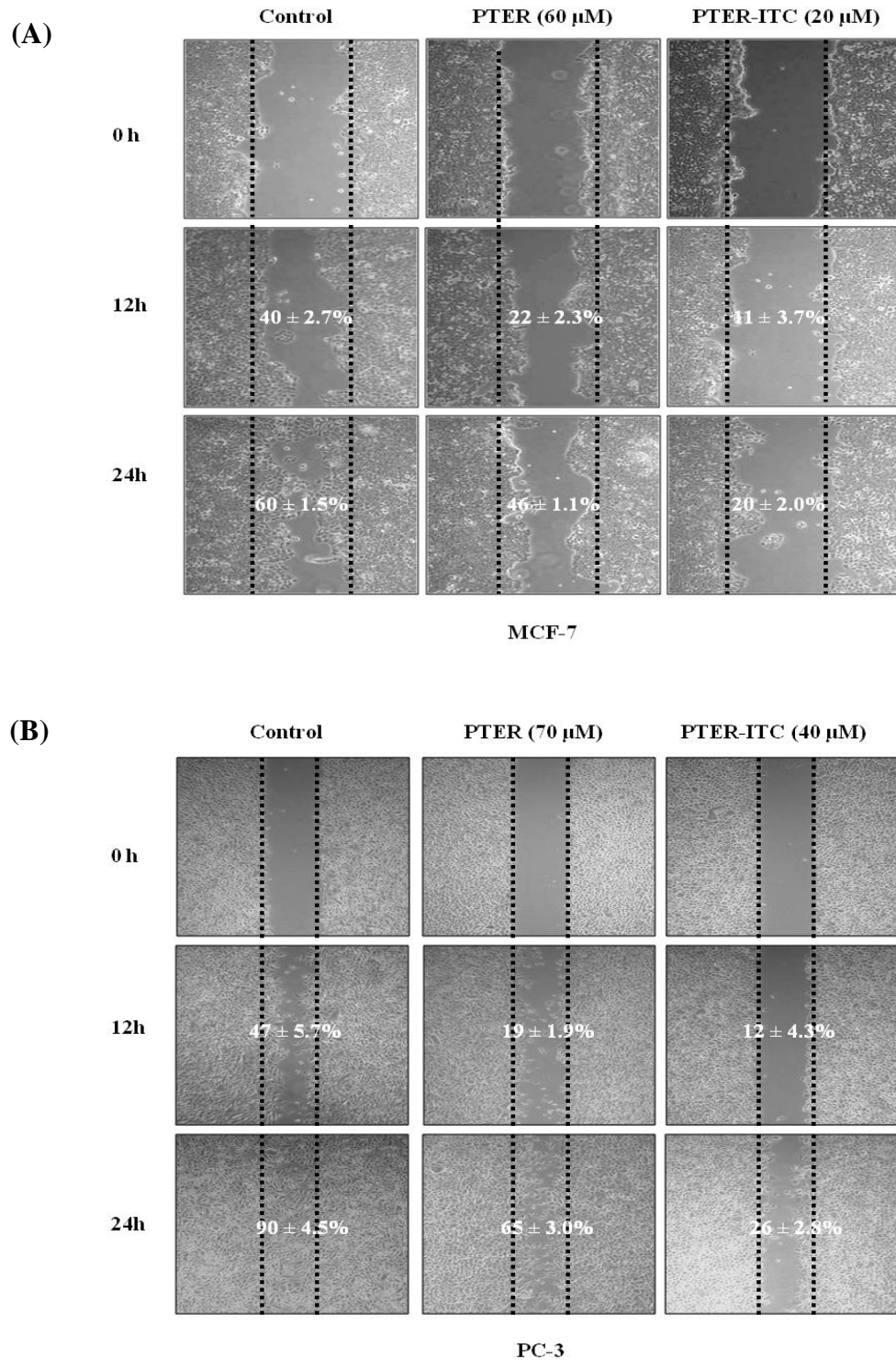
Figure 4.2.6: PTER-ITC induced suppression of the migration of (A) MCF-7 and (B) PC-3 cells. All cells were treated with 5 µg/mL mitomycin-c to halt cell proliferation, followed by treatment with PTER and PTER-ITC for 24 h. The wound edge images were captured and measured at 0, 12 and 24 h after treatment using T-scratch software, and percentage of migration is indicated as mean ± SEM. The data are representative of three independent experiment groups and viewed at 200X magnification.

anti-cancer activities [Adsule et al., 2010; Wittman et al., 2001; Gupta et al., 2010; Mandeville et al., 2008]. The cellular migration pattern is also an important property of tumor cells where they migrate from a primary site to a secondary organ while causing metastasis [Chua et al., 2010]. The conjugated PTER also showed a significant inhibition in the metastatic potential through reduction in cell migration which was almost 2.3 and 2.5-fold in MCF-7 and PC-3 cells respectively when compared to PTER. Overall, our results convincingly demonstrated that PTER-ITC is a superior inhibitor to PTER on the proliferation and migration of MCF-7 and PC-3 cells in culture.

In order to establish the mechanism by which PTER-ITC and PTER inhibit breast and prostate cancer cell growth, we studied the effects of the two compounds on cellular apoptosis. As a programmed cell death process, apoptosis is a mechanism the organism uses to eliminate unwanted or damaged cells. During cancer development, adequate mutations can allow the mutated cells to evade apoptosis and become cancerous; thus, the induction of apoptosis in pre-cancerous and cancer cells is an effective strategy for cancer treatment and prevention [Fesik SW, 2005]. In the annexin V/PI co-staining assay, we observed that both PTER-ITC and PTER were able to increase apoptotic cell population. However, PTER-ITC showed stronger capacity in inducing cellular apoptosis than PTER in both MCF-7 and PC-3 cells. This was evidenced by increased annexin V positive cell population and increase in DNA fragmentation.

The induction of cell cycle arrest and apoptosis are common mechanisms proposed for the cytotoxic effects of anticancer-drug. Cell cycle arrest can trigger proliferation inhibition and apoptosis in cancer cells (Pu et al., 2002; Chao et al., 2004; Saxena et al., 2013). Flow cytometry analysis showed that the PTER-ITC molecule arrested the MCF-7 and PC-3 cells in S and G2/M phases thus suggesting that the PTER-ITC induced inhibition of cell proliferation involved both cell cycle arrest and apoptosis. During cell cycle, the G2/M checkpoint is a potential target for cancer therapy. It prevents DNA-damaged cells from entering mitosis and allows for the repair of DNA that was damaged in late S or G2 phases prior to mitosis (Wang et al., 2009).

Taken together, our study reveals the superior anti-cancer effects of PTER-ITC to PTER in human breast (MCF-7) and prostate (PC-3) cancer cells in culture. These effects include inhibition of cell viability, inhibition of cell migration, cell cycle arrest and induction of apoptosis. This study thus supports the notion that PTER-ITC is a promising cancer-fighting compound in comparison to PTER and may merit further investigation as a potential chemoprophylactic and therapeutic agent for breast and prostate cancer.

Chapter 5. Role of PTER-ITC in Prevention of Breast Cancer

5.1. Introduction

Breast cancer is the most frequently diagnosed and leading cause of cancer-related mortality among females worldwide [Jemal et al., 2011]. The current standard treatment for breast cancer includes surgery, radiotherapy and multi-targeted therapy which include selective estrogen receptor modulator (tamoxifen) [Morgan et al., 2004]. However, the existing treatment options available for breast cancer are far from satisfactory, which results in poor prognosis. Major issues concerning conventional anticancer chemotherapy are the occurrence of side effects induced by the non-specific targeting of both normal and cancer cells [Gurung et al., 2010; Johnston, 2004], and the emergence of drug-resistant cancer cells [Gibbs, 2004]. Based on this, there has been growing interest in the use of naturally occurring molecules with chemo-preventive and chemotherapeutic properties in cancer treatment [Mann, 2002; Surh, 2003; Koehn and Carter, 2005; Newman and Cragg, 2007; Clardy and Walsh, 2004].

Breast cancer is typically hormone-dependent; exposure to estrogen promotes breast cancer cell growth and proliferation. The effects of estrogen are mediated by the binding of estrogen receptors (ER), ERα and ERβ, which are members of the nuclear receptor superfamily and function as ligand-induced transcription factors [Królik and Milnerowicz, 2012; Liang and Shang, 2013]. ERα is the major ER subtype in mammary epithelium, and it plays an important role in breast cancer progression [Roy and Vadlamudi, 2012]. Upon estrogen binding, ligand-activated ERα binds to the estrogen responsive element (ERE) in the target gene promoter and stimulates gene expression [Hall et al., 2001; Heldring et al., 2007; Gong et al., 2010]. Because estrogen plays a significant role in the stimulation and growth of breast cancer cells, antiestrogens such as the selective ER modulator (SERM) including tamoxifen (TAM), or fulvestrant [ICI 182,780 (ICI)] are used in endocrine therapy for ER-positive breast cancer [Buzdar, 2001]. ERα may also regulate breast cancer cells in a manner independent of its ability to act as a transcription factor termed non-genomic signaling. The nongenomic effects of estrogen can regulate different cellular processes, such as proliferation, survival, apoptosis, and differentiated functions in diverse cell-types, including breast cancer cells [Marino et al., 2002; Marino et al., 2003; Acconcia et al., 2005; Migliaccio et al., 1996; Bjornstrom and Sjoberg, 2005; Sun et al., 2001]. In breast cancer cells the activation of phosphatidylinositol 3-kinase (PI3K)/AKT and the Raf/mitogen-activated and extracellular signal-regulated kinase (MEK)/extracellular signal-regulated kinase (ERK) signaling pathways are related to cell growth, cell survival as well as metastasis [Liu et al., 2009; Acconcia et al., 2005; Migliaccio et

al., 1996; Bjornstrom and Sjoberg, 2005; Vander et al., 2009; Santen et al., 2002; Saxena et al., 2013]. Numerous studies from past suggests that PI3K/AKT and Raf/MEK/ERK cascades are interconnected with multiple points of convergence, cross-talk, and feedback loops [Grant, 2008]. Inhibition of either of these pathways can still result in the maintenance of signaling via the other (reciprocal) pathways [Hoeflich et al., 2009; Serra et al., 2011]. The existence of such "escape" mechanisms implies that dual targeting of these pathways may lead to superior efficacy and better clinical outcome in selected patients.

Over the last few years, with the progress of the medicinal chemistry, the hybrid approach has received significant attention since it allows obtaining molecules with improved biological activity with respect to the corresponding lead compounds. Using this approach, a new class of hybrid compound (PTER-ITC) was synthesized and characterized as described in the previous chapter of this thesis. Further this hybrid compound along with its parent molecule was screened for its cytotoxic activity in an array of cancer cell lines. A comparative analysis of the original PTER and conjugate (PTER-ITC) showed a significant elevated action by later as compared to former. Hence, in the present chapter of thesis we made an attempt to understand its mechanism of action using *in vitro* and *in vivo* models in prevention of breast cancer. Our data showed that the pro-apoptotic effect of PTER-ITC is mediated through the activation of caspases, and is correlated with the blockade of the AKT and ERK signaling pathways in MCF-7 cells.

5.2 Brief Methodology

5.2.1 Cell lines

In this study the MCF-7 cells were taken as the representative of the breast cancer cell line for all *in vitro* experiments. The culture conditions have been described in Chapter-3 (3.3.1)

5.2.2 Dose and duration of exposure of test compounds

MCF-7 cells were constantly exposed to PTER-ITC for 24 h at a concentration of 20 μM which was lower than its IC_{50}.

5.2.3 Caspase assay

The assay clearly confirms if there is an activation of caspases in cancerous cells. The effect of PTER-ITC induced apoptosis was therefore checked by this assay. Caspase activity was determined by using ApoTargetTM caspase colorimetric protease assay sampler kit

(Catalog number: KHZ1001; Invitrogen, USA) according to the manufacturer's instructions. Detailed description of the protocol has been given in Chapter-3 (3.6.6).

5.2.4. Treatment of tumor models

The tumor bearing female mice were divided into following groups for further treatments. Treatment was initiated from day 6 after tumor implantation and continued for next 30 days. The animals were otherwise housed with proper food and water ad libitum.

Group-1 Control normal mice

Group-2 Tumor bearing mice (EAC control)

Group-3 Tumor bearing mice treated with PTER (200 mg/kg bw)

Group-4 Tumor bearing mice treated with PTER-ITC (20 mg/kg bw)

Group-5 Tumor bearing mice treated with PTER-ITC (100 mg/kg bw)

Group-6 Tumor bearing mice treated with 5-FU (20 mg/kg bw).

The effect of PTER, 5-FU and PTER-ITC on tumor volume was calculated using the formula $V = 4/3\pi r_1^2 r_2$ where r_1 and r_2 are the radii of the tumor from two directions (Kuttan et al., 1990). Furthermore, the effect of this test chemical on tumor regression was analyzed by analyzing the expression profiles of some marker genes in tumor tissues by RT-PCR and immunoblot analysis.

5.3 Results

5.3.1 PTER-ITC induces caspase dependent apoptosis

In most of the cellular system activation of both extrinsic and intrinsic caspase dependent pathways have been linked to the major mode of cell death [Fadeel and Orrenius, 2005]. To further examine the mechanisms underlying the PTER-ITC-induced death of breast cancer cells, a possible role of caspases in this process were investigated by measuring the enzymatic activities of caspase-7, -8 and -9. While caspase-8 and caspase-9 are essential proteases of extrinsic and intrinsic apoptotic pathways respectively, caspase-7 acts as downstream effectors of both these pathways. Further, caspase-7, a member of the caspase-3 subfamily has been shown to be involved in apoptosis in caspase-3 deficient MCF-7 cells. Our data showed that the PTER-ITC significantly increased caspase-9 and -7 activities while no significant change in caspase-8 activity was observed (Fig. 5.1A) ($p<0.05$). On the other hand, both PTER and 5-FU showed increase in caspase-7, -8 and -9 activities (Fig. 5.1A). The PTER-ITC molecule showed approximately 4.4-fold increase in caspase-9 activity which was about 3.4-fold by that of PTER ($p<0.05$). Furthermore, there was only marginal increase in the level

of caspase-8 which was not significant in case of PTER-ITC while PTER and 5-FU caused 2.5 and 2.7-fold increase in caspase-8 enzyme activities respectively (Fig. 5.1A). Interestingly, the level of caspase-7 activity was increased by 6, 4.4 and 3.6-fold by PTER-ITC, PTER and 5-FU respectively.
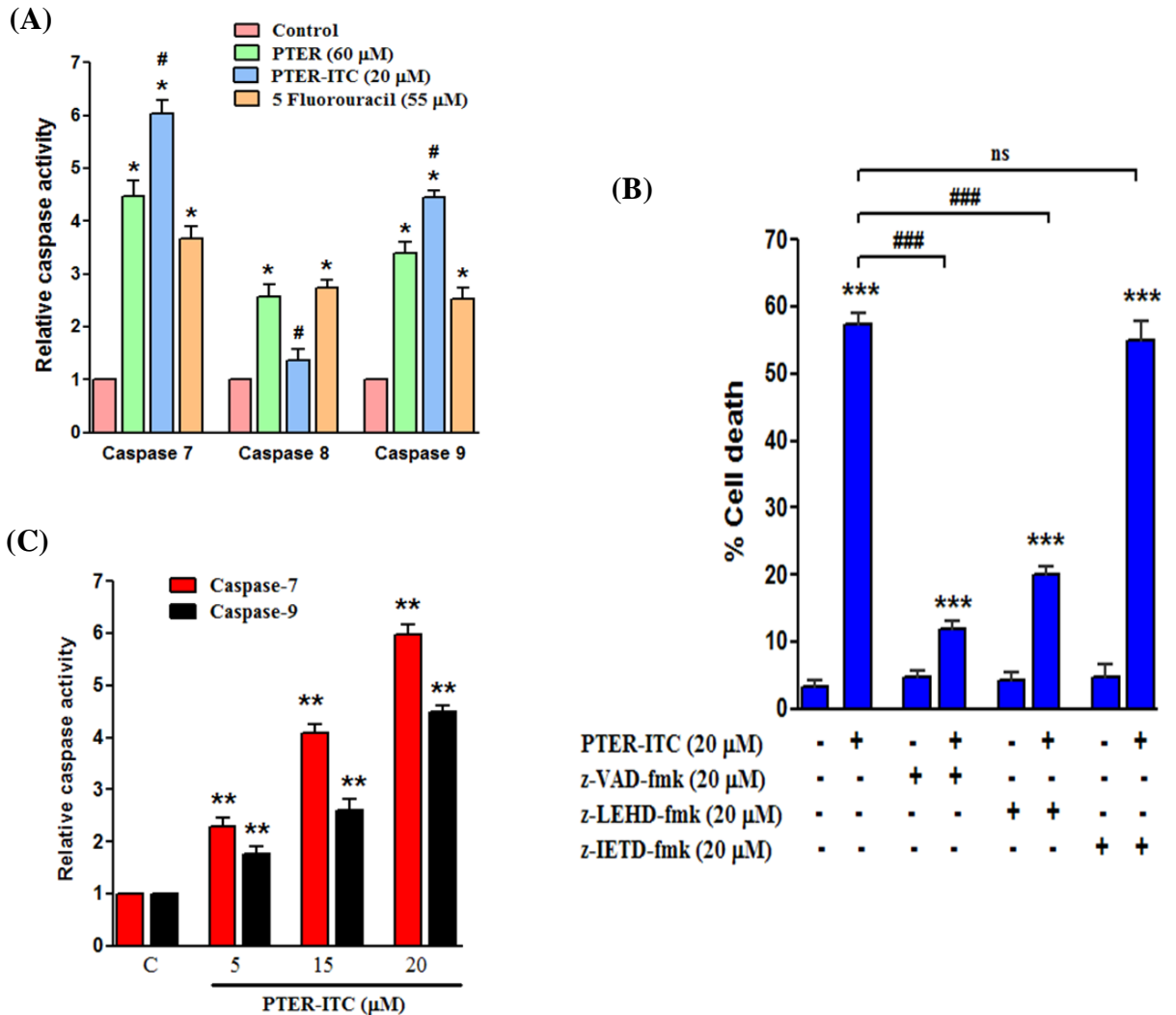
Figure 5.1: Effects of PTER-ITC in regulating the apoptosis of MCF-7 cells. (A) Activation of various caspases by PTER, PTER-ITC and 5-FU. Results are the mean ± SEM of three independent experiments. * and # represents statistically significant difference with respect to control and PTER treated MCF-7 cells respectively for each group at *p<0.05*. (B) Effects of various caspase inhibitors on PTER-ITC-induced apoptosis in MCF-7 cells. The details of the experiment have been described in materials and methods. Data are the mean ± SEM of three independent experiments. *** and ### represents statistically significant difference with respect to control and PTER-ITC treated MCF-7 cells respectively at *p<0.05*. ns, non-significant. (C) Dose dependent effect of PTER-ITC on the activities of caspase-7 and -9. Results are the mean ± SEM of three independent experiments. ** represents statistically significant difference with respect to control for each caspases at *p<0.05*.

Further, in order to determine the specificity of caspase activities for PTER-ITC induced cell death in cultured MCF-7 cells, pharmacological inhibitors of caspases were employed to probe whether they could protect the cells from undergoing apoptosis. As shown in Fig. 5.1B, z-VAD-fmk, a universal caspase inhibitor, showed the most efficient inhibition of apoptosis (up to 76-80%) suggesting that apoptosis is the predominant form of cell death induced by the PTER-ITC. z-LEHD-fmk, a specific inhibitor of caspase-9, also inhibited PTER-ITC induced apoptosis by 66-70% ($p<0.05$) (Fig. 5.1B). In contrast, z-IETD-fmk, a specific inhibitor of caspase-8, was ineffective in blocking the PTER-ITC induced apoptosis. Taken together, these data demonstrates that PTER-ITC induced apoptosis is caspase dependent and specifically caspase-9 is required for mediating this apoptotic cell death in MCF-7 cells.

Based on our finding that caspase-9 is involved in PTER-ITC induced apoptosis, we next assessed the dose dependent effect of PTER-ITC on activities of caspase-9 and its downstream effector (caspase-7). As shown in Fig. 5.1C, a dose dependent increase in caspase-9 and -7 activities were observed with increasing dose of the PTER-ITC. The above data was furthermore validated by immunoblot analysis of cleaved caspase-9 protein where PTER-ITC increased the expression of this protein by about 4.8-fold. PTER and 5-FU on the other hand, showed only 4 and 3-fold increase in the expression of cleaved caspase-9 protein (Fig. 5.3) ($p<0.05$). Together the above data thus suggests that PTER and 5-FU mediates apoptosis by engaging both the transmembrane death receptor dependent extrinsic and mitochondria dependent intrinsic apoptotic pathways while PTER-ITC mediates apoptosis mainly through mitochondrial intrinsic pathway.

5.3.2 Bcl-2 and Bax are involved in apoptosis by PTER-ITC

Bcl-2 forms a heterodimeric complex with apoptotic Bax protein, thereby neutralizing its apoptotic effect. Therefore, the ratio of Bax/Bcl2 is often considered as a decisive factor in determining cell death or survival. Next, when we examined the anti-apoptotic proteins like Bcl-2, Bcl-xL, survivin and AKT, all were found to be significantly down regulated whereas the pro-apoptotic proteins like Bax was significantly up regulated. The PTER-ITC caused about 3.4-fold increase in Bax protein level and 2.5-fold decrease in Bcl-2 level (Fig. 5.2). Comparatively, PTER and 5-FU caused about 2.9 and 2.4-fold increase in Bax and 1.6 and 1.4-fold decreases in Bcl-2 protein levels respectively (Fig. 5.2) ($p<0.05$).

The Jun oncoprotein is a major component of the transcription factor complex, AP-1, which forms homodimers or heterodimers with either Fos (v-Fos, c-Fos, FosB, FosL1, and

FosL2) or activating transcription factor (ATF-2, ATF-3) [Vogt PK, 2001]. Although Jun is known primarily for its growth-promoting activity, it has also been reported to induce apoptosis, a property which it shares with other oncoproteins like Myc, E1A, or E2F. Proapoptotic functions of c-Jun have been reported in neurons, fibroblasts, and endothelial cells, suggesting that cell death is induced both indirectly through its transcriptional regulation of survival/death genes (e.g., Fas ligand) and directly via activation of the caspase cascade, resulting in the cleavage of numerous molecules (e.g., fodrin, poly (ADP-ribose) polymerase (PARP), DNA-dependent protein kinase, and protein kinase C) [Bossy et al., 1997; Kolbue et al., 2000; Ham et al., 1995; Wang et al., 1999]. In our study, the treatment with PTER-ITC and PTER caused about 2.6 and 2-fold increase in the expression of p-c-Jun (Ser 73 phosphorylated c-Jun) respectively, suggesting that AP-1 induction may also be involved in apoptosis caused by this phytochemical (Fig. 5.2) ($p<0.05$).
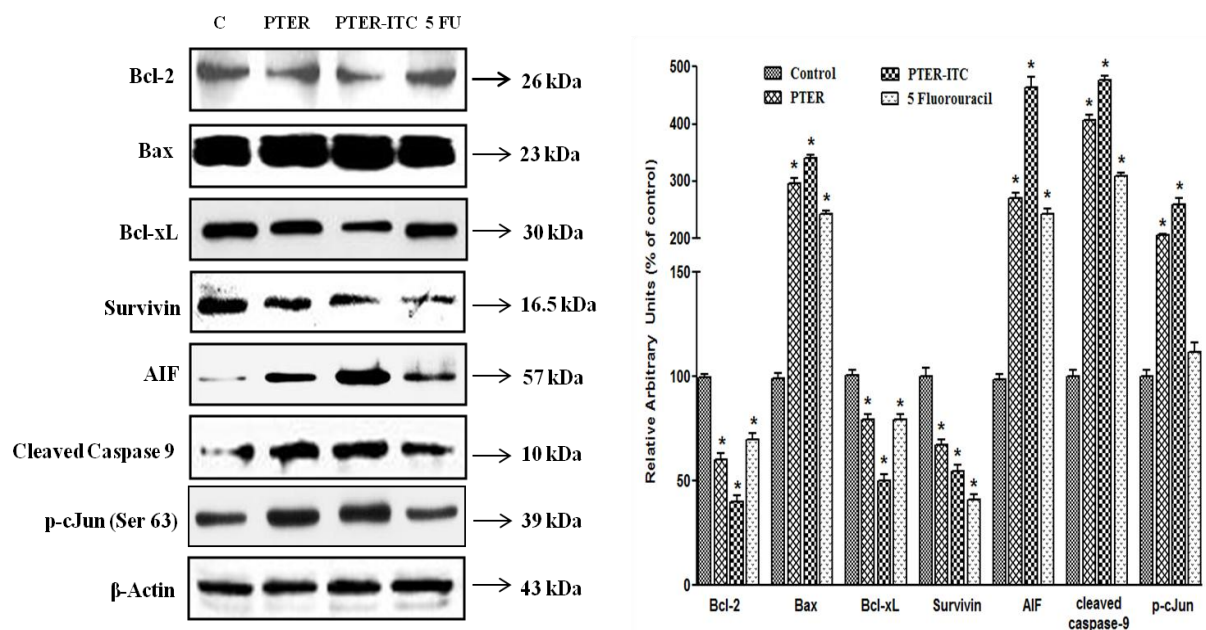
Figure 5.2: Immunoblot analysis for some apoptotic marker and other related genes in response to PTER and PTER-ITC. The histogram in the right panel represents the data as the Relative Arbitrary Units in terms of % over vehicle treated control cells respectively. Results are the mean ± SEM of three independent experiments. * represents statistically significant difference with respect to corresponding control groups at $p<0.05$.

In response to apoptotic stimuli mitochondria releases caspase independent cell effectors such as apoptosis inducing factor (AIF) and endonuclease G [Sean et al., 2004; Banerjee et al., 2012; Prabhu et al., 2013]. AIF translocates from the outer mitochondrial

membrane to the cytosol and to the nucleus, resulting in the induction of nuclear chromatin condensation and DNA fragmentation. Our data showed that the treatment with PTER-ITC caused about 4.6-fold increase in AIF protein expression as compared to 2.7 and 2.4-fold by PTER and 5-FU respectively, suggesting that the caspase-independent mitochondrial apoptotic pathway also might have an important role in apoptotic cell death as induced by these chemicals in MCF-7 cells (Fig. 5.2). The right panel in Fig. 5.2 summarizes the densitometric scanning data for the expression profiles of various proteins.

5.3.3. Cytochrome-c immunofluorescence

The release of cytochrome-c, one of the most important respiratory-chain proteins, from the mitochondria into the cytosol is the hallmark of cells passing through apoptosis. To specify the molecular basis of apoptosis, the release of cytochrome-c into the cytosol was estimated in MCF-7 cells by immunofluorescence analysis. As shown in Fig. 5.3, the intensity of fluorescence in the cytosol of PTER-ITC treated cells was significantly higher than those in PTER and vehicle treated cells. The PTER-ITC and PTER showed 3.2 and 2.1-fold increase in the intensity of immunofluorescence respectively for cytochrome-c as compared to vehicle treated cells (Fig. 5.3, right panel) ($p<0.05$), thus indicating the direct involvement of mitochondrial pathway in response to PTER-ITC.
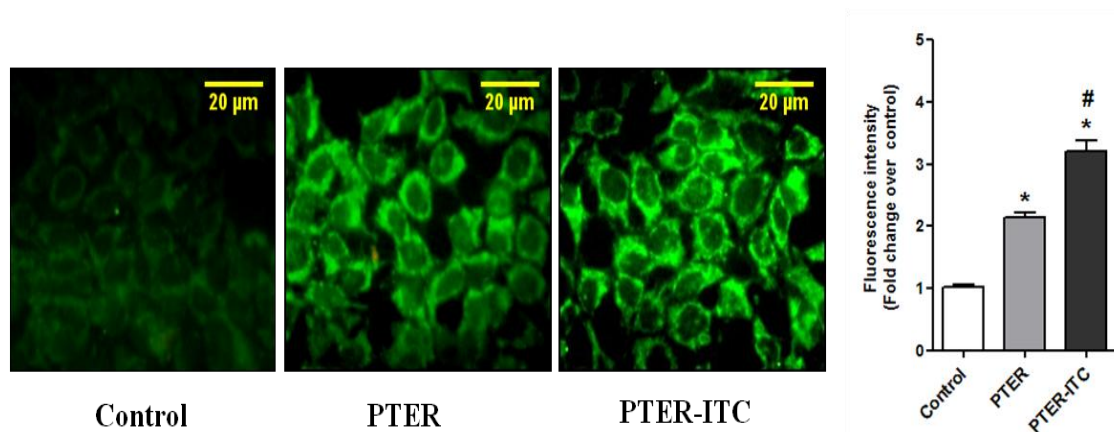
Figure 5.3: Immunofluorescence analysis showing the expression of cytochrome-c in response to PTER (60 µM) and PTER-ITC (20 µM) in MCF-7 cells (200X magnification). The histogram in the right panel of figure represents change in fluorescence intensity expressed as fold change over control. The results are representative of at least two independent experiments. * and # represents statistically significant difference with respect to vehicle control and PTER treated MCF-7 cells respectively at $p<0.05$.

5.3.4. Intracellular ROS levels

In order to check the probable reason for apoptosis in cancer cells, intracellular ROS was measured after treatment with PTER and its conjugate for 24 h. As shown in Fig. 5.4A, the production of ROS was significantly increased by 2.1 and 3-fold in case of PTER and PTER-ITC treated cell respectively as compared to control cells. Interestingly, the PTER-ITC even showed significant increase in ROS production as compared to PTER treated group ($p<0.05$) (Fig. 5.4A). Further, to check the type of reactive oxygen species generated during apoptosis in response to PTER and PTER-ITC, free radical scavengers were used to quench the produced free radicals specifically. As shown in Fig. 5.4A, PTER-ITC and PTER along with 1 mM of sodium azide (scavenger of singlet oxygen) or 1 µM of catalase (H_2O_2 scavengers) reduced the formazone production by about 1.7 and 1.9-fold respectively ($p<0.05$) while 1 mM potassium iodide (scavenger of [OH]$^-$) did not show any significant change ($p<0.01$) in the total ROS production. H_2O_2 (1 µM) was used as a positive control which thereby increased total ROS production by about 3-fold ($p<0.05$) over vehicle treated control. These data thus indicated that the PTER-ITC induced the production of H_2O_2 and singlet oxygen species within treated cells. This result was further validated by DCF-DA method where among conjugated and unconjugated PTER, the conjugate molecule showed increased fluorescence (2-fold) as compared to that of unconjugated ones (1.4-fold) (Fig. 5.4B).

(A)

(B)
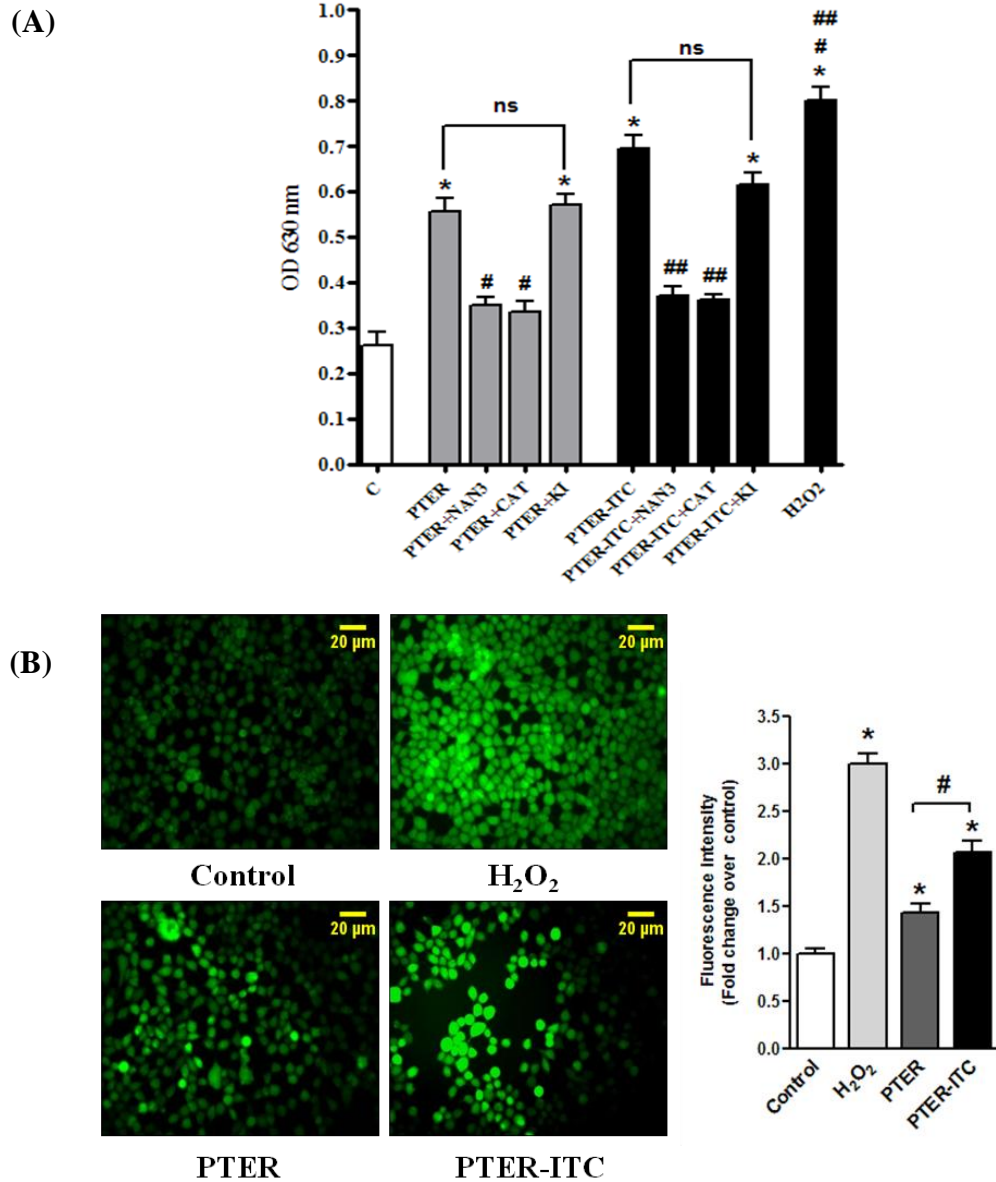
Figure 5.4: Effect of PTER-ITC on ROS production in MCF-7 cells. (A) Production of reduced formazone due to ROS generation in the presence and absence of free radical scavengers. Values are mean $\pm$ SEM of three independent experiments each performed in triplicates. *, # and ## represents statistically significant difference with respect to vehicle, PTER and PTER-ITC treated MCF-7 cells respectively at $p<0.05$. ns, non-significant. (B) ROS accumulation within cells in response to various drug treatments as estimated by H2-DCF-DA staining of treated cells (100X magnifications). The histogram in the right panel of figure represents changes in fluorescence intensities represented as fold change over control. * and # represents statistically significant difference with respect to vehicle and PTER treated cells respectively at $p<0.05$. C, vehicle; NaN$_3$, sodium azide; Cat, catalase; KI, potassium iodide; H$_2$O$_2$, hydrogen peroxide.

5.3.5. Effects of PTER-ITC on phosphorylation status of AKT and ERK

In order to confirm the specific mechanisms involved in apoptosis of these cells in response to PTER-ITC, we examined the effect of PTER-ITC on the AKT and ERK signalling pathways. The AKT signaling pathway is one of the most critical pathways in regulating cell survival [Gioeli et al., 1999]. Phosphorylation of AKT provides cells with a survival signal that allows them to withstand apoptotic stimuli [Abreu-Martin et al., 1999]. Our data showed that both PTER-ITC and PTER significantly decreased the phosphorylation of AKT at Serine 473 residue causing about 1.8 and 1.5-fold reduction in p-AKT/AKT ratios respectively after 24 h of treatment (Fig. 5.5A, $p<0.05$). In the next stage we checked the time dependent regulation of phosphorylation of AKT by 20 μM PTER-ITC. Our data showed that there was a significant decrease in the activation of AKT with increasing time and interestingly the PTER-ITC resulted in a significant decline in the activation of AKT at 12 h which was more prominent with subsequent time lapse (Fig. 5.5B, $p<0.05$). To evaluate whether down-regulation of this kinase is responsible for PTER-ITC-induced cell death, the effect of AKT kinase inhibitor was evaluated. Our data showed that MCF-7 cells treated with different doses of PTER-ITC (5, 15 and 20 μM) in presence and absence of 5 μM AKT 1/2 kinase inhibitor (A6730), caused a dose dependent decrease in AKT and p-AKT protein levels which was almost abolished in presence of AKT 1/2 kinase inhibitor (Fig. 5.6A). To further confirm the involvement of AKT in PTER-ITC induced cell death we next examined the effect of PTER-ITC on the expression levels of active caspase-9 and survivin, a pro and anti-apoptotic protein respectively, downstream of AKT pathway. PTER-ITC treatment caused dose dependent decrease in survivin expression levels which was further drastically inhibited in the presence of A6730. On the other hand, the PTER-ITC caused a dose dependent increase in cleaved caspase-9 levels which was further enhanced in presence of AKT kinase inhibitor (Fig. 5.6A). These results suggested that inhibition of AKT is associated with down regulation of survivin and up regulation of active caspase-9, ultimately leading to apoptosis of MCF-7 cells.
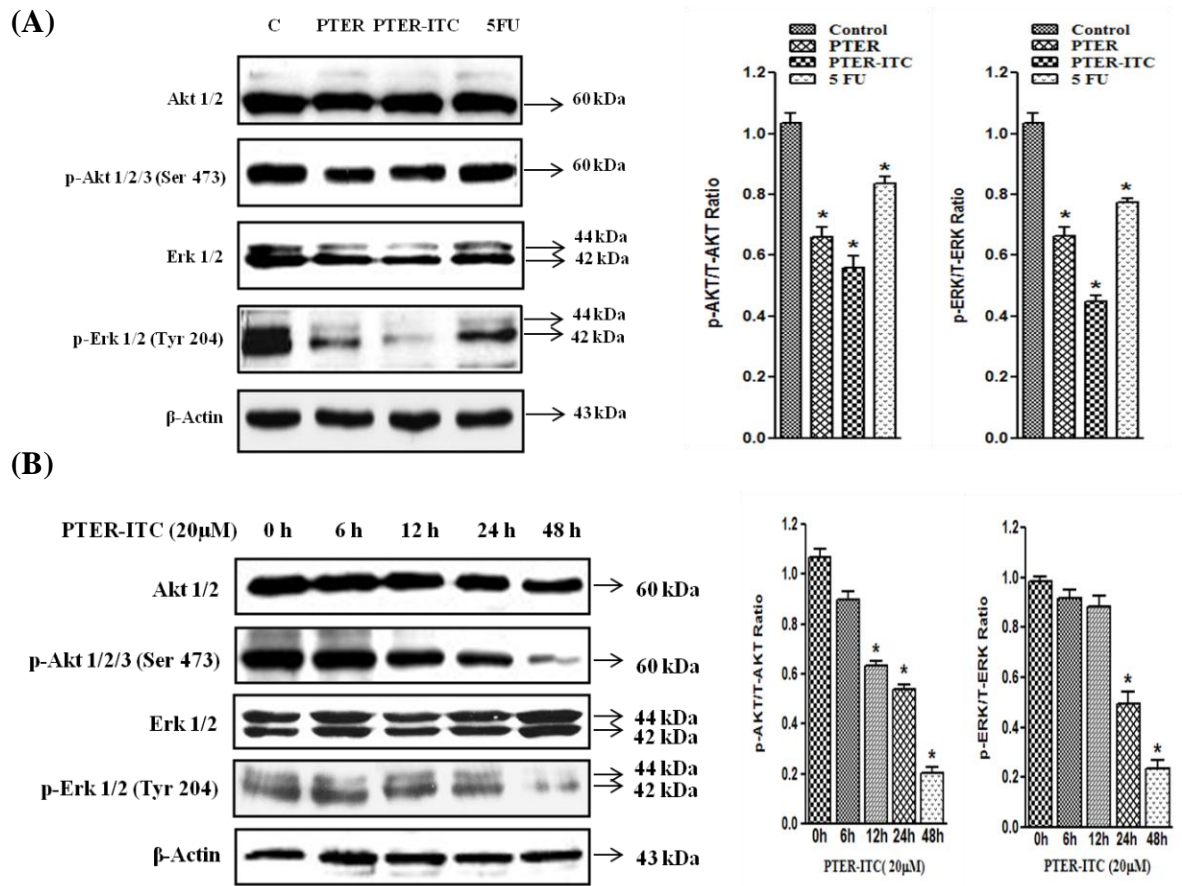
Figure 5.5: Effect of PTER-ITC on PI3K/AKT and MAPK/ERK pathways in MCF-7 cells. (A) Representative immunoblot showing the effects of PTER and PTER-ITC on activation of AKT and ERK pathways. (B) Representative immunoblot showing time dependent effect of PTER-ITC on the activation of AKT and MAPK/ERK pathways in MCF-7 cells. MCF-7 cells were treated with 20 μM PTER-ITC for different time periods (0, 6, 12, 24 and 48 h). Cells were then harvested at various time points and lysates were used for immunoblot analysis. The histogram in the right panel of each figure represents the data as the Relative Arbitrary Units in terms of % over vehicle treated control cells respectively. Results are the mean ± SEM of three independent experiments. * represents statistically significant difference with respect to control at $p < 0.05$.
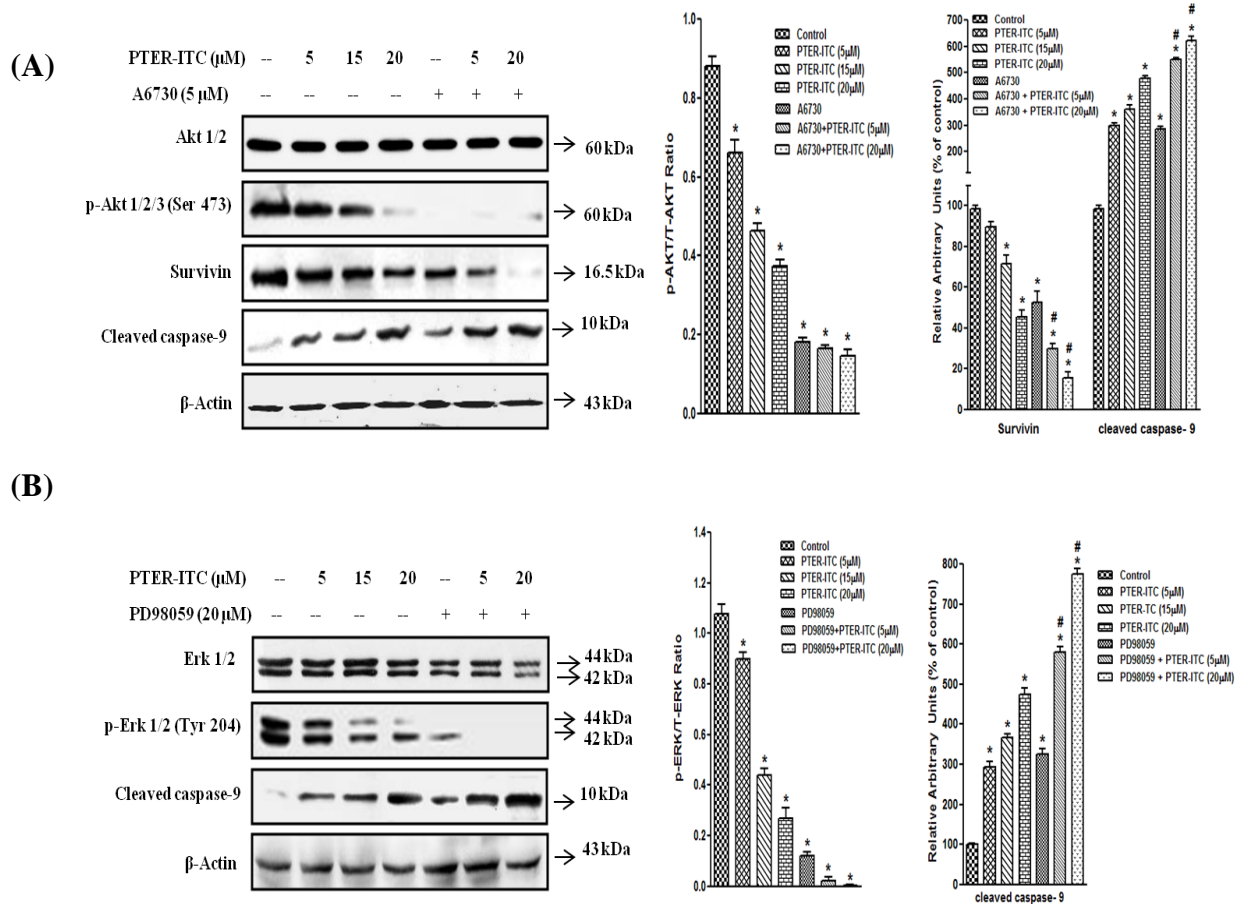
Figure 5.6: Effects of various inhibitors in regulating PTER-ITC induced apoptosis in MCF-7 cells. Representative immunoblot analysis depicting the effect of (A) AKT 1/2 kinase inhibitor (A6730) and (B) MAP Kinase inhibitor (PD98059) on PTER-ITC treated cells. The cells were pre-treated with A6730 (5 μM) or PD98059 (20 μM) for 1 h before 24 h incubation with 20 μM PTER-ITC (total inhibitor exposure time was 25 h) followed by immunoblot analysis with lysates. The histogram in the right panel of each figure represents the data as Relative Arbitrary Units in terms of % over control. Results are the mean ± SEM of three independent experiments. * and # represents statistically significant difference with respect to vehicle treated control and only A6730 or PD98059 treated control groups respectively at *p*<0.05.

The ERK1/2 signalling pathway has also been known to regulate cell proliferation and differentiation and hence its inhibition could lead to the induction of apoptosis [Gao et al., 2006]. Therefore we next checked if MAPK pathways were (in)activated in PTER-ITC treated MCF-7 cells. Interestingly, our data showed that the PTER-ITC caused almost 2.3-fold reduction in the p-ERK/ERK ratio while it was 1.5-fold with that of PTER (Fig. 5.5A). To investigate the possible role of ERK pathway in PTER-ITC-induced cell growth inhibition, we analysed the time and dose-dependent effects of PTER-ITC on the expression and phosphorylation of ERK. As shown in Fig. 5.5B, a time course analysis represented that p-ERK/ERK ratio remained constant till 12 h and significantly decreased at 24h and was almost abolished at 48 h (Fig. 5.5B). To further investigate the role of ERK dependent pathway in PTER-ITC induced cell death, MCF-7 cells were treated with or without PD98059, an ERK specific inhibitor, for 24 h and then the protein expression levels were determined. As shown in Figure 5.6B, the PTER-ITC treatment significantly inhibited the phosphorylation of ERK in MCF-7 cells at a concentration of 5 μM with more prominent effects at further higher doses. Further, the expression of phosphorylated ERK was almost abolished by co-treatment with PTER-ITC and PD98059 at concentration of 5 μM and above. Interestingly, the PTER-ITC molecule caused a dose dependent increase in cleaved caspase-9 expression also which was further enhanced in presence of ERK inhibitor suggesting a direct involvement of ERK pathway in apoptosis induced by PTER-ITC (Figure 5.6B, $p<0.05$).

5.3.6 AKT and MAPK inhibitors sensitized MCF-7 cells to PTER-ITC induced apoptosis

To experimentally verify the role of AKT, ERK and c-Jun in PTER-ITC-induced apoptosis, MCF-7 cells were pre-treated for 1 h with specific inhibitors for AKT (A6730), ERK (PD98059) and JNK (SP600125), an upstream activator of c-Jun. Subsequently, the inhibitor treated cells were exposed to 20 μM PTER-ITC, and then the caspase-9 activity and cell death was measured using Ac-LEHD-pNA as substrate (Fig. 5.7B) and MTT assay (Fig. 5.7A) respectively. As shown in Fig, 5.7A, in comparison to control cells, the percentage of dead cells were significantly higher in cells exposed to 20 μM PTER-ITC which was significantly inhibited by JNK inhibitor SP600125 ($p<0.05$). On the contrary, co-treatment of cells with AKT or ERK inhibitors and PTER-ITC resulted in higher number of dead cells as compared to cells treated with PTER-ITC alone. Consistent with these results, pre-treatment with A6730 and PD98059 increased caspase-9 enzyme activity compared to cells treated with PTER-ITC alone (Fig. 5.7B).These results suggests an important role of AKT, ERK and c-Jun on PTER-ITC

induced apoptosis, where the stimulation of c-Jun and inactivation of AKT and ERK induces the apoptosis in these cells.
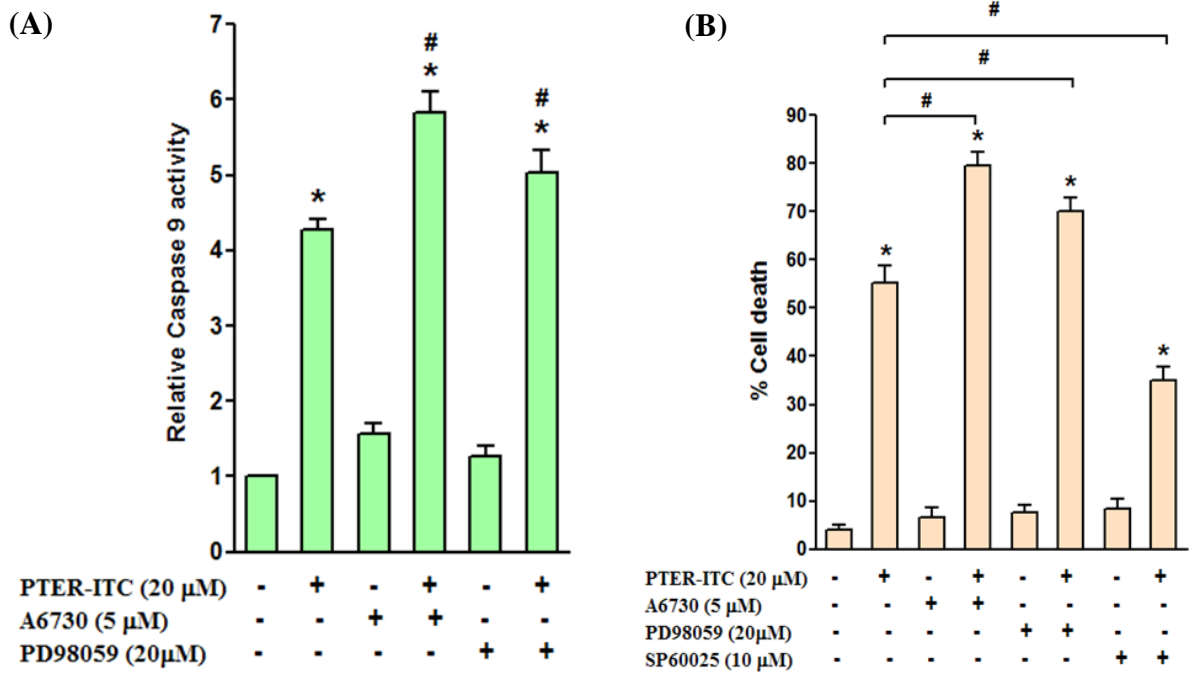
Figure 5.7: Effects of inhibitors of MAPK (PD98059), AKT (A6730) and JNK (SP600125) on PTER-ITC induced cell death (A) and caspase-9 activity (B) in MCF-7 cells. Data are mean ± SEM of three independent experiments. * and # indicates significantly different with respect to control and only PTER-ITC treated groups respectively at $p<0.05$.

5.3.7. Effect of PTER-ITC on Ehrlich ascitic cell induced tumor bearing mice

5.3.7.1. Effects on tumor volume

Our data showed that both PTER and PTER-ITC caused significant reduction in solid tumor volume as compared to untreated tumor group. Tumor group animals when treated with PTER-ITC at a dose of 100 mg/kg bw showed significantly reduced tumor volume by approximately 5-fold after 30 days of treatment which was comparable or even better than positive control i.e. 5-FU treated animals (Table 5.1) ($p <0.05$).

Table 5.1: Effect of PTER and PTER–ITC on tumor volume in Ehrlich ascitic cell tumor bearing mice

Design of treatment	Solid tumor volume (mL)[a]		
	10th day	20th day	30th day
Tumor control	2.96±0.12	4.54±0.61	6.54±0.05
PTER (200 mg/kg BW)[d]	2.05±0.14	2.54±0.05[c]	2.65±0.03[b]
PTER-ITC (20 mg/kg BW)	2.44±0.25	3.54±0.24	3.74±0.21[b]
PTER-ITC (100 mg/kg BW)	1.54±0.21[b]	1.84±0.52[b]	1.34±0.12[b]
5 FU (20 mg/kg BW)[e]	1.52±0.33 [b]	1.90±0.61[b]	1.44±0.11[b]

[a] All values are mean ± SEM
[b] *p<0.001* between tumor control and tumor treated group
[c] *p<0.01* between tumor control and tumor treated group.
[d] PTER, Pterostilbene; [e] 5 FU, 5-Fluorouracil

5.3.7.2. PTER-ITC suppresses VEGF expression and up regulates caspase-3 and Bax expressions

It is already reported that the progressions of tumors are linked to angiogenesis. Out of several factors which plays critical role in this process of angiogenesis VEGF is the most prominent one of them all. Administration of an inhibitor of angiogenesis, which is not directly linked to cytotoxicity of tumor cells, can even increase tumor cell apoptosis, decreased VEGF production, and regression of tumor growth either by inhibiting endothelial cell proliferation or by inducing tumor and/or endothelial cell apoptosis [Ferrara N, 2004]. Therefore, the effect of PTER-ITC on VEGF expression in solid Ehrlich tumor growth was analyzed using RT-PCR (Fig. 5.8A) and immunoblot analysis (Fig. 5.8B). A profound reduction in VEGF protein expression was observed in solid tumor from mice treated with PTER-ITC at 100 mg/kg bw (about 2-fold) and the extent of this inhibitory effect was almost similar to 5-FU but greater in magnitude than PTER treatment ($p<0.05$) (Fig. 5.8B). Further, in order to check if the regression in tumor growth by PTER-ITC was due to its induction of apoptosis in tumor cells, we analyzed the levels of cleaved caspase-3 and Bax in those tumor samples. As shown in Fig. 5.8, PTER-ITC molecule at the highest dose tested, significantly enhanced the expression of

cleaved caspase-3 and Bax protein as compared to untreated tumor group ($p<0.05$) indicating its prominent effects even *in vivo*.
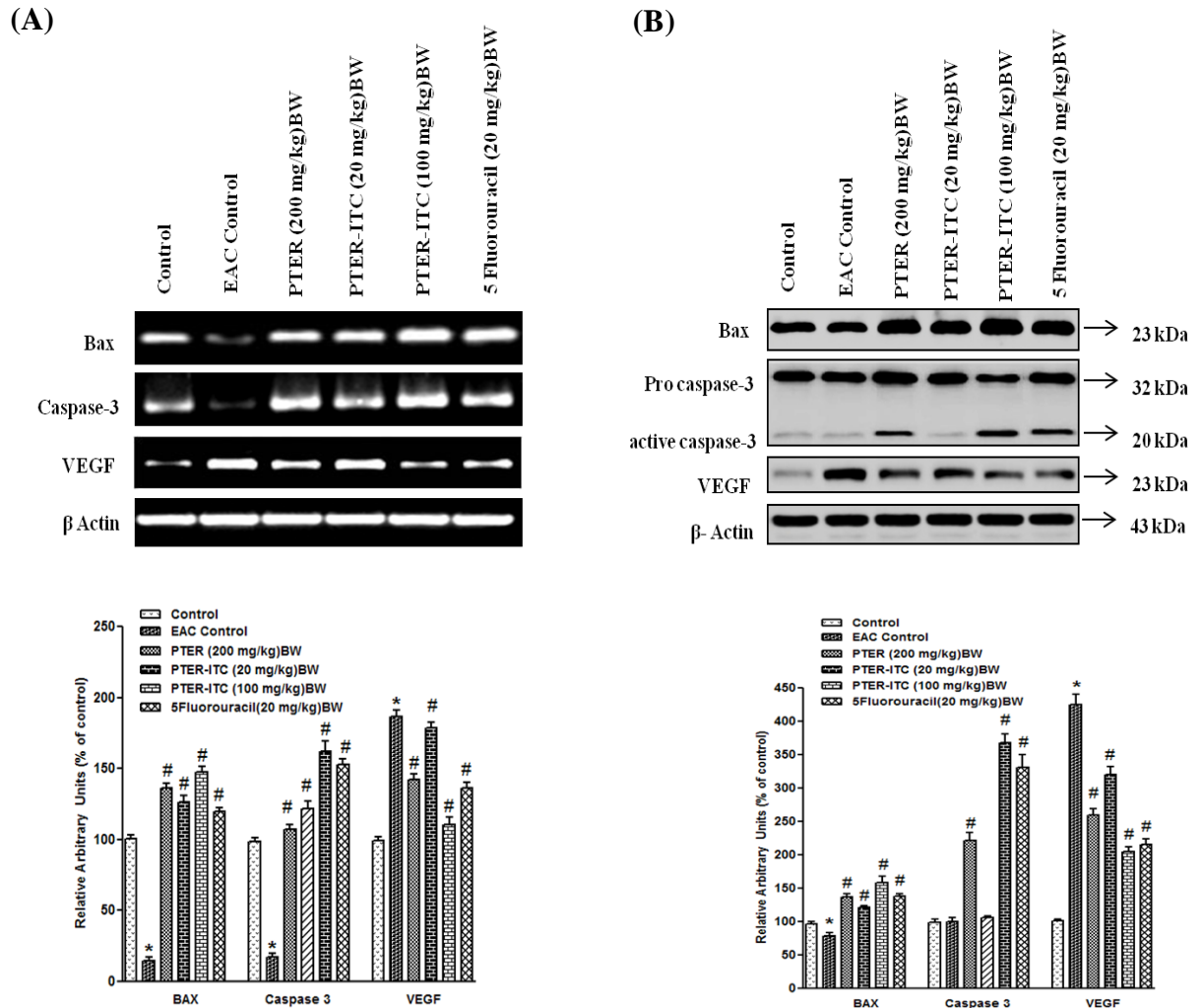
Figure 5.8: Effect of PTER and its conjugate in regulating tumor regression *in vivo*. (A) RT-PCR and (B) Immunoblot analysis for the expression of apoptosis and angiogenesis marker genes in tumor tissues of mice treated with PTER, PTER-ITC and 5-FU. The lower panel indicates the data expressed as Relative Arbitrary Units in terms of % over control where results are the mean ± SEM of three independent experiments. * and # represents statistically significant difference with respect to normal and EAC control groups respectively for each genes at $p<0.05$. EAC, Ehrlich ascitic cell induced tumor mice.

5.3.7.3. Histopathology of conjugated PTER treated mice

In the next phase of study histopathological analysis was performed for various tissues to check if the PTER-ITC treatment renders any toxic effects on the animals during the course of therapy. Our data on liver sections from various experimental groups of animals are illustrated in Fig. 5.9. The hepatic sections from normal animals revealed normal liver parenchyma with the typical architecture characterized by granulated cytoplasm, central vein (CV) and small uniform nuclei. On the contrary, the mice injected with EAC alone showed abnormal architecture with the presence of irregular-shaped cytoplasm, disorganized hepatocytes, widened sinusoidal space and enlarged hyper chromatic nuclei. Interestingly, the cellular architecture of liver sections from mice that received PTER-ITC at 100 mg/kg BW was almost comparable with that of the normal animals. The hepatocytes from this group had compact cytoplasm. Furthermore, the liver cells were mostly mononucleated with regular sized nuclei. Liver sections of mice treated with PTER and 5-FU also showed almost similar cellular architecture as that of normal animals except that the sections showed few widened sinusoidal spaces (Fig. 5.9A).

As shown in Fig. 5.9B, histopathological sections of kidney from untreated (control) mouse showed glomerular capsule (G) with parietal and visceral layer separated by capsular space. In addition, distal and proximal convoluted tubules along with collecting tubule were also visible. The histological section of kidney in tumor bearing mice showed reduced glomerulus, vacuolation in epithelial cells and increased gap in Bowman's space of glomerulus. Interestingly, PTER and PTER-ITC treatment restored the Bowman space of glomerulus and most of normal intact histological structure in kidney (Fig. 5.9B).

When tested for spleen, as shown in Fig. 5.9C, control mice showed normal and preserved red pulp (R), white pulp (W) and megakaryocytes. Infusion of EAC to mice resulted in lymphoid hyperplasia in white pulps (W) of spleen and also there was multiple numbers of immature megakaryocytes in the white pulps. On the other hand, the hyperplasia was much milder in case of animals treated either with PTER or PTER-ITC (as shown by the reappearance of R along with W), thus indicating their effects in ameliorating the damage caused by the tumors (Fig. 5.9C).
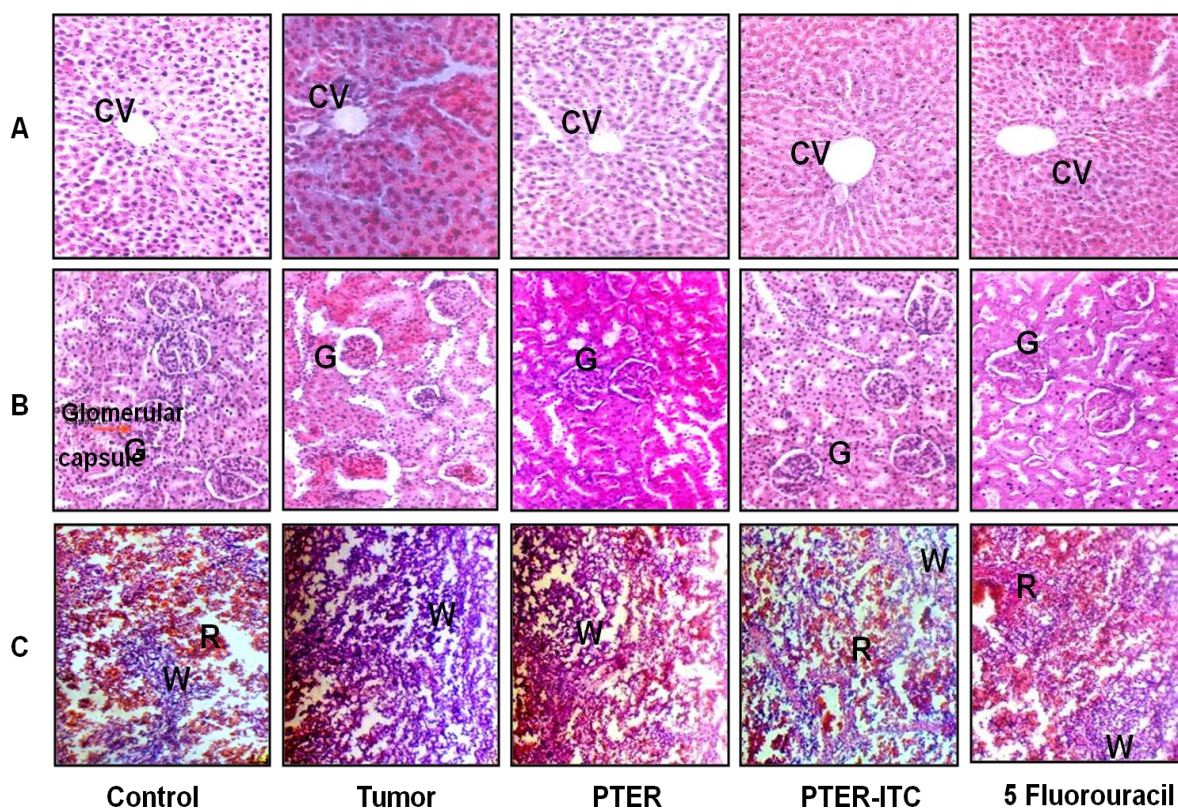
Figure 5.9: Histopathological analysis for (A) Liver (B) Kidney and (C) Spleen tissues from various groups of animals treated with/without compounds. The sections were stained with H&E and observed at 400X magnification. CV, central veins; W, white pulps; R, red pulps; G, glomerulus capsule.

5.4 Discussion

Breast cancer is the most common malignancy and the most common cause of cancer death in elderly women. Chemoprevention with dietary compounds and their synthetic analogs has emerged as an attractive strategy to prevent carcinogenic progression to invasive cancer. In the previous chapter we synthesized a novel derivative of PTER and performed its initial screening as anticancer agent in MCF-7 and PC-3 cells. In the present chapter of this thesis, an attempt was made to understand the mechanism of action of this novel compound in prevention of breast cancer. The present data clearly showed that PTER-ITC conjugate, a hybrid molecule between PTER and ITC, exhibited more potent anti-proliferative and pro-apoptotic effects both *in vitro* and *in vivo* at a comparatively lower dose as compared to its parent molecule, PTER. Our results also provide evidence supporting AKT and ERK as key protein kinases for regulating the apoptotic sensitivity of MCF-7 cells to PTER-ITC.

There are two distinct but interconnected pathways, namely, death receptor and mitochondria-mediated pathways in the regulation of apoptosis. While caspase-9 is involved in the intrinsic pathway, caspase-8 is typically associated with the initiation of the death-receptor pathways which are independent of mitochondria [Chen and Wang, 2002; Hengartner MO, 2000]. Previous studies have shown that PTER could inhibit cell cycle progression and cause apoptosis in human breast cancer cells. Here we tested the effect of PTER-ITC on intrinsic and extrinsic apoptotic pathways in MCF-7 cells. Our data showed that the PTER-ITC molecule displayed specificity by significantly increasing only caspase-9 activity while not activating caspase-8. Moreover, increase in caspase-9 activity led to subsequent activation of the downstream caspase-7, an apoptotic executioner. Pharmacological inhibition of caspase-9 almost completely protected the cells from PTER-ITC induced apoptosis while inhibition of caspase-8 had little or no effect, indicating the possibility that PTER-ITC induced apoptosis is specific to the mitochondrial intrinsic pathway. On the other hand, PTER and 5-FU showed up-regulation of caspase-8 and caspase-9 coupled with subsequent increase in caspase-7 activation, indicative of activation of both intrinsic and extrinsic pathways which was in contrary to the PTER-ITC.

The key element in the intrinsic pathway is the efflux of cytochrome-c from mitochondria to cytosol. Once cytochrome c is in the cytosol, it together with Apaf-1 activates caspase-9, and the latter then activates caspase-3 that finally leads to apoptosis [Nijhawan et al., 1997]. In the present study, the immunofluorescence data for cytochrome-c showed a significant increase of this protein in the cytosol of treated cells as compared with PTER and untreated cells. Thus suggesting that mitochondrial release of cytochrome-c was triggered by this phytochemical. The sensitivity of cells to apoptotic stimuli depends on the balance of pro and anti-apoptotic Bcl-2 proteins which are controlled by levels of cellular damage or stress [Raff M, 1998]. Therefore, increasing levels of pro-apoptotic proteins such as Bid, Bax, and Bak, while decreasing levels of anti-apoptotic protein for instance, Bcl-2, Bcl-xL and survivin is particularly important in promoting a cell's susceptibility to apoptosis [Chen and Wang, 2002; Raff N, 1998]. In the present study PTER-ITC and PTER induced apoptosis was associated with increase in the level of Bax protein which heterodimerizes with, and thereby inhibits, Bcl-2 expression. Changes in the ratio of Bax/Bcl-2 stimulate the release of cytochrome-c from mitochondria into cytosol which then interacts with Apaf-1 and leads to the activation of caspase-9 finally causing cell death. Similar activity of PTER has been reported previously in human gastric [Pan et al., 2007] and breast carcinoma cells [Chakraborty et al.,

2010]. Moreover, increased AIF expression showed that PTER-ITC molecule not only caused caspase dependent but also caspase independent apoptosis.

ROS normally exist in all aerobic cells in balance with biochemical antioxidants. Oxidative stress occurs when this critical balance is disrupted because of excess ROS production and/or antioxidant depletion [Kondo et al., 2006]. Many chemotherapeutic agents may be selectively toxic to tumor cells because they increase oxidant stress and enhance these already stressed cells beyond their limit [Moon et al., 2009; Kim et al., 2005; Lee et al., 2009]. Cytotoxic ROS signaling appears to be triggered by the activation of mitochondria-dependent cell death pathway through activation of MAPK pathways and the proapoptotic protein Bax, with subsequent mitochondrial membrane permeabilization and cell death [Gomez-Lazaro et al., 2007; Manohar et al., 2013]. Our results suggest that the PTER-ITC induced apoptosis might be initiated by generation of ROS which then leads to the disruption of mitochondrial membrane potential and release of cytochrome c into the cytosol and finally activating caspase-9/-3 cascade.

Several protein kinase pathways have been known to regulate cell proliferation and survival. MAPK and PI3K/AKT pathways are the major oxidative stress sensitive signal transduction pathways in most cell types [Simstein et al., 2003; Carvalho et al., 2004]. MAPKs, a family of serine-threonine protein kinases, have been implicated in apoptosis and cell cycle regulation signaling in diverse cell models [[Simstein et al., 2003; Carvalho et al., 2004; Boldt et al., 2002]. The MAPK family includes three kinase members, namely, c-Jun NH2-terminal protein kinase/stress activated protein kinase (JNK/SAPKs), p38 MAPK, and extracellular signal-regulated kinase (ERK). The ERK1/2 signaling pathway is activated by mitogens and growth factors through a Ras/Raf/MEK signaling and regulates cell proliferation, survival and cell differentiation [Gioeli et al., 1999]. The inhibition of ERK1/2 pathway has been reported to cause induction of apoptosis [Albreu-Martin et al., 1999]. In addition to MAPKs, another protein kinase, AKT, can mediate cell growth via the phosphorylation of a variety of substrates including Bad, glycogen synthase kinase-3 (GSK-3) and FOXO transcription factors [Lawlor and Alessi, 2001; El Touny and Banerjee, 2007]. Previous studies have shown that PTER inhibits (HRG)-β1-mediated motility and invasion of MCF-7 cells through the down-regulation of MMP-9 expression that is associated with the ERK, p38, and AKT signaling pathways in breast cancer cells [Pan et al., 2011]. However, there have been no studies on the mechanism of action of PTER and ITC conjugate towards the (in)activation of PI3K/AKT and ERK/MAPK pathways in MCF-7 cells. The PI3K/AKT signaling pathway inhibits apoptosis by inactivating important members of the apoptotic cascade, including

caspase-9, pro-apoptotic Bad [Brunet et al., 1999] and survivin [Kim et al., 2004]. In the present study, our findings established a mechanistic link between the MAPK pathway, AKT, and PTER-ITC induced apoptosis in MCF-7 cells through down regulation of survivin. The PTER-ITC conjugate induced a dose dependent down-regulation of PI3K/AKT, survivin, and ERK. Interestingly, the expression of survivin was significantly decreased after the maximal down-regulation of p-AKT. Further, when the cells were stimulated with AKT kinase inhibitor (A6730) and the ERK specific inhibitor (PD98059) alone and with different concentrations of drug both the inhibitors further enhanced the cell growth inhibitory effect and apoptosis that was already induced by PTER-ITC molecule alone. These data suggests that the PTER-ITC treatment inhibits cell growth and enhances apoptosis via AKT and ERK/MAPK pathways in MCF-7 cells. Further the levels of survivin and caspase-9 were regulated by PTER-ITC via the PI3K/AKT pathway. Collectively, our results suggest that the modulation of ERK and AKT phosphorylation contribute to the anti-cancer effect of this PTER-ITC conjugate molecule.

In the next phase of the study PTER and PTER-ITC at different doses were tested *in vivo* against EAC induced tumor in Swiss albino mice. Ascitic fluid is direct source of nutrition for tumor cells and a rapid increase in ascitic fluid with tumor would be a mean to meet the nutritional requirement of tumor cells [Rajeshwar et al., 2005]. Treatment with PTER and PTER-ITC inhibited tumor volume and also increased the lifespan of tumor bearing mice. Further, to understand the underlying mechanism for this regression in tumor volume we checked the expression level of apoptotic marker proteins like caspase-3 and Bax in tumor samples. Our data showed that the expressions of apoptotic marker proteins were up-regulated after treatment with PTER-ITC. These results clearly support the anti-tumor action of the PTER-ITC.

In vivo experimental studies have already shown that tumor growth and metastasis are dependent on angiogenesis [Folkman J, 2007]. Angiogenesis is a property of most solid tumors and is necessary for their continued growth. Thus inhibiting tumor angiogenesis may halt the tumor growth and decrease metastatic potential of tumors. Further, it has been earlier reported that ascitic tumor growth including EAC cells are angiogenesis dependent [Luo et al., 1998] and VEGF being a permeability factor plays a fundamental role in the fluid accumulation and tumor growth in ascitic tumor. By secreting VEGF, the permeability of pre-existing micro vessel lining of peritoneal cavity is enhanced which stimulates ascites formation thereby tumor progression. Inhibition of fluid accumulation, tumor growth, and micro vessel density by neutralization of VEGF has been demonstrated underlining the importance of VEGF in malignant ascites formation [Messiano et al., 1998; Kim et al., 1993]. Consistent with the

previous reports, our studies also demonstrated that the PTER-ITC inhibited tumor angiogenesis by inhibiting the expression of VEGF in tumor tissue samples and thus reducing the tumor volume in EAC bearing mice. These observations indicate that PTER-ITC possess both anti-tumor and anti-angiogenic activities.

The results presented here clearly shows that PTER-ITC conjugate is an effective inhibitor of cell growth/proliferation and inducer of apoptosis in human breast cancer cells by acting at various targets like activation of AIF, Bax, caspase-9, p-c-Jun and decreasing Bcl2, p-AKT and p-ERK levels. Based on the present data it could be speculated that PTER-ITC is much more efficacious than both PTER and 5-FU. Further, its strong anti-cancer activity at a much lower dose as compared to its other counterpart (PTER) even after 24 h of stimulation reflects its increased efficacy with a scope for further improvements like combinatorial therapy along with other anti-cancer drugs. PTER-ITC induces apoptosis by enhancing the expression of apoptotic genes both at transcriptional and translational levels as characterized by over expression of Bax, change in mitochondrial membrane potential and subsequent release of cytochrome-c from mitochondria into cytoplasm. Moreover, both PI3K/AKT and MAPK/ERK pathways played an important role on PTER-ITC induced apoptosis of MCF-7 cells. The inhibition of AKT pathway by PTER-ITC resulted in inhibition of survivin expression and up regulation of active caspase-9, a downstream target of the PI3K/AKT pathway. Increase in reactive oxygen species production may be another reason for induction of apoptosis by this compound. Further, reduction in ascitic tumor volume on treatment with PTER-ITC showed the anti-tumor properties of this compound on EAC bearing mice. To the best of our knowledge this is the first ever report where PTER has been conjugated with an ITC group to make a hybrid molecule having potent anti-cancer properties. Our results thus suggest a novel strategy of combining PTER and ITC which may benefit patients with breast cancer with minimum side effects. However, further in depth research including animal experimentation on breast tumor models are needed in order to fully understand the inhibition of tumor progression and/or treatment of breast cancer and other human malignancies with this compound before considered for clinical trials.

Chapter 6. PTER-ITC Mediates PPARγ Dependent Apoptosis

6.1 Introduction

The incidence of cancer, in particular breast cancer, continues to be the focus of worldwide attention. Breast cancer is the most frequently occurring cancer and the leading cause of cancer deaths among women, with an estimated 1,383,500 new cases and 458,400 deaths annually [Jemal et al., 2011]. Many treatment options, including surgery, radiation therapy, hormone therapy, chemotherapy, and targeted therapy, are associated with serious side effects [Sjövall al., 2010; Moore S, 2007; Odle TG, 2014 and deRuiter et al., 2014]. Since cancer cells exhibit deregulation of many cell signaling pathways, treatments using agents that target only one specific pathway usually fail in cancer therapy. Several targets can be modulated simultaneously by a combination of drugs with different modes of action, or using a single drug that modulates several targets of this multifactorial disease [Sarkar et al., 2009].

Peroxisome proliferator-activated receptors (PPAR) are ligand-binding transcription factors of the nuclear receptor superfamily, which includes receptors for steroids, thyroids and retinoids [Hans and Romans, 2007; Sertzing et al., 2007]. Three types of PPAR have been identified (α, β, γ), each encoded by distinct genes and expressed differently in many parts of the body [Sertzing et al., 2007]. They form heterodimers with the retinoid X receptor, and these complexes subsequently bind to a specific DNA sequence, the peroxisome proliferating response element (PPRE) that is located in the promoter region of PPARγ target genes and modulates their transcription [Tachibana et al., 2008]. PPARγ is expressed strongly in adipose tissue and is a master regulator of adipocyte differentiation [Lehrke and Lazar, 2005]. In addition to its role in adipogenesis, PPARγ is an important transcriptional regulator of glucose and lipid metabolism, and is implicated in the regulation of insulin sensitivity, atherosclerosis, and inflammation [Lehrke and Lazar, 2005; Semple et al., 2006]. PPARγ is also expressed in tissues such as breast, colon, lung, ovary, prostate and thyroid, where it regulates cell proliferation, differentiation, and apoptosis [Zhang et al., 2005; Elstner et al., 1998; Schmidt et al., 2010].

Although it remains unclear whether PPAR are oncogenes or tumor suppressors, research has focused on this receptor because of its involvement in various metabolic disorders associated with cancer risk [Oyekan 2011; Wilding 2012; Chen et al., 2012]. The anti-proliferative effect of PPARγ is reported in various cancer cell lines including breast [Woo et al.,2011., Yin et al., 2001; Kumar et al., 2009; Venkatachalam et al., 2009], colon [Sarraf et al., 1998], prostate [Kubota et al., 1998] and non-small cell lung cancer [Chang and Szabo, 2000].

Ligand-induced PPARγ activation can induce apoptosis in breast [Cui et al., 2007; Kumar et al., 2009; Elstner et al., 1998, and Kim et al., 2006], prostate [Kubota et al., 1998] and non-small cell lung cancer [Chang and Szabo, 2000], and also PPARγ ligand activation is reported to inhibit breast cancer cell invasion and metastasis [Liu et al., 2003; Panigrahy et al., 2002]. However results of many studies and clinical trials have raised questions regarding the role of PPARγ in anticancer therapies, since its ligands involve both PPARγ-dependent and -independent pathways for their action [Han and Roman, 2007].

Previous studies showed that thiazolidinediones can inhibit proliferation and induce differentiation-like changes in breast cancer cell lines both *in vitro* and in xenografted nude mice [Mueller et al., 1998; Elstner et al., 1998]. Alternately, Abe et al. showed that troglitazone, a PPARγ ligand, can inhibit KU812 leukemia cell growth independently of PPARγ involvement [Abe et al., 2002]. In addition to *in vitro* studies, *in vivo* administration of PPARγ ligands also produced varying results. The use of troglitazone was reported to inhibit MCF-7 tumor growth in triple-negative immunodeficient mice [Elstner et al., 1998] and in DMBA-induced mammary tumorigenesis [Pighetti et al., 2001], and administration of a PPARγ ligand (GW7845) also inhibited development of carcinogen-induced breast cancer in rats [Suh et al., 1999]. In contrast, a study by Lefebvre et al. showed that PPARγ ligands, including troglitazone and BRL-49653, promoted colon tumor development in C57BL/6JAPCMin/+ mice, raising the possibility that PPARγ acts as a collaborative oncogene in certain circumstances [Lefebvre et al., 1998]. It thus appears that PPARγ activation or inhibition can have distinct roles in tumorigenesis, depending on the cancer model examined. Hence determining possible crosstalk between PPARγ and its ligand in cancer is critical for the development of more effective therapy.

Trans-3,5-dimethoxy-4-hydroxystilbene (PTER) is an antioxidant found primarily in blueberries. This naturally occurring dimethyl ether analog of resveratrol (RESV) has higher oral bioavailability and enhanced potency than RESV [Kapetanovic et al., 2011]. Based on its anti-neoplastic properties in several common malignancies, studies suggest that PTER has the hallmark characteristics of an effective anticancer agent [McCormack and McFadden, 2012; Chakraborty et al., 2010; Chakraborty et al., 2012; Li et al., 2013, Mena et al., 2012]. Our recent study, as reported in previous chapter showed that PTER-ITC conjugate, a novel class of hybrid compound synthesized by appending an isothiocyanate moiety to the PTER backbone, can induce greater cytotoxicity in tumor cells at a much lower dose than the PTER parent compound [Nikhil et al., 2014a]. As PPARγ mediates anti-tumor activity in a variety of cancer types, we hypothesized that PTER-ITC could modulate the activity of PPARγ pathway in

breast cancer cells and inhibit tumor cell growth. Our results show that PTER-ITC induced apoptosis in breast cancer cells through caspase activation, which increased the Bax/Bcl-2 ratio and downregulated survivin. Our molecular docking study also demonstrated that PTER-ITC make contact with amino acids within the ligand-binding pocket of PPARγ that are crucial for its activation. We found that PPARγ activation has an important role in PTER-ITC-induced apoptosis and reduced survivin levels. Our studies thus provide evidence for the usefulness of PTER-ITC in breast cancer therapy involving various pathways, including PPARγ.

6.2 Brief Methodology

6.2.1 Cell lines and culture

Three breast cancer cell lines (MCF-7, MDA-MB-231 and T47D) with distinct characteristics were obtained from the National Centre for Cell Science (NCCS; Pune, India). MCF-7 and T47D are estrogen receptor (ER)-positive and lack HER-2 expression, while MDA-MB-231 is ER-negative and has low HER-2 expression. MCF-7 cells express wild-type p53, whereas MDA-MB-231 and T47D express mutant p53. All three cell lines express PPARγ protein.

6.2.2 Luciferase assay

PPARγ activity was studied by luciferase assay as described earlier (Woo et al., 2011). Briefly, cells were seeded at density of ~4 x 10^4 cells/well in 12-well microtiter plates, and incubated overnight. Cells were then incubated in serum-free DMEM for ≥1 h before transfection with PPREx3-tk-Luc (three PPRE from rat acyl-CoA oxidase promoter under the control of the Herpes simplex virus thymidine kinase promoter) and Renilla-luc plasmids as an internal control. For PPAR study, cells were transfected with 25 ng pcMX-PPARα, pcMX-PPARβ and pcMX-PPARγ plasmids, each with 250 ng of reporter gene plasmid using Polyfect transfection reagent (Qiagen), according to instructions. Transfected cells were exposed to vehicle, various concentrations of PTER, PTER-ITC and PPAR agonist or antagonist in charcoal-stripped medium (24 h). Cells were then lysed and luciferase activity measured according to the manufacturer's instructions (Promega, Madison, WI). Triplicates were measured for each experimental point; variability was <10%. Luciferase values for each lysate were normalized to Renilla luciferase activity.

6.3 Results

6.3.1 Differential PPARγ expression in distinct breast cancer cell lines

Three breast cancer cell lines (MCF-7, MDA-MB-231, T47D) were analyzed for PPARγ expression. RT-PCR results showed that *PPARγ* transcription was highest in MDA-MB-231 cells compared to the other two cell lines (Fig. 6.1, left). In accordance, we found that PPARγ protein expression was also higher in MDA-MB-231 cells, followed by MCF-7 and T47D cell lines (Fig. 6.1, right). Based on these results, we selected MCF-7 and MDA-MB-231 cells as *in vitro* models for the remaining part of the study.
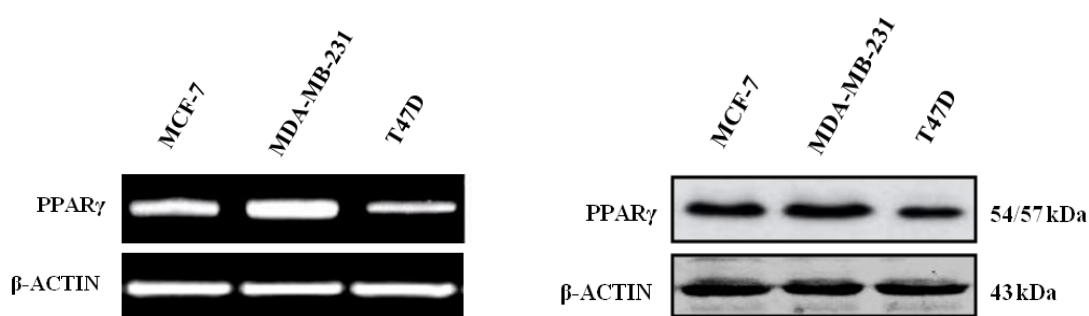
Figure 6.1: PPARγ expression in three breast cancer cell lines as determined by RT-PCR (left) and immunoblot analysis (right).

6.3.2 PPARγ is involved in PTER-ITC-induced inhibition of cell proliferation

MCF-7 and MDA-MB-231 cells were treated with increasing concentrations (1-60 μM) of PTER and PTER-ITC for 24 h and cell survival was determined by MTT assay. Our data showed that treatment of these cells with PTER and PTER-ITC resulted in dose-dependent inhibition of cell proliferation, which was more pronounced after PTER-ITC treatment compared to vehicle-treated control cells in both the cell lines (Fig. 6.2 A, B). In MCF-7 cells treated with 10 and 20 μM PTER-ITC, viable cell numbers decreased from 75% to 55%, which was about 92% and 85% respectively, after PTER treatment (Fig. 6.2C). Preincubation of cells with 10 μM GW9662 (a PPARγ antagonist) increased cell survival from 75% to 87% in the presence of 10 μM PTER-ITC, which was 55% to 67% in the case of 20 μM PTER-ITC ($p<0.05$) (Fig. 6.2C). PTER treatment did not lead to improvement in viability when cells were pretreated with GW9662. Results were similar for MDA-MB-231 cells, in which with 10 μM GW9662 pretreatment increased cell survival from 82% to 97% in the presence of 10 μM PTER-ITC, and 70% to 87% after 20 μM PTER-ITC treatment ($p<0.05$) (Fig. 6.2D).
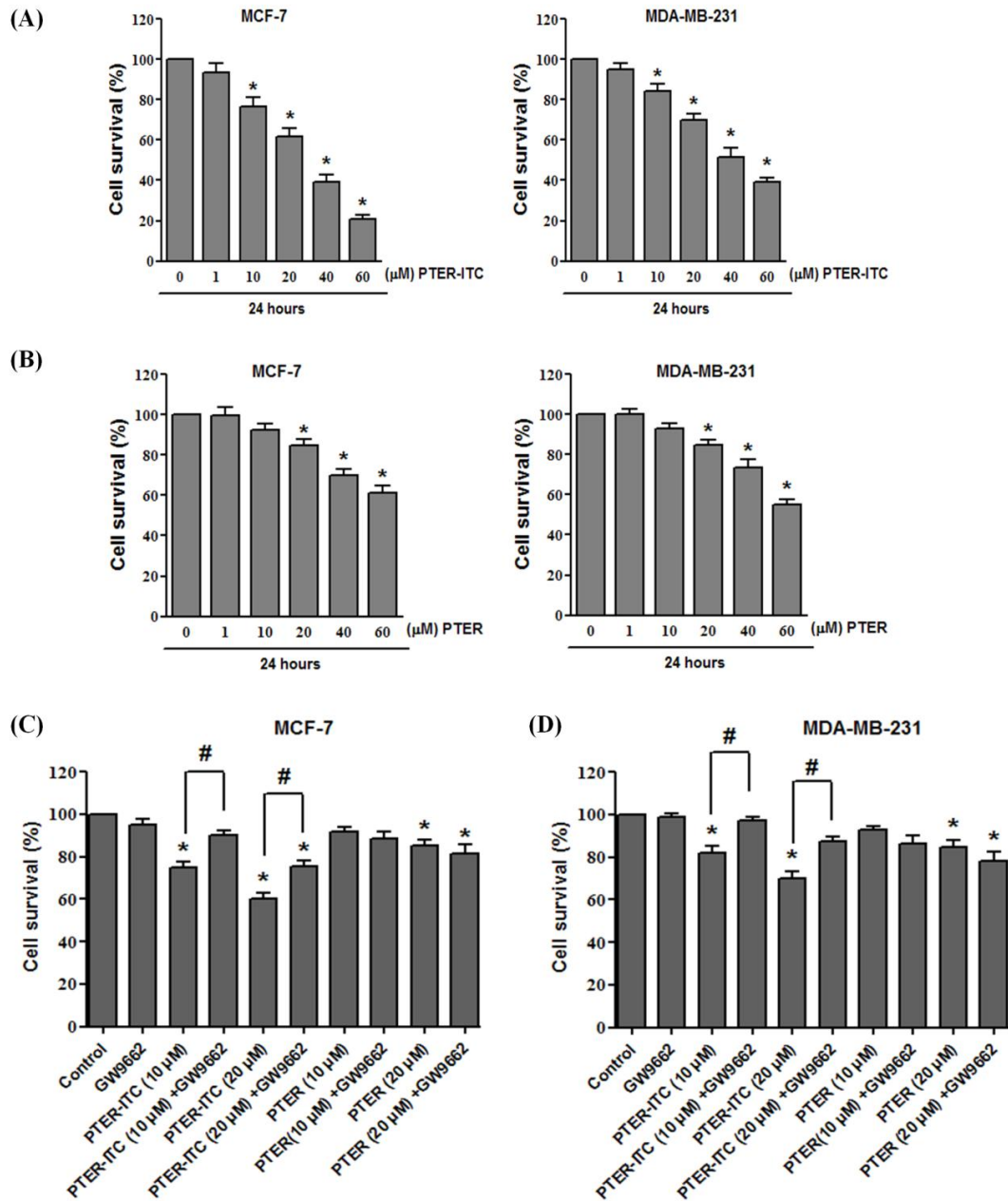
Figure 6.2: Effect of PTER and PTER-ITC on viability of breast cancer cells (A) Cytotoxicity induced by increasing doses of PTER-ITC and (B) PTER in breast cancer cells as determined by MTT assay. Effect of GW9662 on survival of (C) MCF-7 and (D) MDA-MB-231 cells alone and in the presence of PTER-ITC and PTER. Data are shown as mean ± SEM of three independent experiments. * and # indicate statistically significant differences with respect to controls (vehicle-treated) and only PTER-ITC treated groups, respectively at $p<0.05$.

6.3.3 PTER-ITC upregulates PPARγ expression and activity

To examine changes in PPARγ mRNA and protein expression following exposure to different drugs, we used RT-PCR, immunoblot and immunofluorescence techniques. In MCF-7 cells, the *PPARγ* transcript level increased in response to PTER-ITC in a dose-dependent manner, which was ~1.5-fold at the highest dose tested (Fig. 6.3A). In contrast, PTER showed no significant increase, while the PPARγ agonist rosiglitazone caused a 1.7-fold upregulation in its expression, as anticipated. Results were similar in MDA-MB-231 cells, in which PTER-ITC, PTER and rosiglitazone showed 1.6-, 1.1- and 1.8-fold increases in PPARγ mRNA levels at a 20 μM concentration (Fig. 6.3B). This result was validated by immunoblot analysis, in which we observed a dose-dependent increase in PPARγ protein expression after PTER-ITC treatment in MCF-7 (2.1- to 2.8-fold) and MDA-MB-231 cells (1.5- to 2.6-fold) (Fig. 6.3C, D) ($p<0.05$). Treatment with 20 μM PTER had little or no effect, while treatment with same dose of rosiglitazone led to a significant increase in PPARγ expression in MCF-7 and MDA-MB-231 cells ($p<0.05$).

Immunofluorescence analysis of PPARγ localization also showed increased nuclear accumulation of PPARγ for PTER-ITC- and rosiglitazone-treated MCF-7 (Fig. 6.4A) and MDAMB-231 cells (Fig. 6.4B) compared to control cells, which was markedly inhibited by GW9662. PTER treatment led to no increase in PPARγ expression or activity. These data showed that PPARγ expression was upregulated by PTER-ITC at both the transcriptional and translational levels.

6.3.4 PPARγ participates in PTER-ITC-mediated upregulation of the PTEN tumor suppressor gene

To determine the effect of PTER, PTER-ITC and rosiglitazone on the expression pattern of the tumor suppressor gene PTEN, we treated MCF-7 and MDA-MB-231 cells with various concentrations of drugs for 24 h. RT-PCR and immunoblot analysis showed that PTER-ITC increased PTEN expression at both the transcriptional (Fig. 6.3A, B) and translational levels (Fig. 6.3C, D) in a dose-dependent manner ($p<0.05$). The most effective dose was 20 μM PTER-ITC, which caused an increase almost comparable to that of rosiglitazone. There was little or no difference in the relative level of PTEN in the PTER-treated group compared to vehicle treated controls (Fig. 6.3C, D) ($p<0.05$).
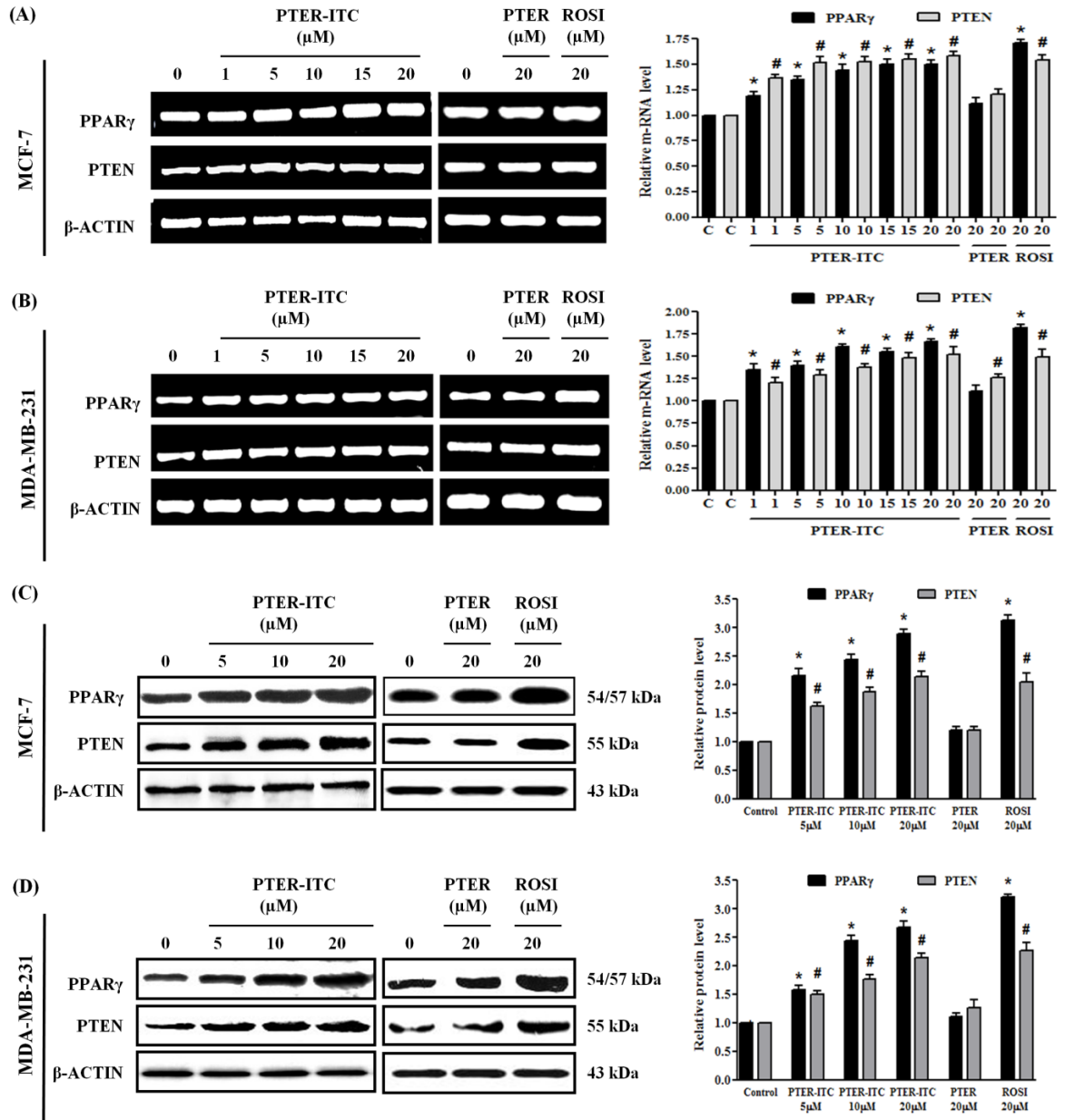
Figure 6.3: PTER-ITC upregulates PPARγ and PTEN expression levels. (A) Effect of PTER-ITC, PTER and rosiglitazone on PPARγ and PTEN mRNA expression as determined by RT-PCR in MCF-7 and (B) MDA-MB-231 cells. Effect of PTER-ITC, PTER and rosiglitazone on PPARγ and PTEN protein expression as determined by immunoblot analysis in (C) MCF-7 and (D) MDA-MB-231 cells. Histogram (right panel in each figure) shows relative band intensities normalized to the corresponding β actin level. Data are expressed as x-fold increase relative to control; values shown as mean ± SEM of three independent experiments. * and # indicate statistically significant differences with respect to controls for PPARγ and PTEN proteins, respectively. $p<0.05$; ROSI, rosiglitazone.

145
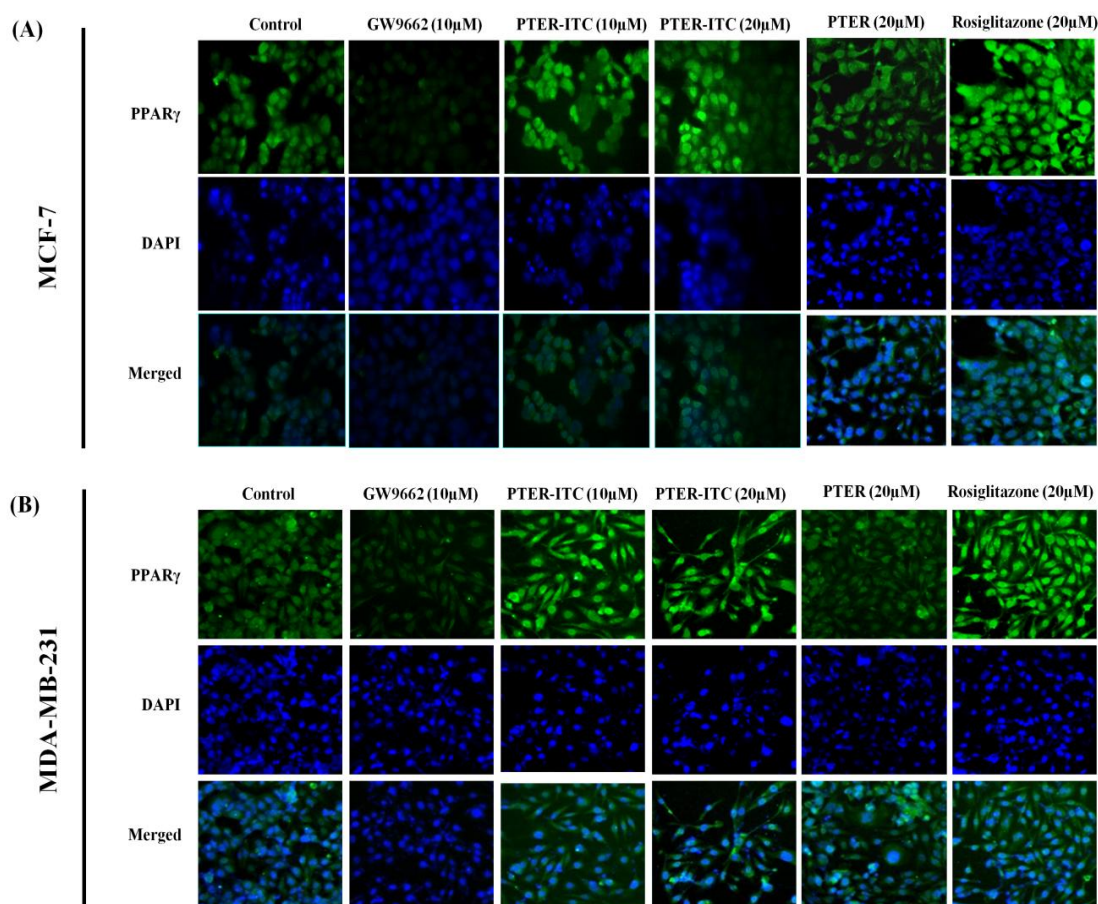
Figure 6.4: Induction of PPARγ expression in response to different treatments. Immunofluorescence analysis to detect PPARγ protein in (A) MCF-7 and (B) MDA-MB-231 breast cancer cells after treatment with GW9662, PTER-ITC, PTER and rosiglitazone. Figures show one representative experiment of three performed. Magnification, 200 ×.

6.3.5 PTER-ITC increased PPARγ and PPARβ activity in MCF-7 cells

We used a luciferase reporter-based transactivation assay to study the effect of PTER-ITC on the activity of various PPAR types in breast cancer cells. For this the cells were transfected with plasmids encoding each PPAR protein (pcMX-PPARα, pcMX-PPARβ or pcMX-PPARγ) and with PPRE-tk-Luc and Renilla luciferase plasmids as internal control. The cells were then treated with PTER and PTER-ITC (24 h), followed by extraction of whole-cell lysates for analysis of luciferase activity. Our data showed that PTER-ITC induced PPARβ and PPARγ activities, but had no significant effects on PPARα (Fig. 6.5A; $p<0.05$), whereas PTER induced only PPARα activity, with no significant change in PPARβ and PPARγ activities (Fig. 6.5A; $p<0.05$). Next we examined the specificity of PTER-ITC on PPARγ and PPARβ activities, using their respective agonists and antagonists. The PPARβ antagonist GSK0660 did not reverse PTER-ITC-induced PPARβ activity (Fig. 6.5B), suggesting that the PTER-ITC

effect on PPARβ was non-specific. Interestingly the PPARγ antagonist, GW9662 reversed PTER-ITC-induced PPARγ activity significantly (Fig. 6.5C), as well as the activity of rosiglitazone, a PPARγ agonist (Fig. 6.5C, right). These data suggested that PTER-ITC activity is mediated mainly via the PPARγ but not the PPARβ pathway.
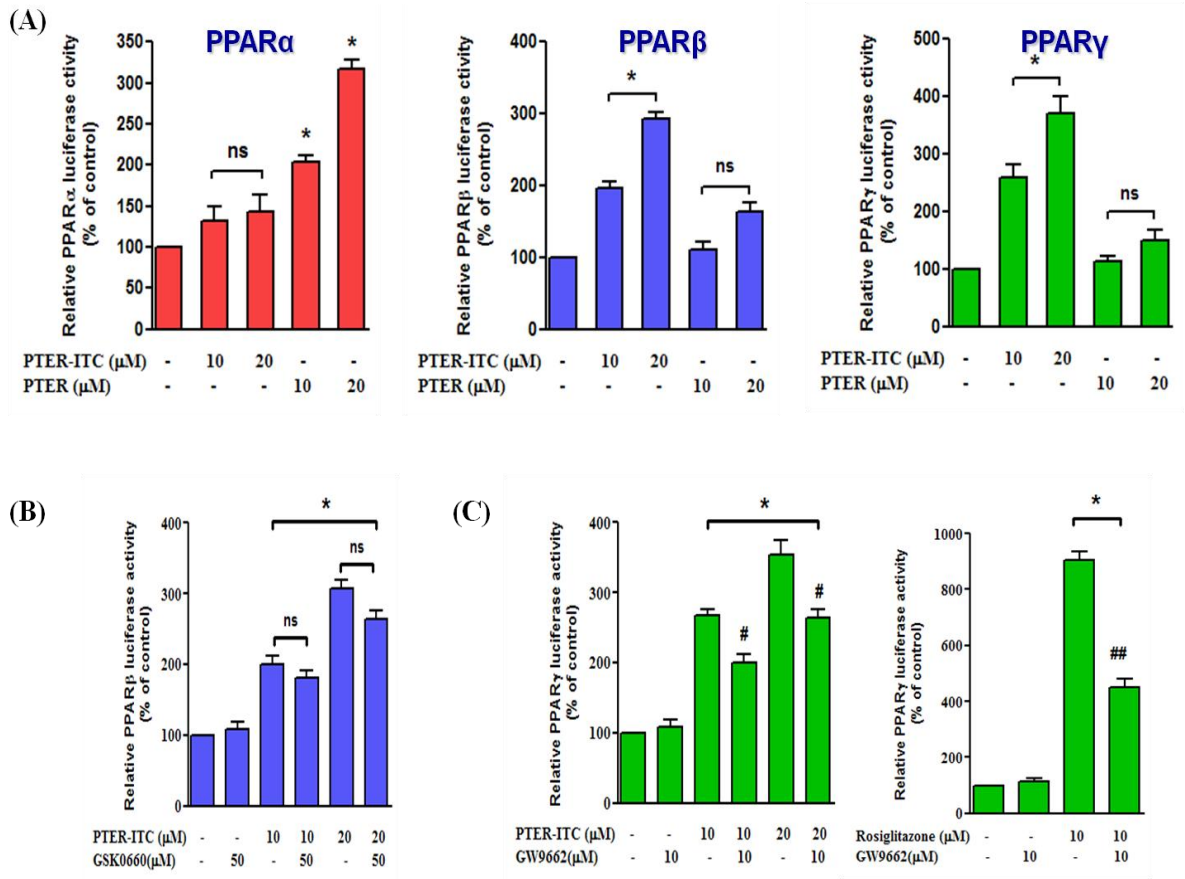
Figure 6.5: PTER-ITC alters PPAR activity (A) Effect of PTER-ITC and PTER on the activity of various PPAR in MCF-7 cells, as determined by transactivation assay. Data are expressed as a percentage of PPAR activity relative to the respective control. Values shown as mean ± SEM of three independent experiments. * indicates significant difference relative to vehicle-treated control; $p<0.05$. (B) Effect of PPARβ inhibitor (GSK0660) and (C) PPARγ inhibitor (GW9662) and activator (rosiglitazone) on PTER-ITC-induced transactivation of PPAR. Cells were transfected with pcMX-PPARβ/γ plasmids, together with PPRE-tk-luc and Renilla plasmids (18 h). Cells were then pre-treated with GSK0660/GW9662 (4 h), followed by PTER-ITC/rosiglitazone treatment (24 h). Data are expressed as percentages of PPARβ/γ activity relative to the vehicle-treated control. Values are shown as mean ± SEM of three independent experiments. *, # and ## indicate statistically significant difference compared to respective controls, only PTER-ITC (either 10 or 20 μM) and rosiglitazone-treated groups, respectively; $p<0.05$. ns, not significant.

6.3.6 Effects of PTER-ITC on MCF-7 cell differentiation

PPARγ activation induces cells to a more differentiated, less malignant state and causes extensive lipid accumulation in cultured breast cancer cells [Mueller et al., 1998]. We thus used Oil Red O staining to test whether addition of PTER-ITC and rosiglitazone in MCF-7 cells also induces their differentiation. Untreated MCF-7 cells showed nominal lipid accumulation as measured by Oil Red O staining (Fig. 6.6, left). In contrast, rosiglitazone treatment (10 μM) strongly induced lipid accumulation; PTER-ITC treatment also caused a dose-dependent increase in lipid accumulation, albeit to a lesser extent than rosiglitazone (Fig. 6.6). Maximum lipid accumulation was found at 5 μM PTER-ITC (Fig. 6.6, right).
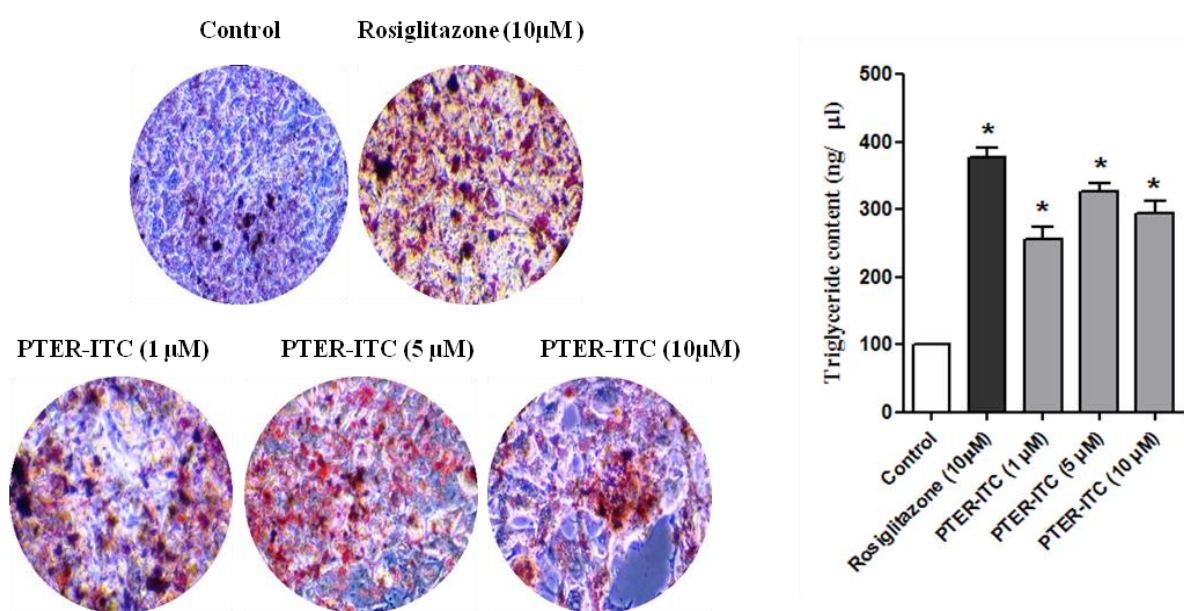
Figure 6.6: PTER-ITC induces differentiation of MCF-7 cells. Oil Red O staining showing lipid accumulation in MCF-7 cells treated with different doses of PTER-ITC and rosiglitazone (10 μM), observed by light microscopy (200x). Histogram (right) shows spectrophotometric estimation of intracellular neutral lipids. Values shown are mean ± SEM of two independent experiments. * indicates significant difference relative to vehicle-treated controls; $p<0.05$.

6.3.7 Molecular modeling of PPARγ LBD/PTER-ITC binding

Since PTER-ITC increased PPARγ transactivation by acting as a selective PPARγ ligand, we used molecular docking analysis to further study PPARγ LBD (ligand-binding domain)/PTER-ITC interaction at the cellular level. PTER-ITC, its parent compound (PTER), and RESV were docked into the PPARγ LBD. The binding mode of each ligand to PPARγ LBD is shown in Fig. 6.7A, with their respective docking scores and interaction energies in

Table 6.1. The terms "XP Glidescore or docking score" and "Emodel" were used to denote interactions between ligand and receptor. Based on these two scores, we observed that the PTER-ITC molecule might have better binding affinity for PPARγ (Table 6.1). In terms of interaction with different residues, PTER-ITC showed better performance than PTER and RESV. In the best-docked position, PTER-ITC formed two hydrogen bonds with the receptor, involving residues His323 and Tyr327 (Table 6.1; Fig. 6.7B). In addition, through extensive hydrophobic interactions, it bound more firmly to the receptor than the other two ligands (Fig. 6.7C). Tyr473 is involved in hydrogen bond formation with both PTER and RESV, indicating a similar orientation of the two molecules, which is also evident from close analysis of their docking positions (Fig. 6.7A). Besides hydrogen bonds and hydrophobic interactions, PTER-ITC is also involved in the formation of π-π stacking between LBD residues His449 and Phe282 and their central benzene rings. This stacking could stabilize PTER-ITC after binding and strengthen the interaction. Similar stacking is partially observed in PTER, which involves only His449.

Table 6.1 Hydrogen bonds and hydrophobic interactions between ligand and PPAR-γ ligand binding domain (LBD). Average Van der Waals (Vdw), Electrostatic (Coul) and model energy (Emodel) of ligands after docking. The corresponding docking scores are also mentioned.

Ligand	Hydrogen bonds[a]	Hydrophobic bonds[b]	Evdw[c]	Ecoul[d]	Emodel[e]	Docking score
RESV	TYR473 (3.05)	PHE282, CYS285, SER289, PHE360, PHE363, TYR473	-23.2	-3.8	-34.3	-7.30
PTER	TYR473 (2.87)	CYS285, SER289, PHE360, PHE363, HIS449, TYR479	-21.4	-1.8	-30.5	-6.78
PTER-ITC	HIS323 (3.10), TYR 327 (2.96)	ILE281 PHE282, CYS285, ILE326, LEU353, LEU356, PHE360, PHE363, MET364, HIS449, TYR473	-43.4	-6.7	-53.4	-8.46

[a]Bond length in Å is given under parentheses. [b]Only strong hydrophobic contacts forming residues are depicted. [c]Evdw= Van Der Waals interaction energy. [d]Ecoul = Coulomb interaction energy. [e]Emodel = Model energy
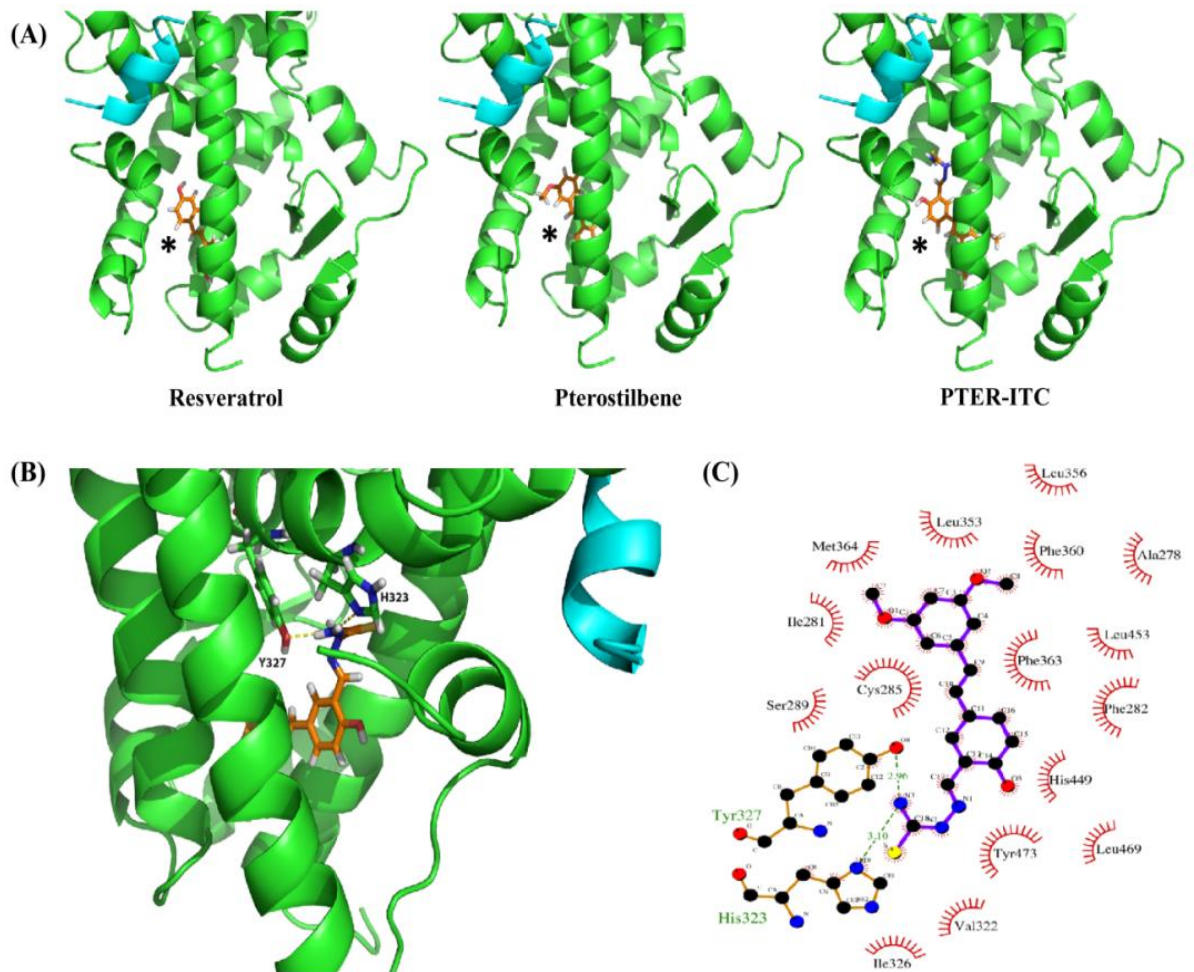
Figure 6.7: Analysis of PTER-ITC docking pattern with PPARγ. (A) Mode of binding of RESV, PTER and PTER-ITC to PPARγ. Note the distinct orientations of the ligands. The broad range of ligand binding ability of PPARγ can be explained in part by the large T shaped ligand binding area, which permits ligands to adopt distinct orientations (figures generated with PyMOL molecular graphics system). (B) Interaction of PTER-ITC within the ligand-binding pocket. Residues H323 and Y327 of protein chain A are involved in hydrogen bond formation with N3 of the ligand. Yellow dashed lines indicate bonding; interacting residues are labeled. (C) Ligand interaction plot showing different hydrophobic and two hydrogen bond interactions of PTER-ITC with PPARγ. Hydrogen bonds are indicated by green dashed lines, with their respective distances.

6.3.8 PPARγ antagonist GW9662 inhibits PTER-ITC-induced apoptosis

We analyzed PTER-ITC apoptosis induction by flow cytometry, using annexin V and propidium iodide (PI) double staining to assess the cause of decreased cell survival after PTER-ITC treatment. We incubated MCF-7 cells with varying concentrations of PTER-ITC, alone or with GW9662 (10 μM; 24 h). PTER-ITC treatment significantly increased the percentage of apoptotic cells, and the effect was partly attenuated by pre-incubation with GW9662 (Fig.

6.8A; $p<0.05$). PTER-ITC also induced apoptosis-associated morphological changes, as cells with condensed nuclei and nuclear fragmentation were apparent after treatment (Fig. 6.8B), which was minimal in vehicle-treated MCF-7 and MDA-MB-231 cells. The apoptotic nuclear changes were clearly reduced in cells pre-treated with 10 μM GW9662 (Fig. 6.8B). These data suggest that blockade of PPARγ activity blunted the drug-induced cell apoptosis.

6.3.9 PTER-ITC induces caspase-dependent apoptosis

Apoptosis is a complex activity that mobilizes a number of molecules, and its mechanisms are classified as caspase-dependent or -independent. The caspase-dependent pathway can be further divided into extrinsic or intrinsic pathways, determined by involvement of caspase-8 or caspase-9, respectively. Both of these pathways involve activation of caspase-3/7, which is important for inducing downstream molecules responsible for DNA cleavage. To further examine the mechanism that underlies PTER-ITC-induced death of breast cancer cells, we studied a possible role for caspase in this process by measuring the enzymatic activity of caspase-3/7, -8 and -9. We observed a gradual increase in caspase-9 and caspase-3/7 activities in MCF-7 and MDA-MB-231 cells treated with 10 and 20 μM PTER-ITC for 24 h (Fig. 6.9A). In contrast, there were no significant changes in caspase-8 activity in MCF-7 cells, whereas we found a dose-dependent increase in activity in MDA-MB-231 cells. Our data thus suggest that PTER-ITC induced activation of the intrinsic caspase pathway in MCF-7 cells, while it induced both extrinsic and intrinsic caspase pathways in MDA-MB-231 cells.

To determine whether caspase activation was involved in PTER-ITC-induced death of cultured breast cancer cells, we used pharmacological caspase inhibitors to test whether they protect cells from undergoing apoptosis. In the case of MDA-MB-231 cells, the general caspase inhibitor Z-VAD-FMK inhibited apoptosis most efficiently (up to 70-80%; Fig. 6.9B, $p<0.05$), suggesting that apoptosis is the predominant form of cell death induced by PTER-ITC in these cells. Z-LEHD-FMK, a specific inhibitor of caspase-9, inhibited PTER-ITC-induced apoptosis by 50-55% ($p<0.05$), while Z-IETD-FMK, a specific inhibitor of caspase-8, inhibited PTER-ITC-induced apoptosis by 65-70% ($p<0.05$). In contrast, Z-LEHD-FMK inhibited PTER-ITC-induced apoptosis by 66-70% in MCF-7 cells, while Z-IETD-FMK did not effectively block PTER-ITC-induced apoptosis in this cell line, which confirmed previous reports (Nikhil et al., 2014a). Our data thus demonstrate that PTER-ITC-induced apoptosis is a caspase-dependent process that involves both caspase-8 and -9 in MDA-MB-231 cells and only caspase-9 in MCF-7 cells.
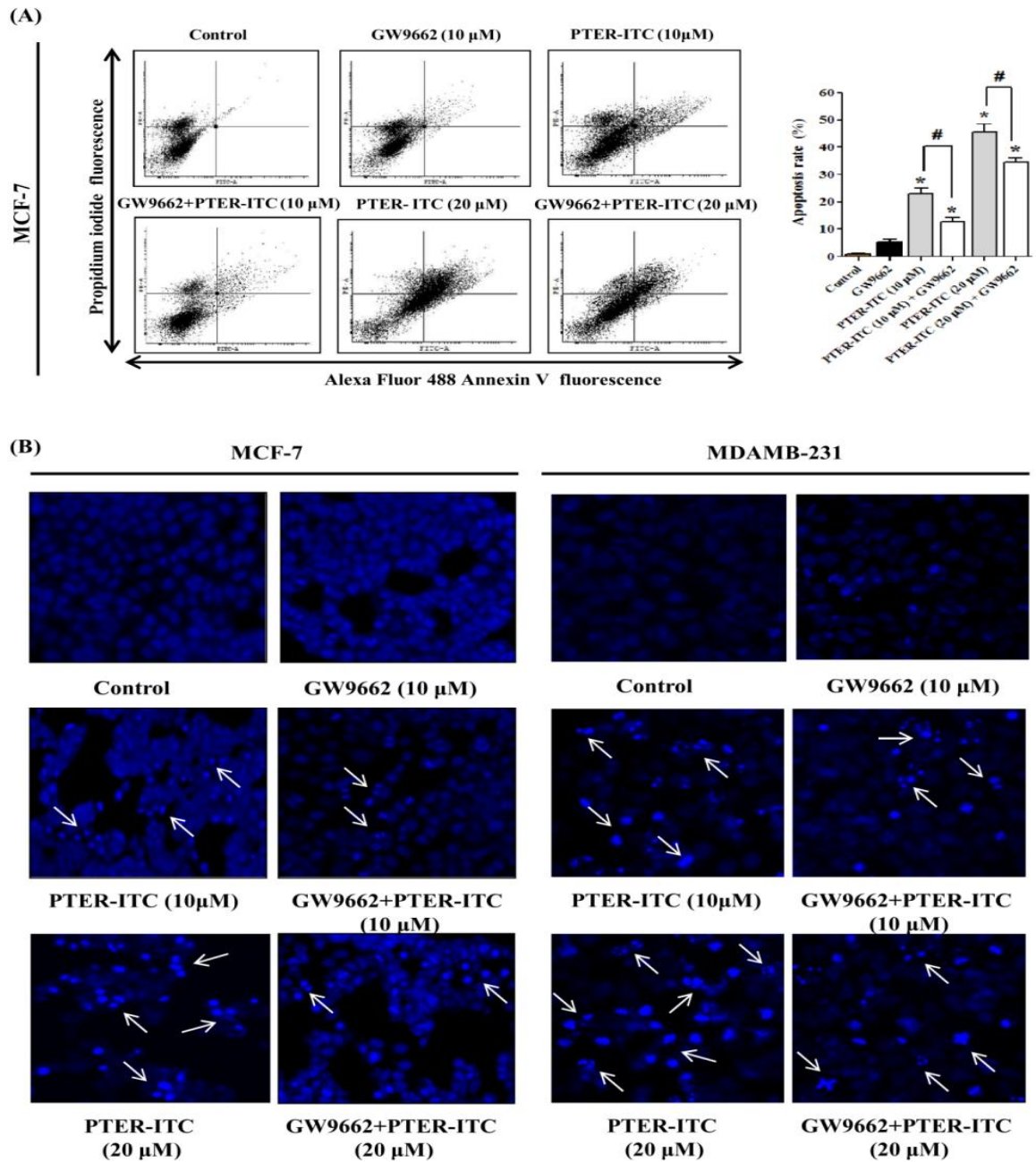
Figure 6.8: PTER-ITC induces PPARγ-dependent apoptosis in breast cancer cells. (A) Representative FACS analysis of cells using annexin V as marker. Histogram (right) shows the apoptosis rate induced by PTER-ITC alone and in the presence of GW9662. Values are mean ± SEM from three independent experiments. * and # indicate statistically significant differences compared to vehicle-treated control and only PTER-ITC treated groups, respectively; $p<0.05$. (B) Apoptosis induced by PTER-ITC alone and in the presence of GW9662, visualized by fluorescence microscopy using DNA-binding fluorochrome DAPI in MCF-7 and MDA-MB-231 breast cancer cells. Figures show a representative experiment of three performed. Magnification, 200 ×. Arrows indicate the formation of apoptotic bodies.
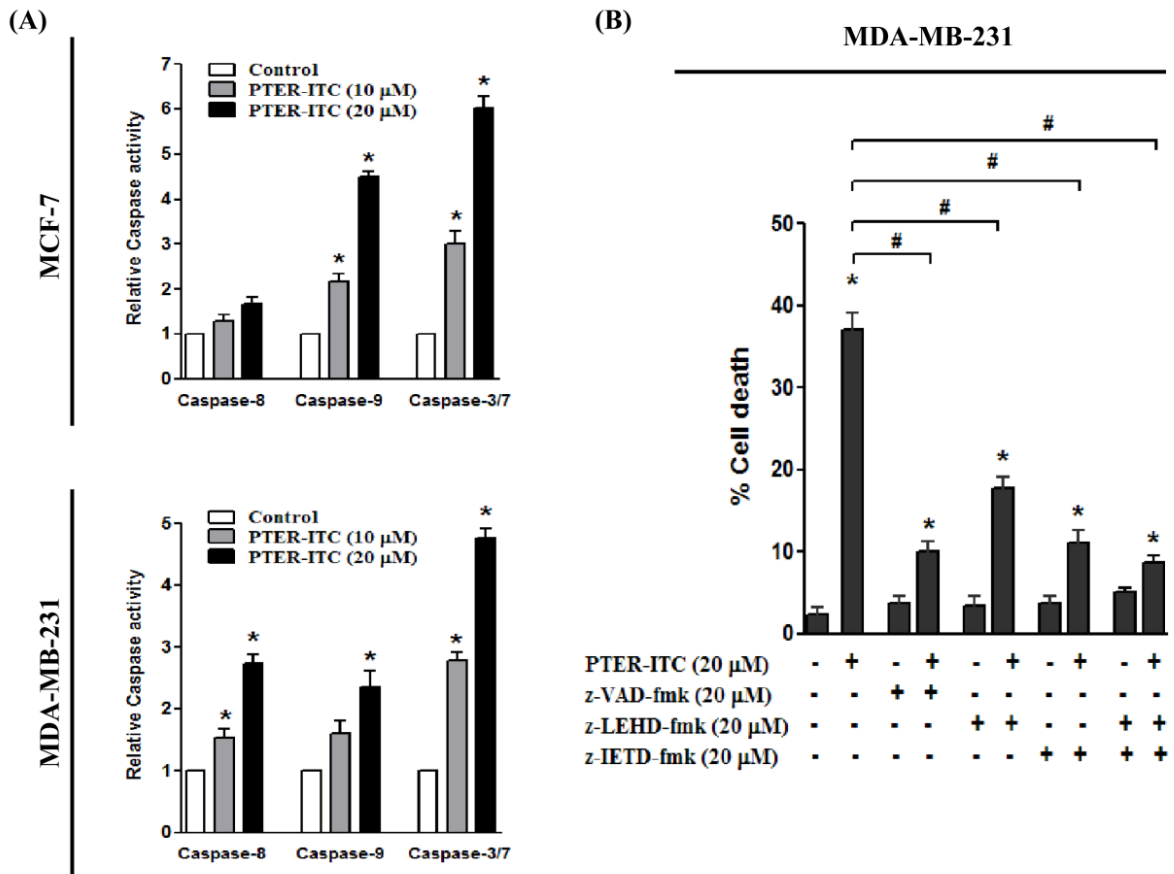
Figure 6.9: PTER-ITC induces caspase-dependent apoptosis in breast cancer cells. (A) Effects of 10 and 20 μM PTER-ITC on caspase-8, -9 and -3/7 activities in MCF-7 and MDA-MB-231 cells. Results are the mean ± SEM of three independent experiments. * indicates statistically significant difference relative to respective controls; $p<0.05$. (B) Effect of caspase inhibitors on PTER-ITC-induced apoptosis in MDA-MB-231 cells. Data shown as mean ± SEM of three independent experiments. * and # indicate statistically significant difference with respect to control and only PTER-ITC-treated cells, respectively; $p<0.05$.

6.3.10 MAPK and JNK are involved in PTER-ITC-induced PPARγ activation and apoptosis

To test for a role of MAPK (mitogen-activated protein kinase) in PTER-ITC-induced PPARγ activation and apoptosis of breast cancer cells, we pre-treated MCF-7 and MDA-MB-231 cells with 20 μM ERK inhibitor (PD98059), 10 μM JNK inhibitor (SP600125) or 10 μM p38 MAPK inhibitor (SB203580) for 1 h, followed by PTER-ITC treatment for an additional 24 h. Total proteins were then isolated for analysis of PPARγ expression patterns. In both breast cancer cell lines, SB203580 and SP600125 pre-treatment completely blocked PTER-ITC-induced PPARγ expression, whereas pre-treatment with PD98059 or DMSO had no effect

(Fig. 6.10A). We therefore suggest that PTER-ITC induces p38 MAPK and JNK pathways to upregulate PPARγ expression in MCF-7 and MDA-MB-231 cells.
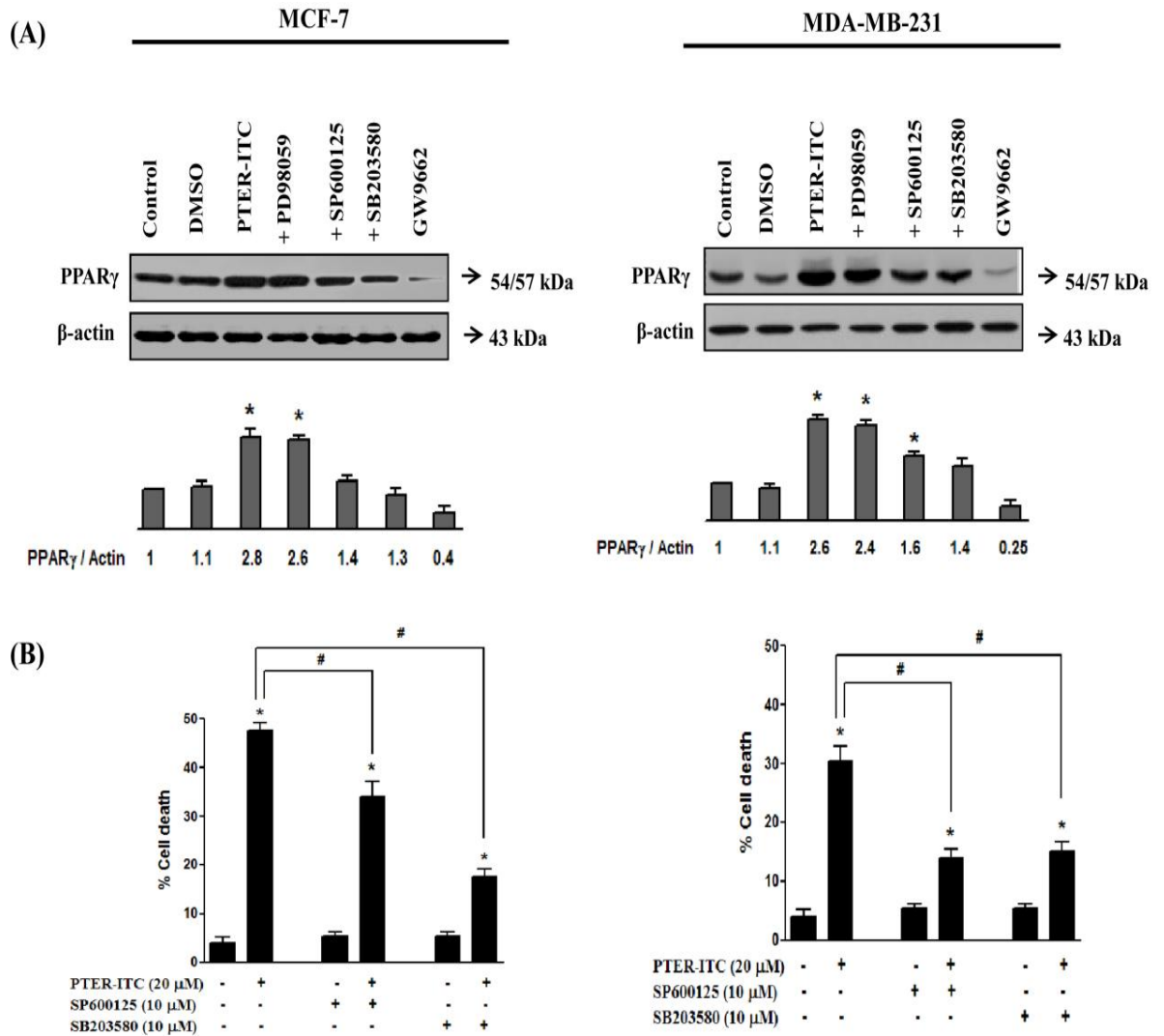
Figure 6.10. PTER-ITC alters PPARγ activity through p38 MAPK and JNK pathways. (A) PTER-ITC induced PPARγ expression in presence of inhibitors of p38 MAPK and JNK pathways in MCF-7 and MDA-MB-231 cells. The experiment was performed in duplicate and yielded similar results. Histogram (bottom) shows relative band intensities normalized to the corresponding β-actin level, where the vehicle-treated group = 1. (B) Effects of p38 MAPK and JNK inhibitors on PTER-ITC-induced apoptosis in MCF-7 and MDA-MB-231 cells. Data are shown as mean ± SEM of three independent experiments. * and # indicate statistically significant difference with respect to vehicle-treated control and only PTER-ITC treated cells, respectively; $p < 0.05$.

Since both p38 MAPK and JNK pathways had important roles in PTER-ITC-induced PPARγ expression, we evaluated whether inhibition of either pathway protected cells from PTER-ITC-induced apoptosis. The breast cancer cells were pre-treated with 10 μM SB203580 (p38 MAPK inhibitor) or SP600125 (JNK inhibitor) for 1 h, followed by PTER-ITC treatment for an additional 24 h, and the percentage of dead cells was determined in an MTT assay. In the case of MCF-7 cells, SB203580 pre-treatment abolished PTER-ITC-induced cell death, which was only partially blocked by the JNK inhibitor (SP600125) (Fig. 6.10B). For MDA-MB-231 cells, inhibition of both p38 MAPK and JNK pathways abolished PTER-ITC-induced cell death. These results confirmed involvement of both p38 MAPK and JNK pathways in PTER-ITC-induced PPARγ activation and apoptosis in MCF-7 and MDA-MB-231 cells, albeit to a lesser extent by the JNK pathway in MCF-7 cells.

6.3.11. PTER-ITC induces apoptosis by targeting PPARγ-related proteins

To elucidate the mode of action of PTER-ITC as an apoptotic agent in the PPARγ-dependent pathway, we next studied its effect on the regulation of PPARγ-related genes in both breast cancer cell lines. PTER-ITC significantly increased PPARγ, PTEN and Bax, and decreased Bcl-2 expression in a dose-dependent manner both at the level of transcription (not shown) and translation (Fig. 6.11A, B). Moreover, PTER-ITC significantly decreased expression of survivin, which blocks caspase-9 and -3, thereby inhibiting apoptosis.

To determine whether the increase in apoptosis and decrease in PPARγ-related genes was due to PTER-ITC-induced PPARγ activation, we performed two sets of experiments. First, we used the PPARγ antagonist GW9662 to block PPARγ pathway activation, followed by 24 h PTER-ITC treatment. Second, PPARγ protein expression was knocked down in MCF-7 and MDA-MB-231 cells by transfection of PPARγ siRNA, followed by 24 h PTER-ITC treatment. Our results showed that MCF-7 and MDA-MB-231 cells in both treatment protocols restored the inhibition of Bcl-2 and survivin caused by PTER-ITC alone (Fig. 6.11A, B) and (Fig. 6.12A, B). In addition, PTER-ITC upregulated Bax and PTEN protein expression in a dose-dependent manner, which was inhibited by the PPARγ antagonist or PPARγ siRNA (Fig. 6.11A, B) (Fig. 6.12A, B), indicating that PTER-ITC modulation of Bax and PTEN is PPARγ-dependent. Furthermore, PTER-ITC induction of cleaved caspase-9 in both MCF-7 and MDAMB-231 cells was attenuated by GW9662 or PPARγ siRNA treatment (Fig. 6.11A, B) and (Fig. 6.12A, B). These data suggest that PTER-ITC induced PPARγ expression, which subsequently enhanced expression of downstream components of this pathway, finally leading to apoptosis.
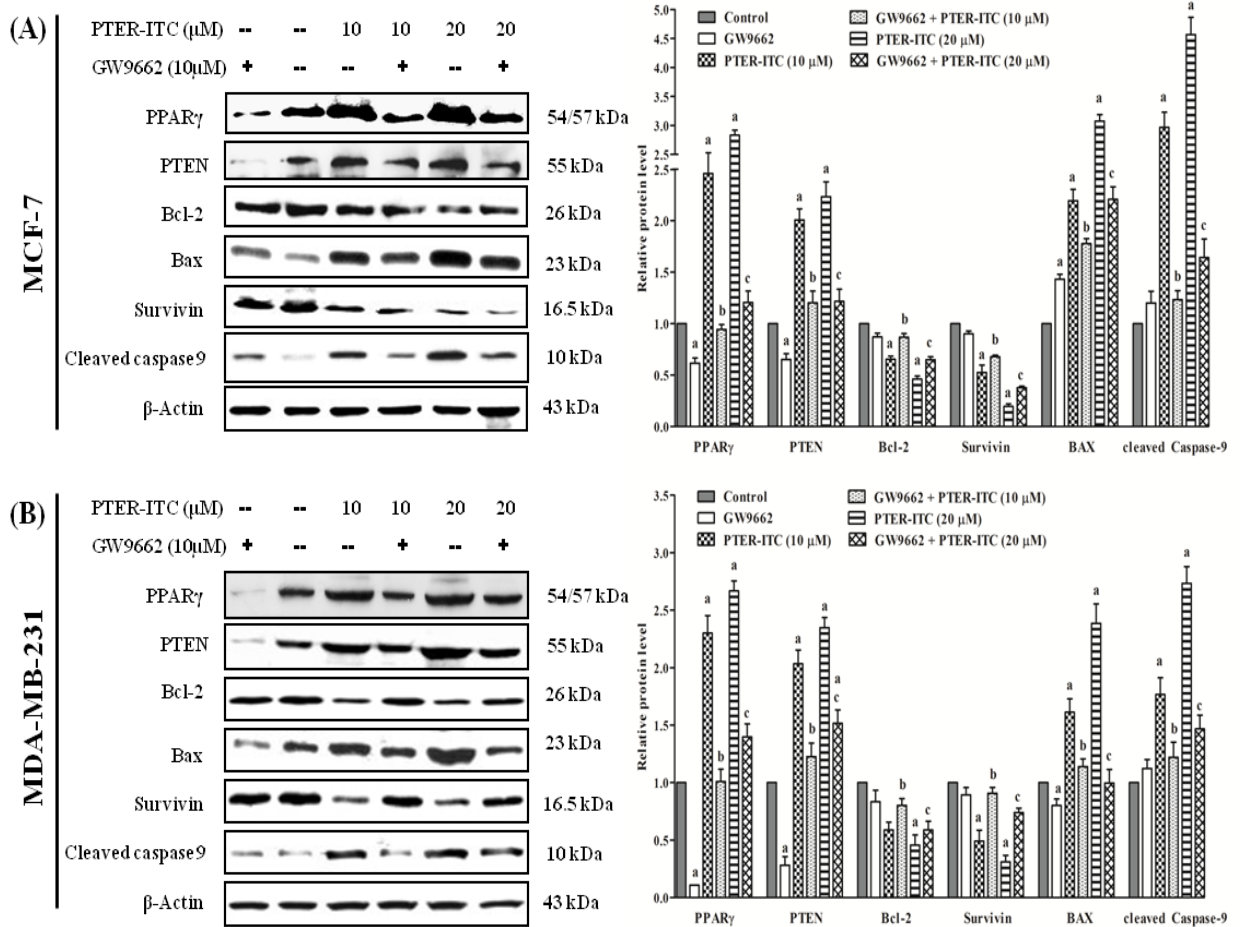
Figure 6.11: PTER-ITC induces apoptosis by targeting PPARγ-related proteins. Immunoblot analysis for apoptotic markers and PPARγ-regulated genes in response to PTER-ITC and GW9662 treatment in (A) MCF-7 and (B) MDA-MB-231 cells. Cells were pre-treated with 10 μM GW9662 (1 h) before treatment with 10 and 20 μM PTER-ITC (24 h). Whole-cell extracts were resolved by SDS-PAGE and probed with indicated antibodies. Expression levels of samples were normalized to the corresponding β-actin levels. Histogram (right panels in each figure) shows data expressed as x-fold change relative to control; bars show mean ± SEM of three independent experiments. a, b and c indicates significant levels of differences with respect to control, 10 and 20 μM only PTER-ITC-treated groups, respectively, for each protein. $p<0.05$.
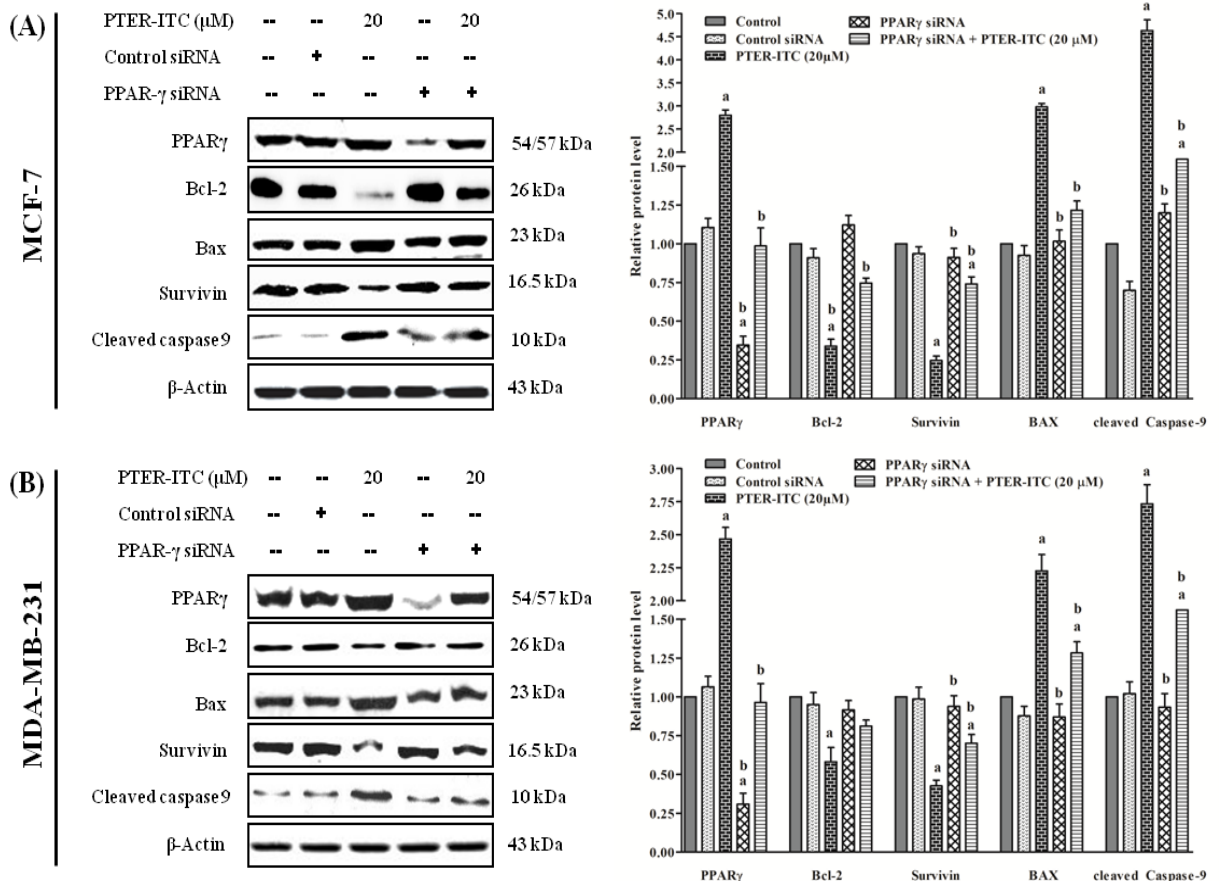
Figure 6.12: PTER-ITC induces apoptosis by targeting PPARγ-related proteins. Immunoblot analysis for apoptotic markers and PPARγ-regulated genes in response to PTER-ITC and PPARγ siRNA treatment. Effect of PPARγ siRNA on PTER-ITC-induced apoptosis of (A) MCF-7 and (B) MDA-MB-231 cells. Both cells were transfected with PPARγ siRNA (final concentration 100 nM). After 24 h, cells were treated with 20 μM PTER-ITC and incubated (24 h). Levels of PPARγ-related proteins were detected in cell lysates by immunoblot analysis. Histogram (right panel in each figure) shows relative band intensities normalized to the corresponding β-actin level. Data are expressed as x-fold change relative to control; bars show mean ± SEM of three independent experiments. a and b indicate significant differences with respect to vehicle-treated control and only 20 μM PTER-ITC-treated groups, respectively; $p < 0.05$.

6.4 Discussion

Breast cancer is the most commonly diagnosed cancer and the second leading cause of cancer death [Ma and Jemal, 2013]. The mortality rate of breast cancer is high because of disease recurrence, which remains the major therapeutic barrier in this cancer type. Although many cytotoxic drugs have been developed for clinical use, cancer chemotherapy is always accompanied by adverse effects, which can be fatal in some cases. Due to the lack of

satisfactory treatment options for breast cancer to date, there is an urgent need to develop preventive approaches for this malignancy. There is a growing interest in combination therapy using multiple anticancer drugs that affect several targets/pathways. A single molecule containing more than one pharmacophore, each with a different mode of action, could be beneficial for cancer treatment. Here, we studied the effectiveness of a new synthetic derivative of pterostilbene, a phytochemical isolated from *Pterocarpus marsupium* stem heart wood, in hormone-dependent (MCF-7) and -independent (MDA-MB-231) breast cancer cell lines.

PPARγ is widely expressed in many tumors and cell lines, and has become a promising target for anticancer therapy. This nuclear receptor has a critical role in breast cancer proliferation, survival, invasion, and metastasis [Woo et al., 2011., Venkatachalam et al., 2009 Kumar et al., 2009; Cui et al., 2007; Elstner et al., 1998; Kim et al., 2006; Liu et al., 2003; Panigrahy et al., 2002]. The effectiveness of PPARγ agonists as anticancer agents has been examined in various cancers including colon, breast, lung, ovary and prostate [Elord and Sun, 2008]. We tested whether PTER-ITC mediates its anti-proliferative and pro-apoptotic effects in breast cancer cells through activation of the PPARγ signaling cascade. Our results showed that PTER-ITC activated PPARγ expression in a dose-dependent manner, followed by downregulation of its anti-apoptotic genes (Bcl-2 and survivin) to induce noteworthy levels of apoptosis in hormone-dependent (MCF-7) and -independent (MDA-MB-231) breast cancer cells.

The PTER-ITC conjugate can be considered more advantageous than existing PPARγ ligands such as rosiglitazone or pioglitazone for breast cancer treatment, as PTER-ITC causes more pronounced cell death at a much lower dose than other ligands [Seargent et al., 2004; Mody et al., 2007; Zhou et al., 2009]. In addition, most (if not all) the other ligands are estrogenic in nature [Talbert et al., 2008], and could thus act as positive factors for ER-dependent breast, ovary and uterine cancers, whereas PTER-ITC is anti-estrogenic at the dose used for this study. Considering these two major points, we consider that the drug could be used at much lower concentrations, which might help reduce the side effects reported for most other PPARγ ligands. PTER-ITC molecule nonetheless requires further validation before use in clinical trials that target the PPARγ pathway.

The most important characteristic of a cancer cell is its ability to sustain proliferation [Kelly et al., 2011]. The pathways that control proliferation in normal cells are altered in most cancers [Evan and Vousden, 2001]. We thus analyzed the effect of PTER-ITC on proliferation of breast cancer cells, and found that PTER-ITC caused significant, dose-dependent inhibition of breast cancer cell growth *in vitro*. This effect was partially reversed, however, when PTER-

ITC was combined with PPARγ antagonists. This result suggests that the PTER-ITC anticancer effects are mediated through the PPARγ activation pathway. These data coincides with findings in several *in vivo* and *in vitro* studies in which PPARγ agonists such as rosiglitazone or troglitazone decreased proliferation of breast cancer cell lines, mediated in part by a PPARγ-dependent mechanism [Kim et al., 2006; Lea et al., 2004].

To elucidate the molecular mechanisms that underlie the anticancer effects observed for PTER-ITC, we studied its effect on activation of PPARγ. To the best of our knowledge, this is the first report showing PTER-ITC participation in the PPARγ-dependent signaling pathway. Our data showed that PTER-ITC increased PPARγ transcriptional and translational activities in MCF-7 and MDA-MB-231 cells. To establish the essential role of PTER-ITC in PPARγ-mediated apoptosis of breast cancer cells, we used PPARγ siRNA and its chemical antagonist to inhibit PPARγ signaling, and demonstrated apoptosis prevention and caspase activation. We also observed an increase in PPARβ activity after PTER-ITC treatment, with no significant reduction after antagonist treatment, suggesting that the increase was non-specific. Although some earlier studies reported involvement of PPARβ activity in tumorigenesis, many others contradicted this idea. The PPARβ ligand GW501516 was reported to promote human hepatocellular growth (Xu et al., 2006), although another study showed that certain PPARβ ligands such as GW0742 and GW501516 reduced growth of MCF-7 and UACC903 cell lines [Girroir et al., 2008]. The role of PPARβ in cancer therapeutics is therefore complex and not yet fully defined [Peters et al., 2012]. Hence the relationship between PTER-ITC and PPARβ could provide an alternative platform to study the involvement of this pathway in cancer therapy.

PPARγ is a phosphoprotein, and many kinase pathways, such as cAMP-dependent protein kinase (PKA), AMP-activated protein kinase (AMPK) and mitogen-activated protein kinase (MAPK) such as ERK, p38 and JNK, have been implicated in the regulation of its phosphorylation [Gardner et al., 2005; Papageorgiou et al., 2007]. Phosphorylation notably inhibits PPARγ ligand-independent and -dependent transcriptional activation [Gardner et al., 2005; Papageorgiou et al., 2007]. Research showed that PPARγ agonists activate different MAPK subfamilies, depending on cell type [Gardner et al., 2005; Lennon et al., 2002; Shah et al., 2004; Teruel et al., 2003] and that these kinases are involved in cell death [Kim et al., 2003; Kim et al., 2006; Li et al., 2005; Motomura et al., 2005]. The role of MAPK signaling pathways in cell death induced by PPARγ agonists is controversial. According to certain studies, PPARγ agonist-induced ERK activation mediates anti-apoptotic signaling [Shan et al., 2004], while others showed its involvement in inducing cell death [Kim et al., 2003; Padilla et al., 2000].

p38 activation by PPARγ agonists is also reported to be regulated differently in various cell types. It has been reported that PPARγ agonists induces p38 activation, leading to apoptosis of cancer cells have been reported in chondrocytes [Shah et al., 2004], human lung cells [Li et al., 2005], liver epithelial cells [Gardner et al., 2003] and skeletal muscle [Kramer et al., 2005]. This coincides with our data, where using pharmaceutical inhibitors, we show that activation of p38 and JNK pathways, but not of ERK, is necessary and sufficient to phosphorylate PPARγ and cause subsequent apoptosis in the breast cancer cell lines studied. At present, we do not know whether PTER-ITC activates p38 and JNK directly, or if it activates other cellular kinase pathways such as PKA and AMPK, which in turn could activate MAPK. Further validation is needed to conclusively establish the pathway(s) involved.

PTEN is a tumor suppressor gene involved in the regulation of cell survival signaling through the phosphatidylinositol 3-kinase (PI3K)/AKT pathway [Carnero et al., 2008]. PI3K/AKT signaling is required for an extremely diverse array of cellular activities that participate mainly in growth, proliferation, apoptosis and survival mechanisms [Vasudevan et al., 2004; Chu et al., 2004]. Activated AKT protects cells from apoptotic death by inactivating compounds of the cell death machinery such as procaspases [Vasudevan et al., 2004]. PTEN exercises its role as a tumor suppressor by antagonizing the PI3K/AKT pathway [Vasudevan et al., 2004]. The PPARγ-dependent increase in PTEN caused by PTER-ITC in our experiments not only indicates that the tumor suppressor gene contributes to the growth-inhibitory activities of the compound, but might also trigger its pro-apoptotic actions.

Our results further showed that PTER-ITC downregulated PPARγ-related genes, including Bcl-2 and survivin. These genes are commonly associated with increased resistance to apoptosis in human cancer cells [Johnstone et al., 2002]. PTER-ITC-induced PPARγ activation was reduced in the presence of GW9662, together with reversal of decreased survivin and Bcl-2 levels. Furthermore, molecular docking analysis suggested that PTER-ITC could interact with amino acid residues within the PPARγ-binding domain, including five polar and eight non-polar residues within the PPARγ ligand-binding pocket that are reported to be critical for its activity. Together these results suggest that PTER-ITC can be considered a PPARγ agonist, and the survivin and Bcl-2 decrease is due to activation of the PPARγ pathway by PTER-ITC.

Two cellular pathways, differentiation and apoptosis, are the main focus in the development of anti-cancer therapies. Induction of differentiation is one potent mechanism by which some cancer therapeutic and chemopreventive agents act [Chamras et al., 2002; Sauer et al., 2005; Sun et al., 2008]. Lipid accumulation in MCF-7 cells is supported by the fact that

tamoxifen and a few other anti-cancer agents such as ansamycins and suberoylanilide hydroxamic acid induce high lipid production (as high as 5-fold in the case of ansamycins) and by triglyceride accumulation, which results in MCF-7 cell differentiation to a more epithelial-like morphology [Munster et al., 2001a; Munster et al., 2001b; Payre et al., 2008]. In a previous study, we showed that long-term exposure to PTER causes growth arrest in MCF-7 cells, which might be linked to mammary carcinoma cell differentiation into normal epithelial cell-like morphology and activation of autophagy [Chakraborty et al., 2012]. In the present study, PTER-ITC also caused differentiation of MCF-7 cells, albeit to a higher level compared to its parent compound PTER than previously reported [Chakraborty et al., 2012]. Based on these data, it can thus be suggested that PTER-ITC inhibits MCF-7 cell growth mainly through apoptosis, while it can also induce differentiation of these breast cancer cells.

In conclusion, this study highlights the anticancer effects of the novel conjugate of PTER and ITC, and shows that the mechanism involves activation of the PPARγ pathway via PTER-ITC binding to the receptor, which affects its regulated gene products. PTER-ITC induces apoptosis by enhancing expression of PPARγ genes at both transcriptional and translational levels, which appears to be triggered at least in part by modulation of PTEN. In addition, activation of caspase-9 and downregulation of Bcl-2 and survivin contribute to PTER-ITC-induced cell death. PTER-ITC exhibits differentiation-promoting as well as anti-proliferative effects on MCF-7 cells. Together these results suggest that the PTER-ITC conjugate acts as a PPARγ agonist and is a promising candidate for cancer therapy, alone or in combination with existing therapies. These preliminary data show that further studies are warranted in *in vitro* and *in vivo* models to elucidate the exact mode of action responsible for the effects of this compound.

Chapter 7. Role of PTER-ITC in Prevention of Prostate Cancer

7.1 Introduction

   Despite significant efforts made towards the ablation of cancers, prostate cancer (PCa) is the most frequently diagnosed cancer and the second leading cause of cancer death among men in the United States, with an estimated 217,730 new cases and 32,050 deaths in 2010 [Jemal et al., 2010]. Although the etiology of PCa remains unknown, elevated levels of steroid hormones, such as androgens and estrogens, as well as growth factors, such as insulin-like growth factor 1, are considered to be important risk factors [Taplin and Balk, 2004; Ho SM, 2004; Renehan et al., 2004]. Androgen ablation therapy has an initial response, but most patients with advanced PCa eventually develop resistance to this therapy and progresses to hormone-refractory prostate cancer (HRPC), for which there is no curative therapy [Bracarda et al., 2005]. Lack of effective treatment options for the management of HRPC reinforce the necessity to develop novel compounds that act singly or in combination.

   Androgen and AR functions play a pivotal role in carcinogenesis and progression of PCa, as well as in normal prostate development [Heinlein and Chang, 2004; Henderson and Feigelson, 2000]. The actions of androgens, such as testosterone and dihydrotestosterone (DHT) are mediated by AR, which is a member of the nuclear receptor super family of ligand-dependent transcription factors [Heinlein and Chang, 2002; Roy et al., 2001]. In addition to androgen, AR activity may also be modified by molecules in other cell signaling pathways. Up regulation of epidermal growth factor receptor (EGFR) and subsequent increases in extracellular-regulated kinase (ERK) and AKT signaling, are implicated in PCa progression [Gay et al., 2010]. AKT regulates the AR signaling pathway by phosphorylation and/or transcriptional regulation of AR. AKT phosphorylates AR at serines 210/213 and 790/791 and finally transactivates its activity. An earlier study showed that inhibition of AKT pathway abrogates the HER-2/neu-induced AR signaling activity [Wen et al., 2000]. These results suggest that AKT is an activator of AR required for androgen-independent survival and growth of PCa cells. Research has shown that inhibition of one or both of these pathways has a more profound effect on tumor cell development and death, making them attractive combinational targets in PCa therapy. Therefore, AR, AKT, and ERK could be potential targets for the treatment of PCa.

   Bioactive food components, in particular, are increasingly being evaluated as potential PCa chemopreventive agents because of their presumed safety (Kris-etherton et al., 2002). One such compound is pterostilbene (PTER), a naturally occurring dimethyl ether analogue of

resveratrol (RESV), which has higher oral bioavailability and enhanced potency as compared to RESV [Kapetanovic et al., 2011]. Several studies have shown that PTER can inhibit the growth of various hormone-responsive cancers, such as breast [Alosi et al., 2010; Chakraborty et al., 2010 Pan et al., 2011] and PCa [Chakraborty et al., 2010; Wang et al., 2010; Lin et al., 2012; Li et al., 2013] both *in vitro* and *in vivo*. Although the anti-metastatic, anti-tumor and anti-leukemic properties of PTER have been well established in breast cancer, there are limited reports on the action of PTER in the proliferation of PCa cells induced by steroid hormones (Wang et al., 2010). Similarly, isothiocyanates (ITCs) are naturally occurring, low molecular weight organic compounds with the general formula R-NCS [Cavell et al., 2011]. These chemoprotective agents are found in a wide variety of cruciferous vegetables like broccoli, cauliflower, cabbage, brussels sprout, and kale [Keum et al., 2004]. Epidemiological studies have suggested that increased consumption of cruciferous vegetables may be protective against PCa risk [Wang et al., 2004; Chiao et al., 2002; Wang et al., 2006; Xiao and Singh, 2002]. However, in spite of compelling epidemiological correlation, the activity of ITCs against PCa cells is yet to be systematically assessed. Since the individual roles of PTER and ITC have already been implicated in PCa, we intended to develop a conjugate of PTER-ITC in search of potent anti-cancer molecules. The PTER-ITC was prepared by appending ITC containing thiosemicarbazide pharmacophore with PTER backbone as described earlier [Nikhil et al., 2014a]. Surprisingly, the PTER-ITC molecule when tested *in vitro*, showed effective cytotoxicity in wide range of cancer cell lines at comparatively lower dose as compared to its parent compound i.e., PTER [Nikhil et al., 2014a]. Further, our study indicated that the anti-proliferative activity of PTER-ITC against human breast cancer cell lines was due to its ability to arrest cells in G2/M phase and activation of caspase, and also correlated with the blockade of AKT and ERK signaling pathways [Nikhil et al., 2014a].

In the present study we examined detailed efficacy and molecular mechanisms of action of PTER-ITC using androgen-dependent (LNCaP) and androgen-independent (PC-3) PCa cells. Further, we also compared the efficacy of PTER-ITC with the parent compound of PTER i.e., RESV. Our study thus identified the newly developed PTER-ITC to be a potent AR-inhibitor that strongly attenuates the growth of PCa cells *in vitro* by modulating AR expression as well as regulating cell cycle progression and apoptosis.

7.2 Brief Methodology

7.2.1 Cell lines and culture

The prostate carcinoma cell lines (AR-positive LNCaP and AR-negative PC-3) and noncancer cell lines (CHO and COS-1) were obtained from the National Centre for Cell Science (NCCS), Pune, India. PC-3, CHO and COS-1 cells were maintained in Dulbecco's modified Eagle's media (DMEM) while LNCaP cells were maintained in RPMI-1640 medium supplemented with 10% foetal bovine serum (FBS) (heat inactivated) under 5% CO_2 at 37°C. All the experiments were performed using LNCaP, PC-3, CHO and COS-1 cells from passage below 29, 34, 20 and 30 respectively. The cells were washed properly before changing the media to steroid-free complete media prior to each treatment with the compounds, unless otherwise stated.

7.2.2 Transfection

The LNCaP cells were grown and transiently transfected with pMMTV-neomycin-luciferase plasmid (300 ng/10^5 cells) in RPMI media supplemented with 10% FBS using polyfect transfection reagent (Qiagen, CA, USA) according to manufacturer's instructions. Then, 24 h after transfection, the cell culture media were changed with media containing 5% charcoal-stripped FBS to reduce the contaminating steroids from the serum and incubated for an additional day before initiating the treatments. In case of PC-3 cells, they were similarly transfected, but in addition to pMMTV-neomycin-luciferase construct, they were also transfected with pSG5-hAR-puro plasmid (full length hAR in pSG5 expression vector) in the ratio of 5:1 as indicated above. For experiments involving co-regulators, 50 ng of co-activator plasmids (25 ng each of GRIP-1 and SRC-1) along with pMMTV-neo-luc (250 ng) were transfected to LNCaP cells. To evaluate the transfection efficiency, 500 ng/10^5 cells of the SV40 promoter-Renilla luciferase (pRL-SV40) vector (Promega Madison, USA) were co-transfected as internal control. The cells were then treated either with vehicle or different concentrations (1-40 µM) of PTER-ITC and/or 10 nM of DHT for 24 h, and the luciferase activity was measured according to the instructions provided in the kit (Promega, Madison, USA). Each experimental point was performed in triplicate and varied by less than 10%. The values of luciferase for each lysates were normalized to the Renilla luciferase activity.

For localization studies, pEGFP-AR plasmid was transfected to LNCaP and PC-3 cells (300 ng/10^5 cells). The cells were then incubated with 10 nM DHT with/ without 10 and 20 µM PTER-ITC and monitored regularly till 12 h under fluorescence microscope (Zeiss, Axiovert 25, Germany).

7.2.3 siRNA transfection

The siRNAs against human AKT and ERK and control siRNA were purchased commercially from Santa Cruz Biotechnology (USA). The LNCaP and PC-3 PCa cells were transfected with siRNAs (at a final concentration of 100 nM) using polyfect transfection reagent (Qiagen, CA, USA) according to manufacturer's instructions. After 24 h of transfection, the cells were washed properly and replaced with fresh medium. The cells were then treated with 20 μM PTER-ITC for 24 h, and finally protein lysates were prepared on completion of treatment. The levels of p-AKT, p-ERK and cleaved caspase-3 expressions were detected by Western blot analysis.

7.3 Results

7.3.1 Inhibition of cell proliferation by PTER-ITC

LNCaP (AR positive) and PC-3 (AR negative) cells were cultured with different concentrations of RESV, PTER and PTER-ITC for 24 h in complete RPMI and DMEM media, respectively. Our data showed that the treatment of LNCaP and PC-3 PCa cells with RESV, PTER and PTER-ITC resulted in a dose dependent inhibition of cell proliferation. As shown in Table 7.1, in case of LNCaP cells, the PTER-ITC resulted in almost 50% reduction in the number of live cells at 40 ± 1.12 μM while it was around 66.4 ± 1.39 and 82.2 ± 2.19 μM in case of PTER and RESV treated cells respectively after 24 h of treatment. Similarly, in case of PC-3 cells the IC_{50} value of PTER-ITC, PTER and RESV was found to be 45 ± 1.50, 75 ± 2.55 and 95.0 ± 1.13 μM respectively after 24 h treatment (Table 7.1). Furthermore, when tested in noncancer cell lines like CHO and COS-1, all the compounds were found to have IC_{50} values above 100 μM concentration. Thus both the cancer cell lines were found to be more sensitive to PTER-ITC treatment as compared to PTER and RESV as depicted by the lower IC_{50} values in all of them. Further, our result showed that PTER-ITC is a potent cytotoxic agent in both AR positive and AR negative cell lines albeit to a marginally higher level in the former as compared to latter.

Table 7.1 Cytotoxicity induced by RESV, PTER and PTER-ITC in noncancer (COS-1, CHO) and prostate cancer (PC-3, LNCaP) cell lines after 24 h exposure as determined by MTT assay.

	IC$_{50}$ Value[a]		
Cell lines	**RESV (µM)[b]**	**PTER (µM)[b]**	**PTER-ITC (µM)[b]**
Prostate cancer			
PC-3	95.0 ± 1.13	75.0 ± 2.55	45.0 ± 1.50[c d]
LNCaP	82.2 ± 2.19	66.4 ± 1.39	40.0 ± 1.12[c d]
Non-cancer			
CHO	> 100 µM	> 100 µM	> 100 µM
COS-1	> 100 µM	> 100 µM	> 100 µM

[a] 50% growth inhibition as determined by MTT assay (24 h drug exposure).
[b] Compound tested in triplicate, data expressed as mean value ± SEM of three independent experiments.
[c] $p < 0.001$ between Resveratrol and PTER-ITC treated group
[d] $p < 0.001$ between PTER and PTER-ITC treated group

7.3.2 Differential sensitivity of PC-3 and LNCaP cells to PTER-ITC induced apoptosis

In milieu of the MTT assay results, we extended our study to examine whether PCa cells undergo apoptosis after PTER-ITC treatment by using Annexin-V/ PI double staining assay and flow cytometry analysis. After PCa cells were incubated with different concentrations of PTER-ITC, the cells were stained with Alexa Fluor 488-conjugated Annexin-V and PI, which can assess the early and late apoptotic cell populations. As shown in Fig. 7.1A, the PTER-ITC produced a dose-dependent increase in the apoptotic cell population in both the PCa cells studied. Treatment of PC-3 cells with increasing doses of PTER-ITC for 24 h resulted in an increase in early apoptotic cells from about 44% to 68% and late apoptotic cells from 12% to 16% at 20 and 40 µM concentrations, as compared to vehicle treated groups respectively (Fig. 7.1A upper panel). Since PC-3 cells lack a functional p53 protein, it was of interest to determine whether the presence of wild type p53 affects cellular sensitivity to the cell death caused by PTER-ITC because p53 is known to regulate apoptosis in different stimuli. We addressed this question by determining the sensitivity of LNCaP cells (wild type p53) towards PTER-ITC-induced apoptosis by FACS analysis. Treatment of LNCaP cells for 24 h with increasing doses of PTER-ITC resulted in a gradual increase of early apoptotic cells

(Annexin V positive only) from 52% to 72% at 20 and 40 µM, respectively (Fig. 7.1A, lower panel). The late apoptotic cells (Annexin V and PI positive) also increased significantly from 8% to 18.5% (Fig. 7.1A, lower panel) as compared to only 0.23% of early apoptotic cells and almost negligible number of late apoptotic cells in the negative control group treated with 0.1% DMSO. The histogram in the right panel (Fig. 7.1B) indicates statistical analysis of three similar independent experiments for both the cell lines. Interestingly, the total number of apoptotic cells was statistically non-significant ($p<0.05$) between LNCaP and PC-3 cells when tested with different concentrations of PTER-ITC, suggesting that p53 protein was not involved in the regulation of PTER-ITC-induced apoptosis of PCa cells.
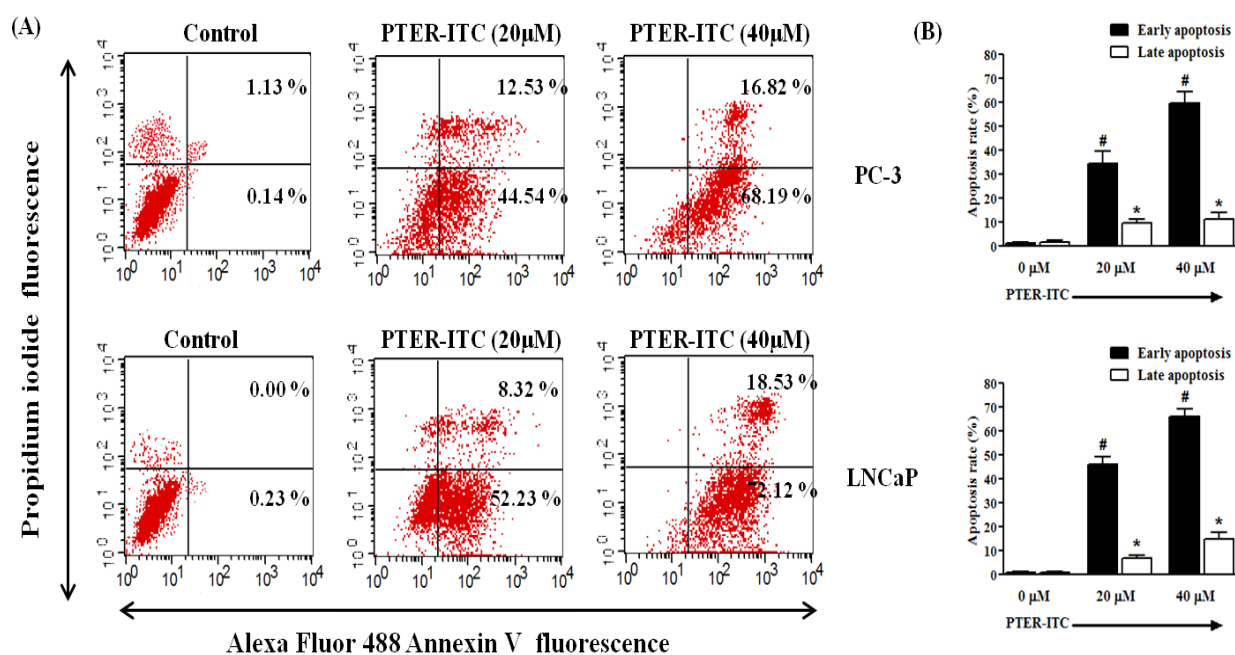
Figure 7.1: Induction of apoptosis by PTER-ITC in prostate cancer cell line. (A) The effect of PTER-ITC on the apoptosis of PC-3 and LNCaP cells as demonstrated by a representative FACS analysis using Annexin V as marker. (B) The histogram showing the data for FACS analysis where the results are the mean ± SEM of three independent experiments. # and * represents statistically significant difference with respect to their specific controls (vehicle treated) for cells in early and late apoptosis respectively at $p<0.05$.

7.3.3 PTER-ITC induced stage specific arrest of prostate cancer cells

Based on the growth and DNA synthesis inhibitory responses of PTER-ITC in PCa cells, we next examined its effect on cell cycle progression. As shown in Fig. 7.2A and 7.2B, treatment of PC-3 and LNCaP cells with increasing doses of PTER-ITC for 24 h resulted in a dose dependent increase in the accumulation of cells in G2/M phase with concomitant decrease in G1 phase cells. In case of PC-3 cells, the effect observed at 40 µM PTER-ITC was the greatest with approximately 50% of the cells being arrested in G2/M phase, compared to only 22% in control group (Fig. 7.2A). A similar trend in G2/M phase arrest was also demonstrated in LNCaP cells (35% in treated cells against 11% in control cells), although the total population of cells could not reach a high level of 50% as observed in PC-3 cells. As shown in Fig. 7.2B, the PTER-ITC treatment resulted in an accumulation of 16–35% of cells in G2/M phase with increasing doses of PTER-ITC. Thus, PTER-ITC-mediated growth inhibition of both PC-3 and LNCaP cells correlated with G2/M phase cell cycle arrest.
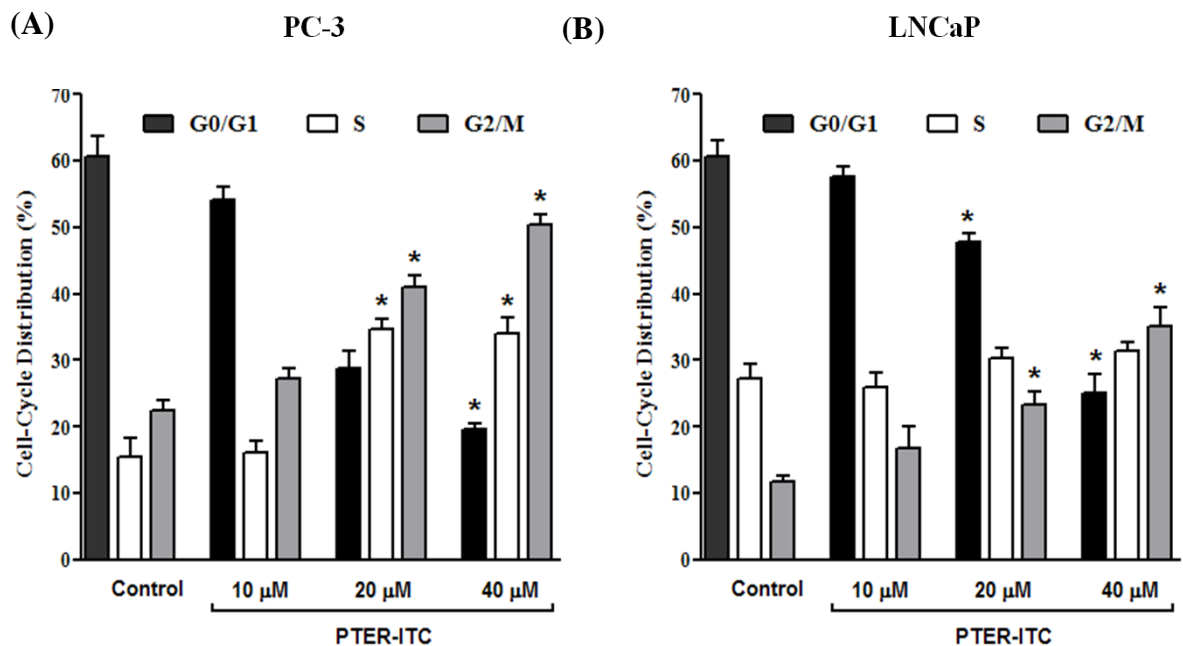
Figure 7.2: PTER-ITC induces G2/M phase cell cycle arrest in prostate cancer cells. (A) Cell cycle distribution of PC-3 and (B) LNCaP cells upon treatment with varying doses of PTER-ITC. Results are presented as mean ± SEM of three independent experiments. * represents statistically significant difference with respect to vehicle treated PC-3 and LNCaP cells respectively corresponding to each stage of cell cycle at $p<0.05$.

7.3.4 PTER-ITC activates caspase-3 via caspase-9

Activation of both extrinsic and intrinsic caspase pathways has already been known to be the major mechanisms of apoptotic cell death in most cellular systems. To better understand the underlying cellular pathways for PTER-ITC-induced death of PCa cells, a possible role of caspase in this process was investigated by measuring the activities of caspase-8, -9, and -3 in these tumor cells. While caspase-8 and caspase-9 are essential proteases of extrinsic and intrinsic apoptotic pathways respectively, caspase-3 acts as downstream effectors of both these pathways. Treatment of PC-3 cells with increasing doses (10, 20 and 40 μM) of PTER-ITC and RESV for 24 h caused a dose-dependent augmentation in caspase-9 and caspase-3 enzyme activities. This increment was comparatively higher in case of PTER-ITC treated cells as compared to cells treated with same dose of RESV (Fig. 7.3A). For caspase-8, although there was marginal increase in its activity at high dose of RESV treatment, no such induction was observed in case of PTER-ITC treatment (Fig. 7.3A). On the contrary, the results obtained in case of LNCaP cells showed a significant increase in all the three caspase i.e. caspase-8, -9 and -3 on PTER-ITC treatment indicative of involvement of both intrinsic (through caspase-9) and extrinsic (through caspase-8) pathways in apoptotic process by the PTER-ITC in this cell line (Fig. 7.3B, left panel). Furthermore, our results indicated that activation of caspase-9 occurs prior to that of caspase-8 (at lower dose), which suggests that the mitochondrial pathway might be essential for PTER-ITC-induced apoptosis. On the other hand, RESV treatment also showed significant increase in caspase -9 and -3 activities but to a lesser extent as compared to the PTER-ITC (Fig. 7.3B, right panel) (*p<0.05*). Thus the above data clearly suggests that PTER-ITC induced apoptosis in PC-3 cells is mediated via the intrinsic pathway, while both the intrinsic and extrinsic pathways contributes to apoptosis in LNCaP cells. Also the PTER-ITC was found to be more effective than RESV in inducing apoptosis in both the PCa cell lines tested.

Furthermore, to elucidate the pathway which was predominant for PTER-ITC-induced apoptosis, pharmacological inhibitors of specific caspases were employed to probe if they could protect the cells from undergoing apoptosis. As shown in Fig. 7.4, Z-VAD-FMK, a general caspase inhibitor, showed significant inhibition of cell death in both PC-3 and LNCaP cells suggesting that apoptosis is the predominant form of cell death induced by the PTER-ITC. In case of PC-3 cells, Z-LEHD-FMK, a specific inhibitor of caspase-9 also inhibited PTER-ITC induced cell death by 73% while Z-IETD-FMK, a specific inhibitor of caspase-8, was completely ineffective in blocking PTER-ITC induced cell death (*p<0.05*) (Fig. 7.4, left panel). Furthermore, in case of LNCaP cells, the inhibitor of caspase-9 almost completely blocked the

PTER-ITC induced apoptosis while inhibitor of caspase-8 only partially inhibited it (Fig. 7.4, right panel). The PTER-ITC induced cell death was most prominently inhibited when the cells were pre-treated with both caspase-8 and caspase-9 inhibitors. Together, these data further strengthens our finding that PTER-ITC induced apoptosis involves caspase -9/-8/-3 and caspase-9/-3 pathways in LNCaP and PC-3 cells respectively.
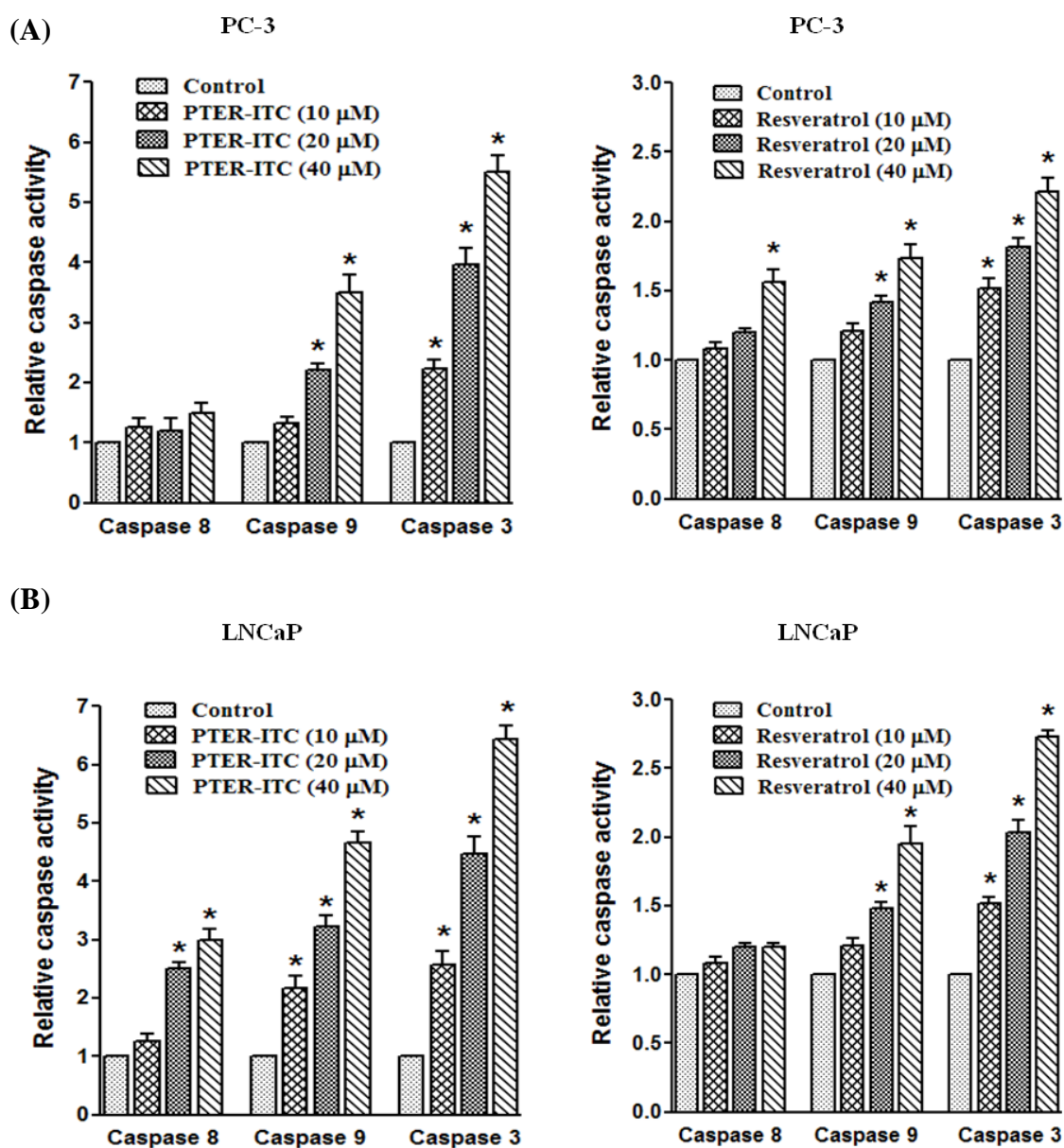
Figure 7.3: PTER-ITC induces caspase dependent cell death in prostate cancer cells (A) The effects of varying doses of PTER-ITC (left panel) and resveratrol (right panel) on caspase-8, -9 and -3 activities in PC-3 and (B) LNCaP cells. Results are the mean ± SEM of three independent experiments. * represents statistically significant difference with respect to control cells for respective caspases tested at $p<0.05$.
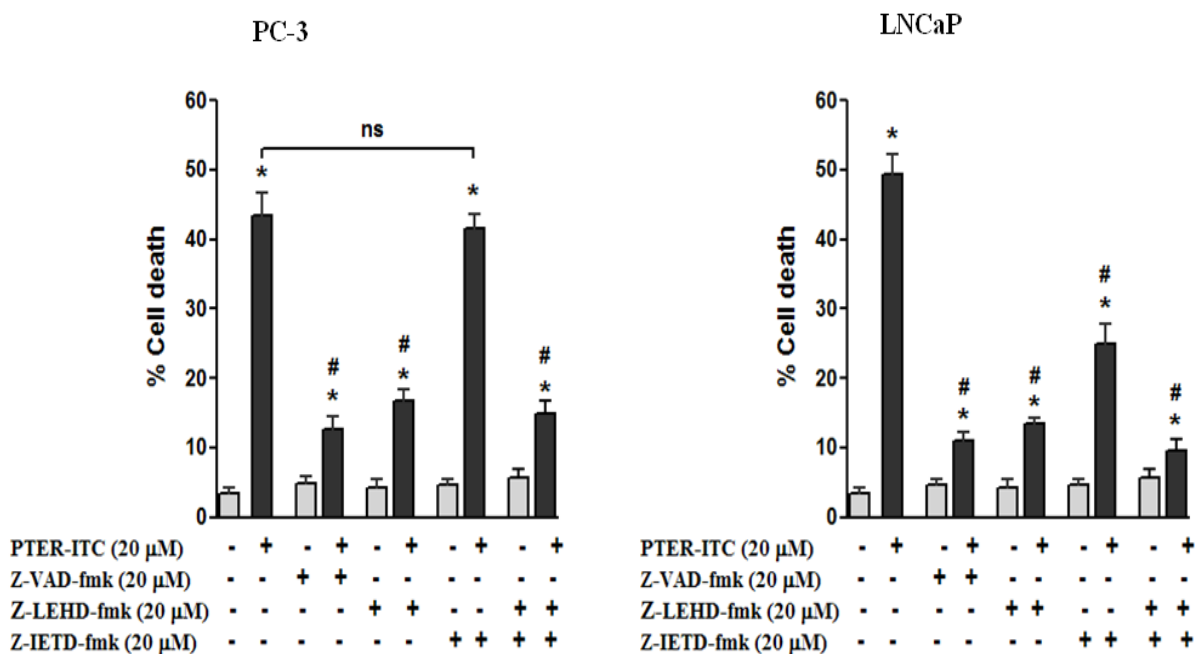
Figure 7.4: The effect of caspase inhibitors on PTER-ITC-induced cell death in PC-3 and LNCaP cells. The cells were pre-treated with 20 µM of respective caspase inhibitors: Z-LEHDFMK (caspase-9 inhibitor); Z-IETDFMK (caspase-8 inhibitor); and Z-VAD-FMK (general caspase inhibitor) for 1 h before the addition of 20 µM PTER-ITC. Cell death was measured 24 h after PTER-ITC treatment using MTT assay. Data are the mean ± SEM of three independent experiments. * and # represents statistically significant difference with respect to control (vehicle) and PTER-ITC treated cells respectively for each cell lines at $p<0.05$. ns, non-significant.

7.3.5 Bcl-2 and Bax are involved in apoptosis by PTER-ITC

Bcl-2 forms a heterodimeric complex with apoptotic Bax protein, thereby neutralizing its apoptotic effect. Therefore, the ratio of Bax/Bcl2 is often considered as a decisive factor in determining cell death or survival. In the present study, treatment of cells with PTER-ITC resulted in a decrease in the expression of *Bcl-2* and *Bcl-xL* with a concomitant increase in *Bax* gene in both LNCaP and PC-3 cells (Fig. 7.5). This resulted in a substantial increase in Bax/Bcl2 ratio, which generally favors apoptosis. As shown in Fig. 7.5, with a concomitant increase in the level of Bax, there was a decrease in Bcl-2 and Bcl-xL levels for both PC-3 (Fig. 7.5A) and LNCaP (Fig. 7.5B) cells, respectively. The increase in Bax level by PTER-ITC coincided with increase in caspase-3 activation, finally leading to apoptosis. It was found that the PTER-ITC showed a marked enhancement of caspase-3 expression by about 8.5- and 6-fold in LNCaP (Fig. 7.5D) and PC-3 (Fig. 7.5C) cells, respectively at highest doses of PTER-ITC treatments. Interestingly, although RESV treatment also significantly enhanced the levels of

caspase-3 expression in both LNCaP (Fig.7.5D) and PC-3 (Fig. 7.5C) cells (4.5- and 3.5-fold respectively) at its highest dose of treatment (40 μM), it was much lower than that caused by the PTER-ITC at the same dose ($p<0.05$). Similar pattern of enhancement was also shown by RESV and PTER-ITC for Bax in both LNCaP (Fig. 7.5D) and PC-3 (Fig. 7.5C) cells. These results suggest that the PTER-ITC-induced apoptosis in PCa cells are partly through Bax-dependent pathway.
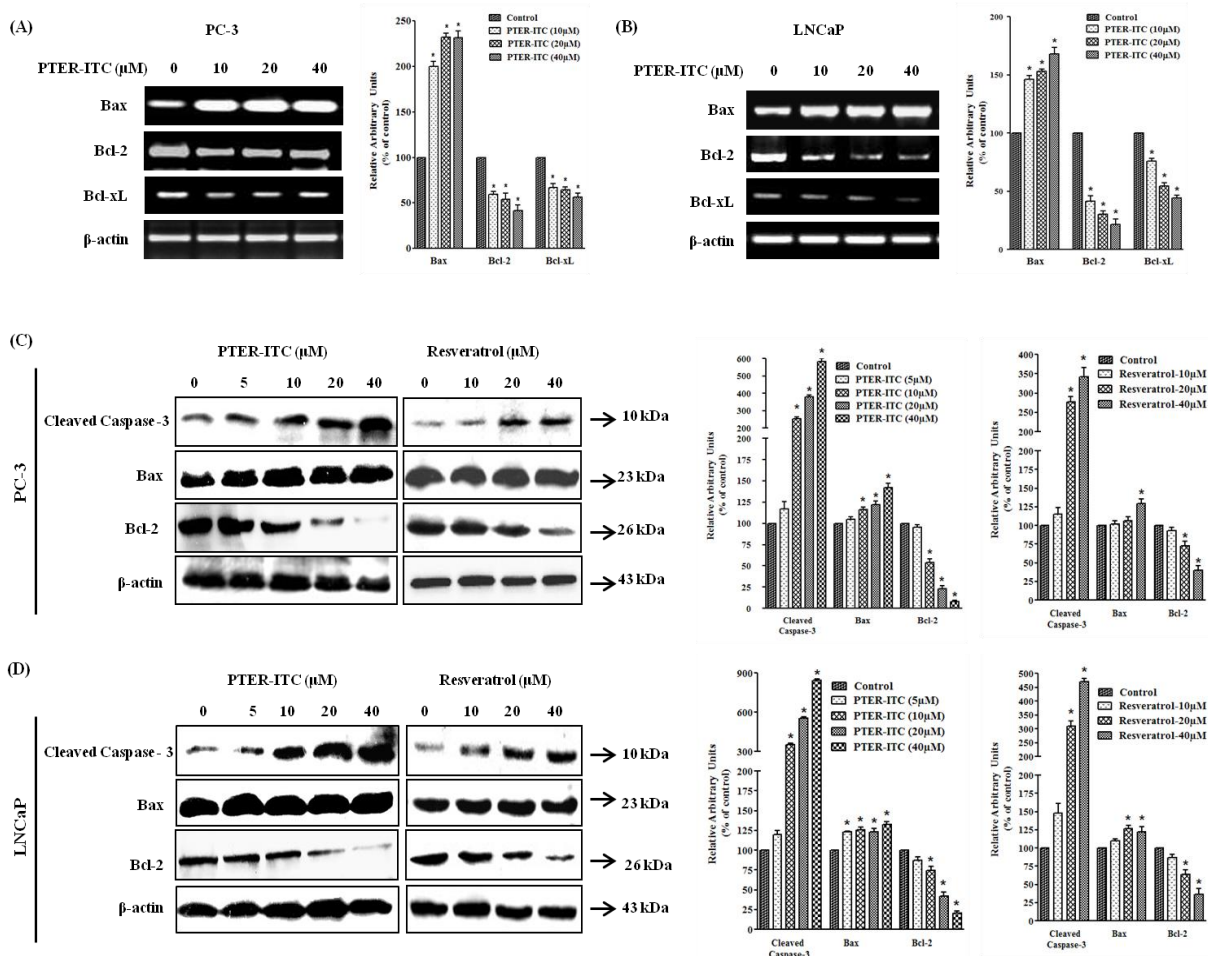
Figure 7.5: Transcriptional and translational analysis of various apoptotic marker genes in response to PTER-ITC. Expression patterns of various apoptotic marker genes in response to varying doses of PTER-ITC treatment as determined by RT-PCR in (A) PC-3 and (B) LNCaP cells. (C) Immunoblot analysis of various apoptotic marker genes in response to different doses of PTER-ITC and resveratrol in PC-3 and (D) LNCaP cells. The histogram on the right panel of each figure represents densitometric analyses of the image data and expressed as percent of control in PTER-ITC treated cells respectively where the results are mean ± SEM of three independent experiments. * represents statistically significant difference with respect to control for each genes at $p<0.05$.

7.3.6 Effect of inhibitor of p53 on PTER-ITC induced apoptosis

Since there was no significant difference in the number of apoptotic cells between PTER-ITC treated LNCaP (wild type p53) and PC-3 (p53 null) cells ($p<0.05$), it was intriguing to check if p53 has any role in PTER-ITC induced apoptosis of PCa cells. For this study we employed a pharmacological approach using specific wild type p53 inhibitor, pifithrin-α (PFT-α). PFT-α is a small molecule that binds to the DNA binding domain of p53, thereby inhibiting its transcriptional activity. For our experiment the LNCaP cells were pre-treated with 20 μM PFT-α for 2 h prior to the addition of 20 and 40 μM of PTER-ITC for next 24 h. Subsequently the drug treated cells were used to check caspase-3 activity and cell death by immunoblot analysis (Fig. 7.6A) and MTT assay (Fig. 7.6B) respectively. As expected, PFT-α significantly down regulated the expression of p53 protein while PTER-ITC treatment caused a dose dependent increase in its expression which, however, was significantly attenuated in presence of PFT-α (Fig. 7.6A).

Further, the expression of cleaved caspase-3 in cells treated with combination of PTER-ITC and PFT-α was almost similar to that of only PTER-ITC treated cells suggesting that p53 was not involved in regulation of PTER-ITC induced apoptosis. Next we determined the effect of p53-inhibition on PTER-ITC induced cell death by using MTT assay. In agreement with the above findings the cell death resulting from a 24 h exposure to 20 and 40 μM PTER-ITC did not differ significantly between LNCaP cells treated with or without PFT-α (Fig. 4B). Collectively, these results demonstrate that PTER-ITC-induced apoptosis and inhibition of cell growth could not be related with the activation of p53 signaling pathway.

(A)

(B)
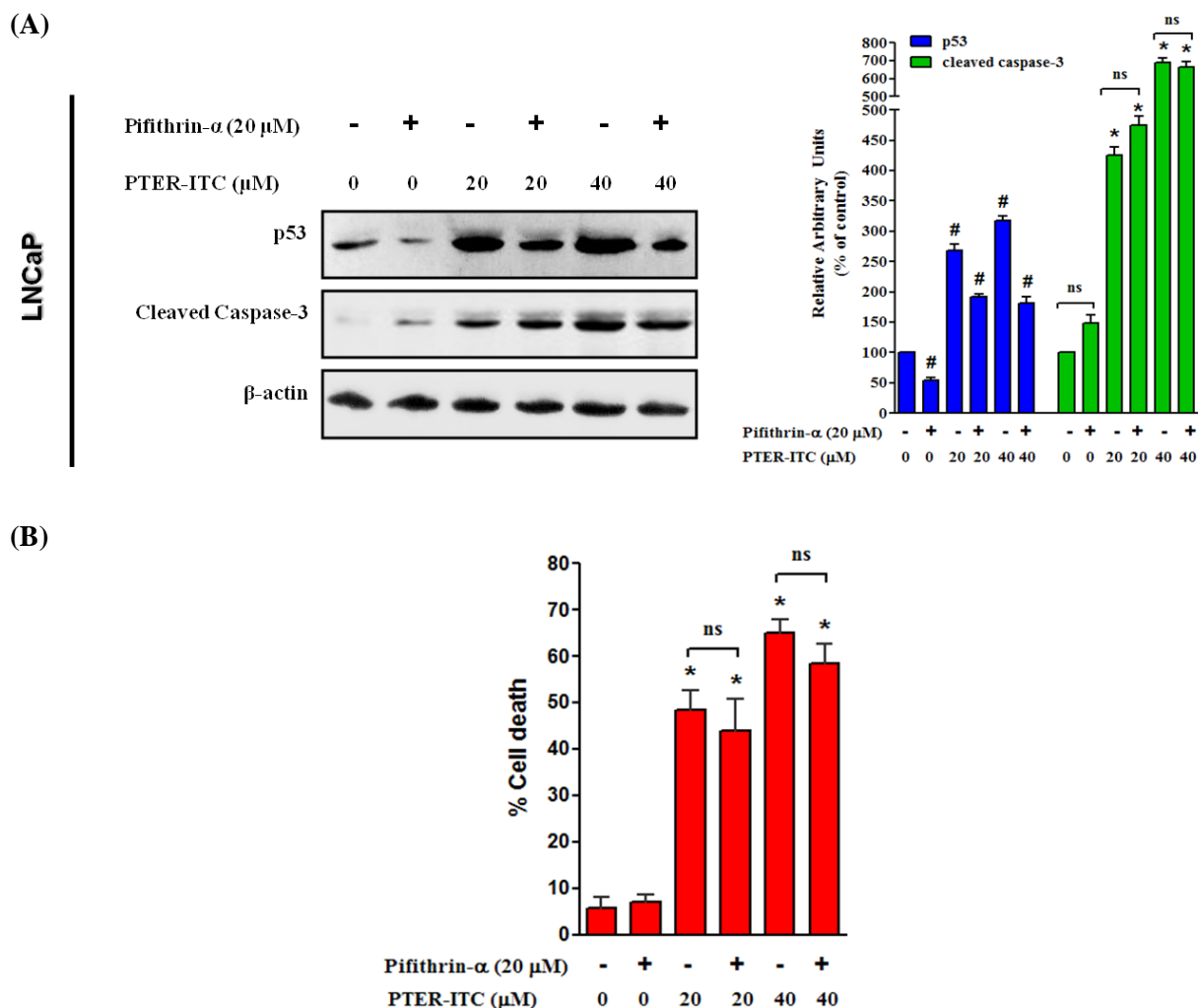
Figure 7.6: Role of p53 protein on PTER-ITC induced cell death in LNCaP cells. Effect of p53 inhibitor (PFT-α) on (A) the expression of apoptotic genes as determined by immunoblot analysis and (B) cell death in PTER-ITC treated LNCaP cells as determined by MTT assay. Data are the mean ± SEM of three independent experiments. # and * indicates significant difference with respect to the controls for p53 and caspsase-3 proteins respectively at *p*<0.05.

7.3.7 Effects of PTER-ITC on phosphorylation status of AKT and ERK1/2

The AKT signaling pathway is one of the most critical pathways in regulating cell survival. Phosphorylation of AKT provides cells with a survival signal that allows them to withstand apoptotic stimuli. Similar to AKT, another signaling molecule, ERK1/2, also regulates the proliferation and differentiation of cells at various stages of cell cycle. It has been earlier reported that inhibition of ERK1/2 pathway could lead to the induction of apoptosis. To probe the involvement of AKT and ERK in regulating apoptosis induced by PTER-ITC and RESV in LNCaP and PC-3 cells, we assessed the effect of PTER-ITC and RESV on the level

of phosphorylated AKT and ERK after 24 h of treatment. Our data showed that PTER-ITC molecule significantly decreased the phosphorylation of AKT at Ser_{473} and ERK at $Tyrosine_{204}$ in a dose-dependent manner in case of PC-3 cells (Fig. 7.7A). The level of p-AKT was decreased by almost 2.2- and 4.4-fold at 20 and 40 μM while the level of p-ERK was reduced to 1.3- and 1.7-fold at similar doses, respectively (Fig. 7.7A) ($p<0.05$). On the other hand, in case of RESV treatment the level of p-AKT decreased by about 1.2- and 1.6-fold at 20 and 40 μM while the level of p-ERK was reduced by 1.3 and 1.8-fold at similar doses, respectively. Furthermore, when tested in LNCaP cells, both RESV and PTER-ITC exposure had negligible effects on the level of p-AKT below 20 μM, while in case of p-ERK, the inhibitory effect was dose-dependent as was observed in PC-3 cells and it was almost completely inhibited at highest dose of PTER-ITC treatment (Fig. 7.7B) ($p<0.05$).
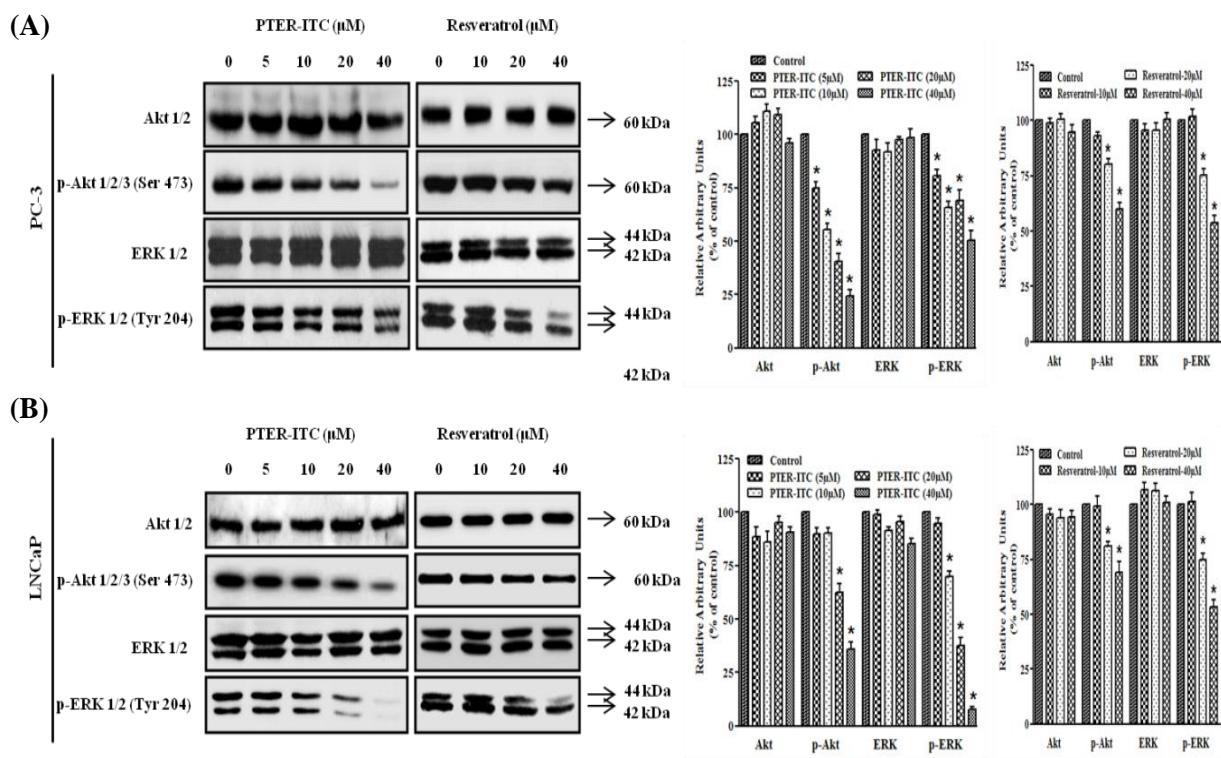
Figure 7.7: Effects of PTER-ITC on phosphorylation status of AKT and ERK1/2 (A) Immunoblot analysis to show the phosphorylation patterns of AKT and ERK in PC-3 and (B) LNCaP cells in response to varying doses of PTER-ITC and resveratrol treatments. The histogram on the right panel of each figure represents densitometric analyses of the image data and expressed as percent of control where the results are mean ± SEM of three independent experiments. * represents statistically significant difference with respect to control for each group at $p<0.05$.

176

7.3.8 Effect of AKT and ERK gene silencing on PTER-ITC-induced apoptosis of PC-3 cells

In order to confirm the role of AKT and ERK in PTER-ITC-induced apoptosis, we silenced both AKT and ERK using their respective siRNAs and examined their effects on the regulation of expression of cleaved caspase-3. The results of siRNA induced silencing of AKT and ERK protein levels were confirmed by immunoblot analysis. As shown in Fig. 7.8A, transfection of PC-3 cells with AKT and ERK specific siRNAs (but not with control siRNA) resulted in approximately 80-90% reduction in the expressions of p-AKT and p-ERK. Treatment of PC-3 cells with 20 μM PTER-ITC resulted in significant increase (3.7-fold) in cleaved caspase-3 protein expressions as compared to control which was enhanced further to 4.8-fold in presence of AKT siRNA ($p<0.05$). Since the combined effects of blockade of AKT by siRNA and PTER-ITC were found to cause enhanced expression of cleaved caspase-3 as compared to their individual responses, it could be suggested that there is direct involvement of AKT dependent pathway in the PTER-ITC induced apoptosis of PC-3 cells. Further, as a single agent the siRNA for ERK increased the expression of caspase-3 by 1.2-fold which was further increased to 3.9-fold in presence of PTER-ITC. However, this increment in caspase-3 expression was similar to that of PTER-ITC alone, suggesting that most probably the PTER-ITC-induced cleavage of caspase-3 did not directly involve ERK pathway at least in PC-3 cells. A similar pattern of results were obtained when A6730 (AKT kinase inhibitor) and PD98059 (ERK inhibitor), were used for blocking AKT and ERK signaling pathways respectively (Fig. 7.9A). Collectively, the data suggested that the PTER-ITC-induced apoptosis of PC-3 cells are mediated mainly through AKT-pathway.

7.3.9 Effect of AKT and ERK gene silencing on PTER-ITC-induced apoptosis of LNCaP cells

To determine whether PTER-ITC-induced apoptosis of LNCaP cells relates to AKT or ERK signaling pathways, the effect of inhibition of AKT and ERK on apoptosis was evaluated in the presence and absence of PTER-ITC in LNCaP cells. As shown in Fig. 7.8B, AKT siRNA, as expected, completely abolished the phosphorylation of AKT and caused a 1.4-fold increase in cleaved caspase-3 protein level. When AKT-silenced LNCaP cells were treated with PTER-ITC, there was about a 4.5-fold increase in cleaved caspase-3 protein level, which was almost comparable to increment caused by PTER-ITC alone. This data suggested that, probably AKT pathway did not play any major role in inducing apoptosis in LNCaP cells. Further, ERK gene silencing showed increase in cleaved caspase-3 level (1.35-fold) when compared to

vehicle treated control. ERK-silenced LNCaP cells when treated with PTER-ITC, it significantly increased the level of cleaved caspase-3 by 6.5-fold, which was about 1.4 times higher than that induced by PTER-ITC alone ($p<0.05$). This results were further validated using pharmacological inhibitors of AKT and ERK where co-treatment of LNCaP cells with PD98059 and PTER-ITC significantly increased the level of cleaved caspase-3, while combining A6730 with the PTER-ITC, did not show any significant increase as compared to only PTER-ITC treated group (Fig. 7.9B). These results thus indicate that in contrary to PC3 cells, ERK played a key role in apoptosis of LNCaP cells by PTER-ITC molecule while AKT inhibition alone was insufficient to induce apoptosis.
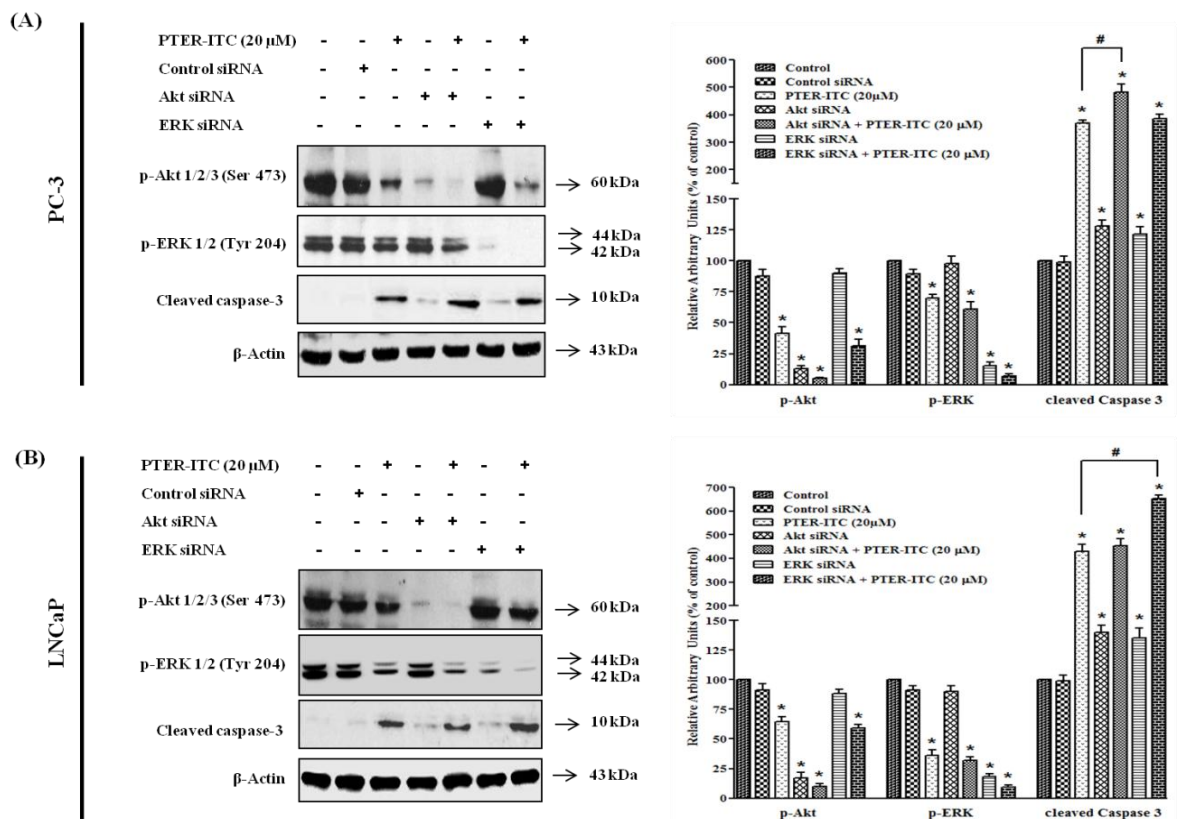
Figure 7.8: Differential role of PI3K/AKT and MAPK/ERK pathways in PTER-ITC induced apoptosis of prostate cancer cells. Effects of siRNA mediated silencing of AKT and ERK on PTER-ITC-induced apoptosis of (A) PC-3 and (B) LNCaP cells. LNCaP and PC-3 PCa cells were transfected with siRNAs (at a final concentration of 100 nM) using polyfect transfection reagent. After 24 h of transfection the cells were treated with 20 μM PTER-ITC and allowed to grow for another 24 h. The cell lysates were prepared and the level of p-AKT, p-ERK and cleaved caspase-3 proteins were detected by immunoblot analysis. The histogram on the right panel of each figure represents densitometric analyses of the image data and expressed as percent of control where the results are mean ± SEM of three independent experiments. * and # represents statistically significant difference with respect to control and 20 μM PTER-ITC treated groups respectively at $p<0.05$.
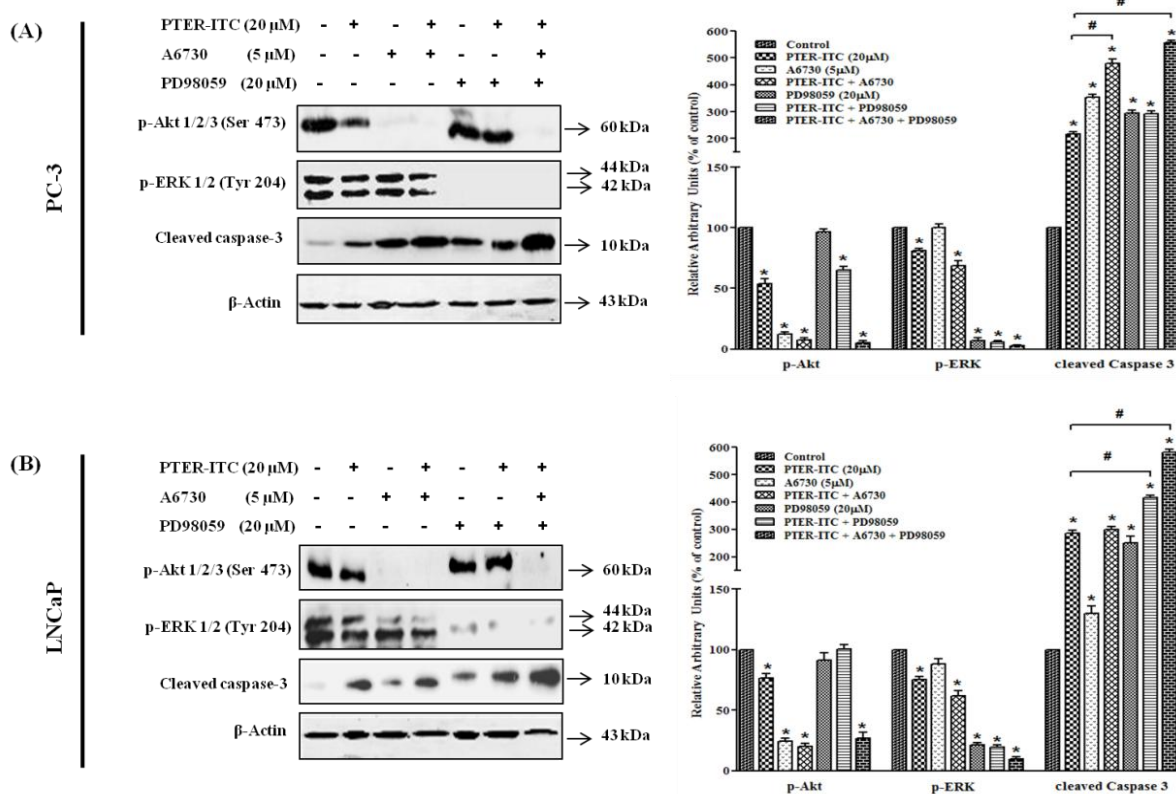
Figure 7.9 Effects of the AKT Kinase inhibitor (A6730) and/or the ERK inhibitor (PD98059) on the PTER-ITC-induced apoptosis of (A) PC-3 and (B) LNCaP cells. The cells were pre-treated with A6730 (5 µM) and/or PD98059 (20 µM) for 1 h before the addition of 20 µM PTER-ITC for additional 24 h (total inhibitor exposure time was 25 h). The collected cell lysates were then immunoblotted using respective antibodies. The histogram on the right panel of each figure represents densitometric analyses of the image data and expressed as percent of control where the results are mean ± SEM of three independent experiments. * and # represents statistically significant difference with respect to control and 20 µM PTER-ITC treated groups respectively at $p<0.05$.

7.3.10 PTER-ITC inhibits expression of AR

Since AR plays a critical role in the initiation and progression of PCa, we analyzed the effects of PTER-ITC on AR expression by reverse transcription-PCR and immunoblot analysis. For this, LNCaP cells, that express endogenous AR, were treated with varying concentrations of PTER-ITC both in presence and absence of 10 nM DHT. As shown in Fig. 7.10A (left panel), the PTER-ITC molecule had no significant effects on the expression of *AR* gene below 40 µM when treated in absence 10 nM DHT. However, interestingly, it demonstrated a dose-dependent inhibition of DHT (10 nM) induced AR transcription, which was reduced by about 1.2-, 1.3- and 1.4-fold ($p<0.05$) in response to 10, 20 and 40 µM of PTER-ITCs, respectively

(Fig. 7.10A, right panel). Further, when we performed the immunoblot analysis of AR with increasing doses of RESV and PTER-ITC treatments, we found a concomitant inhibition of the translation of this protein in response to various doses of the PTER-ITC both in presence and absence of DHT (Fig. 7.10B). Treatment with 10 and 20 μM of PTER-ITC yielded a significant inhibition of AR protein levels by 2- and 5-fold ($p<0.05$), respectively (Fig. 7.10B, left panel) while the same dose of RESV did not show any significant inhibition (Fig. 7.10C, left panel). In addition, the same dose of PTER-ITC also inhibited DHT induced AR protein levels by 1.1- and 1.8-fold (Fig. 7.10B, right panel) while RESV did not show any significant inhibition till 20 μM (Fig. 7.10C, right panel) ($p<0.05$). Thus, the above data clearly suggested that both RESV and PTER-ITC interferes with the translation of AR protein and interestingly, the latter was more potent than the former when tested at same concentrations.
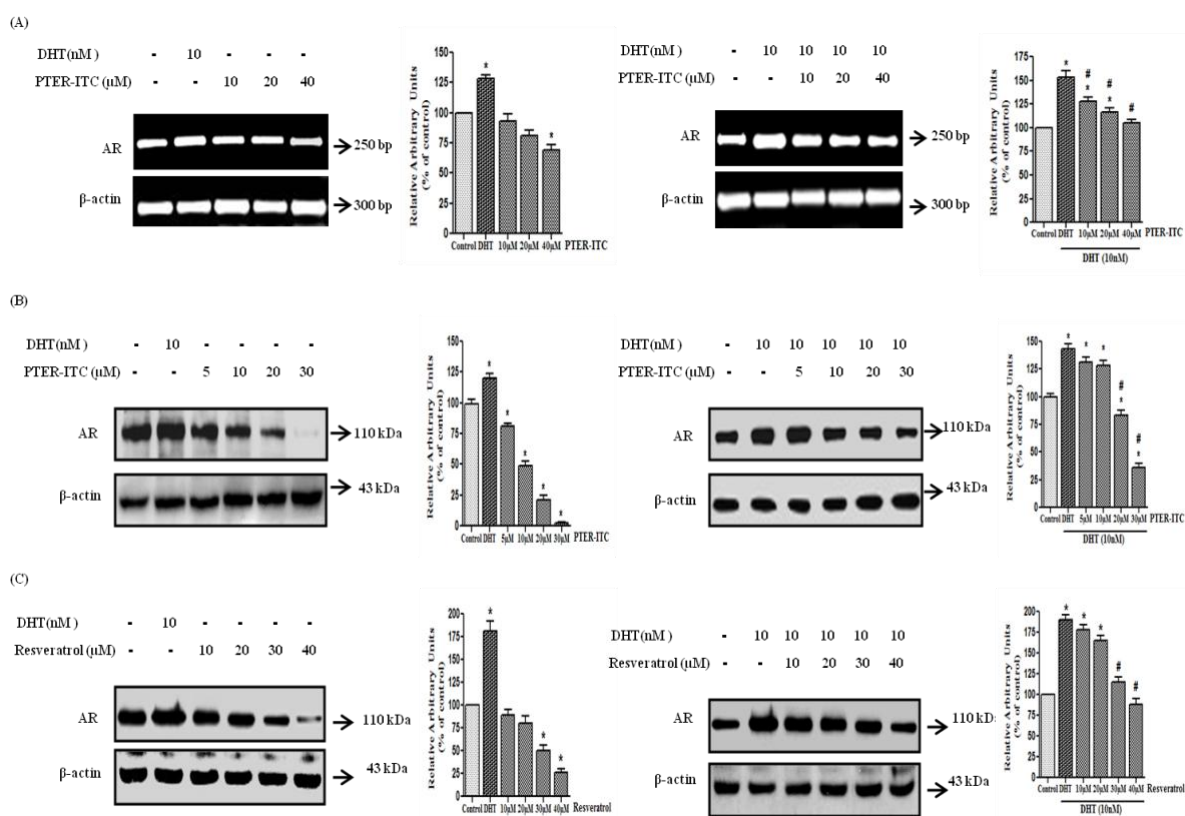
Figure 7.10 Effect of PTER-ITC on androgen receptor expression in LNCaP cells. (A) Regulation of androgen receptor expression in LNCaP cells by varying doses of PTER-ITC as determined by RT-PCR. Immunoblot analysis to show the expression of androgen receptor in response to (B) PTER-ITC and (C) resveratrol. The histogram on the right panel of each figure represents densitometric analyses of the image data and expressed as percent of control where the results are mean ± SEM of three independent experiments. * and # represents statistically significant difference with respect to control and 10 nM DHT respectively at $p<0.05$.

In the next stage of experiment, immunofluorescence staining of LNCaP cells was performed in order to visualize the intensity of endogenous AR expression in this cell. As shown in Fig. 7.11A, treatment of cells with varying doses of PTER-ITC resulted in almost complete abolition of fluorescent intensity in the cells, indicative of its anti-androgenic activity. As expected, DHT caused significant up regulation in the fluorescent intensity while 20 μM RESV showed marginal decrease in AR immunofluorescence which was in accordance to our earlier data.
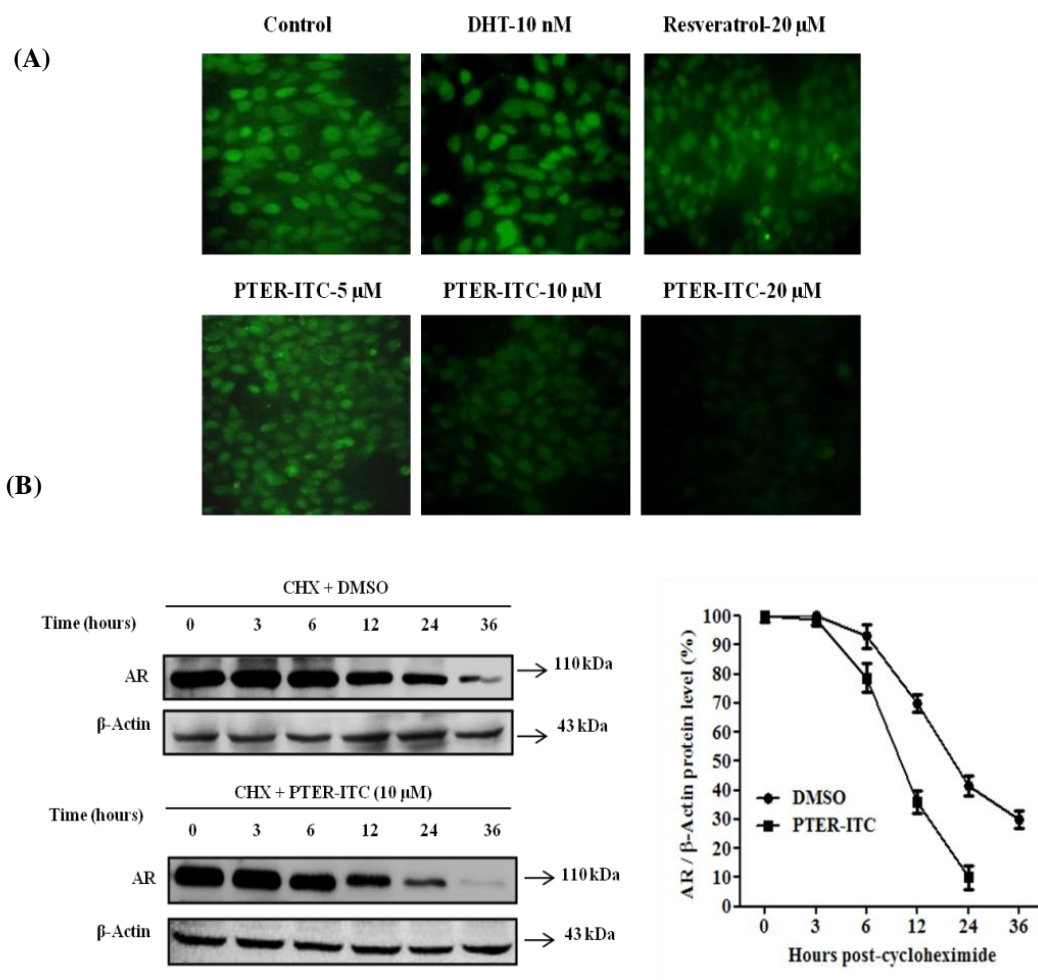
Figure 7.11: Effect of PTER-ITC on androgen receptor expression and turnover in LNCaP cells. (A) Immunofluorescence analysis to show the expression of androgen receptor (400X magnification). (B) Effect of PTER-ITC on androgen receptor protein turnover in LNCaP cells. LNCaP cells were grown to 60-70% confluency and treated with 10 μg/mL protein synthesis inhibitor cycloheximide (30 min pre-treatment) with or without 10 μM PTER-ITC at 0 h. Cells were then harvested at various time points (0, 3, 6 12, 24 and 36 h) and lysates were prepared. Androgen receptor protein levels were determined by immunoblot analysis using anti-androgen receptor antibody and normalized to β-actin control. The results are representative of two independent experiments. CHX, cycloheximide.

7.3.11 PTER-ITC induced decrease in AR half-life

Since PTER-ITC caused a significant dose-dependent decrease in AR protein level, we next focused our efforts on identifying whether post-translational modifications play any role in PTER-ITC-mediated decrease in AR levels. To address this issue, LNCaP cells were treated with protein synthesis inhibitor, cycloheximide (50 µM), with/ without 10 µM concentration of PTER-ITC. At specified time points the cells were harvested and AR protein levels were measured by western blot analysis using anti-AR antibody. As shown in Fig. 7.11B, in PTER-ITC-treated LNCaP cells, the half-life of AR protein was reduced from 20 h to 10 h as observed in the control cells treated with DMSO, suggesting that the observed decrease in AR protein level by PTER-ITC could be due to post-translational degradation.

7.3.12 PTER-TC-induced inhibition of AR-mediated transcription of luciferase activity

In order to check the anti-androgenic activity of PTER-ITC, AR positive LNCaP cells were transiently transfected with pMMTV-neomycin-luciferase construct. Ligand-activated AR binds to androgen response element (ARE) and its functional activation was tested using a luciferase reporter gene linked to MMTV promoter having multiple repeats of AREs. The effect of DHT (10 nM) on the luciferase activity was expressed as 100% transactivation. The PTER-ITC alone (without DHT) did not induce transcriptional activation at any of the concentrations tested (1–40 µM). However, as shown in Fig. 7.12A, the PTER-ITC exhibited a dose-dependent anti-androgenic activity by inhibiting the androgen-induced transactivation by about 73% at the highest dose tested (40 µM) as compared to only DHT treatment. In order to confirm the anti-androgenic activity of PTER-ITC further, similar transactivation assay was also performed in AR negative PC-3 cells co-transfected with pSG5-hAR and pMMTV-neomycin-luciferase constructs. As shown in Fig. 7.12B, consistent with the results described above for LNCaP cells, in this cell line (PC-3) also the DHT-mediated luciferase activity was reduced by 19, 31, 63, 70 and maximum to 80% in the presence of 5, 10, 20, 30 and 40 µM of PTER-ITC, respectively.
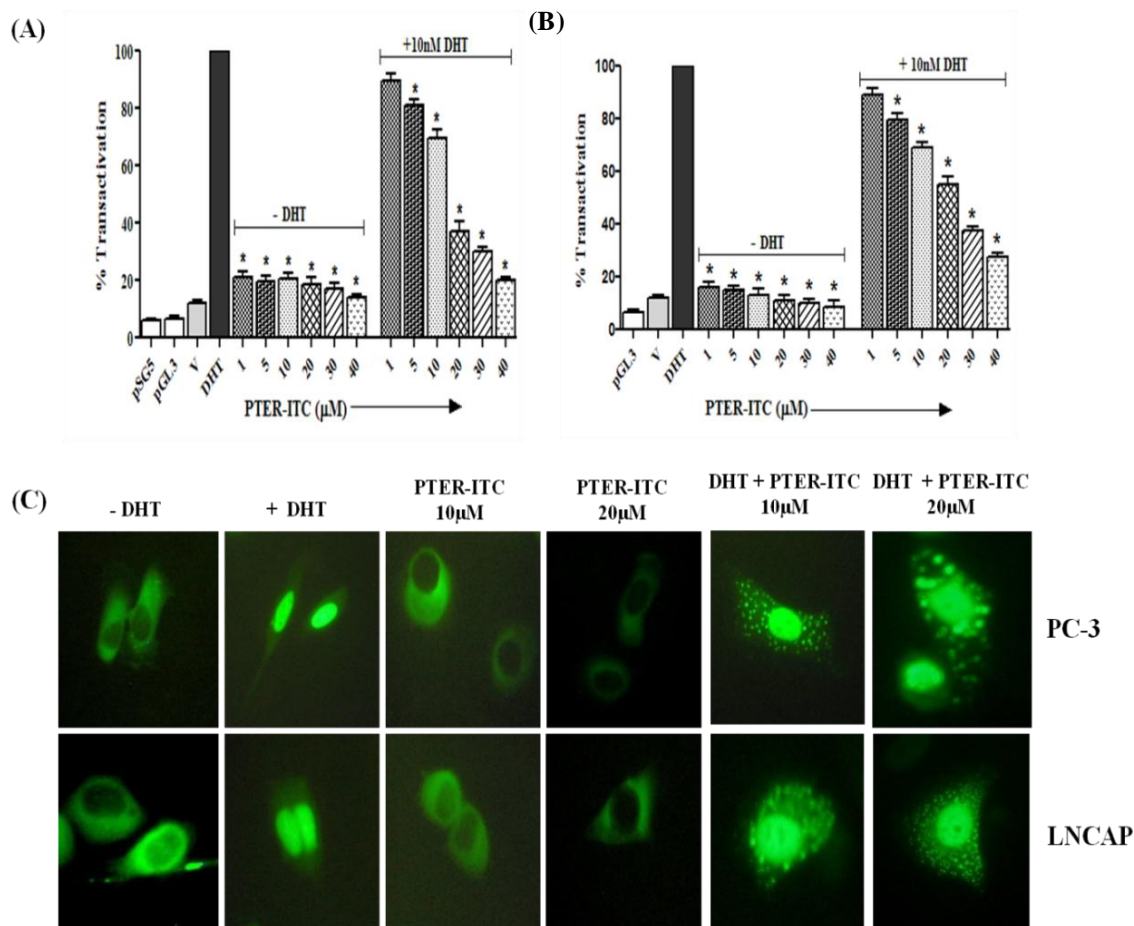
Figure 7.12: PTER-ITC inhibits androgen receptor transactivation and translocation in prostate cancer cells. Effect of PTER-ITC on the transactivation of androgen receptor in presence/absence of 10 nM DHT in (A) androgen receptor positive LNCaP cells and (B) androgen receptor negative PC-3 cells. Luciferase activities are expressed as percentage of transactivation with respect to only 10 nM DHT treated group which is considered as 100%. * indicates statistically significant difference ($p<0.05$) with respect to DHT treated groups. (C) Effect of PTER-ITC on the dynamics of nuclear translocation of androgen receptor as determined by green fluorescent protein (GFP)-androgen receptor construct in presence/absence of 10 nM DHT for 2 h.

7.3.13 Effect of PTER-ITC on the nuclear localization of AR

We next checked the effect of PTER-ITC on the nuclear localization of AR in AR positive (LNCaP) and AR negative (PC-3) cells. Twenty-four hours after transient transfection of pEGFP-AR construct, both PCa cells were treated with 10 nM DHT in the presence and absence of PTER-ITC (10 and 20 µM). Generally, any ligand for AR is expected to cause the nuclear localization of this receptor within a maximum period of 30 min. As shown in Fig. 7.12C, in the absence of androgen, the labeled AR protein was distributed in the cytoplasmic

compartment, which in the presence of 10 nM DHT, was predominantly localized in the nucleus. Interestingly, the distribution of GFP-AR protein in the cells treated with PTER-ITC alone was similar to that of vehicle-treated cells (without DHT), wherein the nuclear translocation of AR was inhibited at both the doses tested. However, as shown in Fig. 7.12C, when the cells are co-treated with DHT and PTER-ITC, the nuclear localization of AR, as induced by DHT, was significantly inhibited by PTER-ITC resulting in the dispersed distribution of AR proteins between the nuclear and the cytoplasmic compartments in both the cell lines. This pattern of distribution could be attributed to the anti-androgenic activity of the PTER-ITC.

7.3.14 The PTER-ITC weakens the interaction between AR and it co-activators: SRC-1 and GRIP-1 in LNCaP cells

It is well documented that the intrinsic ligand-dependent activity of AR is potentiated through its interaction with co-regulators namely SRC-1 and GRIP-1. Since the PTER-ITC repressed AR transcriptional activity and subsequently its transactivation, it is also probable that PTER-ITC might suppress AR transactivation by interrupting the function of its co-activators. Hence, in the next stage alterations in the expression patterns of co-activators (GRIP-1 and SRC-1) were analyzed in response to DHT and PTER-ITC treatment by immunoblot analysis. As shown in Fig. 7.13A, the expression of both the co-activators, GRIP-1 and SRC-1, were greatly reduced in LNCaP cells treated with PTER-ITC. When treated with 10 and 20 μM of PTER-ITC, the expression of SRC-1 protein was decreased by 1.4- and 2.6-fold ($p<0.05$) while the same dose reduced GRIP-1 level by 1.7- and 2.6-fold, respectively ($p<0.05$). As expected, DHT significantly increased the expression of SRC-1 (1.2-fold) ($p<0.05$), however, there was no significant change in the expression of GRIP-1.

Furthermore, to check if the PTER-ITC interferes with the direct interaction of co-activators (SRC-1 and GRIP-1) to AR, co-immunoprecipitation analysis was performed in LNCaP cells, which has endogenous AR. As shown in Fig. 7.13B, lysates immunoprecipitated with AR antibody showed decreased band intensities for SRC-1 and GRIP-1 with increasing doses of PTER-ITC, suggesting reduced interaction of AR-SRC-1 and AR-GRIP-1 in presence of PTER-ITC. As expected, 10 nM DHT in turn showed enhanced interactions with those co-activators thus validating the co-immunoprecipitation assay. No detectable proteins were shown in immunocomplexes precipitated with normal IgG. Together, these data indicate that the PTER-ITC-induced suppression of AR transactivation may not be only through the direct

suppression of AR expression, but also by the inhibition of expression and their subsequent interaction with its co-activators like SRC-1 and GRIP-1.
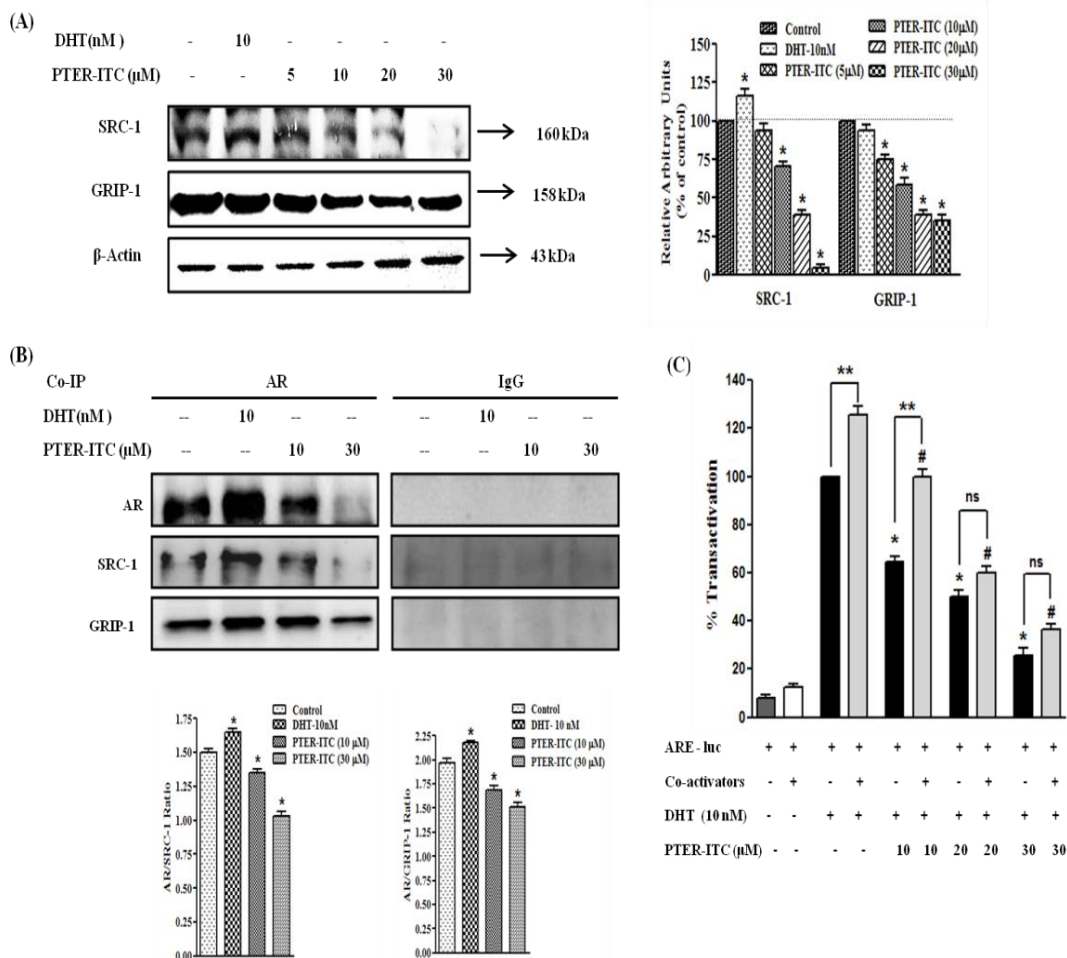
Figure 7.13: PTER-ITC weakens the interaction between androgen receptor and its co-activators. (A) Immunoblot analysis for the expression of androgen receptor co-regulators in response to PTER-ITC in LNCaP cells and the histogram on the right panel of the figure represents densitometric analyses of the image data and expressed as percent of control in PTER-ITC treated cells where the results are mean ± SEM of three independent experiments. * represents statistically significant difference with respect to control ($p<0.05$). (B) Effects of PTER-ITC on the interactions of androgen receptor and its co-activators (SRC-1 and GRIP-1) as determined by co-immunoprecipitation analysis. Histogram in the lower panel represents ratio of androgen receptor to that of co-activators where results are mean ± SEM of three independent experiments. * represents statistically significant difference with respect to control ($p<0.05$). (C) Effect of PTER-ITC on DHT induced transactivation of androgen receptor in presence/absence of co-regulators (SRC-1 and GRIP-1) in androgen receptor positive LNCaP cells. Luciferase activities are expressed as percentage of transactivation with respect to only DHT treated group which is considered as 100%. * and # indicates statistically significant difference from DHT treated cells in absence and presence of co-regulators respectively and ** indicates significant level of difference between two adjacent groups with and without co-activator at $p<0.05$. ns, non-significant.

Since the PTER-ITC decreased DHT-mediated AR transactivation and further down-regulated expressions of its co-activators like SRC-1 and GRIP-1, it was intriguing to check whether the administration of exogenous GRIP-1 and SRC-1 could reverse the effects of PTER-ITC on AR function and PCa cell growth. As shown in Fig 7.13C, the transactivation of AR was significantly enhanced in the presence of co-activators in the cells treated with DHT (1.25-fold) ($p<0.05$), as compared to its responses in the absence of those co-activators. However, when the cells were treated with increasing doses of PTER-ITC (10–30 μM), it caused strong inhibition of DHT-induced AR transactivation in the absence of these co-activators. Our data showed that although the expression of exogenous co-activators rescued the AR-inhibitory activity as caused by the PTER-ITC at low dose of 10 μM (64% vs 102%), it failed to completely revert back this inhibitory effect at 20 and 30 μM concentrations of PTER-ITC where the difference between normal cells (i.e., without co-activator transfected) and co-activator transfected cells was almost non-significant (Fig. 7.13C) ($p<0.05$). These results suggested that the PTER-ITC-mediated reduction of AR activation may be due, at least in part, to a decrease in the expression of AR co-activators and their recruitment to the promoter of the AR target gene.

7.4 Discussion

We have earlier reported that PTER is a potent anticancer molecule with multiple targets of action in breast and PCa cells [Chakraborty et al., 2010, Chakraborty et al., 2012]. On the other hand, ITCs are naturally occurring small molecules that are formed from glucosinolate precursors of cruciferous vegetables. Numerous investigations have shown that naturally occurring ITC and their synthetic analogues retard or inhibit tumor cell growth, both *in vitro* and *in vivo* [Chiao et al., 2002; Fimognari et al., 2009]. The ability of ITC to inhibit tumorigenesis is dependent on its structure, the animal species, target tissues, and the specific carcinogen employed [Wu et al., 2009]. However, the existing literatures are somewhat ambiguous about the chemopreventive activity of ITC which suggests that not all of them are suitable for their use as chemopreventive agents [Fimognari et al., 2009]. Due to their electrophilic reactivity, some ITCs are able to form adducts with DNA and induce mutations and chromosomal aberrations [Fimognari et al., 2012]. PTER on the other hand has not yet been reported to have any genotoxic effects. Based on these reports we hypothesized that by combining PTER with ITC, the newly developed PTER-ITC molecule could bypass some of their individual toxic effects and at the same time would complement each other for inhibition of PCa more efficiently. RESV, a naturally occurring polyphenol is closely related to PTER and

has similar biological activity. The anti–prostate cancer potential of RESV has been well documented in many *in vitro* and *in vivo* studies and a large amount of evidence suggests that it may be a promising molecule in both PCa treatment and prevention [reviewed in Jasinski et al., 2013; Carter et al., 2014]. Hence in the present study, we focused on the characterization of PTER-ITC conjugate, a hybrid molecule from PTER and ITC, for its efficacy as a potent apoptotic and anti-androgenic agent for PCa chemotherapy while directly comparing it to RESV. It is noteworthy to mention here that the response shown by PTER-ITC in this study was much better than that of RESV. The probable reasons for the superior inhibitory effect of PTER-ITC as compared to RESV on PCa cells may be (i) due to the higher binding affinity of the former to same target signaling proteins as that of the latter and or alternatively (ii) the PTER-ITC and RESV may altogether have different protein targets due to differences in their chemical structures.

PCa proceeds through two distinct operationally divisible stages: androgen-dependent and androgen-independent. Therefore, in the present study, two different cell lines, LNCaP (androgen dependent) and PC-3 (androgen independent) were used to study the effect of this PTER-ITC on PCa cells growth and AR regulation. The cell proliferation assay showed that the PTER-ITC molecule caused a dose dependent cytotoxicity in both the cell lines. This cytotoxicity was more or less equally effective in suppressing proliferation of both PC-3 and LNCaP cells. These observations have clinical implications since the majority of human PCa at the time of diagnosis represent androgen-dependent as well as androgen-independent situations. The p53 tumor suppressor protein plays an important role in the regulation of apoptosis by different stimuli [Agarwal et al., 1998; Sheikh and Fornace et al., 2000]. Both p53-dependent and p53-independent apoptosis processes are known to occur in cells due to various insults. To delineate if the PTER-ITC-induced apoptosis in PCa cells are p53-dependent, we compared cancer cell vulnerability against PTER-ITC in p53 positive LNCaP cells. Our functional study showed that the inhibition of p53 by its inhibitor (PFT-α) had no significant effects on the cell death caused by this PTER-ITC, suggesting that the PTER-ITC induced apoptosis of PCa cells are independent of p53. Further, the flow cytometry analysis showed that the PTER-ITC molecule arrested the PCa cells in G2/M phase, suggesting that the PTER-ITC-induced inhibition of cell proliferation involved both cell cycle arrest and apoptosis. During cell cycle, the G2/M checkpoint is a potential target for cancer therapy. It prevents DNA-damaged cells from entering mitosis and allows their repair of DNA that was damaged in late S or G2 phases prior to mitosis [Wang et al., 2009]. Data presented herein indicated that 10 and 20 μM concentrations of PTER-ITC effectively inhibited proliferation of PC-3 and LNCaP cells by

inducing apoptosis and causing cell cycle arrest. Our data are consistent with the results of previous cellular studies using other ITC analogues, such as sulforaphane and phenethyl isothiocyanate, where apoptosis induction, cell cycle arrest and/or molecular changes associated with growth inhibition were observed at a concentration of 50 μM or lower [Chiao et al., 2002; Xiao et al., 2002].

Previous studies have shown that AKT and ERK-MAPK signaling pathways function cooperatively to promote prostate tumorigenicity and androgen independency [Hui et al., 2006]. The AKT pathway can be activated by various growth factors and plays a crucial role in promoting growth and blocking apoptosis in various cancer models including PCa [Addanki et al., 2003; Sinha et al., 2006; Agarwal et al., 2013]. Although the precise anti-apoptotic effects of AKT are still not very well understood, it has already been reported that activated AKT can phosphorylate several apoptosis-regulating proteins including BAD, a member of pro-apoptotic Bcl-2 family [Fresno et al., 2004; del Paso et al., 1997; Touny et al., 2007]. BAD promotes cell death by interacting with anti-apoptotic Bcl-2 members such as Bcl-xL, which allows the multidomain pro-apoptotic Bcl-2 family members like Bax and Bak to aggregate and cause release of apoptogenic molecules (e.g., cytochrome c) from mitochondria to the cytosol culminating into caspase activation and cell death [Cheng et al., 2001]. In the present study, it could be speculated that the PTER-ITC induced inactivation of AKT by decreasing the level of phosphorylated-AKT in a concentration-dependent manner and further reduction in the levels of Bcl-2, Bcl-xL and concomitant increase in the expressions of Bax followed by caspase-9 and caspase-3, as a whole, contributed to the promotion of apoptosis in these two cell lines. Survival-signaling cascade in many cells involves PI-3-kinase, AKT, and also cross-communication between PI-3-kinase and ERKs [Ballif and Blenis, 2001]. Since sustained activation of ERK1/2 is necessary for cell survival and proliferation [Ballif and Blenis, 2001], suppression of ERK activation by any agent can mediate apoptosis, which may be linked to subsequent inhibition of Bcl-2 in PCa cells [Caraglia et al., 2007; Zelivianski et al., 2003]. The current data is in accordance to the previous report where it was speculated that the inhibition of p-ERK1/2 and Bcl-2 by PTER-ITC may be another pathway for apoptosis in PCa cells [Caraglia et al., 2007; Zelivianski et al., 2003]. In conclusion, the current data suggests the involvement of at least two different protein kinase pathways for regulating induction of apoptosis by the PTER-ITC in these two different PCa cells.

The AR is a key regulator in the development and growth of PCa and current therapeutic strategies utilizes anti-androgens that prevent AR activation and/or disrupt endogenous androgen production. However, several reports showed that these therapies

ultimately fail as a result of AR activation by non-steroidal physiological signals as well as the existence of mutant ARs in PCa cells that can be activated by non-androgenic steroids and certain growth factors [Grigoryev et al., 2000; Yeh et al., 1999; Kang et al., 2001; Sharma et al., 2007]. Thus, there is an urgent need for testing new therapies based on different mechanisms to target AR signaling for androgen-dependent PCa. Treatment that aims at reducing AR expression may represent an attractive approach to target androgen signaling in PCa [Amin et al., 2014]. Our results demonstrated that the PTER-ITC disrupts androgen signaling at multiple stages of AR signaling pathways including its transcription, translation and degradation as a part of its growth arrest program in LNCaP cells. Thus, it could be presumed that the PTER-ITC is one of the few compounds along with RESV [Harada et al., 2007], tea polyphenol EGCG [Ren et al., 2000], luteolin [Chiu et al., 2008], andrographolide [Liu et al., 2011], emodin [Cha et al., 2005] and indole-3-carbinol [Hsu et al., 2005], which also disrupts AR cellular activities by down regulating its transcription as well as translation.

The transactivation function of AR can be regulated by several co-regulators (co-activators and co-repressors) [Papaioannou et al., 2005; Baniahmad A, 2005; Sipilä et al., 2011]. These proteins do not directly bind to DNA and are recruited to the promoter regions of the AR-target genes through protein-protein interactions with AR. Therefore, a decrease in the expression levels of AR co-activators or the interruption of their interaction with AR in PCa cells could contribute to inhibition of AR signaling and ultimately the growth of PCa cells [Agoulnik et al., 2005]. The first identified member of the co-activator family that regulated steroid receptor action was SRC-1 [Onate et al., 1995; Amazit et al., 2003], which is functional in many different tissue types and enhances transcriptional activity of AR in a ligand-dependent manner [Heinlein and Chang, 2002]. Co-regulators such as GRIP-1 and SRC-1 interact with AR to enhance ligand-dependent transactivation of AR. The expression of SRC-1 and GRIP-1 increases in cancer and recurrent PCa after medical or surgical castration [Gregory et al., 2001], suggesting that GRIP-1 and SRC-1 may be involved in the development and progression of PCa. In this connection, it is worth mentioning here that the PTER-ITC significantly decreased the expression of both SRC-1 and GRIP-1 and also interrupted the interaction of AR with SRC-1 and GRIP-1 as shown by co-immunoprecipitation analysis. Further, transfection with exogenous SRC-1 and GRIP-1 also could not restore the inhibition caused by the PTER-ITC at higher doses, suggesting that some other co-regulators may also be involved in PTER-ITC-induced decrease in AR regulation. From the above results, it could be hypothesized that most probably, not only the PTER-ITC has anti-AR activity due to its receptor antagonizing

properties, but it might also inhibit some other interacting proteins (mainly co-activators like SRC and GRIP-1), which in turn regulates the AR transcriptional activity.

Finally we checked if the PTER-ITC has any effect on the localization of AR to the nucleus. Our data showed that the PTER-ITC at higher doses (10-20 μM) prominently inhibited the nuclear localization of AR after 2 h incubation with it. A similar pattern of inhibition was also reported in COS-1 cells where the nuclear-localized fluorescently labeled AR decreased after incubation with 40 μM emodin for 2 h (an anthraquinone derivative isolated mainly from the root and rhizome of *Rheum palmatum)* [Cha et al., 2005]. However, in case of PTER-ITC and DHT co-treatments, a prominent cytoplasmic fluorescence was observed with a decrease in nuclear intensity. This may be either due to inhibition of nuclear import of AR or augmentation of nuclear export of AR. A similar pattern of inhibition was reported in case of RESV where the nuclear-localized AR decreased after incubation with 10 μM RESV for 24 h, but not for 3 h [Harada et al., 2007]. This result was further validated by electrophoretic mobility shift assay where the PTER-ITC treatments decreased the binding activity of AR to its cognate response element of *PSA* gene (data not shown). However, based on these data it is difficult to confirm if this is mainly due the inhibition of nuclear translocation of the activated AR or a physical interference of AR association with the ARE through modulation of co-regulators other than SRC-1 and GRIP-1. Further detailed analysis in this regards are warranted to specifically designate the anti-androgenic effect of this PTER-ITC using *in vitro* and *in vivo* AR-knockin/ knockout animal models.

Based on the above findings, it could be concluded that PTER-ITC inhibits the AR-regulated pathways in PCa cells involving various signaling cascades. The PTER-ITC significantly inhibited cell proliferation, induced apoptosis, cell cycle arrest, down regulated the expression of AR and abrogated DHT induced activation in PCa cells. Our findings further support the differential involvement of these protein kinase pathways (AKT and ERK) in regulating apoptosis induction by PTER-ITC in these two different PCa cells. Moreover, results on steroid sex hormones are consistent with PTER-induced inhibition of PCa cells as shown by Wang et al. [2010]. Hence the current data provides a new set of information which states that the PTER-ITC inhibits androgen activity on LNCaP cells. To the best of our knowledge, this is the first study to show that PTER-ITC acts as AR antagonist not only by regulating its expression, but also by preventing its entry into the nucleus followed by recruitment of co-activators. Thus, our results suggest that a novel strategy of combining PTER and ITC may benefit patients with PCa. However, further in depth research including animal experimentation on prostate tumor models are needed in order to fully understand the inhibition of tumor

progression and/or treatment of PCa and other human malignancies with this compound before considering it for clinical trials.

Chapter 8.1 Isolation and characterization of HUVECs from umbilical cord

8.1.1 Introduction

Endothelial cells, the cells derived from blood vessels are involved in exchange of metabolites between blood and the tissues, in blood haemostasis, wound healing and also provide a non-thrombogenic surface [Aird WC, 2013; Sumpio et al., 2002; Pober and Sessa, 2007]. They play an important role in mediating both normal physiology and patho-physiology in human body thus providing a classic model system to study many aspects of endothelial function and disease like normal, abnormal and tumor-associated angiogenesis, oxidative stress, hypoxia, inflammation related pathways and cardiovascular-related complications. These cells are also used as a model to study mode of action of various compounds in preventing these complications [Aird WC, 2013; Sumpio et al., 2002; Pober and Sessa, 2007; Rhim et al., 1996].

HUVEC are most readily available (post-partum waste) source for macrovascular endothelial cells which cover the internal surface of arteries, veins, lymphatic vessels and capillaries. Various methods have been developed and established for isolation and primary culture of HUVECs [Baudin et al., 2007; Siow RCM, 2012]. Important information can be obtained from these primary cultures as long as they retain the characteristics present *in vivo*. Sub-culturing is required for collecting large quantities of cells for various biochemical studies, cell growth properties etc. Culturing of endothelial cells is also meaningful for a variety of applications such as for lining the lumen of a synthetic or tissue engineered vascular graft, making use of their inhibitory properties on platelet adhesion and clotting. Further, they are also considered as a potential target for vascular gene therapy both *in vitro* and *in vivo* because they release proteins directly into blood stream [Bouis et al., 2001]. The current study thus deals with isolation, culture and characterization of HUVEC cells, which represents a keystone for further research on these cells.

8.1.2 Brief Methodology

8.1.2.1 Isolation of HUVECs

HUVECs were isolated from umbilical cord as described in the Materials and Methods section.

8.1.2.2 Characterization of isolated HUVECs

Analysis of marker genes for HUVECs was performed by RT-PCR. The genes selected were CD31 and Von Willebrand factor.

CD31, also designated as platelet endothelial cell adhesion molecule 1 (PECAM-1) is a 130-kDa transmembrane glycoprotein and a member of the immunoglobulin superfamily. This protein is a constituent of the endothelial intercellular junction and is located on the surface of platelets, monocytes, macrophages, and neutrophils. It plays an important role in the adhesion cascade between endothelial cells during angiogenesis and between endothelial cell and inflammatory cells during inflammation in facilitating leucocyte migration.

Von Willebrand factor (vWF) is a glycoprotein that is expressed exclusively on EC where it shows a granular pattern of reactivity. It is stored in Weibel-Palade bodies. It mediates platelet adhesion to subendothelium at sites of vascular injury and binds and stabilizes factor VIII in the circulation [Alles and Bosslet 1988; Yamamoto et al. 1998].

8.1.2.3 Karyotyping

For karyotyping of the isolated cells metaphase chromosomes were prepared according the method detailed in the Materials and Methods section.

8.1.3 Results

8.1.3.1 Morphological identification of HUVEC

Routine evaluation of the quality and growth state of the HUVEC was achieved using an inverted phase microscope. The primary HUVECs became attached completely after 24 h and were confluent after 4 days *in vitro* (Fig. 8.1.1 and 8.1.2). The cells grew as confluent monolayers with cobblestone morphology and were homogenous, closely apposed, large, flat, and polygonal. HUVECs display a characteristic ovoid nucleus with two to three prominent nucleoli and perinuclear granules. When maintained at confluence for an extended period of time, these cells became tightly packed but did not show any tendency to overlap or overgrow one another. With increase in number of passage, cells gradually became larger in size and cell density at confluence decreased. There was also an increased frequency of giant, multinucleated cells and a decreased tendency to form a confluent monolayer.

Magnification = 50 X   Magnification = 100 X

Magnification = 200 X   Magnification = 400 X
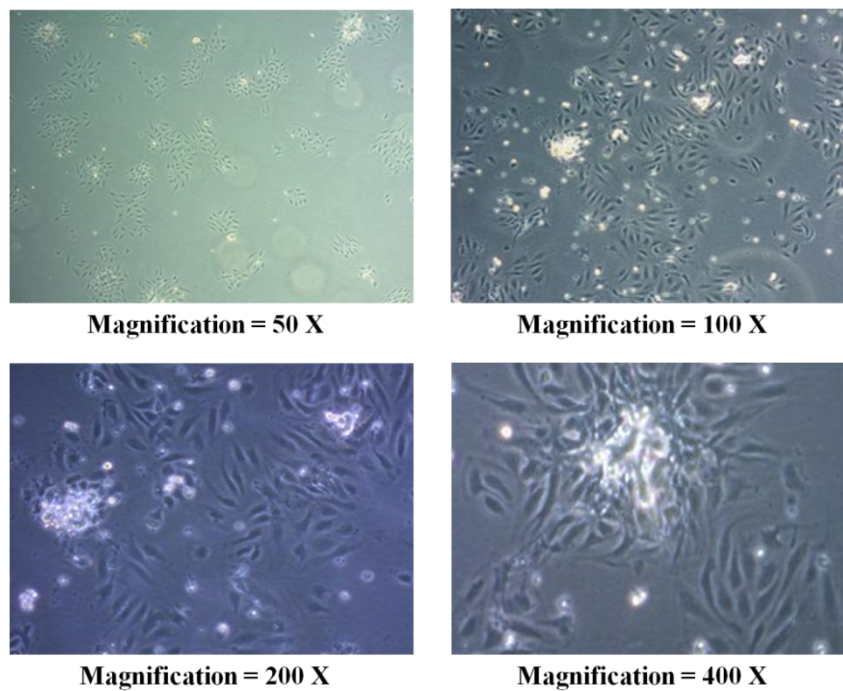
Figure 8.1.1: Phase contrast photomicrograph of a primary culture of HUVEC 48 h after isolation and culture showing colonies of polygonal closely opposed cells.

Magnification = 50 X   Magnification = 100 X

Magnification = 200 X   Magnification = 400 X
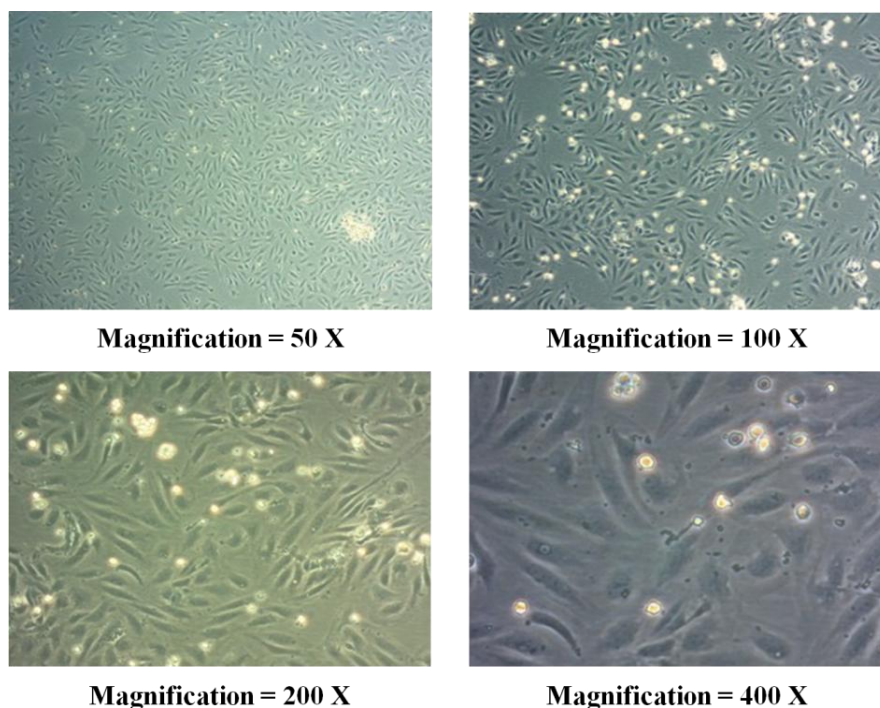
Figure 8.1.2: Phase contrast photomicrograph of HUVECs after 4 days of culture. The cells are confluent and display cobblestone morphology.

8.1.3.2 Characterization of HUVEC

The isolated HUVEC were characterized using specific endothelial cell marker like CD31 and vWF. While vWF protein is present exclusively on endothelial cells, CD31 is located on surface of platelets, monocytes, macrophages, neutrophils and on endothelial intercellular junction. When checked for HUVEC markers, the isolated cells showed positive expression for CD31 and vWF genes (Fig. 8.1.3). When expression of these endothelial cell marker were checked in the nonaggressive MCF-7 and aggressive MDA-MB-231 breast cancer cell lines, both the cells were found to express modest amount of these marker protein (Fig. 8.1.3).

VEGF is a critical factor in vasculogenesis and angiogenesis, and has been shown to be expressed by melanoma cells in a majority of metastases. VEGF is also found to play an important role in autocrine growth regulation of HUVEC [Imaizumi et al., 2000]. Thus when the isolated cell were checked for VEGF expression in different serum conditions the cells were found to express VEGF protein which was predominantly located inside the nucleus (Fig. 8.1.4).
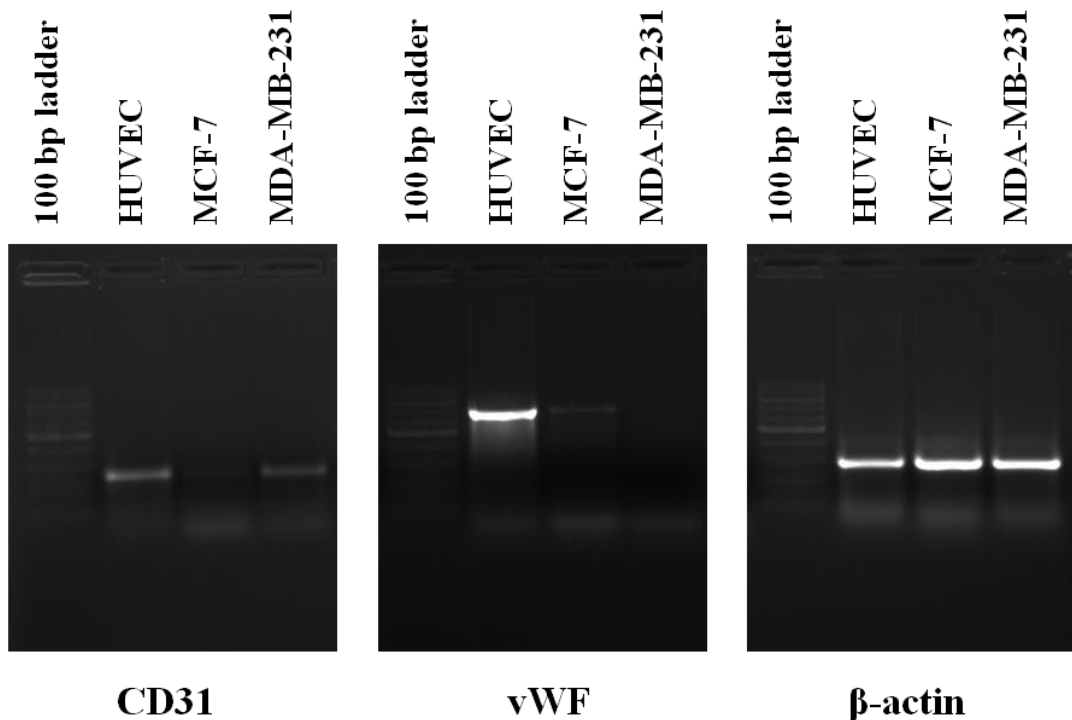
Figure 8.1.3: Transcriptional analysis for the expression of endothelial cell marker genes in isolated HUVECs at passage 1.
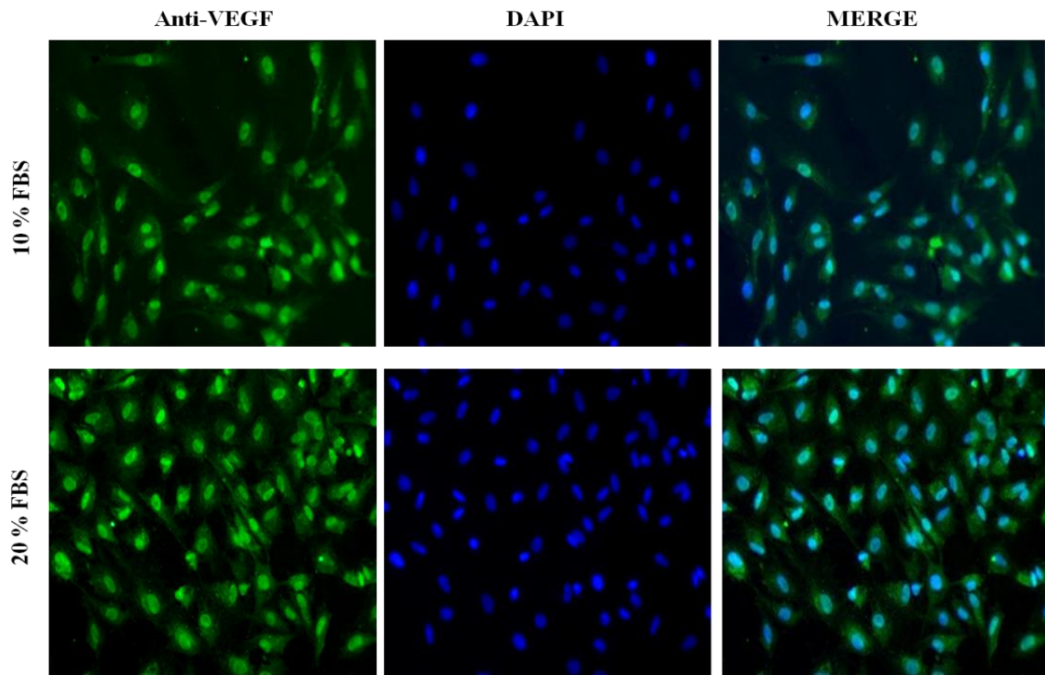
Figure 8.1.4: VEGF immunofluorescence in HUVEC when cultured in different serum conditions at Passage 1.

8.1.3.3 Karyotyping of isolated cells

The karyotypic analysis further showed the normal diploid karyotype of these isolated cells having 46 chromosomes (Fig. 8.1.5).
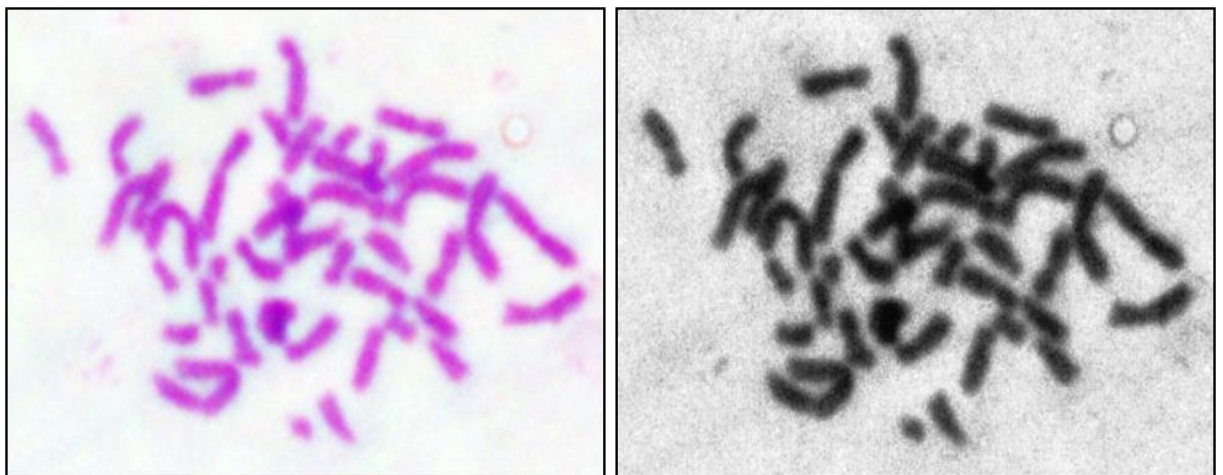
Figure 8.1.5: Representative analysis of metaphase chromosomes from isolated HUVEC at 40X objective.

8.1.4 Discussion

Endothelial dysfunction has been linked to many human diseases, ranging from inflammation, obesity and diabetes to cancer cell metastasis. Therefore, reliable endothelial cell lines have been sought for many years. Endothelial cell culture provides a powerful tool for studying the properties of endothelial cells and contributes significantly in understanding the role of these cells in vasoregulation, haemostasis, leucocytes adhesion, extravasation and angiogenesis. In addition to providing a uniform model to study endothelial cell function, they also have the advantage of providing a starting point for the generation of subsequent sublines selected by function or altered by transformation. Umbilical veins are probably the most widely used source for human endothelial cells, since they are more easily available than many other vessels, they are free from any pathological process and they are physiologically more relevant than many established cell lines.

HUVECs provide a classic model system to study many aspects of endothelial function and disease, such as normal, abnormal and tumor-associated angiogenesis, oxidative stress, hypoxia and inflammation related pathways in endothelia under normal and pathological conditions, cardiovascular-related complications associated with various diseases, mode of action and cardiovascular protection effects of various compounds, etc. The present chapter of this thesis deals with isolation and characterization of HUVECs from umbilical cord sample. The isolated cells were confirmed to be HUVEC since they possessed specific endothelial cell characteristics. Firstly, the isolated cells when grown in endothelial culture medium formed typical cobblestone pattern consistent with their endothelial lineage. Secondly, the cells were found to show strong expression for CD31, a ubiquitous endothelial cell marker important in cell-cell adhesion, and vWF, a glycoprotein that mediates platelet adhesion to subendothelium at sites of vascular injury and binds and stabilizes factor VIII in the circulation.

Cell lines of human origin are particularly valuable because there is limited access to human tissue. Thus in this chapter a successful isolation of the HUVECs was achieved for use in subsequent studies. During early passages, these cells possess the morphological characteristics of vascular endothelial cells and express a number of surface markers consistent with their endothelial cell origin. These cells may be useful in studying the pathophysiology and cellular mechanisms involved in neovascularisation and angiogenesis.

Chapter 8.2 Anti-angiogenic effect of PTER-ITC

8.2.1 Introduction

Angiogenesis, the formation of new blood vessels from pre-existing vasculature, is a tightly regulated process which involves endothelial cell proliferation, migration and organization into capillaries [Lamalice et al., 2007]. While physiologic angiogenesis is essential for embryonic vascular development, wound healing and organ regeneration, pathologic angiogenesis plays an important role in pathogenesis of many diseases, such as solid tumors, atherosclerosis, diabetic retinopathy and rheumatoid arthritis [Quesada et al., 2006; Dong et al., 2007; Lin et al., 2012]. Tumor angiogenesis also plays a vital role in cancer cell survival, growth, and development of distant metastases since the newly generated blood vessels supplies adequate oxygen and nutrition to the growing tumor mass, a prerequisite for initiation of metastatic spread [Hoff and Machado et al., 2012; Nishida et al., 2006]. Thus targeting angiogenesis is an exciting and attractive area in the treatment of cancer.

The mechanism of angiogenesis involves a coordinated signaling pathway between multiple extracellular factors and their respective cell surface receptors, as well as intracellular effectors [Weis and Cheresh, 2011]. On the extracellular level, vascular endothelial growth factor (VEGF) is the most important growth factor during angiogenesis [Moens et al., 2014]. In addition, the vascular endothelium appears to be a target organ for estradiol (E2), since it possesses a highly expressed E2 receptor system [Venkov et al., 1996; Arnal et al., 2010]. Previous studies have demonstrated that estrogen receptor (ER) expressed in endothelial cells mediates angiogenesis through both classical genomic, and rapid non-genomic, mechanisms [Kim-Schulze et al., 1996; Losordo and Isner, 2001; Kim et al., 2008]. The mechanisms involved in the proangiogenic effects of estrogen are probably multifactorial including up regulation of expression of both VEGF and its receptor mediated augmentation of NO synthesis, induction of expression of vascular adhesion molecules and integrins and inhibiting endothelial cell apoptosis. At physiological concentrations ligands of ER such as estrogen has been shown to possess angiogenic properties by inducing stimulation of cell attachment, migration and proliferation of endothelial cells [Morales et al., 1995; Oviedo et al., 2010].

Thrombospondins-1 (TSP-1), the first naturally occurring angiogenic inhibitor to be discovered, is a multifunctional extracellular matrix protein and is synthesized and secreted by fibroblasts, endothelial cells, tumor cells, and others [Armstrong and Bornstein, 2003; Ren et al., 2005; Zhang and Lawler , 2007]. It has been shown to play a critical role in inhibiting angiogenesis [Bornstein, 2009], resulting in the inhibition of tumor growth and experimental

metastasis [Armstrong and Bornstein, 2003; Volpert, 2000; Nor et al., 2000]. In endothelial cells, TSP-1 inhibits migration *in vitro* and induces apoptosis both *in vivo* and *in vitro* [Nor et al., 2000; Garside et al 2010; Rega et al., 2009]. TSP-1 has been found to inhibit angiogenesis in association with increased expression of Bax, decreased expression of Bcl-2 and the processing of caspase-3 into smaller proapoptotic forms in endothelial cells [Armstrong and Bornstein, 2003; Zhang and Lawler , 2007]. Since TSP-1 plays a critical role in inhibition of angiogenesis therefore agent that can up regulate TSP-1 can play beneficial role in anti-angiogenic therapy for cancer.

Resveratrol (trans-3,4',5-trihydroxystilbene; RESV), a naturally polyphenolic phytoalexin found in grapes, cranberries, peanuts and other dietary constituents, has a wide spectrum of anticancer activities both *in vitro* and *in vivo* [Bishayee, 2009; Shukla and Singh, 2011]. In recent years, RESV has been found to possess angiogenesis regulating properties [Chen and Tseng, 2007; Wang et al., 2010; Trapp et al., 2010]. Unfortunately, RESV can induce either pro- or anti-angiogenic effects depending on the situation, applied dosage and cell type [Chen and Tseng, 2007; Wang et al., 2010]. In addition, RESV has a low oral adsorption and metabolic stability because it has three hydroxyl groups (Fig. 1A) [Walle et al., 2004]. Structural modifications of the RESV are needed to increase its bioavailability while preserving its beneficial activities. Pterostilbene (3,5-dimethoxy-4'-hydroxystilbene; PTER), a naturally-occurring dimethylated analog of RESV is significantly more bioavailable than RESV after being ingested [Lin et al., 2009] and shows pleiotropic health benefits, including anti-oxidant, anti-inflammatory, anti-aging, cardioprotective, and neuroprotective activities [Brisdelli et al., 2009]. However, previous studies have shown that PTER (10–40 µM) had no obvious effect on HUVEC proliferation and migration, as well as newly formed micro vessels in chick chorioallantoic membrane (CAMs) indicating that PTER does not possess anti-proliferative and anti-angiogenic activities as compared with its analog, RESV [Zhang et al., 2013].

Due to the widespread use and importance of stilbenes, which are small molecules, new and active stilbenes are still being looked for. In our recent studies, we synthesized a PTER derivative, PTER-isothiocyanate (PTER-ITC) (Fig. 1A), with improved potency and specificity compared with the PTER and studied its role in breast [Nikhil et al., 2014a; Nikhil et al., 2014c] and prostate cancer [Nikhil et al., 2014b] prevention. The present study thus aimed to evaluate the effect of PTER-ITC on angiogenesis induced by female sex steroids, particularly 17β-E2, on Human umbilical vein endothelial cells (HUVECs). As TSP-1 mediates anti-angiogenic activity in endothelial cells by inhibiting its migration and inducing apoptosis, we hypothesized that PTER-ITC could modulate the activity of TSP-1 in HUVECs cells and

inhibits 17β-E2 induced angiogenesis. Our results show that the inhibitory effect of PTER-ITC on 17β-E2 induced angiogenesis is associated, at least in part, with inhibition of cell migration and induction of endothelial cell apoptosis and through targeting TSP-1. Our result further showed that PTER-ITC prevented 17β-E2 induced TSP-1 downregulation by targeting MAPK pathway.

8.2.2 Brief Methodology

8.2.2.1 Cell culture

HUVECs were isolated from human umbilical cord veins by collagenase treatment as described in Chapter-3 (3.3.2). HUVEC below passages 3 was used in our experiments. The cells were washed properly before changing the media to steroid-free complete media prior to each treatment with the compounds, unless otherwise stated.

8.2.2.2 Flow cytometry

Induction of apoptosis in HUVECs caused by RESV and PTER-ITC was quantitatively determined by flow cytometry using Annexin V-conjugated Alexa fluor 488 Vybrant apoptosis kit according the procedure described in Chapter 3 (3.6.1).

8.2.2.3 Acridine orange/Ethidium bromide screening assays

The HUVECs were incubated with the test compound for 24 h and thereafter analyzed for chromatin condensation by AO/EB staining and observed under fluorescent microscope. Detailed protocol of the assay is mentioned previously in chapter 3 (3.6.2).

8.2.2.4 Endothelial cell migration assay: Wound healing assay

We used a wound healing assay to determine the chemotactic motility of HUVECs. The HUVECs were cultured in 6-well plates until they reached 90% confluence. Thereafter, the cells were rinsed with PBS and then serum starved for 6 h. The media was then removed and equal size 'wound' was created using pipette tip and then rinsed with PBS to remove detached cells. The medium with the indicated concentrations of test compound along with 17β-E2 (10 nM) was then added for 24 h incubation in presence of mitomycin-c (2 μg/mL) to control alteration in cell proliferation. The microscopic observations of the cells were recorded at different time interval after treatment. The images were captured using fluorescent microscope (Zeiss, Axiovert 25, Germany) under 100X magnification and analyzed using T-Scratch software v7.8.

8.2.2.5 Endothelial cell invasion assay

Cell invasion assay was performed using Transwell chambers (Corning, MA, USA) with 6.5-mm diameter polycarbonate filters (8 µm pore size). HUVECs (2×10^4 cells/well) suspended in 100 µL serum free RPMI1640 medium were seeded to each insert (upper chamber), and the bottom chamber contained 600 µL of complete RPMI1640 medium supplemented with 10 nM 17β-E2. RESV and PTER-ITC at different concentrations (5–20 µM) was added into the medium of lower and upper chambers. The plate was then placed at 37°C in 5% CO_2/95% air for 12 h. Thereafter the non-migrating cells were removed from the upper surface of the membrane by gentle scrubbing using cotton tipped swabs. Migrated cells on the lower surface of membrane were then fixed with cold 4% paraformaldehyde, permeabilized with 100% methanol and stained with giemsa stain for 15 min and finally washed with PBS. Afterward, the filter was mounted onto glass slides and the invasive cells on the lower side of the filter were counted under 100X magnification from three random fields. Migration was normalized to percent migration, with migration in the presence of 17β-E2 representing the scale of 100%.

8.2.3. Results

8.2.3.1 ER expression in HUVEC

17β-E2 exerts its genomic effects through two distinct classical ERs, ER-α and ER-β. To determine the status of ER in HUVECs, an immunoblot analysis was performed. As shown in Fig. 1B both types of ER are expressed on HUVECs. The antibody against the COOH-terminus of the ER-α detected two major bands at approximately 66 and 50 kDa, while the antibody against ER-β detected a single band (56 kDa) as previously described in HUVECs by Caliceti and colleagues [9]. Unlike MCF-7 breast cancer cells, which express negligible levels of ER-β, the HUVECs utilized in our study express comparable amount of ER-α and β.

8.2.3.2 Effect of PTER-ITC on 17β-E2 induced HUVEC cell proliferation

Endothelial cell proliferation is one of the complex multistep processes involved in angiogenesis. To assess the effect of RESV and PTER-ITC on 17β-E2 induced HUVEC proliferation we performed *in vitro* growth studies. The HUVECs were treated with various concentrations of RESV and PTER-ITC for 24 h in presence and absence of 17β-E2 and the cell viability was measured by MTT assay. As shown in Fig. 1C, HUVEC proliferation was not significantly decreased by any of the concentration of RESV (1-80 µM) either in presence or absence of 17β-E2 (10 nM) ($p<0.05$). In contrast, PTER-ITC reduced 17β-E2 induced HUVEC

cell proliferation in a dose dependent manner which however reached statistical significance at 20 μM concentration (Fig. 1C, right panel) (*p*<0.05).
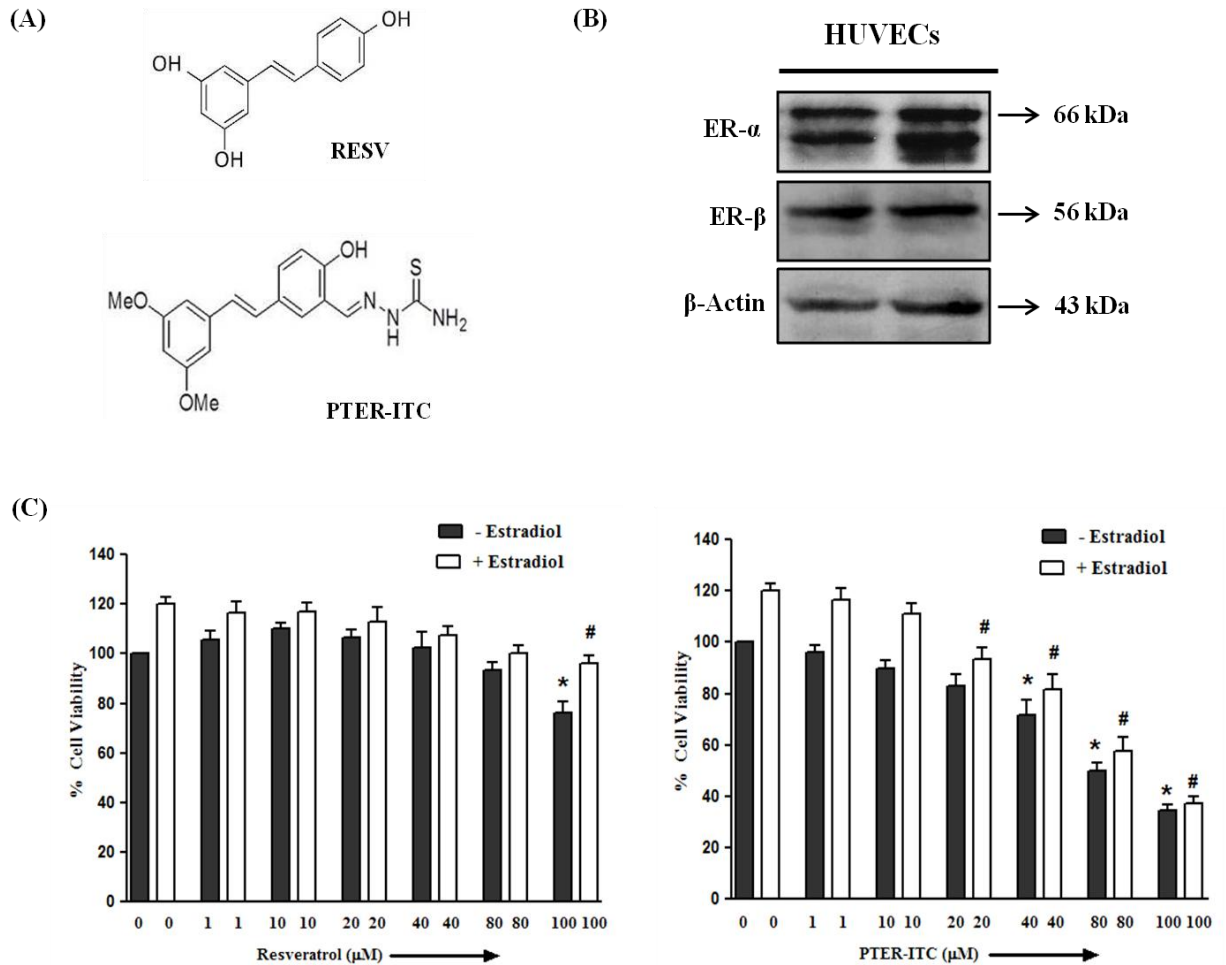
Figure 8.2.1. PTER-ITC inhibits 17β-E2 induced HUVEC cell proliferation. (A) Chemical structure of RESV and PTER-ITC. (B) Representative immunoblots of HUVEC lysates showing the expression of both ER subtypes and their corresponding actin loading control bands. (C) Effect of RESV and PTER-ITC on cell viability in HUVEC cells. Cells were treated with indicated concentrations of PTER and PTER-ITC in the presence or absence of 17β-E2 (10 nM) for 24 h. Cell viability was evaluated using the MTT assay, and the results are expressed as percentage of surviving cells over the control group. Data are the mean ± SEM of three independent experiments. The symbols, * and #, represent statistically significant difference with respect to vehicle and 17β-E2 treated control groups respectively at *p*<0.05.

8.2.3.3 PTER-ITC inhibits 17β-E2 induced migration and invasion of HUVECs

Cell migration is a key step in angiogenesis, therefore we next investigated the effect of both RESV and PTER-ITC on 17β-E2 induced migratory ability of endothelial cells using a monolayer-culture wound-healing assay. A 'wound' was created with a pipette tip and the migration of endothelial cells to fill up the 'wound' was recorded by microscopic observations. As shown in Fig. 2A, 24 h after the 'wound' was created the vehicle-treated and 17β-E2 treated cells had completely filled in the cleared area. On the other hand PTER-ITC was found to be more potent and efficacious (inhibiting migration at 5 μM by 50%) than RESV (which significantly reduced migration only at the highest concentration by 35%). Representative migration images are shown in Fig. 2B.

Invasion is one of the key steps in the process of metastasis. To determine whether PTER-ITC was capable of influencing the invasion ability of HUVECs transwell assays was performed. As shown in Fig. 2C, large number of cells migrated to the lower side of membrane in the transwell chamber after stimulation with 17β-E2. However, 17β-E2 induced HUVEC migration was significantly reduced by PTER-ITC at low dose of 5 μM (25%) and 10 μM (49%). On the other hand, RESV in the concentration range of 5–10 μM failed to significantly block HUVEC migration.
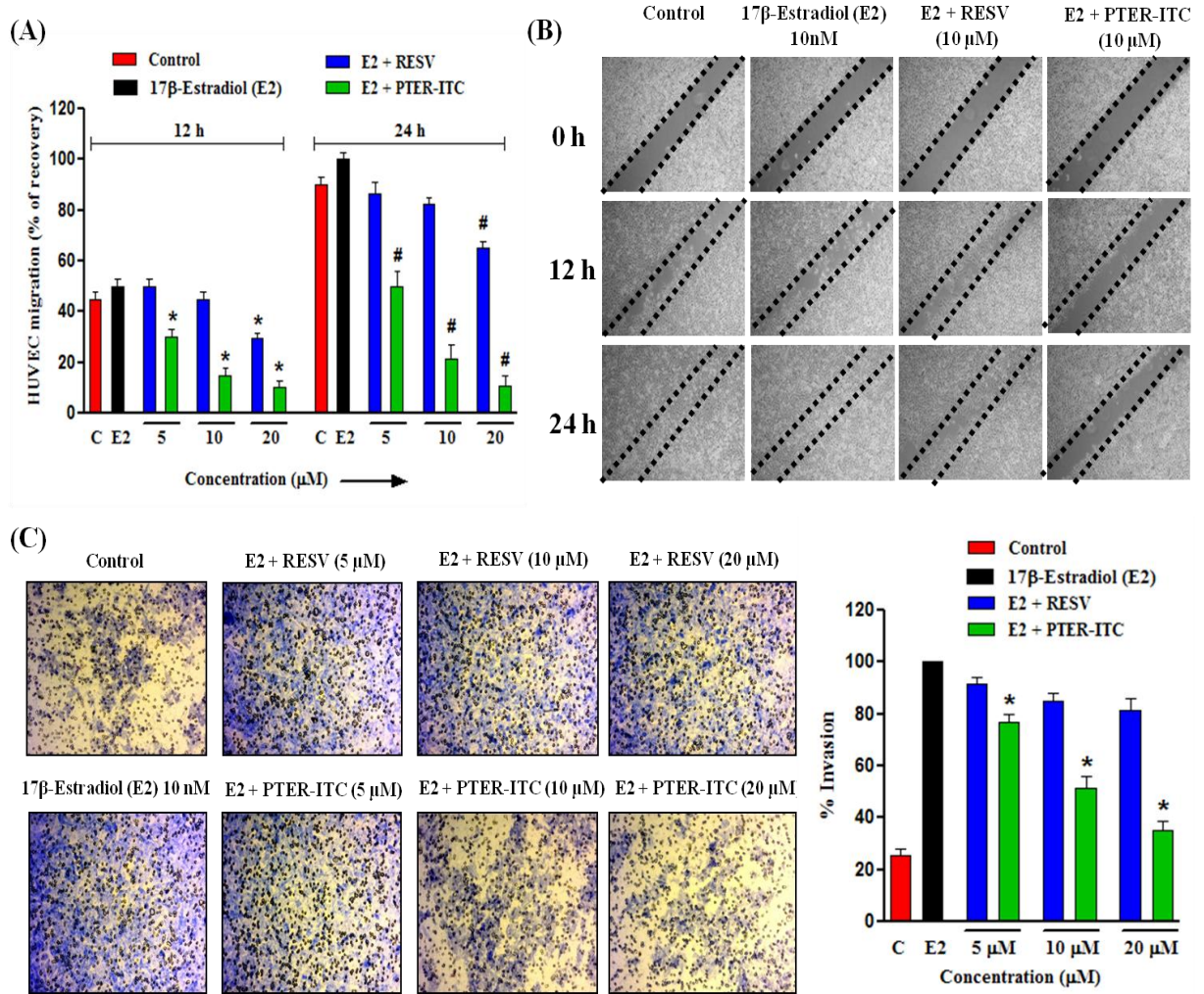
Figure 8.2.2. PTER-ITC inhibits 17β-E2 induced migration and invasion of HUVEC. (A) Comparative effect of RESV and PTER-ITC on the migratory potential of 17β-E2 treated HUVECs as analyzed by wound healing assay. Results are the mean ± SEM of three independent experiments. The symbols, * and #, represent statistically significant difference with respect to only 17β-E2 treated group after 12 and 24 h respectively at $p<0.05$. (B) Representative images of wounds treated with 17β-E2, RESV or PTER-ITC after 24 h of treatment. (C) Comparative effect of RESV and PTER-ITC on 17β-E2 induced invasion of HUVEC by transwell invasion assay after 12 h of treatment. Representative fields were photographed at 100X magnification. The histogram in the right panels of figure represents the quantitative effect of RESV and PTER-ITC on 17β-E2 induced HUVEC invasion. Migration was normalized to percent migration, with migration in the presence of 17β-E2 representing the scale of 100%. Results are the mean ± SEM of three independent experiments. * represent statistically significant difference with respect to only 17β-E2 treated group ($p<0.05$).

8.2.3.4 PTER-ITC potentiates apoptosis in HUVECs

To elucidate the possible mechanism of PTER-ITC-induced anti-angiogenesis, we next investigated the effect of PTER-ITC on HUVEC apoptosis by using Annexin-V/PI double staining assay and flow cytometry analysis. For this HUVEC cells were exposed to different concentrations of RESV and PTER-ITC (10–40 µM) in presence of 17β-E2 for 24 h. Thereafter the cells were stained with Alexa Fluor 488-conjugated Annexin-V and PI, which can assess the early and late apoptotic cell populations. As shown in Fig. 3A, PTER-ITC produced a dose-dependent increase in the apoptotic cell population. Treatment of HUVECs with increasing doses of PTER-ITC resulted in an increase in apoptotic cells from about 25.5% to 43% at 20 and 40 µM concentrations, as compared to vehicle treated groups respectively. RESV on the other hand did not cause any significant increase in apoptotic cell death at any of the dose tested.

To further confirm the above results AO/EtBr staining was performed, AO permeates all cells and makes the nucleus appear green while EB is taken up by the cells only when the cytoplasmic membrane integrity is lost as in late apoptosis or in necrosis staining the nucleus red. As shown in the Fig. 3B, the vehicle and 17β-E2 treated group had maximum number of viable cells showing acridine orange staining with normal cell morphology. On the contrary, the PTER-ITC treated cells showed dose dependent increase in number of EB stained cells while RESV at the highest dose showed very few apoptotic cells.

8.2.3.5 Mechanisms underlying PTER-ITC induced apoptosis in HUVEC

We further investigated the mechanism underlying the apoptotic effect of PTER-ITC in HUVECs by measuring the enzymatic activity of caspase-3, -8 and -9 following PTER-ITC treatment. Our result showed a gradual dose dependent increase in caspase-9 and caspase-3 activities following PTER-ITC treatment, while there was no significant change in caspase-8 activity in HUVECs (Fig. 4A) ($p<0.05$). Western blot analysis showed that the expression level of cleaved caspase-3 gradually increased as the concentration of PTER-ITC increased from 10 µM to 40 µM (Fig. 4B) ($p<0.05$). Our data thus suggests that PTERITC induced activation of the intrinsic caspase pathway in HUVECs.

We next examined the expression of Bcl-2 family proteins in PTER-ITC treated HUVECs cells in a dose-dependent manner. Western blotting analysis revealed that PTER-ITC treatment suppresses the expression of anti-apoptotic proteins such as Bcl-2 and survivin while increasing the expression levels of pro-apoptotic proteins such as Bax (Fig. 4B) ($p<0.05$). Some studies have also demonstrated functional links between p53 expression and endothelial cell

apoptosis [Zhang et al., 2012]. In our study, Western blot analysis showed that the level of p53 was up regulated in HUVECs incubated with PTER-ITC for 24 h (Fig. 4B). These data clearly suggest that PTER-ITC inhibited cell viability and potentiated apoptosis in HUVECs by modulating the levels of pro-apoptotic and anti-apoptotic molecules.
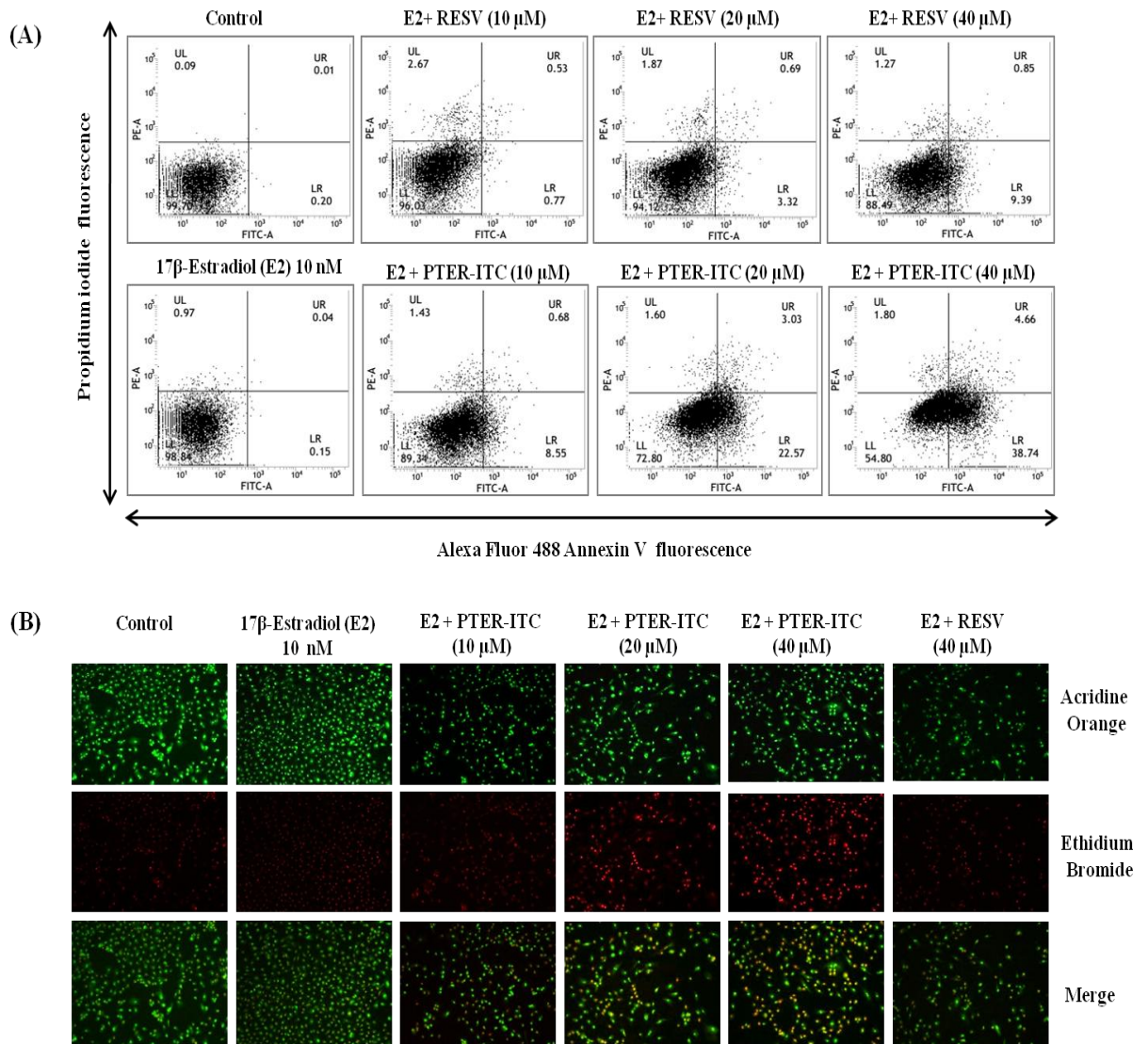
Figure 8.2.3. PTER-ITC induced HUVEC apoptosis. (A) The effect of RESV and PTER-ITC on the apoptosis of HUVEC cells as demonstrated by a representative FACS analysis using Annexin V as marker. (B) Evaluation of apoptosis by using Acridine orange/Ethidium bromide staining on HUVECs treated with RESV, PTER-ITC for 24 h. The green staining indicates that the cell membrane integrity does not allow the entry of ethidium bromide in the cytoplasm. Apoptotic cells are stained red due to the entrance of the Ethidium bromide. The nuclear staining was visualized at 100X magnification of fluorescent microscope. The experiment was performed in triplicate and a representative data is presented.
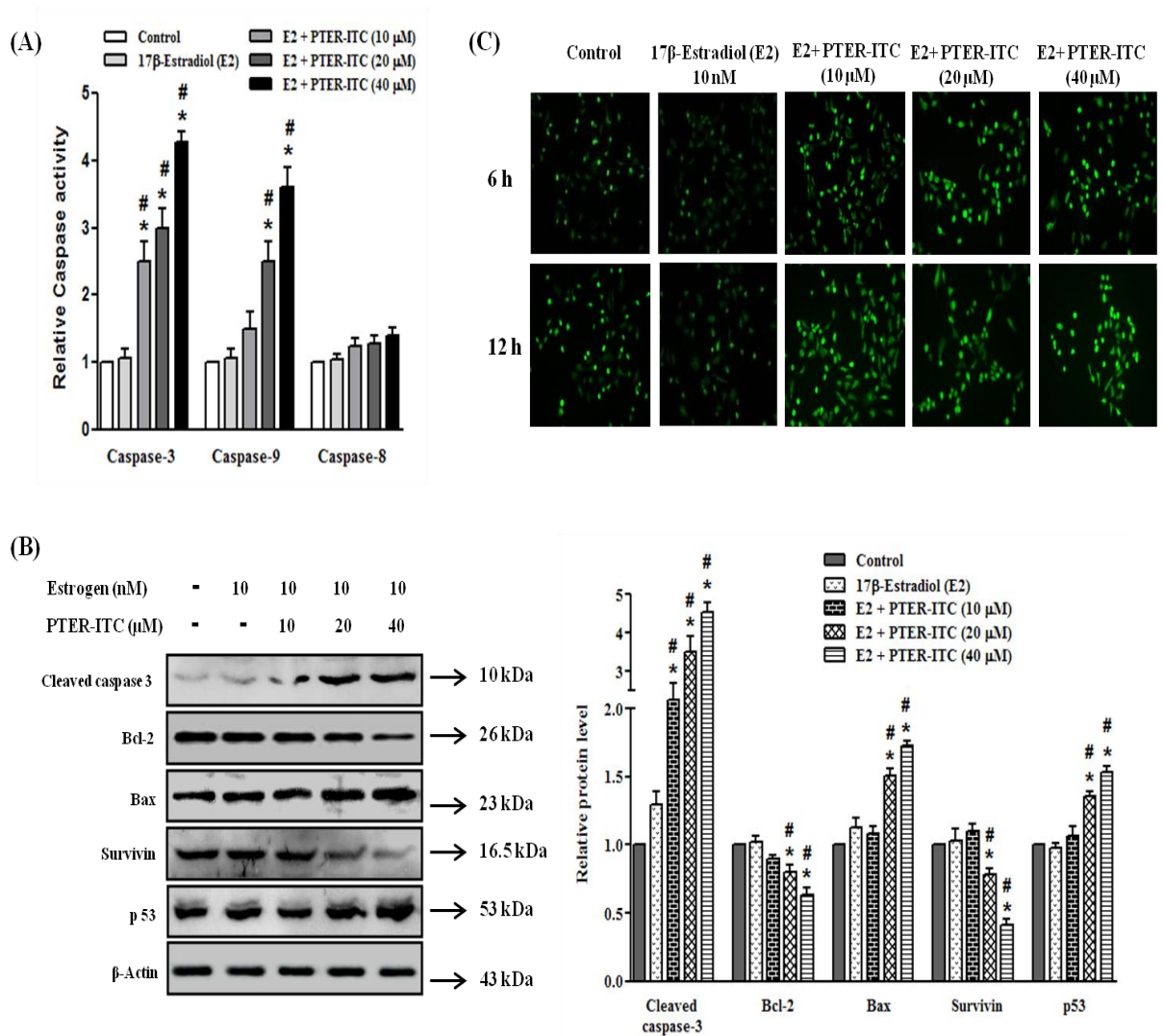
Figure 8.2.4. Effects of the PTER-ITC in regulating apoptosis of HUVECs. (A) The effects of varying doses of PTER-ITC on caspase-3, -9 and -8 activities in HUVECs. Results are the mean ± SEM of three independent experiments. * and #, represent statistically significant difference with respect to control and 17β-E2 treated group respectively at $p<0.05$. (B) Expression patterns of various apoptotic marker genes in response to varying doses of PTER-ITC in 17β-E2 treated HUVECs as determined by immunoblot analysis. Histogram in the right panel shows relative band intensities normalized to the corresponding β-actin level. Data are expressed as x-fold change relative to vehicle treated control; bars show mean ± SEM of three independent experiments. The symbols, * and #, represent statistically significant difference with respect to control and 17β-E2 treated group respectively at $p<0.05$. (C) Representative figure showing ROS accumulation within HUVEC cells in response to various doses of PTER-ITC as estimated by H2-DCF-DA staining (100X magnifications).

8.2.3.6 Reactive oxygen species (ROS) was involved in PTER-ITC induced apoptosis of HUVECs

To investigate whether intracellular ROS is involved in the apoptotic pathway caused by PTER-ITC, we performed a time-course study to determine levels of intracellular ROS levels, which also has been implicated in induction of apoptosis. As shown in Fig. 4C, preincubation of HUVEC cells for 6 and 12 h with 17β-E2 alone (10 nM), resulted in decrease in fluorescence intensity. However when the cells were preincubated with both E2 and various doses of PTER-ITC, inhibitory effect of E2 was prevented leading to increased ROS production (Fig. 4C) ($p<0.05$).

8.2.3.7 Effect of PTER-ITC on 17β-E2 induced VEGF and VEGF receptor expression

Estrogen has been shown to enhance *in vitro* angiogenesis associated events in HUVECs. Thus to examine the mechanism of action of PTER-ITC as an inhibitor of 17β-E2 enhanced angiogenesis, we determined whether PTER-ITC inhibited VEGF expression levels in HUVECs by RT-PCR, immunofluorescence and immunoblot analysis. For this, HUVECs cells were treated with varying concentrations of PTER-ITC in presence of 10 nM 17β-E2. As shown in Fig. 5A, both 17β-E2 and PTER-ITC molecule had no significant effects on the expression levels of *VEGF* gene. Further, when we performed the immunoblot analysis of VEGF we discovered that the levels of VEGF were significantly up regulated by 17β-E2 treatments. However, we found a concomitant inhibition of the translation of this protein in response to increasing doses of PTER-ITC (Fig. 5B) ($p<0.05$). In the next stage of experiment, immunofluorescence staining of HUVECs was performed in order to visualize the intensity of endogenous VEGF expression in this cell. As shown in Fig. 6A, 17β-E2 caused significant up regulation in the fluorescent intensity while treatment of cells with varying doses of PTER-ITC resulted in decrease in fluorescent intensity in the cells which was in accordance to our earlier data.

VEGF is known to exert its angiogenic effects via two tyrosine kinase receptors, VEGFR-1 (flt-1) and VEGFR-2 (flk-1/KDR). We therefore set up an experiment to investigate the effects of PTER-ITC on 17β-E2 induced VEGF signaling in HUVECs. For this we treated HUVECs with 17β-E2 or a combination of 17β-E2 and PTER-ITC for 24 h and measured cellular expression of VEGFR-1 and VEGFR-2 using semi-quantitative RT-PCR. As shown in Fig. 5A there was moderate levels of *VEGFR-1* and *VEGFR-2* gene expression in HUVECs. However, we could not find any significant differences in the expression of VEGFR-2 or VEGFR-1 mRNAs between only 17β-E2 and the 17β-E2+PTER-ITC co-treated groups. This

result thus suggests that the anti-angiogenic activity of PTER-ITC is not due to 17β-E2 induced VEGF/VEGFR2 signaling in HUVECs.
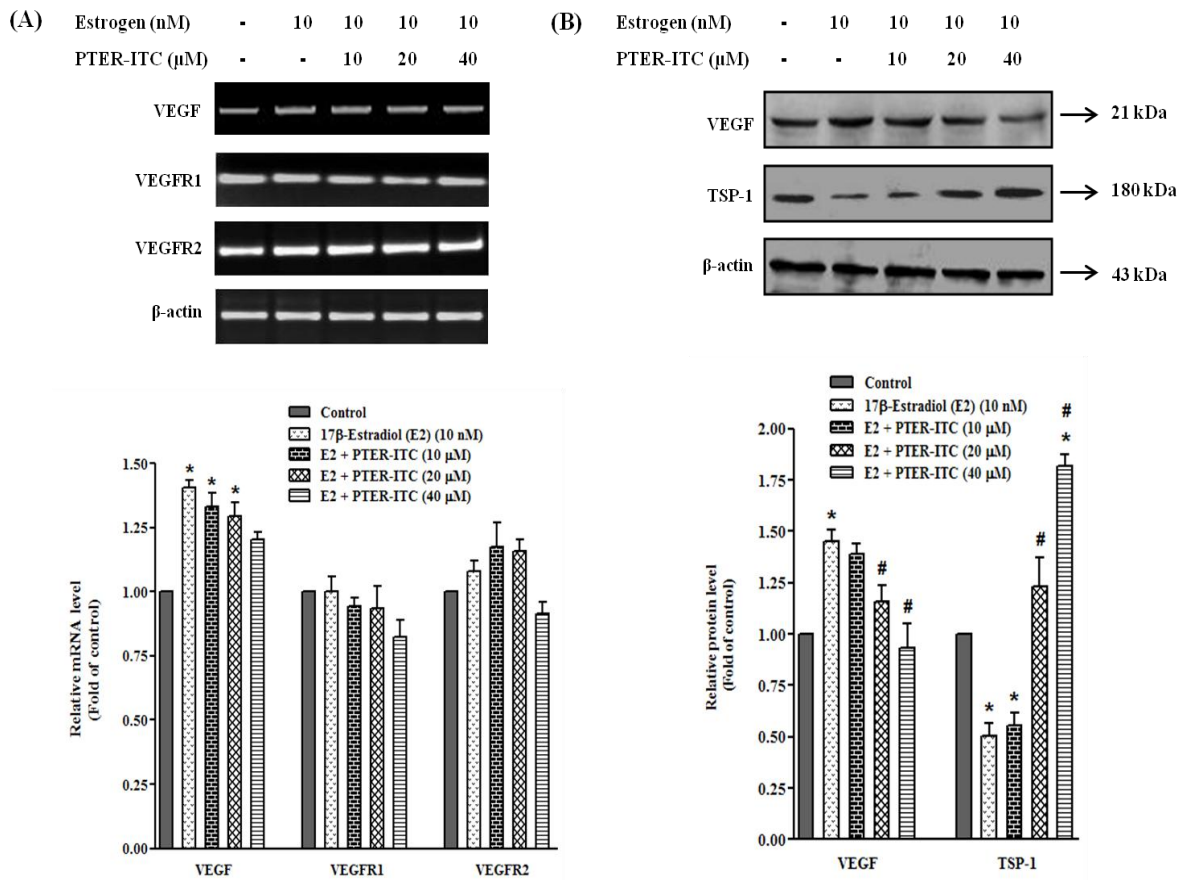
Figure 8.2.5. Effect of PTER-ITC on 17β-E2 induced VEGF signaling in HUVECs. (A) Expression patterns of VEGF and its receptor in response to varying doses of PTER-ITC treatment as determined by RT-PCR in 17β-E2 treated HUVEC cells. (B) Immunoblot analysis to show the expression pattern of VEGF and TSP-1 protein in response to different doses of PTER-ITC in 17β-E2 treated HUVECs. Histogram (lower panel in each figure) shows relative band intensities normalized to the corresponding β-actin level. Data are expressed as x-fold change relative to control; bars show mean ± SEM of three independent experiments. The symbols, * and #, represent statistically significant difference with respect to control and 17β-E2 treated group respectively at $p<0.05$.

8.2.3.8 PTER-ITC upregulates TSP-1 expression levels in HUVEC

Since VEGF signaling did not contribute to 17β-E2 induced anti-angiogenic activity of PTER-ITC we next focussed our work on TSP-1, a most potent angiogenic regulator that plays a critical role in inhibition of angiogenesis. TSP-1 has been shown to inhibit cellular proliferation, motility and morphogenesis in endothelial cells while its downregulation may cause switch to an angiogenic phenotype. A previous study showed reduction in migration and

proliferation of HUVECs with increase in TSP-1 protein concentration in culture medium when stimulated with 17β-E2 [Sengupta et al., 2004]. Here we checked the effect of PTER-ITC on 17β-E2 induced TSP-1 expression levels in HUVEC. As shown in Figure 5B, protein levels of TSP-1 in cell lysates was decreased by 17β-E2 treatment after 2 h of treatment. However, this inhibition was restored back with increasing dose of PTER-ITC which was almost 1.8-fold at the highest dose tested. These results indicate that PTER-ITC increases the expression of TSP-1 in HUVECs in a dose-dependent manner and also prevents 17β-E2 induced TSP-1 downregulation.

8.2.3.9 Effect of PTER-ITC on ER expression level in HUVECs

Since 17β-E2 has been shown to down-regulate the expression of TSP-1 by interacting with ER therefore we next checked the effect of PTER-ITC on ER expression level in HUVECs. The results in Figure 6B clearly revealed that ER-α and ER-β levels in HUVEC were increased with 17β-E2 treatment. However, the increment in ER-α expression level was decreased by concomitant exposure to 17β-E2 and increasing dose of PTER-ITC. On the contrary, the expression level of ER-β increased only marginally which was statistically non-significant. These results thus indicate that PTER-ITC prevents 17β-E2 induced TSP-1 downregulation by targeting mainly ER-α.
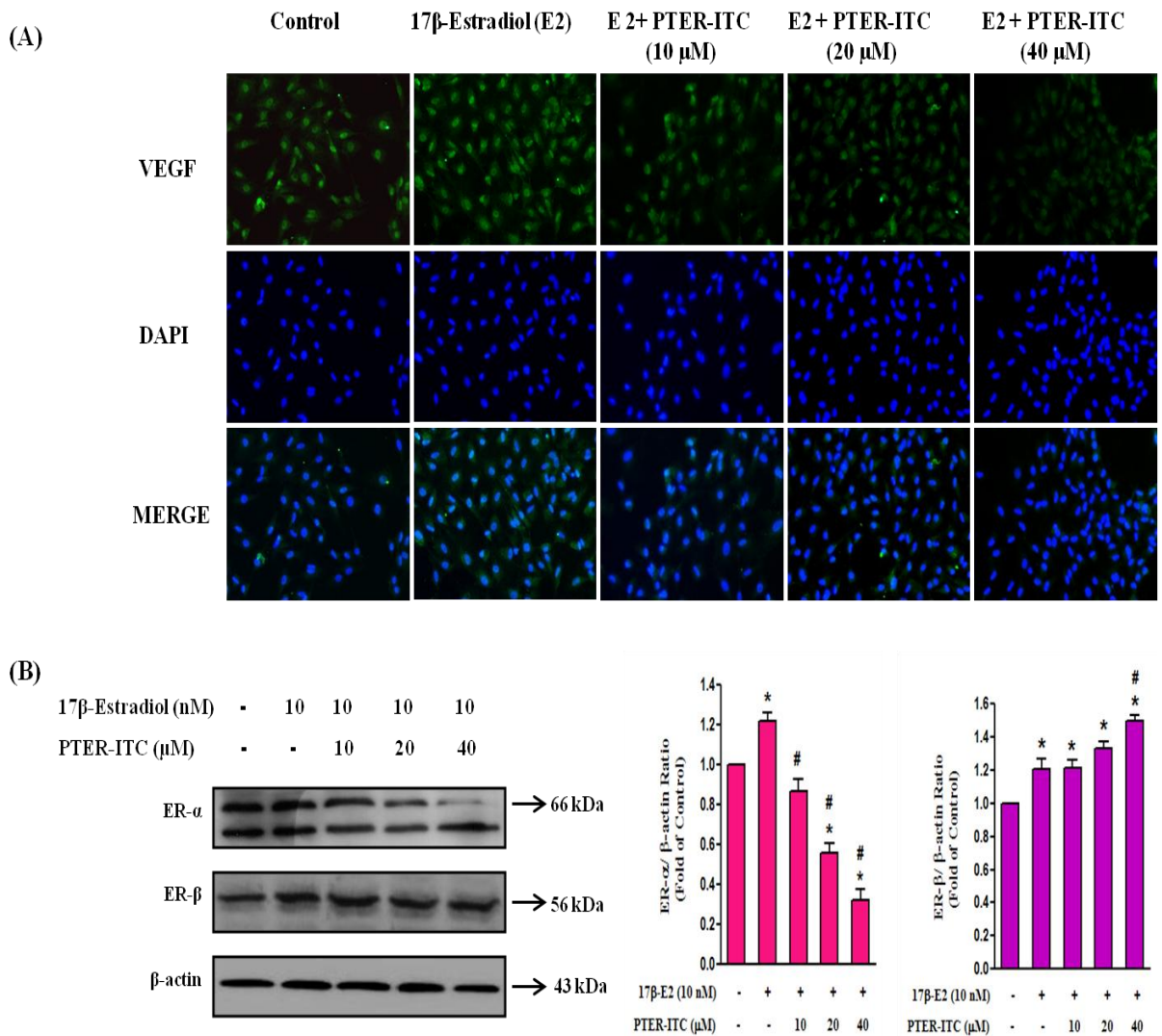
Figure 8.2.6. Effect of PTER-ITC on 17β-E2 induced VEGF and ER expression level in HUVECs. (A) Immunofluorescence analysis to detect VEGF protein in HUVECs after treatment with 17β-E2 and PTER-ITC. Figures show one representative experiment of three performed. Magnification, 200X. (B) Effect of various doses of PTER-ITC on 17β-E2 induced ER-α and ER-β expression level in HUVECs. Histogram (right panel) shows relative band intensities normalized to the corresponding β-actin level. Data are expressed as x-fold change relative to control; bars show mean ± SEM of three independent experiments. The symbols, * and #, represent statistically significant difference with respect to control and 17β-E2 treated group respectively at *p*<0.05.

8.2.3.10 Effect of PTER-ITC on 17β-E2 induced MAPK activation

The diverse actions of estrogens are mediated through a classical ER-mediated genomic pathway or via plasma membrane estrogen-receptor-mediated non-genomic pathway through involving activation of PI3K/AKT and MAPK signaling pathways in endothelial cells [Razandi and Pedram, 2000; Klinge et al., 2005]. Both membrane and nuclear ER are present in HUVECs [Sengupta et al., 2004]. To further explore the mechanism of PTER-ITC action, we determined its effect on downstream signaling pathways in the MAPK cascade which are activated by 17β-E2. The phosphorylation of three MAPKs (ERK, JNK and p38) was increased after 17β-E2 treatment (Fig. 7A) ($p<0.05$). However, co-treatment with PTER-ITC attenuated the 17β-E2 induced phosphorylation of JNK and ERK, while simultaneously increasing the expression of p38 MAPK (Fig. 7A).

8.2.3.11 Effect of PI3K/AKT and MAPKs inhibitors on 17β-E2 induced TSP-1 expression

To probe that the inhibition of TSP-1 expression is related to the downregulation of PI3K/AKT and MAPKs pathways, we examined the effect of PI3K/AKT and MAPKs inhibitors on their expressions. For this analysis Wortmannin (PI3K inhibitor), PD98059 (ERK inhibitor), SP600125 (JNK inhibitor), and SB203580 (p38 inhibitor) were employed. The cells were pretreated with specific inhibitors for 1 h prior to 2 h treatment with 17β-E2 and PTER-ITC. As shown in Figure 7B, 17β-E2-induced TSP-1 downregulation was unaffected by wortmannin and SB203580 but was significantly prevented by PD98059 and SP600125. These results suggested that activation of ERK and JNK is required for 17β-E2-induced TSP-1 downregulation and the PTER-ITC exerts its anti-angiogenic effect by inhibiting these pathways.

8.2.3.12 ERK and JNK inhibitors sensitized HUVEC cells to PTER-ITC induced apoptosis

To probe that the inhibition of HUVEC proliferation is related to the downregulation of MAPKs, we examined the effect of MAPKs inhibitors on 17β-E2 induced HUVEC proliferation. For this HUVEC cells were pre-treated with PD98059 (ERK inhibitor), 10 μM SB203580 (p38 MAPK inhibitor) or SP600125 (JNK inhibitor) for 1 h. Subsequently, the inhibitor treated cells were exposed to 20 μM PTER-ITC along with 10 nM 17β-E2, and then the caspase-3 activity and cell death was measured using Ac-LEHD-pNA as substrate (Fig. 8A) and FACS analysis (Fig. 8B). As shown in Fig. 8B, in comparison to control cells, the percentage of dead cells were significantly higher in cells exposed to 20 μM PTER-ITC which was significantly inhibited by p38 inhibitor SB203580 ($p<0.05$). On the contrary, co-treatment

of cells with JNK or ERK inhibitors and PTER-ITC resulted in higher number of apoptotic cells as compared to cells treated with PTER-ITC alone. Consistent with these results, pre-treatment with SP600125 and PD98059 increased caspase-3 enzyme activity compared to cells treated with PTER-ITC alone (Fig. 8A).These results suggests an important role of JNK and ERK on PTER-ITC induced HUVECs apoptosis.
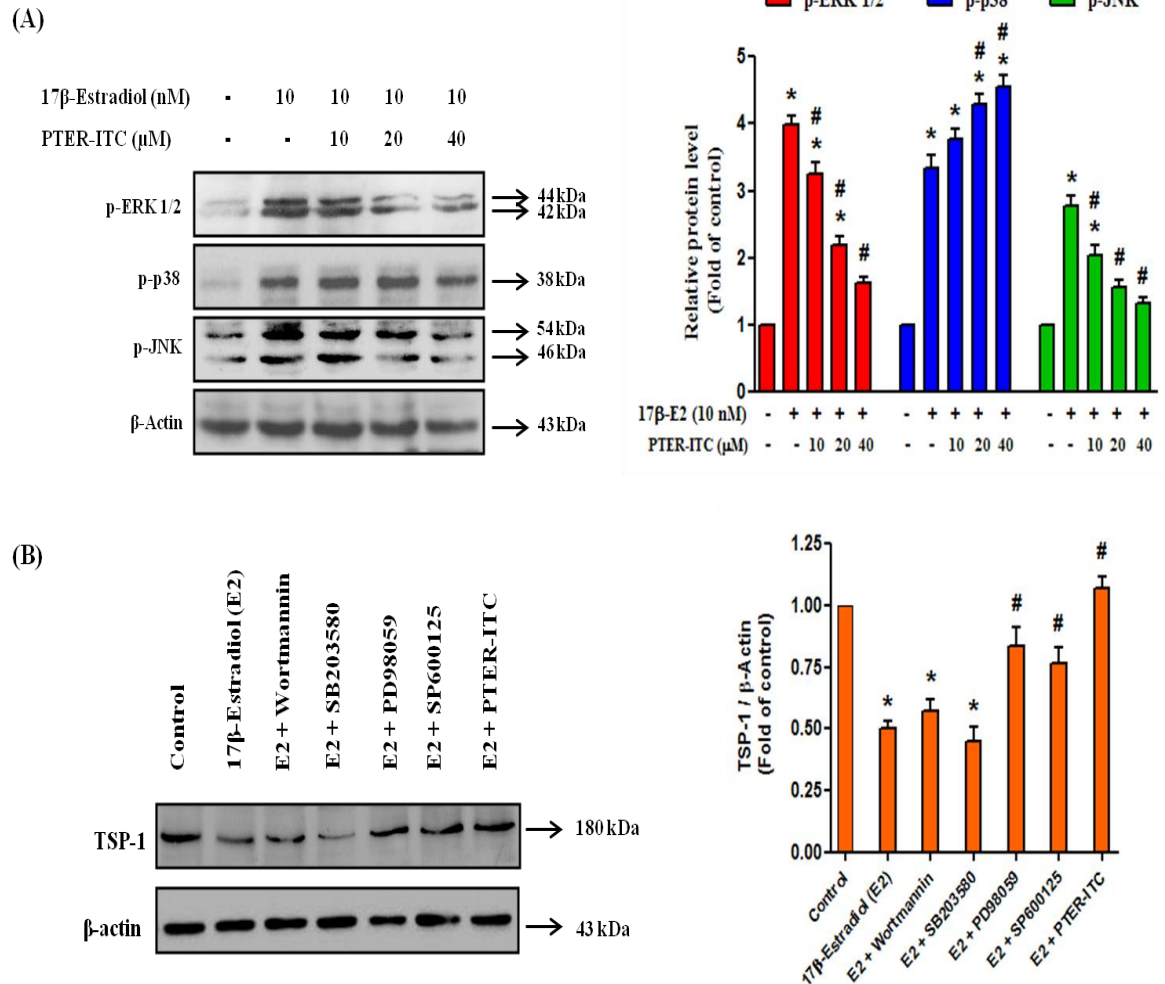
Figure 8.2.7. Effects of PTER-ITC on 17β-E2 induced phosphorylation of MAPKs and AKT signaling pathways in HUVECs. (A) Effect of PTER-ITC on 17β-E2 induced activation of MAPK signaling pathways. (B) Effect of PI3K/AKT inhibitor, MAPK inhibitors and PTER-ITC on 17β-E2-induced alteration of TSP-1 expression level in HUVECs. The cells were pretreated with inhibitors of PI3K/AKT (wortmannin), ERK (PD98059), p38 (SB203580) and JNK (SP600125) or PTER-ITC for 1 h then stimulated with 17β-E2 for next 1 h. Subsequently the whole cell lysates were prepared and the expression levels of TSP-1was determined by immunoblot analysis. Histogram (right panel in each figure) shows relative band intensities normalized to the corresponding β-actin level. Data are expressed as x-fold change relative to control; bars show mean ± SEM of three independent experiments. The symbols, * and #, represent statistically significant difference with respect to control and 17β-E2 treated group respectively at $p<0.05$.

8.2.3.13 PTER-ITC inhibits 17β-E2-stimulated angiogenesis in vivo

Considering that the effect of PTER-ITC on HUVECs *in vitro* cannot be directly translated into its *in vivo* anti-angiogenic activity, we further assessed the *in vivo* anti-angiogenic activity of PTER-ITC using chick CAM angiogenesis assays. As shown in Fig 8C in the chick CAM model, newly formed microvessels regressed in the areas near the PTER-ITC- treatment (shown by arrows) supporting its strong anti-angiogenic effect *in vivo*.
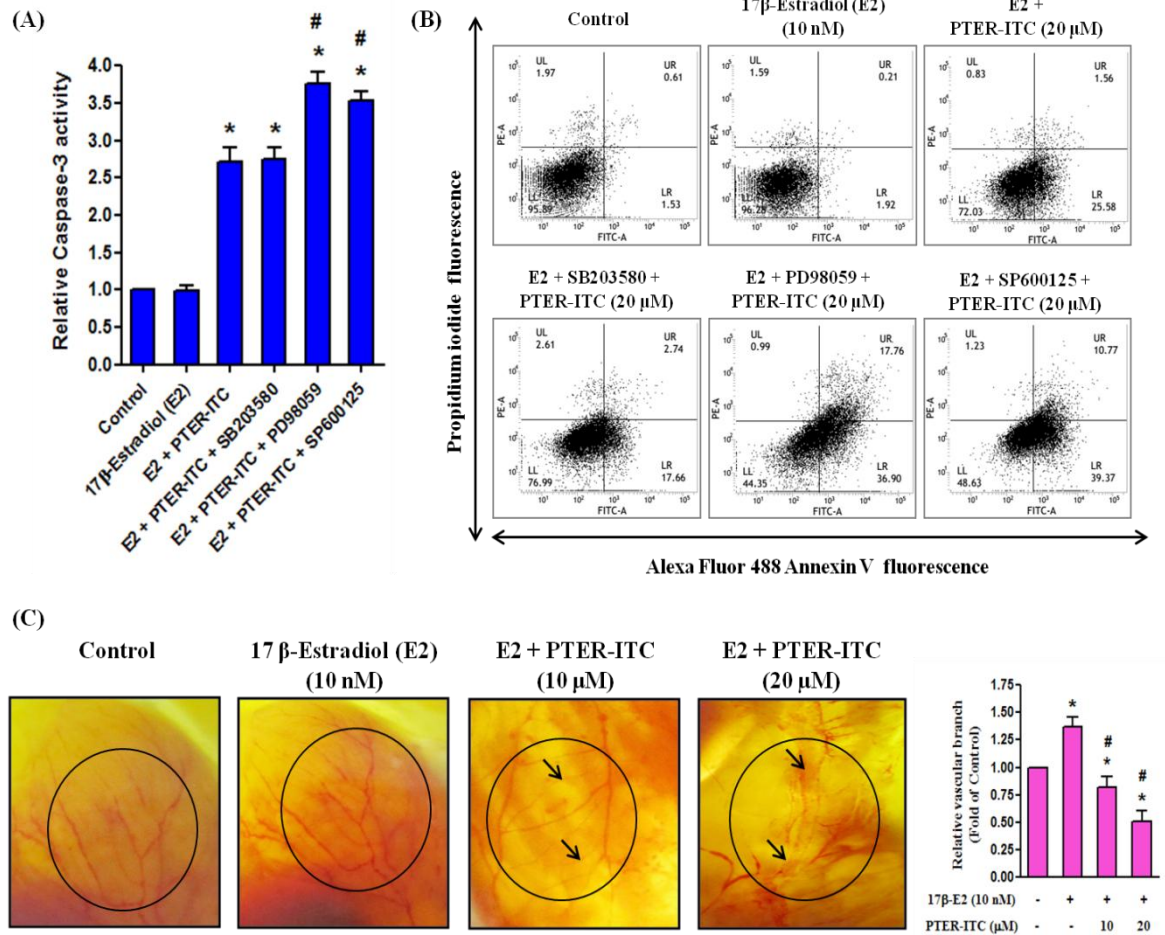
Figure 8.2.8. Effects of MAPK inhibitors in regulating PTER-ITC induced apoptosis in HUVECs and CAM assay. (A) Effects of inhibitors of ERK (PD98059), p38 (SB203580) and JNK (SP600125) on PTER-ITC induced Caspase-3 activity and (B) Apoptosis in HUVEC cells as determined by FACS. Data are mean ± SEM of three independent experiments. The symbols, * and #, represent statistically significant difference with respect to control and 17β-E2 treated group respectively at *p*<0.05. (C) In vivo CAM assay showing inhibitory effect of PTER-ITC on 17β-E2 induced angiogenesis in vivo. Figures show one representative experiment of two performed. The vascular branch in CAM was quantified by angiogenesis-measuring software. The symbols, * and #, represent statistically significant difference with respect to control and 17β-E2 treated group respectively at *p*<0.05.

8.2.4 Discussions

Sex steroid hormones are fundamental regulators of cell growth, proliferation, and migration. Many *in vitro* and *in vivo* studies demonstrate that estrogen and other growth factors promote angiogenesis in endothelial cells via the ER. Estrogen-ER binding also induces endothelial cell proliferation and migration opening the possibility of the use of ER competitors as possible anti-angiogenic agents. An increasing number of clinically relevant drugs have been developed from natural source, by structural modification of natural compounds or by the synthesis of new compounds designed following a natural compound as model [Gordaliza, 2007]. In the present study a novel RESV derivative was tested for its anti-angiogenic action in 17β-E2 stimulated HUVECs while directly comparing it to RESV. Our result showed that PTER-ITC (10–30 μM) could effectively inhibit 17β-E2 induced HUVEC proliferation, migration and invasion at comparatively lower dose than RESV. The chicken egg chorioallantoic membrane (CAM) assay further indicated that PTER-ITC treatment inhibited ex-vivo angiogenesis. In addition, the present study showed for the first time that the anti-angiogenic properties of PTER-ITC was due to the suppression of 17β-E2-stimulated ERK and JNK pathways leading to up-regulation of TSP-1 and finally apoptosis of HUVECs.

Proliferation and migration are two important events in the process of angiogenesis. Female sex hormone i.e. 17β-E2 has been shown to enhance HUVEC cell proliferation and migration via binding to ER [Straub, 2007]. In the present study, we demonstrate for the first time that PTER-ITC at low concentration can effectively suppress HUVEC proliferation as observed by MTT assay. We also showed that PTER-ITC strongly decreases 17β-E2-induced HUVEC migration and invasion *in vitro*.

Induction of endothelial cell apoptosis is an important anti-angiogenic mechanism [Brakenhielm et al., 2004; Chavakis and Dimmeler, 2002]. For example, kringle 5 of human plasminogen (K5), an angiogenic inhibitor, has been shown to induce endothelial cell apoptosis [Nguyen et al., 2007]. In addition, the estrogen metabolite 2-methoxyestradiol has been shown to be a potent anti-angiogenic agent mediated by actions on cytoskeletal structure and by increasing endothelial cell apoptosis [Yue et al., 1997; Tsukamoto et al., 1998]. Whether or not programmed cell death contributes to the inhibition of proliferation of endothelial cells with PTER-ITC treatment was investigated by FACS and immunoblot analysis. Our data suggest that PTER-ITC induced apoptosis in HUVECs in a dose-dependent manner. Cell survival is maintained by a delicate balance between anti-apoptotic and pro-apoptotic stimuli. The present study shows that PTER-ITC treatment not only up-regulated caspase-3 and Bax expressions but also decreased Bcl-2 and survivin levels in HUVECs.

p53 tumor suppressor protein is another key protein in HUVEC apoptosis and plays an important role in apoptosis signal transduction pathways in diverse cell types including HUVECs [Dai et al., 2012; Xuan et al., 2011; Lorenzo et al., 2002]. Numerous studies have provided strong support for a proposal that ROS could act as upstream signal of p53 leading to apoptosis in endothelial cells [Cheng et al., 2007; Liu and Sun, 2010]. Moreover, mitochondria are the most important intracellular source of ROS and play a key role in the regulation of cell death pathways [Gogvadze et al., 2009]. Elevated ROS levels can also decrease mitochondrial membrane potential, thus leading to the release of cytochrome C and apoptosis-inducing factors. We found increased levels of ROS in cells treated with different concentrations of PTER-ITC in HUVECs in presence of 17β-E2 after 6 and 12 h of treatment.

Angiogenesis is regulated by a balance between pro-angiogenic and anti-angiogenic factors, which are produced and secreted by various cell types. TSP-1 is a naturally occurring angiogenesis inhibitor which induces endothelial cell apoptosis by activating the caspase dependent death pathway [Jimenez et al., 2000]. 17β-E2, a natural estrogen, is capable of transiently suppressing expression and secretion of an angiogenic inhibitor, TSP-1, in human endothelial cells [Sengupta et al., 2004]. Since PTER-ITC was found to cause dose dependent increase in TSP-1 protein level as well HUVEC cell apoptosis therefore, it was intriguing to see whether PTER-ITC could modulate 17β-E2 induced TSP-1 expression level. For this, human endothelial cells were exposed to 17β-E2 in the presence or absence of PTER-ITC and TSP-1 protein levels were determined. The results showed that 17β-E2-induced suppression of TSP-1 protein expression could be prevented by PTER-ITC, suggesting that PTER-ITC could directly target ER or ER signaling in HUVECs. The next important issue was how PTER-ITC could prevent 17β-E2 induced TSP-1 expression level. Our data showed that 17β-E2-ER complex modulates the expression of TSP-1 in endothelial cells through non-genomic pathways by activating ERK1/2 and JNK signaling pathways. Using specific pharmaceutical inhibitors, we showed that modulation of ERK and JNK pathways, but not p38 and AKT pathway, is necessary and sufficient to increase TSP-1 expression and cause subsequent apoptosis in HUVECs.

In its entirety, the result from the current study suggests that PTER-ITC is a potential anti-angiogenic agent when compared to RESV. The anti-angiogenic action of PTER-ITC involves inhibition of 17β-E2 induced proliferation, migration, and invasion in HUVECs. In addition, PTER-ITC prevented 17β-E2 induced down-regulation of TSP-1, by targeting MAPK pathway causing HUVEC apoptosis. These findings suggest that PTER-ITC may be excellent leads for the development of anti-angiogenic and anti-cancer drugs.

Chapter 9. PTER-ITC as Anti-inflammatory Agent

9.1 Introduction

Inflammation is the defense mechanism of the body to harmful stimuli, such as tissue damage, trauma, and infection, mediated by activated immune cells such as macrophages and monocytes [Medzhitov, 2008]. There are two stages of inflammation: acute and chronic. Acute inflammation is a normal and helpful component of physiologic response to injury. However, chronic inflammation is persistent inflammation that becomes excessive and has been associated with a wide variety of diseases including atherosclerosis, asthma, psoriasis, rheumatoid arthritis, inflammatory bowel disease, obesity, and cancer [Lawrence, 2009]. Inflammatory responses play decisive roles at different stages of tumor development including initiation, promotion, malignant conversion, invasion, and metastasis [Grivennikov et al., 2010]. Different pro-inflammatory mediators and cytokines can promote tumor development and progression. Therefore, the inhibition of pro-inflammatory mediator production and the suppression of mechanisms responsible for the activation of inflammatory responses are regarded as clinical strategies for the treatment of chronic inflammation and related disease like cancer.

Inflammation can be mediated by inflammatory cytokines which include interleukin (IL)-1β, IL-6, tumor necrosis factor (TNF)-α, interferon (IFN)-γ, IL-12, IL-18 and related inflammatory mediator, such as nitric oxide (NO), and prostaglandin E2 (PGE2), which are produced by inducible nitric oxide synthase (iNOS) and cyclooxygenase (COX), respectively [Lin et al., 2007]. The key pro-inflammatory stimuli include mitogens, cytokines, UV irradiation, and bacterial lipopolysaccharide (LPS) which modulate their effects by inducing the activation of transcription factor NFκB [Karin and Ben-Neriah, 2000; Muller et al., 1993]. In the absence of stimuli, in most cells, NFκB is associated with inhibitor proteins, IκBs and remains sequestered in the cytosol. Exposure to stimuli leads to the activation of the upstream IκB kinase complexes (IKKs), resulting in rapid phosphorylation and proteolytic degradation of IκB to release NFκB, which then translocates to the nucleus and binds to its specific DNA sequence present in promoters of various target genes and initiates their transcription [Karin and Ben-Neriah, 2000]. NFκB activates a number of rapid response genes involved in the inflammatory response including iNOS, COX-2, IL-1β, IL-6, and TNF-α. Production of pro-inflammatory mediators and cytokines by these NFκB response genes may reflect the degree of inflammation and has been suggested to be a measure to assess the effect of chemopreventive agents on the inflammatory processes [Aggarwal et al., 2006].

219

COX is a rate-limiting enzyme for the conversion of arachiodonic acids to prostaglandins such as PGE2. Two isoforms of COX, which are namely COX-1 and COX-2, have been characterized. A third COX isoform produced as an alternate splice variant of COX-1 has recently been identified as COX-3 (or COX-1b) [Aid and Bosetti, 2011]. COX-1 is expressed constitutively in many types of cells and maintains normal physiological functions. In contrast, COX-2 is an inducible enzyme, which is up-regulated by pro-inflammatory stimuli, including mitogens, cytokines, and bacterial lipopolysaccharide (LPS) in response to infection or inflammatory diseases [Dinarello, 2010]. Evidences from numerous studies indicated that COX-2 is primarily associated with inflammatory disease and is induced in various premalignant and malignant tissues, suggesting that COX-2 plays an important role in inflammation and tumorigenesis [de SouzaPereira, 2009; Sarkar et al., 2007]. Thus, developing drugs which inhibit the COX-2 expression is considered to be a promising approach to protect against inflammation and tumorigenesis.

Nitric oxide synthase (NOS) is an enzyme that catalyzes L-arginine to produce nitric oxide (NO). There are mainly three types of NOS isoforms, which are reported to be present in different tissues [Gao et al., 2007; Biswas and Kabir, 1998; Yang et al., 2003]. Endothelial nitric oxide synthase (eNOS) and neuronal nitric oxide synthase (nNOS) are constitutively expressed in the vascular endothelium, central, and peripheral neurons. Inducible nitric oxide synthase (iNOS), on the other hand, is only induced by various inflammatory stimuli such as LPS and inflammatory cytokines in macrophages, endothelial cells, and hepatocytes [Alderton et al., 2001]. iNOS catalyzes the reaction of formation of NO in large amount, which plays an important role in various forms of inflammation and carcinogenesis [Fukumura et al., 2006]. Therefore, iNOS catalyzed NO overproduction may reflect the degree of inflammation, and provides a measure to assess the effect of chemo-preventive agents on the inflammatory process. The induction of iNOS is mainly regulated by transactivation of the iNOS promoter by transcription factors including NFκB and activating protein-1 (AP-1), which are essential transcription factors to activate many other genes related to the regulation of the inflammatory responses [Aggarwal et al., 2006].

LPS is the principal component of the outer membrane of Gram-negative bacteria and can activate a wide variety of immunological responses. Mechanistically, LPS activates toll-like receptor (TLR)-4, which is expressed on pro-inflammatory cells, to build signaling complexes including CD14, LPS-binding protein (LBP), and myeloid differential protein (MD)-2 [Takeda et al., 2005]. Activation of TLR-4 leads to the activation of two different signaling pathways: the myeloid differentiation factor-88 (MyD88)-dependent pathway and the

TIR domain-containing adaptor inducing interferon-β (TRIF)-dependent pathway. Toll-interleukin 1 receptor domain containing adaptor protein (TIRAP) is involved in the MyD88-dependent pathway via TLR4. The MyD88-dependent pathway results in TGF- β-activated kinase 1 (TAK1) phosphorylation. In turn, the phosphorylation of MAPKs and the IκB kinase (IKK) complex ultimately activates several transcription factors, such as NF-κB and AP-1, which induce expression of iNOS and COX-2 and coordinate the induction of many inflammatory mediators [Akira et al., 2004].

Recently, we have reported a new class of hybrid compound (PTER-ITC) by coupling isothiocyanate (ITC) containing thiosemicarbazide pharmacophore with PTER backbone [Nikhil et al., 2014a]. Subsequently we tested for its cancer chemopreventive potential in both breast and prostate cancer cells [Nikhil et al., 2014a; Nikhil et al., 2014b; Nikhil et al., 2014c]. Since inflammatory pathways are critical targets in both prevention and therapy of cancer therefore in the present study, we tested for its anti-inflammatory potential in LPS stimulated RAW264.7 macrophages along with the parent compound PTER. In addition, the *in vitro* data was further supported by the *in vivo* studies on λ-carrageenan-induced rat paw edema model.

9.2 Brief Methodology

9.2.1 Cell culture

RAW 264.7 cells were maintained in Dulbecco's modified Eagle's media (DMEM) supplemented with 10% fetal bovine serum (heat inactivated) (both from Invitrogen, Carlsbad, CA, USA) and 1% antibiotic (100 U/mL of penicillin and 100 μg/mL streptomycin) (Himedia, Mumbai, India) mix at 37 ℃ in humidified atmosphere in a CO2 incubator.

9.2.2 Assessment of cellular NO production

RAW264.7 (1×10^5) cells were seeded in 24-well plates, and then pretreated with different concentrations of PTER and PTER-ITC for 1 h. After 1 h, the cells were stimulated with LPS (1 μg/mL) for the next 18 h. After the incubation period the NO production was determined by assaying the accumulation of nitrite, the primary stable breakdown product of NO, in the culture medium with the Griess reagent [mixture of equal volume of 1% sulfanilamide in 5% H3PO4 and 0.1% N-(1-naphthyl) ethylenediamine dihydrochloride in H2O]. The amount of nitrite produced was quantified spectrophotometrically at 540 nm using a microplate reader (BMG Labtech, Germany). Concentration of nitrite was determined using a standard curve of sodium nitrite prepared in the culture medium.

9.2.3 Determination of cytokine production

RAW 264.7 cells were seeded in a 24 well plate at a density of 1.5×10^5 cells/ml per well. The cells were pre-treated with different concentrations of PTER and PTER-ITC for 2 h and stimulated with 1 µg/ml LPS for 18 h. Then the culture medium was collected and centrifuged at 1000 g for 5 min to obtain cell-free supernatant. Supernatants were stored at -80 °C before being assessed for various cytokines. The concentration of PGE_2 released into medium was detected by commercially available ELISA kits (R&D Systems) according to the manufacturer's instructions.

9.2.4 Luciferase assay for COX-2, AP-1 and NFκB transcriptional activity

In order to determine whether NFκB, AP-1, and COX-2 signaling pathways were involved in the anti-inflammatory action of PTER-ITC, RAW264.7 cells were seeded in a 12 well plate at a concentration of 1×10^5 cells/well and incubated for 24 h before transfection. The signal transduction pathway was determined using a pathway profiling luciferase system (BD Biosciences Clontech, UK). This system contains seven different luciferase reporter vectors, each with a specific cis-acting DNA sequence (enhancer element) upstream of the luciferase gene, and one construct (pTAL) without any enhancer element upstream of luciferase reporter gene to be used as negative control. Thus, when a reporter plasmid is transfected into mammalian cells and induced externally by a ligand the activation of endogenous protein kinases will result in binding of the transcription factors to corresponding enhancer elements which in turn stimulates reporter gene expression. The key cis-acting elements tested in the study were: activator protein 1 (AP1) and nuclear factor of κB (NFκB). All these specific cis-acting DNA binding sequences were located upstream of the TATA-like promoter (pTAL) region from the herpes simplex virus thymidine kinase (HSV-TK) promoter. The vector pTAL was used as null vector which did not have any cis-acting elements in its promoter region and was a negative control in the assay. The cells were then transfected with 200 ng/well of firefly reporter plasmid pNFκB-luciferase, pAP1-luciferase or phPES2(–327/+59)-luciferase, a firefly luciferase reporter construct containing the human COX-2 gene promoter fragment, and 0.6 ng/well of β-gal internal control plasmid using Polyfect transfection reagent (Qiagen, CA, USA). After 20 h of transfection, the cells were washed with fresh medium and treated with different concentrations of PTER-ITC for 1 h followed by stimulation with LPS (1 µg/mL) for the next 6 h. On completion of the treatment, cells were lysed with the lysis buffer (0.6M NaCl, 0.1 M EDTA, 0.2 M $MgSO_4$, 0.2 M DTT, 0.1% Triton X-100, 0.08 M Tricine), and the luminescence was measured using luciferin as a substrate. Each experiment was performed in triplicates, and the results varied by less than 10%. The value of luciferase activity for each

lysates was normalized to the β-gal activity. Luciferase inductions in response to treated cells were expressed as percentage fold induction in luciferase activity with respect to only LPS treated cell which was considered as 100%.

9.2.5 Electrophoretic mobility shift assay (EMSA)

To investigate the inhibitory effect of PTER-ITC on NFκB and AP-1 DNA binding ability, an EMSA assay was performed. Briefly, 10 µg nuclear extracts prepared from RAW 264.7 cells were incubated in a total volume of 15 µl at room temperature for 30 min in 5X binding buffer (750 mM KCl, 0.5 mM dithiothreitol, 0.5 mM EDTA, 50 mM Tris, pH 7.4) and 1 µM concentration of double-stranded oligonucleotide. Then, 15 µl of the EMSA reaction was loaded onto a 6 % of native polyacrylamide gel, and electrophoresis was carried out in 1X TBE buffer at room temperature. The gel was analyzed by using a fluorescence based EMSA kit (Molecular Probes, USA). The gels were then stained with fluorescent dyes and visualized by a gel documentation system (BioRad, USA).

9.2.6 Preparation of tissue samples for western blot analysis

Six hours after carrageenan injection, the rats were sacrificed by cervical dislocation under ether anesthesia, and paw tissue were collected for immunoblot analysis. Soft tissues removed from individual mouse paws were washed with ice cold PBS and homogenized in ice cold lysis buffer (50 mM Tris, pH 7.5, 150 mM NaCl, 1% Triton X-100, 100µg/mL PMSF). The homogenates were then centrifuged at 12,000 g for 20 min at 4°C, and the supernatant was collected for western blot analysis. Western blot was done according to the standard protocol as described above.

9.2.7 Measurement of nitric oxide in paw edema

For measurement of nitric oxide in paw edema homogenized tissue samples were diluted four times with distilled water and deproteinized by adding 1/20 volume of zinc sulfate (300 mg/mL) to a final concentration of 15 mg/mL. After centrifuging at 10,000g for 5 min at room temperature, 100 µL of supernatant was added into a microtiter plate, followed by 100 µL of Griess reagent. After 10 min of color development at room temperature, the absorbance was measured at 540 nm with a microplate reader (BMG Labtech, Germany). Concentration of nitrite was determined by using a standard curve of sodium nitrite.

9.2.8 Quantification of PGE$_2$ in paw tissue

The rat paw tissues were collected 6 hours after inducing the inflammation by carrageenan and homogenized (1g/4ml) in extraction buffer containing 1mM of

phenylmethylsulfonyl fluoride, 1 µg/ml of aprotinin and 0.05% Tween-20 in phosphate-buffered saline (PBS). The homogenate was centrifuged at 5000 g for 15 min and the supernatants were stored at −80 °C until analysis. PGE_2 levels were estimated using commercially available ELISA kits (R&D Systems) according to the manufacturer's instructions.

9.3 Results

9.3.1 Effect of PTER and PTER-ITC on cell viability in RAW264.7 cells

To determine whether PTER and PTER-ITC have potential cytotoxicity on RAW264.7 cells, the cell viability was evaluated using MTT assay. For this RAW264.7 cells were seeded in a 96 well plate followed by treatments with different concentration of test compound (1-30 µM) in the presence and absence of LPS for 24 h followed by MTT assay. Our result showed that PTER treatment without LPS stimulation did not show any significant toxicity till 30 µM as compared to untreated cells (Fig. 9.1) ($p<0.05$). On the other hand, treatment with PTER-ITC did not show any toxicity till 20 µM, while the cell viability was reduced to 80-85% when the dose was increased to 30 µM (Fig. 9.1A) ($p<0.05$). However, LPS alone or in combination of drugs did not show any significant cytotoxicity to the cells till 20 µM. Considering the above data in all the subsequent *in vitro* experiments the dosage for both PTER and PTER-ITC were below 20 µM.

9.3.2 Effect of PTER and PTER-ITC on LPS-induced nitric oxide and PGE_2 production

To investigate whether PTER and PTER-ITC have any role in inflammatory process, initially, we measured its inhibitory effects on the production of NO and PGE_2 level. For this RAW264.7 cells were pretreated with 5 and 10 µM of PTER and PTER-ITC for 1 h followed by treatment with LPS (1µg/ml) for another 18 h. As shown in Fig. 9.2A, the stimulation of RAW264.7 cells with LPS alone led to a significant increase in the levels of NO in the media. However, pretreatment of RAW264.7 cells with PTER and PTER-ITC inhibited LPS-induced NO production in a dose dependent manner. While treatment with 5 and 10 µM of PTER reduced NO production by 37% and 70%, the treatment with the same dose of PTER-ITC showed more significant reduction of 70% and 88%, respectively (Fig. 9.2A) ($p<0.05$). Similarly when checked for PGE_2 level in LPS treated RAW264.7 cells, 5 and 10 µM of PTER reduced PGE_2 production by 20% and 33%, while the treatment with the same dose of PTER-ITC showed more significant reduction of 46% and 66%, respectively (Fig. 9.2B) ($p<0.05$). Next, in order to check if this inhibition was dose dependent, RAW264.7 cells were pretreated with different doses of PTER-ITC (for 1 h) followed by LPS treatment for 18 h and then

checked for NO and PGE$_2$ production. Our results showed that PTER-ITC treatment reduced LPS induced NO (Fig. 9.2C) and PGE$_2$ (Fig. 9.2D) production in a dose dependent manner where it was inhibited by almost 93 and 76% respectively at the highest dose tested ($p<0.05$).
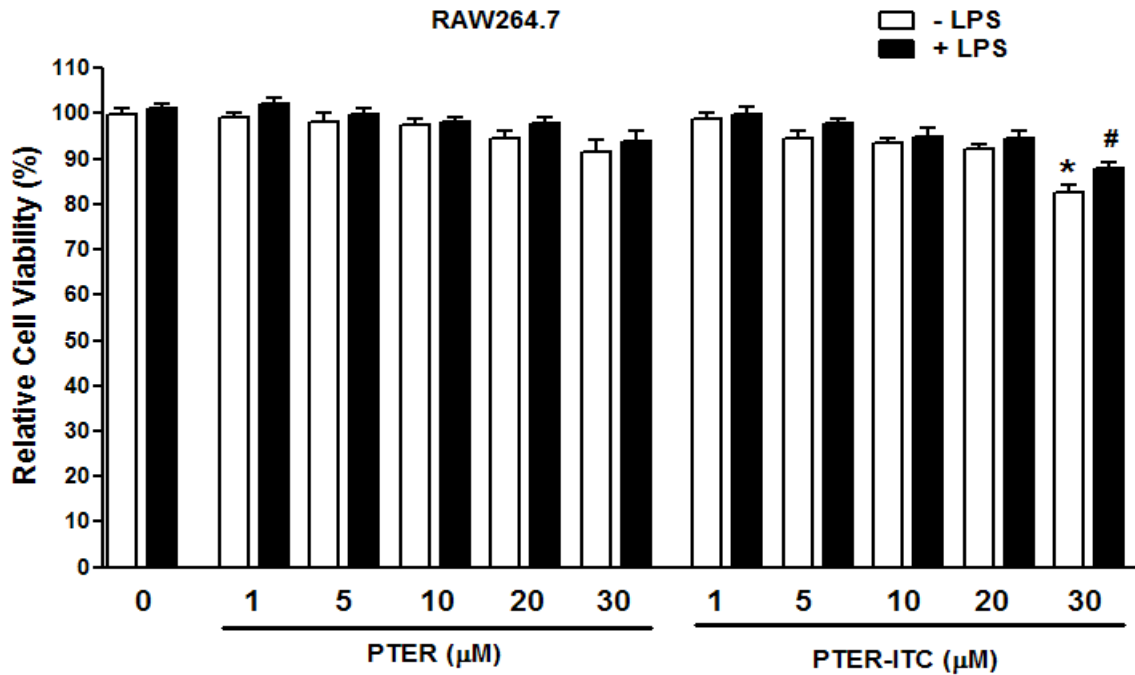
Figure 9.1: Effect of PTER and PTER-ITC on cell viability in RAW264.7 cells. Cells were treated with indicated concentrations of PTER and PTER-ITC in the presence or absence of LPS (1 µg/mL) for 24 h. Cell viability was evaluated using the MTT assay, and the results are expressed as percentage of surviving cells over the control group. Data are the mean ± SEM of three independent experiments. The symbols, * and #, represent statistically significant difference with respect to LPS untreated and treated control group respectively at $p<0.05$.
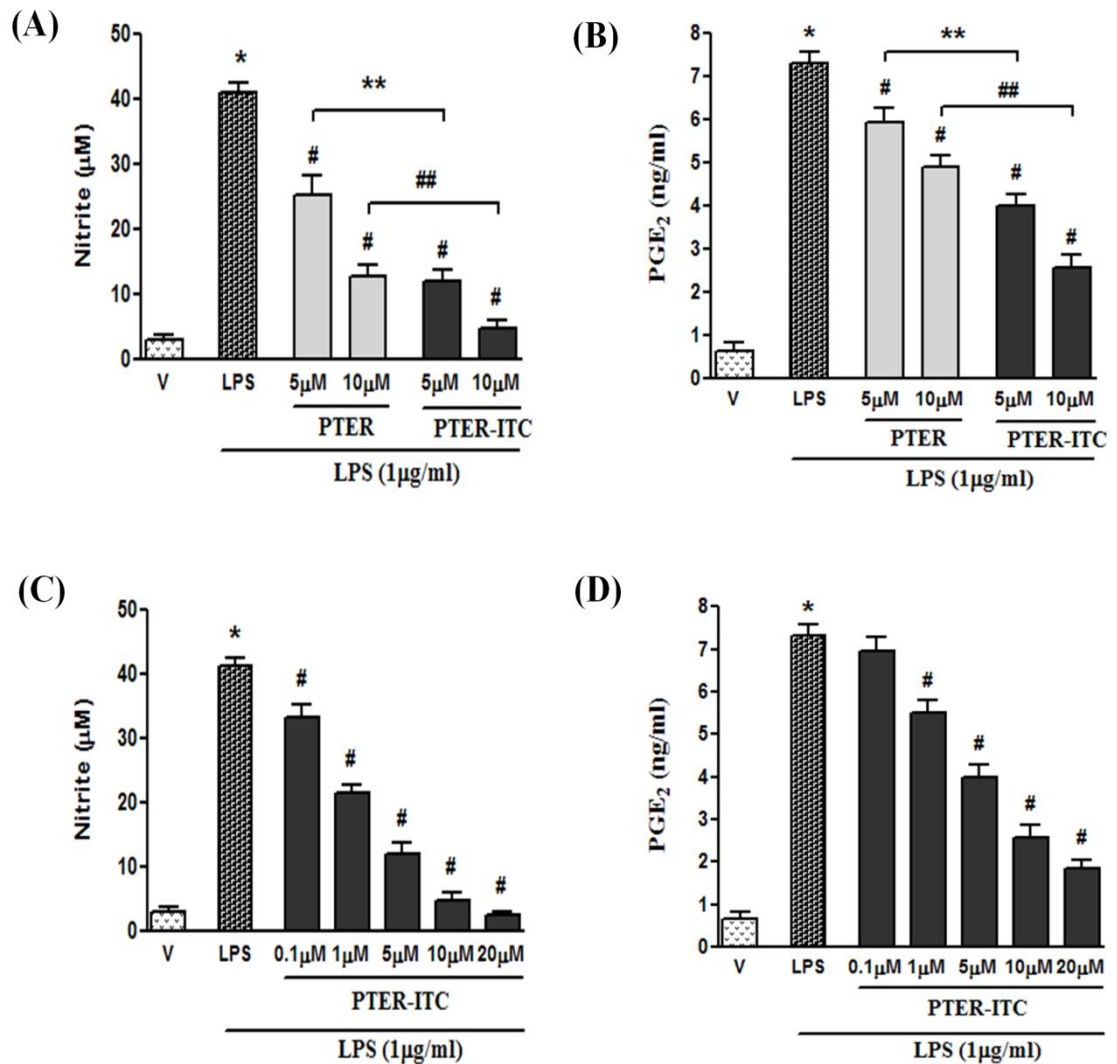
Figure 9.2: Effect of PTER and PTER-ITC on inflammatory mediators in RAW 264.7 cells. (A) Comparative analysis of 5 and 10 μM of PTER and PTER-ITC on nitric oxide and (B) PGE$_2$ production in LPS stimulated RAW 264.7. (C) Dose dependent effect of PTER-ITC on nitric oxide and (D) PGE$_2$ production in LPS activated RAW 264.7 cells. Cells were pretreated with PTER and PTER-ITC for 1 h, and then stimulated with LPS (1 μg/ml) for 18 h. The amount of nitrite concentration and PGE$_2$ level in the medium was determined by Griess reaction and ELISA kit respectively as described in methods. Data are the mean ± SEM of three independent experiments. $*p < 0.05$ vs. vehicle treatment; $\#p < 0.05$ vs. LPS treatment; $**p < 0.05$ vs. 5 μM PTER; $\#\#p < 0.05$ vs. 10 μM PTER.

9.3.3 Effects of PTER and PTER-ITC on iNOS and COX-2 expression levels in LPS-stimulated RAW264.7 macrophages

Since iNOS and COX-2 are the two enzymes involved in the production and formation of inflammatory mediators like NO and PGE2 respectively, we next investigated the effect of PTER and PTER-ITC on LPS induced up-regulation of iNOS and COX-2 using RT-PCR (Fig. 9.3A) and western blot (Fig. 9.3B) analysis. RT-PCR results clearly showed that COX-2 and iNOS mRNA levels were significantly increased by LPS treatment. However, this increase was significantly inhibited by about 50% and 40%, respectively for COX-2 and iNOS with 5 µM of PTER-ITC which was further reduced with increasing dose (10 µM). PTER, on the other hand, did not show any significant reduction at 5 µM, while both COX-2 and iNOS mRNA levels were significantly inhibited at 10 µM by 55% and 30%, respectively (Fig. 9.3A) ($p<0.05$). To confirm whether PTER and PTER-ITC regulate expression of COX-2 and iNOS at the level of translation as well, we next performed immunoblot analysis. Our results showed that both PTER and PTER-ITC significantly attenuated the expression of both COX-2 and iNOS protein levels at both the dose tested. PTER at 10 µM inhibited the LPS-induced COX-2 and iNOS expressions by approximately 55% and 30%, respectively. On the contrary, PTER-ITC at the same dose showed more prominent inhibition where COX-2 and iNOS protein levels were inhibited by 70% and 80%, respectively. Thus, these results suggest that the expressions of both these enzymes were significantly reduced in both PTER-ITC and PTER treated plates and interestingly, it was significantly more prominent in the former as compared to the latter (Fig. 9.3B) ($p<0.05$).

To further confirm whether PTER-ITC regulates the expression of COX-2 at the level of transcription and translation, we next performed its promoter activity and immunofluorescence analysis, respectively. For the promoter assay, RAW264.7 cells were transfected with reporter constructs of COX-2 and then treated with various concentrations of PTER-ITC for 1 h, exposed to LPS for 6 h, and assayed for luciferase reporter activities. The resulting data showed that PTER-ITC suppressed the LPS-induced activation of COX-2 in a dose dependent manner (Fig. 9.4A), indicating that PTER-ITC may inhibit expression of COX-2 by suppressing the activation of transcriptional factors. In case of immunofluorescence analysis, the cells treated with varying doses of PTER-ITC resulted in dose dependent inhibition of fluorescence intensity which was almost completely abolished at the highest dose tested, indicative of its anti-inflammatory activity (Fig 9.4B).
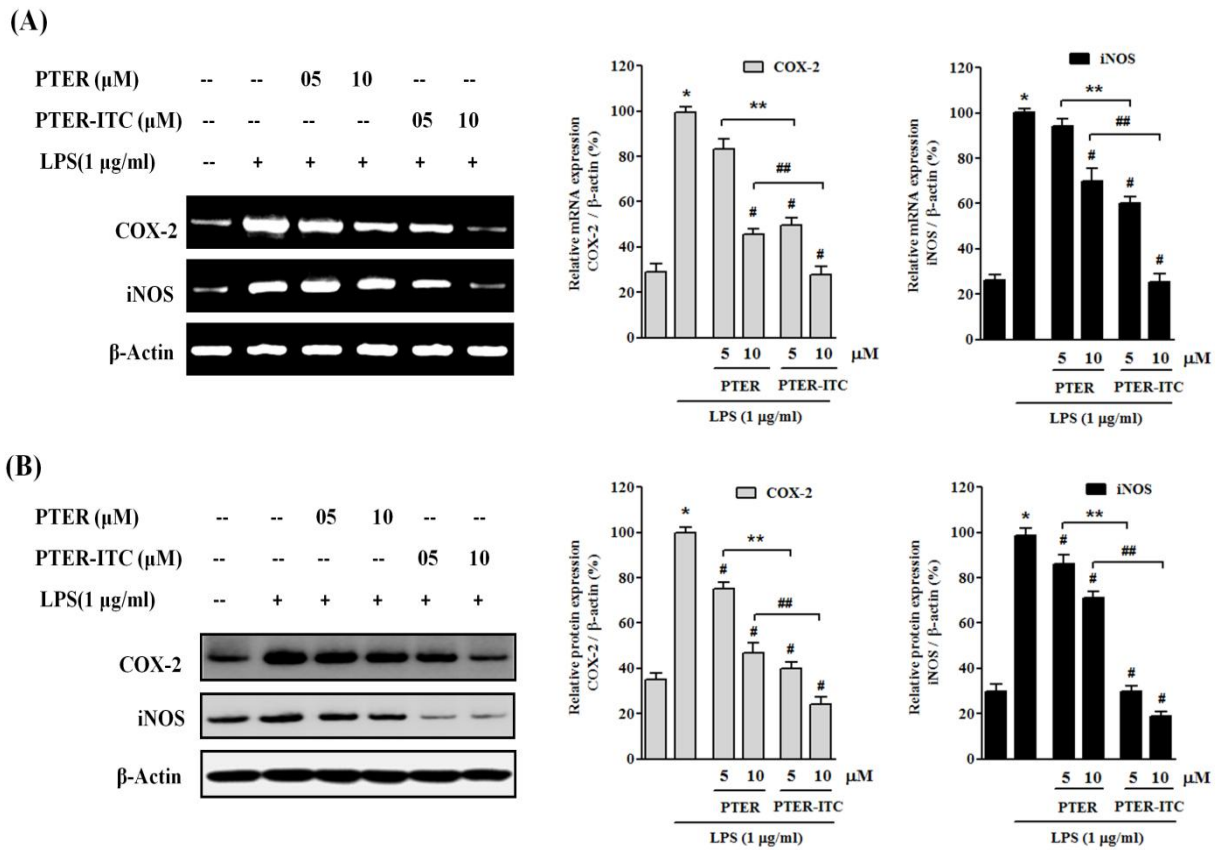
Figure 9.3: Effect of PTER and PTER-ITC on inflammatory enzymes in RAW 264.7 cells. Inhibitory effect of 5 and 10 μM of PTER and PTER-ITC on (A) mRNA and (B) protein expression levels of COX-2 and iNOS in LPS-stimulated RAW264.7 cells. The histogram in the right panels of each figure represents densitometric analyses of the image data and expressed as percent over LPS treated group. Results are the mean ± SEM of three independent experiments. *$p < 0.05$ vs. vehicle treatment; #$p < 0.05$ vs. LPS treatment; **$p < 0.05$ vs. 5 μM PTER; ##$p < 0.05$ vs. 10 μM PTER.

(A)

(B)
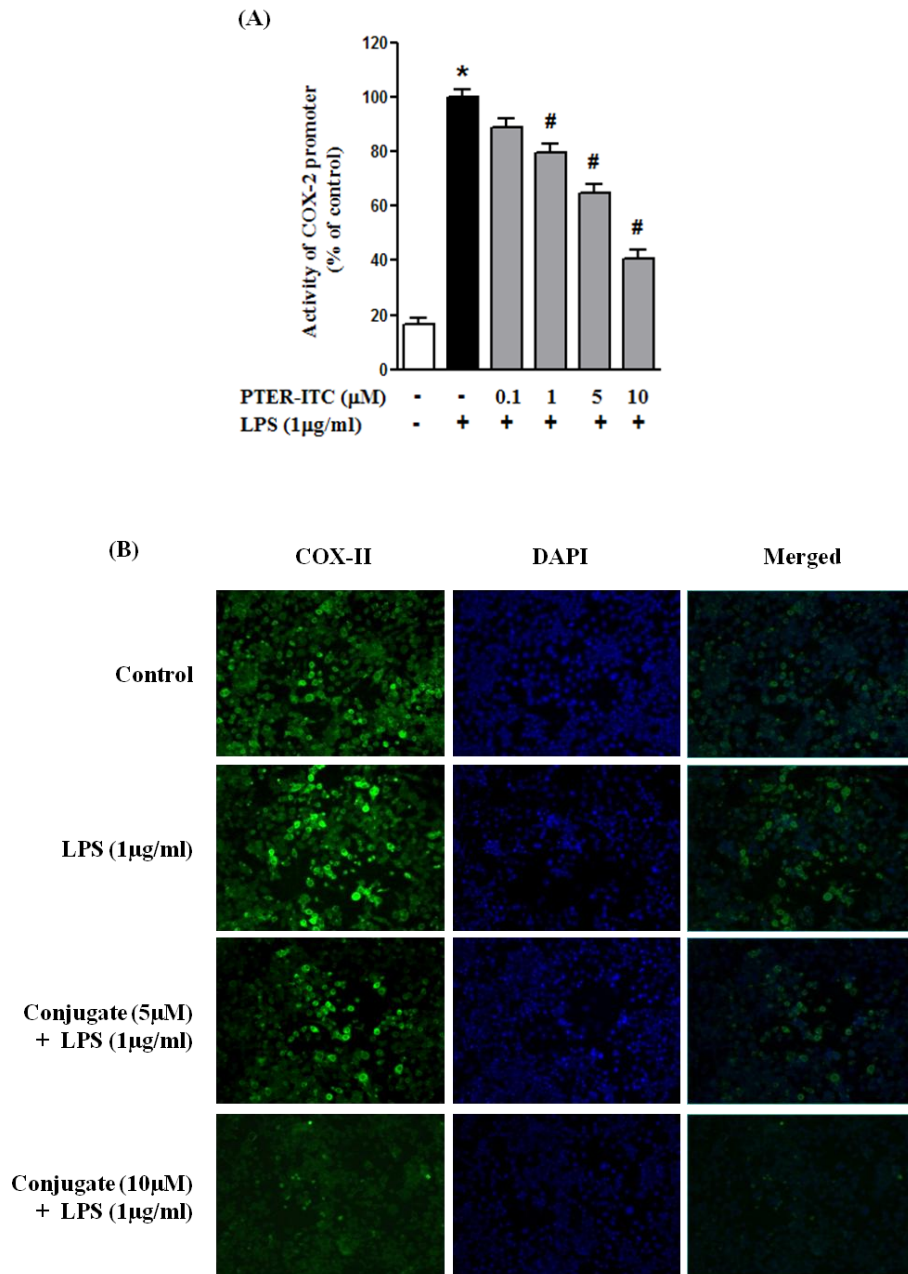
Figure 9.4: Dose dependent effect of PTER-ITC on LPS induced COX-2 promoter activity and expression (A) COX-2 promoter activity showing the inhibitory effect of PTER-ITC on LPS mediated activation of COX-2 promoter. RAW 264.7 cells were transfected with phPES2(–327/+59)-Luc, a firefly luciferase reporter construct containing the human COX-2 gene promoter fragment site. The transfected cells were treated with various doses of PTER-ITC for 1 h followed by LPS treatment for 6 h, and their relative luciferase activities were measured. The values are expressed as the means ± SEM from three individual experiments. The symbols, * and #, represent statistically significant difference with respect to control and LPS treated group respectively at $p<0.05$. (B) Immunofluorescence image for protein expression of COX-2 in RAW264.7 cells.

9.3.4 PTER-ITC reduced LPS-induced transcriptional activity of NFκB in RAW264.7 cells

To investigate the molecular mechanism of the PTER-ITC mediated inhibition of iNOS and COX-2 transcription, the NFκB transcriptional activity was investigated using NFκB transactivation assay. For this assay, RAW264.7 cells were transfected with NFκB-luc plasmid followed by stimulation with LPS either in the presence or absence of different doses of PTER-ITC, and the promoter activity was subsequently measured. As shown in Fig. 9.5A, PTER-ITC inhibited the LPS-induced transcriptional activation of NFκB in a dose-dependent manner which was maximum at 10 μM (almost 70%) ($p<0.05$), suggesting that its ability to inhibit NFκB transactivation may underlie its anti-inflammatory effects.

9.3.5 PTER-ITC inhibited degradation and phosphorylation of Ikβ-α and p-NFκB p65 translocation in LPS stimulated RAW264.7 cells.

In the next phase, we examined the effect of PTER-ITC on the phosphorylation status of LPS induced IκB-α. Our results showed that LPS treatment caused phosphorylation of IκB-α protein which was significant even at 5 min and reached maximum at 10 min followed by gradual degradation thereafter (Fig. 9.5B, upper panel). Once it was confirmed that LPS showed maximal activity at 10 min, in the next set of experiments, RAW264.7 cells were pretreated with PTER-ITC for 1 h prior to the exposure with 1 μg/mL of LPS for another 10 min. Our results also showed that PTER-ITC significantly inhibited the phosphorylation of IκB-α in a dose dependent manner (Fig. 9.5B, lower panel). These results suggested that PTER-ITC might inhibit NFκB activation via blocking LPS-induced phosphorylation and degradation of IκB-α (Fig. 9.5B). On this basis, we further examined the nuclear translocation of p65, a part of p65/p50 heterodimer, subsequently. As shown in Fig. 9.5C, PTER-ITC significantly inhibited LPS-induced nuclear translocation of phosphorylated NFκB p65 dose dependently with subsequent increase its accumulation in the cytoplasm. This data further confirmed the inhibitory action of PTER-ITC on NFκB translocation into the nucleus.

As p65 is the major component of NFκB which is activated by LPS in macrophages, we also examined the effect of PTER-ITC on binding of p65 to DNA oligonucleotides containing NFκB consensus sequence by EMSA. The stimulation of cells with LPS alone led to a significant increase in NFκB DNA-binding activity (Fig. 9.5D, right panel). However, PTER-ITC dose dependently retarded NFκB-DNA binding activity after pre-treatment with it for 1 h followed by stimulation with LPS for another 6 h. PTER-ITC showed about 25% and 40% inhibitions at 5 and 10 μM, respectively (Fig. 9.5D, right panel).
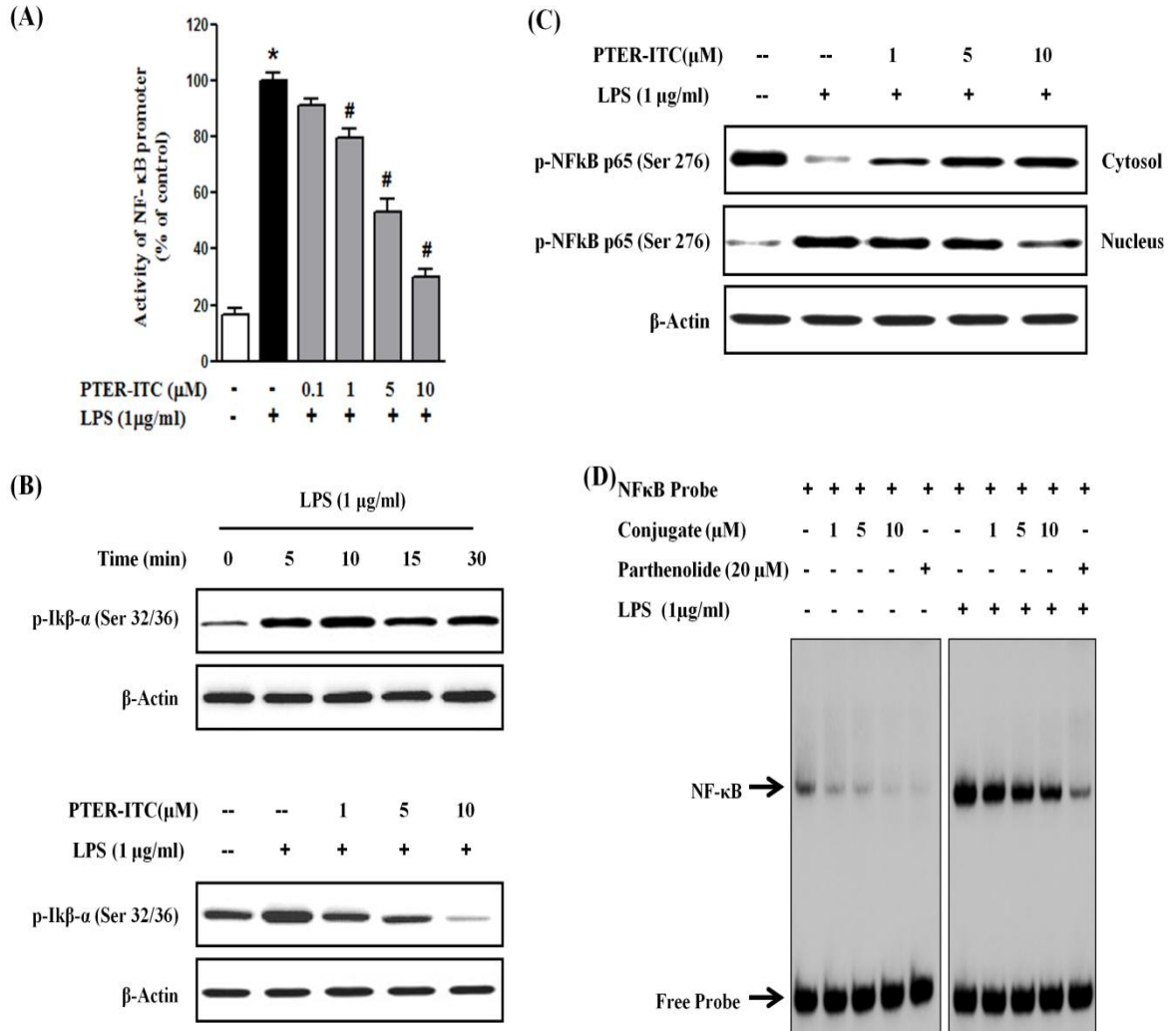
Figure 9.5: Effect of PTER-ITC on promoter activity of NFκB and nuclear translocation of p-NFκB p65 in LPS-stimulated RAW264.7 cells. (A) RAW 264.7 cells transfected with NFκB-responsive luciferase reporter construct (pNFκB-luc) were pretreated with the indicated concentrations of PTER-ITC for 1 h then exposed to LPS (1μg/mL). After 6 h of incubation, the luciferase activity was measured. The values are expressed as the means ± SEM from three individual experiments. The symbols, * and #, represent statistically significant difference with respect to control and LPS treated group respectively at $p<0.05$. (B) The time course and dose dependent effect of LPS and PTER-ITC respectively on phosphorylation of IκB-α in RAW 264.7 cells. (C) Effect of PTER-ITC on nuclear translocation of p-NFκB p65 in LPS-stimulated RAW264.7 cells. The cells were pretreated with PTER-ITC for 1 h prior to the 10 min LPS treatment. The cytoplasmic and nuclear extracts were prepared for the Western blot analysis of p-NFκB p65. Western blots are representative of three independent experiments (D) Dose dependent effect of PTER-ITC on binding of NFκB protein to its consensus binding sequence as determined by EMSA. Arrow indicates binding of NFκB to DNA. The results shown are representative of three independent experiments.
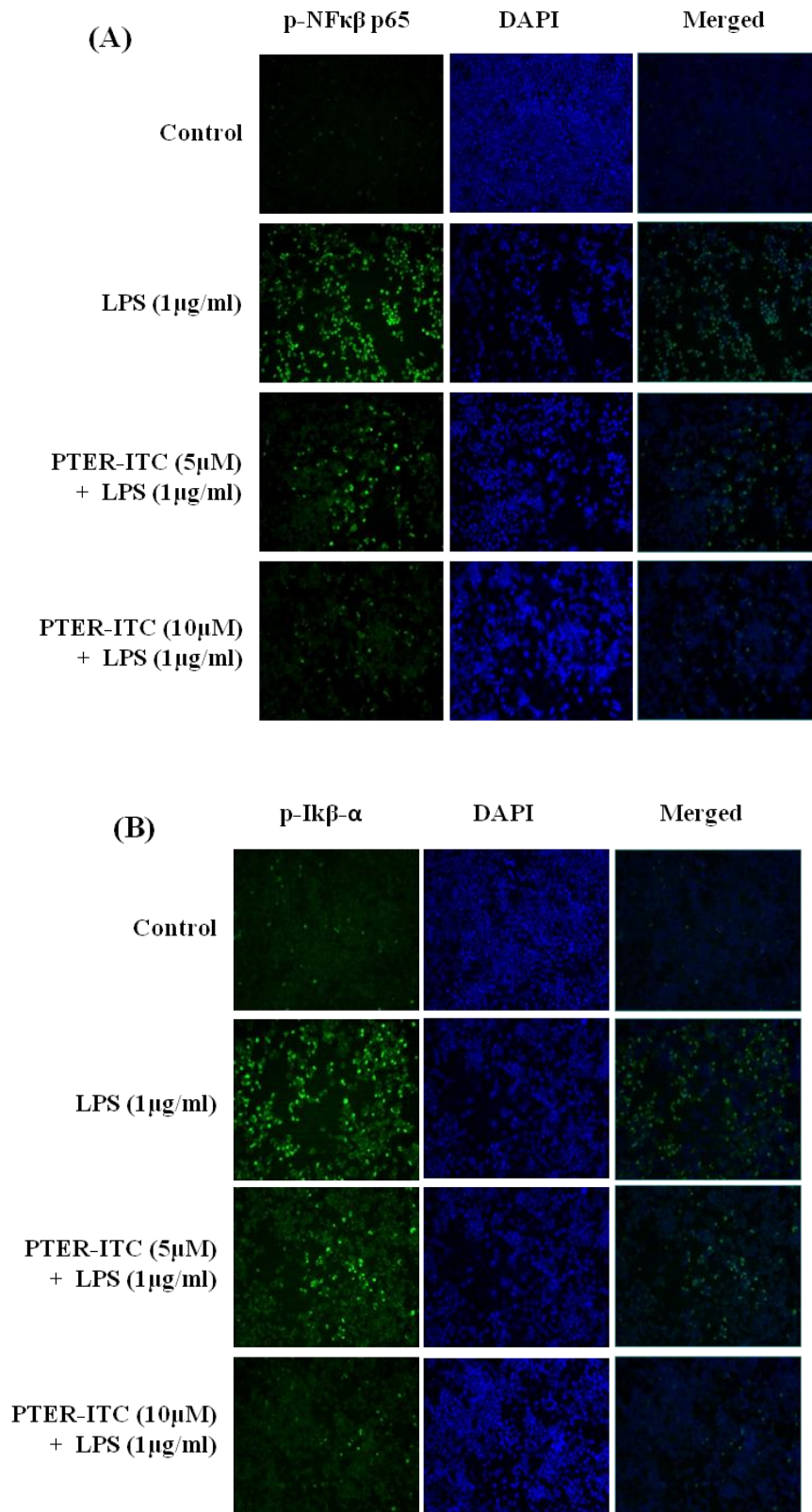
Figure 9.6: Effect of PTER-ITC on LPS induced p-NFκB p65 nuclear translocation and p-IκB-α expression. Immunofluorescence analysis for the detection of (A) p-NFκB p65 protein and (B) p-IκB-α in RAW 264.7 cells after treatment with different dose PTER-ITC followed by LPS stimulation for 6 h.

Parthenolide treatment (20 μM), on the other hand, suppressed the binding of p65 to the NFκB sites by 75% as compared to LPS-induced cells (Fig. 9.5D, right panel). These results indicated that PTER-ITC suppresses the expression of iNOS and COX-2 through the attenuation of the DNA binding activity of the transcription factor NFκB. The above results were further supported by the decrease in fluorescence intensity of p-NFκBp65 (Fig. 9.6A) and p-IκB-α (Fig. 9.6B) protein after treatment with varying doses of PTER-ITC.

9.3.6 Effects of PTER-ITC on the phosphorylation of MAPKs and AKT

The three MAPKs, ERK, p38 and JNK, are known to be activated by LPS, and several studies have shown that the phosphorylation of MAPKs and the subsequent activation of AP-1 are also involved in LPS-induced iNOS and COX-2 expression [Guha and Mackman, 2001]. To investigate if PTER-ITC can modulate this signaling pathway the potential involvement of MAPK was examined. A time course experiment showed that phosphorylation of ERK, JNK and p38 and AKT was increased from 10 to 30 min after LPS treatment. However, 1 h pre-treatment with PTER-ITC significantly attenuated the LPS induced phosphorylation of JNK, p38, and ERK ($p<0.05$) (Fig. 9.7). In contrast, the expression of non phosphorylated ERK, JNK, p38 MAPK and AKT was unaffected by LPS or by combination of PTER-ITC and LPS (Fig. 9.7). Among all three MAPKs, the inhibitory effect of PTER-ITC was maximum for the phosphorylation of JNK and ERK.
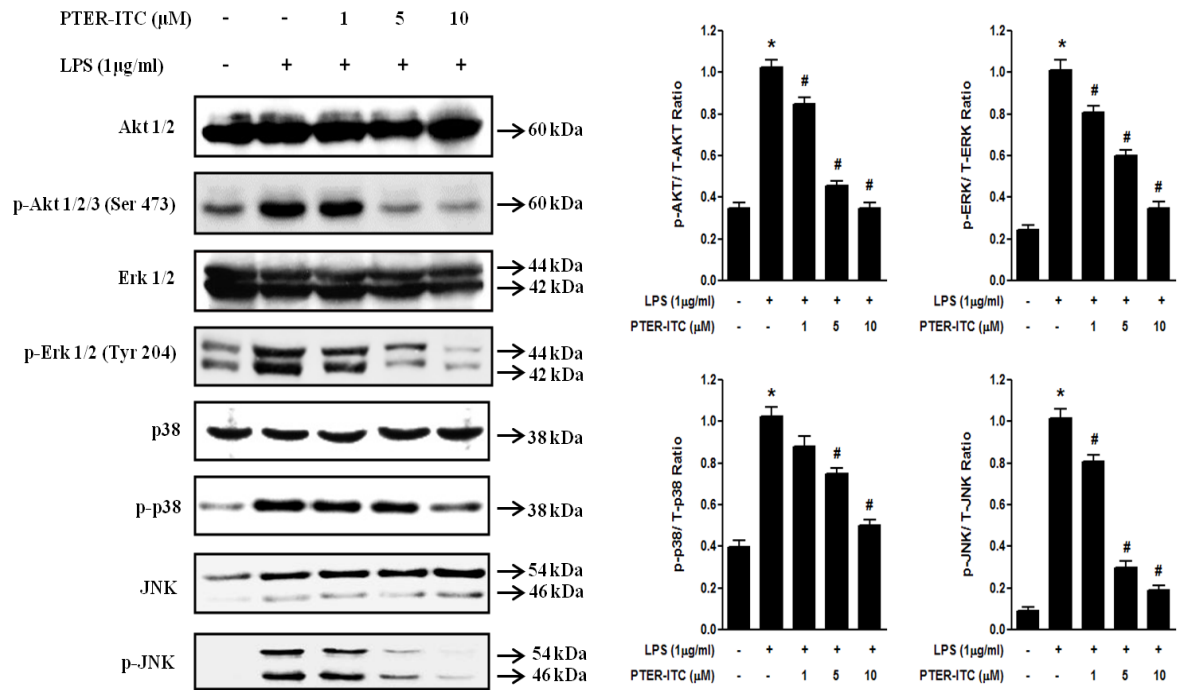
Figure 9.7: Effect of PTER-ITC on LPS-induced phosphorylation of MAPKs and AKT signaling pathways in RAW264.7 cells. RAW264.7 cells were treated with different concentration of PTER-ITC (1, 5, and 10 μM) for 1 h, and then exposed to 1μg/mL LPS for 30 min. Protein expression was detected with their respective antibodies. The right panel indicates the ratio of phosphorylated and unphosphorylated form of respective kinase. Results are the mean ± SEM of three independent experiments. The symbols, * and #, represent statistically significant difference with respect to control and LPS treated group ($p<0.05$).

9.3.7 Effects of PTER-ITC on activation of AP-1 in LPS-activated RAW 264.7 cells

The inflammatory mediators, such as iNOS, COX-2, IL-6, TNF-α along with many other genes are mediated not only by NFκB but also by AP-1 (activator protein-1). MAPK signaling pathway regulates AP-1 activity by increasing the transcription and phosphorylation of AP-1 protein. To determine if AP-1 is involved in the inhibition of those inflammatory factors by PTER-ITC, AP-1 based promoter assay was performed to assess the transcriptional activity of AP-1. For this, RAW264.7 cells were transfected with pAP1-luc plasmid (Promega, USA), and then treated with different doses of PTER-ITC followed by stimulation with LPS. Subsequently, we measured the promoter activity to reveal the transcriptional activation of AP-1. As shown in Fig. 9.8A, PTER-ITC inhibited the LPS-induced transcriptional activation of AP-1 in a dose-dependent manner, suggesting that its ability to inhibit AP-1 transactivation may underlie its anti-inflammatory effects. Next EMSA was performed to assess the DNA-

binding activity of AP-1. As shown in Fig. 9.8B, PTER-ITC significantly inhibited the LPS-induced AP-1 DNA-binding activity which was more prominent in a dose dependent manner. These results indicated that PTER-ITC also suppresses inflammatory mediators through the inhibition of MAPK signaling pathways and the attenuation of the DNA-binding activity of the transcription factor AP-1.
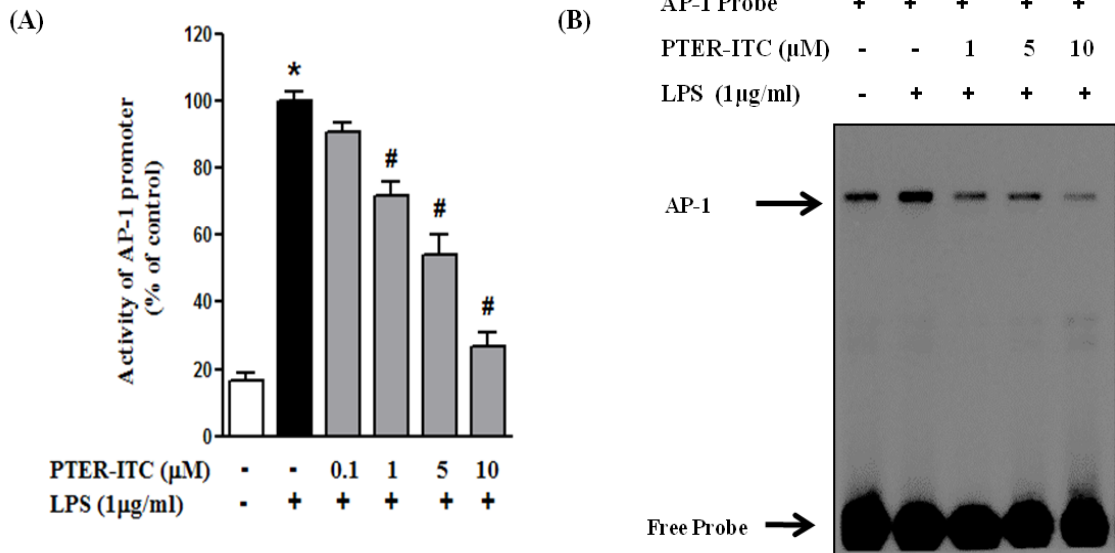
Figure 9.8: Effect of PTER-ITC on AP-1 DNA binding activity and ROS production in LPS stimulated RAW 264.7 cells. (A) Inhibitory effect of PTER-ITC on LPS mediated activation of AP-1. RAW 264.7 cells were transfected with an AP-1-responsive luciferase reporter gene (pAP-1-Luc). The transfected cells were treated with various doses of PTER-ITC for 1 h followed by LPS treatment for 6 h, and their relative luciferase activities were measured. The values are expressed as the means ± SEM from three individual experiments. The symbols, * and #, represent statistically significant difference with respect to control and LPS treated group ($p<0.05$) (B) The nuclear extracts were assayed for AP-1 DNA-binding activity by the EMSA. The results shown are representative of three independent experiments.

9.3.8 PTER-ITC reduces LPS induced intracellular ROS production

ROS plays important role in pro-inflammatory cytokine production and NFκB activation in LPS treated macrophages; hence, inhibition of ROS production is a popular therapeutic target for many inflammatory diseases. Therefore, we tested the effect of PTER-ITC on LPS-induced intracellular ROS production. As shown in Fig. 9.9, PTER-ITC inhibited LPS-induced ROS production in a dose-dependent manner. These data suggest that PTER-ITC inhibits LPS-induced intracellular ROS production; the suppression of which may weaken the

downstream NFκB activity and accordingly, reduces various biochemical events that otherwise may cause excessive oxidative and inflammatory damages.
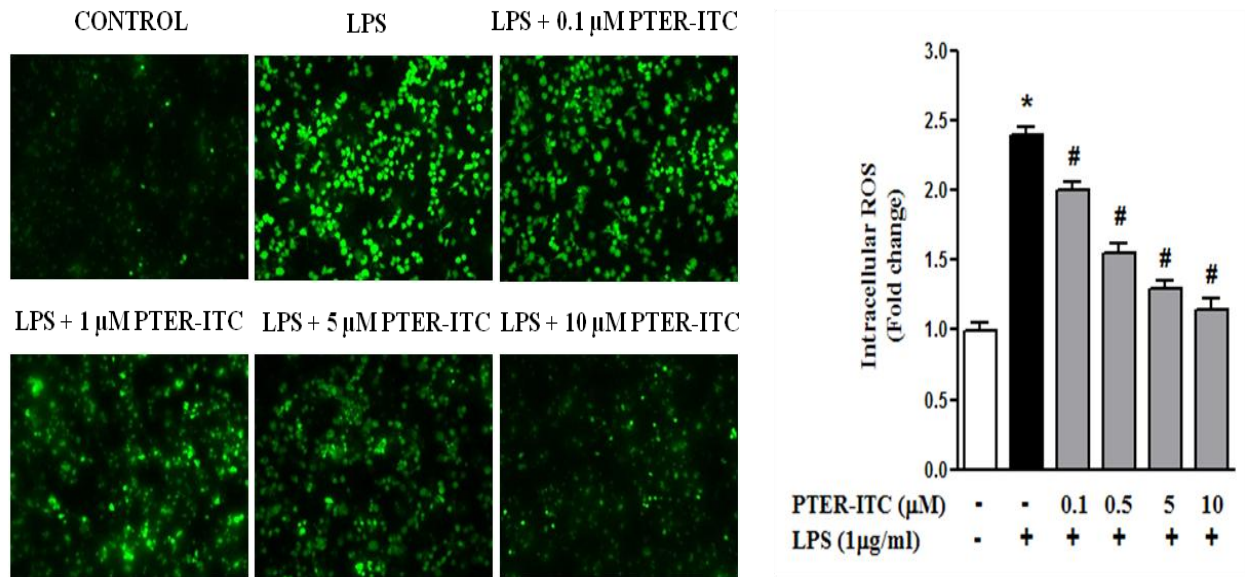
Figure 9.9: ROS accumulation within cells in response to different doses of PTER-ITC treatments as estimated by H2-DCF-DA staining of treated cells (100X magnifications). The histogram in the right panels of figure represents changes in fluorescence intensity represented as fold change over control. The symbols, * and #, represent statistically significant difference with respect to vehicle and PTER treated cells, respectively at $p<0.05$.

9.3.9 Effect of NFκB, AKT, and MAPKs inhibitors on LPS-induced NO production and iNOS and COX-2 expressions

To probe that the inhibition of iNOS and COX-2 expression is related to the downregulation of NFκB, MAPKs and AP-1 pathways, we examined the effect of NFκB, AKT, and MAPKs inhibitors on their expressions. For this analysis, Parthenolide (NFκB inhibitor), A6730 (AKT inhibitor), PD98059 (ERK inhibitor), SP600125 (JNK inhibitor), and SB203580 (p38 inhibitor) were employed. The cells were pretreated with specific inhibitors and PTER-ITC before the addition of LPS. The LPS induced increase in iNOS and COX-2 levels were unaffected by PD98059, but was significantly inhibited by SB203580 and SP600125 (Fig. 9.10B). Estimation of NO levels from the culture supernatant of the above experiments showed that pretreatment with SB203580 and SP600125 profoundly inhibited the LPS-induced NO production, while PD98059 exhibited little effect. As shown in Fig. 9.10A, pretreatment with SB203580, SP600125, and PD98059 showed 35%, 45%, and marginal reduction, respectively,

in NO production. Likewise, pretreatment with Parthenolide and A6730 also reduced the production of nitrite by 75% and 60%, respectively (Fig. 9.10A). These results suggested that activation of p38 and JNK in conjunction with NFκB and AKT may contribute to NO production in the LPS-stimulated RAW 264.7 cells and the PTER-ITC exerts its anti-inflammatory effect by inhibiting these pathways.

(A)

(B)

LPS (1μg/ml)	-	+	+	+	+	+	+	+
Parthenolide (10 μM)	-	-	+	-	-	-	-	-
A6730 (10 μM)	-	-	-	+	-	-	-	-
SP600125 (10 μM)	-	-	-	-	+	-	-	-
SB203580 (20 μM)	-	-	-	-	-	+	-	-
PD98059 (20 μM)	-	-	-	-	-	-	+	-
PTER-ITC (5 μM)	-	-	-	-	-	-	-	+
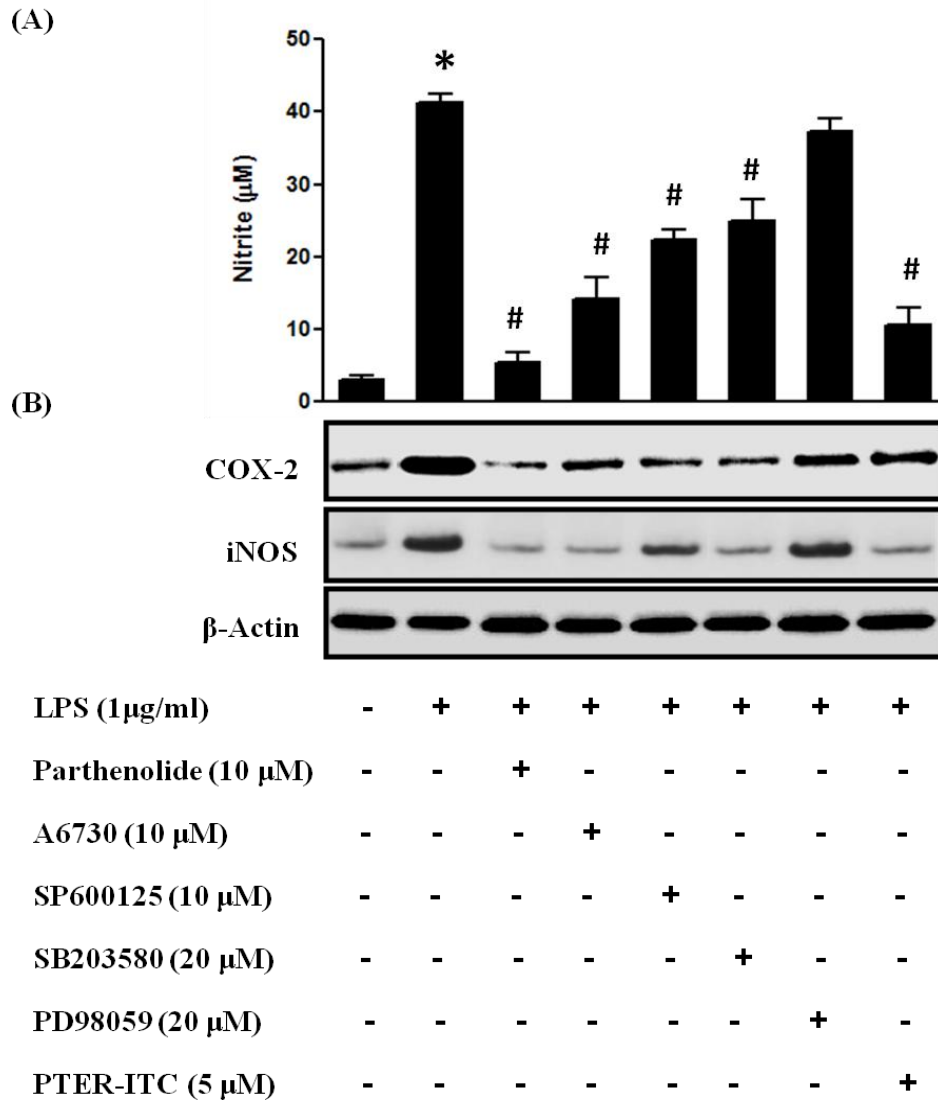
Figure 9.10: Effects of NFκB, AKT, and MAPKs inhibitors on LPS-induced alteration of different inflammatory mediators in RAW 264.7 macrophage cells. (A) Nitrite level (B) COX-2 and iNOS expressions. The cells were pretreated with inhibitors or PTER-ITC for 1 h then stimulated with LPS for 18 h. The amount of NO in the medium was measured using a Griess reagent. The whole cell extracts were prepared and the expression levels of iNOS and COX-2 were determined by Western blot analysis. The values are expressed as the mean±SEM from three individual experiments. The symbols, * and #, represent statistically significant difference with respect to control and LPS treated group ($p < 0.05$).

9.3.10 Inhibitory effects of PTER and PTER-ITC on carrageenan-induced rat paw edema

To evaluate the anti-inflammatory effects of PTER and PTER-ITC *in vivo*, we used the carrageenan-induced paw edema animal model, which is one of the classical models for verifying the efficacy of anti-inflammatory drugs. The subplantar injection of carrageenan led to a time dependent increase in the paw size as shown in Fig 9.11A. The paw volume was measured using a plethysmometer from 0 h to 5 h after carrageenan injection. Indomethacin, a common non-steroidal anti-inflammatory drug, was used as a positive control. Pretreatment with 10 mg/kg of indomethacin showed significant reduction in paw volume after 2 h of carrageenan stimulation. Oral administration PTER-ITC at a dose of 10 and 50 mg/kg bw effectively reduced paw edema starting from 2 and 4 h post carrageenan injection respectively. As observed, the effect of PTER-ITC at the dose of 50 mg/kg on the time course of inflammation was similar to that of positive control indomethacin. Interestingly, pretreatment with 50 mg/kg PTER also decreased paw edema after 3 h of carrageenan stimulation, but the effect was comparatively lower than that of PTER-ITC at the same dose (Fig. 9.11A).

9.3.11 Inhibitory effect of PTER and PTER-ITC on nitric oxide production in carrageenan-induced paw edema model

The L-arginine-NO pathway has been proposed to play an important role in the carrageenan-induced inflammatory response, and the expression of the inducible isoform of NO synthase as an important mediator of inflammation. Our data showed that the NO level increased significantly in edema tissue after 6 h of carrageenan injection, and this increment was markedly reversed by pretreatment with PTER-ITC at 50 mg/kg ($p<0.05$). This inhibitory potency was almost similar to that of positive control of indomethacin at 10 mg/kg dose. Treatment with PTER, on the other hand, also decreased NO production but to a lesser extent than PTER-ITC (Fig. 9.11B).

9.3.12 Inhibitory effect of PTER and PTER-ITC on PGE_2 production in carrageenan-induced paw edema model

PGE_2 is a very important mediator of all types of inflammation and is responsible for increased prostaglandin production in inflamed tissue. Hence we subsequently checked for PGE_2 level in inflamed paw tissue 6 h after carrageenan injection. As shown in Fig 9.11C carrageenan injection, as expected, caused a marked (approx. 2.7 fold) increase in hind paw PGE_2 concentration. However, pretreatment with PTER and PTER-ITC at a dose of 50 mg/kg effectively reduced hind paw PGE_2 concentrations by 23 and 44% respectively. Indomethacin on the other hand reduced PGE_2 production by 50%. Thus from above result it was clear that

PTER-ITC was more potent than PTER as an inhibitor of PGE_2 formation but exhibited similar efficacy to indomethacin (Fig. 9.11C).
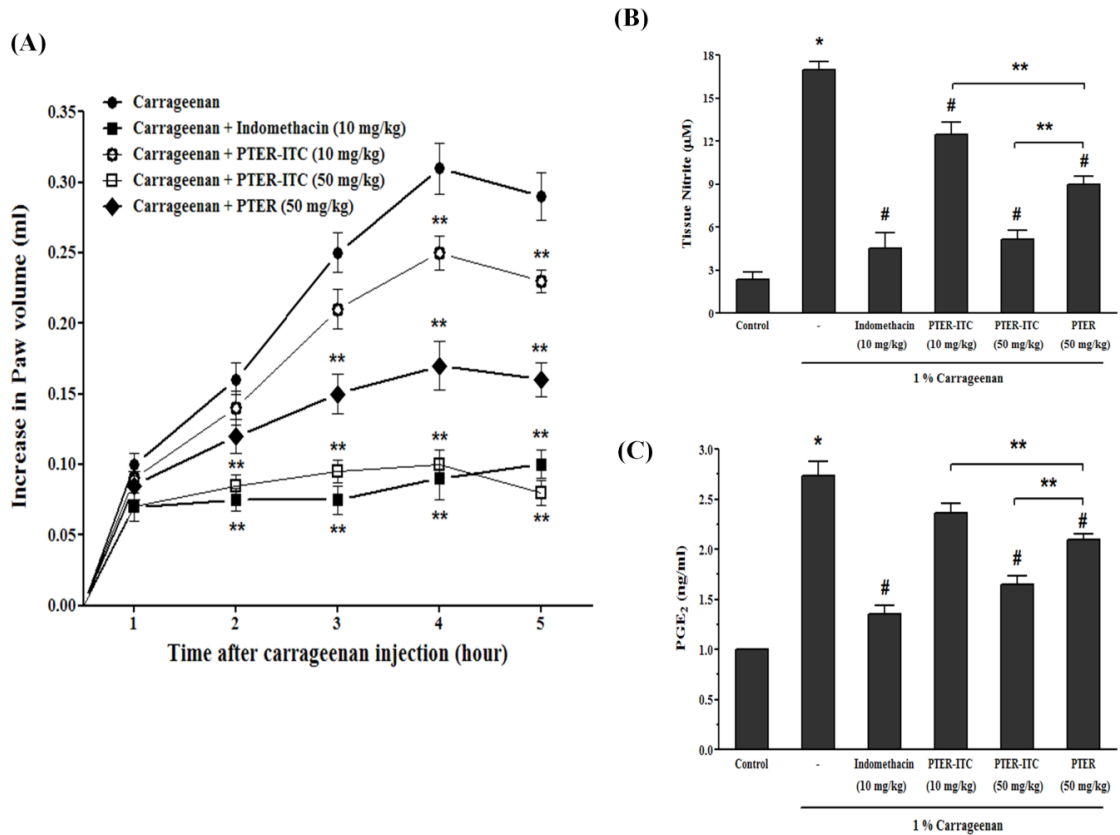
Figure 9.11: Anti-inflammatory effect of PTER and PTER-ITC *in vivo*. (A) The effect of PTER, PTER-ITC and indomethacin on the paw size in carrageenan-induced paw edema model. Rats were pretreated orally with different drugs for 30 min before injection with 1% carrageenan. **$p < 0.05$ vs. carrageenan treated group at different time intervals. (B) PTER-ITC inhibits tissue content of NO and (C) PGE_2 in carrageenan-induced paw edema model. *$p < 0.05$ vs. control; #$p < 0.05$ vs. carrageenan treated group; **$p < 0.05$ vs. PTER treated group

9.3.13 Inhibitory effect of PTER and PTER-ITC on iNOS and COX-2 expressions in the Carrageenan-induced paw edema model

The experimental results obtained showed that 50 mg/kg of PTER and PTER-ITC can significantly inhibit both iNOS and COX-2 protein expression in edema of paw as compared to the only carrageenan-treated group (Fig. 9.12C). The experiments showed an average of 46% and 70% down-regulation of the iNOS and COX-2 proteins, respectively, after treatment with PTER-ITC at 50 mg/kg BW. On the other hand, treatment with the same dose of PTER inhibited iNOS and COX-2 proteins by 23% and 50%, respectively, as compared to the

carrageenan-treated group (Fig. 9.12). In addition, the protein expressions showed an average of 25% and 84% down regulation of the iNOS and COX-2 proteins, respectively, after treatment with indomethacin at 10 mg/kg compared to the carrageenan treated group (Fig. 9.12). Thus, the efficacy of PTER-ITC (50 mg/kg) in down-regulating the expression of iNOS and COX-2 proteins was more or less similar to that of indomethacin (10 mg/kg).
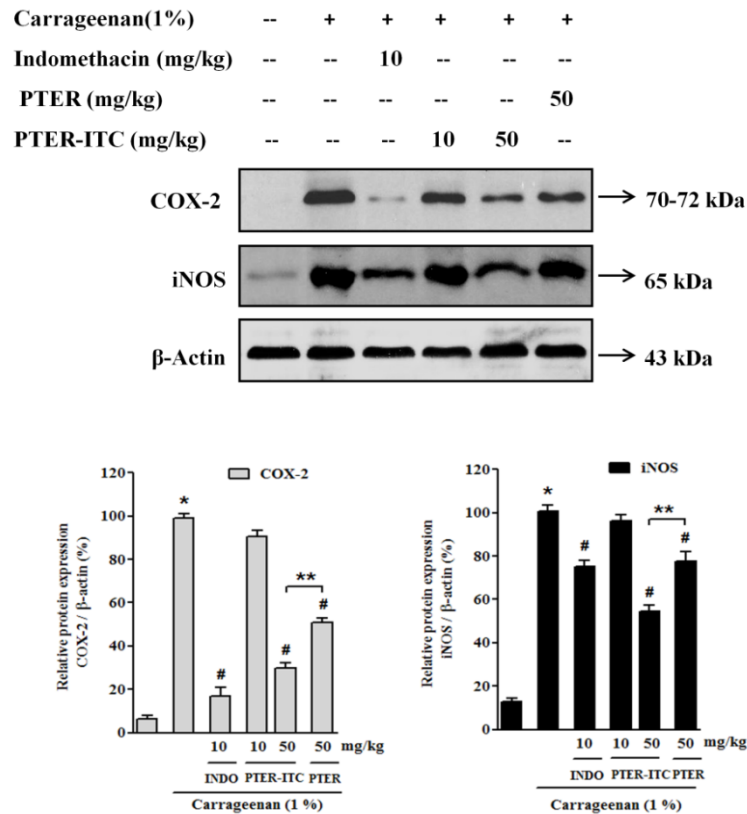
Figure 9.12: Western blot showing COX-2 and iNOS protein expression in carrageenan induced paw edema model. The values are expressed as the mean±SEM from three individual experiments. *$p < 0.05$ vs. control; #$p < 0.05$ vs. carrageenan treated group; **$p < 0.05$ vs. PTER treated group.

9.4 Discussion

Inflammatory responses play decisive roles at different stages of tumor development. The inflammatory state is necessary to maintain and promote cancer progression and accomplish the full malignant phenotype such as tumor tissue remodeling, angiogenesis, metastasis, and the suppression of the innate anti-cancer immune responses [Grivennikov et al., 2010]. Twin drug is defined as a compound that contains two pharmacophore components exerting pharmacological effects in a molecule. It is considered to be a promising drug design strategy and has led quite interesting results [Wermuth, 2008]. Based on the evidence that

PTER-ITC showed little toxicity to normal cells [Nikhil et al., 2014a; Nikhil et al., 2014b; Nikhil et al., 2014c] and the close relationship between inflammation and cancer, the current study was designed to explore the anti-inflammatory effects of PTER-ITC using mouse macrophage cell line RAW264.7 and carrageenan induced rat paw edema as the inflammatory model. Our data showed that non-toxic doses of PTER-ITC could inhibit inflammatory responses against LPS-stimulated RAW264.7 cells. Further, to the best of our knowledge, the present study showed for the first time that the anti-inflammatory properties of PTER-ITC was due to the suppression of LPS-stimulated JNK, p38 MAPK, AKT, and NFκB pathways in RAW264.7 macrophages.

Epidemiological studies have revealed that chronic inflammation predisposes to different forms of cancer. Chronic inflammation causes the increase of pro-inflammatory mediators including COX-2 and iNOS which are responsible for increased levels of prostaglandins (PGs) and nitric oxide (NO), respectively, and various cytokines like TNF-α, IL-1β, and IL-6. To explore the mechanisms underlying the anti-inflammatory action of this conjugate, we examined the effect of PTER-ITC on inflammation related macrophage functions. It has been previously reported that PTER at a dose of 10 μM inhibits LPS induced iNOS and COX-2 mRNA and protein levels which leads to decrease in NO_2 and PGE_2 productions, respectively [Pan et al., 2008]. Our data are consistent with the above finding and further states that modification of PTER by adding an ITC group further enhances its potency. Treatment with 5 and 10 μM of PTER and PTER-ITC showed most significant inhibition with the latter, suggesting that PTER-ITC was more efficient in suppressing the production of inflammatory mediators. Furthermore, the promoter assay and immunofluorescence analysis of COX-2 confirmed that inhibitory effects of PTER-ITC curtail the expression of COX-2 at the level of both transcription and translation.

The transcriptional regulation of NO, PGE2, iNOS, COX-2, and inflammatory cytokines such as TNF-α and IL-1β is a tightly controlled event. A variety of transcription factors including NFκB and AP1 are known to be involved in the transcriptional regulation of these inflammatory cytokines [Aggarwal et al., 2006]. Specifically, the regulation of iNOS and COX-2 via the NFκB pathway is an important mechanism in inflammatory response. From the NFκB reporter gene assay and EMSA experiment, we found that PTER-ITC exhibited an inhibitory effect on NFκB activation. In un-stimulated cells, NFκB was retained in the cytoplasm by binding to the IκB-α. The process of NFκB activation includes degradation through phosphorylation and subsequent nuclear localization of RelA subunit of NFκB. The central role of IκB-α and p65 for NFκB signaling makes them attractive targets for

development of NFκB specific drugs. Therefore, the phosphorylation of IκB-α and translocation of p65 in RAW264.7 cell were measured in this study. LPS stimulation dramatically increased the phosphorylation of IκB-α followed by translocation of p65 into nucleus. However, LPS-induced IκB-α phosphorylation and nuclear translocation of p65 were significantly blocked by pretreatment with PTER-ITC. These collective findings suggested that PTER-ITC might inhibit NFκB activation by blocking LPS-induced phosphorylation and degradation of IκB, and p65 nuclear translocation.

Mitogen-activated protein kinase (MAPK) signaling pathways play important roles in many biological processes, including inflammation, apoptosis, proliferation, and differentiation. The MAPKs include extracellular signal-regulated kinases (ERKs), c-Jun N-terminal kinases (JNKs), and p38 kinase [Gaestel et al., 2007; Torres and Forman, 2003]. Multiple lines of evidence have demonstrated MAPKs play a critical role in regulating expression of COX-2 and iNOS induced by many cytokines and inflammatory products such as LPS, leading to autoimmune and inflammatory diseases [Gaestel et al., 2007; Torres and Forman, 2003; Chakraborty et al., 2014]. Hence, we next examined the effect of PTER-ITC on LPS induce phosphorylation of MAPKs and AKT in RAW 264.7 cells. The results revealed that PTER-ITC suppressed the phosphorylation of ERK, JNK and p38 MAPK as well as that of AKT in LPS-induced inflammatory response of RAW264.7 cells. Our results with p38, JNK, ERK, and AKT inhibitors as well as NFκB specific inhibitor confirmed that the LPS-stimulated increase in iNOS and COX-2 expressions as well as nitrite generation were due to activation of p38, JNK, AKT and NFκB, and PTER-ITC was capable of block these.

During inflammation, activated macrophages largely increase the oxygen uptake resulting in massive accumulation of ROS. ROS has been proposed as the signaling molecules in cellular events and is critical for LPS-induced inflammation [Pan et al., 2014]. The ROS targets the cysteines within the proteins and alters the kinase activation, which further activates redox-sensitive IKK and MAPKs. N-acetyl-l-cysteine (NAC), a synthetic antioxidant, abrogates the activation of NFκB, AP-1, and MAPKs by suppressing ROS. Similar effects have also been revealed using natural antioxidants such as carnosol [Lo et al., 2002] and glycitein [Kang et al., 2007]. In this study, PTER-ITC significantly inhibited LPS-induced ROS production in RAW 264.7 cells. However, whether PTER-ITC inhibited the generation of ROS or scavenged ROS directly, remained unclear. In conclusion, decrease in ROS production by PTER-ITC resulted in weakened downstream signaling activities, lower production of inflammatory mediators, and finally causing reduced cell damage.

Carrageenan-induced rat paw edema model is a suitable test for evaluating anti-inflammatory activity of a given drug. Carrageenan is a strong chemical used for the release of inflammatory and proinflammatory mediators (prostaglandins, leukotrienes, histamine, bradykinin, TNF-α) [Wills, 1969]. The edema develops following the injection of carrageenan and serves as an index of acute inflammatory changes which can be determined from the differences in paw thickness measured immediately after the injection and then every hour. The edema induced by carrageenan is believed to be biphasic with the first phase (1–4 h) involving the release of serotonin and histamine and a prostaglandins, cyclooxygenase products mediated second phase [Tohda et al., 2006]. In the present study, statistical analysis revealed that 10 mg/kg of indomethacin and 50 mg/kg of PTER-ITC significantly inhibited the development of edema 3 h after treatment (Fig 9.11A). Previous studies have shown that carrageenan-induced inflammation in rats increased the production of NO in plasma and the expression of iNOS and COX-2 in paw tissues. We found that Carrageenan induced NO production was decreased significantly by treatment with 50 mg/kg of PTER and PTER-ITC suggesting that the anti-inflammatory mechanism of this compound may be through the L-arginine-NO pathway. Further, our immunoblot results showed that the expressions of COX-2 and iNOS were significantly increased in rats paw tissues after carrageenan-induced inflammation when compared with control rats (without inflammation) which is in agreement with other studies showing increased expressions of COX-2 and iNOS in the paw tissues of mouse and rats submitted to carrageenan-induced inflammation [Huang et al., 2012; Nantel et al., 1999]. We showed that pretreatment with PTER-ITC significantly reduced the expressions of COX-2 and iNOS dose-dependently in rat paw tissues which was similar to the reduction effect with indomethacin.

In conclusion, the *in vitro* and *in vivo* studies demonstrated for the first time to the best of our knowledge that PTER-ITC suppresses NO and PGE2 synthesis through the downregulation of iNOS and COX-2 genes. The inhibition in iNOS and COX-2 expressions is related to down regulation of both IKK/NFκB and MAPK/AP-1 signaling pathways. In addition, our results also suggest that these effects may be related to the inhibition of LPS-induced ROS production. Taken together, all these results indicate the potentiality of PTER-ITC as an anti-inflammatory drug candidate. However, further studies involving more detailed *in vivo* pharmacokinetics and bioavailability related studies are warranted to conclusively prove the efficacy of this conjugate for the therapeutic applications where the data obtained from this study could be used as a base.

Chapter 10. PTER-ITC as Anti-osteoclastogenic Agent

10.1 Introduction

Bone undergoes constant turnover and a balance (homeostasis) is maintained by osteoblasts (creating bone) and osteoclasts (destroying bone). Osteoclasts are unique bone-resorbing cells derived from cells of monocyte-macrophage lineage. Excessive bone resorption by osteoclasts leads to an imbalance in bone remodeling and causes bone lytic diseases such as osteoporosis, Paget's disease, periodontitis, erosive arthritis, hypercalcemia, and cancer metastasis to the bone [Novack and Teitelbaum, 2008]. Current drugs used to treat osteoporosis include bisphosphonates, calcitonin and estrogen. These drugs are all bone resorption inhibitors, which maintain bone mass by inhibiting the function of osteoclasts [Rodan and Martin, 2002; Maatta et al., 2013; Roshandel et al., 2010]. Since the osteoclasts are responsible for bone resorption, therefore, they are one of the main targets for treatment of osteoporosis.

Many factors are involved in osteoclast differentiation. Receptor activator of nuclear factor (NF)-κB (RANK), its ligand RANKL and the decoy receptor osteoprotegerin (OPG) are essential and central regulators of osteoclast development and functions. RANKL is expressed on the surface of osteoblastic/stromal cells and by various types of cancer cells, and is directly involved in the differentiation of monocyte macrophages into osteoclasts [M. Baudhuin et al., 2013; Sigl and Penninger, 2014]. In the physiological milieu when RANKL binds to RANK, it undergoes trimerization and then binds to an adaptor molecule, TNF receptor-associated factor 6 (TRAF6), which then results in the activation of several downstream signaling cascades, including the nuclear factor-kB (NF-kB), mitogen activated protein kinases (MAPK), activating protein 1 (AP-1) and nuclear factor of activated T cells (NFATc1) resulting in the formation of multinucleated bone-resorbing osteoclasts [Takayanagi et al., 2002; Wada et al., 2006].

Bone metastases are a frequent complication of cancer, occurring in up to 70% of patients with advanced breast or prostate cancer [Coleman and Rubens, 1987; El Touny and Banerjee, 2009] and approximately 15-30% of patients with carcinoma of the lung, colon, stomach, bladder, uterus, rectum, thyroid, or kidney. Bone metastasis makes bone more fragile and leads to pathologic fractures and spinal compression [Maatta et al., 2013]. This osteolysis is associated with severe bone pain, which may be intractable. It is estimated that 350,000 people die with bone metastases each year in the United States [Mundy, 2002]. Furthermore, once tumors metastasize to bone, they are usually incurable. For instance, only 20% of patients with breast cancer are still alive 5 years after the diagnosis of bone metastasis [Coleman, 2001]. RANKL has been shown to play a major role in bone metastasis [Onishi et al., 2010], and thus

is an important therapeutic target. So, designing novel drugs that target RANK-RANKL and their signaling pathways in osteoclasts could potentially revolutionize the treatment of cancerous bone metastases, not to mention other diseases associated with bone loss such as arthritis, tooth loss, and osteoporosis. Antibodie against RANKL, for example denosumab [Cummings et al., 2009; Roshandel et al., 2011], have recently been approved by the FDA for the treatment of osteoporosis and for the prevention of skeletal-related events in patients with bone metastases from solid tumors. However, these antibodies require continuous injection and have numerous side effects, which highlight the need for safer therapeutic alternatives.

Trans-3, 4′, 5-trihydroxystilbene or Resveratrol (RESV) is a polyphenol produced by certain plant species, including nut, berries and grapes in response to environmental stress by the action of enzyme, stilbene synthase [Borriello et al., 2013]. RESV possesses significant anti-inflammatory and antioxidant properties, which may benefit bone health. Studies showed that RESV increased osteoblast proliferation and differentiation [Boissy et al., 2005; Lee et al., 2010] and decreased osteoclast differentiation [Lee at al., 2010; He et al., 2010]. Given the limited bioavailability of RESV after oral administration, the high concentrations required to obtain the desired effects, its potential toxicity and complex mechanisms of actions RESV analogues may offer advantages over the parent compound.

Pterostilbene (PTER) is a naturally-occurring dimethylated analog of RESV and shows pleiotropic health benefits, including anti-oxidant, anti-inflammatory, anti-aging, cardioprotective, and neuroprotective activities [Brisdelli et al., 2009]. However, PTER is significantly more bioavailable than RESV after being ingested [Lin et al., 2009]. Due to the widespread use and importance of stilbenes, which are small molecules, new and active stilbenes are still being looked for. In our recent studies, we synthesized a PTER derivative, PTER-isothiocyanate (PTER-ITC), with improved potency and specificity compared with the PTER and studied its role in breast [Nikhil et al., 2014a; Nikhil et al., 2014c] and prostate cancer [Nikhil et al., 2014b] prevention. Additionally in the previous chapter, we reported that PTER-ITC anti-inflammatory properties are probably due to its ability to inhibit the NFkB signalling pathway, which has also been demonstrated to be a major mediator of bone loss [Xu et al., 2009]. In the present study, we investigated whether PTER-ITC, in addition to inhibiting RANKL–induced NFκB avtivation would also inhibit RANKL-induced osteoclastogenesis and found that PTER-ITC acts as a RANKL-mediated osteoclastogenesis inhibitor. This inhibitory effect appears to be due to suppression of reactive oxygen species (ROS) generation and further PTER-ITC also blocked RANKL-induced signaling pathways (MAPKs and NFκB) which were required for osteoclast differentiation.

10.2 Brief Methodology

10.2.1 Osteoclast differentiation and Tartrate-resistant acid phosphatase (TRAP) staining

Murine RAW264.7 cells were grown in DMEM supplemented with 10% FBS and 1% penicillin/streptomycin. For differentiation of osteoclasts, RAW264.7 cells (2×10^4, in 24-well plate) were cultured in the presence of RANKL (50 ng/mL) for 6 days. The culture medium was replaced every 2 days. After completion of differentiation, the cells were fixed and stained for TRAP activity. The TRAP positive multinucleated cells containing two or more nuclei were considered to be osteoclast-like cells, and were counted under the inverted microscope (Axiovert 25, Zeiss).

10.2.2 Measurement of intracellular ROS levels

Intracellular ROS production was determined using DCFH-DA, a flurogenic probe for general ROS such as hydrogen peroxide, peroxynitrite and hydroxyl radical. In brief, RAW264.7 cells were grown and treated with different concentration of PTER-ITC (1-20 µM) for 2 h before stimulation with 50 ng/mL of RANKL. After 1 h of co-incubation, these cells were subsequently incubated with DCFH-DA (at a final concentration of 10 µM) for 30 min at 37°C. Thereafter the cells were washed with PBS twice and intracellular ROS accumulation was observed and photographed using a fluorescent microscope (Axiovert 25, Zeiss).

The quantitative amount of ROS production in RAW264.7 cells was also analyzed by fluorescence-activated cell-sorting (FACS). For this RAW264.7 cells were grown and treated as described above. Thereafter the cells were washed with PBS and incubated with DCFH-DA (at a final concentration of 10 µM) for 30 min at 37°C. Cells were then scraped off, washed in PBS and the fluorescence intensity was analyzed by FACS [FACSverse TM (BD Biosciences, San Jose, CA)].

10.3 Results

10.3.1 Effect of PTER-ITC on cell viability

RAW264.7 cells were treated with different concentration (1–100 µM) of PTER-ITC for 24 h and 72 h, and cell viability was determined by MTT assay. As shown in Fig. 1B PTER-ITC had no cytotoxic effect on the cells at any of the dose tested after 24 h time period. However, when the cells were treated for longer period (72 h), PTER-ITC was found to reduce the cell numbers, at dose above 30 µM. Hence, in order to exclude PTER-ITC-mediated cytotoxicity, non-lethal concentrations (< 30µM) were used in subsequent experiments.

10.3.2 PTER-ITC inhibits RANKL-induced osteoclastogenesis in RAW264.7 cells

In the next phase whether PTER-ITC could inhibit RANKL induced osteoclastogenesis was investigated. For this osteoclast precursor RAW264.7 cells were treated with different concentrations (5, 10, 15 and 20 μM) of PTER-ITC in presence of RANKL and allowed to differentiate into osteoclasts for 6 days. As shown in Figure 10.1B, RANKL induced formation of osteoclasts in control cells. In contrast differentiation into osteoclast was significantly reduced in the presence of PTER-ITC which was dose dependent. As little as 5 μM concentration of PTER-ITC had significant inhibitory effect on RANKL induced osteoclast formation.

To determine whether PTER-ITC inhibits osteoclastogenesis in a time-dependent manner, RAW264.7 cells were incubated with PTER-ITC for 3, 4, or 5 days and allowed to differentiate into osteoclasts by RANKL. Morphological observations clearly demonstrated that RAW264.7 cells differentiated into osteoclasts after RANKL addition, and that PTER-ITC inhibited this differentiation (Fig. 10.2). The extent of suppression was measured by counting the number of TRAP-positive osteoclasts per well (Fig. 10.2). We observed that RANKL induced osteoclast differentiation in a time-dependent manner, with a maximum of TRAP positive osteoclasts per well at day 5 (Fig. 10.2). On the other hand, PTER-ITC decreased the number of TRAP-positive osteoclasts in a dose-dependent manner, with a strong inhibition at 20 μM at all days examined (Fig. 10.2).
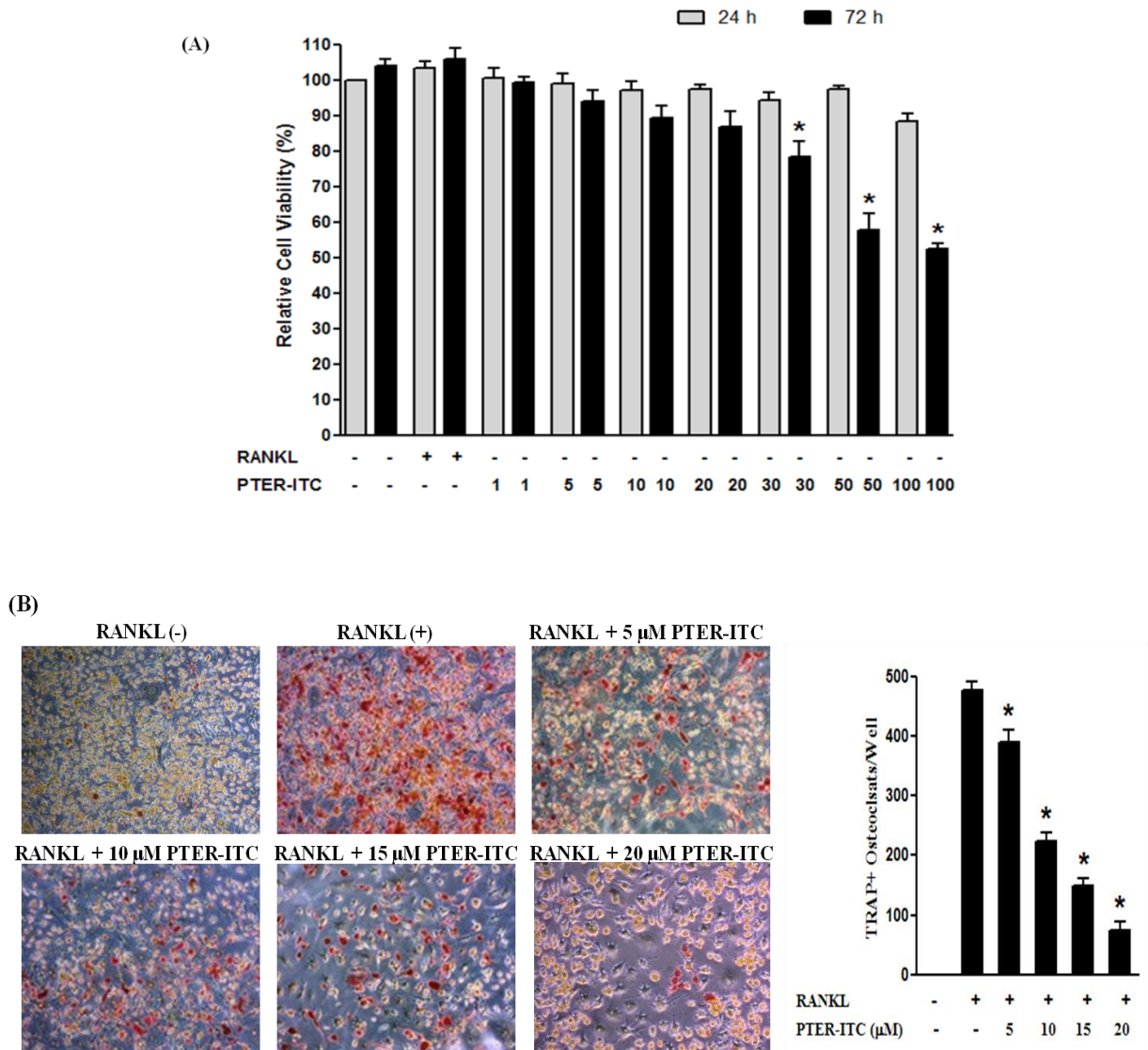
Figure 10.1: PTER-ITC inhibited RANKL induced osteoclastogenesis of RAW264.7 cells without significant toxicity. (A) Effect of PTER-ITC on cell viability in RAW264.7 cells. Cell viability was evaluated using MTT assay and the results are expressed as percentage of surviving cells over the control group. Data are the mean ± SEM of three independent experiments. * represents statistically significant difference compared to control group; $p < 0.05$. (B) Effect of PTER-ITC on RANKL induced osteoclast differentiation. RAW 264.7 cells were cultured for six days with 50 ng/mL RANKL plus indicated concentration of PTER-ITC. Cells were fixed and TRAP staining was performed. TRAP-positive cells were photographed (100X magnifications). Histogram on the right panel shows quantification of multinucleated osteoclasts (i.e., those containing two or more nuclei). Values are mean ± SEM from three independent experiments. * indicate statistically significant differences compared to only RANKL treated groups; $p < 0.05$.
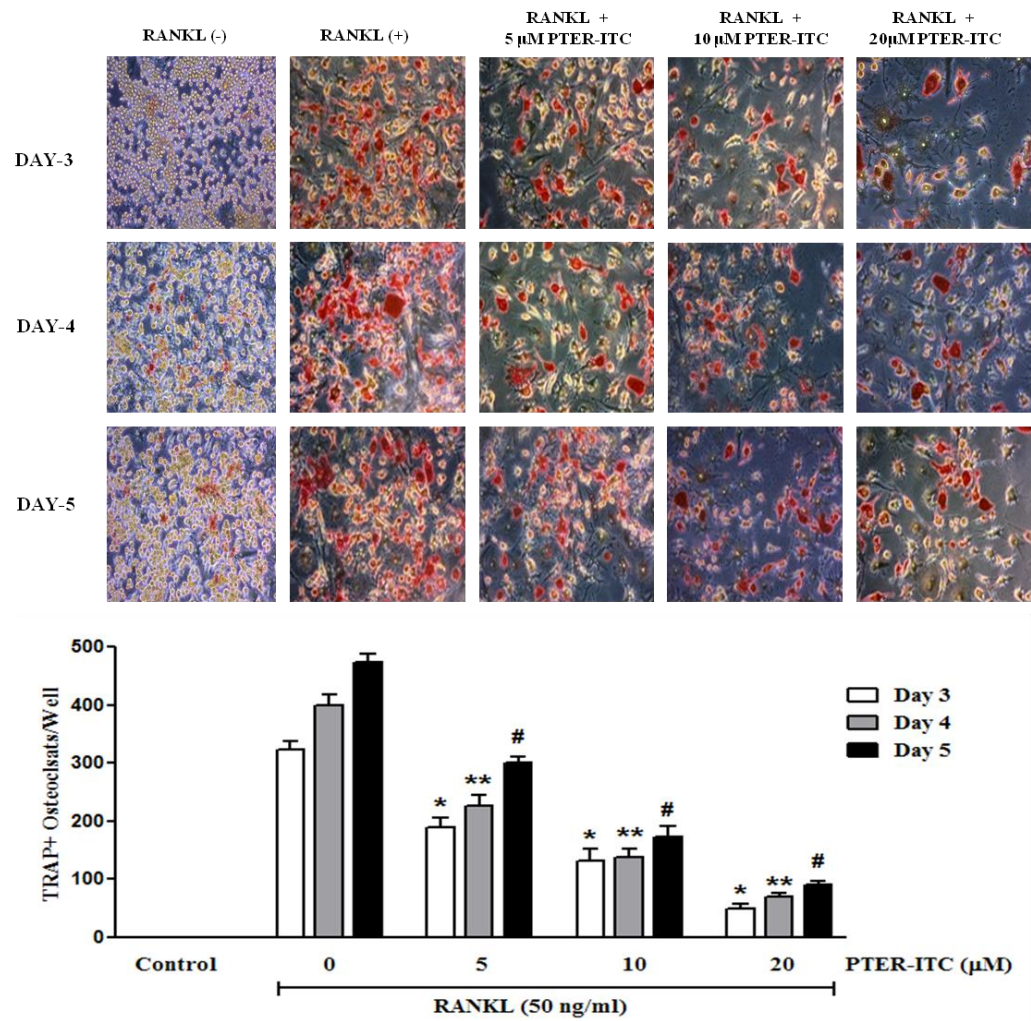
Figure 10.2: PTER-ITC inhibits RANKL induced osteoclastogenesis. RAW264.7 cells were incubated with RANK alone (50 ng/mL) or with RANKL plus PTER-ITC (5, 10 and 20 µM) for 3, 4 or 5 days and then stained for TRAP expression. TRAP-positive cells were photographed (100X magnifications). Histogram on the lower panel shows quantification of multinucleated osteoclast (i.e., those containing two or more nuclei) Values are mean ± SEM from three independent experiments. *, ** and # indicate statistically significant differences compared to only RANKL treated groups at day 3, 4 and 5 days respectively, $p<0.05$.

10.3.3 PTER-ITC inhibits osteoclastogenesis induced by tumor cells

Osteoclastogenesis is commonly linked with various cancers including breast cancer through the activation of RANK-RANKL signaling pathway [Chikatsu et al., 2000]. Breast cancer cell lines like MDA-MB-468 cells are known to constitutively express NF-κB and RANKL. Hence, in the next part of the study we next investigated whether PTER-ITC inhibits tumor cell-induced osteoclastogenesis of RAW264.7 cells. Our result indicated that incubating monocytes with MDA-MB-468 cells induced osteoclast differentiation, and that PTER-ITC suppressed this differentiation (Fig. 10.3). These results indicate that osteoclastogenesis induced by tumor cells is significantly suppressed by the presence of PTER-ITC.
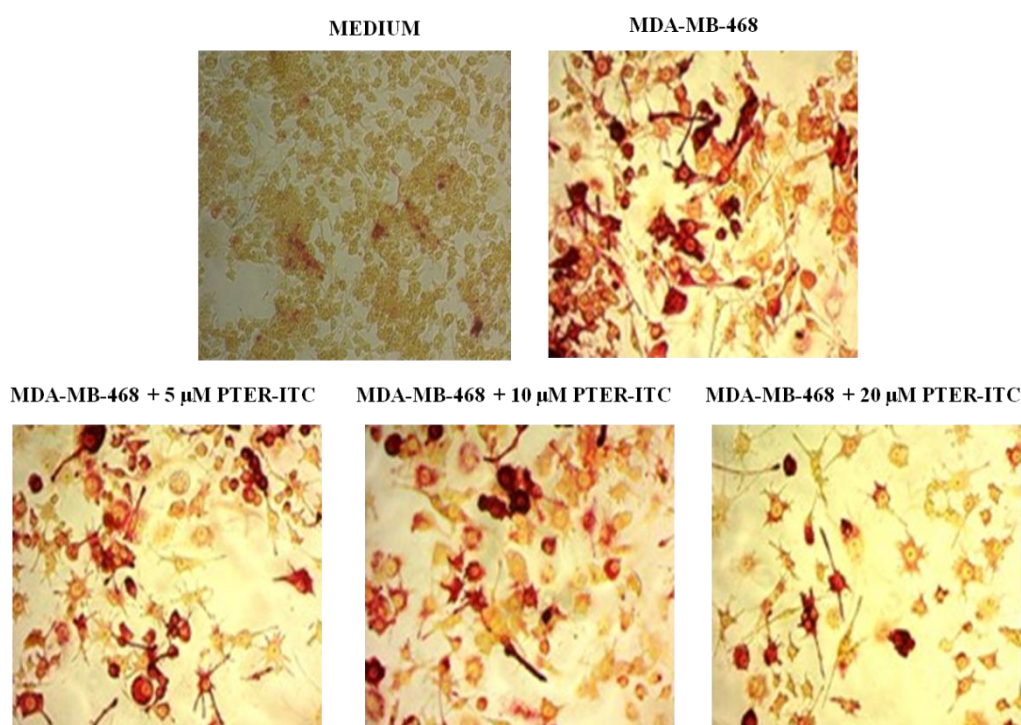
Figure 10.3: PTER-ITC suppressed osteoclastogenesis induced by tumor cells. RAW264.7 cells were incubated in the presence of MDA-MB-468 cells and exposed to PTER-ITC for 5 days, and finally stained for TRAP expression. Figures show one representative experiment of three performed.

10.3.4 Effects of PTER-ITC on expression of osteoclastic marker gene in RANKL stimulated RAW264.7 cells

To further evaluate the osteoclastic changes, we examined the effect PTER-ITC on mRNA expression levels of osteoclast specific genes using semi-quantative RT-PCR. The osteoclastic markers including TRAP, CTSK and MMP 9 were significantly up regulated upon treatment with RANKL. However, the upregulation of osteoclastic marker genes was attenuated in the presence of varying dose of PTER-ITC (Fig. 10.4).
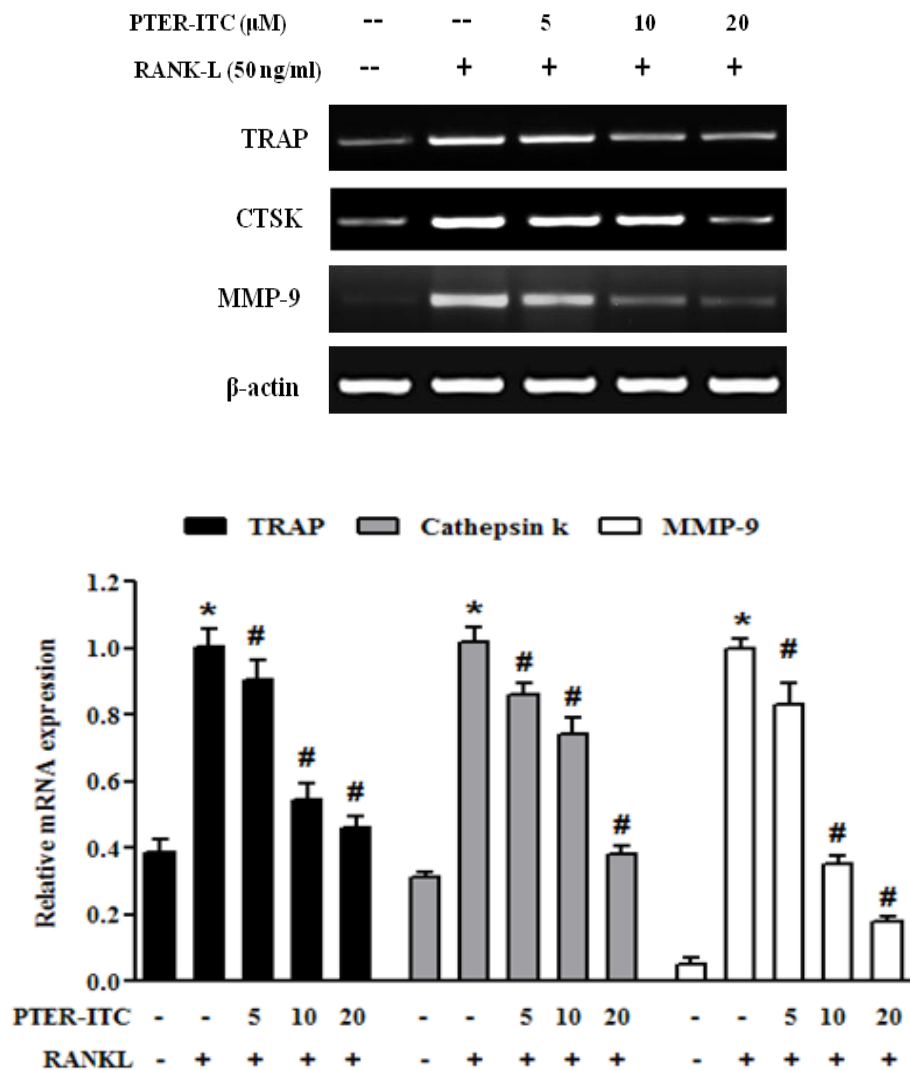
Figure 10.4: PTER-ITC inhibited RANKL induced mRNA expression levels of osteoclasts related genes. RAW264.7 cells were cultured with the indicated concentration of PTER-ITC in presence of RANKL (50 ng/mL). After 5 days of culture, the levels of osteoclasts related genes were determined by RT-PCR. Histogram (lower panel) shows relative band intensities normalized to the corresponding β-actin level. Bar shows mean ± SEM of three independent experiments. * and # indicate statistically significant differences with respect to control and only RANKL treated group respectively, $p<0.05$

10.3.5 PTER-ITC inhibits RANKL-induced osteoclast specific transcription factors

c-Fos and NFATc1 are considered to be two of the most important osteoclast specific transcription factors. The NFATc1 gene has been identified as the most strongly induced transcription factor after RANKL stimulation and is considered to be the master regulator of osteoclastogenesis. To elucidate the molecular mechanisms of the effect of PTER-ITC on osteoclastogenesis, we examined whether PTER-ITC modulates these transcription factors by RT-PCR in RANKL-stimulated RAW264.7 cells. In accord with previous results, treatment with RANKL significantly upregulated both c-Fos and NFATc1 mRNA levels while pretreatment with PTER-ITC significantly downregulated RANKL-induced expression of both of the genes.
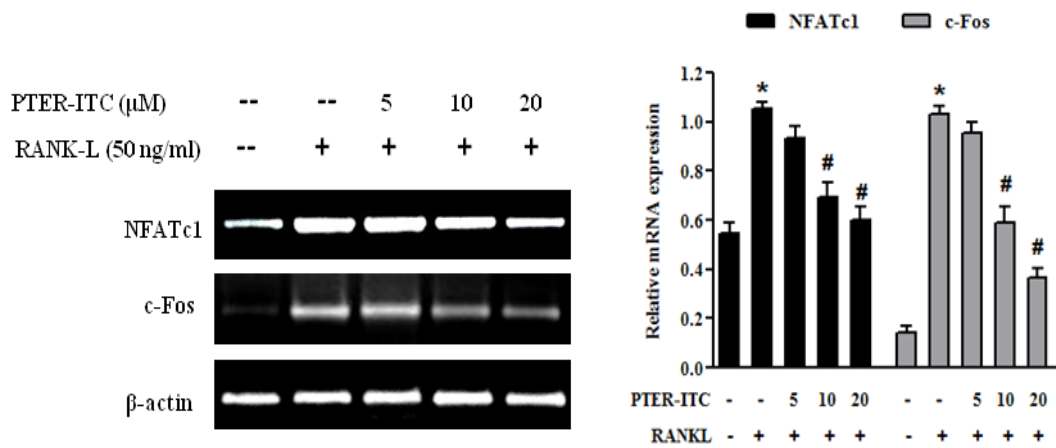
Figure 10.5: Inhibition of transcription of NFATc1 and c-Fos expression by PTER-ITC. RAW264.7 cells were preincubated with vehicle or indicated concentration of PTER-ITC for 2 h and then treated with RANKL (50 ng/mL) for another 48 h. Total RNA was isolated and RT-PCR was performed to detect NFATc1 and c-Fos mRNA levels with β-actin mRNA as endogenous control. Histogram (right panel) shows relative band intensities normalized to the corresponding β-actin level. Bars show mean ± SEM of three independent experiments. * and # indicate significant differences with respect to vehicle control and only RANKL-treated groups, respectively at $p<0.05$.

10.3.6 Effects of PTER-ITC on ROS generation stimulated by RANKL

Since it is known that intracellular ROS production is correlated with RANKL stimulated osteoclastogenesis [Lee et al., 2005; Ha et al., 2004; Kharkwal et al., 2012], we investigated whether PTER-ITC inhibits ROS production during RANKL-mediated osteoclast differentiation using a cell-permeable, oxidation-sensitive dye, DCFH-DA. Our data showed that the production of ROS was increased by stimulation with RANKL and this increase was dose dependently inhibited by PTER-ITC (Fig. 10.6A and 10.6B).
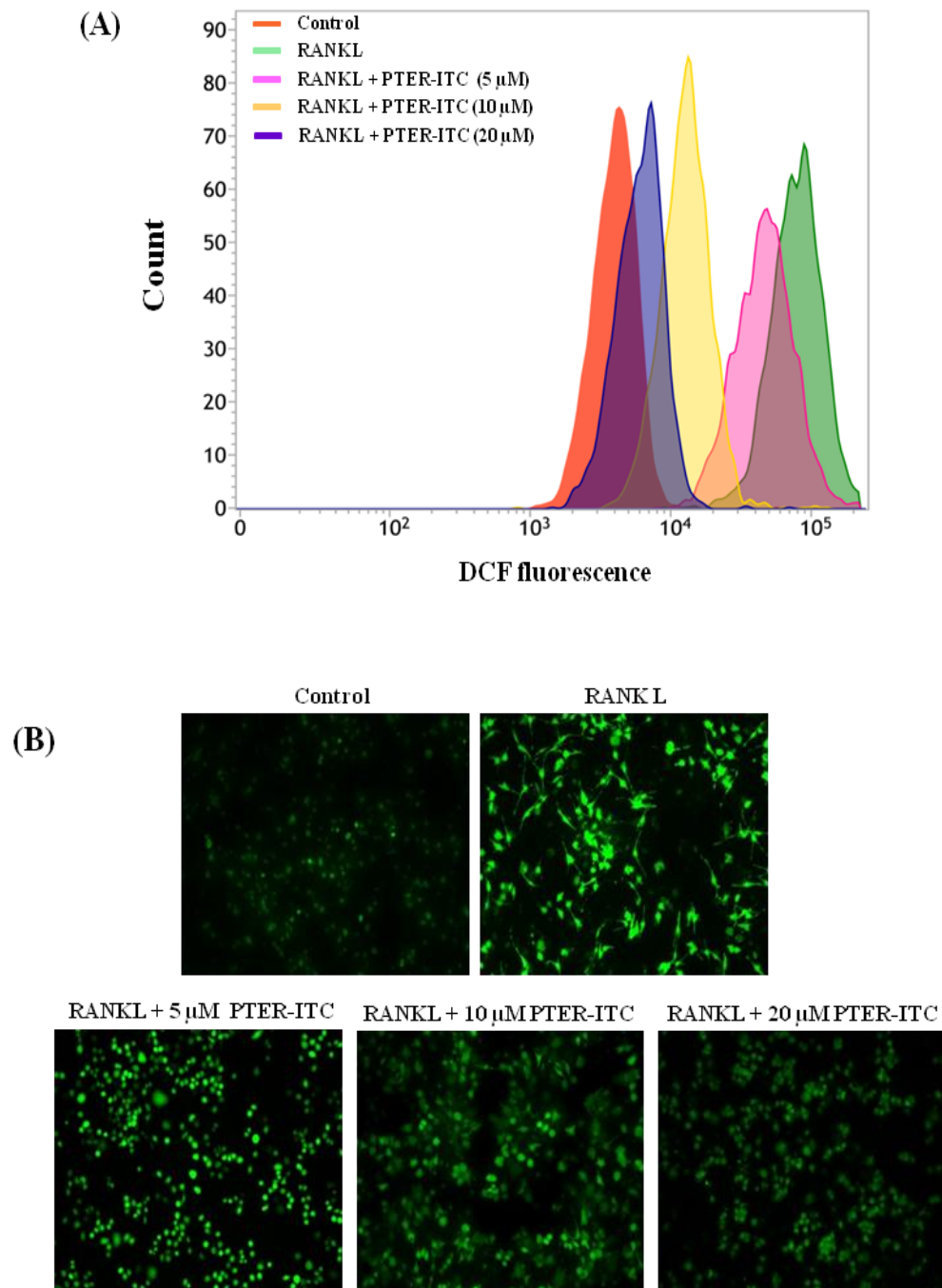
Figure 10.6 PTER-ITC inhibited RANKL induced ROS production. (A) FACS analysis of ROS generation using DCFH-DA in cells exposed to RANKL (50 ng/mL) with or without PTER-ITC pretreatment. The figure was obtained from three independent experiments with similar pattern. (B) ROS accumulation within cells in response to different doses of PTER-ITC treatments as estimated by H2-DCF-DA staining (100X magnifications).

10.3.7 PTER-ITC inhibits early RANKL signalling pathway in RAW264.7 cells

RANKL induces the activation of 3 well-known MAPKs and NFκB in osteoclast precursors and this activation is required for early osteoclast differentiation. To understand the probable mechanisms by which PTER-ITC inhibits osteoclastogenesis, we investigated the effect of PTER-ITC on MAPKs and NFκB activation in macrophages. For this RAW264.7 cells were pre-treated with 5, 10 and 20 μM of PTER-ITC for 2 h and then stimulated with 50 ng/mL RANKL for 30 min. Our result showed that RANKL strongly activated p38 MAPK, ERK 1/2, and JNK phosphorylation in RAW264.7, whereas the RANKL-induced phosphorylation was inhibited by PTER-ITC, most effectively for JNK, followed by ERK 1/2, with no significant change for p38 MAPK (Fig. 10.7).
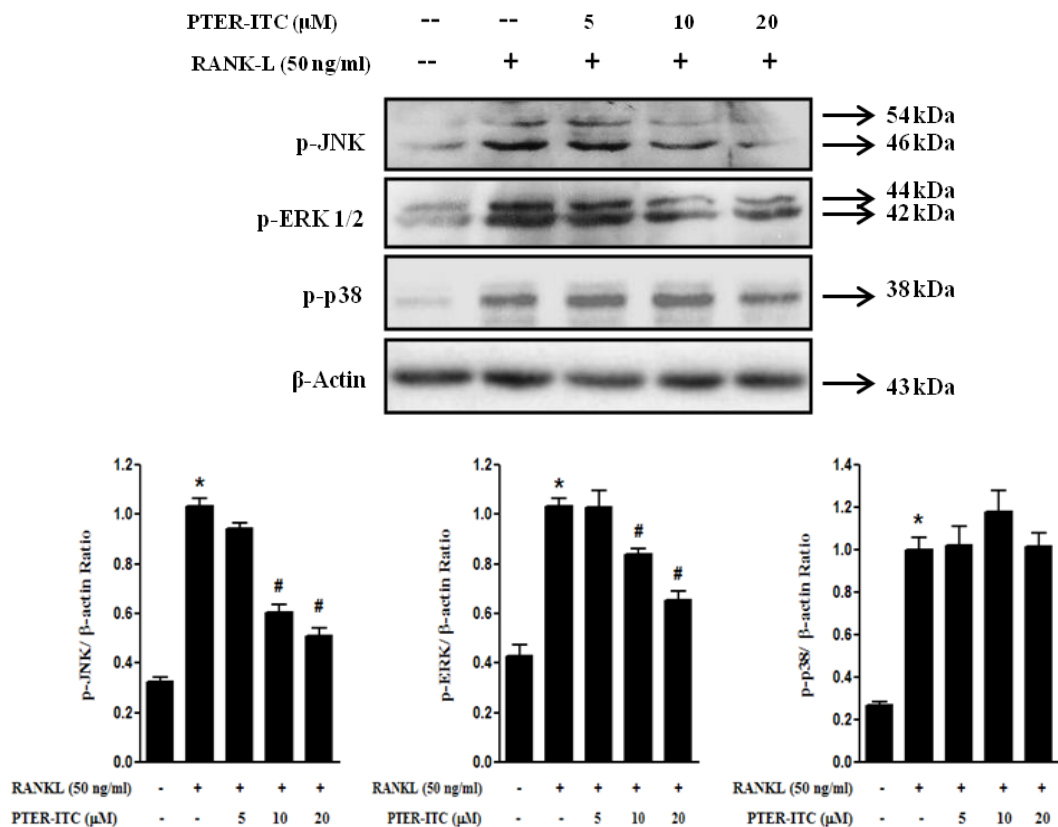
Figure 10.7 PTER-ITC inhibit RANKL induced MAPK signaling pathways. RAW264.7 cells were preincubated with the indicated concentrations of PTER-ITC for 2 h, and then treated with 50 ng/mL RANKL for 30 min. Total protein was then extracted and subjected to western blot analysis. Histogram (lower panel) shows relative band intensities normalized to the corresponding β-actin level. Bars show mean ± SEM of three independent experiments. * and # indicate significant differences with respect to vehicle control and only RANKL-treated groups, respectively at $p<0.05$.

RANKL-induced NFκB activation is essential in initiating osteoclast differentiation. To determine whether PTER-ITC inhibited NFκB mediated osteoclastogenesis, we investigated NFκB activation in RAW264.7 cells affected by PTER-ITC employing two different approach. First, using immunoblot analysis, we showed that PTER-ITC reduced RANKL-induced phosphorylation and degradation IκBα (Fig. 10.8; upper panel), as well as the subsequent nuclear translocation of NFκB subunit (Fig. 10.8; lower panel). Secondly, we performed immunofluorescence staining of p65 with or without PTER-ITC treatment. As shown in Fig. 10.9, in the absence of RANKL, most p65 subunits were located in the cytoplasm. Upon RANKL stimulation, almost all p65 units were located in the nucleus after 30 min of incubation. However, the RANKL induced p65 nuclear translocation was blocked when the cells were pretreated with PTER-IC. These results indicated that PTER-ITC could inhibit RANKL-mediated activation of the NFκB pathway. A similar pattern of inhibition of migration of p65 units was seen in immunoblot analysis as well (Fig. 10.8) whether PTER-ITC inhibited the migration of p65 subunit.
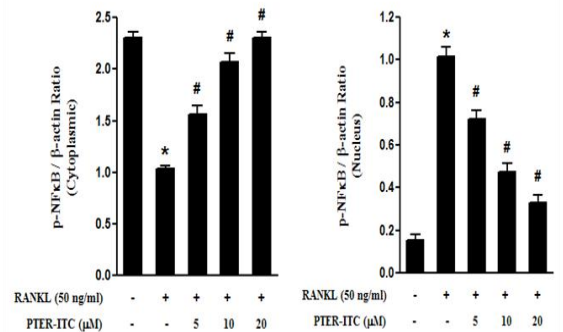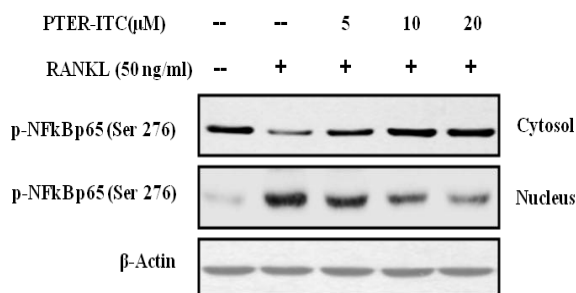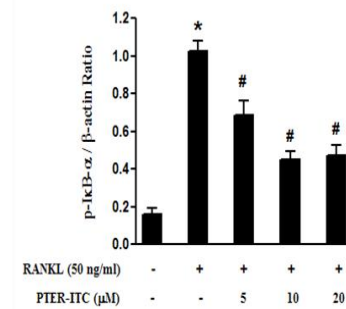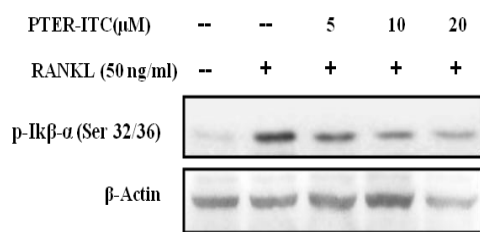
Figure 10.8 PTER-ITC inhibit RANKL induce NFκB/IκB signaling pathways. RAW264.7 cells were preincubated with indicated concentrations of PTER-ITC for 2 h, and then treated with 50 ng/mL RANKL for 30 min. Total, cytoplasmic, or nuclear protein was then extracted, and subjected to western blot analysis using antibodies against p-NFκB p65, p-Ikβ-α or β-actin. Histogram on right panel of each figure shows relative band intensities normalized to the corresponding β-actin level. Bars show mean ± SEM of three independent experiments. * and # indicate significant differences with respect to vehicle control and only RANKL-treated groups, respectively at $p < 0.05$.
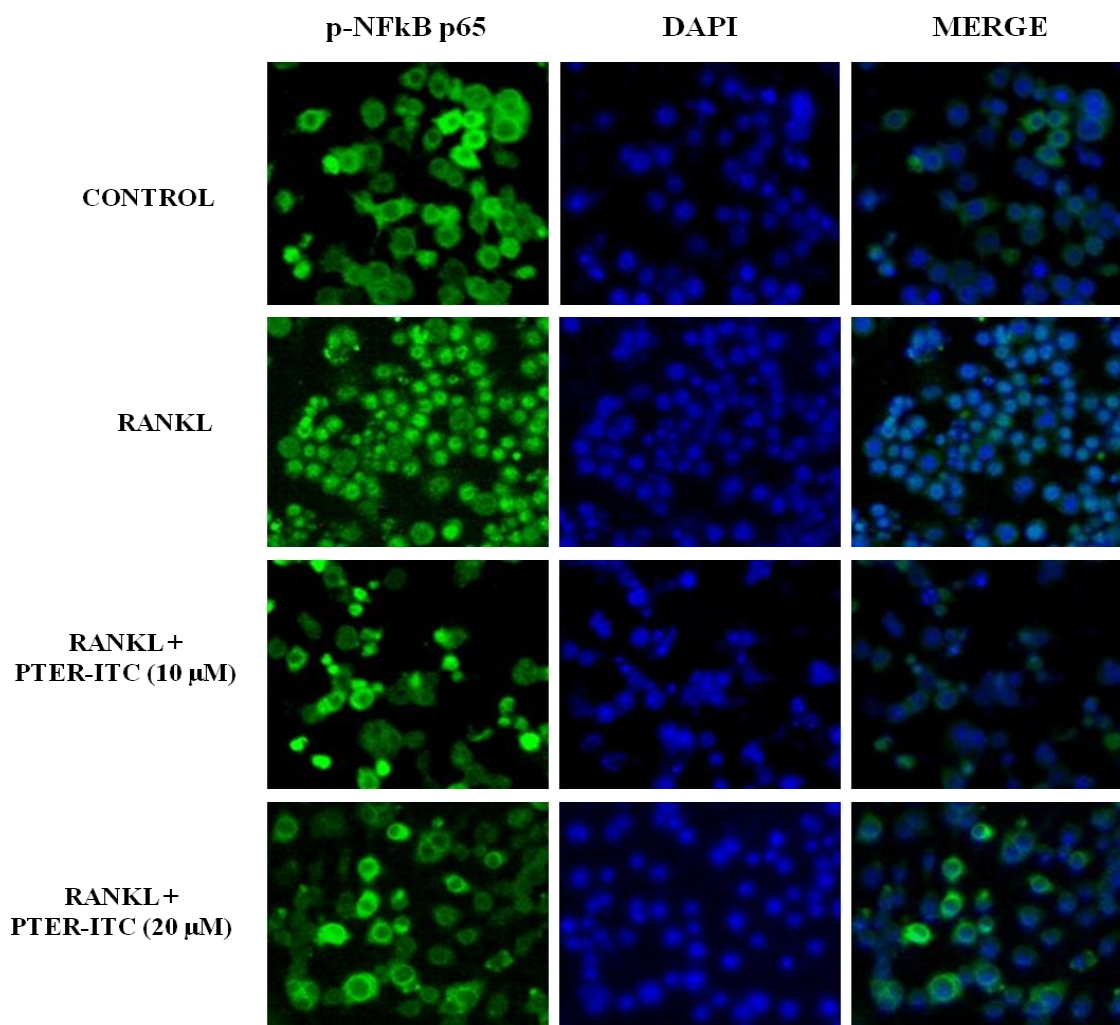
Figure 10.9: Nuclear translocation of p-NFκB p65 was detected by immunofluorescence analysis in cultured RAW264.7 cells. RAW264.7 cells were incubated with 10 and 20 μM PTER-ITC for 2 h, and then treated with 50 ng/mL RANKL for 30 min. Immunofluorescence staining was performed to locate p-NFκB p65 (green). Nuclear counter-staining was performed using DAPI (blue).

10.4 Discussion

Bone is constantly regenerated through continuous formation by osteoblasts and resorption by osteoclasts, which is termed remodeling. Excessive bone resorption plays a central role in pathologic bone [Novack and Teitelbaum, 2008]. Thus safe, efficacious, and affordable compounds that can inhibit bone loss are needed. To date, various drugs have been developed and applied to treat bone loss related diseases. One such compound is RESV, a polyphenolic phytoestrogen with osteogenic and osteoinductive properties [Boissy et al., 2005; Lee et al., 2010; He et al., 2010]. Despite its promising properties, RESV's rapid metabolism and low bioavailability have precluded its advancement to clinical use [Aggarwal et al., 2004].

Structural modifications of RESV may lead to analogues with improved potency and specificity compared with the parental agent, thereby being more tolerable and safer. In this study, we used a synthetic derivative of PTER (an analogue of resveratrol) and tested its effect on osteoclasts differentiation *in vitro*. For this study, we used homogeneous, clonal population of murine monocytic cell RAW264.7 and stimulated it with RANKL to differentiate it into osteoclasts in the presence of PTER-ITC. Our result showed that PTER-ITC inhibits RANKL induced osteoclast differentiation without causing any significant decrease in viability of RAW264.7 cells.

In bone regulation, RANKL-induced intracellular ROS production serves to regulate the RANKL signaling pathways required for osteoclast differentiation and act as an upstream component of signaling pathways that mediate osteoclast activation and survival [Ha et al., 2004; Lee et al., 2005]. Here, we show that ROS was generated within RAW264.7 cells during RANKL simulated osteoclast differentiation. This ROS production during RANKL-simulated osteoclast differentiation decreased distinctly when the RAW264.7 cells were pretreated with PTER-ITC. From these findings, we hypothesized that PTER-ITC might suppress osteoclast differentiation by scavenging the generated intracellular ROS, which acts as a secondary messenger in the RANKL osteoclast differentiation signaling pathway.

Several transcription factors have been suggested to mediate the induction of genes implicated in osteoclastic differentiation in response to RANKL. The NFκB, c-Fos and NFATc1 transcription factor functions downstream of RANKL signaling for osteoclasts differentiation. The c-Fos/c-Jun/NFATc1 pathway plays a critical and essential role in osteoclast development, and the lack of any of these three components arrests osteoclastogenesis [Teitelbaum, 2004]. In this study, RANKL-induced expression of c-Fos and NFATc1 was dramatically down-regulated with pretreatment with PTER-ITC. NFATc1 can regulate the expression of a number of genes associated with osteoclast differentiation and function, such as TRAP, latent transforming growth factor b–binding protein3 (LTBP3), chloride channel (ClC7), MMP9, CTR, Cathepsin K and c-Src. In this study, we examined the NFATc1-regulated gene expression, such as TRAP, MMP9 and CTSK. Our data showed that the expression of all these genes was decreased by PTER-ITC, suggesting that PTER-ITC affects not only the expression of NFATc1 but also regulated the downstream gene expressions.

The importance of NFκB in RANKL/RANK pathways for osteoclastogenesis is well understood by the findings from genetic and pharmacological studies. The classical NFκB signaling pathway involves activation of the, IκB kinase (IKK) complex, which phosphorylates IκBα and targets it for ubiquitin-dependent degradation [Asagiri and Takayanagi, 2007; Kim et

al., 2010]. In a previous study, we reported that PTER-ITC anti-inflammatory properties are probably due to its ability to inhibit the NFκB signalling pathway, which has also been demonstrated to be a major mediator of bone loss [Xu et al., 2009]. For example, mice lacking the NFκB subunits p50 and p52 and mice deficient in IKKβ show severe osteopetrosis caused by failure of osteoclast formation [Franzoso et al., 1997; Zheng et al., 2006]. Furthermore, AbuAmer and colleagues reported that a IκB super-suppressor blocked osteoclast differentiation and activation [Abu-Amer et al., 2001], and that a dominant-negative IκB protein lacking the NH2-terminal phosphorylation site lowered NFκB activation and suppressed recruitment of osteoclasts [Clohisy et al., 2003]. Therefore, a compound that inhibits NFκB is very likely to be able to inhibit osteoclastogenesis as well. Our results showed that PTER-ITC inhibited cytoplasmic degradation of IκBα and the nuclear translocation of p50 and p65 proteins, resulting in reduced levels of NFκB transactivation. The results indicated that inhibition of the NFκB-dependent pathway is one of the mechanisms involved in the antiosteoclastogenic effect of PTER-ITC. Besides the NFκB pathway RANKL stimulation has been shown to activate three major subfamilies of MAPKs (p38 MAPK, ERK 1/2 and JNK). These MAPKs also play pivotal roles in the development of osteoclasts, and are thus key molecular targets for therapeutic application in inflammatory bone disease [Stevenson et al., 2011]. In this current study, we demonstrated that PTER-ITC inhibited RANKL-induced phosphorylation of JNK and ERK in RAW264.7 cell suggesting that PTER-ITC could suppress MAPK cascades.

In our study, PTER-ITC inhibited osteoclastogenesis induced by breast cancercells, indicating that this compound is an attractive potential agent for treating patients with metastasis to the bone. Bisphosphonates are the current standard treatment for patients with bone metastasis or cancer-related bone disease [Terpos and Rahemtulla, 2004; Neville-Webbe and Coleman, 2010]. However, not all patients respond to bisphosphonates, and toxicities such as renal impairment or osteonecrosis of the jaw can preclude the use of bisphosphonates [Kyle et al., 2007]. The RANKL antibody denosumab (Prolia), a humanized monoclonal antibody against RANKL, was recently approved by the US Food and Drug Administration for the treatment and prevention of post menopausal osteoporosis and bone loss in patients with hormone-treated prostate or breast cancer [Body et al., 2006]. However, denosumab carries black box warnings for serious side effects, such as severe jawbone problems (osteonecrosis), skin problems (dermatitis, rash, eczema and serious skin infections) and hypocalcaemia. In addition, this antibody treatment is expensive. Therefore, safe treatments for bone loss are still needed.

In summary, the present study demonstrated that PTER-ITC inhibits RANKL and breast cancer cell induced osteoclastogenesis *in vitro*. PTER-ITC prevents RANKL-induced activation of MAPKs and transcription factors such as NFκB, c-Fos and NFATc1. Although additional experiments are needed to confirm the efficacy of PTER-ITC in treating disease conditions *in vivo*, our results indicate that PTER-ITC has potential as a therapy for disorders associated with bone loss. Our future goal is to examine the potential of PTER-ITC against osteoclastogenesis using clinically relevant animal models before proceeding to cancer patients.

Chapter 11. Summary

Cancer, defined as an uncontrolled growth of abnormal cells, is an unbeaten health challenge for the humankind. Our current understanding that cancer is a systemic multifactorial disease has led us to consider that targeting a single gene may not be effective in eradicating cancer. Worldwide, the prevalence of cancer is still on rise and requires an appropriate strategy to reduce the morbidity and mortality arising from such disease. A recent approach for the rational design of new drug candidates called combinational therapy (hybrid drug) approach, has gained increasing attention by many research groups across the globe [Nepali et al., 2014]. These hybrid drugs have the capacity to interact with multiple targets as one single molecule, lowering the risk of drug-drug interactions and minimizing drug resistance. The present thesis deals with synthesis, characterization and understanding the mode of action of one such hybrid compound developed in our laboratory for prevention of breast and prostate cancer. The current chapter depicts the major findings of this entire thesis to provide an overview of this thesis work and its implications in prevention of cancer and associated malignancies.

Phytochemicals represent a good alternative to the use of cytotoxic chemicals for chemotherapy. These molecules are able to induce apoptosis in cancer cells without affecting the normal cells of the body, an ability which makes them suitable candidates for further research into their underlying anti-cancer effects and their possible modes of actions [Lee et al., 2011; Lee et al., 2014; Shukla et al., 2014]. Given the complex nature of the cancer disease, a combination of the haptophoric moieties (groups responsible for immunogenic response) of two or more such phytochemicals could be a better approach to chemotherapy, than single agent based therapies. Such hybrid molecules can block the spread of cancer by multiple modes or pathways. The naturally occurring RESV and ITC attract great attention due to their wide range of biological properties, including anticancer, antileukemic, antibacterial and anti-inflammatory activities. However, the existing literatures are somewhat ambiguous about the chemopreventive activity of ITC which suggests that not all of them are suitable for their use as chemopreventive agents [Fimognari et al., 2004]. Due to their electrophilic reactivity, some ITCs are able to form adducts with DNA and induce mutations and chromosomal aberrations [Fimognari et al., 2012]. RESV on the other hand requires high concentration to obtain the desired effects, has potential toxicity and complex mechanisms of actions [Aggarwal et al., 2004]. Based on these reports and biological importance of these phytochemicals we hypothesized that by combining PTER (analogue of RESV) with ITC, the newly developed conjugate molecule could bypass some of their individual toxic effects and at the same time

261

would complement each other for cancer prevention. In order to prepare such a hybrid compound we searched for the pharmacophores which contain ITC motif and found it in thiosemicarbazide moiety which is biologically very potent in mediating anticancer effects through pleiotropic mechanisms similar to ITC. Thus a novel conjugate was prepared by appending ITC containing thiosemicarbazide pharmacophore to the PTER backbone. The synthesized hybrid was characterized by IR, NMR, and Mass spectroscopy and its purity was confirmed through HPLC. The synthesized conjugate molecule (PTER-ITC) and parent molecule, PTER were initially tested for their cytotoxic activity in selected human cancer cell lines of breast and prostate cancer origin by MTT assay. Our results showed that both PTER and PTER-ITC caused a dose dependent inhibition in the viability of the cancer cells and the PTER-ITC molecule was more effective at a comparatively lower dose than PTER in various cancer cell lines tested. These data are consistent with various other conjugate molecules already under investigation for their anti-cancer activities [Adsule et al., 2010; Wittman et al., 2001; Gupta et al., 2010; Mandeville et al., 2008].

The next obvious question answered was whether the conjugate molecule also caused apoptosis. It was found that the PTER-ITC caused more efficient apoptosis which was linked to the up regulation of caspase activity and cell membrane blebbing even more strongly than PTER and 5-FU in MCF-7 breast cancer cells. PTER-ITC displayed specificity by significantly increasing only caspase-9 activity while not activating caspase-8. Pharmacological inhibition of caspase-9 almost completely protected the cells from PTER-ITC induced apoptosis while inhibition of caspase-8 had little or no effect, indicating the possibility that PTER-ITC induced apoptosis is specific to the mitochondrial intrinsic pathway. On the other hand, PTER and 5-FU showed up-regulation of caspase-8 and caspase-9 coupled with subsequent increase in caspase-7 activation, indicative of activation of both intrinsic and extrinsic pathways which was in contrary to the PTER-ITC. PTER-ITC induces apoptosis by enhancing the expression of apoptotic genes both at transcriptional and translational levels as characterized by over expression of Bax, change in mitochondrial membrane potential and subsequent release of cytochrome-c from mitochondria into cytoplasm.

The developments of breast cancers are regulated by steroid hormones (mainly estrogen and progesterone) and hence majority of researches are focused on the development of anti-hormone therapies like tamoxifen. However, the biggest challenge is development of clinical resistance to these anti estrogen therapies [Sommer et al., 2001]. These limitations can be addressed with hybrid drugs which have multiple targets of action. The present data showed that PTER-ITC arrested the growth of ER positive breast cancer cell lines and was more

specifically antagonistic to ER. Several protein kinase pathways have been known to regulate cell proliferation and survival. MAPK and PI3K/AKT pathways are the major oxidative stress sensitive signal transduction pathways in most cell types including breast cancer [Acconcia et al., 2006; Björnström and Maria, 2005; Fernando and Wimalsena, 2004; Santen et al., 2002]. In the present study, our findings established a mechanistic link between the MAPK pathway, AKT, and PTER-ITC induced apoptosis in MCF-7 cells through down regulation of survivin. PTER-ITC induced a dose dependent down-regulation of PI3K/AKT, survivin, and ERK. These data suggests that the PTER-ITC treatment inhibits cell growth and enhances apoptosis via AKT and ERK/MAPK pathways in MCF-7 cells. Further the levels of survivin and caspase-9 were regulated by PTER-ITC via the PI3K/AKT pathway. Collectively, our results suggest that the modulation of ERK and AKT phosphorylation contribute to the anti-cancer effect of this PTER-ITC conjugate molecule (Fig. 11.1).
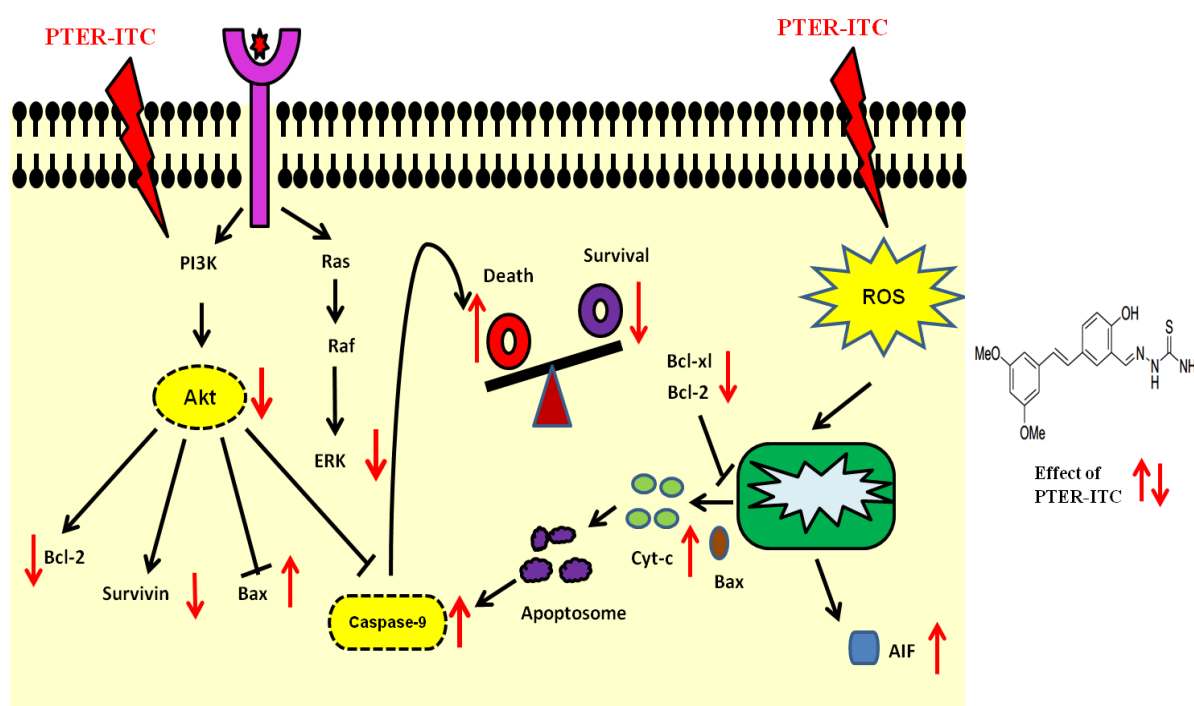
Figure 11.1: Schematic diagram representing the apoptotic pathways activated by PTER-ITC. (All markings in red show the direct regulatory action of PTER-ITC, either activation or inhibition; black arrows represent the normal pathways) PTER-ITC induces apoptosis in human breast cancer cells by acting at various cellular targets like activation of AIF, Bax, caspase-9 and decreasing Bcl2, surviving, p-Akt and p-ERK levels.

In the next phase of the study, the conjugated and non-conjugated PTER at different doses were tested *in vivo* against EAC induced tumor in Swiss albino mice. EAC is a murine spontaneous breast cancer cell that serves as the original tumor from which an ascitic variant was obtained. EAC resembles human tumors and is used in many studies as experimental model to study the antitumor or anti-angiogenic activities of drugs or natural compounds [AL Abdan, 2012; Silva et al., 2004; Ferreira et al., 2007]. Treatment with PTER and its conjugate inhibited tumor volume and also increased the lifespan of tumor bearing mice. Further, the expression level of apoptotic marker proteins like caspase-3 and Bax in tumor containing mice was suppressed upon PTER-ITC treatment suggesting the antitumor activity of this compound.

Peroxisome proliferator-activated receptors (PPAR) are a family of ligand-binding transcription factors of the nuclear receptor superfamily, which includes PPARα, PPARβ, and PPARγ [Hans and Roman, 2007; Sertznig et al., 2007]. They form heterodimers with the retinoid X receptor, and these complexes subsequently bind to a specific DNA sequence, the peroxisome proliferating response element (PPRE) of target gene promoter [Tachibana et al., 2008]. PPARγ is expressed strongly in adipose tissue and is a master regulator of adipocyte differentiation [Lehrke and Lazar, 2005]. In addition, PPARγ is also expressed in tissues such as breast, prostate, lung, ovary, thyroid, colon, tumor and cancer cell lines where it regulates cell proliferation, differentiation, and apoptosis [Zhang et al., 2005; Elstner et al., 1998; Schmidt et al., 2010]. Numerous studies have shown that both PPARγ and its agonist play an important role in prevention of breast cancer, thus acting as a tumor suppressor [Elstner et al., 1998; Woo et al., 2011; Kumar et al., 2009; Venkatachalam et al., 2009; Cui et al., 2007; Kim et al., 2006; Liu et al., 2003; Panigrahy et al., 2002]. Due to such critical role of PPARγ in breast cancer proliferation, survival, invasion, and metastasis we next continued our work to see whether PTER-ITC mediates its anti-proliferative and pro-apoptotic effects in breast cancer cells through activation of the PPARγ signaling cascade.

Three breast cancer cell lines (MCF-7, MDA-MB-231 and T47D) with distinct characteristics were chosen for this study. MCF-7 and T47D are estrogen receptor (ER)-positive and lack HER-2 expression, while MDA-MB-231 is ER-negative and has low HER-2 expression. All three cell lines were found to express PPARγ protein with maximum expression in MDA-MB-231 cells, followed by MCF-7 and T47D cell lines. Based on these both MCF-7 and MD-MB-231 cells were selected as *in vitro* models for the remaining part of the study. Initially we used a luciferase reporter-based transactivation assay to study the effect of PTER, PTER-ITC on the activity of various PPAR subtypes in breast cancer cells. Our result showed that PTER-ITC induced PPARβ and PPARγ activities, but had no significant effects on

264

PPARα, whereas PTER induced PPARα activity, with no significant change in PPARβ and PPARγ. This result was further supported by increased PPARγ transcriptional and translational activities in MCF-7 and MDA-MB-231 cells upon PTER-ITC treatment. Furthermore, molecular docking analysis suggested that PTER-ITC could interact with amino acid residues within the PPARγ-binding domain, including five polar and eight non-polar residues within the PPARγ ligand-binding pocket that are reported to be critical for its activity. Next we analyzed the effect of PTER-ITC on proliferation of breast cancer cells, and found that PTER-ITC caused significant, dose-dependent inhibition of both the breast cancer cell growth *in vitro*. This effect was however partially reversed when PTER-ITC was combined with PPARγ antagonists (GW9662) suggesting that the anticancer effects of PTER-ITC are mediated through the PPARγ activation pathway. These results were in accordance with several *in vivo* and *in vitro* studies in which PPARγ agonists such as rosiglitazone or troglitazone were reported to decrease proliferation of breast cancer cell lines, mediated in part by a PPARγ-dependent mechanism [Cui et al., 2007; Lea et al., 2004]. To establish the essential role of PTER-ITC in PPARγ-mediated apoptosis of breast cancer cells, we used both PPARγ siRNA and its chemical antagonist to inhibit PPARγ signaling, and demonstrated prevention of apoptosis and caspase activation.

PPARγ is a phosphoprotein, and its genomic activity is modulated in addition to ligand binding and many kinase pathways, such as cAMP-dependent protein kinase (PKA), AMP-activated protein kinase (AMPK) and mitogen-activated protein kinase (MAPK) such as ERK, p38 and JNK [Gardner et al., 2005; Papageorgiou et al., 2007]. To decipher the role of these protein kinase pathways in PTER-ITC induced PPAR activation and finally apoptosis of breast cancer cells we used pharmacological approach. Our results showed that activation of p38 and JNK pathways, but not of ERK, is necessary and sufficient to phosphorylate PPARγ and cause subsequent apoptosis in the breast cancer cell lines studied (Fig.11.2). At present, it is difficult to predict whether PTER-ITC activates p38 and JNK directly, or if it activates other cellular kinase pathways such as PKA and AMPK, which in turn could activate MAPK. Further validation is needed to conclusively establish the pathway(s) involved.
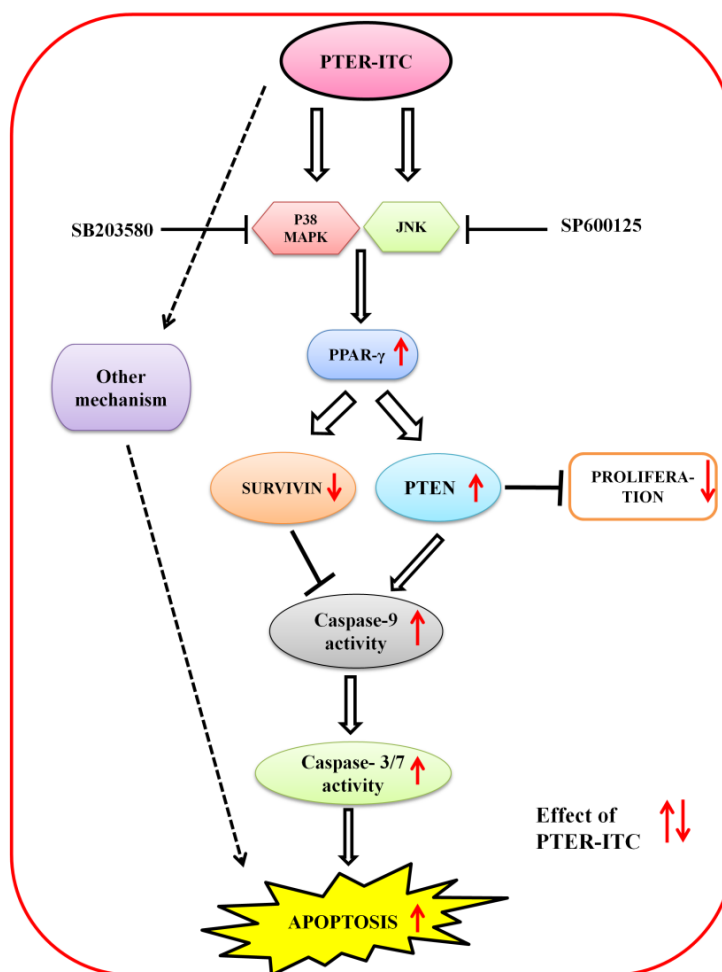
Figure 11.2: Possible mode of action of PTER-ITC-induced apoptosis and cell growth inhibition in breast cancer cells. PTER-ITC activates p38 MAPK and JNK, which in turn up regulate PPARγ expression and receptor activity. PPARγ decreases survivin and up regulates PTEN expressions, both of which in turn increases caspase-9 activities, leading to increased caspase-3/7 activity, which finally results in cell death.

As reported earlier the effect of PTER-ITC was not only restricted to inhibition of breast cancer but was also found to inhibit prostate cancer (PCa) therefore in the next part of the thesis we studied the mechanism of PTER-ITC on inhibition of PCa and the underlying mechanism. PCa proceeds through two distinct operationally divisible stages: androgen-dependent and androgen-independent. therefore, in the present study, two different cell lines, LNCaP (androgen dependent) and PC-3 (androgen independent) were used to study the effect of PTER-ITC on PCa cells growth and AR regulation. The cell proliferation assay showed that PTER-ITC caused a dose dependent cytotoxicity in both the cell lines which was independent of p53. Both PI3K/AKT and MAPK/ERK pathways played an important and differential role in

PTER-ITC-induced apoptosis of these PCa cells (Fig. 11.3). While the inhibitor of AKT (A6730) or AKT-specific small interference RNA (siRNA) greatly sensitized PC-3 cells to PTER-ITC-induced apoptosis, on the contrary, apoptosis was accelerated by inhibition of ERK (by PD98059 or ERK siRNA) in case of LNCaP cells, both ultimately culminating in the expression of cleaved caspase-3 protein and finally apoptosis of these PCa cells.

The AR is a key regulator in the development and growth of PCa and current therapeutic strategies utilizes anti-androgens that prevent AR activation and/or disrupt endogenous androgen production [Ahmed et al., 2014; Santos et al., 2004; Wong et al., 2014; Knuuttila et al., 2014]. Hence the effect of PTER-ITC on AR regulated growth was worth investigating. It was found from the present study that PTER-ITC is anti-androgenic in nature. PTER-ITC was found to disrupt androgen signaling at multiple stages of AR signaling pathways including its transcription, translation and degradation as a part of its growth arrest program in LNCaP cells. The antagonistic activity of PTER-ITC for AR was further linked to the inhibition of ligand induced nuclear localizations of AR. Our data showed that the PTER-ITC at doses (10-20 µM) prominently inhibited the nuclear localization of AR after 2 h incubation with it. However, in case of PTER-ITC and DHT co-treatments, a prominent cytoplasmic fluorescence was observed with a decrease in nuclear intensity. This may be either due to inhibition of nuclear import of AR or augmentation of nuclear export of AR. A similar pattern of inhibition was reported in case of RESV where the nuclear-localized AR decreased after incubation with 10 µM RESV for 24 h, but not for 3 h [Harada et al., 2007]. All these data suggested that PTER-ITC has a potent anti-androgenic activity (Fig. 11.3). This is the preliminary evidence in this direction which needs further validation which is beyond the scope of this thesis. However, if this concept of anti-androgenic activity of PTER-ITC is explored further for the development of anticancer molecule it may provide a drug with high efficacy but with least side effect since is active at a very low dose.
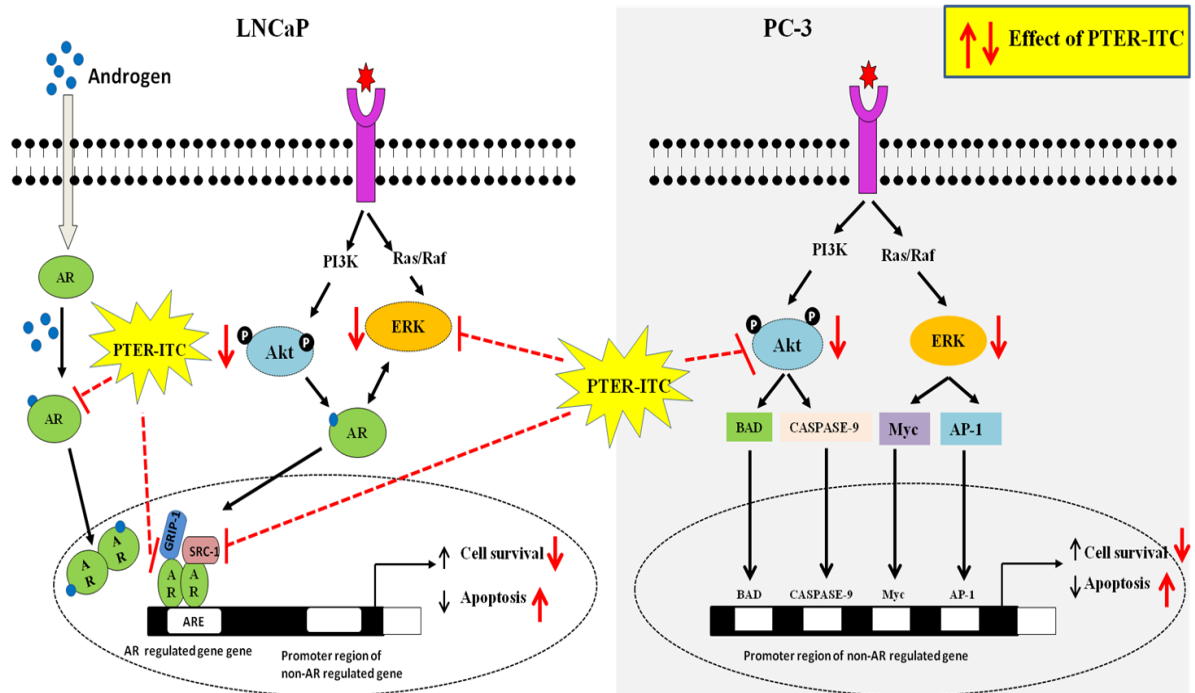
Figure 11.3: Proposed scheme for PTER-ITC mediated actions on LNCaP and PC-3 prostate cancer cells. PTER-ITC inhibits both androgen receptor and ERK signaling and finally contributing to its downstream effects of decreased cell viability and increased apoptosis in androgen receptor positive LNCaP cells. In case of androgen receptor negative PC-3 cells, inhibition of AKT and its downstream targets contributes to PTER-ITC mediated decrease in cell viability and increased apoptosis.

Angiogenesis, the process of new blood vessel formation, plays a central role in both local tumor growth and distant metastasis in cancer. The new vessels not only help to meet the growing metabolic demands of the tumor by supplying additional nutrients, but also provide potential routes for tumor dissemination and metastasis. Considering these perspectives, targeting tumor neovascularization is a favorable strategy for cancer therapy. Angiogenesis is tightly controlled by a balance between a variety of proangiogenic proteins such as VEGF, bFGF, PDGF, pleiotrophin, and antiangiogenic proteins such as TSP-1. TSP-1 is a potent endogenous inhibitors of angiogenesis that acts through direct effects on endothelial cell migration, proliferation, survival, and activating apoptotic pathways. Multiple lines of evidence suggest that estrogen directly modulates angiogenesis via effects on endothelial cells through the estrogen receptor. In addition various other studies have shown that VEGF expression can be up-regulated by estrogen in human breast tumor epithelial cell lines and that transcriptional regulation of this gene is mediated through a classical ER-α [Maity et al., 2001; Sengupta et al., 2002; Mueller et al., 2000]. TSP-1 has been shown to disrupt estrogen-induced endothelial cell proliferation and migration.

HUVECs are a valuable model of *in vitro* angiogenesis because of their ability to form capillary like structures called tubes in response to appropriate stimuli. Hence we next investigated the potential PTER-ITC conjugate, a novel RESVderivative, to inhibit angiogenesis induced by female sex steroids, particularly 17β-Estradiol (E2), on HUVEC and to elucidate TSP-1 involvement in PTER-ITC action.. Our results showed that PTER-ITC significantly inhibited 17β-E2-stimulated proliferation of HUVECs and induced apoptosis as determined by annexinV/propidium iodide staining and cleaved caspase-3 expression. Furthermore PTER-ITC also inhibited endothelial cell migration and invasion. In contrast RESV failed to inhibit 17β-E2 induced HUVECs proliferation and angiogenesis inhibition at similar dose. PTER-ITC was also found to increase TSP-1 protein expression levels in a dose-dependent manner which was however counteracted by co-incubation with p38MAPK or JNK inhibitors, suggesting involvement of these pathways in PTER-ITC action. These results suggest that the inhibitory effect of PTER-ITC on 17β-E2 induced angiogenesis is associated, at least in part, with its induction of endothelial cell apoptosis and inhibition of cell migration through targeting TSP-1.

One of the problems encountered by angiogenesis researchers has been the difficulty of finding suitable methods for assessing the *in vivo* effects of angiogenic regulators. The chick chorioallantoic membrane (CAM) assay is probably the most widely used *in vivo* assay for studying angiogenesis [Staton et al., 2004]. CAM assay was therefore performed for further evaluation of *in vivo* antiangiogenic activity of PTER-ITC. As speculated PTER-ITC significantly inhibited neovascularization ex vivo in CAM assay. In its entirety, the result from the current study suggests that PTER-ITC is a potential anti-angiogenic agent when compared to RESV. Thus PTER-ITC could be served as a potential lead compound for developing a class of new drugs targeting angiogenesis-related diseases.

Inflammatory response plays an important role not only in the normal physiology, but also has decisive roles at different stages of tumor development including initiation, promotion, malignant conversion, invasion, and metastasis [Grivennikov et al., 2010]. Different pro-inflammatory mediators and cytokines can promote tumor development and progression. Therefore, the inhibition of pro-inflammatory mediator production and the suppression of mechanisms responsible for the activation of inflammatory responses are regarded as clinical strategies for the treatment of chronic inflammation and related disease like cancer. PTER-ITC was found to be an effective inducer of apoptosis in human breast and prostate cancer cells affecting various cellular targets. This motivated us further to investigate its anti-inflammatory potential followed by understanding its probable mode of action. The newly developed

compound was tested for its anti-inflammatory actions in lipopolysachharide (LPS) stimulated RAW264.7 macrophages and carrageenan induced rat paw edema models. Our result showed that non-toxic doses of PTER-ITC could inhibit inflammatory responses against LPS-stimulated RAW264.7 cells. PTER-ITC inhibited the expression of inducible nitric oxide synthase (iNOS) and cyclooxygenase-2 (COX-2) as well as the downstream products like nitric oxide (NO), at much lower doses as compared to parent compound i.e. PTER. This effect was found to be associated with the inhibition of phosphorylation/degradation of IκB-α and nuclear translocation of the p-NFκB p65. Further, analysis of upstream regulators showed that inhibition of PI3K/AKT and MAPKs blocked the activation of NFκB (Fig. 11.4). The regulation of NFκB activity by MAPK seems to be dependent on ROS and free radicals as messenger molecule [Chung et al., 2006]. The ROS targets the cysteines within the proteins and alters the kinase activation, which further activates redox-sensitive IKK and MAPKs. N-acetyl-l-cysteine (NAC), a synthetic antioxidant, abrogates the activation of NFκB, AP-1, and MAPKs by suppressing ROS. Similar effects have also been revealed using natural antioxidants such as carnosol [Lo et al., 2002] and glycitein [Kang et al., 2007]. In this study, PTER-ITC significantly inhibited LPS-induced ROS production in RAW 264.7 cells. However, whether PTER-ITC inhibited the generation of ROS or scavenging ROS directly remained unclear. In conclusion, decrease in ROS production by PTER-ITC resulted in weakened downstream signaling activities, lower production of inflammatory mediators, and finally causing reduced cell damage.

Carrageenan-induced rat paw edema model is a suitable test for evaluating anti-inflammatory activity of a given drug. Carrageenan is a strong chemical used for the release of inflammatory and proinflammatory mediators (prostaglandins, leukotrienes, histamine, bradykinin, TNF-α) [Wills, 1969]. The edema develops following the injection of carrageenan and serves as an index of acute inflammatory changes which can be determined from the differences in paw thickness measured immediately after the injection and then every hour. In the present study, statistical analysis revealed that 10 mg/kg of indomethacin and 50 mg/kg of PTER-ITC significantly inhibited the development of edema 3 h after treatment followed by decreased level of the tissue content of NO, iNOS, and expression of COX-2 proteins within the tissues after λ-carrageenan stimulation. Taken together, our findings provide the possibility that synthetic PTER-ITC conjugate might have enhanced cancer chemopreventive potential based on its stronger anti-NFκB and anti-inflammatory activities as compared to its natural counterpart, i.e., PTER. Thus, PTER-ITC can

be used as a useful therapeutic agent to cure inflammation and inflammation-associated diseases.
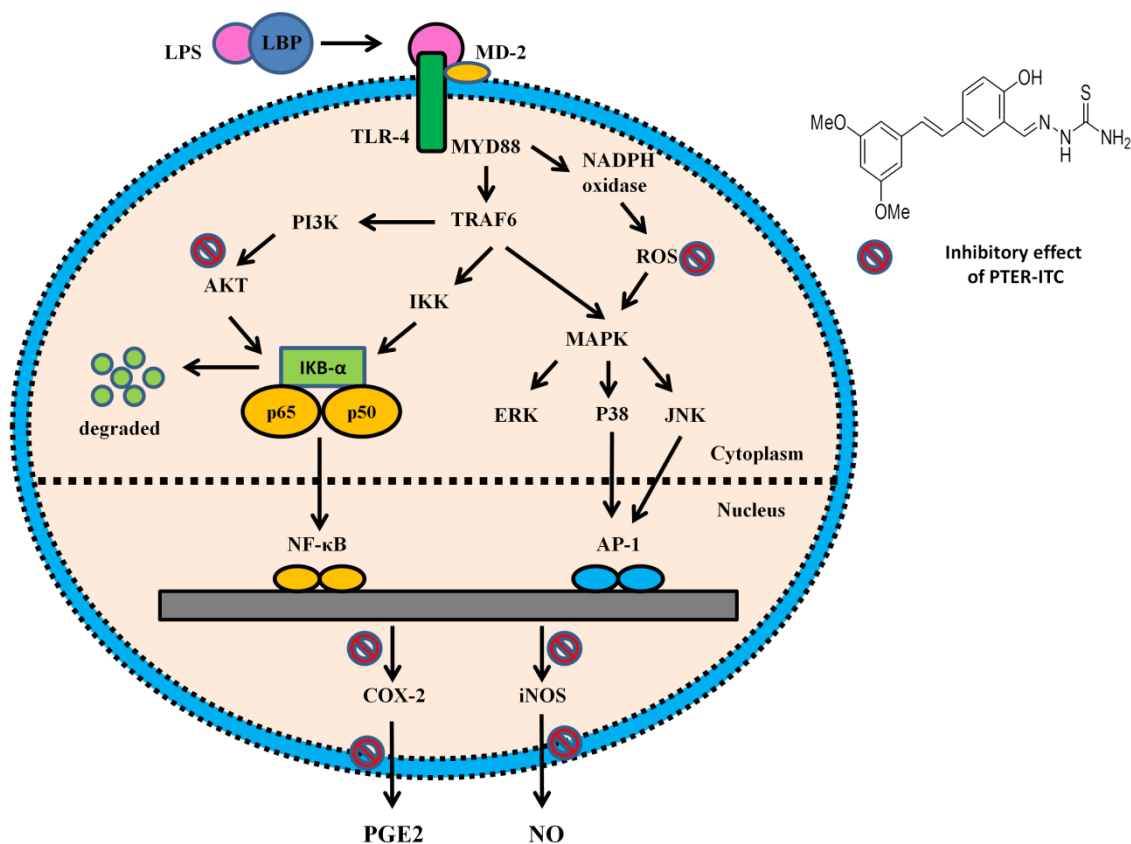
Figure.11.4. A schematic diagram showing the mechanism underlying the inhibitory action of PTER-ITC on pathways involved in inflammation. TLR-4 stimulation by LPS activates an intracellular signaling cascade that involves the recruitment of MyD88 (myeloid differentiation primary response gene-88) and results in the phosphorylation of TRAF-6 (tumor-necrosis-factor-receptor-associated factor 6). TRAF-6 then activates NFκB and MAPK pathways leading to the increased transcription of iNOS and COX-2, and subsequently causes increased production of proinflammatory mediators like PGE2 and NO. The red circle indicates the inhibition by PTER-ITC.

Many common diseases cause loss of bone, either locally in focal lesions, or more generally throughout the skeleton. Bone destruction is a common feature of cancers that invade bone (e.g. breast cancer and prostate cancer) but is also seen in inflammatory diseases both chronic (e.g. rheumatoid arthritis) and in acute bacterial infections. Central to all bone destruction in health and disease is the osteoclast cell, which is related to macrophages but is specialized to resorb (destroy) bone. Both in inflammation and in cancer, the number of osteoclasts increase greatly, resulting in bone loss. It is critical to block this bone destruction,

and to do so in a way that does not impair bone formation as many current anti-osteoclastic therapies do. Receptor activator of nuclear factor-κB (NFκB) ligand (RANKL), a member of the tumor necrosis factor superfamily has been implicated as a major mediator of bone resorption, and agents that can suppress this RANKL signaling have the potential to inhibit bone resorption or osteoclastogenesis.

As reported above, PTER-ITC could suppress cell growth and induce apoptosis in both breast and prostate cancer cells. Further it was also found to inhibit inflammatory responses against LPS-stimulated RAW264.7 cells and carrageenan induced rat paw edema. Next we wanted to explore whether PTER-ITC has a therapeutic effect on bone loss. We examined the effects of PTER-ITC on osteoclast differentiation and the related cellular mechanisms using *in vitro* experimental systems. RAW 264.7, a murine monocytic cell line was used since it undergoes differentiation to osteoclasts when exposed to RANKL. Our *in vitro* study showed that PTER-ITC suppressed the differentiation of monocytes to osteoclasts in a dose and time-dependent manner. Additionally, the expression of osteoclasts marker genes, such as tartarate-resistant acid phosphatase (*TRAP*), cathepsin K (*CTSK*), matrix metalloproteinase 9 (*MMP-9*) and transcription factors *c-Fos*, nuclear factor of activated T cells cytoplasm 1 (*NFATc1*) were also diminished by PTER-ITC (Fig. 11.5). Mechanistically PTER-ITC abrogated the phosphorylation of MAPKs (ERK and JNK), and inhibited RANKL induced activation of NFκB by suppressing IκBα phosphorylation and preventing NFκB/p65 nuclear translocation (Fig. 11.5). This study thus identifies PTER-ITC as an inhibitor of osteoclast formation and provides evidence that PTER-ITC might be an alternative medicine for preventing osteoporosis and cancer associated bone loss.
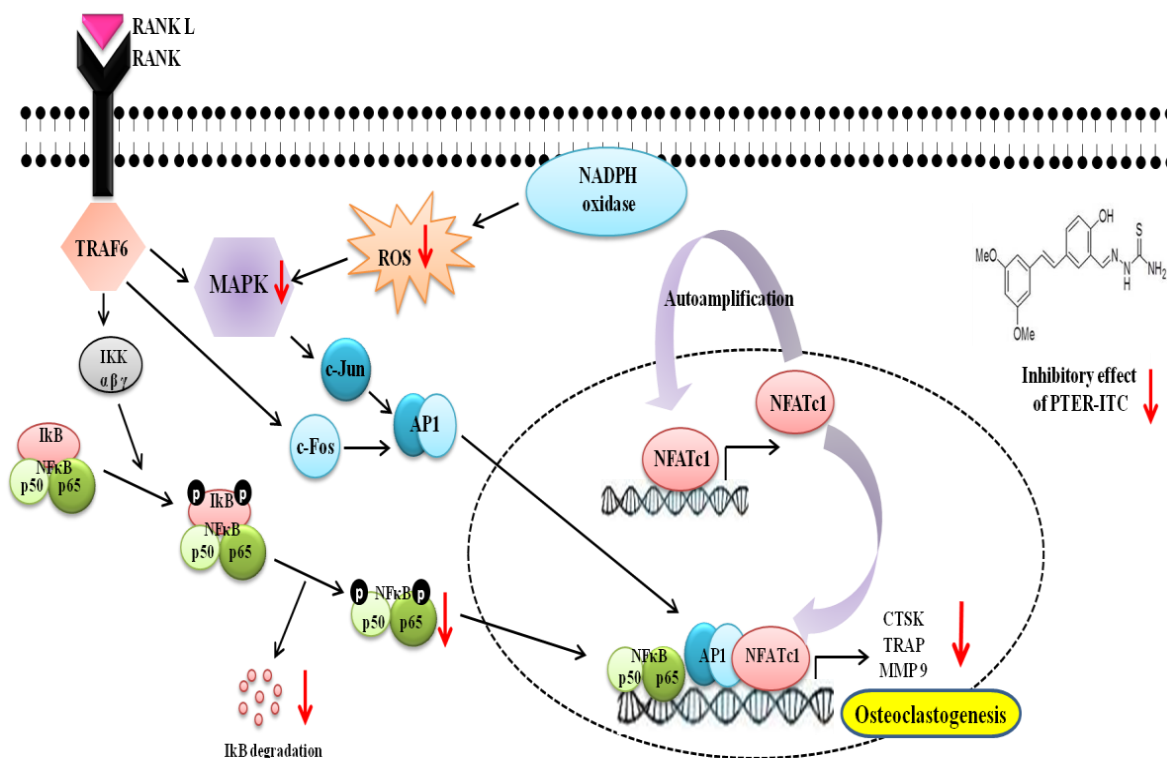
Figure.11.5. A schematic diagram showing the mechanism by which PTER-ITC inhibits osteoclast differentiation and function. RANKL-RANK signaling induces NFATc1 gene expression by the NF-kB and MAPK/AP-1 signaling pathways and then regulates osteoclastogenesis related–gene expression, such as TRAP, CTSK and MMP-9 etc. PTER-ITC on the other hand inhibits RANKL induced NF-kB and MAPK/AP-1 signaling pathways and, subsequently causes suppression of NFATc1 expression leading to inhibition of osteoclastogenesis.

In conclusion, in the present thesis a novel class of hybrid compound was screened for its anticancer properties with special emphasis on breast and prostate cancer. In addition an attempt was made to understand the anti-inflammatory and anti-osteoclastogenic potential of this molecule using both *in vitro* and *in vivo* approach. Altogether, our study reveals the superior anti-cancer effects of PTER-ITC conjugate to PTER in human breast and prostate cancer and associated complications. This study supports the notion that PTER-ITC conjugate is a promising cancer-fighting dietary component due to its stronger anti-carcinogenic effects at very low dose in comparison to PTER. Thus PTER conjugate can be suggested either alone or in combination with other clinically tested anticancer drugs to check for the synergistic effect that might potentially allow clinical chemotherapeutic dose reduction, thereby reducing toxicity while maintaining its efficacy. The information as reported in this thesis could for sure provide a platform for taking up this novel compound for further detailed preclinical and clinical studies

to test their efficacy in human systems. PTER derivative could be considered as a potential lead molecule to be patented for chemoprevention, chemosensitization, radiosensitization and / or cancer interception.

Chapter 12. Bibliography

1. Abe A, Kiriyama Y, Hirano M, Miura T, Kamiya H, Harashima H, Tokumitsu Y. Troglitazone suppresses cell growth of KU812 cells independently of PPAR gamma. Eur J Pharmacol. 2002, 436(1-2):7-13.

2. Abreu-Martin MT, Chari A, Palladino AA, Craft NA, Sawyers CL. Mitogen-activated protein kinase kinase kinase 1 activates androgen receptor-dependent transcription and apoptosis in prostate cancer. Mol Cell Biol. 1999, 19(7):5143-54.

3. Abu-Amer Y, Dowdy SF, Ross FP, Clohisy JC, Teitelbaum SL. TAT fusion proteins containing tyrosine 42-deleted IkappaBalpha arrest osteoclastogenesis. J Biol Chem. 2001, 276(32):30499-503.

4. Acconcia F, Kumar R. Signaling regulation of genomic and nongenomic functions of estrogen receptors. Cancer Lett. 2006, 238(1):1-14.

5. Acconcia F, Totta P, Ogawa S, Cardillo I, Inoue S, Leone S, Trentalance A, Muramatsu M, Marino M. Survival versus apoptotic 17beta-estradiol effect: role of ER alpha and ER beta activated non-genomic signaling. J Cell Physiol. 2005, 203(1):193-201.

6. Adams J, Palombella VJ, Elliott PJ. Proteasome inhibition: a new strategy in cancer treatment. Invest New Drugs. 2000, 18(2):109-21.

7. Adams JM, Cory S. The Bcl-2 apoptotic switch in cancer development and therapy. Oncogene. 2007, 26(9):1324-37.

8. Adsule S, Banerjee S, Ahmed F, Padhye S, Sarkar FH. Hybrid anticancer agents: isothiocyanate-progesterone conjugates as chemotherapeutic agents and insights into their cytotoxicities. Bioorg Med Chem Lett. 2010, 20(3):1247-51.

9. Agarwal ML, Taylor WR, Chernov MV, Chernova OB, Stark GR. The p53 network. J Biol Chem. 1998, 273(1):1-4.

10. Agarwal S, Amin KS, Jagadeesh S, Baishay G, Rao PG, Barua NC, Bhattacharya S, Banerjee PP. Mahanine restores RASSF1A expression by down-regulating DNMT1 and DNMT3B in prostate cancer cells. Mol Cancer. 2013, 12(1):99.

11. Aggarwal BB, Bhardwaj A, Aggarwal RS, Seeram NP, Shishodia S, Takada Y. Role of resveratrol in prevention and therapy of cancer: preclinical and clinical studies. Anticancer Res. 2004, 24(5A):2783-840.

12. Aggarwal BB, Ichikawa H, Garodia P, Weerasinghe P, Sethi G, Bhatt ID, Pandey MK, Shishodia S, Nair MG. From traditional Ayurvedic medicine to modern medicine:

identification of therapeutic targets for suppression of inflammation and cancer.Expert Opin Ther Targets. 2006, 10(1):87-118.

13. Aggarwal BB, Shishodia S, Sandur SK, Pandey MK, Sethi G. Inflammation andcancer: how hot is the link? Biochem Pharmacol. 2006, 72(11):1605-21.

14. Aggarwal BB, Shishodia S. Molecular targets of dietary agents for prevention and therapy of cancer. Biochem Pharmacol. 2006, 71(10):1397-421.

15. Agoulnik IU, Vaid A, Bingman WE 3rd, Erdeme H, Frolov A, Smith CL, Ayala G,Ittmann MM, Weigel NL. Role of SRC-1 in the promotion of prostate cancer cell growth and tumor progression. Cancer Res. 2005, 65(17):7959-67.

16. Ahmed A, Ali S, Sarkar FH. Advances in androgen receptor targeted therapy for prostate cancer. J Cell Physiol. 2014, 229(3):271-6.

17. Aïd S, Bosetti F. Targeting cyclooxygenases-1 and -2 in neuroinflammation: Therapeutic implications. Biochimie. 2011, 93(1):46-51.

18. Aird WC. Endothelial cell heterogeneity. Cold Spring Harb Perspect Med. 2012, 2(1):a006429.

19. Aka JA, Lin SX. Comparison of functional proteomic analyses of human breast cancer cell lines T47D and MCF7. PLoS One. 2012, 7(2):e31532.

20. Akira S, Takeda K. Toll-like receptor signalling. Nat Rev Immunol. 2004, 4(7):499-511.

21. Al Abdan M. Alfa-lipoic acid controls tumor growth and modulates hepatic redox state in Ehrlich-ascites-carcinoma-bearing mice. ScientificWorld Journal. 2012:509838.

22. Alderton WK, Cooper CE, Knowles RG. Nitric oxide synthases: structure, function and inhibition. Biochem J. 2001, 357(Pt 3):593-615.

23. Allred DC. Ductal carcinoma in situ: terminology, classification, and natural history. J Natl Cancer Inst Monogr. 2010, 41:134-8.

24. Alosi JA, McDonald DE, Schneider JS, Privette AR, McFadden DW. Pterostilbene inhibits breast cancer in vitro through mitochondrial depolarization and induction of caspase-dependent apoptosis. J Surg Res. 2010, 161(2):195-201.

25. Amazit L, Alj Y, Tyagi RK, Chauchereau A, Loosfelt H, Pichon C, Pantel J, Foulon-Guinchard E, Leclerc P, Milgrom E, Guiochon-Mantel A. Subcellular localization and mechanisms of nucleocytoplasmic trafficking of steroid receptor coactivator-1. J Biol Chem. 2003, 278(34):32195-203.

26. Amin KS, Jagadeesh S, Baishya G, Rao PG, Barua NC, Bhattacharya S, Banerjee PP. A naturally derived small molecule disrupts ligand-dependent and ligand-independent androgen receptor signaling in human prostate cancer cells. Mol Cancer Ther. 2014, 13(2):341-52.

27. Amit I, Citri A, Shay T, Lu Y, Katz M, Zhang F, Tarcic G, Siwak D, Lahad J,Jacob-Hirsch J, Amariglio N, Vaisman N, Segal E, Rechavi G, Alon U, Mills GB, Domany E, Yarden Y. A module of negative feedback regulators defines growth factor signaling. Nat Genet. 2007, 39(4):503-12.

28. Ansonoff MA, Etgen AM. Estradiol elevates protein kinase C catalytic activity in the preoptic area of female rats. Endocrinology. 1998, 139(7):3050-6.

29. Apantaku LM. Breast-conserving surgery for breast cancer. Am Fam Physician. 2002, 66(12):2271-8.

30. Ardestani SK, Inserra P, Solkoff D, Watson RR. The role of cytokines and chemokines on tumor progression: A review. Cancer Detect Prev. 1999, 23(3):215-25.

31. Armstrong LC, Bornstein P. Thrombospondins 1 and 2 function as inhibitors of angiogenesis. Matrix Biol. 2003, 22(1):63-71.

32. Arnal JF, Fontaine C, Billon-Galés A, Favre J, Laurell H, Lenfant F, Gourdy, P. Estrogen receptors and endothelium. Arteriosclerosis, thrombosis, and vascular biology. 2010, 30(8):1506-1512.

33. Asagiri M, Takayanagi H. The molecular understanding of osteoclast differentiation. Bone. 2007, 40(2):251-64.

34. Athar M, Back JH, Tang X, Kim KH, Kopelovich L, Bickers DR, Kim AL. Resveratrol: a review of preclinical studies for human cancer prevention. Toxicol Appl Pharmacol. 2007, 224(3):274-83.

35. Azmi AS, Bhat SH, Hadi SM. Resveratrol-Cu(II) induced DNA breakage in human peripheral lymphocytes: implications for anticancer properties. FEBS Lett. 2005, 579(14):3131-5.

36. Babior BM. Phagocytes and oxidative stress. Am J Med. 2000, 109(1):33-44.

37. Baer-Dubowska W. Cancer chemo preventive agents-drugs for the 21st century? Acta Pol. Pharm. 2006, 63:369-373.

38. Baeriswyl V, Christofori G. The angiogenic switch in carcinogenesis. Semin Cancer Biol. 2009, 19(5):329-37.

39. Baldwin AS Jr. The NF-kappa B and I kappa B proteins: new discoveries and insights. Annu Rev Immunol. 1996, 14:649-83.

40. Balkwill F, Mantovani A. Inflammation and cancer: back to Virchow? Lancet. 2001, 357(9255):539-45.

41. Balkwill F. Tumor necrosis factor or tumor promoting factor? Cytokine Growth Factor Rev. 2002, 13(2):135-41.

42. Ballif BA, Blenis J. Molecular mechanisms mediating mammalian mitogen-activated protein kinase (MAPK) kinase (MEK)-MAPK cell survival signals. Cell Growth Differ. 2001, 12(8):397-408.

43. Banerjee H, Das A, Srivastava S, Mattoo HR, Thyagarajan K, Khalsa JK, Tanwar S, Das DS, Majumdar SS, George A, Bal V, Durdik JM, Rath S. A role for apoptosis-inducing factor in T cell development. J Exp Med. 2012, 209(9).

44. Banerjee N, Banerjee S, Sen R, Bandyopadhyay A, Sarma N, Majumder P, Das JK, Chatterjee M, Kabir SN, Giri AK. Chronic arsenic exposure impairs macrophage functions in the exposed individuals. J Clin Immunol. 2009, 29(5):582-94.

45. Baniahmad A. Nuclear hormone receptor co-repressors. J Steroid Biochem Mol Biol. 2005, 93(2-5):89-97.

46. Barnes DE, Lindahl T. Repair and genetic consequences of endogenous DNA base damage in mammalian cells. Annu Rev Genet. 2004, 38:445-76.

47. Barth TF, Martin-Subero JI, Joos S, Menz CK, Hasel C, Mechtersheimer G, Parwaresch RM, Lichter P, Siebert R, Möoller P. Gains of 2p involving the REL locus correlate with nuclear c-Rel protein accumulation in neoplastic cells of classical Hodgkin lymphoma. Blood. 2003, 101(9):3681-6.

48. Baud'huin M, Duplomb L, Teletchea S, Lamoureux F, Ruiz-Velasco C, Maillasson M, Redini F, Heymann MF, Heymann D. Osteoprotegerin: multiple partners for multiple functions. Cytokine Growth Factor Rev. 2013, 24(5):401-9.

49. Baudin B, Bruneel A, Bosselut N, Vaubourdolle M. A protocol for isolation and culture of human umbilical vein endothelial cells. Nat Protoc. 2007, 2(3):481-5.

50. Baur JA, Sinclair DA. Therapeutic potential of resveratrol: the in vivo evidence. Nat Rev Drug Discov. 2006, 5(6):493-506.

51. Beadle G, Baade P, Fritschi L. Acute myeloid leukemia after breast cancer: a population-based comparison with hematological malignances and other cancers. Ann Oncol. 2009, 20(1):103-9.

52. Becker C, Fantini MC, Schramm C, Lehr HA, Wirtz S, Nikolaev A, Burg J, Strand S, Kiesslich R, Huber S, Ito H, Nishimoto N, Yoshizaki K, Kishimoto T, Galle PR,

Blessing M, Rose-John S, Neurath MF. TGF-beta suppresses tumor progression in colon cancer by inhibition of IL-6 trans-signaling. Immunity. 2004, 21(4):491-501.

53. Benchimol S. p53-dependent pathways of apoptosis. Cell Death Differ. 2001, 8(11):1049-51.

54. Ben-Neriah Y, Karin M. Inflammation meets cancer, with NF-κB as the matchmaker. Nat Immunol. 2011, 12(8):715-23.

55. Bentle MS, Reinicke KE, Bey EA, Spitz DR, Boothman DA. Calcium-dependent modulation of poly(ADP-ribose) polymerase-1 alters cellular metabolism and DNA repair. J Biol Chem. 2006, 281(44):33684-96.

56. Berman HM, Westbrook J, Feng Z, Gilliland G, Bhat TN, Weissig H, Shindyalov IN, Bourne PE. The Protein Data Bank. Nucleic Acids Res. 2000, 28(1):235-42.

57. Bhakkiyalakshmi E, Shalini D, Sekar TV, Rajaguru P, Paulmurugan R, Ramkumar KM. Therapeutic potential of pterostilbene against pancreatic beta-cell apoptosis mediated through Nrf2. Br J Pharmacol. 2014, 171(7):1747-57.

58. Bilton RL, Booker GW. The subtle side to hypoxia inducible factor (HIFalpha) regulation. Eur J Biochem. 2003, 270(5):791-8.

59. Bird BR, Swain SM. Cardiac toxicity in breast cancer survivors: review of potential cardiac problems. Clin Cancer Res. 2008, 14(1):14-24.

60. Bishayee A. Cancer prevention and treatment with resveratrol: from rodent studies to clinical trials. Cancer Prev Res (Phila). 2009, 2(5):409-18.

61. Biswas S, Kabir SN, Pal AK. The role of nitric oxide in the process of implantation in rats. J Reprod Fertil. 1998, 114(1):157-61.

62. Björnström L, Sjöberg M. Mechanisms of estrogen receptor signaling: convergence of genomic and nongenomic actions on target genes. Mol Endocrinol. 2005, 19(4):833-42.

63. Blows FM, Driver KE, Schmidt MK, Broeks A, van Leeuwen FE, Wesseling J, Cheang MC, Gelmon K, Nielsen TO, Blomqvist C, Heikkilä P, Heikkinen T, Nevanlinna H, Akslen LA, Bégin LR, Foulkes WD, Couch FJ, Wang X, Cafourek V, Olson JE, Baglietto L, Giles GG, Severi G, McLean CA, Southey MC, Rakha E, Green AR, Ellis IO, Sherman ME, Lissowska J, Anderson WF, Cox A, Cross SS, Reed MW, Provenzano E, Dawson SJ, Dunning AM, Humphreys M, Easton DF, García-Closas M, Caldas C, Pharoah PD, Huntsman D. Subtyping of breast cancer by immunohistochemistry to investigate a relationship between subtype and short and

long term survival: a collaborative analysis of data for 10,159 cases from 12 studies. PLoS Med. 2010, 7(5):e1000279.

64. Bode AM, Dong Z. Cancer prevention research - then and now. Nat Rev Cancer. 2009, 9(7):508-16.

65. Body JJ, Facon T, Coleman RE, Lipton A, Geurs F, Fan M, Holloway D, Peterson MC, Bekker PJ. A study of the biological receptor activator of nuclear factor-kappaB ligand inhibitor, denosumab, in patients with multiple myeloma or bone metastases from breast cancer. Clin Cancer Res. 2006, 12(4):1221-8.

66. Bogdan C. Nitric oxide and the immune response. Nat Immunol. 2001, 2(10):907-16.

67. Bogdan C. Nitric oxide and the regulation of gene expression. Trends Cell Biol. 2001, 11(2):66-75.

68. Boissy P, Andersen TL, Abdallah BM, Kassem M, Plesner T, Delaissé JM. Resveratrol inhibits myeloma cell growth, prevents osteoclast formation, and promotes osteoblast differentiation. Cancer Res. 2005, 65(21):9943-52.

69. Boldt S, Weidle UH, Kolch W. The role of MAPK pathways in the action of chemotherapeutic drugs. Carcinogenesis. 2002, 23(11):1831-8.

70. Bonaccorsi L, Muratori M, Carloni V, Marchiani S, Formigli L, Forti G, Baldi E. The androgen receptor associates with the epidermal growth factor receptor in androgen-sensitive prostate cancer cells. Steroids. 2004, 69(8-9):549-52.

71. Boocock DJ, Faust GE, Patel KR, Schinas AM, Brown VA, Ducharme MP, Booth TD,Crowell JA, Perloff M, Gescher AJ, Steward WP, Brenner DE. Phase I dose escalation pharmacokinetic study in healthy volunteers of resveratrol, a potential cancer chemopreventive agent. Cancer Epidemiol Biomarkers Prev. 2007, 16(6):1246-52.

72. Bornstein P. Thrombospondins as matricellular modulators of cell function. J Clin Invest. 2001, 107(8):929-34.

73. Bornstein P. Thrombospondins function as regulators of angiogenesis. J Cell Commun Signal 2009, 3:189-200.

74. Borriello A, Bencivenga D, Caldarelli I, Tramontano A, Borgia A, Pirozzi AV, Oliva A, Della Ragione F. Resveratrol and cancer treatment: is hormesis a yet unsolved matter? Curr Pharm Des. 2013, 19(30):5384-93.

75. Bossy-Wetzel E, Bakiri L, Yaniv M. Induction of apoptosis by the transcription factor c-Jun. EMBO J. 1997, 16(7):1695-709.

76. Boughey JC, Buzdar AU, Hunt KK. Recent advances in the hormonal treatment of breast cancer. Curr Probl Surg. 2008, 45(1):13-55.

77. Bouïs D, Hospers GA, Meijer C, Molema G, Mulder NH. Endothelium in vitro: a review of human vascular endothelial cell lines for blood vessel-related research. Angiogenesis. 2001, 4(2):91-102.

78. Bracarda S, de Cobelli O, Greco C, Prayer-Galetti T, Valdagni R, Gatta G, de Braud F, Bartsch G. Cancer of the prostate. Crit Rev Oncol Hematol. 2005, 56(3):379-96.

79. Bråkenhielm E, Veitonmäki N, Cao R, Kihara S, Matsuzawa Y, Zhivotovsky B, Funahashi T, Cao Y. Adiponectin-induced antiangiogenesis and antitumor activity involve caspase-mediated endothelial cell apoptosis. Proc Natl Acad Sci U S A. 2004, 101(8): 2476-81.

80. Brisdelli F, D'Andrea G, Bozzi A. Resveratrol: a natural polyphenol with multiple chemopreventive properties. Curr Drug Metab. 2009, 10(6):530-46.

81. Brivanlou AH, Darnell JE Jr. Signal transduction and the control of gene expression. Science. 2002, 295(5556):813-8.

82. Brunet A, Bonni A, Zigmond MJ, Lin MZ, Juo P, Hu LS, Anderson MJ, Arden KC, Blenis J, Greenberg ME. Akt promotes cell survival by phosphorylating and inhibiting a Forkhead transcription factor. Cell. 1999, 96(6):857-68.

83. Burkhart DL, Sage J. Cellular mechanisms of tumour suppression by the retinoblastoma gene. Nature Reviews Cancer. 2008, 8(9):671-682.

84. Burns J, Gardner PT, O'Neil J, Crawford S, Morecroft I, McPhail DB, Lister C, Matthews D, MacLean MR, Lean ME, Duthie GG, Crozier A. Relationship among antioxidant activity, vasodilation capacity, and phenolic content of red wines. J Agric Food Chem. 2000, 48(2):220-30.

85. Burri PH, Hlushchuk R, Djonov V. Intussusceptive angiogenesis: its emergence, its characteristics, and its significance. Dev Dyn. 2004, 231(3):474-88.

86. Buzdar AU. Endocrine therapy in the treatment of metastatic breast cancer. Semin Oncol. 2001, 28(3):291-304.

87. Caamaño J, Hunter CA. NF-kappaB family of transcription factors: central regulators of innate and adaptive immune functions. Clin Microbiol Rev. 2002, 15(3):414-29.

88. Caliceti C, Aquila G, Pannella M, Morelli MB, Fortini C, Pinton P, Bonora M, Hrelia S, Pannuti A, Miele L, Rizzo P, Ferrari R. 17β-estradiol enhances signalling mediated by VEGF-A-delta-like ligand 4-notch1 axis in human endothelial cells. PLoS One. 2013, 8(8):e71440.

89. Caraglia M, Marra M, Leonetti C, Meo G, D'Alessandro AM, Baldi A, Santini D, Tonini G, Bertieri R, Zupi G, Budillon A, Abbruzzese A. R115777 (Zarnestra)/Zoledronic acid (Zometa) cooperation on inhibition of prostate cancer proliferation is paralleled by Erk/Akt inactivation and reduced Bcl-2 and bad phosphorylation. J Cell Physiol. 2007, 211(2):533-43.

90. Carnero A, Blanco-Aparicio C, Renner O, Link W, Leal JF. The PTEN/PI3K/AKT signalling pathway in cancer, therapeutic implications. Curr Cancer Drug Targets. 2008, 8(3):187-98.

91. Carr AM, Lambert S. Replication stress-induced genome instability: the dark side of replication maintenance by homologous recombination. J Mol Biol. 2013, 425(23):4733-44.

92. Carter LG, D'Orazio JA, Pearson KJ. Resveratrol and cancer: focus on in vivo evidence. Endocr Relat Cancer. 2014, 21(3):R209-25

93. Carvalho H, Evelson P, Sigaud S, González-Flecha B. Mitogen-activated protein kinases modulate H(2)O(2)-induced apoptosis in primary rat alveolar epithelial cells. J Cell Biochem. 2004, 92(3):502-13.

94. Castle PE, Hillier SL, Rabe LK, Hildesheim A, Herrero R, Bratti MC, Sherman ME, Burk RD, Rodriguez AC, Alfaro M, Hutchinson ML, Morales J, Schiffman M. An association of cervical inflammation with high-grade cervical neoplasia in women infected with oncogenic human papillomavirus (HPV). Cancer Epidemiol Biomarkers Prev. 2001, 10(10):1021-7.

95. Cavell BE, Syed Alwi SS, Donlevy A, Packham G. Anti-angiogenic effects of dietary isothiocyanates: mechanisms of action and implications for human health. Biochem Pharmacol. 2011, 81(3):327-36.

96. Cha TL, Qiu L, Chen CT, Wen Y, Hung MC. Emodin down-regulates androgen receptor and inhibits prostate cancer cell growth. Cancer Res. 2005, 65(6):2287-95.

97. Chakraborty A, Bodipati N, Demonacos MK, Peddinti R, Ghosh K, Roy P. Long term induction by pterostilbene results in autophagy and cellular differentiation in MCF-7 cells via ROS dependent pathway. Mol Cell Endocrinol. 2012, 355(1):25-40.

98. Chakraborty A, Gupta N, Ghosh K, Roy P. In vitro evaluation of the cytotoxic, anti-proliferative and anti-oxidant properties of pterostilbene isolated from Pterocarpus marsupium. Toxicol In Vitro. 2010, 24(4):1215-28.

99. Chakraborty P, Saraswat G, Kabir SN. α-Dihydroxychalcone-glycoside (α-DHC) isolated from the heartwood of Pterocarpus marsupium inhibits LPS induced MAPK

activation and up regulates HO-1 expression in murine RAW 264.7 macrophage. Toxicol Appl Pharmacol. 2014, 277(1):95-107.

100. Chamras H, Ardashian A, Heber D, Glaspy JA. Fatty acid modulation of MCF-7 human breast cancer cell proliferation, apoptosis and differentiation. J Nutr Biochem. 2002, 13(12):711-716.

101. Chan LS, Daruwalla J, Christophi C. Selective targeting of the tumour vasculature. ANZ J Surg. 2008, 78(11):955-67.

102. Chang TH, Szabo E. Induction of differentiation and apoptosis by ligands of peroxisome proliferator-activated receptor gamma in non-small cell lung cancer.Cancer Res. 2000, 60(4):1129-38.

103. Chao JI, Kuo PC, Hsu TS. Down-regulation of survivin in nitric oxide-induced cell growth inhibition and apoptosis of the human lung carcinoma cells. J Biol Chem. 2004, 279(19):20267-76.

104. Chari RV. Targeted delivery of chemotherapeutics: tumor-activated prodrug therapy. Adv Drug Deliv Rev. 1998, 31(1-2):89-104.

105. Chavakis E, Dimmeler S. Regulation of endothelial cell survival and apoptosis during angiogenesis. Arteriosclerosis, thrombosis, and vascular biology. 2002, 22(6):887-893.

106. Chechlinska M, Kowalewska M, Nowak R. Systemic inflammation as a confounding factor in cancer biomarker discovery and validation. Nat Rev Cancer. 2010, 10(1):2-3.

107. Chen CC, Rosenbloom CL, Anderson DC, Manning AM. Selective inhibition of E-selectin, vascular cell adhesion molecule-1 and intercellular adhesion molecule-1 expression by inhibitors of I kappa B-alpha phosphorylation. J Immunol. 1995, 155(7):3538-45.

108. Chen M, Wang J. Initiator caspases in apoptosis signaling pathways. Apoptosis. 2002, 7(4):313-9.

109. Chen RJ, Tsai SJ, Ho CT, Pan MH, Ho YS, Wu CH, Wang YJ. Chemopreventive effects of pterostilbene on urethane-induced lung carcinogenesis in mice via the inhibition of EGFR-mediated pathways and the induction of apoptosis and autophagy. J Agric Food Chem. 2012, 60(46):11533-41.

110. Chen Y, Tseng SH. Review. Pro- and anti-angiogenesis effects of resveratrol. In Vivo. 2007, 21(2):365-70.

111. Chen YC, Wu JS, Tsai HD, Huang CY, Chen JJ, Sun GY, Lin TN. Peroxisome proliferator-activated receptor gamma (PPAR-γ) and neurodegenerative disorders. Mol Neurobiol. 2012, 46(1):114-24.

112. Cheng EH, Wei MC, Weiler S, Flavell RA, Mak TW, Lindsten T, Korsmeyer SJ. BCL-2, BCL-X(L) sequester BH3 domain-only molecules preventing BAX- and BAK-mediated mitochondrial apoptosis. Mol Cell. 2001, 8(3):705-11.

113. Cheng J, Cui R, Chen CH, Du J. Oxidized low-density lipoprotein stimulates p53-dependent activation of proapoptotic Bax leading to apoptosis of differentiated endothelial progenitor cells. Endocrinology. 2007, 148(5):2085-94.

114. Chiao JW, Chung FL, Kancherla R, Ahmed T, Mittelman A, Conaway CC. Sulforaphane and its metabolite mediate growth arrest and apoptosis in human prostate cancer cells. Int J Oncol. 2002, 20(3):631-6.

115. Chikatsu N, Takeuchi Y, Tamura Y, Fukumoto S, Yano K, Tsuda E, Ogata E, Fujita T. Interactions between cancer and bone marrow cells induce osteoclast differentiation factor expression and osteoclast-like cell formation in vitro. Biochem Biophys Res Commun. 2000, 267(2):632-7.

116. Chiou YS, Tsai ML, Nagabhushanam K, Wang YJ, Wu CH, Ho CT, Pan MH. Pterostilbene is more potent than resveratrol in preventing azoxymethane (AOM)-induced colon tumorigenesis via activation of the NF-E2-related factor 2 (Nrf2)-mediated antioxidant signaling pathway. J Agric Food Chem. 2011, 59(6):2725-33.

117. Chiu FL, Lin JK. Downregulation of androgen receptor expression by luteolin causes inhibition of cell proliferation and induction of apoptosis in human prostate cancer cells and xenografts. Prostate. 2008, 68(1):61-71.

118. Chomczynski P, Sacchi N. Single-step method of RNA isolation by acid guanidinium thiocyanate-phenol-chloroform extraction. Anal Biochem. 1987, 162(1):156-9.

119. Chong J, Poutaraud A, and Hugueney P. Metabolism and roles of stilbenes in plants. Plant Science. 2009, 177(3):143-155.

120. Chu EC, Chai J, Tarnawski AS. NSAIDs activate PTEN and other phosphatases in human colon cancer cells: novel mechanism for chemopreventive action of NSAIDs. Biochem Biophys Res Commun. 2004, 320(3):875-9.

121. Chua AW, Hay HS, Rajendran P, Shanmugam MK, Li F, Bist P, Koay ES, Lim LH, Kumar AP, Sethi G. Butein downregulates chemokine receptor CXCR4 expression and function through suppression of NF-κB activation in breast and pancreatic tumor cells. Biochem Pharmacol. 2010, 80(10):1553-62.

122. Chung HY, Sung B, Jung KJ, Zou Y, Yu BP. The molecular inflammatory process in aging. Antioxid Redox Signal. 2006, 8(3-4):572-81.

123. Chung YC, Chang YF. Serum interleukin-6 levels reflect the disease status of colorectal cancer. J Surg Oncol. 2003, 83(4):222-6.

124. Cinar B, Mukhopadhyay NK, Meng G, Freeman MR. Phosphoinositide 3-kinase-independent non-genomic signals transit from the androgen receptor to Akt1 in membrane raft microdomains. J Biol Chem. 2007, 282(40):29584-93.

125. Claesson-Welsh L, Welsh M, Ito N, Anand-Apte B, Soker S, Zetter B, O'Reilly M, Folkman J. Angiostatin induces endothelial cell apoptosis and activation of focal adhesion kinase independently of the integrin-binding motif RGD. Proc Natl Acad Sci U S A. 1998, 95(10):5579-83.

126. Clardy J, Walsh C. Lessons from natural molecules. Nature. 2004, 432(7019):829-37.

127. Clarke JD, Dashwood RH, Ho E. Multi-targeted prevention of cancer by sulforaphane. Cancer Lett. 2008, 269(2):291-304.

128. Clohisy JC, Roy BC, Biondo C, Frazier E, Willis D, Teitelbaum SL, Abu-Amer Y. Direct inhibition of NF-kappa B blocks bone erosion associated with inflammatory arthritis. J Immunol. 2003, 171(10):5547-53.

129. Closa D, Folch-Puy E. Oxygen free radicals and the systemic inflammatory response. IUBMB Life. 2004, 56(4):185-91.

130. Coleman RE, Rubens RD. The clinical course of bone metastases from breast cancer. Br J Cancer. 1987, 55(1):61-6.

131. Coleman RE. Metastatic bone disease: clinical features, pathophysiology and treatment strategies. Cancer Treat Rev. 2001, 27(3):165-76.

132. Colotta F, Allavena P, Sica A, Garlanda C, Mantovani A. Cancer-related inflammation, the seventh hallmark of cancer: links to genetic instability.Carcinogenesis. 2009, 30(7):1073-81.

133. Courtois G, Gilmore TD. Mutations in the NF-kappaB signaling pathway: implications for human disease. Oncogene. 2006, 25(51):6831-43.

134. Cui Y, Lu Z, Bai L, Shi Z, Zhao WE, Zhao B. beta-Carotene induces apoptosis and up-regulates peroxisome proliferator-activated receptor gamma expression and reactive oxygen species production in MCF-7 cancer cells. Eur J Cancer. 2007, 43(17):2590-601.

135. Cummings SR, San Martin J, McClung MR, Siris ES, Eastell R, Reid IR, Delmas P, Zoog HB, Austin M, Wang A, Kutilek S, Adami S, Zanchetta J, Libanati C, Siddhanti S, Christiansen C, FREEDOM Trial. Denosumab for prevention of fractures in postmenopausal women with osteoporosis. N Engl J Med. 2009, 361(8):756-65.

136. Dai F, Chen Y, Song Y, Huang L, Zhai D, Dong Y, Lai L, Zhang T, Li D, Pang X, Liu M, Yi Z. A natural small molecule harmine inhibits angiogenesis and suppresses tumour growth through activation of p53 in endothelial cells. PLoS One. 2012, 7(12):e52162.

137. D'Amato RJ, Loughnan MS, Flynn E, Folkman J. Thalidomide is an inhibitor of angiogenesis. Proc Natl Acad Sci U S A. 1994, 91(9):4082-5

138. Daniel D, Meyer-Morse N, Bergsland EK, Dehne K, Coussens LM, Hanahan D. Immune enhancement of skin carcinogenesis by CD4+ T cells. J Exp Med. 2003, 197(8):1017-28.

139. Dasgupta S, Bhattacharya S, Biswas A, Majumdar SS, Mukhopadhyay S, Ray S, Bhattacharya S. NF-kappaB mediates lipid-induced fetuin-A expression in hepatocytes that impairs adipocyte function effecting insulin resistance. Biochem J. 2010, 429(3):451-62.

140. Daverey A, Saxena R, Tewari S, Goel SK, Dwivedi A. Expression of estrogen receptor co-regulators SRC-1, RIP140 and NCoR and their interaction with estrogen receptor in rat uterus, under the influence of ormeloxifene. J Steroid Biochem Mol Biol. 2009, 116(1-2):93-101.

141. Davies MA, Samuels Y. Analysis of the genome to personalize therapy for melanoma. Oncogene. 2010, 29(41):5545-55.

142. de Ruiter MB, Reneman L, Boogerd W, Veltman DJ, Caan M, Douaud G, Lavini C, Linn SC, Boven E, van Dam FS, Schagen SB. Late effects of high-dose adjuvant chemotherapy on white and gray matter in breast cancer survivors: converging results from multimodal magnetic resonance imaging. Hum Brain Mapp. 2012, 33(12):2971-83.

143. de Souza Pereira R. Selective cyclooxygenase-2 (COX-2) inhibitors used for preventing or regressing cancer. Recent Pat Anticancer Drug Discov. 2009, 4(2):157-63.

144. DeBerardinis RJ, Lum JJ, Hatzivassiliou G, Thompson CB. The biology of cancer: metabolic reprogramming fuels cell growth and proliferation. Cell Metab. 2008, 7(1):11-20.

145. del Peso L, González-García M, Page C, Herrera R, Nuñez G.Interleukin-3-induced phosphorylation of BAD through the protein kinase Akt. Science. 1997, 278(5338):687-9.

146. Demaria S, Pikarsky E, Karin M, Coussens LM, Chen YC, El-Omar EM, Trinchieri G, Dubinett SM, Mao JT, Szabo E, Krieg A, Weiner GJ, Fox BA, Coukos G, Wang E, Abraham RT, Carbone M, Lotze MT. Cancer and inflammation: promise for biologic therapy. J Immunother. 2010, 33(4):335-51.

147. DeSantis CE, Lin CC, Mariotto AB, Rebecca L, Siegel KD. Stein JL. Kramer RA, Anthony S. Robbins and Ahmedin Jemal. Cancer statistics, 2014. CA: a cancer journal for clinicians 2014, 64: 9-29.

148. Dev K, Gautam SK, Giri SK, Kumar A, Yadav A, Verma V, Kumar P, Singh B. Isolation, culturing and characterization of feeder-independent amniotic fluid stem cells in buffalo (Bubalus bubalis). Res Vet Sci. 2012, 93(2):743-8.

149. Dhanabal M, Ramchandran R, Volk R, Stillman IE, Lombardo M, Iruela-Arispe ML, Simons M, Sukhatme VP. Endostatin: yeast production, mutants, and antitumor effect in renal cell carcinoma. Cancer Res. 1999, 59(1):189-97.

150. Dikshit P, Chatterjee M, Goswami A, Mishra A, Jana NR. Aspirin induces apoptosis through the inhibition of proteasome function. J Biol Chem. 2006, 281(39):29228-35.

151. Dinarello CA. Anti-inflammatory Agents: Present and Future. Cell. 2010, 140(6):935-50.

152. Dohle DS, Pasa SD, Gustmann S, Laub M, Wissler JH, Jennissen HP, Dünker N. Chick ex ovo culture and ex ovo CAM assay: how it really works. J Vis Exp. 2009, (33).

153. Dolcet X, Llobet D, Pallares J, Matias-Guiu X. NF-kB in development and progression of human cancer. Virchows Arch. 2005, 446(5):475-82.

154. Dong X, Han ZC, Yang R. Angiogenesis and antiangiogenic therapy in hematologic malignancies. Crit Rev Oncol Hematol. 2007, 62(2):105-18.

155. Dos Santos EG, Dieudonne MN, Pecquery R, Le Moal V, Giudicelli Y, Lacasa D.Rapid nongenomic E2 effects on p42/p44 MAPK, activator protein-1, and cAMP response element binding protein in rat white adipocytes. Endocrinology. 2002, 143(3):930-40.

156. Dranoff G. Cytokines in cancer pathogenesis and cancer therapy. Nat Rev Cancer. 2004, 4(1):11-22.

157. Driggers PH, Segars JH. Estrogen action and cytoplasmic signaling pathways. Part II: the role of growth factors and phosphorylation in estrogen signaling. Trends Endocrinol Metab. 2002, 13(10):422-7.

158. Dumitrescu RG, Cotarla I. Understanding breast cancer risk -- where do we stand in 2005? J Cell Mol Med. 2005, 9(1):208-21.

159. Eberhart CE, Coffey RJ, Radhika A, Giardiello FM, Ferrenbach S, DuBois RN. Up-regulation of cyclooxygenase 2 gene expression in human colorectal adenomas and adenocarcinomas. Gastroenterology. 1994, 107(4):1183-8.

160. El Touny LH, Banerjee PP. Akt GSK-3 pathway as a target in genistein-induced inhibition of TRAMP prostate cancer progression toward a poorly differentiated phenotype. Carcinogenesis. 2007, 28(8):1710-7.

161. El Touny LH, Banerjee PP. Identification of a biphasic role for genistein in the regulation of prostate cancer growth and metastasis. Cancer Res. 2009, 69(8):3695-703.

162. Elrod HA, Sun SY. PPARgamma and Apoptosis in Cancer. PPAR Res. 2008, 2008:704165.

163. Elstner E, Müller C, Koshizuka K, Williamson EA, Park D, Asou H, Shintaku P, Said JW, Heber D, Koeffler HP. Ligands for peroxisome proliferator-activated receptorgamma and retinoic acid receptor inhibit growth and induce apoptosis of human breast cancer cells in vitro and in BNX mice. Proc Natl Acad Sci U S A. 1998, 95(15):8806-11.

164. Eltzschig HK, Carmeliet P. Hypoxia and inflammation. N Engl J Med. 2011, 364(7):656-65.

165. Evan GI, Vousden KH. Proliferation, cell cycle and apoptosis in cancer. Nature. 2001, 411(6835):342-8.

166. Evans WP, Warren Burhenne LJ, Laurie L, O'Shaughnessy KF, Castellino RA. Invasive lobular carcinoma of the breast: mammographic characteristics and computer-aided detection. Radiology. 2002, 225(1):182-9.

167. Fadeel B, Orrenius S. Apoptosis: a basic biological phenomenon with wide-ranging implications in human disease. J Intern Med. 2005, 258(6):479-517.

168. Fahey JW, Zalcmann AT, Talalay P. The chemical diversity and distribution of glucosinolates and isothiocyanates among plants. Phytochemistry. 2001, 56(1):5-51.

169. Falleti MG, Sanfilippo A, Maruff P, Weih L, Phillips KA. The nature and severity of cognitive impairment associated with adjuvant chemotherapy in women with breast cancer: a meta-analysis of the current literature. Brain Cogn. 2005, 59(1):60-70.

170. Farhat MY, Abi-Younes S, Dingaan B, Vargas R, Ramwell PW. Estradiol increases cyclic adenosine monophosphate in rat pulmonary vascular smooth muscle cells by a nongenomic mechanism. J Pharmacol Exp Ther. 1996, 276(2):652-7.

171. Federico A, Morgillo F, Tuccillo C, Ciardiello F, Loguercio C. Chronic inflammation and oxidative stress in human carcinogenesis. Int J Cancer. 2007, 121(11):2381-6.

172. Fernando RI, Wimalasena J. Estradiol abrogates apoptosis in breast cancer cells through inactivation of BAD: Ras-dependent nongenomic pathways requiring signaling through ERK and Akt. Mol Biol Cell. 2004, 15(7):3266-84.

173. Feron O. Pyruvate into lactate and back: from the Warburg effect to symbiotic energy fuel exchange in cancer cells. Radiother Oncol. 2009, 92(3):329-33.

174. Ferrara N, Carver-Moore K, Chen H, Dowd M, Lu L, O'Shea KS, Powell-Braxton L, Hillan KJ, Moore MW. Heterozygous embryonic lethality induced by targeted inactivation of the VEGF gene. Nature. 1996, 380(6573):439-42.

175. Ferrara N. Vascular endothelial growth factor. Arterioscler Thromb Vasc Biol. 2009, 29(6):789-91.

176. Ferrara N. Vascular endothelial growth factor: basic science and clinical progress. Endocr Rev. 2004, 25(4):581-611.

177. Ferrara N. VEGF as a therapeutic target in cancer. Oncology. 2005, 69 Suppl 3:11-6.

178. Ferreira E, da Silva AE, Serakides R, Gomes MG, Cassali GD. Ehrlich tumor as model to study artificial hyperthyroidism influence on breast cancer. Pathol Res Pract. 2007, 203(1):39-44.

179. Fesik SW. Promoting apoptosis as a strategy for cancer drug discovery. Nat Rev Cancer. 2005, 5(11):876-85.

180. Fimognari C, Lenzi M, Hrelia P. Apoptosis induction by sulfur-containing compounds in malignant and nonmalignant human cells. Environ Mol Mutagen. 2009, 50(3):171-89.

181. Fimognari C, Nüsse M, Berti F, Iori R, Cantelli-Forti G, Hrelia P. Isothiocyanates as novel cytotoxic and cytostatic agents: molecular pathway on human transformed and non-transformed cells. Biochem Pharmacol. 2004, 68(6):1133-8.

182. Fimognari C, Turrini E, Ferruzzi L, Lenzi M, Hrelia P. Natural isothiocyanates: genotoxic potential versus chemoprevention. Mutat Res. 2012, 750(2):107-31.

183. Fisher B, Anderson S, Bryant J, Margolese RG, Deutsch M, Fisher ER, Jeong JH, Wolmark N. Twenty-year follow-up of a randomized trial comparing total

mastectomy, lumpectomy, and lumpectomy plus irradiation for the treatment of invasive breast cancer. N Engl J Med. 2002, 347(16):1233-41.

184. Folkman J. Angiogenesis in cancer, vascular, rheumatoid and other disease. Nat Med. 1995, 1(1):27-31.

185. Folkman J. Angiogenesis: an organizing principle for drug discovery? Nat Rev Drug Discov. 2007, 6(4):273-86.

186. Folkman J. Antiangiogenesis in cancer therapy--endostatin and its mechanisms of action. Exp Cell Res. 2006, 312(5):594-607.

187. Folkman J. Seminars in Medicine of the Beth Israel Hospital, Boston. Clinical applications of research on angiogenesis. N Engl J Med. 1995, 333 (26):1757-63.

188. Folkman J. What is the evidence that tumors are angiogenesis dependent? J Natl Cancer Inst. 1990, 82(1):4-6.

189. Franzoso G, Carlson L, Xing L, Poljak L, Shores EW, Brown KD, Leonardi A, Tran T, Boyce BF, Siebenlist U. Requirement for NF-kappaB in osteoclast and B-cell development. Genes Dev. 1997, 11(24):3482-96.

190. Fresno Vara JA, Casado E, de Castro J, Cejas P, Belda-Iniesta C, González-Barón M. PI3K/Akt signalling pathway and cancer. Cancer Treat Rev. 2004, 30(2):193-204.

191. Friesner RA, Murphy RB, Repasky MP, Frye LL, Greenwood JR, Halgren TA, Sanschagrin PC, Mainz DT. Extra precision glide: docking and scoring incorporating a model of hydrophobic enclosure for protein-ligand complexes. J Med Chem. 2006 Oct 19, 49(21):6177-96.

192. Fukumura D, Kashiwagi S, Jain RK. The role of nitric oxide in tumour progression. Nat Rev Cancer. 2006 Jul, 6(7):521-34.

193. Fulda S. Resveratrol and derivatives for the prevention and treatment of cancer. Drug Discov Today. 2010, 15(17-18):757-65.

194. Gaestel M, Mengel A, Bothe U, Asadullah K. Protein kinases as small molecule inhibitor targets in inflammation. Curr Med Chem. 2007, 14(21):2214-34.

195. Gan Y, Shi C, Inge L, Hibner M, Balducci J, Huang Y. Differential roles of ERK and Akt pathways in regulation of EGFR-mediated signaling and motility in prostate cancer cells. Oncogene. 2010, 29(35):4947-58.

196. Gao H, Ouyang X, Banach-Petrosky WA, Gerald WL, Shen MM, Abate-Shen C. Combinatorial activities of Akt and B-Raf/Erk signaling in a mouse model of androgen-independent prostate cancer. Proc Natl Acad Sci U S A. 2006, 103(39):14477-82.

197. Gao YT, Panda SP, Roman LJ, Martásek P, Ishimura Y, Masters BS. Oxygen metabolism by neuronal nitric-oxide synthase. J Biol Chem. 2007, 282 (11):7921-9.

198. García-Zepeda SP, García-Villa E, Díaz-Chávez J, Hernández-Pando R, Gariglio P. Resveratrol induces cell death in cervical cancer cells through apoptosis and autophagy. Eur J Cancer Prev. 2013, 22(6):577-84.

199. Gardner OS, Dewar BJ, Earp HS, Samet JM, Graves LM. Dependence of peroxisome proliferator-activated receptor ligand-induced mitogen-activated protein kinase signaling on epidermal growth factor receptor transactivation. J Biol Chem. 2003, 278(47):46261-9.

200. Gardner OS, Dewar BJ, Graves LM. Activation of mitogen-activated protein kinases by peroxisome proliferator-activated receptor ligands: an example of nongenomic signaling. Mol Pharmacol. 2005, 68(4):933-41.

201. Garside SA, Harlow CR, Hillier SG, Fraser HM, Thomas FH. Thrombospondin-1 inhibits angiogenesis and promotes follicular atresia in a novel in vitro angiogenesis assay. Endocrinology. 2010, 151(3):1280-9.

202. Gediya LK, Njar VC. Promise and challenges in drug discovery and development of hybrid anticancer drugs. Expert Opin Drug Discov. 2009, 4(11):1099-111.

203. Geller DA, Billiar TR. Molecular biology of nitric oxide synthases. Cancer Metastasis Rev. 1998, 17(1):7-23.

204. Giatromanolaki A, Koukourakis MI, Sivridis E, Chlouverakis G, Vourvouhaki E, Turley H, Harris AL, Gatter KC. Activated VEGFR2/KDR pathway in tumour cells and tumour associated vessels of colorectal cancer. Eur J Clin Invest. 2007, 37(11):878-86.

205. Gibbs JB. Mechanism-based target identification and drug discovery in cancer research. Science. 2000, 287(5460):1969-73.

206. Gilmore TD, Cormier C, Jean-Jacques J, Gapuzan ME. Malignant transformation of primary chicken spleen cells by human transcription factor c-Rel. Oncogene. 2001, 20(48):7098-103.

207. Gioeli D, Mandell JW, Petroni GR, Frierson HF Jr, Weber MJ. Activation of mitogen-activated protein kinase associated with prostate cancer progression. Cancer Res. 1999, 59(2):279-84.

208. Girroir EE, Hollingshead HE, Billin AN, Willson TM, Robertson GP, Sharma AK, Amin S, Gonzalez FJ, Peters JM. Peroxisome proliferator-activated receptor-beta/delta

(PPARbeta/delta) ligands inhibit growth of UACC903 and MCF7 human cancer cell lines. Toxicology. 2008, 243(1-2):236-43.

209. Gjertson CK, Albertsen PC. Use and assessment of PSA in prostate cancer. Med Clin North Am. 2011, 95(1):191-200.

210. Gogvadze V, Orrenius S, Zhivotovsky B. Mitochondria as targets for chemotherapy. Apoptosis. 2009, 14(4):624-40.

211. Goh PP, Sze DM, Roufogalis BD. Molecular and cellular regulators of cancer angiogenesis. Curr Cancer Drug Targets. 2007, 7(8):743-58.

212. Gomes FG, Nedel F, Alves AM, Nör JE, Tarquinio SB. Tumor angiogenesis and lymphangiogenesis: tumor/endothelial crosstalk and cellular/microenvironmental signaling mechanisms. Life Sci. 2013, 92(2):101-7.

213. Gomez-Lazaro M, Fernandez-Gomez FJ, Jordán J. p53: twenty five years understanding the mechanism of genome protection. J Physiol Biochem. 2004, 60(4):287-307.

214. Gomez-Lazaro M, Galindo MF, Melero-Fernandez de Mera RM, Fernandez-Gómez FJ, Concannon CG, Segura MF, Comella JX, Prehn JH, Jordan J. Reactive oxygen species and p38 mitogen-activated protein kinase activate Bax to induce mitochondrial cytochrome c release and apoptosis in response to malonate. Mol Pharmacol. 2007, 71(3):736-43.

215. Gong EY, Park E, Lee K. Hakai acts as a coregulator of estrogen receptor alpha in breast cancer cells. Cancer Sci. 2010, 101(9):2019-25.

216. Gordaliza M. Natural products as leads to anticancer drugs. Clin Transl Oncol. 2007, 9(12):767-76.

217. Gos M, Miłoszewska J, Przybyszewska M. Epithelial-mesenchymal transition in cancer progression. Postepy Biochem. 2009, 55(2):121-8.

218. Gosslau A, Chen M, Ho CT, Chen KY. A methoxy derivative of resveratrol analogue selectively induced activation of the mitochondrial apoptotic pathway in transformed firoblasts. Br J Cancer 2005, 92 (3): 513-21.

219. Grant S. Co targeting survival signaling pathways in cancer. J Clin Invest. 2008, 118 (9) 3003-3006.

220. Gregory CW, He B, Johnson RT, Ford OH, Mohler JL, French FS, Wilson EM. A mechanism for androgen receptor-mediated prostate cancer recurrence after androgen deprivation therapy. Cancer Res. 2001, 61(11):4315-9.

221. Grigoryev DN, Long BJ, Njar VC, Brodie AH. Pregnenolone stimulates LNCaP prostate cancer cell growth via the mutated androgen receptor. J Steroid Biochem Mol Biol. 2000, 75(1):1-10.

222. Grivennikov SI, Greten FR, Karin M. Immunity, inflammation, and cancer. Cell. 2010, 140(6):883-99

223. Guha M, Mackman N. LPS induction of gene expression in human monocytes. Cell Signal. 2001, 13(2):85-94.

224. Guo S, Colbert LS, Fuller M, Zhang Y, Gonzalez-Perez RR. Vascular endothelial growth factor receptor-2 in breast cancer. Biochim Biophys Acta. 2010, 1806(1):108-21.

225. Gupta A, Saha P, Descôteaux C, Leblanc V, Asselin E, Bérubé G. Design, synthesis and biological evaluation of estradiol-chlorambucil hybrids as anticancer agents. Bioorg Med Chem Lett. 2010, 20(5):1614-8.

226. Gurung RL, Lim SN, Khaw AK, Soon JF, Shenoy K, Mohamed Ali S, Jayapal M, Sethu S, Baskar R, Hande MP. Thymoquinone induces telomere shortening, DNA damage and apoptosis in human glioblastoma cells. PLoS One. 2010, 5(8):e12124.

227. Guttridge DC, Albanese C, Reuther JY, Pestell RG, Baldwin AS Jr. NF-kappaB controls cell growth and differentiation through ranscriptional regulation of cyclin D1. Mol Cell Biol. 1999, 19(8):5785-99.

228. Ha H, Kwak HB, Lee SW, Jin HM, Kim HM, Kim HH, Lee ZH. Reactive oxygen species mediate RANK signaling in osteoclasts. Exp Cell Res. 2004, 301(2):119-27.

229. Hajdu SI. A note from history: landmarks in history of cancer, part 1. Cancer. 2011, 117(5):1097-102.

230. Half E, Tang XM, Gwyn K, Sahin A, Wathen K, Sinicrope FA. Cyclooxygenase-2 expression in human breast cancers and adjacent ductal carcinoma in situ. Cancer Res. 2002, 62(6):1676-81.

231. Hall JM, Couse JF, Korach KS. The multifaceted mechanisms of estradiol and estrogen receptor signaling. J Biol Chem. 2001, 276(40):36869-72.

232. Ham J, Babij C, Whitfield J, Pfarr CM, Lallemand D, Yaniv M, Rubin LL. A c-Jun dominant negative mutant protects sympathetic neurons against programmed cell death. Neuron. 1995, 14(5):927-39.

233. Han S, Roman J. Peroxisome proliferator-activated receptor gamma: a novel target for cancer therapeutics? Anticancer Drugs. 2007, 18(3):237-44.

234. Hanahan D, Folkman J. Patterns and emerging mechanisms of the angiogenic switch during tumorigenesis. Cell. 1996, 86(3):353-64.

235. Hanahan D, Weinberg RA. Hallmarks of cancer: the next generation. Cell. 2011, 144(5):646-74.

236. Hanahan D, Weinberg RA. The hallmarks of cancer. Cell. 2000, 100(1):57-70.

237. Hansen TV, Skattebøl L, Organic Syntheses, 2005, 82, 267-271.

238. Harada N, Murata Y, Yamaji R, Miura T, Inui H, Nakano Y. Resveratrol down-regulates the androgen receptor at the post-translational level in prostate cancer cells. J Nutr Sci Vitaminol (Tokyo). 2007, 53(6):556-60.

239. Hart JH, Shrimpton DM. Role of stilbenes in resistance of wood to decay. Phytopathology 1979, 69:1138-1143.

240. He X, Andersson G, Lindgren U, Li Y. Resveratrol prevents RANKL-induced osteoclast differentiation of murine osteoclast progenitor RAW 264.7 cells through inhibition of ROS production. Biochem Biophys Res Commun. 2010, 401(3):356-62.

241. Head J, Johnston SR. New targets for therapy in breast cancer: farnesyltransferase inhibitors. Breast Cancer Res. 2004, 6(6):262-8.

242. Heinlein CA, Chang C. Androgen receptor (AR) coregulators: an overview. Endocr Rev. 2002, 23(2):175-200.

243. Heinlein CA, Chang C. Androgen receptor in prostate cancer. Endocr Rev. 2004, 25(2):276-308.

244. Heldring N, Pike A, Andersson S, Matthews J, Cheng G, Hartman J, Tujague M, Ström A, Treuter E, Warner M, Gustafsson JA. Estrogen receptors: how do they signal and what are their targets. Physiol Rev. 2007, 87(3):905-31.

245. Hellwig-Bürgel T, Stiehl DP, Wagner AE, Metzen E, Jelkmann W. Review: hypoxia-inducible factor-1 (HIF-1): a novel transcription factor in immune reactions. J Interferon Cytokine Res. 2005, 25(6):297-310.

246. Henderson BE, Feigelson HS. Hormonal carcinogenesis. Carcinogenesis. 2000, 21(3):427-33.

247. Hengartner MO. The biochemistry of apoptosis. Nature. 2000, 407(6805):770-6.

248. Hennessy BT, Smith DL, Ram PT, Lu Y, Mills GB. Exploiting the PI3K/AKT pathway for cancer drug discovery. Nat Rev Drug Discov. 2005, 4(12):988-1004.

249. Hettmann T, DiDonato J, Karin M, Leiden JM. An essential role for nuclear factor kappaB in promoting double positive thymocyte apoptosis. J Exp Med. 1999, 189(1):145-58.

250. Hida T, Yatabe Y, Achiwa H, Muramatsu H, Kozaki K, Nakamura S, Ogawa M, Mitsudomi T, Sugiura T, Takahashi T. Increased expression of cyclooxygenase 2 occurs frequently in human lung cancers, specifically in adenocarcinomas. Cancer Res. 1998, 58(17):3761-4.

251. Higgins KJ, Abdelrahim M, Liu S, Yoon K, Safe S. Regulation of vascular endothelial growth factor receptor-2 expression in pancreatic cancer cells by Sp proteins. Biochem Biophys Res Commun. 2006, 345(1):292-301.

252. Hinz M, Krappmann D, Eichten A, Heder A, Scheidereit C, Strauss M. NF-kappaB function in growth control: regulation of cyclin D1 expression and G0/G1-to-S-phase transition. Mol Cell Biol. 1999, 19(4):2690-8.

253. Ho SM. Estrogens and anti-estrogens: key mediators of prostate carcinogenesis and new therapeutic candidates. J Cell Biochem. 2004, 91(3):491-503.

254. Hoeflich KP, O'Brien C, Boyd Z, Cavet G, Guerrero S, Jung K, Januario T, Savage H, Punnoose E, Truong T, Zhou W, Berry L, Murray L, Amler L, Belvin M, Friedman LS, Lackner MR. In vivo antitumor activity of MEK and phosphatidylinositol 3-kinase inhibitors in basal-like breast cancer models. Clin Cancer Res. 2009, 15(14):4649-64.

255. Hoff PM, Machado KK. Role of angiogenesis in the pathogenesis of cancer. Cancer Treat Rev. 2012, 38(7):825-33.

256. Holmgren L, O'Reilly MS, Folkman J. Dormancy of micrometastases: balanced proliferation and apoptosis in the presence of angiogenesis suppression. Nat Med. 1995, 1(2):149-53.

257. Hong BH, Wu CH, Yeh CT, Yen GC. Invadopodia-associated proteins blockade as a novel mechanism for 6-shogaol and pterostilbene to reduce breast cancer cell motility and invasion. Mol Nutr Food Res. 2013, 57(5):886-95.

258. Hopkins AL. Network pharmacology: the next paradigm in drug discovery. Nat Chem Biol. 2008, 4(11):682-90.

259. Hsieh MJ, Lin CW, Yang SF, Sheu GT, Yu YY, Chen MK, Chiou HL. A combination of pterostilbene with autophagy inhibitors exerts efficient apoptotic characteristics in both chemosensitive and chemoresistant lung cancer cells. Toxicol Sci. 2014, 137(1):65-75.

260. Hsu JC, Zhang J, Dev A, Wing A, Bjeldanes LF, Firestone GL. Indole-3-carbinol inhibition of androgen receptor expression and downregulation of androgen responsiveness in human prostate cancer cells. Carcinogenesis. 2005, 26(11):1896-904.

261. Hsu PP, Sabatini DM. Cancer cell metabolism: Warburg and beyond. Cell. 2008, 134(5):703-7.

262. Hu Z, Fan C, Oh DS, Marron JS, He X, Qaqish BF, Livasy C, Carey LA, Reynolds E, Dressler L, Nobel A, Parker J, Ewend MG, Sawyer LR, Wu J, Liu Y, Nanda R, Tretiakova M, Ruiz Orrico A, Dreher D, Palazzo JP, Perreard L, Nelson E, Mone M, Hansen H, Mullins M, Quackenbush JF, Ellis MJ, Olopade OI, Bernard PS, Perou CM. The molecular portraits of breast tumors are conserved across microarray platforms. BMC Genomics. 2006, 7:96.

263. Huang C, Li J, Ma WY, Dong Z. JNK activation is required for JB6 cell transformation induced by tumor necrosis factor-alpha but not by 12-O-tetradecanoylphorbol-13-acetate. J Biol Chem. 1999, 274(42):29672-6.

264. Huang CS, Ho CT, Tu SH, Pan MH, Chuang CH, Chang HW, Chang CH, Wu CH, Ho YS. Long-term ethanol exposure-induced hepatocellular carcinoma cell migration and invasion through lysyl oxidase activation are attenuated by combined treatment with pterostilbene and curcumin analogues. J Agric Food Chem. 2013, 61(18):4326-35.

265. Huang GJ, Pan CH, Wu CH. Sclareol exhibits anti-inflammatory activity in both lipopolysaccharide-stimulated macrophages and the λ-carrageenan-induced paw edema model. J Nat Prod. 2012, 75(1):54-9.

266. Hudson JD, Shoaibi MA, Maestro R, Carnero A, Hannon GJ, Beach DH. A proinflammatory cytokine inhibits p53 tumor suppressor activity. J Exp Med. 1999, 190(10):1375-82.

267. Hussain SP, Hofseth LJ, Harris CC. Radical causes of cancer. Nat Rev Cancer. 2003, 3(4):276-85.

268. Hwang D, Scollard D, Byrne J, Levine E. Expression of cyclooxygenase-1 and cyclooxygenase-2 in human breast cancer. J Natl Cancer Inst. 1998, 90(6):455-60.

269. Inoue K, Slaton JW, Eve BY, Kim SJ, Perrotte P, Balbay MD, Yano S, Bar-Eli M, Radinsky R, Pettaway CA, Dinney CP. Interleukin 8 expression regulates tumorigenicity and metastases in androgen-independent prostate cancer. Clin Cancer Res. 2000, 6(5):2104-19.

270. Ishii K, Hamamoto H, Kamimura M, Nakamura Y, Noda H, Imamura K, Mita K, Sekimizu K. Insect cytokine paralytic peptide (PP) induces cellular and humoral immune responses in the silkworm Bombyx mori. J Biol Chem. 2010, 285(37):28635-42.

271. Jackson SP, Bartek J. The DNA-damage response in human biology and disease. Nature. 2009, 461(7267):1071-8.

272. Jaiswal M, LaRusso NF, Burgart LJ, Gores GJ. Inflammatory cytokines induce DNA damage and inhibit DNA repair in cholangiocarcinoma cells by a nitric oxide-dependent mechanism. Cancer Res. 2000, 60(1):184-90.

273. Jana NR, Dikshit P, Goswami A, Nukina N. Inhibition of proteasomal function by curcumin induces apoptosis through mitochondrial pathway. J Biol Chem. 2004, 279(12):11680-5.

274. Jana NR, Zemskov EA, Wang Gh, Nukina N. Altered proteasomal function due to the expression of polyglutamine-expanded truncated N-terminal huntingtin induces apoptosis by caspase activation through mitochondrial cytochrome c release. Hum Mol Genet. 2001, 10(10):1049-59.

275. Jang M, Cai L, Udeani GO, Slowing KV, Thomas CF, Beecher CW, Fong HH, Farnsworth NR, Kinghorn AD, Mehta RG, Moon RC, Pezzuto JM. Cancer chemopreventive activity of resveratrol, a natural product derived from grapes. Science. 1997, 275(5297):218-20.

276. Jasiński M, Jasińska L, Ogrodowczyk M. Resveratrol in prostate diseases – a short review. Cent European J Urol. 2013, 66(2):144-9.

277. Jemal A, Bray F, Center MM, Ferlay J, Ward E, Forman D. Global cancer statistics. CA Cancer J Clin. 2011, 61(2):69-90

278. Jemal A, Siegel R, Xu J, Ward E. Cancer statistics, 2010. CA Cancer J Clin. 2010, 60(5):277-300.

279. Jia LT, Chen SY, Yang AG. Cancer gene therapy targeting cellular apoptosis machinery. Cancer Treat Rev. 2012, 38(7):868-76.

280. Jiang BH, Liu LZ. PI3K/PTEN signaling in angiogenesis and tumorigenesis. Adv Cancer Res. 2009, 102:19-65.

281. Jiménez B, Volpert OV, Crawford SE, Febbraio M, Silverstein RL, Bouck N. Signals leading to apoptosis-dependent inhibition of neovascularization by thrombospondin-1. Nat Med. 2000, 6(1):41-8.

282. Johnstone RW, Ruefli AA, Lowe SW. Apoptosis: a link between cancer genetics and chemotherapy. Cell. 2002, 108(2):153-64.

283. Jones RG, Thompson CB. Tumor suppressors and cell metabolism: a recipe for cancer growth. Genes Dev. 2009, 23(5):537-48.

284. Jorgenson WL, Maxwell DS, Julian TR. Development and testing of the OPLS all atom force field on conformational energetic and properties of organic liquids. J Am Chem Soc. 1996, 118: 11225-11236.

285. Kang HY, Lin HK, Hu YC, Yeh S, Huang KE, Chang C. From transforming growth factor-beta signaling to androgen action: identification of Smad3 as an androgen receptor coregulator in prostate cancer cells. Proc Natl Acad Sci U S A. 2001, 98(6):3018-23.

286. Kang KA, Zhang R, Piao MJ, Lee KH, Kim BJ, Kim SY, Kim HS, Kim DH, You HJ, Hyun JW. Inhibitory effects of glycitein on hydrogen peroxide induced cell damage by scavenging reactive oxygen species and inhibiting c-Jun N-terminal kinase. Free Radic Res. 2007, 41(6):720-9.

287. Kang KS, Wang P, Yamabe N, Fukui M, Jay T, Zhu BT. Docosahexaenoic acid induces apoptosis in MCF-7 cells in vitro and in vivo via reactive oxygen species formation and caspase 8 activation. PLoS One. 2010, 5(4):e10296.

288. Kapetanovic IM, Muzzio M, Huang Z, Thompson TN, McCormick DL. Pharmacokinetics, oral bioavailability, and metabolic profile of resveratrol and its dimethylether analog, pterostilbene, in rats. Cancer Chemother Pharmacol. 2011, 68(3):593-601.

289. Karin M, Ben-Neriah Y. Phosphorylation meets ubiquitination: the control of NF-[kappa]B activity. Annu Rev Immunol. 2000, 18:621-63.

290. Karin M, Cao Y, Greten FR, Li ZW. NF-kappaB in cancer: from innocent bystander to major culprit. Nat Rev Cancer. 2002, 2(4):301-10.

291. Katz M, Amit I, Yarden Y. Regulation of MAPKs by growth factors and receptor tyrosine kinases. Biochim Biophys Acta. 2007, 1773(8):1161-76.

292. Kelly PN, Strasser A. The role of Bcl-2 and its pro-survival relatives in tumourigenesis and cancer therapy. Cell Death Differ. 2011, 18(9):1414-24.

293. Kennedy KM, Dewhirst MW. Tumor metabolism of lactate: the influence and therapeutic potential for MCT and CD147 regulation. Future Oncol. 2010, 6(1):127-48.

294. Kerbel R, Folkman J. Clinical translation of angiogenesis inhibitors. Nat Rev Cancer. 2002, 2(10):727-39.

295. Kerr JF, Wyllie AH, Currie AR. Apoptosis: a basic biological phenomenon with wide-ranging implications in tissue kinetics. Br J Cancer. 1972, 26(4):239-57.

296. Keum YS, Jeong WS, Kong AN. Chemoprevention by isothiocyanates and their underlying molecular signaling mechanisms. Mutat Res. 2004, 555(1-2):191-202.

297. Kharkwal G, Chandra V, Fatima I, Dwivedi A. Ormeloxifene inhibits osteoclast differentiation in parallel to downregulating RANKL-induced ROS generation and suppressing the activation of ERK and JNK in murine RAW264.7 cells. J Mol Endocrinol. 2012, 48(3):261-70.

298. Kim BC, Kim HG, Lee SA, Lim S, Park EH, Kim SJ, Lim CJ. Genipin-induced apoptosis in hepatoma cells is mediated by reactive oxygen species/c-Jun NH2-terminal kinase-dependent activation of mitochondrial pathway. Biochem Pharmacol. 2005, 70(9):1398-407.

299. Kim EJ, Park KS, Chung SY, Sheen YY, Moon DC, Song YS, Kim KS, Song S, Yun YP, Lee MK, Oh KW, Yoon DY, Hong JT. Peroxisome proliferator-activated receptor-gamma activator 15-deoxy-Delta12,14-prostaglandin J2 inhibits neuroblastoma cell growth through induction of apoptosis: association with extracellular signal-regulated kinase signal pathway. J Pharmacol Exp Ther. 2003, 307(2):505-17.

300. Kim KH, Moriarty K, Bender JR. Vascular cell signaling by membrane estrogen receptors. Steroids. 2008, 73(9-10):864-9.

301. Kim KJ, Li B, Winer J, Armanini M, Gillett N, Phillips HS, Ferrara N. Inhibition of vascular endothelial growth factor-induced angiogenesis suppresses tumour growth in vivo. Nature. 1993, 362(6423):841-4.

302. Kim KN, Heo SJ, Yoon WJ, Kang SM, Ahn G, Yi TH, Jeon YJ. Fucoxanthin inhibits the inflammatory response by suppressing the activation of NF-κB and MAPKs in lipopolysaccharide-induced RAW 264.7 macrophages. Eur J Pharmacol. 2010, 649(1-3):369-375.

303. Kim KY, Kim SS, Cheon HG. Differential anti-proliferative actions of peroxisome proliferator-activated receptor-gamma agonists in MCF-7 breast cancer cells. Biochem Pharmacol. 2006, 72(5):530-40.

304. Kim S, Kang J, Qiao J, Thomas RP, Evers BM, Chung DH. Phosphatidylinositol 3-kinase inhibition down-regulates survivin and facilitates TRAIL-mediated apoptosis in neuroblastomas. J Pediatr Surg. 2004, 39(4):516-21.

305. Kim SH, Yoo CI, Kim HT, Park JY, Kwon CH, Kim YK. Activation of peroxisome proliferator-activated receptor-gamma (PPARgamma) induces cell death hrough

MAPK-dependent mechanism in osteoblastic cells. Toxicol Appl Pharmacol. 2006, 215(2):198-207.

306. Kim-Schulze S, McGowan KA, Hubchak SC, Cid MC, Martin MB, Kleinman HK, Greene GL, Schnaper HW. Expression of an estrogen receptor by human coronary artery and umbilical vein endothelial cells. Circulation. 1996, 94(6):1402-7.

307. Klinge CM, Blankenship KA, Risinger KE, Bhatnagar S, Noisin EL, Sumanasekera WK, Zhao L, Brey DM, Keynton RS. Resveratrol and estradiol rapidly activate MAPK signaling through estrogen receptors alpha and beta in endothelial cells. J Biol Chem. 2005, 280(9):7460-8.

308. Knuuttila M, Yatkin E, Kallio J, Savolainen S, Laajala TD, Aittokallio T, Oksala R, Häkkinen M, Keski-Rahkonen P, Auriola S, Poutanen M, Mäkelä S. Castration induces up-regulation of intratumoral androgen biosynthesis and androgen receptor expression in an orthotopic VCaP human prostate cancer xenograft model. Am J Pathol. 2014, 184(8):2163-73.

309. Koehn FE, Carter GT. The evolving role of natural products in drug discovery. Nat Rev Drug Discov. 2005, 4(3):206-20.

310. Kolbus A, Herr I, Schreiber M, Debatin KM, Wagner EF, Angel P. c-Jun-dependent CD95-L expression is a rate-limiting step in the induction of apoptosis by alkylating agents. Mol Cell Biol. 2000, 20(2):575-82.

311. Kondo N, Nakamura H, Masutani H, Yodoi J. Redox regulation of human thioredoxin network. Antioxid Redox Signal. 2006, 8(9-10):1881-90.

312. Kops GJ, Weaver BA, Cleveland DW. On the road to cancer: aneuploidy and the mitotic checkpoint. Nat Rev Cancer. 2005, 5(10):773-85.

313. Korkina LG, De Luca C, Kostyuk VA, Pastore S. Plant polyphenols and tumors: from mechanisms to therapies, prevention, and protection against toxicity of anti-cancer treatments. Curr Med Chem. 2009, 16(30):3943-65.

314. Krämer DK, Al-Khalili L, Perrini S, Skogsberg J, Wretenberg P, Kannisto K, Wallberg-Henriksson H, Ehrenborg E, Zierath JR, Krook A. Direct activation of glucose transport in primary human myotubes after activation of peroxisome proliferator-activated receptor delta. Diabetes. 2005, 54(4):1157-63.

315. Kris-Etherton PM, Hecker KD, Bonanome A, Coval SM, Binkoski AE, Hilpert KF, Griel AE, Etherton TD. Bioactive compounds in foods: their role in the prevention of cardiovascular disease and cancer. Am J Med. 2002, 113 Suppl 9B:71S-88S.

316. Królik M, Milnerowicz H. The effect of using estrogens in the light of scientific research. Adv Clin Exp Med. 2012, 21(4):535-43.

317. Kubota T, Koshizuka K, Williamson EA, Asou H, Said JW, Holden S, Miyoshi I, Koeffler HP. Ligand for peroxisome proliferator-activated receptor gamma (troglitazone) has potent antitumor effect against human prostate cancer both in vitro and in vivo. Cancer Res. 1998, 58(15):3344-52.

318. Kühnel F, Zender L, Paul Y, Tietze MK, Trautwein C, Manns M, Kubicka S. NFkappaB mediates apoptosis through transcriptional activation of Fas (CD95) in adenoviral hepatitis. J Biol Chem. 2000, 275(9):6421-7.

319. Kumar AP, Garcia GE, Ghosh R, Rajnarayanan RV, Alworth WL, Slaga TJ. 4-Hydroxy-3-methoxybenzoic acid methyl ester: a curcumin derivative targets Akt/NF kappa B cell survival signaling pathway: potential for prostate cancer management. Neoplasia. 2003, 5(3):255-66.

320. Kumar AP, Quake AL, Chang MK, Zhou T, Lim KS, Singh R, Hewitt RE, Salto-Tellez M, Pervaiz S, Clément MV. Repression of NHE1 expression by PPARgamma activation is a potential new approach for specific inhibition of the growth of tumor cells in vitro and in vivo. Cancer Res. 2009, 69(22):8636-44.

321. Kumar S, Saradhi M, Chaturvedi NK, Tyagi RK. Intracellular localization and nucleocytoplasmic trafficking of steroid receptors: an overview. Mol Cell Endocrinol. 2006, 246(1-2):147-56.

322. Kundu N, Fulton AM. Selective cyclooxygenase (COX)-1 or COX-2 inhibitors control metastatic disease in a murine model of breast cancer. Cancer Res. 2002, 62(8):2343-6.

323. Kupzig S, Walker SA, Cullen PJ. The frequencies of calcium oscillations are optimized for efficient calcium-mediated activation of Ras and the ERK/MAPK cascade. Proc Natl Acad Sci U S A. 2005, 102(21):7577-82.

324. Kuttan G, Vasudevan DM, Kuttan R. Effect of a preparation from Viscum album on tumor development in vitro and in mice. J Ethnopharmacol. 1990, 29(1):35-41.

325. Kyle RA, Yee GC, Somerfield MR, Flynn PJ, Halabi S, Jagannath S, Orlowski RZ, Roodman DG, Twilde P, Anderson K, American Society of Clinical Oncology. American Society of Clinical Oncology 2007 clinical practice guideline update on the role of bisphosphonates in multiple myeloma. J Clin Oncol. 2007, 25(17):2464-72.

326. Lamalice L, Le Boeuf F, Huot J. Endothelial cell migration during angiogenesis. Circ Res 2007, 100:782-794.

327. Lamb P, Crawford L. Characterization of the human p53 gene. Mol Cell Biol. 1986, 6(5):1379-85.

328. Lander R, Nordin K, LaBonne C. The F-box protein Ppa is a common regulator of core EMT factors Twist, Snail, Slug, and Sip1. J Cell Biol. 2011, 194(1):17-25.

329. Langcake P, Pryce RJ. A new class of phytoalexins from grapevines. Experientia. 1977, 33(2):151-2.

330. Lareu RR, Lacher MD, Bradley CK, Sridaran R, Friis RR, Dharmarajan AM. Regulated expression of inhibitor of apoptosis protein 3 in the rat corpus luteum. Biol Reprod. 2003, 68(6):2232-40.

331. Lawlor MA, Alessi DR. PKB/Akt: a key mediator of cell proliferation, survival and insulin responses? J Cell Sci. 2001, 114(Pt 16):2903-10.

332. Lawrence T. The nuclear factor NF-kappaB pathway in inflammation. Cold Spring Harb Perspect Biol. 2009, 1(6):a001651.

333. Lea MA, Sura M, Desbordes C. Inhibition of cell proliferation by potential peroxisome proliferator-activated receptor (PPAR) gamma agonists and antagonists. Anticancer Res. 2004, 24(5A):2765-71.

334. Lee HJ, Chattopadhyay S, Gong EY, Ahn RS, Lee K. Antiandrogenic effects of bisphenol A and nonylphenol on the function of androgen receptor. Toxicol Sci. 2003, 75(1):40-6.

335. Lee JH, Khor TO, Shu L, Su ZY, Fuentes F, Kong AN. Dietary phytochemicals and cancer prevention: Nrf2 signaling, epigenetics, and cell death mechanisms in blocking cancer initiation and progression. Pharmacol Ther. 2013, 137(2):153-71.

336. Lee KW, Bode AM, Dong Z. Molecular targets of phytochemicals for cancer prevention. Nat Rev Cancer. 2011, 11(3):211-8.

337. Lee NK, Choi YG, Baik JY, Han SY, Jeong DW, Bae YS, Kim N, Lee SY. A crucial role for reactive oxygen species in RANKL-induced osteoclast differentiation. Blood. 2005, 106(3):852-9.

338. Lee SK, Nam KA, Hoe YH, Min HY, Kim EY, Ko H, Song S, Lee T, Kim S. Synthesis and evaluation of cytotoxicity of stilbene analogues. Arch Pharm Res. 2003, 26(4):253-7.

339. Lee WY, Liu KW, Yeung JH. Reactive oxygen species-mediated kinase activation by dihydrotanshinone in tanshinones-induced apoptosis in HepG2 cells. Cancer Lett. 2009, 285(1):46-57.

340. Lee YS, Kim YS, Lee SY, Kim GH, Kim BJ, Lee SH, Lee KU, Kim GS, Kim SW, Koh JM. AMP kinase acts as a negative regulator of RANKL in the differentiation of osteoclasts. Bone. 2010, 47(5):926-37

341. Lefebvre AM, Chen I, Desreumaux P, Najib J, Fruchart JC, Geboes K, Briggs M, Heyman R, Auwerx J. Activation of the peroxisome proliferator-activated receptor gamma promotes the development of colon tumors in C57BL/6J-APCMin/+ mice. Nat Med. 1998, 4(9):1053-7.

342. Lehrke M, Lazar MA. The many faces of PPARgamma. Cell. 2005, 123(6):993-9.

343. Lemmon MA, Schlessinger J. Cell signaling by receptor tyrosine kinases. Cell. 2010, 141(7):1117-34.

344. Lennon AM, Ramaugé M, Dessouroux A, Pierre M. MAP kinase cascades are activated in astrocytes and preadipocytes by 15-deoxy-Delta(12-14)-prostaglandin J(2) and the thiazolidinedione ciglitazone through peroxisome proliferator activator receptor gamma-independent mechanisms involving reactive oxygenated species. J Biol Chem. 2002, 277(33):29681-5.

345. Lespagnard L, Gancberg D, Rouas G, Leclercq G, de Saint-Aubain Somerhausen N, Di Leo A, Piccart M, Verhest A, Larsimont D. Tumor-infiltrating dendritic cells in adenocarcinomas of the breast: a study of 143 neoplasms with a correlation to usual prognostic factors and to clinical outcome. Int J Cancer. 1999, 84(3):309-14.

346. Li K, Dias SJ, Rimando AM, Dhar S, Mizuno CS, Penman AD, Lewin JR, Levenson AS. Pterostilbene acts through metastasis-associated protein 1 to inhibit tumor growth, progression and metastasis in prostate cancer. PLoS One. 2013, 8(3):e57542.

347. Li L, Wu T, Liu Z. [Integration of extra-nuclear and nuclear estrogen receptor actions]. Sheng Wu Yi Xue Gong Cheng Xue Za Zhi. 2010, 27(4):958-following 60.

348. Li M, Lee TW, Mok TS, Warner TD, Yim AP, Chen GG. Activation of peroxisome proliferator-activated receptor-gamma by troglitazone (TGZ) inhibits human lung cell growth. J Cell Biochem. 2005, 96(4):760-74.

349. Li P, Nijhawan D, Budihardjo I, Srinivasula SM, Ahmad M, Alnemri ES, Wang X. Cytochrome c and dATP-dependent formation of Apaf-1/caspase-9 complex initiates an apoptotic protease cascade. Cell. 1997, 91(4):479-89.

350. Li Q, Verma IM. NF-kappaB regulation in the immune system. Nat Rev Immunol. 2002, 2(10):725-34.

351. Liang J, Shang Y. Estrogen and cancer. Annu Rev Physiol. 2013, 75:225-40.

352. Lim YP, Lim TT, Chan YL, Song AC, Yeo BH, Vojtesek B, Coomber D, Rajagopal G, Lane D. The p53 knowledgebase: an integrated information resource for p53 research. Oncogene. 2007, 26(11):1517-21.

353. Lin C, Wu M, Dong J. Quercetin-4'-O-β-D-glucopyranoside (QODG) inhibits angiogenesis by suppressing VEGFR2-mediated signaling in zebrafish and endothelial cells. PLoS One. 2012, 7(2):e31708.

354. Lin HS, Yue BD, Ho PC. Determination of pterostilbene in rat plasma by a simple HPLC-UV method and its application in pre-clinical pharmacokinetic study. Biomed Chromatogr. 2009, 23(12):1308-15.

355. Lin VC, Tsai YC, Lin JN, Fan LL, Pan MH, Ho CT, Wu JY, Way TD. Activation of AMPK by pterostilbene suppresses lipogenesis and cell-cycle progression in p53 positive and negative human prostate cancer cells. J Agric Food Chem. 2012, 60(25):6399-407.

356. Lin WW, Karin M. A cytokine-mediated link between innate immunity, inflammation, and cancer. J Clin Invest. 2007, 117(5):1175-83.

357. Liu C, Nadiminty N, Tummala R, Chun JY, Lou W, Zhu Y, Sun M, Evans CP, Zhou Q, Gao AC. Andrographolide targets androgen receptor pathway in castration-resistant prostate cancer. Genes Cancer. 2011, 2(2):151-9.

358. Liu H, Zang C, Fenner MH, Possinger K, Elstner E. PPARgamma ligands and ATRA inhibit the invasion of human breast cancer cells in vitro. Breast Cancer Res Treat. 2003, 79(1):63-74.

359. Liu P, Cheng H, Roberts TM, Zhao JJ. Targeting the phosphoinositide 3-kinase pathway in cancer Nat Rev Drug Discov. 2009, 8 (8): 627–644.

360. Liu P, Liang H, Xia Q, Li P, Kong H, Lei P, Wang S, Tu Z. Resveratrol induces apoptosis of pancreatic cancers cells by inhibiting miR-21 regulation of BCL-2 expression. Clin Transl Oncol. 2013, 15(9):741-6.

361. Liu X, Sun J. Endothelial cells dysfunction induced by silica nanoparticles through oxidative stress via JNK/P53 and NF-kappaB pathways. Biomaterials. 2010, 31(32):8198-209.

362. Liu Y, Wang L, Wu Y, Lv C, Li X, Cao X, Yang M, Feng D, Luo Z. Pterostilbene exerts antitumor activity against human osteosarcoma cells by inhibiting the JAK2/STAT3 signaling pathway. Toxicology. 2013, 304:120-31.

363. Lo AH, Liang YC, Lin-Shiau SY, Ho CT, Lin JK. Carnosol, an antioxidant in rosemary, suppresses inducible nitric oxide synthase through down-regulating nuclear factor-kappaB in mouse macrophages. Carcinogenesis. 2002, 23(6):983-91.

364. Locksley RM, Killeen N, Lenardo MJ. The TNF and TNF receptor superfamilies: integrating mammalian biology. Cell. 2001, 104(4):487-501.

365. Lorenzo E, Ruiz-Ruiz C, Quesada AJ, Hernández G, Rodríguez A, López-Rivas A, Redondo JM. Doxorubicin induces apoptosis and CD95 gene expression in human primary endothelial cells through a p53-dependent mechanism. J Biol Chem. 2002, 277(13):10883-92.

366. Losordo DW, Isner JM Estrogen and angiogenesis: A review. Arterioscler Thromb Vasc Biol. 2001, 21:6-12.

367. Low KC, Tergaonkar V. Telomerase: central regulator of all of the hallmarks of cancer. Trends Biochem Sci. 2013, 38(9):426-34.

368. Luca M, Huang S, Gershenwald JE, Singh RK, Reich R, Bar-Eli M. Expression of interleukin-8 by human melanoma cells up-regulates MMP-2 activity and increases tumor growth and metastasis. Am J Pathol. 1997, 151(4):1105-13.

369. Lucas R, Holmgren L, Garcia I, Jimenez B, Mandriota SJ, Borlat F, Sim BK, Wu Z, Grau GE, Shing Y, Soff GA, Bouck N, Pepper MS. Multiple forms of angiostatin induce apoptosis in endothelial cells. Blood. 1998, 92(12):4730-41.

370. Luo JC, Yamaguchi S, Shinkai A, Shitara K, Shibuya M. Significant expression of vascular endothelial growth factor/vascular permeability factor in mouse ascites tumors. Cancer Res. 1998, 58(12):2652-60.

371. Ma J, Jemal A (2013). Breast Cancer Statistics. In Breast Cancer Metastasis and Drug Resistance (pp. 1-18). Springer New York.

372. Määttä JA, Büki KG, Gu G, Alanne MH, Vääräniemi J, Liljenbäck H, Poutanen M, Härkönen P, Väänänen K. Inactivation of estrogen receptor α in bone-forming cells induces bone loss in female mice. FASEB J. 2013, 27(2):478-88.

373. Määttä JA, Büki KG, Ivaska KK, Nieminen-Pihala V, Elo TD, Kähkönen T, Poutanen M, Härkönen P, Väänänen K. Inactivation of the androgen receptor in bone-forming cells leads to trabecular bone loss in adult female mice. Bonekey Rep. 2013, 2:440.

374. Mac Gabhann F, Popel AS. Systems biology of vascular endothelial growth factors. Microcirculation. 2008, 15(8):715-38.

375. Madsen CD, Sahai E. Cancer dissemination-lessons from leukocytes. Dev Cell. 2010, 19(1):13-26.

376. Maity A, Sall W, Koch CJ, Oprysko PR, Evans SM. Low pO2 and beta-estradiol induce VEGF in MCF-7 and MCF-7-5C cells: relationship to in vivo hypoxia. Breast Cancer Res Treat. 2001, 67(1):51-60.

377. Maity R, Sharma J, Jana NR. Capsaicin induces apoptosis through ubiquitin-proteasome system dysfunction. J Cell Biochem. 2010, 109(5):933-42.

378. Maiuri MC, Zalckvar E, Kimchi A, Kroemer G. Self-eating and self-killing: crosstalk between autophagy and apoptosis. Nat Rev Mol Cell Biol. 2007, 8(9):741-52.

379. Mak KK, Wu AT, Lee WH, Chang TC, Chiou JF, Wang LS, Wu CH, Huang CY, Shieh YS, Chao TY, Ho CT, Yen GC, Yeh CT. Pterostilbene, a bioactive component of blueberries, suppresses the generation of breast cancer stem cells within tumor microenvironment and metastasis via modulating NF-κB/microRNA 448 circuit. Mol Nutr Food Res. 2013, 57(7):1123-34.

380. Maldonado V, Meléndez-Zajgla J, Ortega A. Modulation of NF-kappa B, and Bcl-2 in apoptosis induced by cisplatin in HeLa cells. Mutat Res. 1997, 381(1):67-75.

381. Mandriota SJ, Jussila L, Jeltsch M, Compagni A, Baetens D, Prevo R, Banerji S, Huarte J, Montesano R, Jackson DG, Orci L, Alitalo K, Christofori G, Pepper MS. Vascular endothelial growth factor-C-mediated lymphangiogenesis promotes tumour metastasis. EMBO J. 2001, 20(4):672-82.

382. Mann J. Natural products in cancer chemotherapy: past, present and future. Nat Rev Cancer. 2002, 2(2):143-8.

383. Manna PR, Huhtaniemi IT, Stocco DM. Mechanisms of protein kinase C signaling in the modulation of 3',5'-cyclic adenosine monophosphate-mediated steroidogenesis in mouse gonadal cells. Endocrinology. 2009, 150(7):3308-17.

384. Mannal PW, Alosi JA, Schneider JG, McDonald DE, McFadden DW. Pterostilbene inhibits pancreatic cancer in vitro. J Gastrointest Surg. 2010, 14(5):873-9.

385. Manohar M, Fatima I, Saxena R, Chandra V, Sankhwar PL, Dwivedi A. (-)-Epigallocatechin-3-gallate induces apoptosis in human endometrial adenocarcinoma cells via ROS generation and p38 MAP kinase activation. J Nutr Biochem. 2013, 24(6):940-7.

386. Mantovani A, Allavena P, Sica A, Balkwill F. Cancer-related inflammation. Nature. 2008, 454(7203):436-44.

387. Marino M, Acconcia F, Bresciani F, Weisz A, Trentalance A. Distinct nongenomic signal transduction pathways controlled by 17beta-estradiol regulate DNA synthesis

and cyclin D(1) gene transcription in HepG2 cells. Mol Biol Cell. 2002, 13(10):3720-9.

388. Marino M, Acconcia F, Trentalance A. Biphasic estradiol-induced AKT phosphorylation is modulated by PTEN via MAP kinase in HepG2 cells. Mol Biol Cell. 2003, 14(6):2583-91.

389. Marino M, Ficca R, Ascenzi P, Trentalance A. Nitric oxide inhibits selectively the 17beta-estradiol-induced gene expression without affecting nongenomic events in HeLa cells. Biochem Biophys Res Commun. 2001, 286(3):529-33.

390. Marino M, Pallottini V, Trentalance A. Estrogens cause rapid activation of IP3-PKC-alpha signal transduction pathway in HEPG2 cells. Biochem Biophys Res Commun. 1998, 245(1):254-8.

391. Marnett LJ. Oxy radicals and DNA damage. Carcinogenesis 2000, 2 1(3):361–70.

392. Martin TA, Goyal A, Watkins G, Jiang WG. Expression of the transcription factors snail, slug, and twist and their clinical significance in human breast cancer. Ann Surg Oncol. 2005, 12(6):488-96.

393. Maynard S, Schurman SH, Harboe C, de Souza-Pinto NC, Bohr VA. Base excision repair of oxidative DNA damage and association with cancer and aging. Carcinogenesis. 2009, 30(1):2-10.

394. Mayur YC, Peters GJ, Prasad VV, Lemo C, Sathish NK. Design of new drug molecules to be used in reversing multidrug resistance in cancer cells. Curr Cancer Drug Targets. 2009, 9(3):298-306.

395. McCormack D, Mannal P, McDonald D, Tighe S, Hanson J, McFadden D. Genomic analysis of pterostilbene predicts its antiproliferative effects against pancreatic cancer in vitro and in vivo. J Gastrointest Surg. 2012, 16(6):1136-43.

396. McCormack D, McFadden D. A review of pterostilbene antioxidant activity and disease modification. Oxid Med Cell Longev. 2013, 2013:575482.

397. McCormack D, McFadden D. Pterostilbene and cancer: current review. J Surg Res. 2012, 173(2):e53-61.

398. Medzhitov R. Origin and physiological roles of inflammation. Nature. 2008, 454(7203):428-35.

399. Melagraki G, Afantitis A, Igglessi-Markopoulou O, Detsi A, Koufaki M, Kontogiorgis C, Hadjipavlou-Litina DJ. Synthesis and evaluation of the antioxidant and anti-inflammatory activity of novel coumarin-3-aminoamides and their alpha-lipoic acid adducts. Eur J Med Chem. 2009, 44(7):3020-6.

400. Melchior F, Kindl H. Coordinate- and elicitor-dependent expression of stilbene synthase and phenylalanine ammonia-lyase genes in Vitis cv. Optima. Arch Biochem Biophys. 1991, 288(2):552-7.

401. Mena S, Rodríguez ML, Ponsoda X, Estrela JM, Jäättela M, Ortega AL. Pterostilbene-induced tumor cytotoxicity: a lysosomal membrane permeabilization-dependent mechanism. PLoS One. 2012, 7(9):e44524.

402. Mesiano S, Ferrara N, Jaffe RB. Role of vascular endothelial growth factor in ovarian cancer: inhibition of ascites formation by immunoneutralization. Am J Pathol. 1998, 153(4):1249-56.

403. Metzen E, Ratcliffe PJ. HIF hydroxylation and cellular oxygen sensing. Biol Chem. 2004, 385(3-4):223-30.

404. Meulmeester E, Jochemsen AG. p53: a guide to apoptosis. Curr Cancer Drug Targets. 2008, 8(2):87-97.

405. Mgbonyebi OP, Russo J, Russo IH. Antiproliferative effect of synthetic resveratrol on human breast epithelial cells. Int J Oncol. 1998, 12(4):865-9.

406. Micalizzi DS, Farabaugh SM, Ford HL. Epithelial-mesenchymal transition in cancer: parallels between normal development and tumor progression. J Mammary Gland Biol Neoplasia. 2010, 15(2):117-34.

407. Micheau O, Tschopp J. Induction of TNF receptor I-mediated apoptosis via two sequential signaling complexes. Cell. 2003, 114(2):181-90.

408. Migliaccio A, Di Domenico M, Castoria G, de Falco A, Bontempo P, Nola E, Auricchio F. Tyrosine kinase/p21ras/MAP-kinase pathway activation by estradiol-receptor complex in MCF-7 cells. EMBO J. 1996, 15(6):1292-300.

409. Mignatti P, Rifkin DB. Plasminogen activators and matrix metalloproteinases in angiogenesis. Enzyme Protein. 1996, 49(1-3):117-37

410. Mills N (2006) ChemDraw Ultra 10.0. J Am Chem Soc 128 (41).

411. Mizejewski GJ. Role of integrins in cancer: survey of expression patterns. Proc Soc Exp Biol Med. 1999, 222(2):124-38.

412. Mody M, Dharker N, Bloomston M, Wang PS, Chou FS, Glickman TS, McCaffrey T, Yang Z, Pumfery A, Lee D, Ringel MD, Pinzone JJ. Rosiglitazone sensitizes MDA-MB-231 breast cancer cells to anti-tumour effects of tumour necrosis factor-alpha, CH11 and CYC202. Endocr Relat Cancer. 2007, 14(2):305-15.

413. Moens S, Goveia J, Stapor PC, Cantelmo AR, Carmeliet P. The multifaceted activity of VEGF in angiogenesis–Implications for therapy responses. Cytokine & growth factor reviews. 2014, 25(4), 473-482.

414. Moon DO, Kim MO, Kang SH, Choi YH, Kim GY. Sulforaphane suppresses TNF-alpha-mediated activation of NF-kappaB and induces apoptosis through activation of reactive oxygen species-dependent caspase-3. Cancer Lett. 2009, 274(1):132-42.

415. Moore S. Managing treatment side effects in advanced breast cancer. Semin Oncol Nurs. 2007, 23(4 Suppl 2):S23-30.

416. Mora A, Youn J, Keegan A, Boothby M. NF-kappa B/Rel participation in the lymphokine-dependent proliferation of T lymphoid cells. J Immunol. 2001 Feb 15, 166(4):2218-27.

417. Morales DE, McGowan KA, Grant DS, Maheshwari S, Bhartiya D, Cid MC, Kleinman HK, Schnaper HW. Estrogen promotes angiogenic activity in human umbilical vein endothelial cells in vitro and in a murine model. Circulation 91, no. 3 (1995): 755-763.

418. Morgan G, Ward R, Barton M. The contribution of cytotoxic chemotherapy to 5-year survival in adult malignancies. Clin Oncol (R Coll Radiol). 2004, 16(8):549-60.

419. Morley P, Whitfield JF, Vanderhyden BC, Tsang BK, Schwartz JL. A new, nongenomic estrogen action: the rapid release of intracellular calcium. Endocrinology. 1992, 131(3):1305-12.

420. Morphy R, Rankovic Z. Designed multiple ligands. An emerging drug discovery paradigm. J Med Chem. 2005, 48(21):6523-43.

421. Mosmann T. Rapid colorimetric assay for cellular growth and survival: application to proliferation and cytotoxicity assays. J Immunol Methods. 1983, 65(1-2):55-63.

422. Motomura W, Tanno S, Takahashi N, Nagamine M, Fukuda M, Kohgo Y, Okumura T. Involvement of MEK-ERK signaling pathway in the inhibition of cell growth by troglitazone in human pancreatic cancer cells. Biochem Biophys Res Commun. 2005, 332(1):89-94.

423. Mueller E, Sarraf P, Tontonoz P, Evans RM, Martin KJ, Zhang M, Fletcher C, Singer S, Spiegelman BM. Terminal differentiation of human breast cancer through PPAR gamma. Mol Cell. 1998, 1(3):465-70.

424. Mueller MD, Vigne JL, Minchenko A, Lebovic DI, Leitman DC, Taylor RN. Regulation of vascular endothelial growth factor (VEGF) gene transcription by estrogen receptors alpha and beta. Proc Natl Acad Sci U S A. 2000, 97(20):10972-7.

425. Mukai H. Targeted therapy in breast cancer: current status and future directions. Jpn J Clin Oncol. 2010, 40(8):711-6.

426. Mukherjee KL. (2003) Routine biochemical tests and histological techniques. In: Mukherjee, K (Ed), Medical Laboratory Technology, Tata McGraw-Hill Publishing Company Limited, New Delhi 1124-1190

427. Müller A, Homey B, Soto H, Ge N, Catron D, Buchanan ME, McClanahan T, Murphy E, Yuan W, Wagner SN, Barrera JL, Mohar A, Verástegui E, Zlotnik A. Involvement of chemokine receptors in breast cancer metastasis. Nature. 2001, 410(6824):50-6.

428. Müller JM, Ziegler-Heitbrock HW, Baeuerle PA. Nuclear factor kappa B, a mediator of lipopolysaccharide effects. Immunobiology. 1993, 187(3-5):233-56.

429. Mundy GR. Metastasis to bone: causes, consequences and therapeutic opportunities. Nat Rev Cancer. 2002, 2(8):584-93.

430. Münster PN, Srethapakdi M, Moasser MM, Rosen N. Inhibition of heat shock protein 90 function by ansamycins causes the morphological and functional differentiation of breast cancer cells. Cancer Res. 2001, 61(7):2945-52.

431. Munster PN, Troso-Sandoval T, Rosen N, Rifkind R, Marks PA, Richon VM. The histone deacetylase inhibitor suberoylanilide hydroxamic acid induces differentiation of human breast cancer cells. Cancer Res. 2001, 61(23):8492-7.

432. Murias M, Handler N, Erker T, Pleban K, Ecker G, Saiko P, Szekeres T, Jäger W. Resveratrol analogues as selective cyclooxygenase-2 inhibitors: synthesis and structure-activity relationship. Bioorg Med Chem. 2004, 12(21):5571-8.

433. Murias M, Jäger W, Handler N, Erker T, Horvath Z, Szekeres T, Nohl H, Gille L. Antioxidant, prooxidant and cytotoxic activity of hydroxylated resveratrol analogues: structure-activity relationship. Biochem Pharmacol. 2005, 69(6):903-12.

434. Murillo G, Mehta RG. Cruciferous vegetables and cancer prevention. Nutr Cancer. 2001, 41(1-2):17-28.

435. Myung J, Kim KB, Crews CM. The ubiquitin-proteasome pathway and proteasome inhibitors. Med Res Rev. 2001, 21(4):245-73.

436. Nantel F, Denis D, Gordon R, Northey A, Cirino M, Metters KM, Chan CC. Distribution and regulation of cyclooxygenase-2 in carrageenan-induced inflammation. Br J Pharmacol. 1999, 128(4):853-9.

437. Nathan C. Nitric oxide as a secretory product of mammalian cells. FASEB J. 1992, 6(12):3051-64.

438. Negrini S, Gorgoulis VG, Halazonetis TD. Genomic instability-an evolving hallmark of cancer. Nat Rev Mol Cell Biol. 2010, 11(3):220-8.

439. Nelson AR, Fingleton B, Rothenberg ML, Matrisian LM. Matrix metalloproteinases: biologic activity and clinical implications. J Clin Oncol. 2000, 18(5):1135-49.

440. Nepali K, Sharma S, Sharma M, Bedi PM, Dhar KL. Rational approaches, design strategies, structure activity relationship and mechanistic insights for anticancer hybrids. Eur J Med Chem. 2014, 77:422-87.

441. Neufeld G, Cohen T, Gengrinovitch S, Poltorak Z. Vascular endothelial growth factor (VEGF) and its receptors. FASEB J. 1999, 13(1):9-22.

442. Neville-Webbe HL, Coleman RE. Bisphosphonates and RANK ligand inhibitors for the treatment and prevention of metastatic bone disease. Eur J Cancer. 2010, 46(7):1211-22.

443. Newman DJ, Cragg GM. Natural products as sources of new drugs over the last 25 years. J Nat Prod. 2007, 70(3):461-77.

444. Nguyen TM, Subramanian IV, Kelekar A, Ramakrishnan S. Kringle 5 of human plasminogen, an angiogenesis inhibitor, induces both autophagy and apoptotic death in endothelial cells. Blood. 2007, 109(11):4793-802.

445. Nikhil K, Sharan S, Chakraborty A, Bodipati N, Krishna Peddinti R, Roy P. Roleof isothiocyanate conjugate of pterostilbene on the inhibition of MCF-7 cell proliferation and tumor growth in Ehrlich ascitic cell induced tumor bearing mice. Exp Cell Res. 2014, 320(2):311-28.

446. Nikhil K, Sharan S, Chakraborty A, Roy P. Pterostilbene-isothiocyanate conjugate suppresses growth of prostate cancer cells irrespective of androgen receptor status. PLoS One. 2014, 9(4):e93335.

447. Nikhil K, Sharan S, Singh AK, Chakraborty A, Roy P. Anticancer activities of pterostilbene-isothiocyanate conjugate in breast cancer cells: involvement of PPARγ. PLoS One. 2014, 9(8):e104592.

448. Nikoletopoulou V, Markaki M, Palikaras K, Tavernarakis N. Crosstalk between apoptosis, necrosis and autophagy. Biochim Biophys Acta. 2013,1833(12):3448-59

449. Nishida N, Yano H, Nishida T, Kamura T, Kojiro M. Angiogenesis in cancer. Vasc Health Risk Manag. 2006, 2(3):213-9.

450. Nishikawa M. Reactive oxygen species in tumor metastasis. Cancer Lett. 2008. 266(1):53-9.

451. Nör JE, Mitra RS, Sutorik MM, Mooney DJ, Castle VP, Polverini PJ. Thrombospondin-1 induces endothelial cell apoptosis and inhibits angiogenesis by activating the caspase death pathway. J Vasc Res. 2000, 37(3):209-18.

452. Novack DV, Teitelbaum SL. The osteoclast: friend or foe? Annu Rev Pathol. 2008, 3:457-84.

453. Nutakul W, Sobers HS, Qiu P, Dong P, Decker EA, McClements DJ, Xiao H.Inhibitory effects of resveratrol and pterostilbene on human colon cancer cells: a side-by-side comparison. J Agric Food Chem. 2011, 59(20):10964-70

454. O'Brien MA and Kirby R. Apoptosis: A review of pro-apoptotic and anti-apoptotic pathways and dysregulation in disease. Journal of Veterinary Emergency and Critical Care, 2008, 18: 572–585.

455. Odle TG., Adverse effects of breast cancer treatment. Radiologic technology. 2014, 85(3): 297M-319M.

456. Okami J, Yamamoto H, Fujiwara Y, Tsujie M, Kondo M, Noura S, Oshima S, Nagano H, Dono K, Umeshita K, Ishikawa O, Sakon M, Matsuura N, Nakamori S, Monden M. Overexpression of cyclooxygenase-2 in carcinoma of the pancreas. Clin Cancer Res. 1999, 8:2018-24

457. Okamoto T, Schlegel A, Scherer PE, Lisanti MP. Caveolins, a family of scaffolding proteins for organizing "preassembled signaling complexes" at the plasma membrane. J Biol Chem. 1998, 6, 273(10):5419-22.

458. Olsson AK, Johansson I, Akerud H, Einarsson B, Christofferson R, Sasaki T, Timpl R, Claesson-Welsh L. The minimal active domain of endostatin is a heparin-binding motif that mediates inhibition of tumor vascularization. Cancer Res. 2004, 64(24):9012-7.

459. Oñate SA, Tsai SY, Tsai MJ, O'Malley BW. Sequence and characterization of a coactivator for the steroid hormone receptor superfamily. Science. 1995, 270(5240):1354-7.

460. Onishi T, Hayashi N, Theriault RL, Hortobagyi GN, Ueno NT. Future directions of bone-targeted therapy for metastatic breast cancer. Nat Rev Clin Oncol. 2010, 7(11):641-51.

461. O'Reilly MS, Boehm T, Shing Y, Fukai N, Vasios G, Lane WS, Flynn E, Birkhead JR, Olsen BR, Folkman J. Endostatin: an endogenous inhibitor of angiogenesis and tumor growth. Cell. 1997 88(2):277-85.

462. Otozai S, Ishikawa-Fujiwara T, Oda S, Kamei Y, Ryo H, Sato A, Nomura T, Mitani H, Tsujimura T, Inohara H, Todo T. p53-Dependent suppression of genome instability in germ cells. Mutat Res Fundam Mol Mech Mutagen. 2014, 760:24-32.

463. Oviedo PJ, Sobrino A, Laguna-Fernandez A, Novella S, Tarín JJ, García-Pérez MA, Sanchís J, Cano A, Hermenegildo C. Estradiol induces endothelial cell migration and proliferation through estrogen receptor-enhanced RhoA/ROCK pathway. Mol Cell Endocrinol. 2011, 335(2):96-103.

464. Oyekan A PPARs and their effects on the cardiovascular system. Clinical and Experimental Hypertension. 2011, 33(5): 287-293.

465. Pace-Asciak CR, Hahn S, Diamandis EP, Soleas G, Goldberg DM. The red wine phenolics trans-resveratrol and quercetin block human platelet aggregation and eicosanoid synthesis: implications for protection against coronary heart disease.Clin Chim Acta. 1995, 235(2):207-19.

466. Padilla J, Kaur K, Cao HJ, Smith TJ, Phipps RP. Peroxisome proliferator activator receptor-gamma agonists and 15-deoxy-Delta(12,14)(12,14)-PGJ(2) induce apoptosis in normal and malignant B-lineage cells. J Immunol. 2000, 15, 165(12):6941-8.

467. Pan MH, Chang YH, Badmaev V, Nagabhushanam K, Ho CT. Pterostilbene induces apoptosis and cell cycle arrest in human gastric carcinoma cells. J Agric Food Chem. 2007, 55(19):7777-85.

468. Pan MH, Chang YH, Tsai ML, Lai CS, Ho SY, Badmaev V, Ho CT. Pterostilbene suppressed lipopolysaccharide-induced up-expression of iNOS and COX-2 in murine macrophages. J Agric Food Chem. 2008. 56(16), 7502-7509.

469. Pan MH, Chiou YS, Chen WJ, Wang JM, Badmaev V, Ho CT. Pterostilbene inhibited tumor invasion via suppressing multiple signal transduction pathways in human hepatocellular carcinoma cells. Carcinogenesis 2009, 30: 1234-1242.

470. Pan MH, Lin YT, Lin CL, Wei CS, Ho CT, Chen WJ. Suppression of Heregulin-β1/HER2-modulated invasive and aggressive phenotype of breast carcinoma by pterostilbene via inhibition of matrix metalloproteinase-9, p38 kinase cascade and Akt activation. Evid Based Complement Alternat Med. 2011: 562187.

471. Pan X, Cao X, Li N, Xu Y, Wu Q, Bai J, Yin Z, Luo L, Lan L. Forsythin inhibits lipopolysaccharide-induced inflammation by suppressing JAK-STAT and p38 MAPK signalings and ROS production. Inflamm Res. 2014, 63(7):597-608.

472. Panigrahy D, Singer S, Shen LQ, Butterfield CE, Freedman DA, et al. PPAR gamma ligands inhibit primary tumor growth and metastasis by inhibiting angiogenesis. J Clin Invest. 2002, 110: 923-32.

473. Papageorgiou E, Pitulis N, Msaouel P, Lembessis P, Koutsilieris M The non-genomic crosstalk between PPAR-γ ligands and ERK1/2 in cancer cell lines. Expert Opin Ther Targets. 2007, 11(8):1071-85.

474. Papaioannou M, Reeb C, Asim M, Dotzlaw H, Baniahmad A. Co-activator and co-repressor interplay on the human androgen receptor. Andrologia. 2005, 37: 211-212.

475. Parangi S, O'Reilly M, Christofori G, Holmgren L, Grosfeld J, Folkman J, Hanahan D. Angiogenesis therapy of transgenic mice impairs de novo tumor growth. Proc Natl Acad Sci U S A. 1996, 93:2002-2007.

476. Park E, Gong EY, Romanelli MG, Lee K. Suppression of estrogen receptor-alpha transactivation by thyroid transcription factor-2 in breast cancer cells. Biochem Biophys Res Commun. 2012, 421(3):532-7.

477. Park JI, Venteicher AS, Hong JY, Choi J, Jun S, Shkreli M, Chang W, Meng Z, Cheung P, Ji H, McLaughlin M, Veenstra TD, Nusse R, McCrea PD, Artandi SE.Telomerase modulates Wnt signalling by association with target gene chromatin.Nature. 2009:460(7251):66-72.

478. Patan S. Vasculogenesis and angiogenesis. Cancer Treat Res. 2004, 117:3–32.

479. Paul S, Mizuno CS, Lee HJ, Zheng X, Chajkowisk S, Rimoldi JM, Conney A, Suh N, Rimando AM. In vitro and in vivo studies on stilbene analogs as potential treatment agents for colon cancer. Eur. J. Med Chem 2010, 45: 3702-3708.

480. Payré B, de Medina P, Boubekeur N, Mhamdi L, Bertrand-Michel J, Tercé F, Fourquaux I, Goudounèche D, Record M, Poirot M, Silvente-Poirot S. Microsomal antiestrogen-binding site ligands induce growth control and differentiation of human breast cancer cells through the modulation of cholesterol metabolism. Mol Cancer Ther. 2008,7(12):3707-3718

481. Pepper MS. Role of the matrix metalloproteinase and plasminogen activator-plasmin systems in angiogenesis. Arterioscler Thromb Vasc Biol. 2001, 21(7):1104-17.

482. Perkins ND. The Rel/NF-nB family: friend and foe. Trends Biochem Sci 2000, 25:434–40.

483. Perou CM, Borresen-Dale AL. Systems biology and genomics of breast cancer. Cold Spring Harb Perspect Biol. 2011, 3(2).

484. Perou CM, Sørlie T, Eisen MB, van de Rijn M, Jeffrey SS, Rees CA, Pollack JR, Ross DT, Johnsen H, Akslen LA, Fluge O, Pergamenschikov A, Williams C, Zhu SX, Lønning PE, Børresen-Dale AL, Brown PO, Botstein D. Molecular portraits of human breast tumours. Nature. 2000, 406:747-52.

485. Peters JM, Shah YM, Gonzalez FJ. The role of peroxisome proliferator-activated receptors in carcinogenesis and chemoprevention. Nat Rev Cancer.2012, 12(3): 181-195.

486. Petrelli A, Giordano S. From single- to multi-target drugs in cancer therapy: when aspecificity becomes an advantage. Curr Med Chem. 2008, 15(5):422-32.

487. Pettit GR, Grealish MP, Jung MK, Hamel E, Pettit RK, Chapuis JC, Schmidt JM. Antineoplastic agents. 465. Structural modification of resveratrol: sodium resverastatin phosphate.J Med Chem. 2002, 45(12):2534-42.

488. Philip M, Rowley DA, Schreiber H. Inflammation as a tumor promoter in cancer induction. Semin Cancer Biol. 2004,14:433-9

489. Picotto G, Massheimer V, Boland R. Acute stimulation of intestinal cell calcium influx induced by 17β-estradiol via the cAMP messenger system. Mol Cell Endocrinol. 1996, 119:129-134.

490. Pighetti GM, Novosad W, Nicholson C, Hitt DC, Hansens C, Hollingsworth AB, Lerner ML, Brackett D, Lightfoot SA, Gimble JM. Therapeutic treatment of DMBA-induced mammary tumors with PPAR ligands. Anticancer Res. 2001, 21, 825-9.

491. Pober JS, William CS. Evolving functions of endothelial cells in inflammation. Nature Reviews Immunol. 2007, 10, 803-815.

492. Pollard JW. Tumour-educated macrophages promote tumour progression and metastasis. Nat Rev Cancer. 2004, 4:71-478.

493. Poutanen M. Understanding the diversity of sex steroid action. J Endocrinol. 2012, 212(1):1-2.

494. Prabhu SB, Khalsa JK, Banerjee H, Das A, Srivastava S, Mattoo HR, Thyagarajan K, Tanwar S, Das DS, Majumdar SS, George A, Bal V, Durdik JM, Rath S. Role of apoptosis-inducing factor (Aif) in the T cell lineage. Indian J Med Res. 2013, 138(5):577-90.

495. Praga C, Bergh J, Bliss J, Bonneterre J, Cesana B, Coombes RC, Fargeot P, Folin A, Fumoleau P, Giuliani R, Kerbrat P, Hery M, Nilsson J, Onida F, Piccart M, Shepherd L, Therasse P, Wils J, Rogers D. Risk of acute myeloid leukemia and myelodysplastic

syndrome in trials of adjuvant epirubicin for early breast cancer: correlation with doses of epirubicin and cyclophosphamide. J Clin Oncol. 2005, 23(18):4179-4191.

496. Prescott SM, Fitzpatrick FA. Cyclooxygenase-2 and carcinogenesis. Biochim Biophys Acta. 2000, 1470, 69 -78.

497. Provencher-Mandeville J, Descôteaux C, Mandal SK, Leblanc V, Asselin E, Bérubé G. Synthesis of 17beta-estradiol-platinum(II) hybrid molecules showing cytotoxic activity on breast cancer cell lines. Bioorg Med Chem Lett. 2008, 18(7):2282-7.

498. Pu L, Amoscato AA, Bier ME, Lazo JS. Dual G1 and G2 phase inhibition by a novel, selective Cdc25 inhibitor 6-chloro-7-[corrected](2-morpholin-4- ylethylamino)-quinoline-5,8-dione. J Biol Chem. 2002, 277:46877-85.

499. Qian BZ, Pollard JW. Macrophage diversity enhances tumor progression and metastasis. Cell. 2010, 141(1), 39-51.

500. Quesada AR, Munoz-Chapuli R, Medina MA. Anti-angiogenic drugs: From bench to clinical trials. Med Res Rev. 2006, 26(4):483–530.

501. Raff M. Cell suicide for beginners. Nature. 1998, 396: 119-122.

502. Rafii S, Skobe M. Spilitting vessels: Keeping lymph apart from blood. Nature Med. 2003, 9:166-8.

503. Rajeshwar Y, Gupta M, Mazumder UK. Antitumor activity and in vivo antioxidant status of Mucuna pruriens (Fabaceae) seeds against Ehrlich ascites carcinoma in Swiss albino mice. Iran J Pharm Therapeut. 2005, 4, 46-53.

504. Ramos S. Cancer chemoprevention and chemotherapy: dietary polyphenols and signalling pathways Mol Nutr Food Res. 2008, 507–526.

505. Rao SK, Pavicevic Z, Du Z, Kim JG, Fan M, Jiao Y, Rosebush M, Samant S, Gu W, Pfeffer LM, Nosrat CA. Pro-inflammatory genes as biomarkers and therapeutic targets in oral squamous cell carcinoma. J Biol Chem. 2010, 285(42):32512-21.

506. Razandi M, Pedram A, Levin ER. Estrogen signals to the preservation of endothelial cell form and function. J Biol Chem. 2000, 275(49):38540-6.

507. Rebecca SY, Wong A. Apoptosis in cancer: from pathogenesis to treatment. J Exp Clin Cancer Res. 2011. 30, 1-14.

508. Reed JC. Dysregulation of apoptosis in cancer. J Clin Oncol. 1999, 17: 2941-2953.

509. Rege TA, Stewart J Jr, Dranka B, Benveniste EN, Silverstein RL, Gladson CL. Thrombospondin-1-induced apoptosis of brain microvascular endothelial cells can be mediated by TNF-R1. J Cell Physiol. 2009, 218(1):94-103.

510. Rehn M, Veikkola T, Kukk-Valdre E, Nakamura H, Ilmonen M, Lombardo C,Pihlajaniemi T, Alitalo K, Vuori K. Interaction of endostatin with integrins implicated in angiogenesis. Proc Natl Acad Sci. 2001, 30, 98(3):1024-9.

511. Remsberg, C M, Yáñez JA, Ohgami Y, Vega-Villa K R, Rimando AM, Davies NM. Pharmacometrics of pterostilbene: preclinical pharmacokinetics and metabolism, anticancer, antiinflammatory, antioxidant and analgesic activity. Phytother Res. 2008. 22(2), 169-179.

512. Ren B, Yee KO, Lawler J, Khosravi-Far R. Regulation of tumor angiogenesis by thrombospondin-1. Biochim Biophys Acta. 2006, 1765(2):178-88.

513. Ren F, Zhang S, Mitchell SH, Butler R, Young CY. Tea polyphenols down-regulate the expression of the androgen receptor in LNCaP prostate cancer cells. Oncogene. 2000, 19: 1924-1932.

514. Rene Gonzalez R, Watters A, Xu Y, Singh UP, Mann DR, Rueda BR, Penichet ML. Leptin-signaling inhibition results in efficient anti-tumor activity in estrogen receptor positive or negative breast cancer. Breast Cancer Res. 2009, 11(3):R36.

515. Renehan AG, Zwahlen M, Minder C, O'Dwyer ST, Shalet SM, Egger M. Insulin-like growth factor (IGF)-I, IGF binding protein-3, and cancer risk: systematic review and meta-regression analysis. Lancet. 2004 363(9418):1346-53.

516. Rhim JS, Tsai WP, Chen ZQ, Chen Z, Van Waes C, Burger AM, Lautenberger JA. A human vascular endothelial cell model to study angiogenesis and tumorigenesis. Carcinogenesis. 1998, 19(4):673-81.

517. Richie RC & Swanson JO. Breast cancer: a review of the literature. J Insur Med. 2003. 35, 85-101

518. Rimando AM, Kalt W, Magee JB, Dewey J, Ballington JR. Resveratrol, pterostilbene, and piceatannol in Vaccinium berries. J Agric Food Chem. 2004, 52, 4713-4719.

519. Risau W. Development and differentiation of endothelium. Kidney Int Suppl. 1998, 67, S3-6.

520. Risbridger, G P, Davis ID, Birrell S N, Tilley WD. Breast and prostate cancer: more similar than different. Nature Reviews Cancer. 2010, 10(3): 205-212.

521. Ristimaki A, Honkanen N, Jankala H, Sipponen P, Harkonen M. Expression of cyclooxygenase 2 in human gastric cancer. Cancer Res. 1997, 57:1276-80.

522. Robbins RJ. Phenolic acids in foods: an overview of analytical methodology. J. Agric. Food Chem. 2003. 51, 2866–2887.

523. Roberti M, Pizzirani D, Simoni D, Rondanin R, Baruchello R, Bonora C, Buscemi F, Grimaudo S, Tolomeo M. Synthesis and biological evaluation of resveratrol and analogues as apoptosis-inducing agents. J Med Chem. 2003, 46(16):3546-54.

524. Rodan GA, Martin TJ. Therapeutic approaches to bone diseases. Science. 2000, 289(5484):1508-14.

525. Roshandel D, Holliday KL, Pye SR, Boonen S, Borghs H, Vanderschueren D, Huhtaniemi IT, Adams JE, Ward KA, Bartfai G, Casanueva F, Finn JD, Forti G, Giwercman A, Han TS, Kula K, Lean ME, Pendleton N, Punab M, Silman AJ, Wu FC, Thomson W, O'Neill TW; EMAS Study Group. Genetic variation in the RANKL/RANK/OPG signaling pathway is associated with bone turnover and bone mineral density in men. J Bone Miner Res. 2010, 25(8):1830-8.

526. Roshandel D, Holliday KL, Pye SR, Ward KA, Boonen S, Vanderschueren D, Borghs H, Huhtaniemi IT, Adams JE, Bartfai G, Casanueva FF, Finn JD, Forti G, Giwercman A, Han TS, Kula K, Lean ME, Pendleton N, Punab M, Silman AJ, Wu FC, Thomson W, ONeill TW; EMAS Study Group. Influence of polymorphisms in the RANKL/RANK/OPG signaling pathway on volumetric bone mineral density and bone geometry at the forearm in men. Calcif Tissue Int. 2011, 89(6):446-55.

527. Roupe, KA, Remsberg CM, Yáñez JA, Davies, NM. Pharmacometrics of stilbenes: seguing towards the clinic. Curr Clin Pharmacol. 2006, 81-101.

528. Roy AK, Tyagi RK, Song CS, Lavrovsky Y, Ahn SC, Oh TS, Chatterjee B. Androgen receptor: structural domains and functional dynamics after ligand-receptor interaction. Ann N Y Acad Sci. 2001, 949:44-57.

529. Russell KS, Haynes MP, Sinha D, Clerisme E, Bender JR. Human vascular endothelial cells contain membrane binding sites for estradiol, which mediate rapid intracellular signaling. Proc Natl Acad Sci USA. 2000, 97:5930-5935.

530. Saha MN, Qiu L, Chang H. Targeting p53 by small molecules in hematological malignancies. J Hematol Oncol. 2013, 6(1):23.

531. Saha Roy S, Vadlamudi RK. Role of estrogen receptor signaling in breast cancer metastasis. Int J Breast Cancer. 2012, 654698.

532. Sanchez Alcazar JA, Ruiz Cabello J, Hernandez-Munoz I, Pobre PS, Torre P, Siles Rivas E, Garcia I, Kaplan O, Munoz-Yague MT, Solis Herruzo JA. Tumor Necrosis Factor-alpha Increases ATP Content in metabolically inhibited L929 cells preceding cell death. J Biol Chem. 1997, 272: 30167-30177.

533. Sankari S, Leena KM, Masthan N. Aravindha Babu, Tathagata Bhattacharjee, and M. Elumalai. Apoptosis in cancer–an update. Asian Pac J Cancer Prev. 2012, 10:4873-8.

534. Santen RJ, Song RX, McPherson R, Kumar R, Adam L, Jeng MH, Yue W. The role of mitogen-activated protein (MAP) kinase in breast cancer. J Steroid Biochem Mol Biol. 2002, 80(2):239-56.

535. Santos AF, Huang H, Tindall DJ. The androgen receptor: a potential target for therapy of prostate cancer. Steroids. 2004 Feb,69(2):79-85

536. Saraste A, Pulkki K. Morphologic and biochemical hallmarks of apoptosis. Cardiovasc Res. 2000, 45(3):528-37.

537. Sarkar FH, Adsule S, Li Y, Padhye S. Back to the future: COX-2 inhibitors for chemoprevention and cancer therapy. Mini Rev Med Chem. 2007, 7(6):599-608.

538. Sarkar FH, Li Y, Wang Z, Kong D. Cellular signaling perturbation by natural products. Cell Signal. 2009(11):1541-7.

539. Sarraf P, Mueller E, Jones D, King FJ, DeAngelo DJ, Partridge JB, Holden SA, Chen LB, Singer S, Fletcher C, Spiegelman BM. Differentiation and reversal of malignant changes in colon cancer through PPARgamma. Nat Med. 1998, 1046-52.

540. Sashidhara KV, Kumar A, Kumar M, Sarkar J, Sinha S. Synthesis and in vitro evaluation of novel coumarine-chalcone hybrids as potential anticancer agents Bioorg Med Chem. 2010, 7205-7211.

541. Sauer LA, Dauchy RT, Blask DE, Krause JA, Davidson LK, Dauchy EM. Eicosapentaenoic acid suppresses cell proliferation in MCF-7 human breast cancer xenografts in nude rats via a pertussis toxin-sensitive signal transduction pathway. J Nutr. 2005, 135(9):2124-9.

542. Sawyers C. Targeted cancer therapy. Nature. 2004, 432(7015):2947.

543. Saxena R, Chandra V, Manohar M, Hajela K, Debnath U, Prabhakar YS, Saini KS, Konwar R, Kumar S, Megu K, Roy BG, Dwivedi A. Chemotherapeutic Potential of 2-[Piperidinoethoxyphenyl]-3-Phenyl-2H-Benzo(b)pyran in Estrogen Receptor-Negative Breast Cancer Cells: Action via Prevention of EGFR Activation and Combined Inhibition of PI-3-K/Akt/FOXO and MEK/Erk/AP-1 Pathways. PLoS One. 2013, 8(6):e66246.

544. Saxena R, Fatima I, Chandra V, Blesson CS, Kharkwal G, Hussain MK, Hajela K, Roy BG, Dwivedi A. Benzopyran derivative CDRI-85/287 induces G2-M arrest in estrogen receptor-positive breast cancer cells via modulation of estrogen receptors α-

and β-mediated signaling, in parallel to EGFR signaling and suppresses the growth of tumor xenograft. Steroids. 2013, 78(11):1071-86.

545. Schmidt MV, Brüne B, von Knethen A. The Nuclear Hormone Receptor PPAR γ as a Therapeutic Target in Major Diseases. Sci World J. 2010, 10: 2181-2197.

546. Schneider JG, Alosi JA, McDonald DE, McFadden DW. Pterostilbene inhibits breast cancer in vitro through mitochondrial depolarization and induction of caspase-dependent apoptosis. J Surg Res. 2010, 161: 18-22.

547. Schneider MR, Hoeflich A, Fischer JR, Wolf E, Sordat B, Lahm H. Interleukin-6 stimulates colonogenic growth of primary and metastatic human colon carcinoma cells. Cancer Lett. 2000, 151:31-8.

548. Schneider Y, Vincent F, Duranton B, Badolo L, Gossé F, Bergmann C, Seiler N, Raul F. Anti-proliferative effect of resveratrol, a natural component of grapes and wine, on human colonic cancer cells. Cancer Lett. 2000, 158(1):85-91.

549. Schnitt SJ. Classification and prognosis of invasive breast cancer: from morphology to molecular taxonomy. Mod Pathol. 2010, 2:S60-4.

550. Schöppner, A., and Helmut Kindl. Purification and properties of a stilbene synthase from induced cell suspension cultures of peanut. J Biol Chem. 1984, 259(11): 6806-6811.

551. Schrau fstatter I, Hyslop PA, Jackson JH, Cochrane CG. Oxidant- induced DNA damage of target cells. J Clin Invest 1988, 8 2(3):1040-50.

552. Scotton CJ, Wilson JL, Milliken D, Stamp G, Balkwill FR. Epithelial cancer cell migration: a role for chemokine receptors. Cancer Res 2001, 61: 4961-5.

553. Sean PC, Valina L. Dowson, Ruth S. Slack. Role of AIF in caspase-dependent and caspase-independent cell death. Oncogene 2004, 23: 2785-2796.

554. Seargent JM, Yates EA, Gill JH GW9662, a potent antagonist of PPARγ, inhibits growth of breast tumour cells and promotes the anticancer effects of the PPARγ agonist rosiglitazone, independently of PPARγ activation. Brit J Pharmacol. 2004, 143: 933-937.

555. Sebolt-Leopold JS, Herrera R. Targeting the mitogen-activated protein kinase cascade to treat cancer. Nature Reviews. Cancer. 2004, 4: 937-947.

556. Semenza GL. Tumor metabolism: cancer cells give and take lactate. J Clin Invest. 2008, 118, 3835-3837.

557. Semple RK, Chatterjee VK, O'Rahilly S. PPAR gamma and human metabolic disease. J Clin Invest. 2006, 116: 581-589.

558. Sengupta K, Banerjee S, Saxena N, Banerjee SK. Estradiol-induced vascular endothelial growth factor-A expression in breast tumor cells is biphasic and regulated by estrogen receptor-alpha dependent pathway. Int J Oncol. 2003, 22(3):609-14.

559. Sengupta K, Banerjee S, Saxena NK, Banerjee SK. Thombospondin-1 disrupts estrogen-induced endothelial cell proliferation and migration and its expression is suppressed by estradiol. Mol Cancer Res. 2004, 2(3):150-8.

560. Serra V, Scaltriti M, Prudkin L, Eichhorn PJ, Ibrahim YH, Chandarlapaty S, Markman B, Rodriguez O, Guzman M, Rodriguez S, Gili M, Russillo M, Parra JL, Singh S, Arribas J, Rosen N, Baselga J. PI3K inhibition results in enhanced HER signaling and acquired ERK dependency in HER2-overexpressing breast cancer. Oncogene. 2011, 30(22):2547-57.

561. Sertznig, P, Seifert M, Tilgen W, Reichrath J Present concepts and future outlook: Function of peroxisome proliferator-activated receptors (PPARs) for pathogenesis, progression, and therapy of cancer. J cell physiol. 2007, 1: 1-12.

562. Shalaby F, Rossant J, Yamaguchi TP, Gertsenstein M, Wu XF, Breitman ML, & Schuh, AC. Failure of blood-island formation and vasculogenesis in Flk-1-deficient mice. Nature. 1995, 376(6535), 62-66.

563. Shan ZZ, Masuko-Hongo K, Dai SM, Nakamura H, Kato T, Nishioka K. A potential role of 15-deoxy-delta(12,14)-prostaglandin J2 for induction of human articular chondrocyte apoptosis in arthritis. J Biol Chem. 2004, 279(36):37939-50.

564. Sharma M, Hanchate NK, Tyagi RK, Sharma P. Cyclin dependent kinase 5 (Cdk5) mediated inhibition of the MAP kinase pathway results in CREB down regulation and apoptosis in PC12 cells. Biochem Biophys Res Commun. 2007, 358(2):379-84.

565. Sheikh MS and Fornace AJ Role of p53 family members in apoptosis. J Cell Physiol. 2000, 182: 171-181.

566. Sherman W, Day T, Jacobson MP, Friesner RA, Farid R Novel procedure for modelling ligand/receptor induced fit effects. J Med Chem. 2006, 49: 534-553.

567. Sheth S, Jajoo S, Kaur T, Mukherjea D, Sheehan K, Rybak LP, Vickram R. Resveratrol reduces prostate cancer growth and metastasis by inhibiting the Akt/MicroRNA-21 pathway. PLoS One. 2012, 7: e51655.

568. Shibuya M. Tyrosine Kinase Receptor Flt/VEGFR Family Its Characterization Related to Angiogenesis and Cancer. Genes & cancer, 2010, 1(11), 1119-1123.

569. Shirisha K, Patole J, Padhye S, Sinn E, Shishodia S, Aggarwal BB. Copper complexes of Henna-Sulforaphane conjugates as potent antiproliferative agents against human

myeloma KBM-5 cells through blockade of transcription factor NF-κB. Lett. Drug Design Discovery. 2007, 4(4):257-262.

570. Shukla S, Meeran SM, Katiyar SK. Epigenetic regulation by selected dietary phytochemicals in cancer chemoprevention. Cancer Lett. 2014 355(1):9-17.

571. Shukla Y, Singh R. Resveratrol and cellular mechanisms of cancer prevention. Ann N Y Acad Sci. 2011, 1215:1-8.

572. Siegel R, DeSantis C, Virgo K, Stein K, Mariotto A, Smith T, Cooper D, Gansler T, Lerro C, Fedewa S, Lin C, Leach C, Cannady RS, Cho H, Scoppa S, Hachey M,Kirch R, Jemal A, Ward E. Cancer treatment and survivorship statistics, 2012. CA Cancer J Clin. 2012, 62(4):220-41.

573. Sies H. Polyphenols and health: update and perspectives. Arch Biochem Biophys. 2010. 501(1):2-5.

574. Sigl V, Penninger JM. RANKL/RANK - from bone physiology to breast cancer. Cytokine Growth Factor Rev. 2014, 2:205-14.

575. Silva AE, Serakides R, Ferreira E, Moraes JR, Ocarino Nde M, Cassali GD. Effect of hypothyroidism on the solid form of Ehrlich tumor in intact or castrated adult female mice. Arq Bras Endocrinol Metabol. 2004, 48(6):867-74.

576. Simoni D, Roberti M, Invidiata FP, Aiello E, Aiello S, Marchetti P, Baruchello R, Eleopra M, Di Cristina A, Grimaudo S, Gebbia N, Crosta L, Dieli F, Tolomeo M. Stilbene-based anticancer agents: resveratrol analogues active toward HL60 leukemic cells with a non-specific phase mechanism. Bioorg Med Chem Lett. 2006, 16(12):3245-8.

577. Simstein R, Burow M, Parker A, Weldon C, Beckman B. Apoptosis, chemo resistance and breast cancer: insights from the MCF-7 cell model system. Exp Biol Med. 2003, 228:995-1003.

578. Sinha S, Pal BC, Jagadeesh S, Banerjee PP, Bandyopadhaya A, Bhattacharya S. Mahanine inhibits growth and induces apoptosis in prostate cancer cells through the deactivation of Akt and activation of caspases. Prostate. 2006, 66(12):1257-65.

579. Siow RCM. Culture of human endothelial cells from umbilical veins. In Human Cell Culture Protocols. 2012, 265-274.

580. Sipilä P, Krutskikh A, Pujianto DA, Poutanen M, Huhtaniemi IT. Regional expression of androgen receptor coregulators and androgen action in the mouse epididymis. J Androl. 2011, 32(6):711-7.

581. Sjövall K, Strömbec G, Löfgren A, Bendahl PO, Gunnars B Adjuvant radiotherapy of women with breast cancer–Information, support and side-effects. Europ J Onco Nursing. 2010, 14(2):147-153.

582. Slattery ML, Wolff RK, Herrick J, Caan BJ, and Samowitz W, Tumor markers and rectal cancer: support for an inflammation-related pathway. Int J Cancer. 2009, 125 1698-704.

583. Smyth MJ, Cretney E, Kershaw MH, Hayakawa Y. Cytokines in cancer immunity and immunotherapy. Immunol Rev. 2004, 202:275-293.

584. Solomon VR, Hu C, Lee H. Hybrid pharmacophore design and synthesis of isatin-benzothiazole analogs for their anti-breast cancer activity. Bioorg Med Chem. 2009, 17:7585-7592.

585. Song CH, Yang SH, Park E, Cho SH, Gong EY, Khadka DB, Cho WJ, Lee K. Structure-based virtual screening and identification of a novel androgen receptor antagonist. J Biol Chem. 2012, 287(36):30769-80.

586. Song HY, Ngai MH, Song ZY, MacAry PA, Hobley J, Lear MJ. Practical synthesis of maleimides and coumarin-linked probes for protein and antibody labelling via reduction of native disulfides. Org Biomol Chem. 2009, 7(17):3400-6.

587. Sørlie T, Perou CM, Tibshirani R, Aas T, Geisler S, Johnsen H, Hastie T, Eisen MB, van de Rijn M, Jeffrey SS, Thorsen T, Quist H, Matese JC, Brown PO, Botstein D, Lønning PE, Børresen-Dale AL. Gene expression patterns of breast carcinomas distinguish tumor subclasses with clinical implications.

588. Sridaran R, Hisheh S, Dharmarajan AM. Induction of apoptosis by a gonadotropin-releasing hormone agonist during early pregnancy in the rat. Apoptosis. 1998, 3(1):51-7.

589. Stack MS, Gately S, Bafetti LM, Enghild JJ, Soff GA. Angiostatin inhibits endothelial and melanoma cellular invasion by blocking matrix-enhanced plasminogen activation. Biochem J. 1999, 15:340

590. Staton CA, Stribbling SM, Tazzyman S, Hughes R, Brown NJ, Lewis CE. Current methods for assaying angiogenesis in vitro and in vivo. Int J Exp Pathol. 2004, 85(5):233-48.

591. Stevenson DA, Schwarz EL, Carey JC, Viskochil DH, Hanson H, Bauer S, Weng HY, Greene T, Reinker K, Swensen J, Chan RJ, Yang FC, Senbanjo L, Yang Z, Mao R, Pasquali M. Bone resorption in syndromes of the Ras/MAPK pathway. Clin Genet. 2011, 80(6):566-73.

592. Straub RH. The complex role of estrogens in inflammation. Endocr Rev. 2007, 28(5):521-74.

593. Suh N, Wang Y, Williams CR, Risingsong R, Gilmer T, Willson TM, Sporn MB. A new ligand for the peroxisome proliferator-activated receptor-gamma (PPAR-gamma), GW7845, inhibits rat mammary carcinogenesis. Cancer Res. 1999, 59(22):5671-3.

594. Sumpio BE, Riley JT, Dardik A. Cells in focus: endothelial cell. Int J Biochem Cell Biol. 2002, 34(12):1508-12.

595. Sun H, Berquin IM, Owens RT, O'Flaherty JT, Edwards IJ. Peroxisome proliferator-activated receptor gamma-mediated up-regulation of syndecan-1 by n-3 fatty acids promotes apoptosis of human breast cancer cells. Cancer Res. 2008, 68(8): 2912-9.

596. Sun M, Paciga JE, Feldman RI, Yuan Z, Coppola D, Lu YY, Shelley SA, Nicosia SV, Cheng JQ. Phosphatidylinositol-3-OH Kinase (PI3K)/AKT2, activated in breast cancer, regulates and is induced by estrogen receptor alpha (ERalpha) via interaction between ERalpha and PI3K. Cancer Res. 2001, 61(16):5985-91.

597. Surh YJ. Cancer chemoprevention with dietary phytochemicals. Nat Rev Cancer. 2003, 3:768-780.

598. Sweeney C, Li L, Shanmugam R, Bhat-Nakshatri P, Jayaprakasan V, Baldridge LA, Gardner T, Smith M, Nakshatri H, Cheng L. Nuclear factor-kappaB is constitutively activated in prostate cancer in vitro and is overexpressed in prostatic intraepithelial neoplasia and adenocarcinoma of the prostate. Clin Cancer Res. 2004, 10(16):5501-7.

599. Tachibana K, Yamasaki D, Ishimoto K, Doi T. The Role of PPARs in Cancer. PPAR Research. 2008:102737.

600. Tak PP, Firestein GS. NF-κB: a key role in inflammatory diseases. J Clin Invest 2001, 107:7-11.

601. Takahashi A, Matsumoto H, Yuki K, Yasumoto JI, Kajiwara A, Aoki M, Furusawa Y, Ohnishi K, Ohnishi T. High-LET radiation enhanced apoptosis but not necrosis regardless of p53 status. Int J Radiat Oncol Biology Physics 2004, 60: 591-597.

602. Takayanagi H, Kim S, Koga T, Nishina H, Isshiki M, Yoshida H, Saiura A, Isobe M, Yokochi T, Inoue J, Wagner EF, Mak TW, Kodama T, Taniguchi T. Induction and activation of the transcription factor NFATc1 (NFAT2) integrate RANKL signaling in terminal differentiation of osteoclasts. Dev Cell. 2002, 3(6):889-901.

603. Takeda K, Akira S. Toll-like receptors in innate immunity. Int Immunol, 2005. 17(1):1-14.

604. Talbert DR, Allred CD, Zaytseva YY, Kilgore MW Transactivation of ERα by rosiglitazone induces proliferation in breast cancer cells. Breast Cancer Res Treat. 2008, 108(1): 23-33.

605. Tanno S, Ohsaki Y, Nakanishi K, Toyoshima E, & Kikuchi K. Human small cell lung cancer cells express functional VEGF receptors, VEGFR-2 and VEGFR-3. Lung Cancer. 2004, 46(1), 11-19.

606. Taplin ME and Balk SP Androgen receptor: a key molecule in the progression of prostate cancer to hormone independence. J Cell Biochem. 2004, 91: 483-490.

607. Teitelbaum SL. RANKing c-Jun in osteoclast development. J. Clin. Invest. 2004, 114: 463-465.

608. Terpos E, Rahemtulla A. Bisphosphonate treatment for multiple myeloma. Drugs Today (Barc). 2004, 40(1):29-40.

609. Teruel T, Hernandez R, Benito M, Lorenzo M Rosiglitazone and retinoic acid induce uncoupling protein-1 (UCP-1) in a p38 mitogen-activated protein kinase-dependent manner in fetal primary brown adipocytes. J Biol Chem. 2003, 278: 263-269.

610. Thiery JP, Acloque H, Huang RY, Nieto MA. Epithelial-mesenchymal transitions in development and disease. Cell. 2009, 139(5), 871-890.

611. Tice RR, Agurell E, Anderson D, Burlinson B, Hartmann A, Kobayashi H, Miyamae Y, Rojas E, Ryu JC, Sasaki YF. Single cell gel/comet assay: guidelines for in vitro and in vivo genetic toxicology testing. Environ Mol Mutagen. 2000, 35(3):206-21.

612. Tietze LF, Bell HP, Chandrasekhar S. Natural product hybrids as new leads for drug discovery. Angew Chem Int Ed Engl. 2003, 42(34):3996-4028.

613. Tippani R, Prakhya LJ, Porika M, Sirisha K, Abbagani S, Thammidala C, Pterostilbene as a Potential Novel Telomerase Inhibitor: Molecular Docking Studies and its In Vitro Evaluation. Curr Pharm Biotechnol 2014, 14 (12):1027-35.

614. Tohda C, Nakayama N, Hatanaka F, Komatsu K. Comparison of antiinflammatory activities of six curcuma rhizomes: a possible curcuminoid-independent pathway mediated by Curcuma phaeocaulis Extract. Evid Based Complement Alternat Med. 2006, 3(2), 255-260.

615. Tolomeo M, Grimaudo S, Di Cristina A, et al: Pterostilbene and 3'-hydroxypterostilbene are effective apoptosis-inducing agents in MDR and BCR-ABL-expressing leukemia cells. Int J Biochem Cell Biol 37: 1709-1726, 2005.

616. Torres M, Forman HJ. Redox signaling and the MAP kinase pathways. Biofactors. 2003, 17(1-4):287-96.

617. Trapp V, Parmakhtiar B, Papazian V, Willmott L, Fruehauf JP. Anti-angiogenic effects of resveratrol mediated by decreased VEGF and increased TSP1 expression in melanoma-endothelial cell co-culture. Angiogenesis. 2010, 13(4):305-15.

618. Tsujii M, Kawano S, Dubois RN. Cyclooxygenase-2 expression in human colon cancer cells increases metastatic potential. Proc Natl Acad Sci USA 1997, 94:3336-40.

619. Tsukamoto A, Kaneko Y, Yoshida T, Han K, Ichinose M, Kimura S. 2-Methoxyestradiol, an endogenous metabolite of estrogen, enhances apoptosis and beta-galactosidase expression in vascular endothelial cells. Biochem Biophys Res Commun. 1998, 248(1):9-12.

620. Tulika M, Madhu K, and Aruna B. Anticancer Potential of Aqueous Ethanol Seed Extract of Ziziphus mauritiana against cancer cell lines and Ehrlich ascites carcinoma. Evidence-Based Complementary and Alternative Medicine 2011, 2011:11.

621. Udenigwe CC, Ramprasath VR, Aluko RE, Jones PJ. Potential of resveratrol in anticancer and anti-inflammatory therapy. Nutr Rev. 2008, 66(8):445-54.

622. Unni E, Sun S, Nan B, McPhaul MJ, Cheskis B, Mancini MA, Marcelli M. Changes in androgen receptor nongenotropic signaling correlate with transition of LNCaP cells to androgen independence. Cancer Res. 2004, 64(19):7156-68.

623. Vander Heiden MG, Cantley LC, Thompson CB. Understanding the Warburg effect: the metabolic requirements of cell proliferation. Science. 2009, 324(5930):1029-33.

624. Vardy J. Cognitive function in breast cancer survivors. In Adjuvant Therapy for Breast Cancer. 2009, 387-419.

625. Varmus H. The New Era in Cancer Research. Science 2006, 312:1162-1165.

626. Vasudevan KM, Gurumurthy S, Rangnekar VM. Suppression of PTEN expression by NFkappa B prevents apoptosis. Mol Cell Biol. 2004, 24: 1007-1021.

627. Venkatachalam G, Kumar AP, Yue LS, Pervaiz S, Clement MV, Sakharkar MK.Computational identification and experimental validation of PPRE motifs in NHE1 and MnSOD genes of human. BMC Genomics. 2009, 10:3,S5

628. Venkitaraman AR. Cancer susceptibility and the functions of BRCA1 and BRCA2. Cell, 2002. 108(2), 171-182.

629. Venkov CD, Rankin AB, Vaughan DE. Identification of authentic estrogen receptor in cultured endothelial cells. A potential mechanism for steroid hormone regulation of endothelial function. Circulation. 1996, 94(4):727-33.

630. Viatour P, Merville M-P, Bours V, Chariot A. Phosphorylation of NF-kB and InB proteins: implications in cancer and inflammation. Trends Biochem Sci 2005, 30:43–52.

631. Viegas-Junior C, Danuello A, da Silva Bolzani V, Barreiro EJ, Fraga CA. Molecular hybridization: a useful tool in the design of new drug prototypes. Curr Med Chem. 2007, 14(17):1829-52.

632. Vilar S, Quezada E, Santana L, Uriarte E, Yánez M, Fraiz N, Alcaide C, Cano E, Orallo F. Design, synthesis, and vasorelaxant and platelet antiaggregatory activities of coumarin-resveratrol hybrids. Bioorg Med Chem Lett. 2006, 16(2):257-61.

633. Visvanathan, K. The challenges of treating lobular carcinoma in situ. Oncology. 2011, 25, 1058, 1061, 1066

634. Vivanco I, Sawyers CL. The phosphatidylinositol 3-Kinase AKT pathway in human cancer. Nature Reviews. Cancer. 2002, 2: 489–501.

635. Voduc KD, Cheang MC, Tyldesley S, Gelmon K, Nielsen TO, Kennecke H. Breast cancer subtypes and the risk of local and regional relapse. J Clin Oncol. 2010, 28(10):1684-91.

636. Vogt PK. Jun, the oncoprotein. Oncogene. 2001, 20: 2365-77.

637. Volpert OV. Modulation of endothelial cell survival by an inhibitor of angiogenesis thrombospondin-1: a dynamic balance. Cancer Metastasis Rev. 2000, 19(1-2):87-92.

638. Vosper H, Patel L, Graham TL, Khoudoli GA, Hill A, Macphee CH, Pinto I, Smith SA, Suckling KE, Wolf CR, Palmer CN. The peroxisome proliferator-activated receptor δ promotes lipid accumulation in human macrophages. J. Biol. Chem. 2001, 276: 44258–44265.

639. Vurusaner B, Poli G, Basaga H. Tumor suppressor genes and ROS: complex networks of interactions. Free Radical Biology and Medicine, 2012, 52(1):7-18.

640. Wada T, Nakashima T, Hiroshi N, Penninger JM. RANKL-RANK signaling in osteoclastogenesis and bone disease. Trends Mol Med. 2006, 12(1):17-25.

641. Wallace DM, Chisholm GD, Hendry WF. T.N.M. classification for urological tumours (U.I.C.C.) - 1974. Br J Urol. 1975, 47(1):1 -12.

642. Walle T, Hsieh F, DeLegge MH, Oatis JE Jr, Walle UK. High absorption but very low bioavailability of oral resveratrol in humans. Drug Metab Dispos. 2004, 32(12):1377-82.

643. Wang H, Zhou H, Zou Y, Liu Q, Guo C, Gao G, Shao C, Gong Y. Resveratrol modulates angiogenesis through the GSK3β/β-catenin/TCF-dependent pathway in human endothelial cells. Biochem Pharmacol. 2010, 80(9):1386-95.

644. Wang L, Liu D, Ahmed T, Chung FL, Conaway C, Chiao JW. Targeting cell cycle machinery as a molecular mechanism of sulforaphane in prostate cancer prevention. Int J Oncol. 2004, 24(1):187-92.

645. Wang LG, Liu XM, Chiao JW. Repression of androgen receptor in prostate cancer cells by phenethyl isothiocyanate. Carcinogenesis. 2006, 10: 2124-32.

646. Wang M, Jin Y, Ho CT. Evaluation of resveratrol derivatives as potential antioxidants and identification of a reaction product of resveratrol and 2, 2-diphenyl-1-picryhydrazyl radical. J Agric Food Chem. 1999, 47(10):3974-7.

647. Wang N, Verna L, Hardy S, Zhu Y, KS Ma, Birrer MJ, Stemerman MB. c-Jun triggers apoptosis in human vascular endothelial cells. Circ Res.1999, 85: 387-93.

648. Wang TT, Schoene NW, Kim YS, Mizuno CS, Rimando AM Differential effects of resveratrol and its naturally occurring ethylether analogs on cell cycle and apoptosis in human androgen-responsive LNCaP cancer cells. Mol Nutr Food Res. 2010, 54: 335-44.

649. Wang Y, Ji P, Liu J, Broaddus RR, Xue F, Zhang W. Centrosome-associated regulators of the G(2)/M checkpoint as targets for cancer therapy. Mol Cancer. 2009, 8:8.

650. Warburg OH. The Metabolism of Tumours: Investigations from the Kaiser Wilhelm Institute for Biology, Berlin-Dahlem (London, UK: Arnold Constable) 1930.

651. Warburg, O. On respiratory impairment in cancer cells. Science 1956b, 124 (3215), 269–270.

652. Warburg, O. On the origin of cancer cells. Science 1956a, 123(3191): 309-314.

653. Wattenberg LW. Chemoprevention of cancer. Cancer Res. 1985, 45:1-8

654. Watters JJ, Campbell JS, Cunningham MJ, Krebs EG, Dorsa DM. Rapid membrane effects of steroids in neuroblastoma cells: effects of estrogen on mitogen activated protein kinase signalling cascade and c-fos immediate early gene transcription. Endocrinology. 1997, 138:4030-4033.

655. Weinberg OK, Marquez‑Garban DC, Pietras RJ. New approaches to reverse resistance to hormonal therapy in human breast cancer. Drug Resist Updates 2005, 8:219-33.

656. Weis SM, Cheresh DA. Tumor angiogenesis: molecular pathways and therapeutic targets. Nat Med. 2011, 17(11):1359-70.

657. Wen Y, Hu MCT, Makino K, Spohn B, Bartholomeusz G, Yan DH, Hung. HER-2/neu promotes androgen-independent survival and growth of prostate cancer cells through the Akt pathway. Cancer Res. 2000, 60:6841-5.

658. Wenzel E, Soldo T, Erbersdobler H, Somoza V. Bioactivity and metabolism of trans-resveratrol orally administered to Wistar rats. Mol. Nutr. Food Res. 2005, 49: 482–494.

659. Wermuth CG. The Practice of Medicinal Chemistry (third ed.) Elsevier/Academic Press, Amsterdam, Boston. 2008.

660. Wertz IE, Dixit VM. Regulation of death receptor signaling by the ubiquitin system. Cell Death & Differentiation, 2010. 17(1), 14-24.

661. Wickstrom SA, Alitalo K, Keski-Oja J. Endostatin associates with integrin alfa5beta1 and caveolin-1, and activates Src via a tyrosyl phosphatasa-dependent pathway in human endothelial cells. Cancer Res. 2002, 62:5580-9.

662. Wilding JPH. PPAR agonists for the treatment of cardiovascular disease in patients with diabetes. Diabetes, Obesity and Metabolism, 2012. 14(11): 973-982.

663. Wills AL (1969). Release of histamine, kinin and prostaglandins during carrageenin induced inflammation in the rats, Prostaglandins, Peptides and Amins, P. Montagazzaand, E.W. Horton, Eds., pp. 31-48, Academic Press, London, UK.

664. Wilson J, Balkwill F. The role of cytokines in the epithelial cancer microenvironment. Semin Cancer Biol. 2002, 12:113–20.

665. Winter, C A, Risley EA, Nuss, GW. Carrageenan-induced edema in hind paws of rat as an assay for anti-inflammatory drugs. Proc Soc Exp Biol Med. 1962, 111(3), 544-547.

666. Witsch E, Sela M, Yarden Y. Roles for growth factors in cancer progression. Physiology (Bethesda, Md.) 2010. 25(2), 85.

667. Wittman MD, Kadow JF, Vyas DM, Lee FL, Rose WC, Long BH, Fairchild C, Johnston K. Synthesis and antitumor activity of novel paclitaxel-chlorambucil hybrids Bioorg Med Chem Lett 2001, 11: 811-814.

668. Wong YN, Ferraldeschi R, Attard G, de Bono J. Evolution of androgen receptor targeted therapy for advanced prostate cancer. Nat Rev Clin Oncol. 2014, (6):365-76.

669. Woo CC, Loo SY, Gee V, Yap CW, Sethi G, Kumar AP, Tan KH. Anticancer activity of thymoquinone in breast cancer cells: possible involvement of PPAR-γ pathway. Biochem Pharmacol. 2011, 82(5):464-75.

670. Wu S, Boyer CM, Whitaker RS, Berchuck A, Wiener JR, Weinberg JB, Bast RC Jr. Tumor necrosis factor alpha as an autocrine and paracrine growth factor for ovarian cancer: monokine induction of tumor cell proliferation and tumor necrosis factor alpha expression. Cancer Res. 1993, 53(8):1939-44.

671. Wu X, Zhou QH, Xu K Are isothiocyanates potential anti-cancer drugs? Acta Pharmacol Sin. 2009, 30(5): 501-512.

672. Wu, Y, and Zhou BP. TNF-alpha/NF-kappaB/Snail pathway in cancer cell migration and invasion. Br. J. Cancer. 2010, 102:639-44.

673. Xiao D, Singh SV. Phenethyl isothiocyanate-induced apoptosis in p53-deficient PC-3 human prostate cancer cell line is mediated by extracellular signal-regulated kinases. Cancer Res. 2002, 62(13):3615-9.

674. Xu J, Wu HF, Ang ES, Yip K, Woloszyn M, Zheng MH, Tan RX. NF-kappaB modulators in osteolytic bone diseases. Cytokine Growth Factor Rev. 2009, 20(1):7-17.

675. Xu L, Han C, Lim K, Wu T. Cross-talk between peroxisome proliferator-activated receptor delta and cytosolic phospholipase A(2)alpha/cyclooxygenase-2/ prostaglandin E(2) signaling pathways in human hepatocellular carcinoma cells. Cancer Res. 2006, 66:11859-68.

676. Xuan H, Zhao J, Miao J, Li Y, Chu Y, Hu F. Effect of Brazilian propolis on human umbilical vein endothelial cell apoptosis. Food Chem Toxicol. 2011, 49(1):78-85.

677. Yang H, Bhat GK, Wadley R, Wright KL, Chung BM, Whittaker JA, Dharmarajan AM, Sridaran R. Gonadotropin-releasing hormone-agonist inhibits synthesis of nitric oxide and steroidogenesis by luteal cells in the pregnant rat. Biol Reprod. 2003, 68(6):2222-31.

678. Yeh S, Lin HK, Kang HY, Thin TH, Lin MF, Chang C. From HER2/Neu signal cascade to androgen receptor and its coactivators: a novel pathway by induction of androgen target genes through MAP kinase in prostate cancer cells. Proc Natl Acad Sci U S A. 1999, 96(10):5458-63.

679. Yi T, Cho SG, Yi Z, Pang X, Rodriguez M, Wang Y, Sethi G, Aggarwal BB, Liu M. Thymoquinone inhibits tumor angiogenesis and tumor growth through suppressing AKT and ERK signaling pathways. Mol Cancer Ther 2008, 7: 1789-1796.

680. Yin F, Wakino S, Liu Z, Kim S, Hsueh WA, Collins AR, Van Herle AJ, Law RE.Troglitazone inhibits growth of MCF-7 breast carcinoma cells by targeting G1 cell cycle regulators. Biochem Biophys Res Commun. 2001, 286(5):916-22.

681. Yoo SY, Kwon SM. Angiogenesis and its therapeutic opportunities. Mediators Inflamm. 2013, 127170:11.

682. Yu J, Wang Z, Kinzler KW, Vogelstein B, Zhang L. PUMA mediates the apoptotic response to p53 in colorectal cancer cells. Proc Natl Acad Sci U S A. 2003, 100(4):1931-6.

683. Yuan H, Gong A, Young CY. Involvement of transcription factor Sp1 in quercetin-mediated inhibitory effect on the androgen receptor in human prostate cancer cells. Carcinogenesis. 2005, 26(4):793-801.

684. Yue TL, Wang X, Louden CS, Gupta S, Pillarisetti K, Gu JL, Hart TK, Lysko PG, Feuerstein GZ. 2-Methoxyestradiol, an endogenous estrogen metabolite, induces apoptosis in endothelial cells and inhibits angiogenesis: possible role for stress-activated protein kinase signaling pathway and Fas expression. Mol Pharmacol. 1997, 51(6):951-62.

685. Zelivianski S, Spellman M, Kellerman M, Kakitelashvilli V, Zhou XW, Lugo E, Lee MS, Taylor R, Davis TL, Hauke R, Lin MF. ERK inhibitor PD98059 enhances docetaxel-induced apoptosis of androgen-independent human prostate cancer cells. Int J Cancer. 2003, 107(3):478-85.

686. Zhan P, Liu X. Designed multiple ligands: an emerging anti-HIV drug discovery paradigm. Curr Pharm Des. 2009, 15(16):1893-917.

687. Zhang GY, Ahmed N, Riley C, Oliva K, Barker G, Quinn MA, Rice GE. Enhanced expression of peroxisome proliferator-activated receptor gamma in epithelial ovarian carcinoma. Br J Cancer. 2005, 92(1):113-119.

688. Zhang L, Jing H, Cui L, Li H, Zhou B, Zhou G, Dai F. 3,4-Dimethoxystilbene, a resveratrol derivative with anti-angiogenic effect, induces both macroautophagy and apoptosis in endothelial cells. J Cell Biochem. 2013, 114(3):697-707.

689. Zhang Z, Kumar R, Santen RJ, Song RX. The role of adapter protein Shc in estrogen non-genomic action. Steroids.2004, 69(89):523-9.

690. Zheng H, Yu X, Collin-Osdoby P, Osdoby P. RANKL stimulates inducible nitric-oxide synthase expression and nitric oxide production in developing osteoclasts. An autocrine negative feedback mechanism triggered by RANKL-induced interferon-beta via NF-kappaB that restrains osteoclastogenesis and bone resorption. J Biol Chem. 2006, 281(23):15809-20.

691. Zhou J, Zhang W, Liang B, Casimiro MC, Whitaker-Menezes D, Wang M, Lisanti MP, Lanza-Jacoby S, Pestell RG, Wang C. PPAR gamma activation induces autophagy in breast cancer cells. Int J Biochem Cell Biol. 2009, 41(11):2334-42.

692. Zhuang L, Lin J, Lu ML, Solomon KR, Freeman MR. Cholesterol-rich lipid rafts mediate akt-regulated survival in prostate cancer cells. Cancer Res. 2002, 62(8):2227-31.